

**THE SYNTHESIS OF XANTHONE DERIVATIVES  
AND THEIR ENZYMATIC CONVERSION AND  
INHIBITION  
OF AFLATOXIN BIOSYNTHESIS**

by

**ROBERT MOONSAMY GENGAN**

**M.Dip.Tech**

**(M L Sultan Technikon: Kwa-Zulu Natal)**

**submitted in partial fulfilment of the  
requirements for the degree of  
Doctor of Philosophy,  
in the  
Department of Physiology  
University of Natal  
Durban**

## DEDICATION

I dedicate this thesis in memory of my late brother-in-law, Sam Govender, and to my Bhagawan Sri Sathya Sai Baba for helping me to achieve what my ego said could not be done.

*You have to busy yourself with activity in order to use time and skill to the best advantage. The dull and the inert will hesitate to be active, for fear of exhaustion or failure or loss. The emotional, passionate individuals will plunge headlong and crave for quick results and will be disappointed if they do not come in. The balanced persons will be active, because it is their duty; they will not be agitated by anything- failure or success. Seek the light always; be full of confidence and zest. Do not despair; it can never produce results. It only worsens the problem, for it darkens the intellect and plunges you in doubt.*

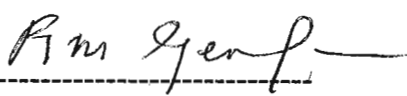
*Sai Baba*

## PREFACE

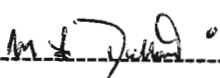
The experimental work described in this thesis was carried out in:

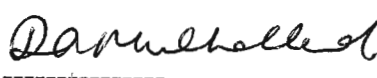
- the Department of Physiology, University of Natal, Durban, under the supervision of Professor Mike F Dutton and
- the Department of Chemistry, M L Sultan Technikon, under the co-supervision of Professor Dulcie A Mulholland.

These studies represent original work by the author and have not been submitted in any form to another University. Where use was made of the work of others it has been duly acknowledged in the text.

  
-----  
Robert Moonsamy Gengan

I hereby certify that the above statement is correct.

  
-----  
Professor M F Dutton

  
-----  
Professor D A Mulholland

## PUBLICATIONS AND PRESENTATIONS

1. Gengan, R.M., Chuturgoon, A.A., Mulholland, D.A. and Dutton, M.F. 1997. The Synthesis of Sterigmatocystin Derivatives. *Frank Warren Conference*, Mtunzini, Kwa-Zulu, Natal (poster presentation).
2. Gengan, R.M., Chuturgoon, A.A., Mulholland, D.A. and Dutton, M.F. 1997. The Conversion of Sterigmatocystin Derivatives to Aflatoxin B<sub>1</sub> in a Cell-Free Enzyme Preparation. *The 6<sup>th</sup> Joint Microbiology and Biochemistry Symposium*, Durban, Kwa-Zulu, Natal (oral presentation).
3. Gengan, R.M., Chuturgoon, A.A., Mulholland, D.A. and Dutton, M.F. 1998. The in Vitro Conversion of Sterigmatocystin and O-Methyl sterigmatocystin to Aflatoxin B<sub>1</sub>. An Improved Method of Cell-Free Enzyme Preparation. *The 10<sup>th</sup> Biennial Conference of the Society for Microbiology*, Durban, Kwa-Zulu, Natal (poster presentation).
4. Gengan, R.M., Chuturgoon, A.A., Mulholland, D.A. and Dutton, M.F. 1999. Synthesis of Sterigmatocystin Derivatives and their Biotransformation to Aflatoxins by a Blocked Mutant of *Aspergillus parasiticus*. *Mycopathologia* 114: 115-122.
5. Gengan, R.M., Chuturgoon, A.A., Mulholland, D.A. and Dutton, M.F. 1998. The Role of O-methyl sterigmatocystin in Aflatoxin B<sub>1</sub> Biosynthesis. *Mycopathologia* (with editors, Ref. No. MYCO 2353-3).
6. Gengan, R.M., Mulholland, D.A., Dutton, M.F. and Chuturgoon, A.A. 1999. The Conversion of Sterigmatocystin and its Derivatives to Aflatoxin B<sub>1</sub> by a Partially Purified Enzyme System (in preparation).

## OTHER CONTRIBUTIONS

1. The Synthesis of Zearlenone Epoxide and its *In Vivo* Cytotoxic Effect in Human Cell Lines. 1996. *M.Med.Sc.* (Naidoo, D).
2. The Synthesis of Aflatoxin B<sub>1</sub> Epoxide and its *In Vivo* Cytotoxic Effect in Human Cell Lines. 1997. *M.Med.Sc.* (Palanee, T).
3. The Synthesis of Aflatoxin B<sub>1</sub> Amino Acid Conjugates and the Development of a High Pressure Liquid Chromatography Method for Analysis. 1998. *M.Med.Sc.* (Selby, S).

## ACKNOWLEDGEMENTS

The kind assistance of the following people who played a role in the successful completion of the study is noted with gratitude:

1. Professor M F Dutton, Head of the Physiology Department, University of Natal, Medical Faculty, Durban, for supervising the study with such expertise that just the correct guidance was given at the appropriate time and the author's initiative was neither sacrificed nor accepted without criticism.
2. Professor D A Mulholland, Associate Professor of the Chemistry Department, University of Natal, Durban, the co-supervisor of the study, for assisting the author in the chemistry aspects of the thesis. Her appraisal of my work and attention to detail has been most valuable.
3. Mr A Chuturgoon, Senior Lecturer of the Biochemistry Department, University of Natal, Medical Faculty, Durban, for all the useful comments and suggestions made regarding all aspects of the study. His willingness to help and share his vast experience and knowledge is indeed noted with gratitude.
4. My wife Shirley and my daughters Kerena and Trinisha, for their patience and understanding shown during my absence whilst undertaking this rigorous study.
5. My parents, brothers and sister for all the sacrifices they made in providing the solid foundation on which I could build my academic career.
6. The academic, technical and secretarial staff of the Department of Chemistry, M L Sultan Technikon, Durban and the Department of Physiology, University of Natal, Durban, for their assistance rendered whenever it was required.
7. The Foundation for Research and Development for the generous study grant during the 5 years of study.

## ABSTRACT

The biosynthesis of Aflatoxin B<sub>1</sub> (AFB<sub>1</sub>) has been the subject of conflicting speculation and numerous reviews. The currently accepted scheme for the aflatoxin pathway is based on data obtained from feeding studies using isotopically labelled precursors. In these studies the conversion of possible intermediate metabolites to AFB<sub>1</sub> by mutants of *Aspergillus parasiticus* illustrated their role as biogenetic precursors. Currently there is now agreement on the identity of most of the intermediate metabolites involved in the biosynthesis of AFB<sub>1</sub>. However, there is a lack of clarity on the details of AFB<sub>1</sub> biosynthesis including the conversion of sterigmatocystin (ST) to AFB<sub>1</sub> via the metabolite *O*-methylsterigmatocystin (OMST). There is no clear cut evidence of the metabolic role of OMST, i.e., either it is a compulsory intermediate or a shunt metabolite and hence part of a metabolic grid.

In order to investigate this step in AFB<sub>1</sub> biosynthesis, ST was isolated from surface cultures of *A. versicolor* (M1101) and purified by silica gel column chromatography and repeated recrystallisation. Sterigmatocystin was characterised by thin layer chromatography (t.l.c.), low resolution mass spectrometry (M.S) and nuclear magnetic resonance spectroscopy (N.M.R). A series of seven derivatives of the free hydroxyl group of ST were synthesised by known chemical reactions, purified by silica gel column chromatography and characterised by high resolution mass spectrometry and proton nuclear magnetic resonance spectroscopy.

A high pressure liquid chromatography (HPLC) method was developed using a fluorescence detector. The optimum parameters for the separation of the four major aflatoxins, namely AFB<sub>1</sub>, AFB<sub>2</sub>, AFG<sub>1</sub> and AFG<sub>2</sub>, using trifluoroacetic acid as the derivatising reagent, were obtained for a reversed phase Prodigy C<sub>18</sub> column with a mobile phase of water: acetonitrile: isopropanol: acetic acid (8: 1: 0.5: 0.5, v/v).

Feeding studies, using whole cells of *A. parasiticus* (Wh1-11-105), showed that ST and the ST derivatives were converted to AFB<sub>1</sub>. A time course study for the conversion of ST and selected ST derivatives to AFB<sub>1</sub> indicated a decrease in the rate of conversion in the order:

*O*-propyl sterigmatocystin (OPROST) > *O*-ethyl sterigmatocystin > *O*-methyl sterigmatocystin > Sterigmatocystin > *O*-benzoyl sterigmatocystin (OBzST).

It was apparent that the “enzyme” responsible for the conversion of the derivatives to AFB<sub>1</sub> did not display a high degree of substrate specificity, since it was unable to recognize the difference between the various alkyl groups, either as ether or ester functional groups.

An HPLC method was developed using a diode array detector. The optimum parameters for the separation of aflatoxin metabolites and the synthesised derivatives were obtained for a reversed phase Lichrosphere RP-18 column with a 30 minute gradient elution program with water and acetonitrile as the mobile phase.

Crude cell-free extracts were prepared by lyophilisation of the mycelia of *A. parasiticus* (Wh1-11-105) with phosphate buffer. The temperature and pH for the conversion of ST to AFB<sub>1</sub>, were found to be optimum at 28°C and 7.2, respectively. The addition of SAM (1.5 mM) and NADPH (1.5 mM) increased the conversion of ST to AFB<sub>1</sub> from 11.21 % to 27.10 %. A time course study with ST, OMST and OPROST showed that the rate of conversion to AFB<sub>1</sub> was close to linear for an incubation time of up to 60 minutes. Approximation of the reaction rate indicated a decrease in the order:

OMST > ST > OPROST.

This indicated that the time course reaction using whole cells was in part a measure of membrane permeability rather than substrate specificity.

Molecular exclusion chromatography was used to separate enzymatic protein from primary and secondary metabolites, small biomolecules and indigenous co-factors (MW < 10 000) and the partially purified “enzyme” was concentrated by dialysis against



solid sucrose. The “enzyme” was subjected to non-denaturing polyacrylamide gel electrophoresis and was found to be made of sub-units ranging from 58 kDa to over 200 kDa. Enzymatic investigations with ST, as substrate, indicated that OMST is a compulsory intermediate in the biosynthesis of AFB<sub>1</sub>. Also, enzymatic investigations of selected ST derivatives showed that the partially purified “enzyme” displayed relative specificity for these substrates, viz., OMST, OPROST and OBzST.

Three xanthenes, namely, 1-hydroxy-3,6-dimethylxanthone, 1-methoxy-3,6-dimethylxanthone and 1-acetyl-3,6-dimethylxanthone were synthesised, purified and characterised spectroscopically. Whole cell studies of *A. parasiticus* (CMI 91019b) and *A. parasiticus* (Wh1-11-105) showed that these xanthenes inhibited AFB<sub>1</sub> production to varying extents. Kinetic studies of cell-free extracts revealed that the 1-methoxy-3,6-dimethylxanthone derivative was a non-competitive inhibitor. The Michaelis Menten constant ( $K_m$ ) of approximately 5.60  $\mu$ M (for OMST) was determined for a cell-free reaction at pH 7.2 and 28 °C.

A Clark oxygen electrode was used to carry out oxygen consumption studies in a partially purified “enzyme” preparation. A calibration system was designed and the enzymatic conversion of OMST to AFB<sub>1</sub> and NADPH consumption were monitored by HPLC and UV spectroscopy, respectively. From the results of these enzymatic reactions, the following stoichiometric relationship was determined:

2 mole oxygen consumed = 1 mole NADPH consumed = 1 mole AFB<sub>1</sub> produced

A tentative mechanism is discussed for the conversion of OMST to AFB<sub>1</sub> which utilizes a monooxygenase and a dioxygenase.



## TABLE OF CONTENTS

	<b>Page</b>
DEDICATION	ii
PREFACE	iii
PUBLICATIONS AND PRESENTATIONS	iv
ACKNOWLEDGEMENTS	v
ABSTRACT	vi-viii
TABLE OF CONTENTS	ix-xiv
LIST OF FIGURES	xv-xxiv
LIST OF TABLES	xxv-xxviii
LIST OF ABBREVIATIONS	xxix-xxx
 <b>CHAPTER ONE</b>	
<b>INTRODUCTION</b>	1-2
 <b>CHAPTER TWO</b>	
<b>LITERATURE REVIEW</b>	
2.1. AFLATOXINS AS SECONDARY METABOLITES	3
2.2. THE HISTORY AND INCIDENCE OF AFLATOXINS	3-4
2.3. THE STRUCTURE OF AFLATOXINS	4-5
2.4. THE STRUCTURE OF STERIGMATOCYSTIN	6-7
2.5. FUNGAL SECONDARY METABOLIC ENZYMES	8
2.5.1. Characteristics of the Enzymes	8-10
2.5.2. Isolation of the Enzymes	10-11
2.5.3. Purification of the Enzymes	12
2.6. AFLATOXIN BIOSYNTHESIS	13-15
2.7. AFLATOXIN BIOSYNTHETIC PATHWAY	13-14
2.7.1. The Polyketide Pathway and Aflatoxin Pathways	16-19

2.7.2. Anthraquinone Synthesis	19-21
2.7.3. Xanthone Synthesis	21-24
2.7.4. Xanthone Transformation to Aflatoxins	25-29
2.8. THE INHIBITION OF AFLATOXIN BIOSYNTHESIS	29-31
2.9. MOLECULAR BIOLOGY OF AFLATOXIN BIOSYNTHESIS	31-34

### **CHAPTER THREE**

#### **PRODUCTION, ISOLATION AND CHARACTERISATION OF STERIGMATOCYSTIN**

3.1. INTRODUCTION	35-36
3.2. MATERIALS AND METHODS	37
3.2.1. Chemicals and Materials	37
3.2.2. General	37
3.2.3. Organism, Medium and Culturing Technique	37-38
3.2.4. Extraction and Purification of Sterigmatocystin	38
3.2.5. Characterisation by Thin Layer Chromatography	38-39
3.2.6. Characterisation by Spectroscopic Techniques	39
3.3. RESULTS AND DISCUSSION	40-44

### **CHAPTER FOUR**

#### **SYNTHESIS AND CHARACTERISATION OF STERIGMATOCYSTIN DERIVATIVES**

4.1. INTRODUCTION	45-46
4.2. MATERIALS AND METHODS	47
4.2.1. Chemicals	47
4.2.2. General	47
4.2.3. General Procedure for Alkylation of Sterigmatocystin	47-48
4.2.4. General Procedure for Esterification	48
4.3. RESULTS AND DISCUSSION	49-56

## **CHAPTER FIVE**

### **DEVELOPMENT OF METHODS FOR HIGH PRESSURE LIQUID CHROMATOGRAPHY**

5.1. INTRODUCTION	57-64
5.2. MATERIALS AND METHODS	65
5.2.1. Chromatographic Equipment	65
5.2.2. Chemicals and Reagents	65
5.2.3. Preparation of Standard Solutions	65-66
5.2.4. The Mobile Phase for Fluorescence Detector	66
5.2.5. The Mobile Phase for Photo Diode Array Detector	66
5.2.6. The Method Used for Quantification of Aflatoxin B <sub>1</sub>	66
5.2.7. Repeatability of Retention Times and Peak Areas	67
5.3. RESULTS AND DISCUSSION	68-87

## **CHAPTER SIX**

### **BIOTRANSFORMATION OF STERIGMATOCYSTIN DERIVATIVES USING WHOLE CELLS**

6.1. INTRODUCTION	88-89
6.2. MATERIALS AND MATHODS	90
6.2.1. Chemicals and Materials	90
6.2.2. Organism, Media and Culture Technique	90
6.2.3. Extraction of Aflatoxins and Sample Preparation for Thin Layer and High Pressure Liquid Chromatography	91
6.3. RESULTS AND DISCUSSION	92-99

## **CHAPTER SEVEN**

### **ENZYMATIC CONVERSION OF STERIGMATOCYSTIN DERIVATIVES USING CELL-FREE EXTRACTS**

7.1. INTRODUCTION	100-101
-------------------	---------

7.2. MATERIALS AND METHODS	102
7.2.1. Chemicals	102
7.2.2. General	102
7.2.3. Culture and Culture Conditions	102
7.2.4. The Preparation of Cell-Free Extracts	103
7.2.5. The Method Used for Enzyme Assays	103-104
7.2.6. Qualitative Analysis by Thin Layer Chromatography	104
7.2.7. Quantification by High Pressure Liquid Chromatography	104
7.2.8. Determination of the Protein Content of the Cell-Free Extract	105
7.2.8.1. Preparation of the Bradford Reagent	105
7.2.8.2. Preparation of the Protein Standard Calibration Graph	105
7.3. RESULTS AND DISCUSSION	106-118

## **CHAPTER EIGHT**

### **PARTIAL PURIFICATION OF CELL-FREE EXTRACT AND ITS ENZYMATIC REACTION**

8.1. INTRODUCTION	119-120
8.2. MATERIALS AND METHODS	121
8.2.1. General	121
8.2.2. Chemicals	121
8.2.3. Preparation of Sephadex Gel	121
8.2.4. Preparation of the Column for Chromatography	121-122
8.2.5. The Method of Dialysis for Concentrating the Protein	122
8.2.6. The Method Used for Enzyme Assays	122
8.2.7. The Method used for Polyacrylamide Gel Electrophoresis	122-123
8.3. RESULTS AND DISCUSSION	124-132

**CHAPTER NINE****SYNTHESIS OF SIMPLE XANTHONES AND THEIR INHIBITION OF AFLATOXIN BIOSYNTHESIS**

9.1. INTRODUCTION	133-145
9.2. MATERIALS AND METHODS	146
9.2.1. General	146
9.2.2. Chemicals	146
9.2.3. Synthesis of Ethyl Salicylate	146-147
9.2.4. Attempted Synthesis of 1-Hydroxyxanthone	147
9.2.5. Attempted Synthesis of 1,8-Dihydroxyxanthone	147-148
9.2.6. Attempted Synthesis of 1-Hydroxy-6,8-Dimethoxyxanthone	148-149
9.2.7. Synthesis of 1-Hydroxy-3,6-dimethylxanthone	149-150
9.2.8. Alkylation of 1-Hydroxy-3,6-dimethylxanthone	150
9.2.9. Acetylation of 1-Hydroxy-3,6-dimethylxanthone	150-151
9.2.10. Organism, Media and Culture Conditions for Whole Cell Reactions	151-152
9.2.11. Extraction of Aflatoxins and Sample Preparation for Thin Layer and High Pressure Liquid Chromatography	152
9.2.12. Preparation of the Cell-Free Extract	152
9.2.13. The Method Used for Enzyme Assays	153
9.2.14. Kinetic Studies of Cell-Free Extracts	153
9.3. RESULTS AND DISCUSSION	154-174

**CHAPTER TEN****THE NATURE OF THE OXYGENASE(S) INVOLVED IN THE CONVERSION OF *O*-METHYL STERIGMATOCYSTIN TO AFLATOXIN B<sub>1</sub>**

10.1 INTRODUCTION	175
10.1.1. The Metabolic Mechanism	175-179
10.1.2. The Oxygen Electrode	179-184
10.2. MATERIALS AND METHODS	185

10.2.1. General	185
10.2.2. Chemicals	185-186
10.2.3. Preparation of the Concentrated Dialysed Enzyme(s)	186
10.2.4. Qualitative Analysis by Thin Layer Chromatography	187
10.2.5. Quantification by High Pressure Liquid Chromatography	187
10.2.6. Quantification of NADPH by Ultra-Violet Spectroscopy	187-188
10.2.7. The Method Used for Oxygen Consumption Studies	188
10.2.7.1. The Operation of the Oxygen Uptake Chamber	188-190
10.2.7.2. The Installation of the Membrane	190
10.2.7.3. Calibration of the Instrument	190-192
10.2.7.4. The Method Used to Determine the Electrode Response to Organic Solvents	193
10.2.7.5. The Method Used for Enzyme Assay with the Clark Oxygen Electrode	193-194
10.3. RESULTS AND DISCUSSION	195-215
 <b>CHAPTER ELEVEN</b>	
<b>GENERAL DISCUSSION</b>	216-224
 <b>REFERENCES</b>	225-233
<b>APPENDICES</b>	234-314

## LIST OF FIGURES

Figure	Page
1. The Structure of Aflatoxins and Closely Related Metabolites	5
2. Xanthone Type Metabolites Found in the Aflatoxin Biosynthetic Pathway	7
3. Incorporation of Molecular Oxygen by Oxygenases	8
4. Conversion of Progesterone to Testosterone Lactone by a Monooxygenase	9
5. Incorporation of Molecular Oxygen by a Dioxygenase	10
6. Proposed Pathway for the Biosynthesis of Aflatoxin B <sub>1</sub>	14
7. The Currently Accepted Pathway for the Biosynthesis of Aflatoxin B <sub>1</sub>	15
8. Transformation of Dehydroacetic Acid to Some Natural Products	16
9. The Acy-Polymalonate Biosynthetic Route for Polketide Biosynthesis	17
10. Schematic Representation of Fatty Acid and Polyketide Biosynthesis	19
11. Hypothetical Scheme for the Assembly of Anthraquinones in <i>Aspergillus sp.</i>	20
12. Schematic Representation of Anthraquinone Derivatives leading to AFB <sub>1</sub> Production	21
13. The Metabolic Scheme for Aflatoxin Biosynthesis Showing Structures of Critical Intermediates	23
14. Possible Steps Involved in the Rearrangement of Anthraquinone to Xanthenes	24
15. Structure of Sterigmatocystin with Labels Derived from Acetate	25
16. The Metabolic Scheme Proposed for the Late Stages of Aflatoxin Biosynthesis	26
17. The Mechanism Proposed by Bhatnagar <i>et al.</i> for the Conversion of <i>O</i> -Methyl sterigmatocystin to Aflatoxin B <sub>1</sub>	27
18. A Mechanism Proposed by Bhatnagar <i>et al.</i> for the Conversion of <i>O</i> -Methyl sterigmatocystin to Aflatoxin B <sub>1</sub> Involving Oxygenases	29
19. The Chemical Structure of Some Compounds Inhibiting Aflatoxin B <sub>1</sub> Production	31
20. The Biosynthetic Pathway of Aflatoxin B <sub>1</sub> Showing the Major Intermediates	



and the Aflatoxin Gene Cluster.	34
21. The Structure of Sterigmatocystin Showing the Numbering System	41
22. The DEPT Spectrum of Sterigmatocystin	235
23. The $^{13}\text{C}$ -NMR Spectrum of Sterigmatocystin	236
24. The HETCOR Spectrum of Sterigmatocystin	237
25. The COSY Spectrum of Sterigmatocystin	238
26. The $^1\text{H}$ -NMR Spectrum of Sterigmatocystin	43
27. The Expanded $^1\text{H}$ -NMR Spectrum of Sterigmatocystin	239
28. The Normalised Mass Spectrum of Sterigmatocystin Using Electron Impact Ionization (70 eV)	44
29. The Stabilization of a Typical Phenoxide Ion by Resonance	45
30. The Structure of Compounds Obtained from Sterigmatocystin	46
31. The Reaction Scheme for the Synthesis of Sterigmatocystin Derivatives	49
32. The Structure of Sterigmatocystin Derivatives	51
33. The $^1\text{H}$ -NMR Spectrum of <i>O</i> -Ethyl sterigmatocystin	240
34. The Expanded $^1\text{H}$ -NMR Spectrum of <i>O</i> -Ethyl sterigmatocystin	242
35. The Normalised Mass Spectrum of <i>O</i> -Ethyl sterigmatocystin	243
36. The $^1\text{H}$ -NMR Spectrum of <i>O</i> -Propyl sterigmatocystin	245
37. The Expanded $^1\text{H}$ -NMR Spectrum of <i>O</i> -Propyl sterigmatocystin	246
38. The Normalised Mass Spectrum of <i>O</i> -Propyl sterigmatocystin	247
39. The $^1\text{H}$ -NMR Spectrum of <i>O</i> -Butyl sterigmatocystin	55
40. The Expanded $^1\text{H}$ -NMR Spectrum of <i>O</i> -Butyl sterigmatocystin	248
41. The Normalised Mass Spectrum of <i>O</i> -Butyl sterigmatocystin	56
42. The $^1\text{H}$ -NMR Spectrum of <i>O</i> -Pentyl sterigmatocystin	250
43. The Expanded $^1\text{H}$ -NMR Spectrum of <i>O</i> -Pentyl sterigmatocystin	251
44. The Normalised Mass Spectrum of <i>O</i> -Pentyl sterigmatocystin	252
45. The $^1\text{H}$ -NMR Spectrum of <i>O</i> -Propenyl sterigmatocystin	254
46. The Expanded $^1\text{H}$ -NMR Spectrum of <i>O</i> -Propenyl sterigmatocystin	255
47. The Normalised Mass Spectrum of <i>O</i> -Propenyl sterigmatocystin	256
48. The $^1\text{H}$ -NMR Spectrum of <i>O</i> -Acetyl sterigmatocystin	258

49. The Normalised Mass Spectrum of <i>O</i> -Acetyl sterigmatocystin	259
50. The <sup>1</sup> H-NMR Spectrum of <i>O</i> -Benzoyl sterigmatocystin	261
51. The Expanded <sup>1</sup> H-NMR Spectrum of <i>O</i> -Benzoyl sterigmatocystin	262
52. The Normalised Mass Spectrum of <i>O</i> -Benzoyl sterigmatocystin	263
53. A Chromatogram with its Characteristic Features	58
54. Structures of the Aflatoxins and Derivatives Produced by TFA	61
55. Isocratic Reversed Phase Chromatogram of Standard Aflatoxins	62
56. The UV 6000LP Optical System	63
57. The Calibration Graph of Aflatoxin B <sub>1</sub> Using the Fluorescence Detector	264
58. The Calibration Graph of Aflatoxin B <sub>1</sub> Using the Diode Array Detector	265
59. The Isocratic Reversed Phase Chromatogram for the Separation of Aflatoxins with the Mobile Phase Water: Acetonitrile: Isopropanol (8:1:1) at a Flow Rate of 1 ml/min.	69
60. The Isocratic Reversed Phase Chromatogram for the Separation of Aflatoxins with the Mobile Phase Water: Acetonitrile: Isopropanol: Acetic Acid (7.95:1:1:0.05) at a Flow Rate of 1 ml/min.	70
61. The Isocratic Reversed Phase Chromatogram for the Separation of Aflatoxins with the Mobile Phase Water: Acetonitrile: Isopropanol: Acetic Acid (7.9:1:1:0.1) at a Flow Rate of 1 ml/min.	70
62. The Isocratic Reversed Phase Chromatogram for the Separation of Aflatoxins with the Mobile Phase Water: Acetonitrile: Isopropanol: Acetic Acid (8.4:1:0.5:0.1) at a Flow Rate of 1 ml/min.	72
63. The Isocratic Reversed Phase Chromatogram for the Separation of Aflatoxins with the Mobile Phase Water: Acetonitrile: Isopropanol: Acetic Acid (8.3:1:0.5:0.2) at a Flow Rate of 1 ml/min.	72
64. The Isocratic Reversed Phase Chromatogram for the Separation of Aflatoxins with the Mobile Phase Water: Acetonitrile: Isopropanol: Acetic Acid (8.2:1:0.5:0.3) at a Flow Rate of 1 ml/min.	73
65. The Isocratic Reversed Phase Chromatogram for the Separation of Aflatoxins with the Mobile Phase Water: Acetonitrile: Isopropanol: Acetic Acid	

(8:1:0.5:0.5) at a Flow Rate of 1 ml/min.	74
66. A Typical Isocratic Reversed Phase Chromatogram of a Pre-Column Derivatised Aflatoxin B <sub>1</sub> Standard Obtained with the Mobile Phase of Water: Acetonitrile: Isopropanol: Acetic Acid (8:1:0.5:0.5) at a Flow Rate of 1 ml/min.	76
67. A Typical Isocratic Reversed Phase Chromatogram of a Blank Run with the Mobile Phase Water: Acetonitrile (2:8) at a Flow Rate of 1 ml/min.	78
68. A Typical Isocratic Reversed Phase Chromatogram of AFB <sub>1</sub> Standard with the Mobile Phase Water: Acetonitrile (2:8) at a Flow Rate of 1 ml/min.	78
69. A Typical Isocratic Reversed Phase Chromatogram for the Separation of AFB <sub>1</sub> in a Cell-Free Extract with the Mobile Phase Water: Acetonitrile (2:8) at a Flow Rate of 1 ml/min.	79
70. A Typical Isocratic Reversed Phase Chromatogram of AFB <sub>1</sub> Standard with the Mobile Phase Water: Acetonitrile (3:7) at a Flow Rate of 1 ml/min.	80
71. A Typical Isocratic Reversed Phase Chromatogram for the Separation of AFB <sub>1</sub> in a Cell-Free Extract with the Mobile Phase Water: Acetonitrile (3:7) at a Flow Rate of 1 ml/min.	81
72. A Typical Isocratic Reversed Phase Chromatogram for the Separation of AFB <sub>1</sub> in a Cell-Free Extract with the Mobile Phase Water: Acetonitrile (3:7) at a Flow Rate of 1 ml/min.	82
73. The Gradient Reversed Phase Chromatogram for the Separation of AFB <sub>1</sub> in a Cell-Free Extract at a Flow Rate of 1 ml/min.	83
74. A Typical Gradient Reversed Phase Chromatogram of AFB <sub>1</sub> Standard at a Flow Rate of 1 ml/min.	84
75. A Typical Gradient Reversed Phase Chromatogram of OMST Standard at a Flow Rate of 1 ml/min.	84
76. A Typical Gradient Reversed Phase Chromatogram of ST Standard at a Flow Rate of 1 ml/min.	85
77. The UV Spectrum of Aflatoxin B <sub>1</sub> Standard	86
78. The UV Spectrum of Sterigmatocystin Standard	268

79. The UV Spectrum of <i>O</i> -Methyl sterigmatocystin Standard	268
80. Scheme for Aflatoxin Biosynthesis and Sites for Blocked Mutants	88
81. Time Course for the Biotransformation of ST and ST Derivatives to AFB <sub>1</sub> in the Culture fluid	95
82. Time Course for the Biotransformation of ST and ST Derivatives to AFB <sub>1</sub> in the Pellet Fraction	97
83. The Liquid Chromatogram for the Conversion of OMST to AFB <sub>1</sub> in Whole Cells of <i>A. parasiticus</i> (Wh1)	270
84. The Liquid Chromatogram for the Conversion of OPROST to AFB <sub>1</sub> in Whole Cells of <i>A. parasiticus</i> (Wh1)	271
85. The Liquid Chromatogram for the Conversion of OEST to AFB <sub>1</sub> in Whole Cells of <i>A. parasiticus</i> (Wh1)	272
86. The Calibration Graph of the Protein Ovalbumin	274
87. The Effect of Cell-Free Extract Protein Concentration on the Conversion of ST to AFB <sub>1</sub> at pH 7.5 and 27 °C for an Incubation Time of 1 Hour	108
88. A Typical Liquid Chromatogram for the Conversion of ST to AFB <sub>1</sub> in a Cell-Free Extract at pH 7.5 and 27 °C for an Incubation Time of 1 Hour	275
89. The Effect of pH of Incubation for the Enzymatic Conversion of ST to AFB <sub>1</sub> at 27 °C for an Incubation Time of 1 Hour	110
90. A Typical Liquid Chromatogram for the Conversion of ST to AFB <sub>1</sub> in a Cell-Free Extract at pH 7.1 and 27 °C for an Incubation Time of 1 Hour	276
91. A Typical Liquid Chromatogram for the Conversion of ST to AFB <sub>1</sub> in a Cell-Free Extract at pH 7.4 and 27 °C for an Incubation Time of 1 Hour	277
92. The Effect of Temperature of Incubation for the Conversion of ST to AFB <sub>1</sub> in a Cell-Free Extract at pH 7.2 for an Incubation Time of 1 Hour	112
93. A Typical Liquid Chromatogram for the Conversion of ST to AFB <sub>1</sub> in a Cell-Free Extract at pH 7.2 and 24 °C for an Incubation Time of 1 Hour	278
94. The Effect of the Addition of Co-Factors (1.5 mM) on the Conversion of ST to AFB <sub>1</sub> in a Cell-Free Extract at pH 7.2 and 28 °C for an Incubation Time of 1 Hour	113

95. A Typical Liquid Chromatogram for the Conversion of ST to AFB<sub>1</sub> in a Cell-Free Extract, in the Presence of NADPH (1.5 mM), at pH 7.2 and 28 °C for an Incubation Time of 1 Hour 279
96. The Conversion of ST, OMST and OPROST to AFB<sub>1</sub> in a Cell-Free Extract, in the Presence of NADPH (1.5 mM ) and SAM (1.5 mM), at pH 7.2 and 28 °C 116
97. A Typical Liquid Chromatogram for the Conversion of ST to AFB<sub>1</sub> in a Cell-Free Extract, at pH 7.2 and 28 °C for an Incubation Time of 45 Minutes 280
98. A Typical Liquid Chromatogram for the Conversion of OMST to AFB<sub>1</sub> in a Cell-Free Extract, at pH 7.2 and 28 °C for an Incubation Time of 60 Minutes 281
99. Protein Elution Profile after Separation of the Cell-Free Extract by Gel Chromatography with Sephadex G-25 124
100. A Typical Liquid Chromatogram of ST in Enzyme Fraction 9-17, at pH 7.2 and 28 °C for an Incubation Time of 5 Hours 284
101. Polyacrylamide Gel Electrophoresis of the Partially Purified Enzyme Fraction 9-30 126
102. A Typical Liquid Chromatogram for the Conversion of ST to AFB<sub>1</sub> in Enzyme Fraction 9-30, after Dialysis, at pH 7.2 and 28 °C for an Incubation Time of 3 Hours 285
103. A Typical Liquid Chromatogram of ST in Enzyme Fraction 9-30, in the Presence of NADPH, at pH 7.2 and 28 °C for an Incubation Time of 3 Hours 286
104. A Typical Liquid Chromatogram for the Conversion of OPROST to AFB<sub>1</sub> in Enzyme Fraction 9-30, in the Presence of NADPH (1.5 mM), at pH 7.2 and 28 °C for an Incubation Time of 3 Hours 287
105. A Typical Liquid Chromatogram for the Conversion of OBzST to AFB<sub>1</sub> in Enzyme Fraction 9-30, in the Presence of NADPH (1.5 mM), at pH 7.2 and 28 °C for an Incubation Time of 3 Hours 288
106. A Proposed Scheme for the Conversion of ST and ST Derivatives to AFB<sub>1</sub> 131



107. The Structure of the Xanthone Nucleus Showing the Numbering System	133
108. The Effect of the Inhibitor on the Enzyme in Competitive Inhibition	136
109. The Effect of Competitive Inhibition on Enzyme Kinetics	138
110. The Effect of the Inhibitor on the Enzyme in Non-Competitive Inhibition	138
111. The Effect of Non-Competitive Inhibition on Enzyme Kinetics	140
112. The Effect of the Inhibitor on the Enzyme in Uncompetitive Inhibition	140
113. The Effect of Uncompetitive Inhibition on Enzyme Kinetics	141
114. The Structures of Four Simple Xanthenes	142
115. The Reaction Scheme for the Synthesis of 1-Hydroxyxanthone	143
116. A Mechanism Postulated by Patel and Trivedi for the Formation of 1-Hydroxyxanthone	144
117. The Reaction Scheme for the Condensation Reaction in the Formation of Simple Xanthenes	145
118. The $^1\text{H}$ -NMR Spectrum of Ethyl Salicylate	289
119. The Expanded $^1\text{H}$ -NMR Spectrum of Ethyl Salicylate	290
120. The $^1\text{H}$ -NMR Spectrum of the Compound Obtained from the Condensation of Ethyl Salicylate with Hydroquinone	291
121. The Normalised Mass Spectrum of 1-Hydroxy-3,6-dimethylxanthone	159
122. The $^1\text{H}$ -NMR Spectrum of 1-Hydroxy-3,6-dimethylxanthone	292
123. The Expanded $^1\text{H}$ -NMR Spectrum of 1-Hydroxy-3,6-dimethylxanthone	293
124. The COSY Spectrum of 1-Hydroxy-3,6-dimethylxanthone	294
125. The IR Spectrum of 1-Hydroxy-3,6-dimethylxanthone	295
126. The Normalised Mass Spectrum of 1-Methoxy-3,6-dimethylxanthone	160
127. The $^1\text{H}$ -NMR Spectrum of 1-Methoxy-3,6-dimethylxanthone	296
128. The Expanded $^1\text{H}$ -NMR Spectrum of 1-Methoxy-3,6-dimethylxanthone	297
129. The Normalised Mass Spectrum of 1-Acetyl-3,6-dimethylxanthone	161
130. The $^1\text{H}$ -NMR Spectrum of 1-Acetyl-3,6-dimethylxanthone	298
131. The Expanded $^1\text{H}$ -NMR Spectrum of 1-Acetyl-3,6-dimethylxanthone	299
132. The Reaction Scheme for the Synthesis of Xanthone Derivatives	157
133. The Structures of 1-Methoxy-3,6-dimethylxanthone and OMST	158

134. A Typical Liquid Chromatogram for the Production AFB <sub>1</sub> in Whole Cells of <i>A. parasiticus</i> (NIX) in the Presence of 1-Acetyl-3,6-dimethylxanthone	300
135. A Typical Liquid Chromatogram for the Production AFB <sub>1</sub> in Whole Cells of <i>A. parasiticus</i> (NIX) in the Presence of 1-Hydroxy-3,6-dimethylxanthone	301
136. A Typical Liquid Chromatogram for the Production of AFB <sub>1</sub> in Whole Cells of <i>A. parasiticus</i> (NIX), in the Presence of 1-Methoxy-3,6-dimethylxanthone	302
137. A Typical Liquid Chromatogram for the Conversion of OMST to AFB <sub>1</sub> in Whole Cells of <i>A. parasiticus</i> (Wh1), in the Presence of 1-Acetyl-3,6-dimethylxanthone	303
138. A Typical Liquid Chromatogram for the Conversion of OMST to AFB <sub>1</sub> in Whole Cells of <i>A. parasiticus</i> (Wh1), in the Presence of 1-Hydroxy-3,6-dimethylxanthone	304
139. A Typical Liquid Chromatogram for the Conversion of OMST to AFB <sub>1</sub> in Whole Cells of <i>A. parasiticus</i> (Wh1), in the Presence of 1-Methoxy-3,6-dimethylxanthone,	305
140. A Typical Liquid Chromatogram for the Conversion of OMST to AFB <sub>1</sub> in a Cell-Free Extract at pH 7.2 and 28 °C for an Incubation Time of 1 Hour	306
141. A Typical Liquid Chromatogram for the Conversion of OMST to AFB <sub>1</sub> in a Cell-Free Extract, in the Presence of 1-Methoxy-3,6-dimethylxanthone, at pH 7.2 and 28 °C for an Incubation Time of 1 Hour	307
142. A Typical Liquid Chromatogram for the Conversion of OMST to AFB <sub>1</sub> in a Cell-Free Extract at pH 7.2 and 28 °C for an Incubation Time of 10 Minutes	308
143. A Typical Liquid Chromatogram for the Conversion of OMST to AFB <sub>1</sub> in a Cell-Free Extract, in the Presence of 1-Methoxy-3,6-dimethylxanthone, at pH 7.2 and 28 °C for an Incubation Time of 10 Minutes	309
144. The Effect of OMST Concentration and of the Addition of 1-Methoxy-3,6-dimethylxanthone (2.75 µM) on the Conversion of OMST to AFB <sub>1</sub> in a Cell-Free Extract at pH 7.2 and 28 °C for an Incubation Time of 10 Minutes	172



145. The Line-Weaver Burk Plot	172
146. A Possible Mode of Attachment of 1-Methoxy-3,6-dimethylxanthone to an Enzyme Center	173
147. The Mechanism Proposed by Chatterjee and Townsend in the Formation of Aflatoxin B <sub>1</sub>	176
148. The Mechanism Proposed by Chatterjee and Townsend and in the Formation of Aflatoxin B <sub>1</sub>	177
149. The Mechanism Proposed by Watanabe and Townsend in the Formation of Aflatoxin B <sub>1</sub>	178
150. A Schematic Diagram of a Clark Oxygen Electrode	180
151. The Characteristic Polarographic Curve	181
152. The Standard Curve of Current and Partial Pressure of Oxygen	182
153. The Effect of Stirring Speed on Current	183
154. The Calibration graph of AFB <sub>1</sub>	310
155. The Calibration graph of NADPH	311
156. The Three Alignment Positions of the Window Valve of the Oxygen Uptake Chamber	189
157. A Diagrammatic Representation of a Modified Calibration Cell for the Clark Oxygen Electrode	191
158. A Recorder Trace of the Enzymatic Conversion of OMST to AFB <sub>1</sub> in a Partially Purified Enzyme, in the Presence of NADPH (0.15 mM), in a Clark Oxygen Electrode	196
159. A Recorder Trace Showing the Response of the Electrode due to the Addition of Deionised Water	198
160. A Recorder Trace Showing the Response of the Electrode due to the Addition of Acetone	198
161. A Recorder Trace Showing the Response of the Electrode due to the Addition of Dimethyl Sulphoxide	199
162. A Recorder Trace Showing the Response of the Electrode due to the Addition of Deionised Water	200

163. A Recorder Trace Showing the Response of the Electrode due to the Addition of Dimethyl Sulphoxide Free of Dissolved Oxygen	200
164. A Recorder Trace Showing the Response of the Electrode due to the Addition of Dimethyl Sulphoxide containing Dissolved Oxygen	201
165. A Recorder Trace of the Partially Purified Enzyme in the Presence of NADPH (0.15 mM) and SAM (0.15 mM)	203
166. A Recorder Trace of the Partially Purified Enzyme in the Presence of ST and Deionised Water	203
167. A Recorder Trace of the Partially Purified Enzyme in the Presence of NADPH (0.15 mM), SAM (0.15 mM) and DMSO	204
168. A Recorder Trace for the Conversion of ST to AFB <sub>1</sub> in a Partially Purified Enzyme in the Presence of NADPH (0.15 mM) and SAM (0.15 mM)	204
169. A Recorder Trace of the Partially Purified Enzyme in the Presence of NADPH (50 µg/50 µl)	207
170. A Recorder Trace of the Partially Purified Enzyme in the Presence of NADPH (50 µg/50 µl) and DMSO	207
171. A Recorder Trace for the Conversion of OMST to AFB <sub>1</sub> in a Partially Purified Enzyme in the Presence of NADPH (50 µg/50 µl)	208
172. A Typical Liquid Chromatogram of Standard AFB <sub>1</sub> with the Mobile Phase Water: Acetonitrile (4:6) at a Flow rate of 1 ml/min.	312
173. A Typical Liquid Chromatogram for the Conversion of OMST to AFB <sub>1</sub> in a Partially Purified Enzyme in the Presence of NADPH (1.5 mM)	313
174. A Typical Liquid Chromatogram for the Conversion of OMST to AFB <sub>1</sub> in a Partially Purified Enzyme in the Presence of NADPH (1.5 mM)	314
175. A Mechanism Proposed by Gengan <i>et al.</i> for the Conversion of OMST to AFB <sub>1</sub>	215

## LIST OF TABLES

Table	Page
1. Examples of Methods Used to Prepare Cell- Free Extracts from <i>Aspergillus</i> species	11
2. Chemical Shift Values of ST Obtained from $^{13}\text{C}$ -NMR Spectrum	41
3. The $^1\text{H}$ -NMR Data of Sterigmatocystin	42
4. The Physical Properties of Sterigmatocystin Derivatives Obtained by Using Aliphatic Iodides and Acid Chlorides as Reagents	50
5. The $^1\text{H}$ -NMR Data of <i>O</i> -Ethyl sterigmatocystin	240
6. The $^1\text{H}$ -NMR Data of <i>O</i> -Propyl sterigmatocystin	244
7. The $^1\text{H}$ -NMR Data of <i>O</i> -Butyl sterigmatocystin	54
8. The $^1\text{H}$ -NMR Data of <i>O</i> -Pentyl sterigmatocystin	249
9. The $^1\text{H}$ -NMR Data of <i>O</i> -Propenyl sterigmatocystin	253
10. The $^1\text{H}$ -NMR Data of <i>O</i> -Acetyl sterigmatocystin	257
11. The $^1\text{H}$ -NMR Data of <i>O</i> -Benzoyl sterigmatocystin	260
12. The HPLC Data Obtained for the Calibration Graph of AFB <sub>1</sub> Using the Fluorescence Detector	264
13. The HPLC Data Obtained for the Calibration Graph of AFB <sub>1</sub> Using the Diode Array Detector	265
14. The HPLC Data for Repeatability of Peak Area and Retention Time with the Fluorescence Detector	266
15. The HPLC Data for Repeatability of Peak Area and Retention Time with the Diode Array Detector	267
16. The Different Concentration of the Mobile Phase Water: Acetonitrile: Isopropanol: Acetic Acid, Used in Reversed Phase Chromatography	71
17. The Gradient Elution Program Used for HPLC Analysis for the Conversion of ST and ST Derivatives to AFB <sub>1</sub> in Cell-Free Extracts	83

18. The Conversion of Selected Substrates to AFB <sub>1</sub> in the Culture Fluid Fraction of Whole Cells of <i>A. parasiticus</i> (Wh1)	94
19. The Conversion of Selected Substrates to AFB <sub>1</sub> in the Pellet Fraction of Whole Cells of <i>A. parasiticus</i> (Wh1)	96
20. The Data for the Calibration Graph of Protein Using the Bradford Assay Method	274
21. The Effect of Cell-Free Extract Protein Concentration on the Conversion of ST to AFB <sub>1</sub> , in Cell-Free Extracts in the Presence of NADPH (1.5 mM) and SAM (1.5 mM), at pH 7.5 and 27 °C for an Incubation Time of 1 Hour	108
22. The Effect of pH of Incubation on the Conversion of ST to AFB <sub>1</sub> in Cell-Free Extracts, in the Presence of NADPH (1.5 mM) and SAM (1.5 mM) at 27 °C for an Incubation Time of 1 Hour	109
23. The Effect of Temperature of Incubation on the Conversion of ST to AFB <sub>1</sub> in Cell-Free Extracts, in the Presence of NADPH (1.5 mM) and SAM (1.5 mM) at pH 7.2 for an Incubation Time of 1 Hour	111
24. The Effect of the Addition of Co-Factors on the Conversion of ST to AFB <sub>1</sub> in Cell-Free Extracts, in the Presence of Co-Factors, at pH 7.2 and 28 °C for an Incubation Time of 1 Hour	113
25. The Conversion of Selected Substrates to AFB <sub>1</sub> in Cell-Free Extracts, in the Presence of NADPH (1.5 mM ) and SAM (1.5 mM ) at pH 7.2 and 28 °C for an Incubation Time of 1 Hour	115
26. The Conversion of ST to AFB <sub>1</sub> in the Enzyme Fraction 9-30, in the Presence of NADPH (1.5 mM ) and SAM (1.5 mM) at pH 7.2 and 28 °C for an Incubation Time of 5 Hours	125
27. The Conversion of ST to AFB <sub>1</sub> in the Enzyme Fraction 9-30 , After Dialysis, in the Presence of NADPH (1.5 mM) and SAM (1.5 mM) at pH 7.2 and 28 °C for an Incubation Time of 3 Hours	127
28. The Enzymatic Reaction of ST in the Enzyme Fraction 9-30 , After Dialysis, at pH 7.2 and 28 °C for an Incubation Time of 3 Hours	128
29. The Conversion of Selected Substrates to AFB <sub>1</sub> in the Enzyme Fraction	

9-30 , After Dialysis, in the Presence of NADPH(1.5 mM) and SAM (1.5 mM) at pH 7.2 and 28 °C for an Incubation Time of 3 Hours	129
30. The <sup>1</sup> H-NMR Data of 1-Hydroxyxanthone	155
31. Whole Cells Reactions of <i>A. parasiticus</i> (CMI), in the Presence of Different Quantities of Xanthone Derivatives, at 25 °C for an Incubation Time of 96 Hours	163
32. The Enzymatic Conversion of OMST to AFB <sub>1</sub> in Whole Cells of <i>A. parasiticus</i> (Wh1), in the Presence of Different Quantities of Xanthone Derivatives, at 25 °C for an Incubation Time of 3 Hours	165
33. The Enzymatic Conversion of OMST to AFB <sub>1</sub> in Cell-Free Extracts, in the Presence of Xanthone Derivatives and NADPH (1.5 mM) at pH 7.2 and 28 °C for an Incubation Time of 1 Hour	166
34. The Enzymatic Conversion of OMST to AFB <sub>1</sub> in Cell-Free Extracts, in the Presence of NADPH (1.5 mM) at pH 7.2 and 28 °C for an Incubation Time of 10 Minutes	168
35. The Enzymatic Conversion of OMST to AFB <sub>1</sub> in Cell-Free Extracts, in the Presence of 3,6-Dimethyl-1-Methoxyxanthone (2.75 μM), and NADPH (1.5 mM) at pH 7.2 and 28 °C for an Incubation Time of 10 Minutes	169
36. The Data Obtained for the Line-Weaver Burk Plot	169
37. The Data for the Calibration Graph of AFB <sub>1</sub>	310
38. The Data for the Calibration Graph of NADPH	311
39. The Effect of Organic Solvents on Electrode Response	197
40. The Effect of Dimethyl Sulphoxide on Electrode Response	200
41. The Enzymatic Conversion of ST to AFB <sub>1</sub> in a Partially Purified Enzyme, in the Presence of NADPH (1.5 mM) and SAM (1.5 mM) at pH 7.2 and 28 °C	202
42. The Enzymatic Conversion of OMST to AFB <sub>1</sub> in a Partially Purified Enzyme in the Presence of NADPH (50 μg/50 μl) at pH 7.2 and 28 °C	206

43. The Enzymatic Conversion of OMST to AFB<sub>1</sub> in a Partially Purified Enzyme in the Presence of NADPH (50 µg/50 µl) at pH 7.2 and 28 °C 208
44. The Mole Ratio of Substrates for the Enzymatic Conversion of OMST to AFB<sub>1</sub> 209



## LIST OF ABBREVIATIONS

ACP	Acyl carrier protein
AFB <sub>1</sub>	Aflatoxin B <sub>1</sub>
AFB <sub>2</sub>	Aflatoxin B <sub>2</sub>
AFB <sub>2a</sub>	Aflatoxin B <sub>2a</sub>
AFG <sub>1</sub>	Aflatoxin G <sub>1</sub>
AFG <sub>2</sub>	Aflatoxin G <sub>2</sub>
AFG <sub>2a</sub>	Aflatoxin G <sub>2a</sub>
AVN	Averantin
<sup>13</sup> C-NMR	Carbon-13 nuclear magnetic resonance
CoA	Co-enzyme A
CEI	Chloroform: ethyl acetate: isopropanol (90: 5: 5)
COSY	Correlated nuclear magnetic resonance spectroscopy
CDCl <sub>3</sub>	Deuteriochloroform
DMSO	Dimethyl Sulphoxide
DAD	Diode array detector
DEPT	Distortionless enhancement by polarization transfer
FAS	Fatty acid synthase
FD	Fluorescence detector
HETCOR	Heteronuclear magnetic resonance spectroscopy
HPLC	High pressure liquid chromatography
Hz	Hertz
IR	Infra red spectroscopy
m.p.	Melting point
MS	Mass spectroscopy
NA	Norsolorinic acid
NAD	Nicotinamide adenine dinucleotide
NADP	Nicotinamide adenine dinucleotide phosphate
OAcST	O-Acetyl sterigmatocystin



OBzST	<i>O</i> -Benzoyl sterigmatocystin
OBUST	<i>O</i> -Butyl sterigmatocystin
OEST	<i>O</i> -Ethyl sterigmatocystin
OMST	<i>O</i> -Methyl sterigmatocystin
OPREST	<i>O</i> -Propenyl sterigmatocystin
OPROST	<i>O</i> -Propyl sterigmatocystin
p.p.b.	Parts per billion
p.p.m.	Parts per million
PAGE	Polyacrylamide gel electrophoresis
PDA	Potato dextrose agar
<sup>1</sup> H-NMR	Proton nuclear magnetic resonance
NADPH	Reduced nicotinamide adenine dinucleotide phosphate
SAM	S-adenosyl methionine
ST	Sterigmatocystin
SDS	Sodium dodecyl sulphate
TCA	Tricarboxylic acid cycle
t.l.c.	Thin layer chromatography
TEF	Toluene: ethyl acetate: formic acid (12: 6: 2)
UV	Ultra violet spectroscopy
VA	Versicolorin A

# CHAPTER ONE

## INTRODUCTION

Aflatoxin B<sub>1</sub> (AFB<sub>1</sub>)(Figure 1, page 5) is the most commonly produced aflatoxin and also the most toxic and carcinogenic<sup>1</sup>. The presence of aflatoxins in a variety of foods and feeds has led to extensive research concerning their production, detoxification and incidence<sup>2</sup>.

The biosynthetic pathway of AFB<sub>1</sub> is considered one of the most complex among aromatic polyketides. An unusual hexanoyl starter unit<sup>3,4</sup> is homologated by the successive addition of malonyl co-enzyme A (CoA) to give the tetrahydroxyanthraquinones. A complex yet chemically efficient sequence of chemical reduction and oxidation steps, which are enzyme catalysed, produces a series of known intermediates leading ultimately to AFB<sub>1</sub>. Some of the details of the pathway are still unclear while in other parts there is conflicting evidence.

Although evidence<sup>5-7</sup> is presented for the biotransformation of sterigmatocystin (ST) (**2a**) (Figure 2, page 7) to AFB<sub>1</sub> via *O*-methylsterigmatocystin (OMST) (**2c**) (Figure 2, page 7), the role of OMST is still uncertain. Cell-free studies<sup>8</sup> have also shown OMST as a side shunt metabolite thus giving rise to confusion in the study of the latter part of the biosynthetic pathway, i.e., either OMST is an obligatory intermediate or a side shunt metabolite and hence part of a metabolic grid. Enzymological studies of the final stages of the biosynthesis thus warranted further attention, since enzyme specificity details would give a better understanding of the role of OMST. Also further research into the means by which other compounds influence aflatoxin synthesis is required since it is potentially beneficial in expanding our understanding of mycotoxigenesis. Such studies are likely to yield knowledge that would lead to identification of key bio-regulatory loci controlling aflatoxin synthesis and development of basic knowledge that could provide insight into new strategies for controlling aflatoxin production.

The objectives of this study were to:

- produce, isolate and characterise ST by spectroscopic techniques
- synthesise xanthone derivatives by converting the free hydroxyl group at C-3 of ST to derivatives homologous to OMST, purify and characterise these derivatives by spectroscopic techniques
- develop high pressure liquid chromatography (HPLC) methods for the quantification of AFB<sub>1</sub>
- investigate the conversion of ST and ST derivatives to AFB<sub>1</sub> in whole cells of *Aspergillus parasiticus* (Wh1-11-105)
- optimise the enzyme activity of crude cell-free extracts and to investigate the conversion of ST and selected ST derivatives to AFB<sub>1</sub>
- remove endogenous co-factors, viz., reduced nicotinamide adenine dinucleotide phosphate (NADPH) and S-adenosyl methionine (SAM), from crude cell-free extracts, concentrate the crude enzyme(s) and determine the specificity of the enzyme(s) with ST and selected ST derivatives
- synthesise, purify and characterise simple xanthenes and determine their inhibition of AFB<sub>1</sub> production in whole cells and cell-free extracts of *A. parasiticus*, and
- determine the nature of the oxygenase(s) involved in the conversion of OMST to AFB<sub>1</sub>.

## CHAPTER TWO

### LITERATURE REVIEW

#### 2.1. AFLATOXINS AS SECONDARY METABOLITES

Mycotoxins are metabolites which are produced by an ubiquitous group of fungi with a filamentous form. These metabolites are poisonous to mammals, birds and fish and have been responsible for illness and even death in the human population and domesticated animals. All mycotoxins, including aflatoxin, belong to a subclass of compounds called secondary metabolites. The aflatoxins are secondary metabolites as they are produced not during active growth of the organism and are not required for any known function in the producing organism<sup>9,10</sup>.

In addition, the aflatoxins satisfy the following criteria to be classified as secondary metabolites:

- The production of aflatoxins is limited to only two types, viz., *A. flavus* and *A. parasiticus* with only certain strains of the species being toxigenic.
- The compounds which are produced are closely related in structure and activity.
- The synthesis of the metabolites fail to appear in the growth phase (trophophase) and is initiated only during the stationary phase (idiophase).
- Aflatoxins are biosynthesised from simple precursors such as acetate and malonate.
- The function of these metabolites in the welfare, development and reproduction of the producing organism is not apparent.

#### 2.2. THE HISTORY AND INCIDENCE OF AFLATOXINS

Aflatoxins are produced by several species of fungi in the genus *Aspergillus*<sup>11</sup>. Prior to the outbreak of the 'Turkey X disease' in England, in 1960, nothing was known about these highly toxic and carcinogenic compounds. The high magnitude of poultry deaths initiated intensive research throughout the world. The cause of the poultry deaths was found to be dietary and was subsequently associated with a Brazilian peanut meal which was the common ingredient in the poultry feed. Feeding experiments with the chloroform extract of

the meal was found to induce the disease in ducklings<sup>12</sup>, and this response was used as the basis of a bioassay<sup>13</sup> for the toxin.

A paper chromatographic technique for detection of the toxin, based on a blue-fluorescing spot under ultra-violet (UV) light, was described by Sargeant *et al.*<sup>11</sup>. Various commodities were screened and the toxin was found to be present in peanuts from many sources. Subsequently *A. flavus* cultures were identified on Ugandan nuts and were shown to produce the toxin named 'aflatoxin' which was initially considered as a single compound. However, production of the toxin by laboratory culture of the organism facilitated its concentration and purification. This revealed that aflatoxin was not a single compound but a mixture of closely related ones which were designated trivial names aflatoxin B<sub>1</sub>, aflatoxin B<sub>2</sub> (AFB<sub>2</sub>), aflatoxin G<sub>1</sub> (AFG<sub>1</sub>) and aflatoxin G<sub>2</sub> (AFG<sub>2</sub>)<sup>14,15</sup>. The distinguishing letters for the aflatoxins relate to the colour of the metabolites under UV fluorescence exhibited on thin layer chromatography (t.l.c.), B being for blue and G for green.

### 2.3 THE STRUCTURE OF AFLATOXINS

Initial chemical investigations of the aflatoxins focused on the structural elucidation of these compounds<sup>15,16</sup>. In a preliminary communication in 1963, Asao *et al.*<sup>16</sup> proposed structures for AFB<sub>1</sub>, AFB<sub>2</sub>, AFG<sub>1</sub> and AFG<sub>2</sub> (Figure 1, page 5); however, the stereochemical aspects of these structures were not considered. A later publication from the same authors<sup>17</sup> furnished proof for the structures proposed earlier.

X-ray crystallographic investigations of the aflatoxins established the *cis*-fusion of the two dihydrofuran rings<sup>18-20</sup>. The absolute configuration of the aflatoxins was determined by Brechbuhler *et al.*<sup>21</sup> in 1967. The basic skeleton of the aflatoxin molecule is a condensed bisfuran/coumarin ring system.

Other aflatoxins (Figure 1, page 5) that have been discovered are aflatoxin M<sub>1</sub> and aflatoxin M<sub>2</sub> which are mammalian metabolites of AFB<sub>1</sub> and AFB<sub>2</sub> respectively. In addition, other aflatoxin derivatives such as aflatoxin B<sub>2a</sub> (AFB<sub>2a</sub>) and aflatoxin G<sub>2a</sub> (AFG<sub>2a</sub>) have been isolated from *A. flavus* cultures by Dutton and Heathcote<sup>22</sup>.

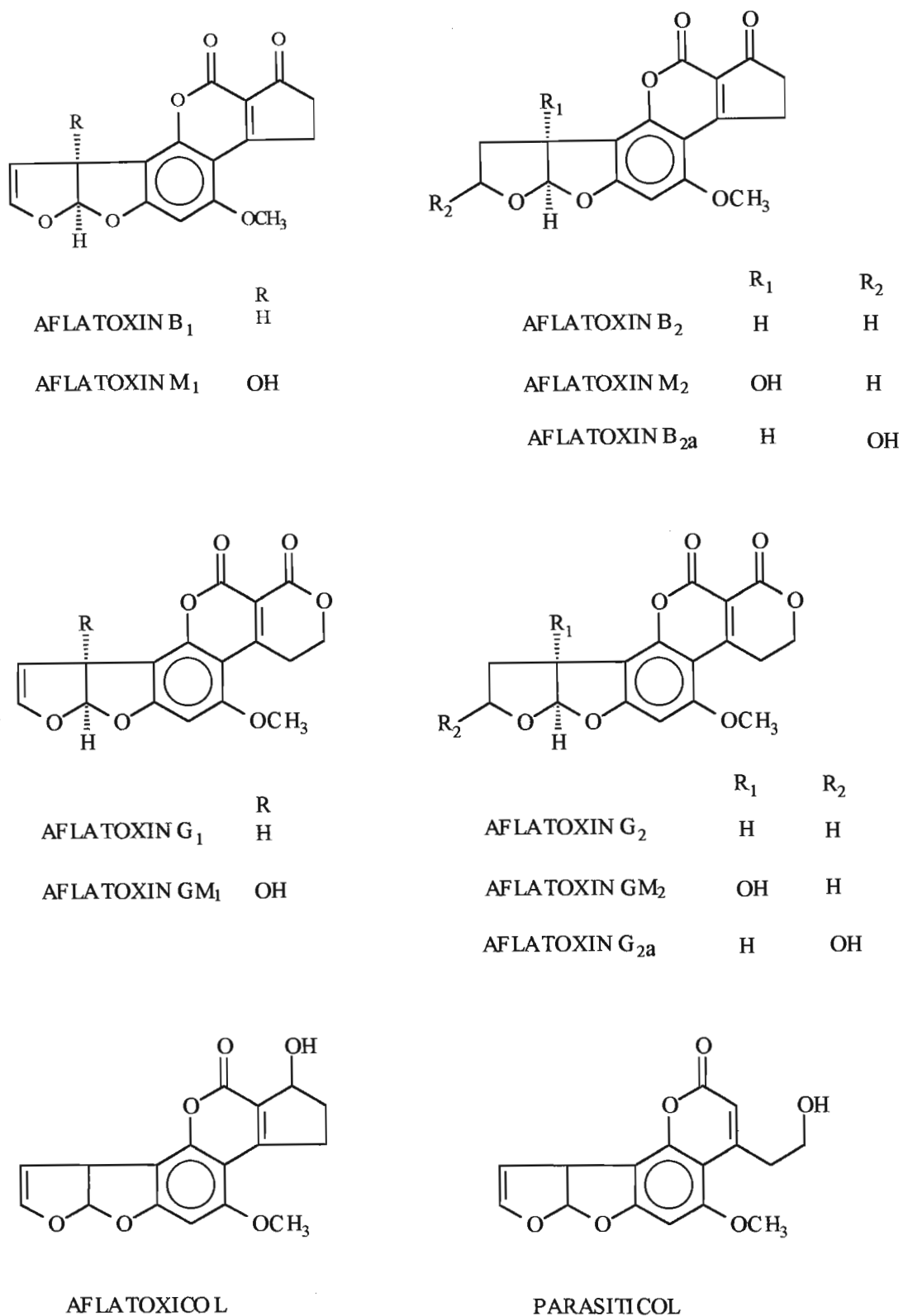


Figure 1. The Structure of Aflatoxins and Closely Related Metabolites<sup>23</sup>.

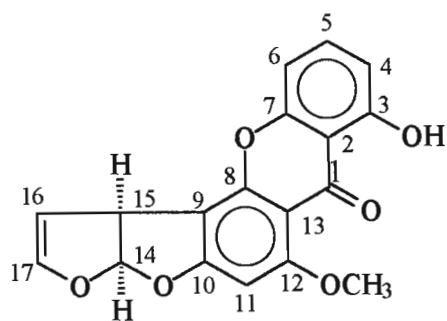
## 2.4. THE STRUCTURE OF STERIGMATOCYSTIN

Sterigmatocystin (**2a**)(Figure 2, page 7) is a mycotoxin which has been proposed<sup>24</sup> as a biogenetic precursor of AFB<sub>1</sub> and is known to be produced by isolates of *A. nidulans*, *A. versicolor*, *Bipolaris sorokiniana* and other related fungi. Sterigmatocystin was first isolated<sup>25</sup> as a yellow crystalline compound from the mycelial mats of *A. versicolor* and was found to be a xanthone derivative.

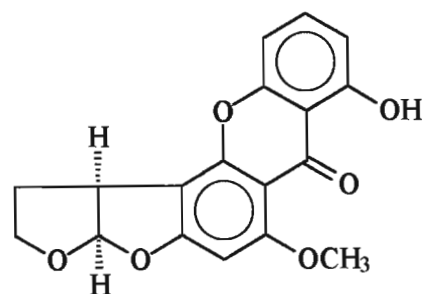
The structure of ST was studied by several groups of researchers and in 1962 it was proposed<sup>26</sup> that the molecule contained a bisdihydrofuran ring system. In 1970 the structure of ST was confirmed<sup>27</sup> by X-ray analysis of the *p*-bromo-benzoate derivative. The absolute configuration of the bisdihydrofuran ring system was confirmed by chemical and X-ray methods<sup>28</sup>, by proton nuclear magnetic resonance spectroscopy (<sup>1</sup>H-NMR) and carbon-13 nuclear magnetic resonance spectroscopy (<sup>13</sup>C-NMR)<sup>29,30</sup>.

Other xanthone type metabolites (Figure 2, page 7) containing a bisdihydrofuran or a dihydro-bisdihydrofuran ring system were isolated from *A. versicolor* and their structures were determined by elemental analysis and spectroscopic methods by different authors. These metabolites are OMST (**2c**)<sup>8</sup>, dihydrodemethylsterigmatocystin (**2f**)<sup>31</sup>, dihydrosterigmatocystin (**2b**)<sup>31</sup>, sterigmatin (**2g**)<sup>32</sup>, 5-methoxysterigmatocystin (**2d**)<sup>33</sup> and demethylsterigmatocystin (**2e**)<sup>34</sup>.

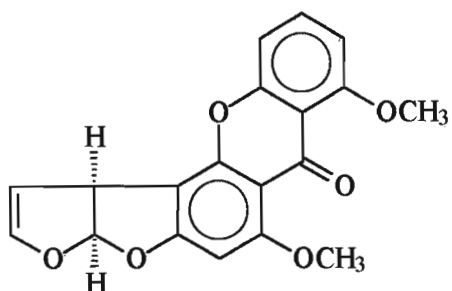




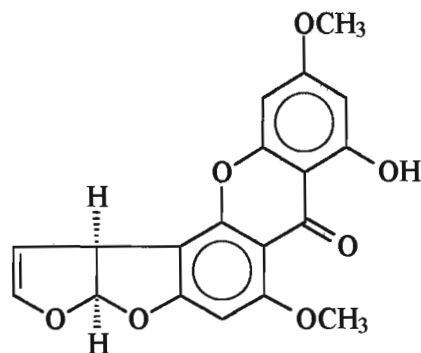
STERIGMATOCYSTIN (2a)



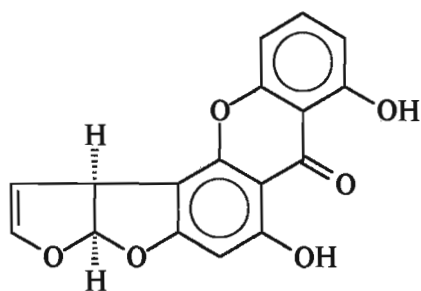
DIHYDROSTERIGMATOCYSTIN (2b)



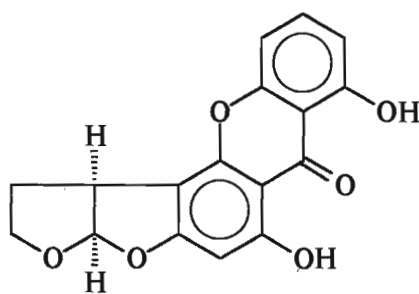
O-METHYLSTERIGMATOCYSTIN (2c)



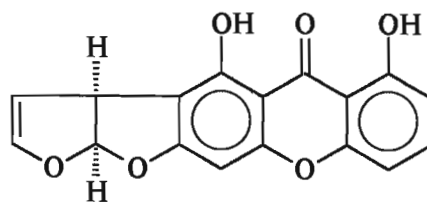
5-METHOXYSTERIGMATOCYSTIN (2d)



DEMETHYLSTERIGMATOCYSTIN (2e)



DIHYDRODEMETHYLSTERIGMATOCYSTIN (2f)



STERIGMATIN (2g)

Figure 2. Xanthone Type Metabolites Found in the Aflatoxin Biosynthetic Pathway<sup>31-34</sup>.

## 2.5. FUNGAL SECONDARY METABOLIC ENZYMES

### 2.5.1. Characteristics of the Enzymes

As far as has been ascertained, the properties of secondary metabolic enzymes are the same as those of their primary counterparts. They are formed by the usual protein biosynthetic machinery and in many cases are subjected to feedback inhibition, induction and catabolic repression<sup>35</sup>. The secondary enzymes use common co-factors and energy storage cells as those of their primary counterpart.

The secondary metabolic enzymes, however, have some special characteristics of their own in that they are only active or formed during the idiophase, i.e., when normal growth has ceased and differentiation has begun<sup>36</sup>. In certain cases they display relative specificity, i.e., an enzyme catalyses analogous reactions with a series of structurally related metabolites, in contrast to primary metabolic enzymes which are absolutely specific<sup>37</sup>. In addition, secondary metabolic activity normally ceases because of synthase decay or feedback inhibition and enzyme repression or both<sup>23</sup>.

The oxidative modification of many mycotoxins are carried out by a group of enzymes called oxygenases. Their catalytic function involves the incorporation of molecular oxygen into the substrate. In general, oxygenases are divided into two classes, viz., monooxygenase and dioxygenase. The monooxygenases are responsible for the incorporation of a single oxygen atom into the substrate (Figure 3) while the other oxygen atom undergoes reduction by reduced nicotinamide adenine dinucleotide phosphate<sup>38</sup> (NADPH).

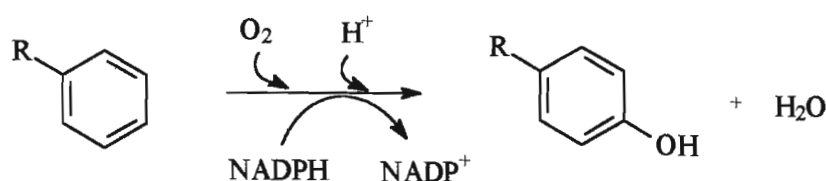


Figure 3. Incorporation of Molecular Oxygen by Monooxygenases<sup>38</sup>.

Many monooxygenases catalyse hydroxylation of aromatic and aliphatic compounds by insertion of an oxygen atom into a C-H bond. They are also capable of catalysing epoxide formation, dealkylation and deamination reactions. In addition, monooxygenases are also responsible for the insertion of an oxygen atom directly into an activated C-C bond of the substrate which has a carbonyl functional group. This reaction results in the formation of lactones, thus emulating the Baeyer-Villiger type of reaction. This type of enzymatic reaction is illustrated by conversion of progesterone via 4-androstene-3,17-dione to testosterone lactone by *Penicilium lilicum*<sup>39</sup> (Figure 4).

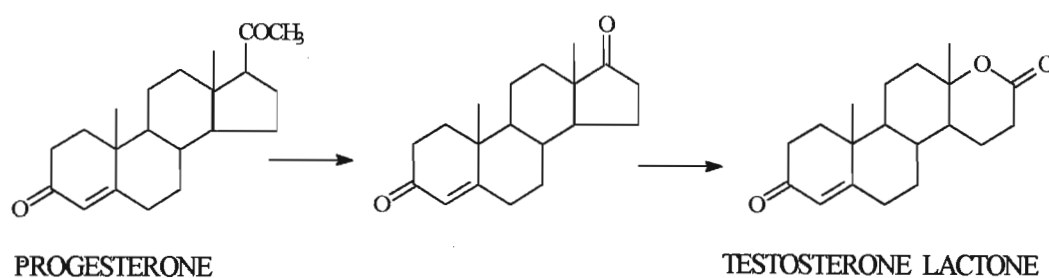


Figure 4. Conversion of Progesterone to Testosterone Lactone by a Monooxygenase<sup>39</sup>.

The biosynthetic pathway leading to the production of aflatoxin follows an orderly sequence of events with known stable and stereochemically correct precursors, this being necessary for successful continuation of the metabolic process. Thus, in the conversion of OMST to AFB<sub>1</sub>, the oxygenases catalyse the oxidation and hence the decarboxylation processes.

After the initial action of the monooxygenase on the substrate, the compound becomes biologically more active in the sense that it is more susceptible to the action of other enzymes, e.g. dioxygenases. The dioxygenases on the other hand are able to incorporate two oxygen atoms into the substrate and are often involved in ring cleavage of aromatic C=C bond between two hydroxylated carbon atoms (“*ortho*” cleavage), or adjacent to a hydroxylated carbon atom (“*meta*” cleavage)<sup>40</sup>. This enzymatic reaction is illustrated in Figure 5 (page 10).

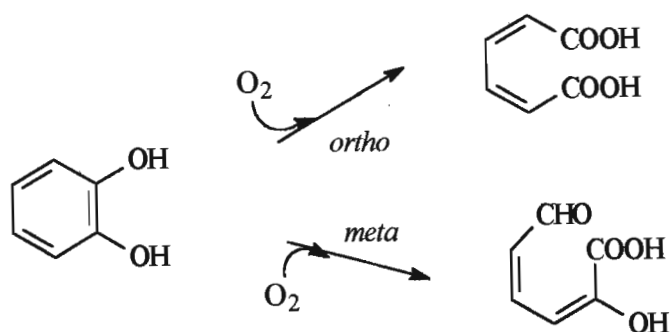


Figure 5. Incorporation of Molecular Oxygen by a Dioxygenase<sup>40</sup>.

Some dioxygenases such as tryptophan 2,3-dioxygenase contain haem as the prosthetic group<sup>41</sup>, while others such as pyrocatechase contain non-haem iron<sup>42</sup>. Enzymes such as quercetine dioxygenase contain copper as a co-factor<sup>43</sup>. All phenolic dioxygenases that have been purified contain non-haem iron as the sole co-factor. It is assumed that iron plays a role in activating the oxygenase as well as the substrate<sup>44</sup>. These enzymes have been found to be inhibited by iron chelating groups<sup>42</sup>. The reaction mechanism for dioxygenase was postulated as follows :- the enzyme containing the ferrous iron combines with an inorganic substrate, resulting in the reduction of the iron, which then reacts with the oxygen to form a ternary complex<sup>44</sup>.

### 2.5.2. Isolation of the Enzymes

The enzymology of fungal secondary metabolism has had a slow start due to the difficulty of obtaining an active cell-free fraction and also the fact that enzymes are present in small concentrations. One of the problems was to determine when to harvest and extract the cells in the growth cycle which, in essence, required investigation into the period in which the trophophase switches to the idiophase<sup>23</sup>. The events which occur during this short time period are extremely complex as they are controlled by repressors, such as carbon and nitrogen sources, energy charge or one of several other regulatory systems<sup>23</sup>.

Another problem which had to be addressed was to choose a method to remove the rigid fungal cell wall without interfering with the cell contents. Although there are many known techniques which are used both in industry and research laboratories<sup>23</sup>, the choice of the

method depends on the particular fungus since enzymes respond differently to a particular method of preparation.

With respect to the aflatoxins, a rotating wire loop with glass beads was used to prepare a system<sup>45</sup> which could convert versiconal acetate to versicolorin A (VA)(Figure 6, page 14). A disruption method with only glass beads was used to prepare a system<sup>46</sup> which could convert ST to AFB<sub>1</sub>. Preparations<sup>6,47</sup> from powdered lyophilised mycelia were used to convert norsolorinic acid (NA) to averantin (AVN) and ST to AFB<sub>1</sub>. The method<sup>48</sup> of lysis of the protoplast was the only technique that could be used in the study of the biosynthesis of AFB<sub>1</sub> from acetate. It was found<sup>23</sup> that the method of the French press destroyed the ability of the homogenate to convert ST to AFB<sub>1</sub>.

Although other methods for preparing active homogenates are available (Table 1), it is apparent that for aflatoxin biosynthesis, a gentle method of cell wall disruption is required. It is possible that these systems require integrated association of enzymes, perhaps connected to structural elements in the intact cells, which are particularly sensitive to disruption. Certainly, procedures designed to give cell-free preparations active in secondary biosynthetic processes have often proved difficult and unreliable but experienced enzymologists have improved techniques considerably in the last two decades.

Table 1. Examples of Methods Used to Prepare Crude-Cell Free Extracts from *Aspergillus* species.

Method	Fungus	Enzyme
Grind (sand) <sup>49</sup>	<i>A. flavus</i>	Oxidase
Grind (sand) <sup>50</sup>	<i>A. parasiticus</i>	Oxidase
Grind (buffer) <sup>51</sup>	<i>A. niger</i>	Oxygenase
Freeze/grind <sup>52</sup>	<i>A. ochraceus</i>	Oxygenase
Freeze/blend <sup>53</sup>	<i>A. niger</i>	Reductase
Freeze/lyophilise <sup>54</sup>	<i>A. niger</i>	Dehydrogenase
Lyophilise/acetone <sup>55</sup>	<i>A. parasiticus</i>	Dehydrogenase
Sonication <sup>56</sup>	<i>A. amstelodami</i>	Reductase
Acetone powder <sup>57</sup>	<i>A. niger</i>	Hydrolase



### 2.5.3. Purification of the Enzymes

In addition to the difficulty of obtaining an active cell-free preparation from the mycelia of filamentous fungi, major hurdles are faced in the purification of the enzymes. The enzymes tend to be rapidly denatured or inactivated by the slightest perturbation from their native environment<sup>23</sup>. In addition, there is a relatively small quantity of the secondary metabolic enzyme in the cell and this together with denaturation during isolation, may have a negative effect in the substrate-product conversion reaction. Thus, at each stage in the purification, optimisation of concentration and stability must be achieved. Suitable methods used for concentrating the enzyme are ultra-filtration and dialysis against sucrose<sup>23</sup>. In the isolation of a methyltransferase system, precipitation with ammonium sulphate was used to non-specifically remove contaminating material<sup>23</sup>. Many different types of stabilizing agents have been used in the isolation of enzymes, including glycerol<sup>58</sup> and thiol reducing agents<sup>59</sup>.

### 2.6. AFLATOXIN BIOSYNTHESIS

Drew and Demain<sup>35</sup> have shown that primary and secondary metabolism are separate and distinct processes. Since the metabolic pathway of primary metabolism produces the precursors required for secondary metabolism, factors that have an effect on primary metabolism will ultimately affect secondary metabolism. Therefore, aflatoxin production is affected by catabolic activity<sup>60,61</sup>, reduced co-enzyme levels<sup>62</sup>, energy charge<sup>63</sup> and metal ions<sup>64</sup>.

Studies into the effect of nutrition on aflatoxin production commenced soon after the discovery of the toxins. It was found that metals such as zinc<sup>64</sup> and magnesium<sup>65</sup> stimulated aflatoxin production. A similar effect was found with the amino acids proline<sup>66</sup> and asparagine<sup>67</sup>, and with a mixture of sucrose and yeast extract<sup>68</sup>. It was found that high levels of inorganic nitrogen<sup>69</sup> and phosphate<sup>67</sup> inhibited aflatoxin production.

Investigation of the effect of zinc on glucose-1-phosphate and mannitol dehydrogenase, obtained from *A. parasiticus*, showed that aflatoxin, rather than fatty acid, biosynthesis was favoured<sup>55,70</sup> because it prevents NADPH formation by inhibition of both of these enzymes.



It was suggested<sup>71,72</sup> that the stimulatory effects of carbohydrates, such as glucose, were mediated through the loss of NADPH formation and by inhibition of the enzymes present in the tricarboxylic acid (TCA) cycle. The low activity of the TCA enzymes reduces acetate oxidation thus making the acetates available for aflatoxin production.

Aflatoxin biosynthesis has been linked to the high activity of pyruvate kinase which can promote the utilization of pyruvate or phosphoenolpyruvate as a source of malonyl coenzyme A (CoA). Furthermore, the kinase activity was found high in toxigenic strains of the fungus and low in non-toxigenic strains<sup>73</sup>.

Bhatnagar *et al.*<sup>74</sup> reported that reduced nicotinamide adenine dinucleotide (NAD) and nicotinamide adenine dinucleotide phosphate (NADP) glutamate dehydrogenase stimulates the generation of idiophase conditions by formation of  $\alpha$ -ketoglutarate which is able to inhibit the TCA cycle.

## 2.7. AFLATOXIN BIOSYNTHETIC PATHWAY

Elucidation of the biosynthetic pathway has involved intensive studies on the structures of various metabolites produced by the fungi as possible intermediate compounds. Incorporation of isotopically labelled precursors and the use of an *A. parasiticus* blocked mutant, which could not produce aflatoxins but accumulated various intermediate compounds, has been used. Most of these investigations were made with whole cell cultures in replacement media. Cell-free extracts have also been used to check the intermediacy of compounds in the aflatoxin pathway and to establish the precursor relationship of metabolites. A variety of precursors and some biosynthetic pathways have been proposed. A pathway<sup>75</sup> of aflatoxin biosynthesis, presented in 1983, is illustrated in Figure 6 (page 14).

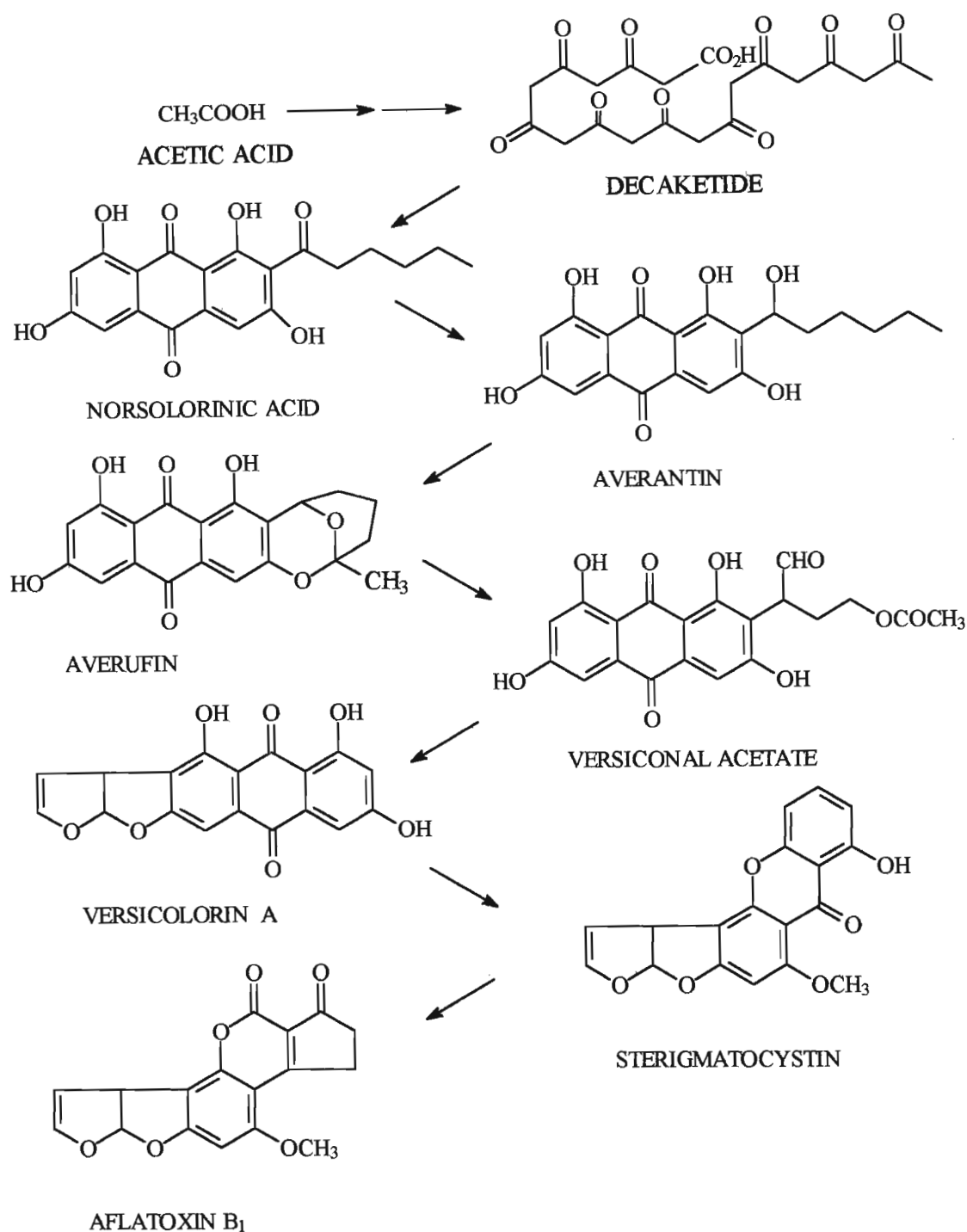


Figure 6. Proposed Pathway<sup>75</sup> for the Biosynthesis of AFB<sub>1</sub>.

Evidence in support of this pathway comes from studies with putative precursors isotopically labelled with  $^{13}\text{C}$ ,  $^{14}\text{C}$ ,  $^2\text{H}$ , or  $^{18}\text{O}$ . The latter three isotopes were the subject of a series of nuclear magnetic resonance studies by Steyn *et al.*<sup>76</sup>. The currently accepted pathway<sup>77</sup> of aflatoxin B<sub>1</sub> biosynthesis is illustrated in Figure 7 (page 15).

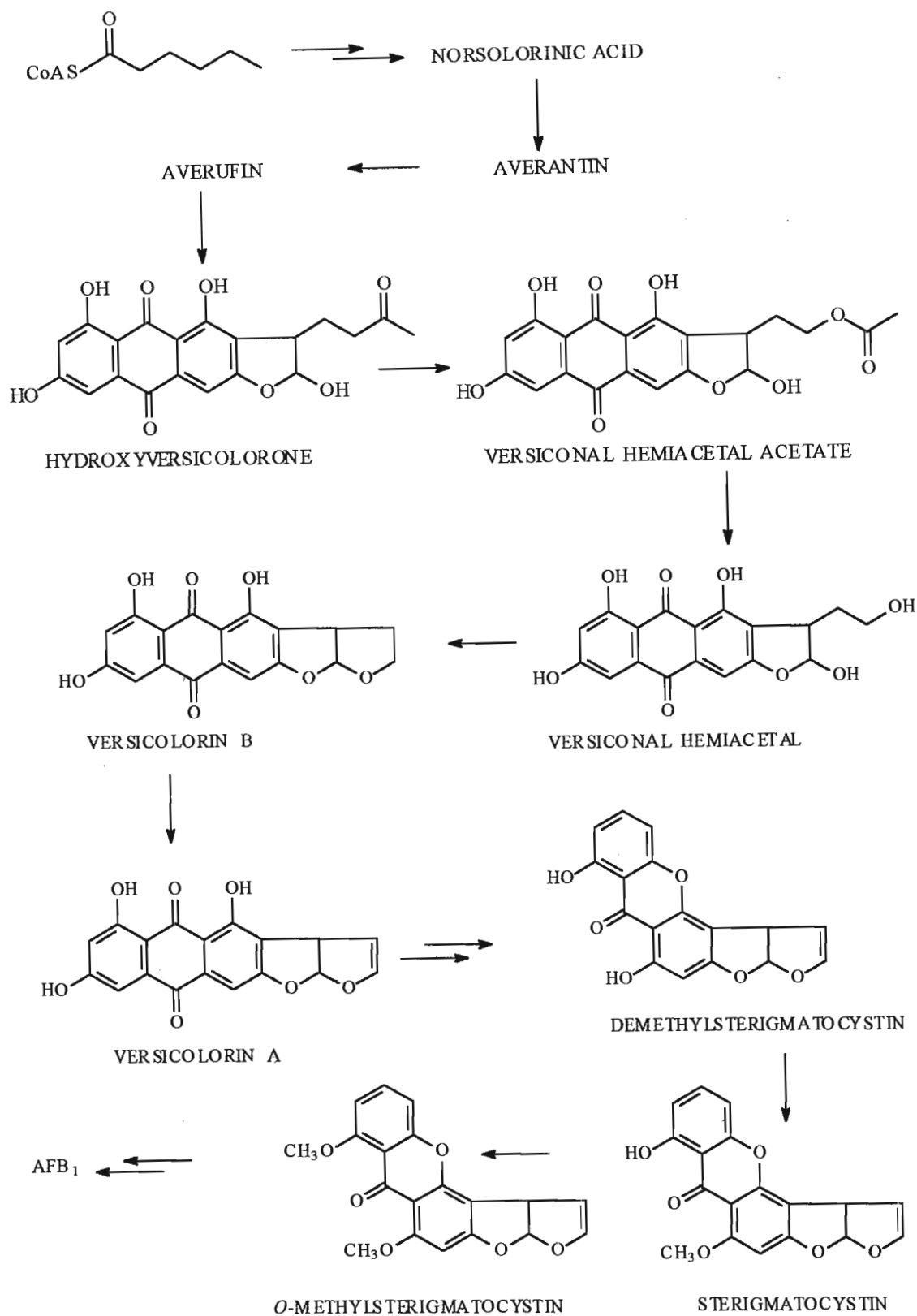


Figure 7. The Currently Accepted Pathway<sup>77</sup> for the Biosynthesis of AFB<sub>1</sub>.

### 2.7.1. The Polyketide and Aflatoxin Pathways

The polyketide route to secondary metabolites may be regarded as the metabolic route most characteristic of the fungi. Many aromatic compounds in nature have structural features arising from head to tail linkage of acetate units via poly- $\beta$ -carbonyl intermediate compounds<sup>78</sup>.

In 1907, Collie<sup>79</sup> used the observation made by previous researchers of the self condensation of ethylacetoacetate into dehydroacetic acid, and thus suggested the polyacetate pathway based on the transformation of dehydroacetic acid to orcinol and compounds resembling natural products (Figure 8).

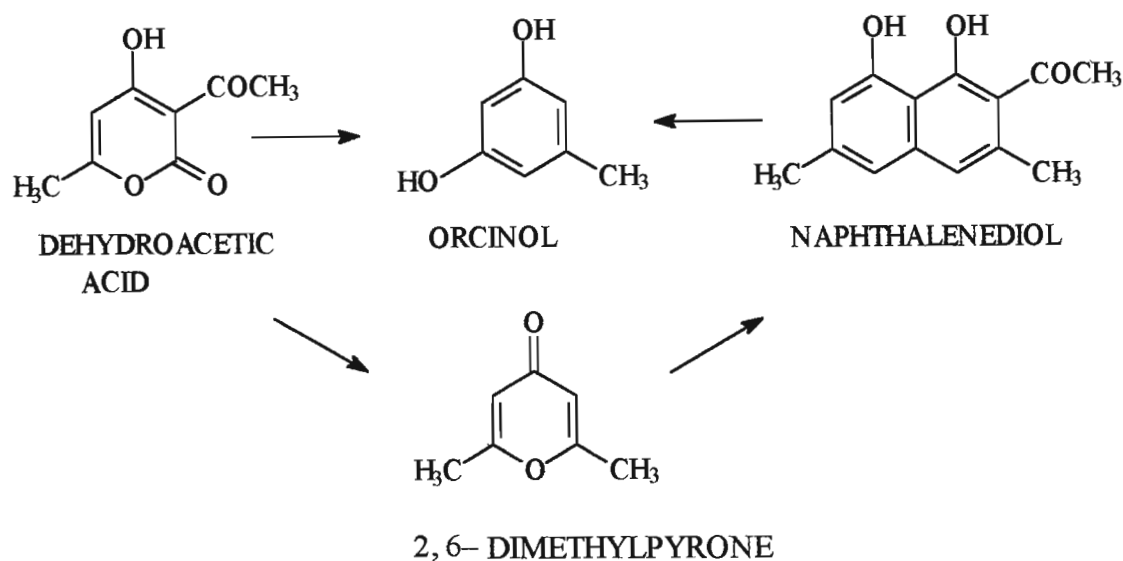


Figure 8. Transformation of Dehydroacetic Acid to Some Natural Products<sup>79</sup>.

This information laid the foundation for the polyketide hypothesis that basic C<sub>2</sub> building blocks give poly- $\beta$ -ketone intermediates from which aromatic metabolites arise by cyclization. However, this hypothesis was limited since it was not based on any biochemical or metabolic data. In 1953 Birch and Donovan<sup>80</sup> provided the experimental proof for the pathway. In order to account for the numerous natural products of possible polyketide origin, Birch and Donovan had to make several hypotheses to deal with secondary

alterations that could occur before or after the formation of the phenolic structure. The current interpretation<sup>81</sup> for polyketide biosynthesis is illustrated in Figure 9.

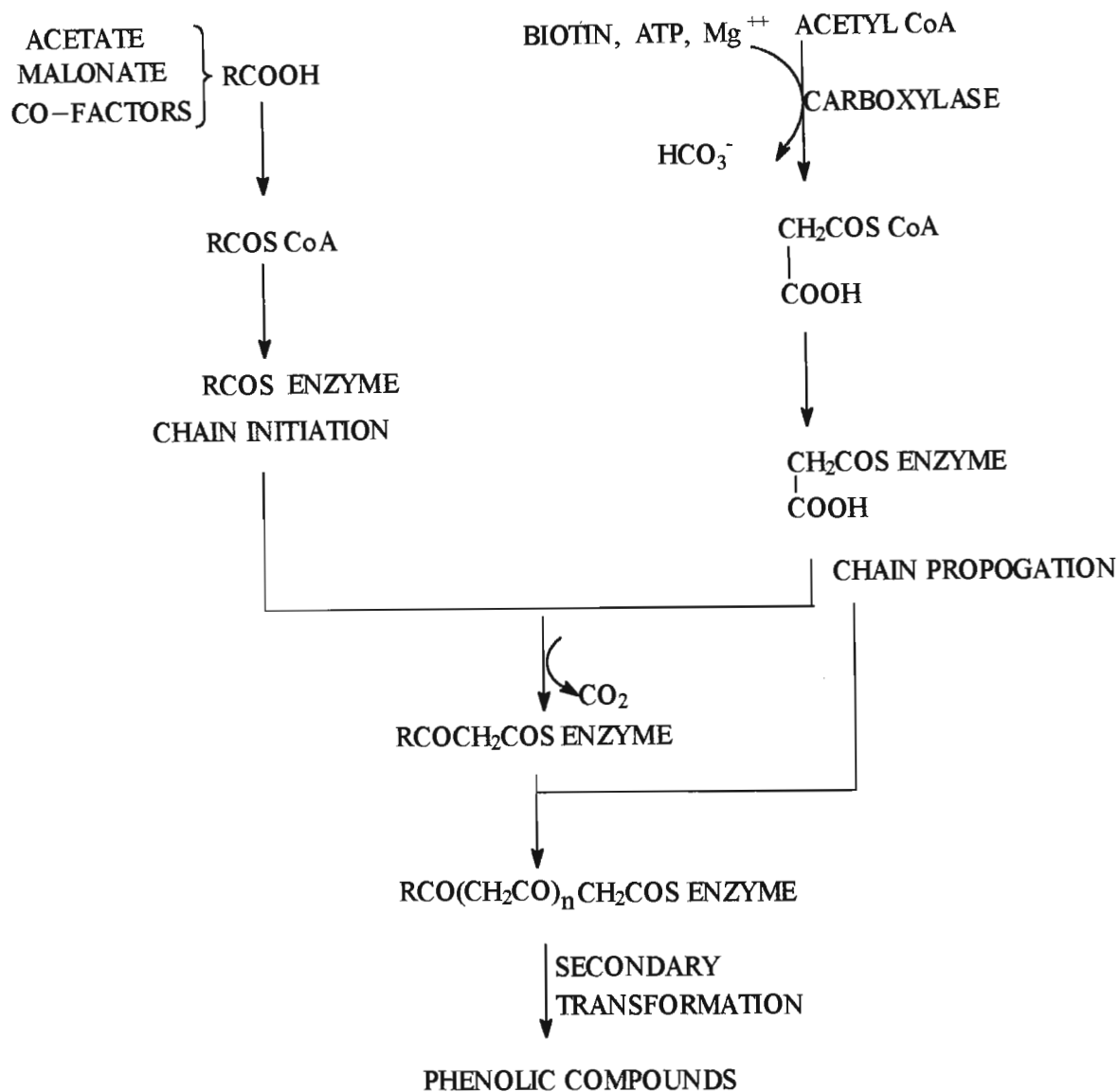


Figure 9. The Acyl-Polymalonate Biosynthetic Route for Polyketide Biosynthesis<sup>81</sup>.

The polyketide synthesis is similar<sup>82</sup> to fatty acid biosynthesis; however, it lacks some of the intermediate reduction steps<sup>81</sup>. The first step in both fatty acid and polyketide biosynthesis is the formation of malonyl CoA from acetyl CoA. Malonyl CoA arises from oxaloacetate via a decarboxylation, catalysed by oxaloacetate dehydrogenase<sup>83</sup>. The second step<sup>84</sup>, common to both syntheses, is chain elongation commencing with the condensation of acetyl CoA and malonyl CoA. This is catalysed by a transferase activity fixed into a multi-enzyme

complex in the form a flexible<sup>9</sup> protein “arm”. The condensation reaction is driven by the release of carbon dioxide.

The fatty acid synthase (FAS) that catalyses this series of reactions varies in its structural organization in different life forms<sup>85</sup>. A schematic representation of the fatty acid and polyketide biosynthesis, showing the different enzymes involved, is presented in Figure 10 (page 19). In most bacteria and in higher plants, FAS is a multienzyme complex (FAS Type II). It consists of separate polypeptides for condensation, ketoreduction, dehydration and enoyl reduction, together with a small polypeptide, the acyl carrier protein (ACP) to which the growing carbon chain is intermittently attached. In addition there are acetyl and malonyl tranferases. In vertebrates, corresponding biochemical functions are carried out by distinct domains on a large multifunctional polypeptide (FAS Type I).

A critical aspect of the FAS/PKS biosynthetic cycle is the translation reaction that transfers the acyl chain from the ACP phosphopantetheine arm to the  $\beta$ -ketoacyl synthase active site. It is not known whether this step is catalysed by a unique transacylase activity or results from an activity of the  $\beta$ -ketoacyl synthase itself<sup>85</sup>.

After reaching the required chain length, stabilization occurs in the formation of an aromatic structure. The formation of this stabilized ring and the release of the phenolic compound from the enzyme complex may occur by an intramolecular condensation reaction or under the influence of an enzyme derived proton<sup>86</sup>. The intramolecular condensation processes that occur can alter the phenolic compounds resulting in the production of diverse types of compounds.



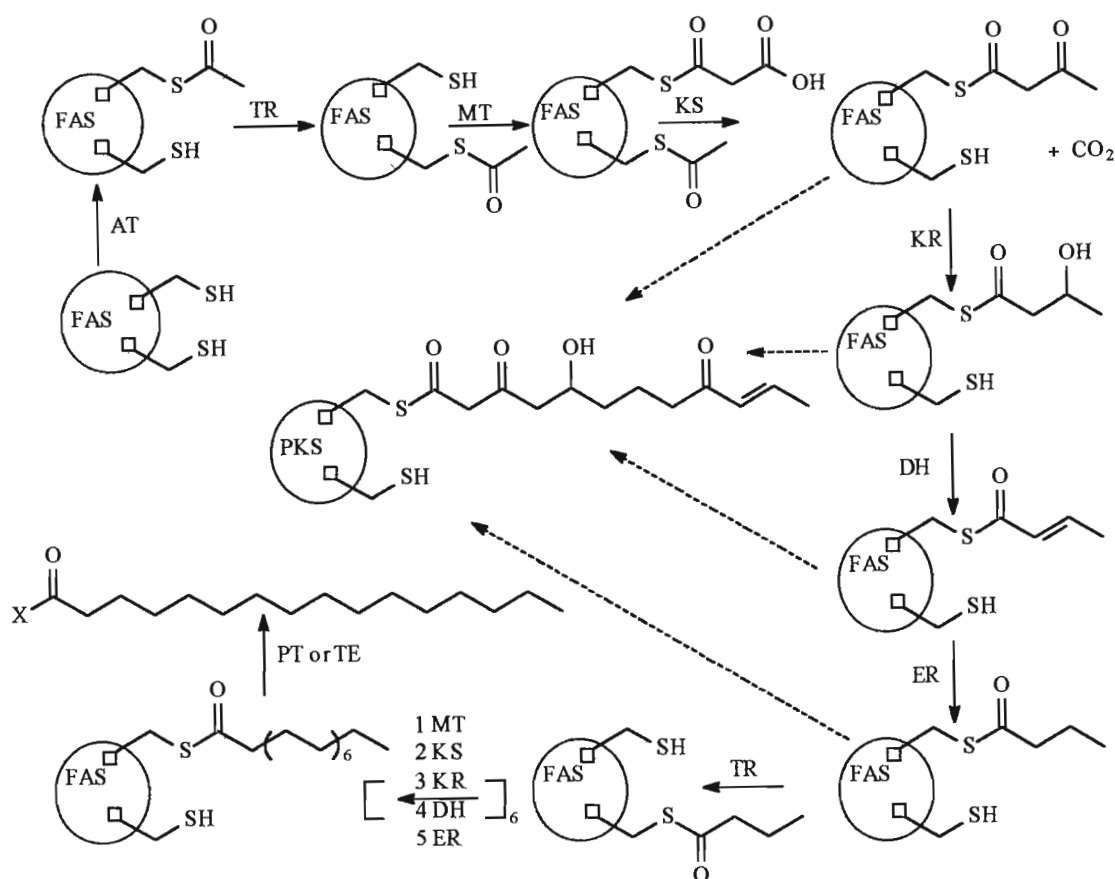


Figure 10. Schematic Representation of Fatty Acid and Polyketide Biosynthesis<sup>85</sup>.

FAS and PKS represents the fatty acid and polyketide synthase, respectively, carrying the β-ketoacyl synthase (□) and the acyl carrying protein (□). The reaction steps are labelled: acetyl transferase (AT), acyl transferase (TR), malonyl transferase (MT), β-ketoacyl synthase (KS), ketoreductase (KR), dehydrase (DH), enoyl reductase (ER), palmitoyl transferase (PT) and thioesterase (TE). CoA (X) or OH (X).

### 2.7.2. Anthraquinone Synthesis

In aflatoxin synthesis, the decaketide formed via the polyketide pathway<sup>9</sup> (Figure 11, page 20) has sites available for modification to form stabilized products. This process is followed by numerous oxidation-reduction steps which results in the release of energy in a process independent to that of fatty acid biosynthesis. The primary driving force for further biosynthetic modification of the polyketide seems to be the synthesis of an end product which is easily released by the fungi<sup>87</sup>.



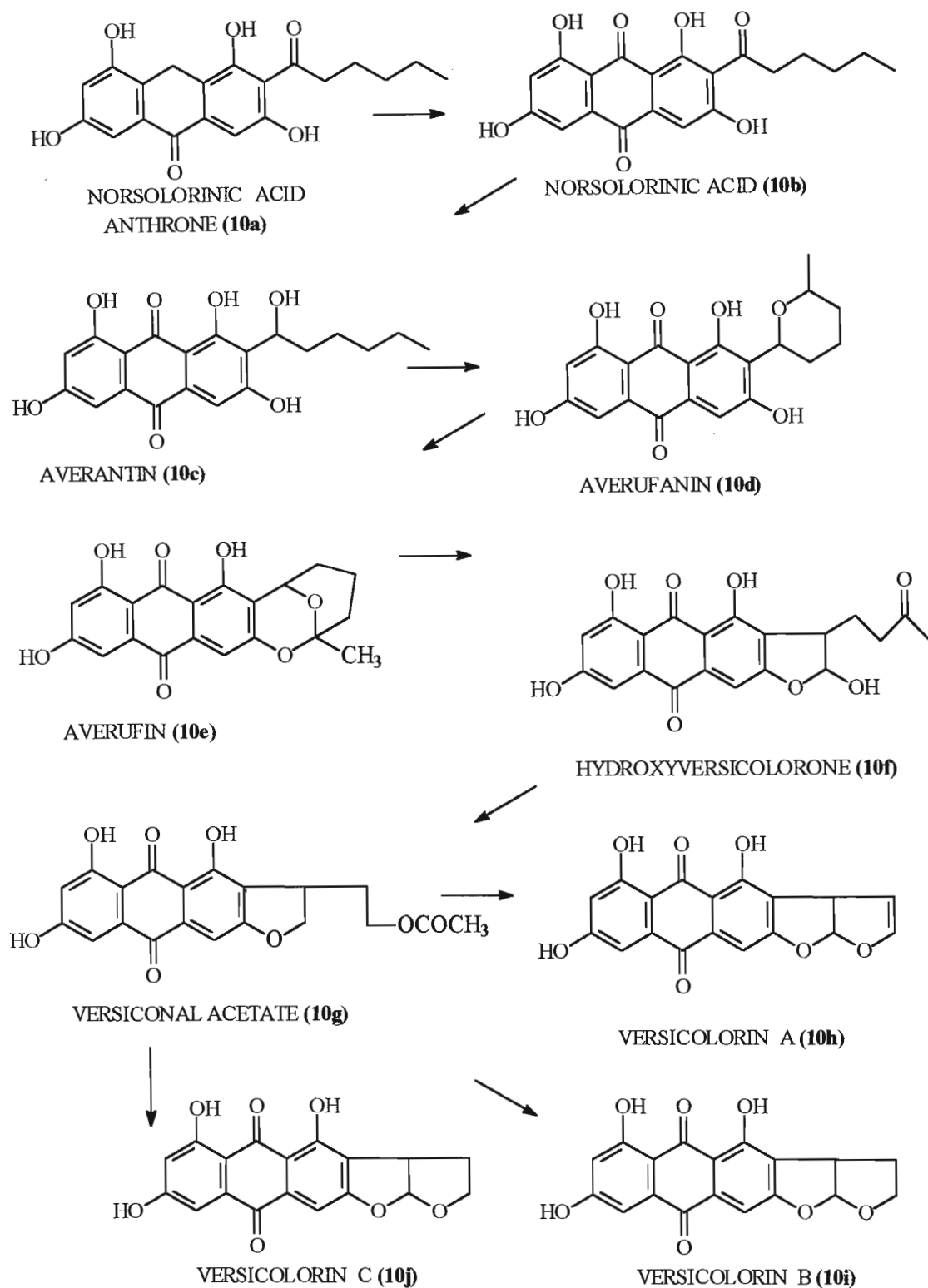


Figure 12. Schematic Representation of Anthraquinone Derivatives<sup>87</sup> leading to AFB<sub>1</sub> Production.

### 2.7.3. Xanthone Synthesis

The biosynthetic pathway of aflatoxins is mostly known and Figure 13 (page 23) shows the latter part leading to the formation of the four major naturally occurring aflatoxins, viz., AFB<sub>1</sub>, AFB<sub>2</sub>, AFG<sub>1</sub> and AFG<sub>2</sub>. In the pathway, the formation of the bisfuran compound from versiconal hemiacetal is completed via the oxidative desaturation of versicolorin B to versicolorin A<sup>88,89</sup>. Aflatoxin B<sub>1</sub> and AFG<sub>1</sub> are produced from demethylsterigmatocystin (DMST), and AFB<sub>2</sub> and AFG<sub>2</sub> are produced from dihydrodemethylsterigmatocystin (DHDMST). Recently, Yabe *et al.*<sup>90</sup> reported on a purified *O*-methyltransferase which catalyses the conversion of DMST to ST and DHDMST to dihydrosterigmatocystin (DHST). Although the mechanisms of the molecular rearrangements in the post-versicolorin A segment of the pathway are not known, important progress has been made to identify the genes in *A. parasiticus* that encode proteins involved in the biosynthesis of aflatoxins (Section 2.9, page 31-34).

Modification of the polyhydroxyanthraquinone compounds involves cleavage of the quinone portion by a Baeyer-Villiger type reaction and subsequent rearrangement to produce the angular xanthone sterigmatocystin<sup>87</sup>. The possible steps involved in this rearrangement, as illustrated in Figure 14 (page 24), include a Baeyer-Villiger oxidation of the quinone portion of the ring, rearrangement with decarboxylation and concomitant deoxygenation to produce demethylsterigmatocystin (**11f**). Methylation of one phenolic hydroxyl group occurs to give ST (**11g**). Of the enzymes present in the xanthone transformation, the methyltransferase has been identified, purified and characterised<sup>91</sup>.

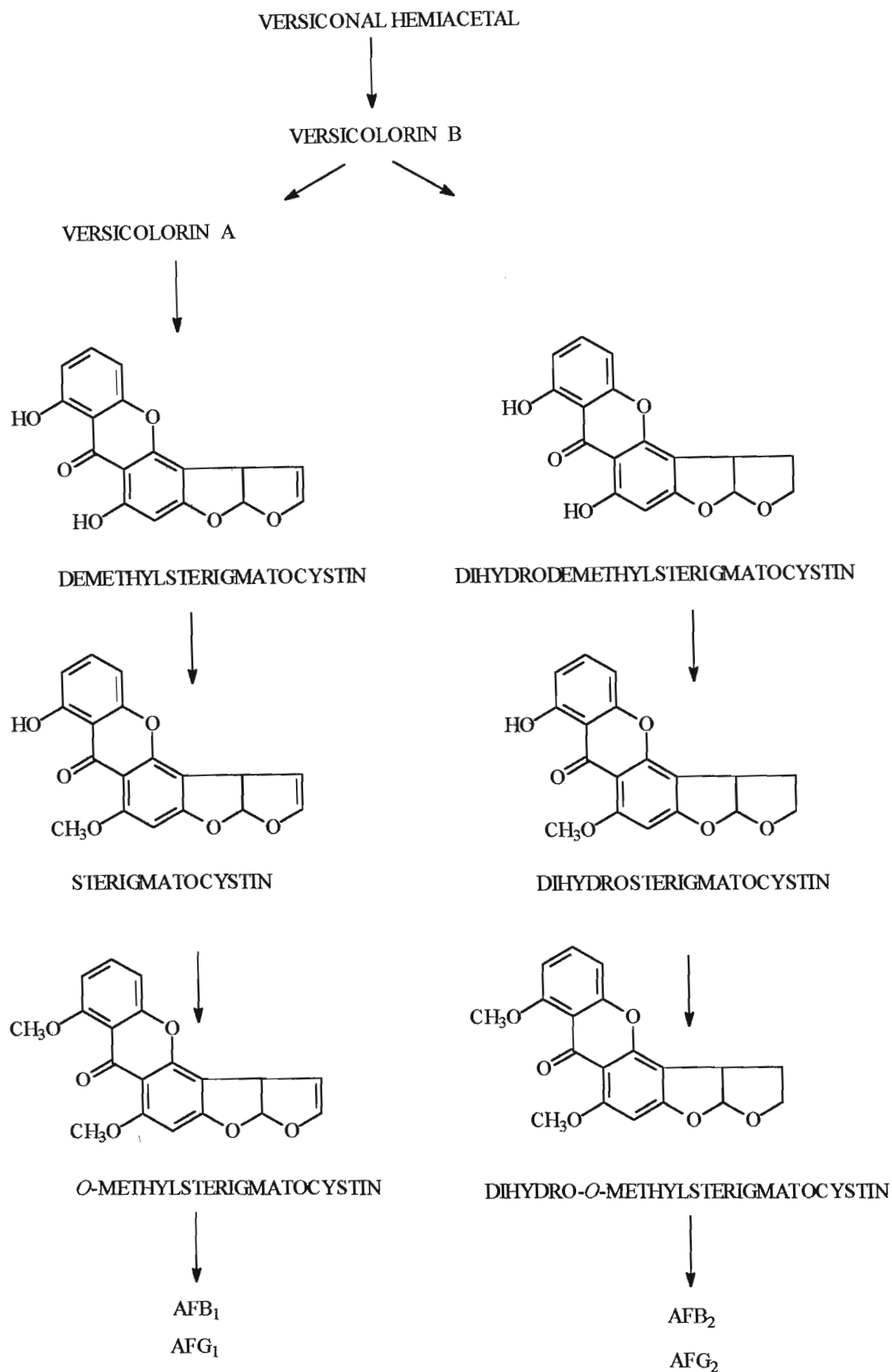


Figure 13. The Metabolic Scheme for Aflatoxin Biosynthesis Showing Structures of Critical Intermediates<sup>90</sup>.

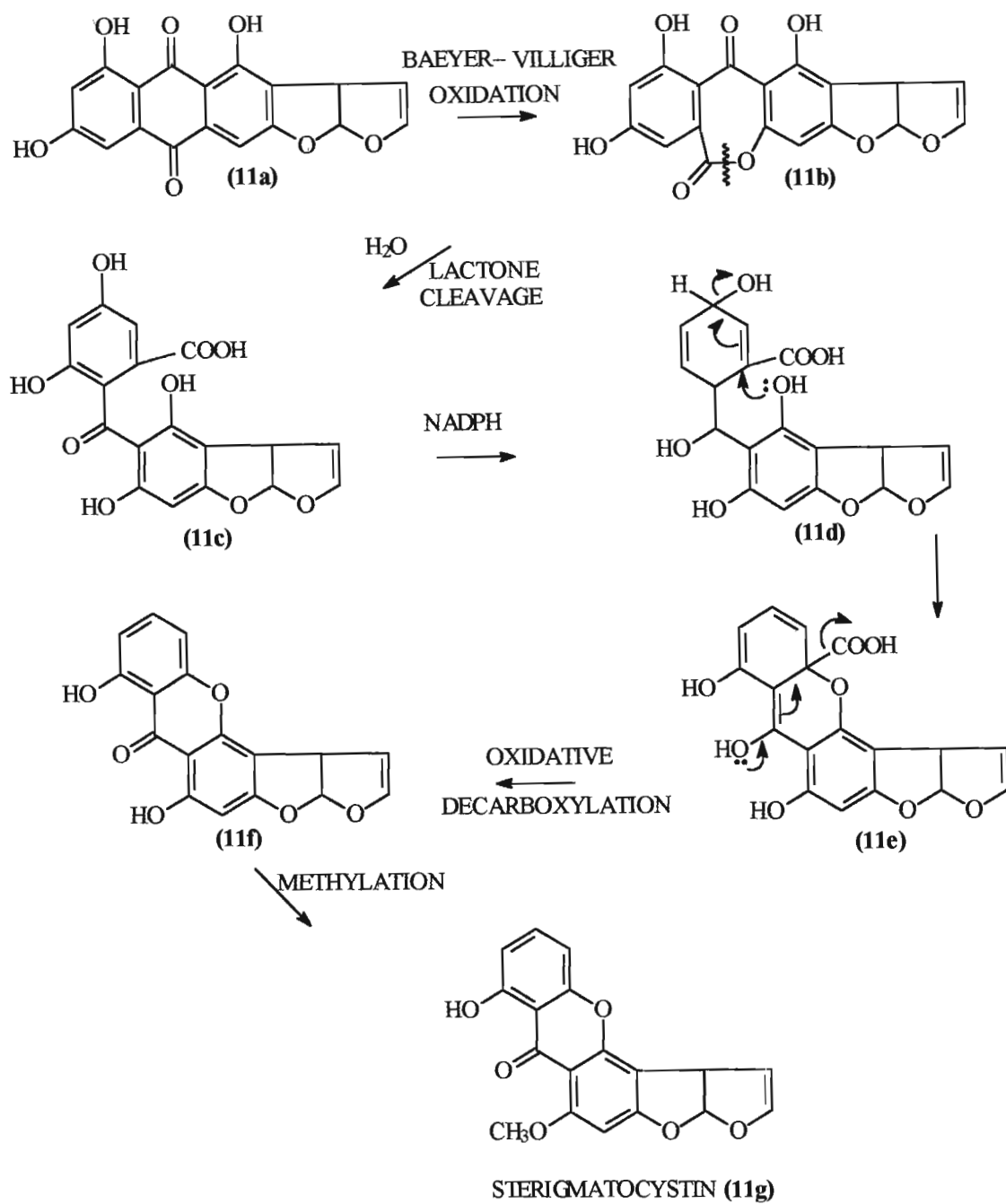


Figure 14. Possible Steps Involved in the Rearrangement of Anthraquinone to Xanthones<sup>87</sup>.



#### 2.7.4. Xanthone Transformation to Aflatoxins

Using  $^{14}\text{C}$ - and  $^{13}\text{C}$ - labelled acetate precursors, biosynthetic studies<sup>92,93</sup> on ST revealed the distribution of labels in the acetate derived skeleton as illustrated in Figure 15. These studies indicate that ST arises from the acetate-malonate pathway with the methoxy group derived from methionine.

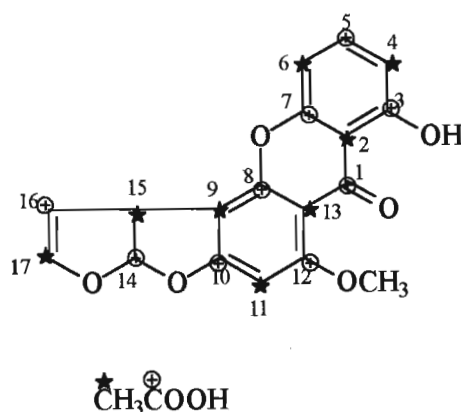


Figure 15. Structure of Sterigmatocystin with Labels Derived from Acetate<sup>92,93</sup>.

In several hypothetical schemes, ST has been proposed<sup>94</sup> as an intermediate in the aflatoxin biochemical pathway. Using the replacement culture technique<sup>95</sup>, it was established that ST could act as a precursor to AFB<sub>1</sub>. There was doubt cast on this theory when a micro-colony technique<sup>96</sup> showed that ST could be a side shunt metabolite.

In 1983, Jeenah and Dutton<sup>6</sup> reported the conversion of ST and OMST to AFB<sub>1</sub> in cell-free extracts. Subsequently Lax *et al.*<sup>97</sup> proposed that OMST is an intermediate between ST and AFB<sub>1</sub>. It was subsequently concluded that the biosynthesis of AFB<sub>1</sub> proceeded by two steps :

- methylation of ST to OMST involving a soluble or loosely bound enzyme, and followed by
- oxidation of OMST to AFB<sub>1</sub> mediated by a membrane-associated enzyme.

The post-microsomal fraction of a cell-free extract showed<sup>48</sup> that DL-ethionine inhibited the production of OMST and subsequently, it was shown<sup>98</sup> that the methylating activity increased in the presence of S-adenosyl methionine (SAM) which is the primary methyl donor for the enzymatic conversion. The enzyme responsible for the conversion was designated a 'methyltransferase'. The microsomal fraction of a cell-free extract showed<sup>98</sup> that NADPH is a co-factor which enhanced the enzyme activity for the conversion of OMST to AFB<sub>1</sub>. This indicated that an oxidation-reduction process occurred in the system and the enzyme responsible for the conversion was subsequently designated an 'oxido-reductase'.

In 1989, Yabe *et al.*<sup>99</sup> reported two distinct *O*-methyltransferase which are involved in aflatoxin biosynthesis, viz., *O*-methyltransferase I and *O*-methyltransferase II. The study demonstrated that DMST and DHDMST are the intermediate precursors in the formation of ST and DMST, respectively (Figure 16).

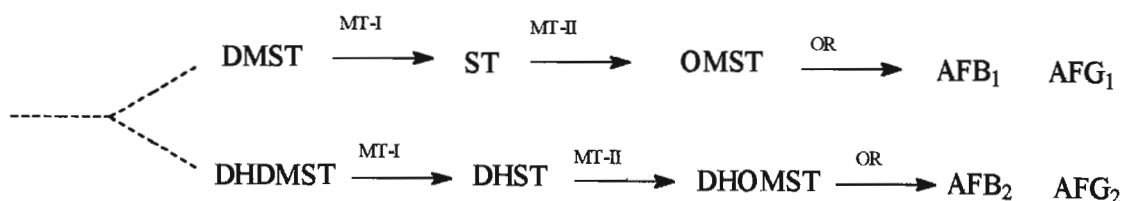


Figure 16. Metabolic Scheme Proposed for the Late Stages of Aflatoxin Biosynthesis<sup>99</sup>.

MT-I = *O*-methyltransferase I ; MT-II = *O*-methyltransferase II ; OR = oxido-reductase.

Bhatnagar *et al.*<sup>100</sup>, in 1989, proposed a mechanism for the conversion of OMST to AFB<sub>1</sub> as illustrated in Figure 17 (page 27).

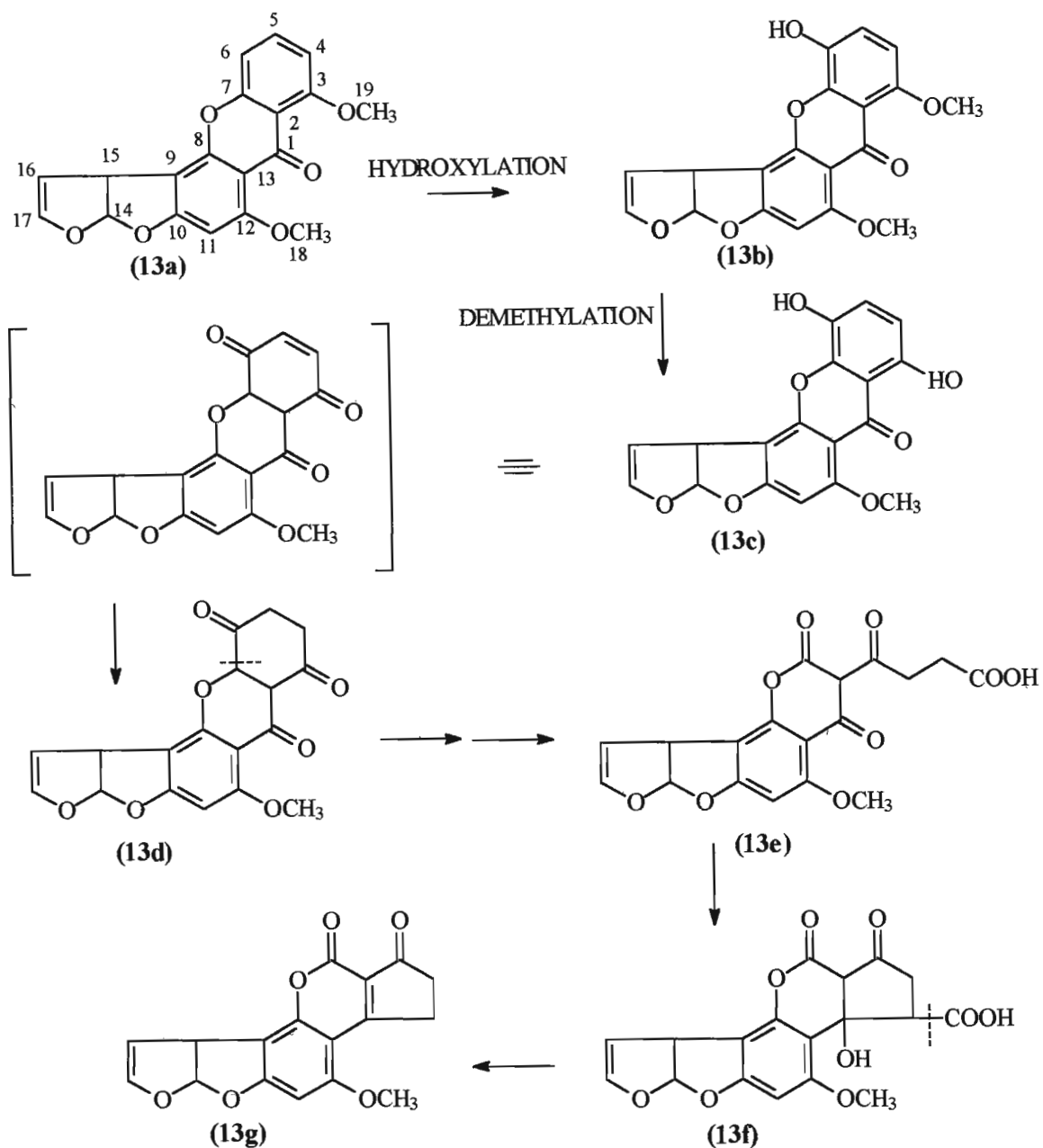


Figure 17. The Mechanism Proposed by Bhatnagar *et al.*<sup>100</sup> for the Conversion of *O*-Methyl sterigmatocystin to Aflatoxin B<sub>1</sub>. Intermediates **13e** and **13f** were proposed by Bu'Lock<sup>101</sup>.

This proposal<sup>100</sup> is supported by the observed disappearance of the -C[<sup>3</sup>H]<sub>3</sub> group from the C-19 position in OMST (**13a**) into the reaction medium during the enzymatic conversion of OMST to AFB<sub>1</sub>.

Currently, there is no chemical rationale for the methylation of ST to OMST. The current line of thinking is that the conversion from a phenolic to an anisolic ring may activate the

ring toward subsequent oxidation by enhanced electron induction of the terminal aromatic ring of ST into the pentenone of AFB<sub>1</sub>. This hypothesis is based on research<sup>102,103</sup> on the enzymatic conversion of N-alkylaniline type compounds by amine oxidases.

The following steps were postulated for the conversion of OMST to AFB<sub>1</sub> :

- OMST may undergo *para*-hydroxylation to yield 10-hydroxy-*O*-methylsterigmatocystin (**13b**) by an oxygenase,
- this could be followed by demethylation to yield 10-hydroxysterigmatocystin (**13c**).
- The quinonoid form of (**13c**) may undergo reduction by NADPH to form the 8,9-dihydroquinoid derivative (**13d**) of ST,
- and (**13d**) would then proceed through the proposed intermediates<sup>101</sup> to produce AFB<sub>1</sub>.

Another possible pathway<sup>87</sup> utilizing a dioxygenase is illustrated in Figure 18 (page 29). According to this proposal the dioxygenase, requiring Fe<sup>2+</sup> for activity, is responsible for catalysing the formation of a deoxetane ring (**14b**) which undergoes ring cleavage to form the carbonyl functional group (**14c**). This is followed by hydrolysis, with the loss of methyl possibly as methanol, and rearrangement such that subsequent cyclisation could occur to produce compound **14e**. The monooxygenase is now able to act on the substrate, in the presence of NADPH, to form cyclopentanone carboxylic acid which finally undergoes decarboxylation to the cyclopentanone ring.

No intermediate metabolites between OMST and AFB<sub>1</sub> have been found, a fact suggesting that the substrate remains part of the oxidative enzyme complex until the cyclopentenone ring is formed.

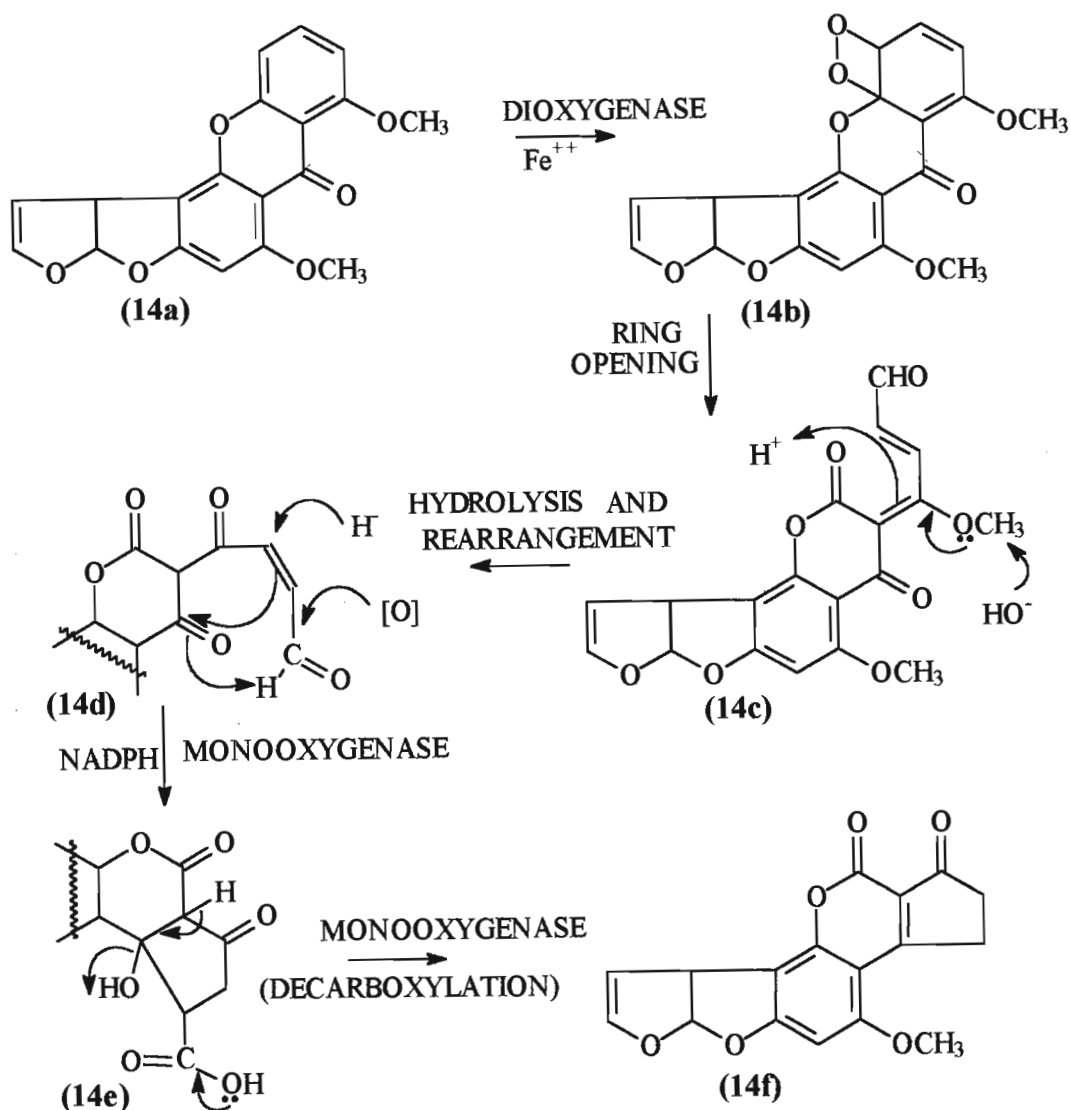


Figure 18. A Mechanism Postulated by Bhatnagar *et al.*<sup>87</sup> for the Conversion of OMST to AFB<sub>1</sub> Involving Oxygenases.

## 2.8. THE INHIBITION OF AFLATOXIN BIOSYNTHESIS

Many compounds<sup>104</sup>, including a number of botanical substances and food preservatives, inhibit aflatoxin biosynthesis by *A. flavus* and *A. parasiticus*. These substances were of interest in that the study of their effects aided in the elucidation of the mechanism involved in or regulating aflatoxin biosynthesis. In most instances the research results obtained for various inhibitors were presented only in terms of fungal growth and aflatoxin production. However, Zaika and Buchanan<sup>105</sup> discussed test substances that exerted additional effects

on the fungus, such as alteration of enzymatic activity, inhibition or stimulation of various metabolic processes or changes in accumulation of metabolites.

Rao and Harein<sup>106</sup> reported dichlorvos (1) (Figure 19, page 31) as the first organophosphate to be associated with aflatoxin inhibition in wheat, rice, peanut and corn. Treatment of aflatoxigenic fungi with dichlorvos was associated with the accumulation of an orange pigment which was subsequently characterized by Cox *et al.*<sup>107</sup> as VHA. Isotopic-labelling studies by Bennett and Christensen<sup>9</sup> indicated that VHA was an intermediate in aflatoxin biosynthesis. Anderson and Dutton<sup>108</sup> reported dichlorvos-like activity for the organophosphates ciodrin (2), naled (3), phosdrin (4), trichlorphon (5) and chlormephos (6)(Figure 19, page 31). These authors suggested that dichlorvos and other organophosphates affecting aflatoxin biosynthesis, acted by inhibiting the fungal oxygenase activity.

Other compounds, such as benzoic acid (7), have also been reported to inhibit aflatoxin synthesis. It has been suggested by Uraih *et al.*<sup>109</sup> that although benzoic acid is a weaker inhibitor than dichlorvos, it may act at the same site as dichlorvos. Two naturally occurring compounds viz., chlobenthiazone (8) and tricyclazole (9) were reported by Wheeler *et al.*<sup>110,111</sup> to inhibit the accumulation of AFB<sub>1</sub>, AFB<sub>2</sub> and AFB<sub>2a</sub> on three wild strains of *A. flavus*. It was suggested by Wheeler *et al.*<sup>110</sup> that chlobenthiazone was responsible for inhibition at a site in the aflatoxin pathway prior to the synthesis of NA. Mahmoud<sup>112</sup> reported the effect of twenty essential oil constituents on *A. flavus* growth and aflatoxin production. The five oil constituents, viz., geraniol (10), nerol (11), citronellol (12), thymol (13) and cinnamaldehyde (14)(Figure 19, page 31) completely inhibited fungal growth and aflatoxin formation.



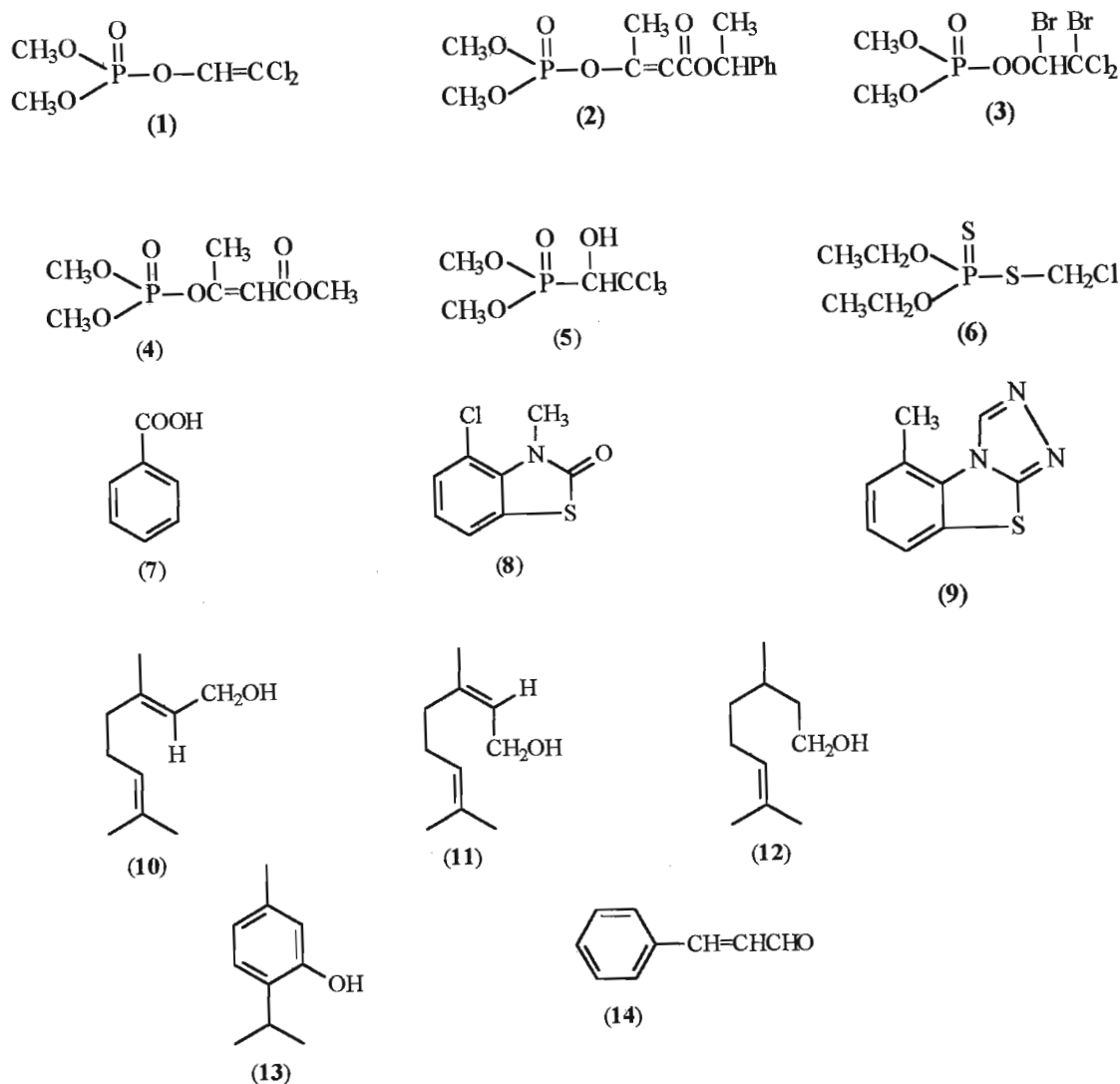


Figure 19. The Chemical Structure of Some Compounds Inhibiting AFB<sub>1</sub> Production.

## 2.9. MOLECULAR BIOLOGY OF AFLATOXIN BIOSYNTHESIS

Recently, efforts in several laboratories have focused on developing an in-depth understanding of the molecular biology of the aflatoxin biosynthetic pathway. This arose due to the difficulty in effectively and economically controlling aflatoxin contamination of food and feed by traditional agricultural methods. Little was known about the genetic basis of aflatoxin production versus non-production, largely because of the asexual nature of the *Aspergillus* species. The recent advent of molecular cloning procedures, however, has provided a means to study the mechanisms of gene expression in these fungi.

Four methods have been used to characterise the aflatoxin pathway on the levels of gene and enzymes<sup>113</sup>:

- complementation of classically generated mutants
- targeted disruption of suspected pathway genes in wild-type species
- purification of biosynthetic enzymes for the isolation of coding sequence through reverse genetics and
- random mutagenesis

The first gene was isolated and described by Chang *et al.*<sup>114</sup>. Rapid and significant progress followed the discovery that genes involved in aflatoxin biosynthesis in both *A. flavus* and *A. parasiticus* are clustered<sup>115,116</sup> (Figure 20, page 34). The cluster in *A. flavus* is located on a 4.9 mb chromosome<sup>117</sup>. Yu *et al.*<sup>118</sup> partially mapped the clusters in *A. parasiticus* and *A. flavus* and estimated the cluster size to be 75 kb. Keller *et al.*<sup>119</sup> discovered that in *A. nidulans* the genes in ST biosynthesis is also clustered. Although the arrangement of the genes within the clusters is different from the aflatoxin gene cluster, the deduced amino acid sequence of the gene products are similar.

Chang *et al.*<sup>120</sup> identified the polyketide synthase gene *pksA* when transforming an NA accumulating strain of *A. parasiticus* with DNA containing fragments of the aflatoxin cluster. Mahanty *et al.*<sup>121</sup> identified the fatty acid synthase gene *fasI* by complementation in *A. parasiticus* strain UVM8. Gene disruption experiments indicated that *fasI* functioned prior to the formation of NA. A second gene, viz., *fas2*, was located adjacent to *fasI*.

Trail *et al.*<sup>122</sup> identified the gene *norI* which encodes a 29 kDa protein with amino acid similarity to dehydrogenases that have a NADPH binding motif. Carey *et al.*<sup>123</sup> identified a cDNA clone corresponding to a gene, *norA*, located on the aflatoxin gene cluster of both *A. parasiticus* and *A. flavus*.

The genes involved in the conversion of AVN to VA are the least defined of the genes in aflatoxin biosynthesis. Yu *et al.*<sup>116</sup> identified the gene *avnA* which encodes a 56.2 kDa cytochrome P450 monooxygenase. The gene *avfI* involved in the conversion of AVF to

VHA was mapped to be a 7kb DNA fragment. Sequence analysis<sup>124</sup> indicated that this DNA fragment contains two genes, viz., *aflB* and *aflW*.

Skory *et al.*<sup>125</sup> used genetic complementation of an *A. parasiticus* mutant, that accumulates VA, to isolate *ver1A* which encodes a NADPH dependent keto-reductase. A second gene, *ver1B*, was identified in *A. parasiticus* that has 95 percent identity to *ver1A*.

Yu *et al.*<sup>126</sup> used an antiserum raised against the purified protein from *A. parasiticus* to screen a cDNA library and isolate the corresponding gene *omt1* involved in the conversion of ST to OMST. The gene *ord1*, involved in the conversion of OMST to AFB<sub>1</sub>, was mapped<sup>127</sup> to a 3.3 kb DNA fragment.

Expression of genes in the aflatoxin biosynthesis cluster is regulated by *aflR*. The gene was isolated from *A. flavus* by Payne *et al.*<sup>128</sup>. In *A. parasiticus*, *aflR* was identified by Chang *et al.*<sup>129</sup>. The protein encoded by *aflR* contains a zinc cluster motif (Cys-Xaa2-Cys-Xaa6-Cys-Xaa6-Cys-Xaa2-Cys-Xaa6-Cys). The zinc cluster motif is involved in the binding of the regulatory protein to the DNA target sequence. A recent review by Keller and Hohn<sup>130</sup> indicated that there are no obvious answers to questions concerning the regulatory and evolutionary significance of the gene cluster. Although clusters contain genes with similar structure and function, the gene order within the cluster and the direction of transcription of some of the corresponding genes are different. A recent review by Payne and Brown<sup>131</sup> indicated that *aflR* is not the only factor involved in pathway regulation. Although *aflR* is the only gene cluster required for transcriptional activation of pathway genes, it appears that other regulatory elements are involved in the temporal expression of the pathway, eg., physiological and nutritional thresholds.

Little is known about the gene(s) involved in the biosynthesis of the aflatoxin G-family, which are only produced by *A. parasiticus*. Biochemical evidence<sup>87</sup> suggests that AFG<sub>1</sub> is produced by a separate pathway branching from ST. Currently there is no evidence indicating that the genes responsible for the branched pathway are within the gene cluster of *A. parasiticus*. However, the genes at the end of the cluster have not been thoroughly characterised.

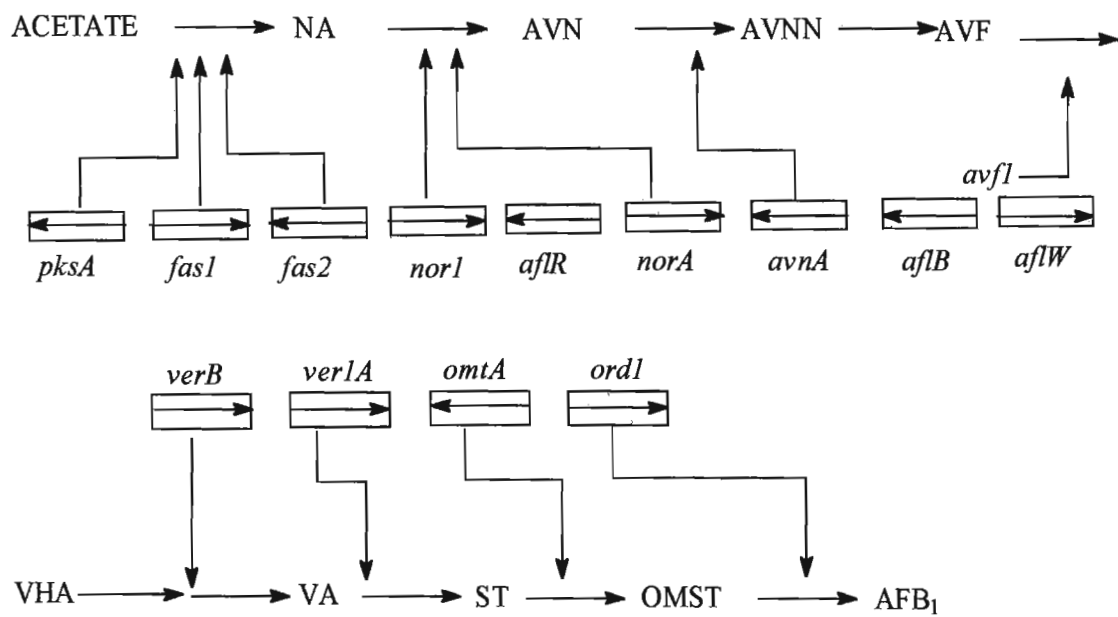


Figure 20. The Biosynthetic Pathway of Aflatoxin B<sub>1</sub>, Showing the Major Intermediates and the Aflatoxin Gene Cluster.

## CHAPTER THREE

### PRODUCTION, ISOLATION AND CHARACTERISATION OF STERIGMATOCYSTIN

#### 3.1. INTRODUCTION

Sterigmatocystin is produced by isolates of *Aspergillus* on both solid substrates and liquid media in varying quantities<sup>132</sup>. It is produced in high yields by strains of the fungi *A. versicolor*, *A. nidulans* and *Bipolaris sorokiniana*<sup>133</sup>. Mutant strains which arise either spontaneously or are obtained artificially by irradiation or treatment with chemical mutagen have also been known to produce ST. The great majority of these differ from the parent stock in only a single gene, which results in the impaired synthesis of a single enzyme. As ST is a secondary metabolite, blocks in the steps leading to its biosynthesis or further metabolism are not limiting to the growth of the organism. This allows for a highly convenient way of identifying precursors and metabolic intermediates without compromising the producing organism.

The production of ST is affected by aeration, the level of atmospheric gases, temperature, moisture content and humidity. The cultivation media of either simple or complex chemical composition are used. A simple medium consists of a solution of mineral salts to which certain defined organic compounds, such as glucose, have been added. In the case of liquid cultures, the composition of the medium and incubation temperature determine the rate of growth and the mass of mycelia produced at the critical time when secondary metabolism comes into prominence. Carbohydrates are the most important nutrient for secondary metabolism as high concentrations in the culture medium result in the formation of abundant acetyl CoA which activates the processes of secondary metabolism.

The preparation of ST from cultures of *A. versicolor* has been discussed in several research reports<sup>132,133</sup>. Davies *et al.*<sup>134</sup> used the surface culture technique to grow the fungus in a solution of sucrose (3 %) and inorganic ions. The flasks were maintained at 30 °C for 21 days and ST was isolated in a yield of 3.3 % (g/g dry mycelia) after successive solvent extractions, chromatography and recrystallisation.

Hsieh and Yang<sup>24</sup>, using *A. versicolor*, investigated three culture techniques and found the standing culture, with its medium not disturbed, produced the highest quantity of ST (27.00 mg/g dry mycelia). The same culture with its medium replaced by a nitrogen free resting cell medium produced less ST (22.09 mg/g dry mycelia). The shaking suspension of mycelia in the resting medium, incubated as a submerged culture, produced the least amount of ST (2.10 mg/g dry mycelia).

Halls and Ayres<sup>135</sup> used various buffers to obtain yields of 1.0 mg/25 ml, in still cultures. Rabie *et al.*<sup>133</sup> found that in liquid media, a maximum of 210 mg/liter was obtained in shake cultures at 25 °C for 20 days. Chatterjee and Townsend<sup>136</sup> found, that of the five media investigated, the production of ST was most successful in Czapek medium and ST production was evident on the sixth day of incubation and tapered off after 24 days.

Barnes *et al.*<sup>137</sup> investigated seven species of *Aspergillus*, two species of *Chaetomium* and one species of *Bipolaris* for the production of ST on a sucrose-salt-phenylalanine (SSP) defined medium and three complex substrates. It was reported that the highest production of ST (361mg/Kg wheat), on a complex substrate, was by *A. versicolor* (SRRC 109) whereas the highest production of ST (7.8 mg/ml SSP) on the defined medium was by *Chaetomium cellulolyticum*.

Since one of the aims of the project was to synthesise ST derivatives (Chapter 4) by chemical transformation of the phenolic group of ST, its production in large quantities was necessary. Due to the high cost of ST, it was necessary to produce the toxin in the laboratory. Thus *A. versicolor*, a producer of ST, was used on liquid culture for this study. The metabolite, once isolated and purified, had to be characterised spectroscopically, viz., by proton nuclear magnetic resonance spectroscopy (<sup>1</sup>H-NMR), carbon-13 nuclear magnetic resonance spectroscopy (<sup>13</sup>C-NMR) and mass spectrometry (MS).

## 3.2. MATERIALS AND METHODS

### 3.2.1. Chemicals and Materials

All chemicals were of reagent grade or analytical grade. Analytical grade solvents were used for extraction and were purchased from Sigma Chemical Suppliers (SA) and Merck NT Laboratory Suppliers (SA). Petri-dishes and disposable plastic pipettes were purchased from Polychem Chemical Co. Thin layer chromatography plates containing fluorescent indicator (F<sub>254</sub>) (Merck Art: 5554) and Silica gel 60 (Merck Art: 9385) were purchased from Merck NT Laboratory Suppliers (SA). Potato dextrose agar (PDA) was purchased from Laboratory and Scientific Chemical Company (SA).

### 3.2.2. General

Melting points are uncorrected and obtained from an Electrothermal IA 9000 digital melting point apparatus. Mass spectra were recorded on a Finnigan Mat GCQ low resolution mass spectrometer operating at an ionization potential of 70 eV. <sup>1</sup>H-NMR and <sup>13</sup>C-NMR spectra were obtained for solutions in deuteriochloroform (CDCl<sub>3</sub>) and recorded on a Varian Gemini 300 spectrometer (75 MHz). The spectra were referenced against the central line of the CDCl<sub>3</sub> singlet at  $\delta_H$  7.24 parts per million (ppm). A Buchi rotary evaporator was used to evaporate solvents *in vacuo*. A New Brunswick Scientific controlled environment incubator shaker and a Nuaire -85°C ultra low freezer were used.

### 3.2.3. Organism, Media and Culturing Technique

The fungus *A. versicolor* (M1101), obtained as a gift from Professor J.W. Bennett of the University of Tulane, was used. Using the normally accepted aseptic techniques, spores of the original culture were inoculated, by means of a bacteriological loop, on potato dextrose agar (15 ml) (Appendix 1, Page 234) in sterile disposable petri dishes. The cultures were incubated at 28°C for 5-7 days or until good sporulation had occurred. The culture was maintained on PDA for up to three months at 4°C.



A spore suspension was prepared in sterile sodium dodecyl sulphate solution (SDS) (0.01%) of approximately  $10^6$  spores per ml. The solution was left standing for 15 minutes and inoculated in fifteen Erlenmeyer flasks (250 ml) containing Reddy's medium<sup>67</sup> (100 ml) (Appendix 2, page 234). The flasks were plugged with cotton wool and incubated in the dark for 24 days at 30 °C as surface cultures.

#### 3.2.4. Extraction and Purification of Sterigmatocystin

The yellow-orange pigmented mycelia pellets from 15 flasks were collected separately on cheesecloth, by pouring the contents of the flask through the cloth, and were filtered *in vacuo*. Sterigmatocystin was extracted from the aqueous phase with chloroform and dried over anhydrous sodium sulphate. The solution was filtered and the chloroform evaporated *in vacuo* to yield a brown solid.

The solid mycelia were suspended in acetone (500 ml) and sonicated to break open the cells. The broken cell suspension was then gently heated at 45 °C for 5 hours to extract ST from the cells. The acetone was filtered, dried over anhydrous sodium sulphate, filtered and evaporated *in vacuo* to yield a yellow brown solid.

The solid pigments were combined and then purified by column chromatography on silica gel 60 using dichloromethane: hexane: ethyl acetate (4:1:1,v/v). The silica slurry was prepared in the eluting solvent and packed into a glass column (1.1 x 30 cm) and equilibrated with the solvent mentioned above. Fractions were monitored by t.l.c. (described below) and those containing ST were bulked, evaporated to dryness *in vacuo* and recrystallised from acetone to yield yellow needles (110 mg), m.p. 245-246 °C (Literature value<sup>134</sup> m.p. 246 °C).

#### 3.2.5. Characterisation by Thin Layer Chromatography

A sample of ST (0.20 mg) was redissolved in chloroform (100 µl) and a portion (20 µl) was spotted onto the origin of a t.l.c. plate (10 x 10 cm aluminium backed silica gel). The plate was developed in chloroform: ethyl acetate: isopropanol (CEI) (90: 5: 5, v/v) and

toluene: ethyl acetate: formic acid (TEF) (12: 6: 2, v/v), air dried and scanned for fluorescence under UV. The t.l.c. plates were then sprayed with aluminium chloride in ethanol (20 %, w/v), heated for 10 minutes at 110 °C and scanned for fluorescence under UV.

### **3.2.6. Characterisation of Sterigmatocystin by Spectroscopic Techniques**

The techniques which were used to characterise ST were :

- nuclear magnetic resonance spectroscopy viz.,  $^1\text{H}$ -NMR,  $^{13}\text{C}$ -NMR, correlated nuclear magnetic resonance spectroscopy (COSY), heteronuclear shift correlation nuclear magnetic resonance spectroscopy (HETCOR) and distortionless enhancement by polarization transfer spectroscopy (DEPT), and
- low resolution mass spectrometry.

### 3.3. RESULTS AND DISCUSSION

Sterigmatocystin production in the liquid medium was evident by t.l.c. (using CEI as the mobile phase) on the seventh day of incubation and aflatoxin metabolites were extracted on day 24 as recommended by Chatterjee and Townsend<sup>136</sup>. Pure crystalline ST was obtained by column chromatography separation and repeated recrystallisations. The yield of ST (7.3 mg/100 ml medium) was lower than the quantity (14 mg/100 ml medium) reported by Chatterjee and Townsend<sup>136</sup>. Since aflatoxin production depends on the carbon source contained in the culture medium<sup>71</sup>, one possible reason for the lower yield may be the different culture medium used in this study, viz., Reddy's medium against the Czapek medium used by Chatterjee and Townsend. Barnes *et al.*<sup>137</sup> reported a yield of 39.0, 1.4 and 12.0 (mg/g substrate) of ST on the three complex substrates: oats, rice and shredded wheat respectively. Also environmental factors such as aeration, length of incubation and illumination may also affect the production of ST.

Thin layer chromatographic analysis of the pure crystals showed the characteristic brick-red fluorescence of ST when viewed under UV ( $R_{f1}$  0.91;  $R_{f2}$  0.83). The fluorescence of ST changed to yellow when the t.l.c. plate was sprayed with the aluminium chloride spray reagent and heated for 10 minutes at 110 °C. The retardation factor ( $R_f$ ) was calculated by using the formula:

$$R_f = \frac{\text{distance between the baseline and the centre of the sample spot}}{\text{distance between the baseline and the solvent front}}$$

It was important to characterise the structure of ST by nuclear magnetic resonance spectroscopy, especially by <sup>1</sup>H-NMR as this was to be used as a tool for the characterisation of the synthesised derivatives (Chapter 4).

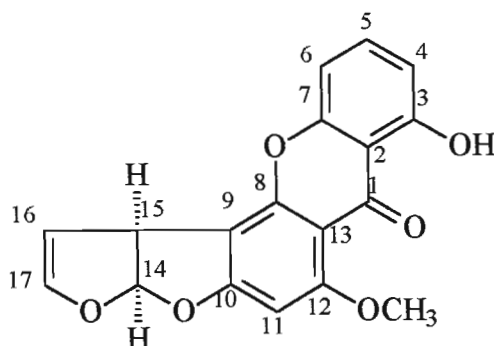


Figure 21. The Structure of Sterigmatocystin Showing the Numbering System.

The DEPT spectrum (Figure 22, Appendix 3, page 235) indicated the nine protonated carbons (1 x CH<sub>3</sub>, 8 x CH). The <sup>13</sup>C-NMR spectrum (Figure 23, Appendix 4, page 236) was analysed and the carbon atoms of ST were assigned (Table 2) according to Steyn and Maes<sup>138</sup>.

Table 2. Chemical Shift Values of ST Obtained from <sup>13</sup>C-NMR Spectrum.

Carbon atom	<sup>a</sup> Chemical shift in p.p.m.		Carbon atom	<sup>a</sup> Chemical shift in p.p.m.	
	Found	<sup>b</sup> Literature value		Found	<sup>b</sup> Literature value
1	181.3	181.1	10	164.6	164.5
2	108.9	108.8	11	90.5	90.4
3	162.3	162.2	12	163.3	163.2
4	111.2	111.1	13	106.0	105.9
5	135.7	135.5	14	113.2	113.2
6	105.9	105.8	15	48.6	48.0
7	155.0	154.8	16	102.5	102.4
8	154.0	153.9	17	145.4	145.3
9	106.5	106.5	OCH <sub>3</sub>	56.8	56.7

<sup>a</sup>Solvent CDCl<sub>3</sub>. <sup>b</sup>Literature value from Reference 113; 125.76 MHz <sup>13</sup>C-NMR data for ST.

The protons coupled to each carbon atom were determined by use of the HETCOR spectrum (Figure 24, Appendix 5, page 237) and coupled protons were determined by use

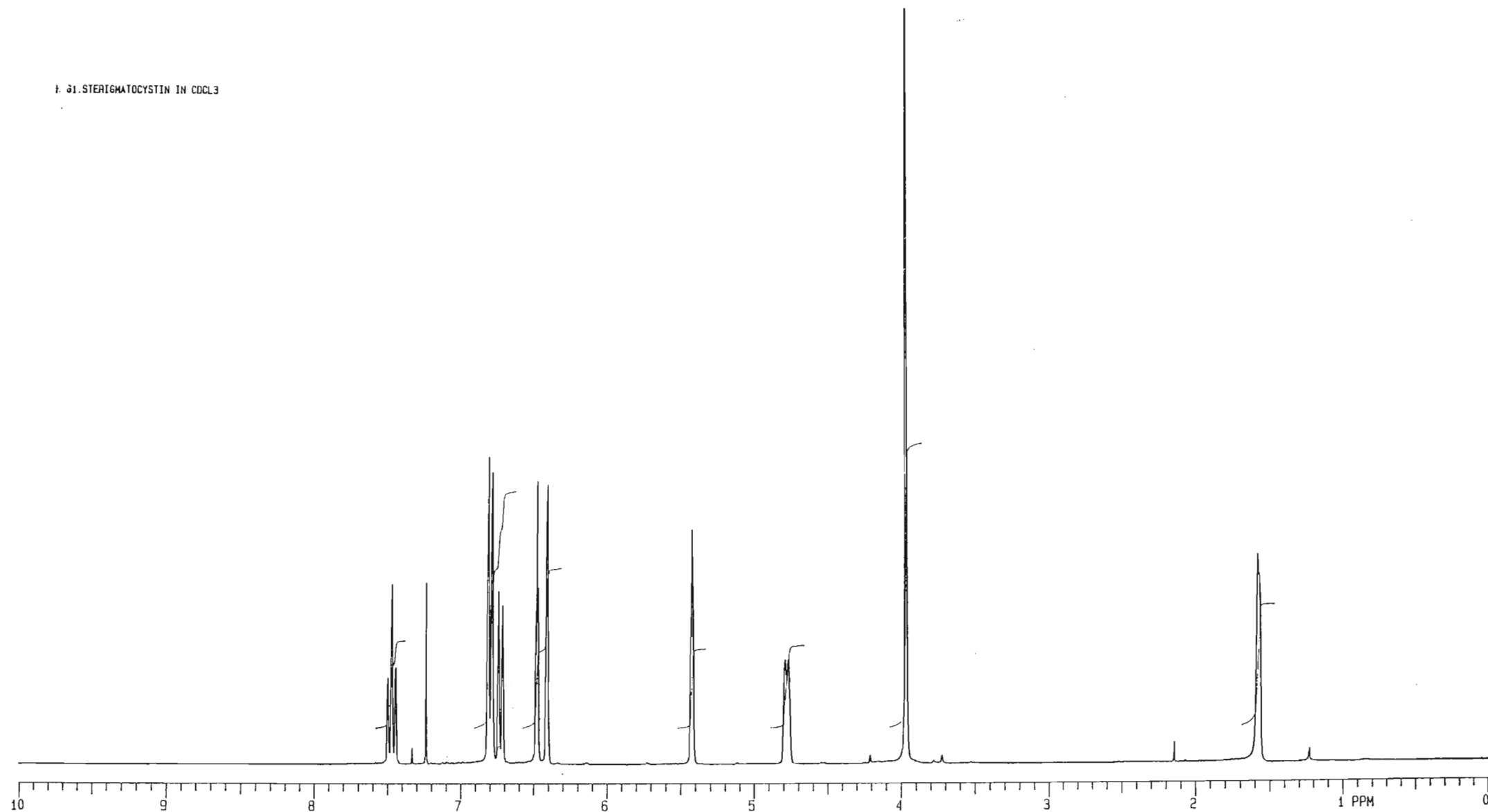
of the COSY spectrum (Figure 25, Appendix 6, page 238). Thus all the protons of ST, except the phenolic proton, were assigned. The  $^1\text{H}$ -NMR data of ST is presented in Table 3 and Figure 26 (page 43) presents the  $^1\text{H}$ -NMR spectrum. The chemical shift and splitting pattern of each proton were comparable to literature values<sup>30,136</sup>. The splitting pattern of those protons occurring at low fields were not clear and therefore the  $^1\text{H}$ -NMR spectrum was expanded and the splitting pattern determined (Figure 27, Appendix 7, page 239).

Table 3. The  $^1\text{H}$ -NMR Data of Sterigmatocystin (300 MHz).

Proton atom	$\delta_{\text{H}}$ <sup>a</sup>			Coupling constant $J(\text{H,H})$ Hz
	Found	<sup>b</sup> Literature	<sup>c</sup> Literature	
H-4	6.81d	6.74dd	6.72dd	7.3
H-5	7.48t	7.84t	7.47dd	8.3
H-6	6.73d	6.80dd	6.78dd	8.2
H-11	6.42s	6.42s	6.38s	-
H-14	6.81d	6.81d	6.80d	7.3
H-15	4.79dd	4.78dt	4.76ddd	-
H-16	5.43dd	5.44t	5.42dd	2.6
H-17	6.48t	6.50t	6.48dd	2.4
OCH <sub>3</sub>	3.97s	3.98s	3.97s	-

<sup>a</sup> $\delta_{\text{H}}$  in p.p.m.; solvent  $\text{CDCl}_3$ . <sup>b</sup>Literature value (100 MHz) from Reference 30. <sup>c</sup>Literature value (300 MHz) from Reference 136. Letters refer to the pattern resulting from one bond (C,H) couplings; s = singlet, d = doublet, t = triplet, dd = double doublet, dt = doublet of triplets, ddd = triple doublet.

1. 31. STERIGMATOCYSTIN IN CDCL<sub>3</sub>



43

Figure 26. The  $^1\text{H}$ -NMR Spectrum of Sterigmatocystin

Mass spectrometry was used to confirm the structure of ST. The normalised mass spectrum is presented in Figure 28. The molecular ion ( $M^+$  peak) is at  $m/z$  324 corresponding to a molecular formula  $C_{18}H_{12}O_6$ . Typical fragments<sup>139</sup> at  $m/z$  306 (loss of  $H_2O$ ) and 295 (loss of  $C_2H_5$ ) were identified.

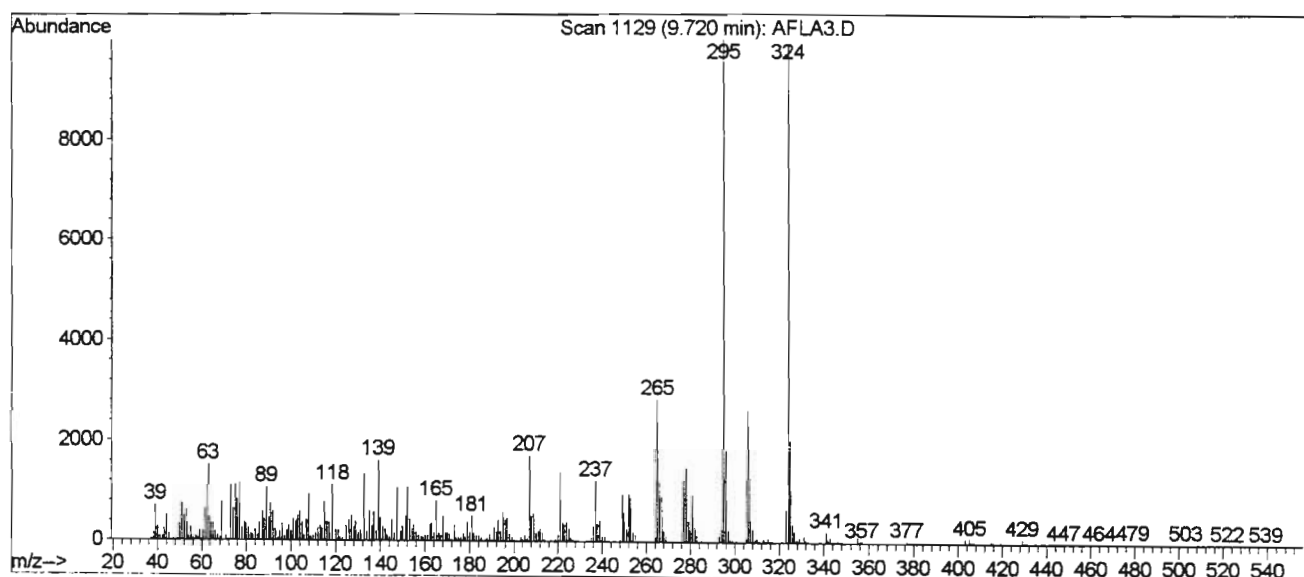


Figure 28. The Normalised Mass Spectrum of Sterigmatocystin Using Electron Impact Ionisation (70eV).



## CHAPTER FOUR

### SYNTHESIS AND CHARACTERISATION OF STERIGMATOCYSTIN DERIVATIVES

#### 4.1. INTRODUCTION

Numerous reports have been published showing the *in vivo* conversion of exogenously added OMST to AFB<sub>1</sub>. However, the question of the intermediacy of the metabolite OMST, i.e., whether it is a compulsory intermediate or one of a set of related substrates displaying enzyme specificity, has not been answered. Thus, in order to elucidate the final step in the AFB<sub>1</sub> biochemical pathway, viz., the conversion of ST to AFB<sub>1</sub> via OMST, ST derivatives had to be prepared. The structures of these compounds had to resemble OMST in order to mimic its *in vivo* conversion to AFB<sub>1</sub>. Therefore it was decided to transform the phenolic group of ST to other functional groups without changing any other part of the structure of ST.

One set of compounds of interest required the conversion of the phenolic group to ether-type compounds by a known chemical reaction, viz., the Williamson synthesis. In a typical Williamson reaction, the phenolic compound is treated with a base to produce a phenoxide ion which undergoes stabilization by resonance (Figure 29). Thus, in the presence of a primary or secondary alkyl halide, a S<sub>N</sub>2 type reaction occurs to form the ether, the product of *O*-alkylation.

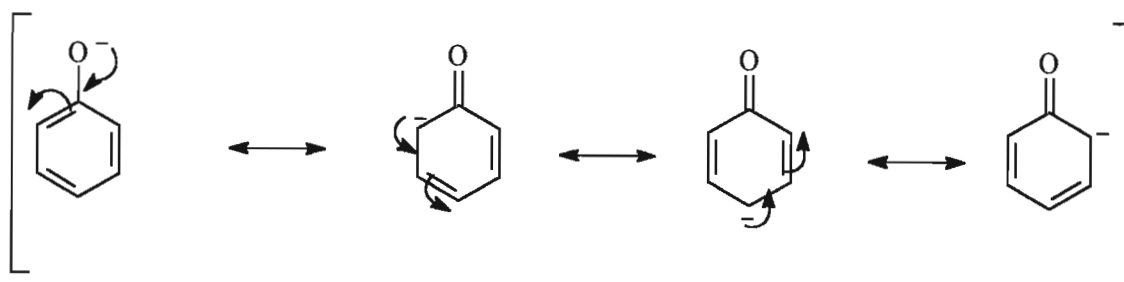


Figure 29. The Stabilization of a Typical Phenoxide Ion by Resonance.

With regards to reactions of ST, it was reported by Davies *et al.*<sup>134</sup> that hot ethanolic potassium hydroxide slowly converted ST into an optically inactive compound, isosterigmatocystin (1) (Figure 30). The structure of (1) was determined by Bullock<sup>140</sup>. Davies *et al.*<sup>134</sup> had to modify the Williamson synthesis by using a mild base, viz., sodium carbonate, in order to synthesise OMST from ST thereby preventing the formation of (1). Therefore in this investigation the method of Davies *et al.*<sup>134</sup> was used to synthesise ST alkyl ether derivatives.

Another set of compounds of interest required the transformation of the phenolic group of ST to the ester functional group. There are various methods available for the formation of an ester. One such method involves the use of an acid derivative, viz., acid chloride, which is very reactive towards a nucleophile. Thus, in the presence of a phenol, the chloride ion becomes a good leaving group resulting in the formation of an ester by a facile addition-elimination reaction.

With regards to ST, it was reported<sup>141</sup> that vigorous refluxing of ST in pyridine with acetic anhydride as reagent, resulted in acetic acid adding to the vinyl ether group to form a 'diacetate' of molecular formula  $C_{22}H_{18}O_9$ . The product could not be hydrogenated and was identified as acetoxymono-*O*-acetyldihydrosterigmatocystin (2) (Figure 30). For the synthesis of sterigmatocystin ester compounds, mild reaction conditions were necessary to avoid undesirable reactions at the fused bisfuran ring. Therefore in this investigation the method by Davies *et al.*<sup>134</sup> was used.

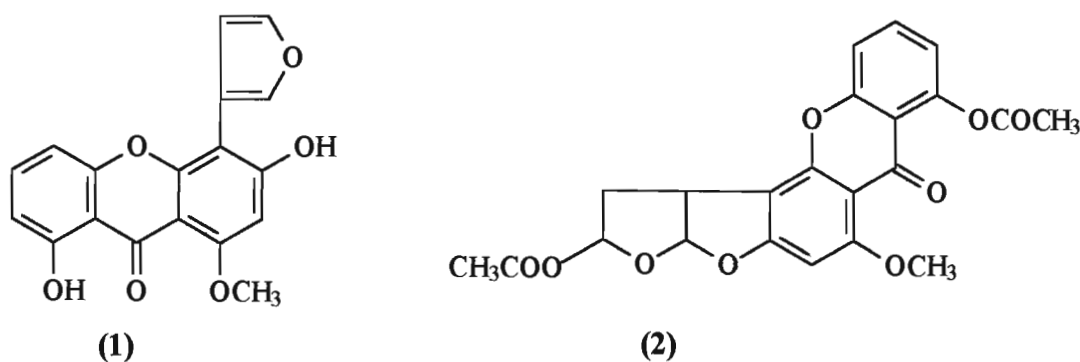


Figure 30. The Structure of Compounds Obtained from Sterigmatocystin.

## 4.2 MATERIALS AND METHODS

### 4.2.1. Chemicals

Analytical grade solvents were purchased from Sigma Chemical Suppliers (SA) and reagent grade solvents from Merck NT Laboratory Suppliers (SA). All other chemicals were purchased from Sigma Chemical Suppliers (SA). Sterigmatocystin was produced by *A. versicolor* (Chapter 3).

### 4.2.2. General

Melting points are uncorrected and obtained using an Electrothermal IA 9000 digital melting point apparatus. High resolution masses and mass spectra were recorded by Dr. P. Boschoff from Cape Technikon, on a Kratos 9/50 mass spectrometer. The MS spectra were recorded using a Hewlett Packard 518A low resolution mass spectrometer operating at an electron voltage of 70 eV. The  $^1\text{H}$ -NMR spectra were recorded in  $\text{CDCl}_3$  on a Varian Gemini 300 Spectrometer (300 MHz). The spectra were referenced against the central line of the deuteriochloroform singlet at  $\delta_{\text{H}}$  7.24 p.p.m. Mass measurements were made by means of a Mettler TG 50 Thermobalance.

Silica gel columns were prepared using silica gel 60 (Merck Art: 9385, particle size 0.04-0.063 mm), and the slurry was packed using the eluting solvents, hexane: dichloromethane: ethyl acetate (4:1:1, v/v). Silica gel (0.2 mm) containing fluorescent indicator (F<sub>254</sub>) on aluminium backed plates (Merck Art: 5554) was used for analytical t.l.c. using the solvent system CEI.

### 4.2.3. General Procedure for Alkylation of Sterigmatocystin<sup>134</sup>

To a solution of ST (10 mg; 30.9  $\mu\text{mol}$ ) in dry acetone (5 ml), was added anhydrous potassium carbonate (10.7 mg; 77.25  $\mu\text{mol}$ ) and the appropriate alkylhalide (100  $\mu\text{l}$ ). The mixture was then heated under reflux for 8 hours. The solids were removed by gravity filtration. The filtrate was dried over anhydrous sodium sulphate, filtered and evaporated

with a stream of nitrogen gas and gentle heat. The oil was neutralized with a solution of ammonia (2 ml of 12.5 %). The addition of deionised water yielded a flocculent precipitate which was filtered, washed and dried. This was purified by column chromatography and recrystallised from methanol.

The alkyl halides used to produce the five novel ST derivatives were: ethyl iodide, propyl iodide, butyl iodide, pentyl iodide and propenyl iodide.

#### **4.2.4. General Procedure for Esterification of Sterigmatocystin<sup>134</sup>**

To a solution of ST (10 mg; 30.9  $\mu\text{mol}$ ) in anhydrous pyridine (5 ml), was slowly added the acid chloride (100  $\mu\text{l}$ ). After the solution was left overnight at room temperature, more acid chloride (30  $\mu\text{l}$ ) was added and left to stand for a further 45 minutes at room temperature. The solution was heated under reflux for 15 minutes, poured onto ice (3 g) and left overnight. The product was extracted with chloroform (3 x 5 ml), washed with 2 M hydrochloric acid (3 x 5 ml) and then with deionised water (3 x 5 ml). Thereafter, evaporation of the chloroform yielded a brown oil which on the addition of ethanol, gave a crude product. This was purified by column chromatography and recrystallised from ethanol.

The acid chlorides used to produce the two ST derivatives were acetyl chloride and benzoyl chloride.

### 4.3. RESULTS AND DISCUSSION

The ST derivatives which were synthesised, and thus selected for further studies, were the simple ether and ester compounds obtained by replacing the phenolic proton of ST (Figure 31). The structure of these synthesised compounds **2b-2h** (Figure 32, page 51) were analogous to OMST.

For the preparation of ethers, sodium carbonate was used as the weak base in a modified Williamson type synthesis. For the preparation of esters, acid chlorides were used and the reaction conducted at room temperature. The reagents which were used in the synthesis and the physical properties of the ST derivatives are presented in Table 4 (page 50).

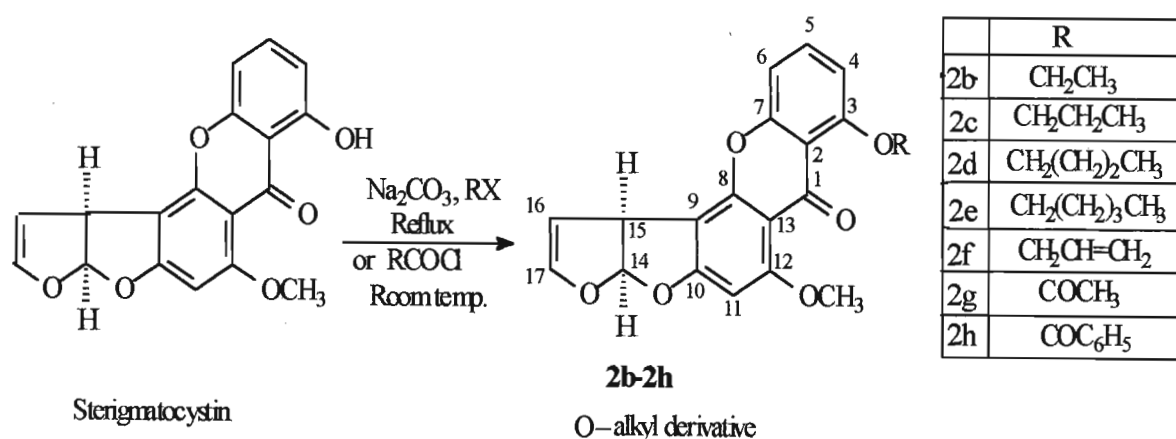


Figure 31. The Reaction Scheme for the Synthesis of Sterigmatocystin Derivatives.

Table 4. The Physical Properties of Sterigmatocystin Derivatives Obtained by Using Aliphatic Iodides and Acid Chlorides as Reagents.

Reagent	Product	<sup>a</sup> Yield (%)	<sup>b</sup> Physical appearance	<sup>c</sup> R <sub>f</sub> value	Melting point (° C)
CH <sub>3</sub> CH <sub>2</sub> I	2b	80	yellow	0.87	253-255
CH <sub>3</sub> CH <sub>2</sub> CH <sub>2</sub> I	2c	84	yellow	0.79	213-215
CH <sub>3</sub> (CH <sub>2</sub> ) <sub>2</sub> CH <sub>2</sub> I	2d	72	pale yellow	0.73	180-182
CH <sub>3</sub> (CH <sub>2</sub> ) <sub>3</sub> CH <sub>2</sub> I	2e	67	pale yellow	0.69	152-154
CH <sub>3</sub> CH=CHI	2f	70	light brown	0.68	204-206
CH <sub>3</sub> COCl	2g	74	colourless	0.63	<sup>d</sup> 139-140
PhCOCl	2h	69	colourless	0.55	<sup>e</sup> 257-259

<sup>a</sup>Yield of pure, isolated product based on ST. <sup>b</sup>Colour of crystalline product. <sup>c</sup>Solvent system CEI.

<sup>d</sup>Literature value<sup>142</sup> m.p. 140 °C. <sup>e</sup>Literature value<sup>134</sup> m.p. 258-260 °C.

To characterise the ST derivatives, <sup>1</sup>H-NMR was selected as the main spectroscopic technique. To accomplish this the <sup>1</sup>H-NMR spectra of the synthesised compounds (**2b-2h**) were compared with that of ST, the protons of which were assigned in Chapter 3 (Table 3, page 42). The identity of the compounds was further confirmed by high resolution mass spectrometry. It must be noted that less than eight milligram quantities of each of the compounds was isolated and purified, and were subsequently used for enzymatic reactions. The synthesis and purification of the new compounds was difficult considering the fact that only 10 mg quantities of ST were used as the substrate. This situation arose due to the difficulty of producing ST (Chapter 3) in sufficient quantity for its use as a substrate.

Each of the nine protons that were assigned for ST (Table 3, page 42) was identified in the ST derivatives (**2b-2h**). The remaining protons for each compound were assigned by examining the splitting patterns, chemical shifts and coupling constants.

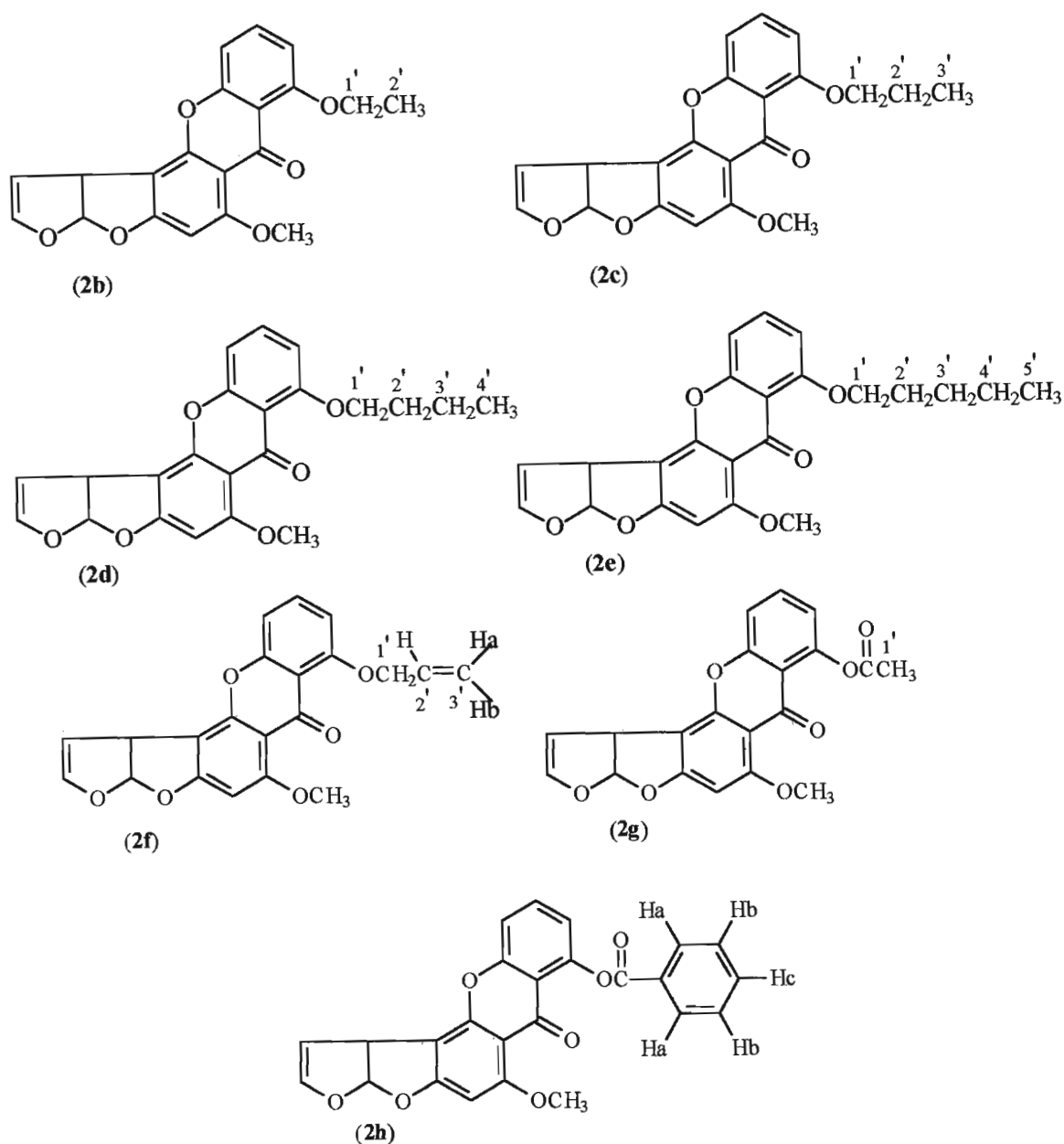


Figure 32. The Structure of Sterigmatocystin Derivatives (2b-2h).

• Compound **2b** (*O*-ethyl sterigmatocystin) (OEST):

The <sup>1</sup>H-NMR data for **2b** are presented in Table 5 (Appendix 8, page 240). The <sup>1</sup>H-NMR spectrum is presented in Figure 33 (Appendix 9, page 241) and the expanded proton spectrum in Figure 34 (Appendix 10, page 242). The two H-1' protons appear as a quartet at  $\delta_H$  4.16 ( $J$  7.0 Hz) whilst the three H-2' protons appear as a triplet at  $\delta_H$  1.53 ( $J$  7.1 Hz). High resolution mass spectrometry showed a molecular ion peak [M<sup>+</sup>] at  $m/z$  352.0973 (C<sub>20</sub>H<sub>16</sub>O<sub>6</sub> requires 352.0946). The low resolution mass spectrum is



presented in Figure 35 (Appendix 11, page 243). The fragment at  $m/z$  337 is due to  $[M-CH_3]^+$  and the fragment at  $m/z$  323 is due to  $[M-CH_2CH_3]^+$ . The fragment at  $m/z$  295 is due to  $[ST-CH_2CH_3]^+$ .

- Compound **2c** (*O*-propyl sterigmatocystin) (OPROST):

The  $^1H$ -NMR data of **2c** are presented in Table 6 (Appendix 12, page 244). The  $^1H$ -NMR spectrum is presented in Figure 36 (Appendix 13, page 245) and the expanded proton spectrum in Figure 37 (Appendix 14, page 246). The two H-1' protons appear as a triplet at  $\delta_H$  4.04 ( $J$  6.6 Hz) and the two H-2' protons appear as a sextet at  $\delta_H$  1.95 ( $J$  6.8 Hz). The remaining three protons appear as a triplet at  $\delta_H$  1.10 ( $J$  7.3 Hz). High resolution mass spectrometry showed a molecular ion peak  $[M]^+$  at  $m/z$  366.1100 ( $C_{21}H_{18}O_6$  requires 366.1107). The low resolution mass spectrum is presented in Figure 38 (Appendix 15, page 247). The fragment at  $m/z$  337 is due to  $[M-CH_2CH_3]^+$  and the fragment at  $m/z$  323 is due to  $[M-CH_2CH_2CH_3]^+$ .

- Compound **2d** (*O*-butyl sterigmatocystin) (OBUST):

The  $^1H$ -NMR data of **2d** are presented in Table 7 (page 54). The  $^1H$ -NMR spectrum is presented in Figure 39 (page 55) and the expanded proton spectrum in Figure 40 (Appendix 16, page 248). The two H-1' protons appear as a triplet at  $\delta_H$  4.08 ( $J$  6.6 Hz). The two H-2' protons and the two H-3' protons appear as multiplets at  $\delta_H$  1.89 and  $\delta_H$  1.57, respectively. The remaining three protons appears as a triplet at  $\delta_H$  0.97 ( $J$  7.3 Hz). High resolution mass spectrometry showed a molecular ion peak  $[M]^+$  at  $m/z$  380.1253 ( $C_{22}H_{20}O_6$  requires 380.1260). The low resolution mass spectrum is presented in Figure 41 (page 56). The fragment at  $m/z$  351 is due to  $[M-CH_2CH_3]^+$  and the fragment at  $m/z$  337 is due to  $[M-CH_2CH_2CH_3]^+$ . The fragment at  $m/z$  323 is due to  $[M-CH_2CH_2CH_2CH_3]^+$ .

- Compound **2e** (*O*-pentyl sterigmatocystin) (OPEST):

The  $^1H$ -NMR data of **2e** are presented in Table 8 (Appendix 17, page 249). The  $^1H$ -NMR spectrum is presented in Figure 42 (Appendix 18, page 250) and the expanded proton

spectrum in Figure 43 (Appendix 19, page 251). The two H-1' protons appear as a triplet at  $\delta_{\text{H}}$  4.07 ( $J$  6.8 Hz). The H-2', H-3' and H-4' protons appear as multiplets at  $\delta_{\text{H}}$  1.92,  $\delta_{\text{H}}$  1.49 and  $\delta_{\text{H}}$  1.39, respectively. The H-5' protons appear as a triplet at  $\delta_{\text{H}}$  0.92 ( $J$  7.3 Hz). High resolution mass spectrometry showed a molecular ion peak  $[\text{M}^+]$  at  $m/z$  394.1427 ( $\text{C}_{23}\text{H}_{22}\text{O}_6$  requires 394.1416). The low resolution mass spectrum is presented in Figure 44 (Appendix 20, page 252). The fragment at  $m/z$  365 is due to  $[\text{M}-\text{CH}_2\text{CH}_3]^+$  and the fragment at  $m/z$  351 is due to  $[\text{M}-\text{CH}_2\text{CH}_2\text{CH}_3]^+$ . The fragment at  $m/z$  323 is due to  $[\text{M}-\text{CH}_2\text{CH}_2\text{CH}_2\text{CH}_2\text{CH}_3]^+$ .

- Compound **2f** (*O*-propenyl sterigmatocystin) (OPREST):

The  $^1\text{H}$ -NMR data of **2f** are presented in Table 9 (Appendix 21, page 253). The  $^1\text{H}$ -NMR spectrum is presented in Figure 45 (Appendix 22, page 254) and the expanded proton spectrum in Figure 46 (Appendix 23, page 255). The two H-1' protons appear as a doublet of triplet at  $\delta_{\text{H}}$  4.70 ( $J$  4.9 Hz; 5.25 Hz). The single H-2' proton appear as a multiplet at  $\delta_{\text{H}}$  6.09. The single H-3'a proton appear as a double doublet at  $\delta_{\text{H}}$  5.60 ( $J$  15.57 Hz; 1.59 Hz). The single H-3'b proton appear as a double doublet at  $\delta_{\text{H}}$  5.30 ( $J$  9.21 Hz; 1.47 Hz). High resolution mass spectrometry showed a molecular ion peak  $[\text{M}^+]$  at  $m/z$  364.0939 ( $\text{C}_{21}\text{H}_{16}\text{O}_6$  requires 364.0947). The low resolution mass spectrum is presented in Figure 47 (Appendix 24, page 256). The fragment at  $m/z$  349 is due to  $[\text{M}-\text{CH}_3]^+$ .

- Compound **2g** (*O*-acetyl sterigmatocystin) (OAcST):

The  $^1\text{H}$ -NMR data of **2g** are presented in Table 10 (Appendix 25, page 257). The  $^1\text{H}$ -NMR spectrum is presented in Figure 48 (Appendix 26, page 258). The three H-1' protons appear as a singlet at  $\delta_{\text{H}}$  2.46. High resolution mass spectrometry showed a molecular ion peak  $[\text{M}^+]$  at  $m/z$  366.0736 ( $\text{C}_{20}\text{H}_{14}\text{O}_6$  requires 366.0739). The low resolution mass spectrum is presented in Figure 49 (Appendix 27, page 259). The fragment at  $m/z$  324 is due to  $[\text{M}-\text{COCH}_2]^+$ . The fragment at  $m/z$  306 is due to  $[\text{M}-\text{CH}_3\text{COOH}]^+$ .

• Compound **2h** (*O*-benzoyl sterigmatocystin) (OBzST):

The  $^1\text{H}$ -NMR data of **2h** are presented in Table 11 (Appendix 28, page 260). The  $^1\text{H}$ -NMR spectrum is presented in Figure 50 (Appendix 29, page 261) and the expanded proton spectrum in Figure 51 (Appendix 30, page 262). The two Ha protons appear as a doublet at  $\delta_{\text{H}}$  8.27 ( $J$  7.2 Hz). The two Hb and single Hc protons appear as multiplets and could not be easily assigned from the  $^1\text{H}$ -NMR spectra. High resolution mass spectrometry showed a molecular ion peak  $[\text{M}^+]$  at  $m/z$  428.0891 ( $\text{C}_{25}\text{H}_{16}\text{O}_6$  requires 428.0895). The low resolution mass spectrum is presented in Figure 52 (Appendix 31, page 263). The fragment at  $m/z$  323 is due to  $[\text{M}-\text{COC}_6\text{H}_5]^+$ .

The  $^1\text{H}$ -NMR data of a typical ST derivative, viz., OBUST is presented in Table 7. The  $^1\text{H}$ -NMR spectrum of OBUST is presented in Figure 39 (page 55). The normalized mass spectrum, showing the fragmentation pattern, is presented in Figure 41 (page 56).

Table 7. The  $^1\text{H}$ -NMR Data of OBUST.

Proton atom	Chemical Shift $\delta_{\text{H}}$ (p.p.m.)	Splitting Pattern	Coupling constant $J(\text{H,H})$ Hz
H-4	6.90	doublet	7.9
H-5	7.45	triplet	8.3
H-6	6.73	doublet	8.2
H-11	6.37	singlet	-
H-14	6.70	doublet	7.1
H-15	4.77	double doublet	2.8, 2.1
H-16	5.42	double doublet	2.6, 2.5
H-17	6.47	triplet	4.2
$\text{OCH}_3$	3.97	singlet	-
H-1'	4.08	triplet	6.6
H-2'	1.89	multiplet	
H-3'	1.57	multiplet	
H-4'	0.97	triplet	7.3

R6BUST-2 IN CDCL<sub>3</sub>

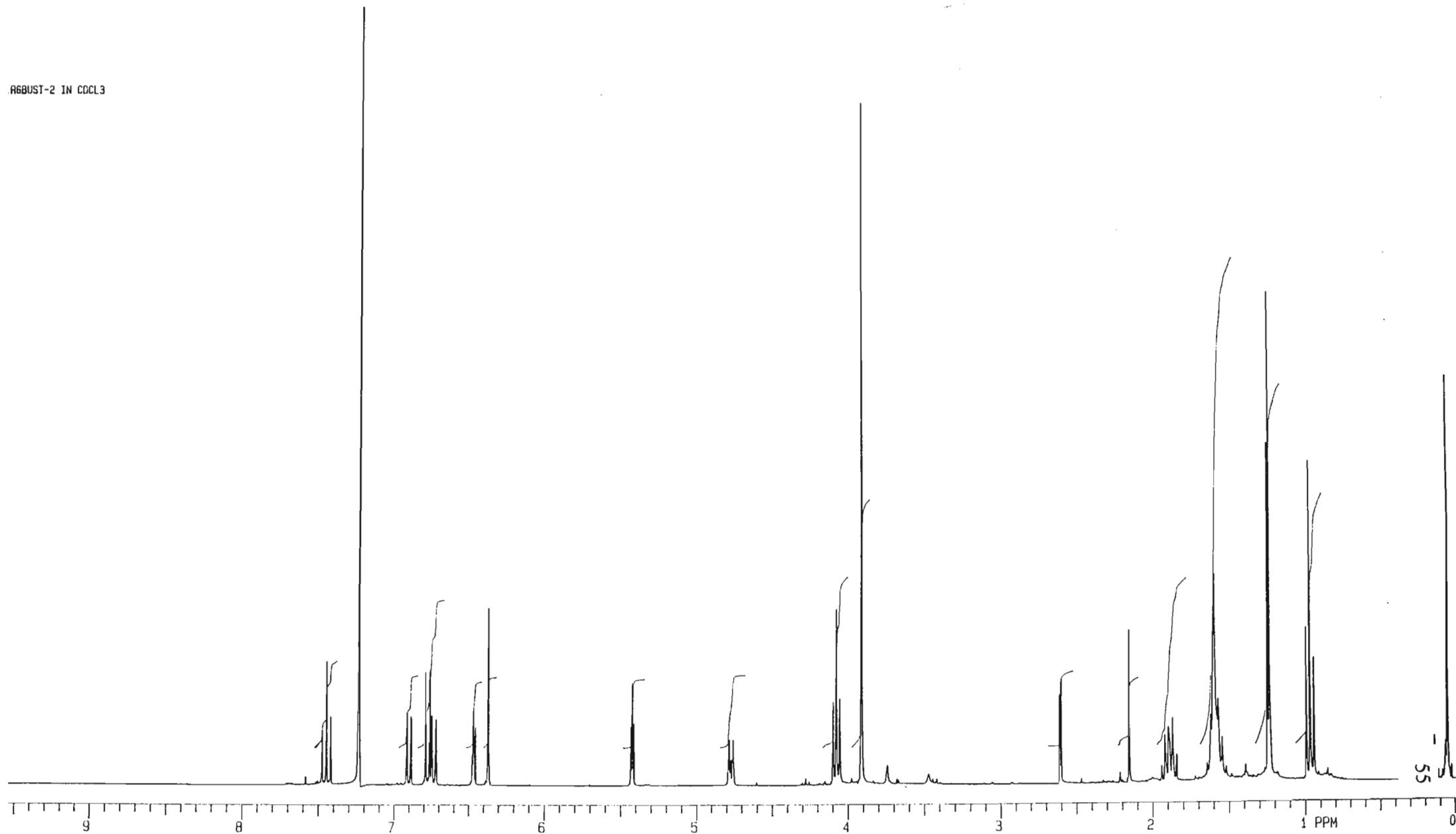


Figure 39. The <sup>1</sup>H-NMR Spectrum of *O*-Butyl sterigmatocystin

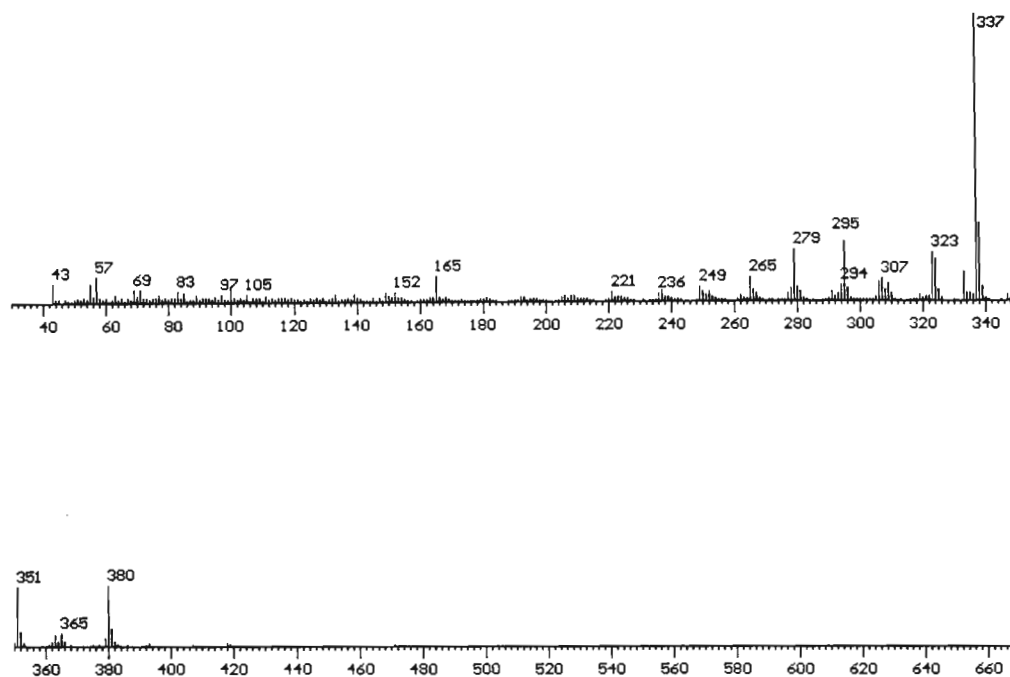


Figure 41. The Normalized Mass Spectrum of *O*-Butyl sterigmatocystin.

Thus seven alkyl/aryl derivatives of sterigmatocystin were synthesised by reacting the phenolic group of ST with alkyl halides or acid chlorides using mild reaction conditions. These derivatives were characterised by  $^1\text{H}$ -NMR and MS.

## CHAPTER FIVE

### DEVELOPMENT OF METHODS FOR HIGH PRESSURE LIQUID CHROMATOGRAPHY

#### 5.1. INTRODUCTION

Chromatography is a separation method which is used to resolve individual components from a mixture. This process involves the selective distribution of components between two heterogeneous (immiscible) phases, viz., the stationary phase and mobile phase. The stationary phase is a dispersed medium, which usually has a relatively large surface area, through which the mobile phase is allowed to flow. The mobile phase can be either a gas or liquid. The techniques gas chromatography and liquid chromatography therefore indicate the type of mobile phase which is used in the separation process.

All chromatographic separations are based upon the differences in the extent to which components (solutes) are partitioned between the mobile phase and the stationary phase. This equilibrium process is quantitatively described by means of a partition coefficient  $K_i$ , for each solute in the sample as:

$$K_i = \frac{C_{i,s}}{C_{i,m}}$$

where  $C_{i,s}$  is the concentration of solute in the stationary phase and  $C_{i,m}$  is the concentration of solute in the mobile phase.

The distribution of each solute between the stationary phase and mobile phase is described by the capacity factor ( $k'$ )

$$k' = \frac{x_{i,s}}{x_{i,m}} = K_i \left( V_s / V_m \right) = \frac{K_i}{\beta}$$

where  $x$  represents the masses of components in each phase,  $V_s$  and  $V_m$  are the volumes of the stationary phase and mobile phases, respectively, and  $\beta$  is the phase ratio of the column.

A typical chromatogram and its characteristic features is presented in Figure 53 .

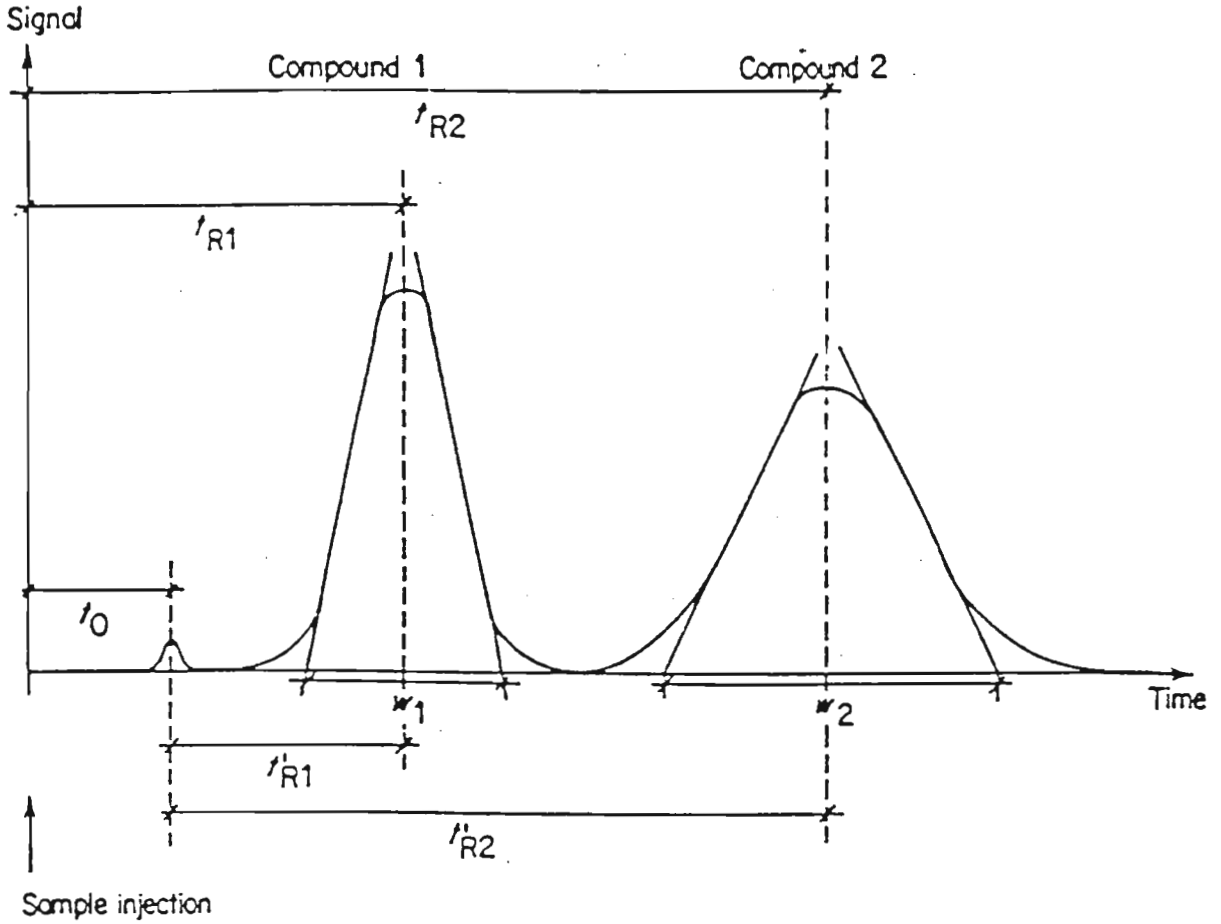


Figure 53. A Chromatogram with its Characteristic Features.

The time required by the mobile phase to pass through the column is the dead time or retention time of an unretained solute and is denoted by  $t_o$ . The peak width at the baseline is  $w$ . The average linear flow velocity,  $u$  can be calculated as

$$u = \frac{L}{t_o}$$

where  $L$  is the column length. The retention time  $t_r$  is the period between sample injection



and recording of the peak maximum while  $t_r$  is the net retention time. The retention time of a solute is a function of mobile phase flow velocity and column length. Two components are separated if they have different retention times.

The capacity factor, which is a measure of retention of sample components, can be used to characterise a component and this is expressed as:

$$k' = \frac{t_r - t_o}{t_o}$$

The ease of separating two different components on a column is expressed as selectivity,  $\alpha$

$$\alpha = \frac{k'_2}{k'_1}$$

where  $k'_1$  and  $k'_2$  are the capacity factors of each component and  $k'_2$  is the capacity factor of the later eluting component. The capacity factor can be conceptualised as spacing between peak maxima. A large  $\alpha$  indicates that the components are separated and as  $\alpha$  approaches unity, the peaks fuse.

The resolution between two components describes the magnitude of separation and is expressed as:

$$R = \frac{2(t_2 - t_1)}{(w_{b1} + w_{b2})}$$

High pressure liquid chromatography (HPLC) is a versatile technique which may use any one of the principles of adsorption, partition, ion-exchange, exclusion or affinity chromatography. The only requirement is that the sample components to be separated must be soluble in some solvent, and that components differ from each other in some clearly defined way, e.g., polarity, charge, size, etc. In general, components are detected by their absorption of light in either the visible or ultra-violet region, but HPLC detectors are also available to measure fluorescence, radioactivity, electrochemical potential or refractive index. High pressure liquid chromatography has advantages over traditional low-pressure ("open column") liquid chromatography in improved speed, resolution, sensitivity and

reproducibility. These advantages together with improved instrument automation have been responsible for the emergence of HPLC as the most widely used chromatographic technique in modern biochemistry.

With regard to the analysis of aflatoxin metabolites, found in agricultural products in trace quantities, traditional methods use t.l.c. procedures. Thin layer chromatography has been used as a rapid screening method for toxic compounds. The disadvantages of this approach are:

- the lack of quantitative precision<sup>143</sup>;
- the photochemical decomposition of aflatoxins<sup>144,145</sup>
- health hazards due to harmful vapours in the air<sup>146</sup> and
- the day to day variation in the resolution of aflatoxins on the t.l.c. plate<sup>147</sup>.

High performance liquid chromatography techniques have been developed and subsequently employed for routine use since it has achieved better accuracy, sensitivity, and reliability. In addition, it completely eliminates aflatoxin exposure to air and light and thus minimises degradation.

Numerous reports have been published<sup>148-153</sup> discussing HPLC parameters and conditions for aflatoxin analysis by normal phase techniques. Detection of aflatoxins was achieved with UV absorption at 365 nm, however, some attempts in completely resolving a mixture of AFB<sub>1</sub>, AFB<sub>2</sub>, AFG<sub>1</sub> and AFG<sub>2</sub> were not successful. In addition, only a few reports on aflatoxin levels less than 20 parts per billion (p.p.b.), in food extracts, were actually tested. Also, sample extracts often produce background interference in the UV detection at low contamination levels. This seriously limits the sensitivity of the technique and necessitates further rigorous sample clean-up. Usually, normal phase HPLC systems make use of a silica gel adsorption packing material and a water-saturated organic solvent as a component for the mobile phase. Reproducibility<sup>147,152</sup> in the separation of the four aflatoxins by this approach has proven difficult due to the inability to maintain saturated conditions which are temperature dependant.

In reversed phase HPLC, which commonly uses C<sub>18</sub> columns, water is used as the primary

solvent. Thus, variations caused by the non-uniformity in the normal phase HPLC due to a water saturated solvent is avoided. However, in aqueous solvents the fluorescence of AFB<sub>1</sub> and AFG<sub>1</sub> species is diminished, and derivatisation procedures are therefore required for these compounds.

Pre-column derivatisation using trifluoroacetic acid (TFA) is simple<sup>154</sup> and efficient since the reaction occurs within a few minutes at room temperature. In this reaction the conversion of the non-fluorescent AFB<sub>1</sub> (1) and AFG<sub>1</sub> (3) to the highly fluorescent AFB<sub>2a</sub> (2) and AFG<sub>2a</sub> (4) (Figure 54) increases the sensitivity at picogram levels for quantitative analysis. Although the retention of the compounds in reversed phase systems changes by the derivatisation, generally the required adaptation of the chromatographic conditions is negligible. An important advantage of this method of derivatisation is that it provides immediate structural confirmation of AFB<sub>1</sub> and AFG<sub>1</sub> without going through an independent additional analysis. In addition, sample background components, seen in the UV adsorption mode, do not fluoresce under the reversed phase conditions<sup>149</sup>. A disadvantage of the TFA method is that it is specific to the quantification of AFB<sub>1</sub> and AFB<sub>2</sub>. Thus other metabolites of the aflatoxin pathway are not detected since they are not suited for derivatisation.

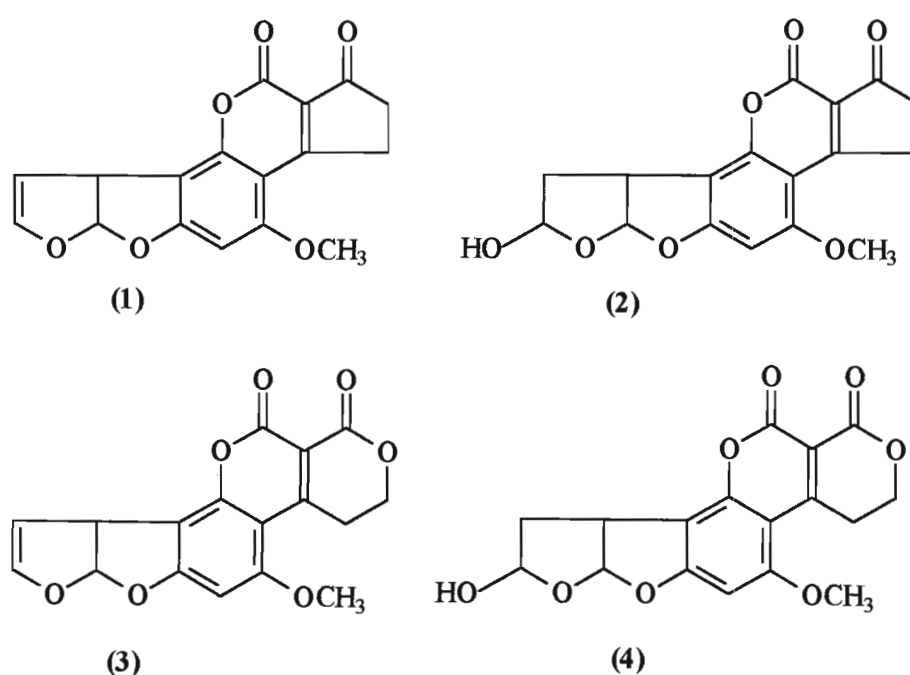


Figure 54. Structures of the Aflatoxins<sup>23</sup> and Derivatives Produced by TFA.

Typical chromatograms<sup>149</sup> of a mixture of standard aflatoxins is presented in Figure 55. These chromatograms shows the order of elution of the derivatised and underivatised metabolites, in increasing retention times, as:

$$\text{AFG}_{2a} < \text{AFB}_{2a} < \text{AFG}_2 < \text{AFB}_2$$

which therefore indicates that the order of elution of the underivatised metabolites as:

$$\text{AFG}_1 < \text{AFB}_1 < \text{AFG}_2 < \text{AFB}_2$$

Chromatograms A and B indicates the increase in sensitivity that is obtained by converting  $\text{AFB}_1$  and  $\text{AFG}_1$  to  $\text{AFB}_{2a}$  and  $\text{AFG}_{2a}$ , respectively. Chromatograms B and C indicates the increase in the quantity of  $\text{AFB}_{2a}$  and  $\text{AFG}_{2a}$  when the reaction with TFA is left for a longer time.

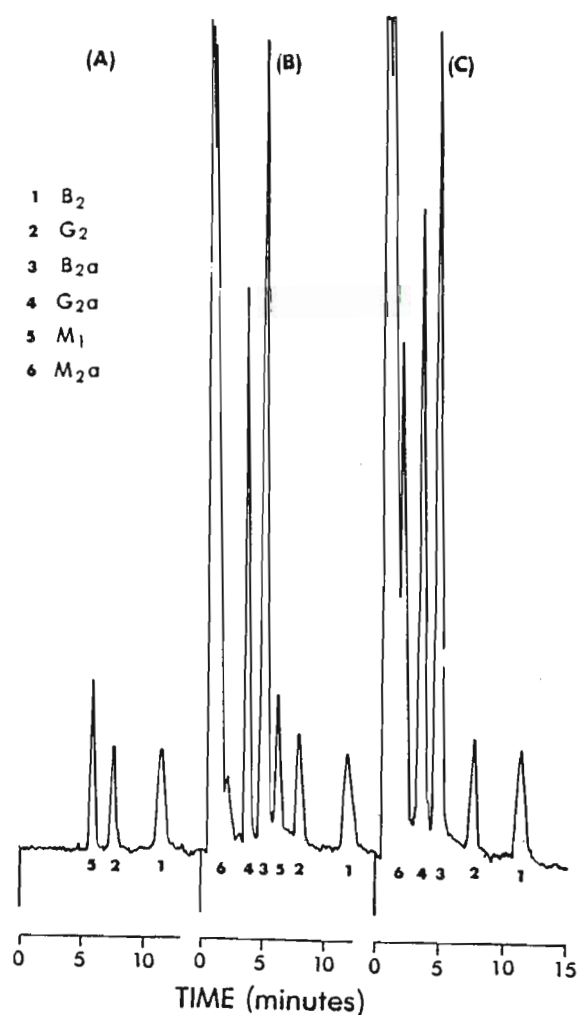


Figure 55. Isocratic Reversed Phase Chromatograms of Standard Aflatoxins. (A) Untreated with TFA. (B) Treated with TFA for 1 Minute and Dilution with the Mobile Phase. (C) Treated with TFA for 20 Minutes and Dilution with the Mobile Phase.

One of the aims of the project was to quantitatively monitor the *in vivo* conversion of ST and selected synthesised derivatives (synthesis is described in Chapter 4) to AFB<sub>1</sub>. Although the separation of aflatoxins by HPLC is relatively simple and well defined, optimisation of the separation and detection conditions was important in order to minimise requirements for sample clean-up. The pre-column derivatisation method, using TFA, was the method of choice in the absence of post-column instrumentation. Hence, the fluorescence detector was selected for part of the study, viz., whole cell reactions (Chapter 6). Subsequently, with the purchase of a new diode array detector (Spectra SYSTEM UV6000LP), another HPLC method was developed and was used in the study of cell-free and whole cell reactions (Chapters 7, 8 and 9).

The use of a diode array detector is suitable when quantification of different metabolic substrates is required. An advantage of this technique is that a single chromatographic run is able to provide a spectrum which can be analysed at several wavelengths simultaneously<sup>155</sup>.

The optical system of the Spectra SYSTEM UV6000LP detector is presented in Figure 56.

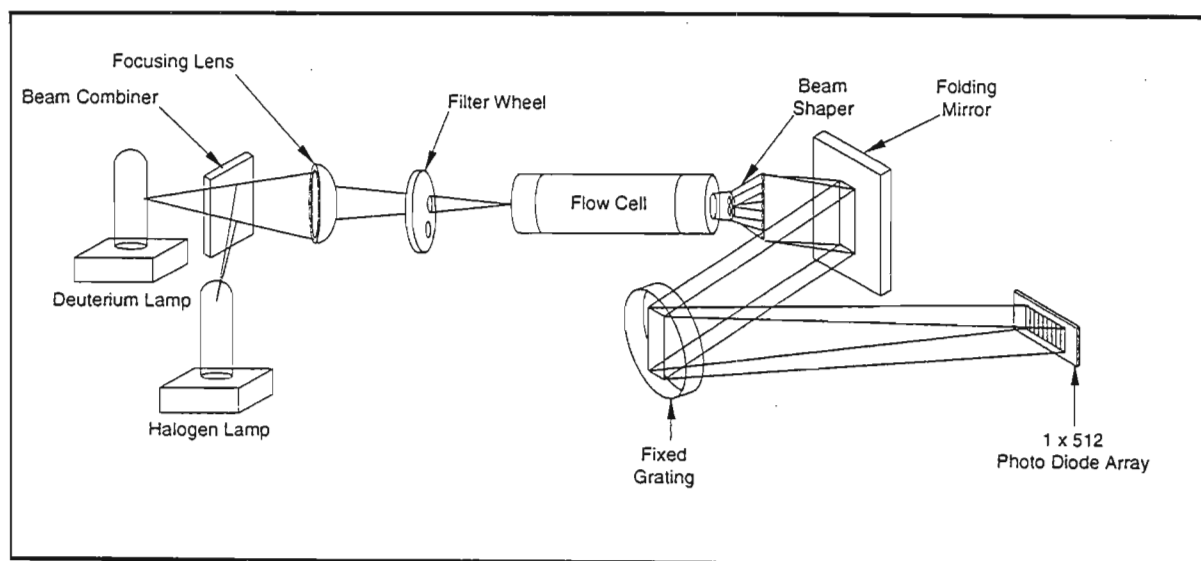


Figure 56. The UV6000LP Optical System.

The dual-light source included a deuterium lamp for detection in the ultra-violet wavelength range (190-350 nm) and a tungsten-halogen lamp for detection in the visible wavelength range (350-800 nm). The optical bench consisted of a beam combiner, focusing lens, filter wheel, flow-cell, beam shaper, folding mirror and grating. The function of the beam combiner is to reflect the light coming from the tungsten-halogen lamp so that it is parallel to and coincident with the light from the deuterium lamp. The combined beam is then focused on the inlet window of the flow-cell through the filter wheel. The light focused on the inlet window of the flow-cell travels down the cell, is partially absorbed by the sample flowing through the cell, and exits into the beam shaper. The beam shaper transfers the light to the grater for greater light throughput than the mechanical slit used in conventional photo-diode array detectors. The spectrum from the grating is focused on the 512 element photo-diode array. The diode array is continuously scanned at a rate of 20 hertz and the light intensity at each diode is converted to a 20-bit digital word and stored in a dual-port random access memory on the CPU PCBA.

The Spectra SYSTEM UV6000LP detector, used in this study, is unique in that it contains a LightPipe flow-cell (50 mm length) optical path which is five times the normal industry standard length (10 mm). Also the interior surface of the cell is lined with a chemically inert coating which has a refractive index lower than that for HPLC mobile phases thereby allowing the transmitted light to be channelled through the flow-cell. In addition any divergent light is redirected back into the flow-cell bore so that no light is absorbed by the flow-cell's interior. Thus with the new technological LightPipe detection, the UV6000LP detector is able to deliver a 400 % increase in sensitivity over other photo-diode array detectors (Saunders, M., Analytical Reporter Issue No.1/1998 page 20). While the longer flow-cell path length enhances the signal, the negligible loss of light reduces noise thereby resulting in a higher signal-to-noise ratio.

## **5.2. MATERIALS AND METHODS**

### **5.2.1. Chromatographic Equipment**

High pressure liquid chromatography was performed on the following two instruments:

- A Perkin Elmer Liquid Chromatograph, with a 20  $\mu$ l injection loop, equipped with a Perkin Elmer Binary LC pump and linked to a Hewlett Packard Programmable fluorescence detector and a Hewlett Packard Desk-jet 600 printer were used.

A stainless steel (150 mm x 4.60 mm) column packed with 5  $\mu$ m particle C<sub>18</sub>-bonded Silica reverse phase was used. The fluorescence excitation and emission wavelengths were set at 325 and 420 nm, respectively.

- A Spectra Physics UV 6000 LP System, with a 20  $\mu$ l injection loop, linked to a diode array detector and a Hewlett Packard desk-jet 600 C printer were used. The chromatography columns, investigated on this system were:

- C<sub>18</sub> Prodigy (150 x 4.60 mm), 5  $\mu$ m, spherical
- C<sub>18</sub> Lichrosphere (250 x 4.60 mm), 5  $\mu$ m, spherical

### **5.2.2. Chemicals and Reagents**

All analytical grade solvents were used for HPLC and purchased from Sigma Chemical Suppliers (SA). Trifluoroacetic acid, OMST, AFB<sub>1</sub>, AFB<sub>2</sub>, AFG<sub>1</sub>, and AFG<sub>2</sub> were purchased from Sigma Chemical Suppliers (SA). Disposable micro-pipette tips were purchased from Polychem Chemical Co.(SA). Deionised water and HPLC grade water were provided by a Milli-Q-Reagent Grade Water System (Millipore SA). Millipore 0.45  $\mu$ m membrane filters were purchased from Millipore SA.

### **5.2.3. Preparation of Standard Solutions**

For the fluorescence detector, a stock solution of 0.3  $\mu$ g/ml AFB<sub>1</sub> was prepared in a 10 ml volumetric flask. A 333.3  $\mu$ l aliquot was transferred, by means of a micro-pipette, to a 10 ml volumetric flask and evaporated to dryness under a gentle stream of N<sub>2</sub>. Trifluoroacetic acid (100  $\mu$ l) was added, shaken briefly and allowed to stand for 5 minutes. The solution

was diluted with acetonitrile to yield a 10 p.p.b. AFB<sub>2a</sub> solution. Similarly, standard solutions of AFB<sub>2a</sub> were prepared in the range 20-1000 p.p.b.

For the diode array detector, standard solutions of AFB<sub>1</sub> were prepared in the range 20-5000 p.p.b. by serial dilution with acetonitrile..

#### **5.2.4. The Mobile Phase for Fluorescence Detector**

Isocratic conditions were used for the different combinations of water, isopropanol and acetonitrile. Results were unsatisfactory and thus different combinations of water, acetonitrile, isopropanol and acetic acid were used (see results and discussion).

#### **5.2.5. The Mobile Phase for Diode Array Detector**

Two columns (mentioned in Section 5.2.1., page 65) were investigated. Different combinations of water and acetonitrile were used to develop a gradient elution program (see results and discussion).

#### **5.2.6. The Method Used for Quantification of Aflatoxin B<sub>1</sub>**

The external calibration method was used by plotting concentration in p.p.b. versus average integrated peak area in mV.s. The best fit straight line was obtained by using linear regression analysis. The data and calibration graph of AFB<sub>2a</sub>, using the fluorescence detector, are presented in Table 12 (Appendix 32, page 264) and Figure 57 (Appendix 33, page 264), respectively.

The data and calibration graph of AFB<sub>1</sub>, using the diode array detector, are presented Table 13 (Appendix 34, page 265) and Figure 58 (Appendix 35, page 265), respectively.

Aflatoxin B<sub>1</sub> was monitored at its optimum detection wavelength viz., at 360 nm.



### **5.2.7. Repeatability of Retention Times and Peak Areas**

A standard containing 0.3 µg/ml of AFB<sub>1</sub> was derivatised with TFA (200 µl) as described previously. The solution was diluted accurately to volume and eight injections (20 µl) were made using the fluorescence detection, excitation at 325 nm and emission at 420 nm. The retention time and peak area (Table 14, Appendix 36, page 266) were recorded.

A standard solution containing 0.2 µg/ml of AFB<sub>1</sub> was prepared and eight injections (20 µl) were made using the diode array detector. The retention time and peak area (Table 15, Appendix 37, page 267) were recorded.

### 5.3. RESULTS AND DISCUSSION

Previous<sup>156</sup> studies, based on the reaction between TFA and the metabolites AFB<sub>1</sub> and AFG<sub>1</sub> showed that in order to achieve reproducibility, the reaction was required to proceed for approximately 5 minutes. As mentioned earlier (page 61) AFB<sub>1</sub> is converted to AFB<sub>2a</sub> whilst AFG<sub>1</sub> is converted to AFG<sub>2a</sub>. Based on earlier studies, the reaction in this study was also carried out for 5 minutes. In addition, the samples were prepared and injected immediately to avoid degradation of AFB<sub>2a</sub> and AFG<sub>2a</sub> in the HPLC solvent.

The parameters selected for optimisation of HPLC, using the fluorescence detector, were the excitation wavelength, emission wavelength, column and mobile phase. The column which was selected in this study was a reversed phase C<sub>18</sub> Prodigy ODS-2 of 5 microns. The excitation and emission wavelengths were set at 325 nm and 420 nm, respectively, after optimising the detector for the strongest fluorescent intensity of AFB<sub>2a</sub>.

Manabe *et al.*<sup>157</sup> reported that the fluorescence of aflatoxins was enhanced by increasing the concentration of organic acid in the mobile phase. Therefore in this study, acetic acid was used as one of the components of the aqueous mobile phase. However, high concentrations of acids could not be used due to the risk of damaging some of the components of the HPLC system. Hence the solvent system selected for analysis consisted of an aqueous solution of acetonitrile, isopropanol and acetic acid.

To ensure proper resolution between the major aflatoxins in a minimum time, the correct proportion of the mobile phase components had to be established. Different combination of the solvents for the separation of the four aflatoxins, were attempted. It was found that a mobile phase consisting of water : acetonitrile : isopropanol (8 : 1 : 1) and a flow rate of 1 ml/min. resulted in poor resolution of the four metabolites since there was co-elution of AFG<sub>2a</sub> (retention time = 3.82), AFB<sub>2a</sub> (retention time = 4.11) and AFG<sub>2</sub> (retention time = 4.63). The chromatogram is presented in Figure 59 (page 69). The metabolites were identified by comparing their retention time with those of authentic standards.

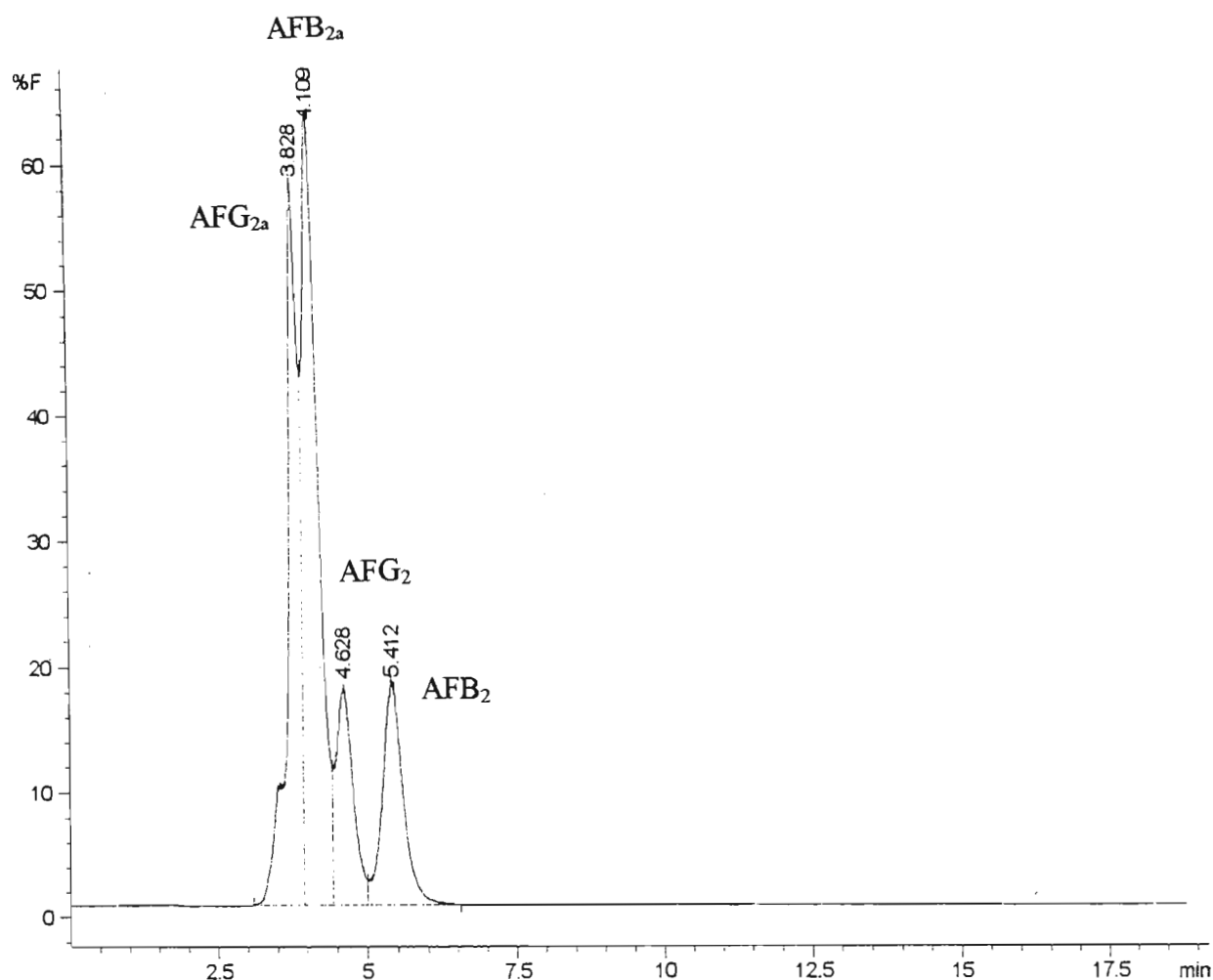


Figure 59. The Isocratic Reversed Phase Chromatogram for the Separation of Aflatoxins with the Mobile Phase Water: Acetonitrile: Isopropanol (8:1:1) at a Flow Rate of 1 ml/min.

The addition of acetic acid (0.5 %) to the mobile phase resulted in an improvement in the separation of the four metabolites (Figure 60, page 70). However, only AFB<sub>2</sub> was base-line resolved from the other metabolites. The other three metabolites appeared as fused peaks. By increasing the concentration of acetic acid (1 %) in the mobile phase it was found that the separation of the four metabolites was further improved and AFB<sub>2</sub> was base-line resolved from AFG<sub>2</sub>. The chromatogram is presented in Figure 61 (page 70).

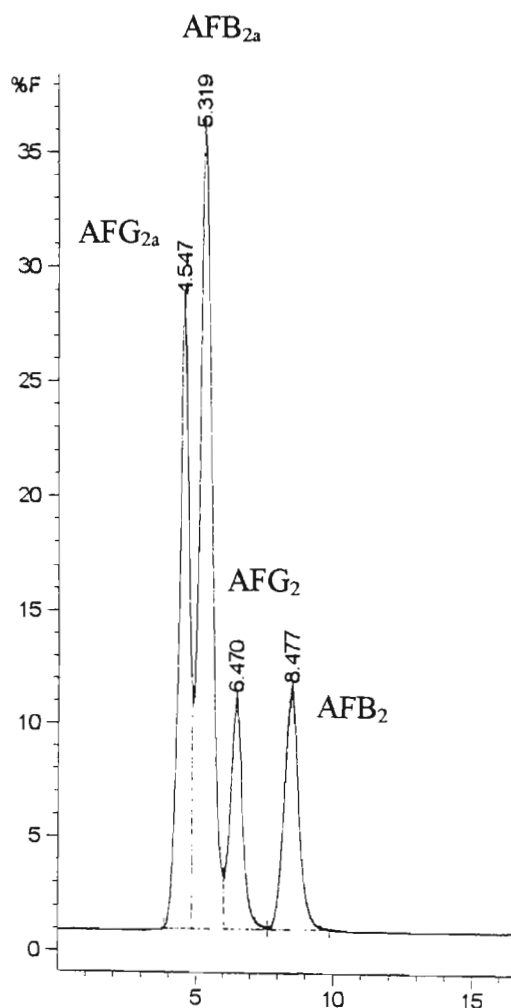


Figure 60. The Isocratic Reversed Phase Chromatogram for the Separation of Aflatoxins with the Mobile Phase Water: Acetonitrile: Isopropanol: Acetic Acid (7.95: 1: 1: 0.05) at a Flow Rate of 1 ml/min.

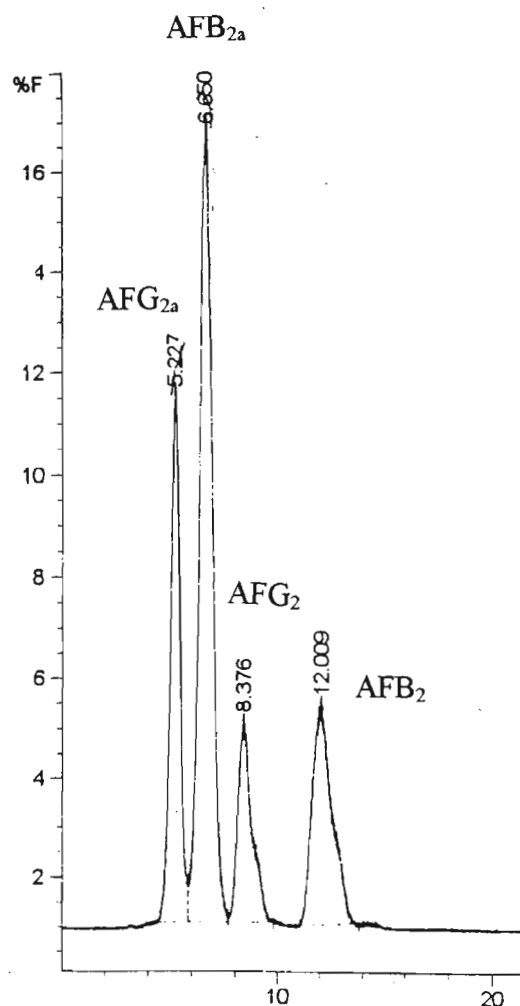


Figure 61. The Isocratic Reversed Phase Chromatogram for the Separation of Aflatoxins with the Mobile Phase Water: Acetonitrile: Acetic Acid: Isopropanol: (7.9: 1: 1: 0.1) at a Flow Rate of 1 ml/min.

Having established that acetic acid could improve the separation of the four metabolites, the mobile phase components were varied in order to achieve optimum resolution of the metabolites. The different concentration of mobile phase is presented in Table 16 (page 71).

Table 16. The Different Concentration of the Mobile Phase Water: Acetonitrile: Isopropanol: Acetic Acid Used in Reversed Phase Chromatography.

Mobile Phase (water: acetonitrile: isopropanol: acetic acid)	Figure Number
8.4: 1: 0.5: 0.1	62, page 71
8.3: 1: 0.5: 0.2	63, page 72
8.2: 1: 0.5: 0.3	64, page 73
8: 1: 0.5: 0.5	65, page 74

The chromatogram presented below (Figure 62) indicates that increasing the quantity of acetic acid by small increments resulted in an overall improvement in the separation and resolution of the metabolites.

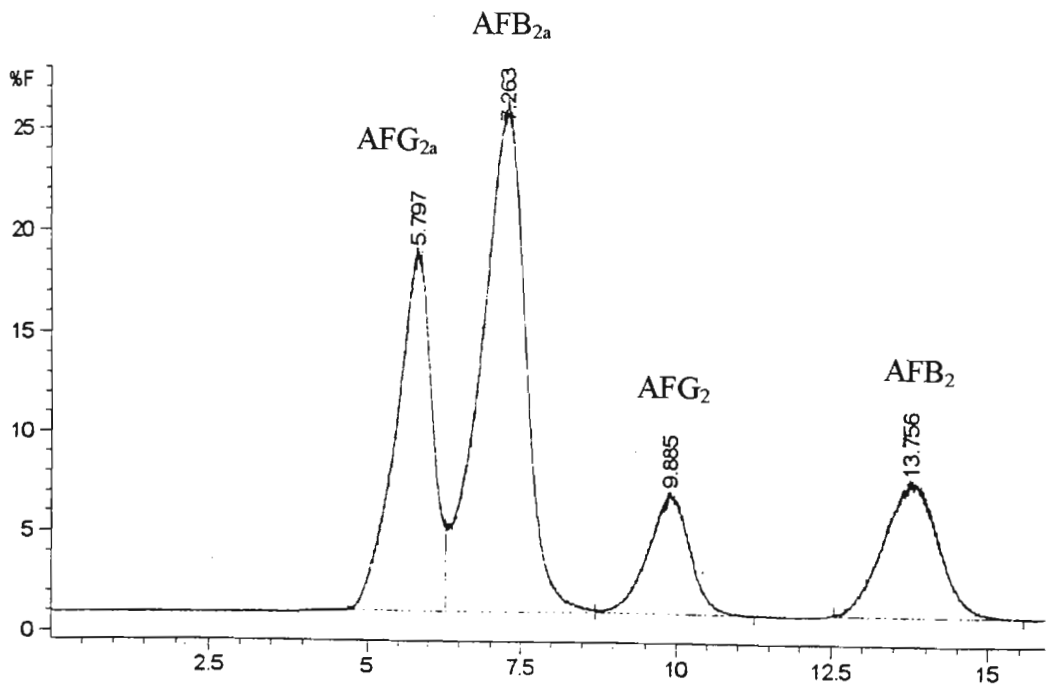


Figure 62. The Isocratic Reversed Phase Chromatogram for the Separation of Aflatoxins with the Mobile Phase of Water: Acetonitrile : Isopropanol: Acetic Acid (8.4: 1: 0.5: 0.1) at a Flow Rate of 1 ml/min.

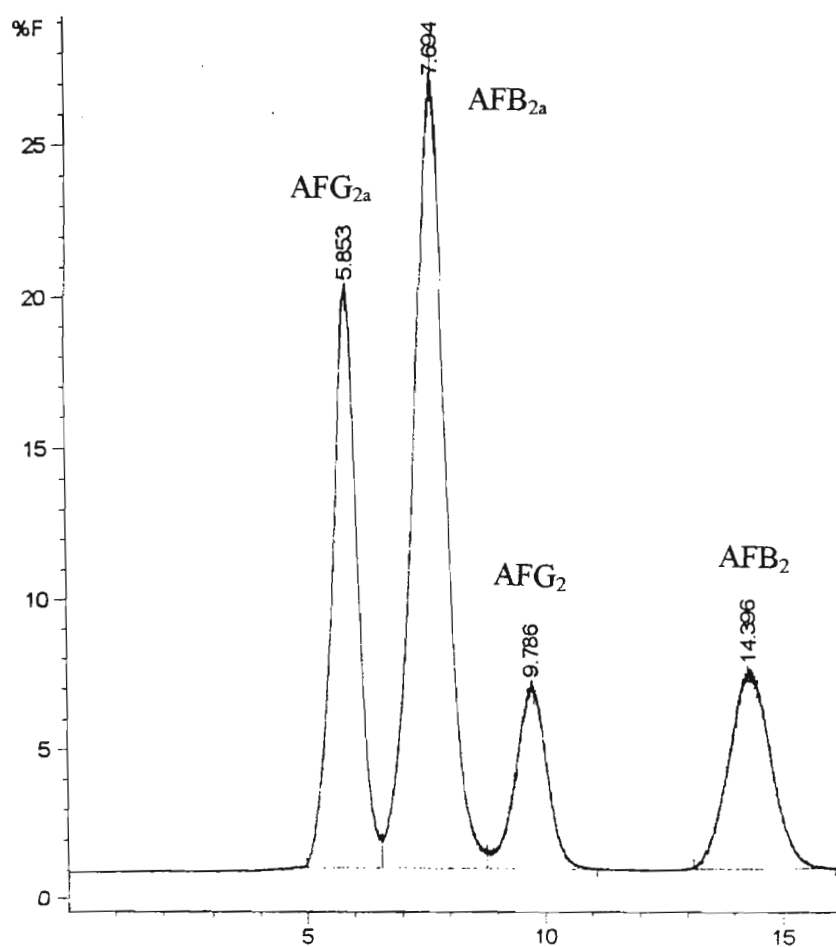


Figure 63. The Isocratic Reversed Phase Chromatogram for the Separation of Aflatoxins with the Mobile Phase of Water: Acetonitrile : Isopropanol: Acetic Acid (8.3: 1: 0.5: 0.2) at a Flow Rate of 1 ml/min.

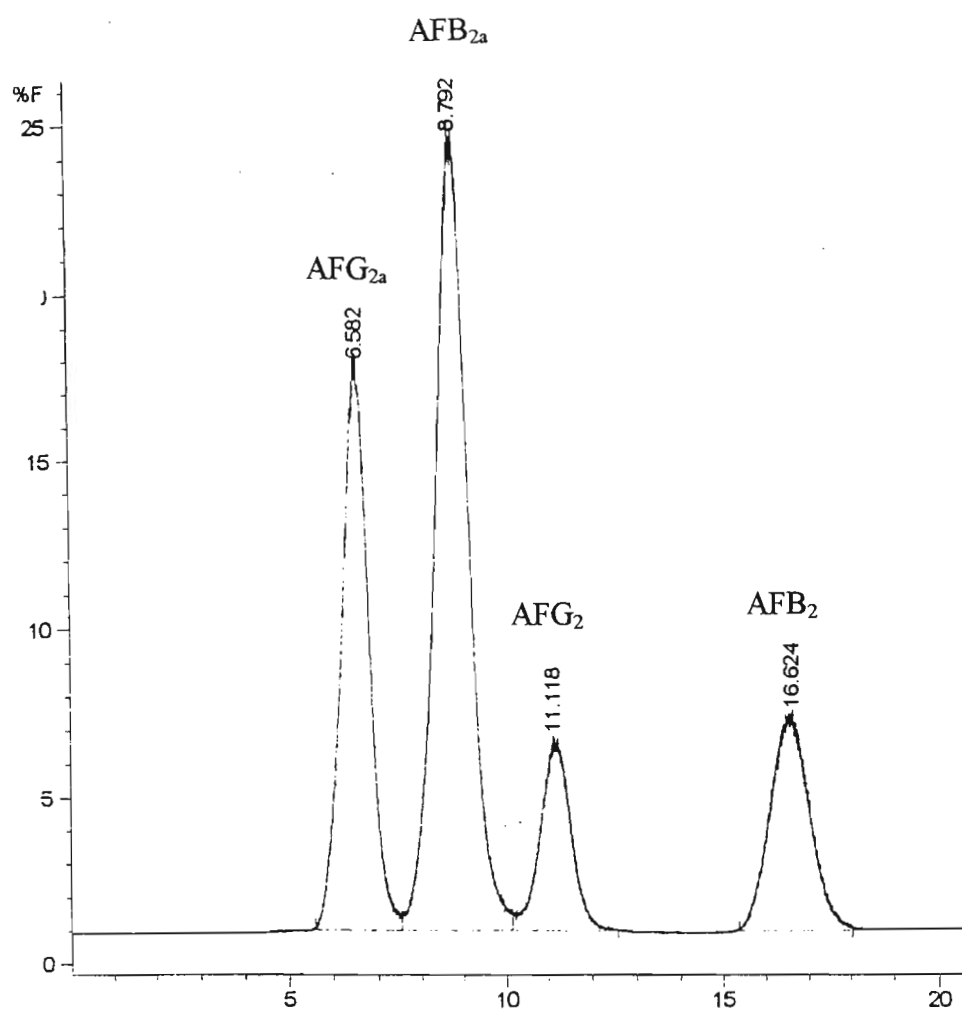


Figure 64. The Isocratic Reversed Phase Chromatogram for the Separation of Aflatoxins with the Mobile Phase of Water: Acetonitrile : Isopropanol: Acetic Acid (8.2: 1: 0.5: 0.3) at a Flow Rate of 1 ml/min.

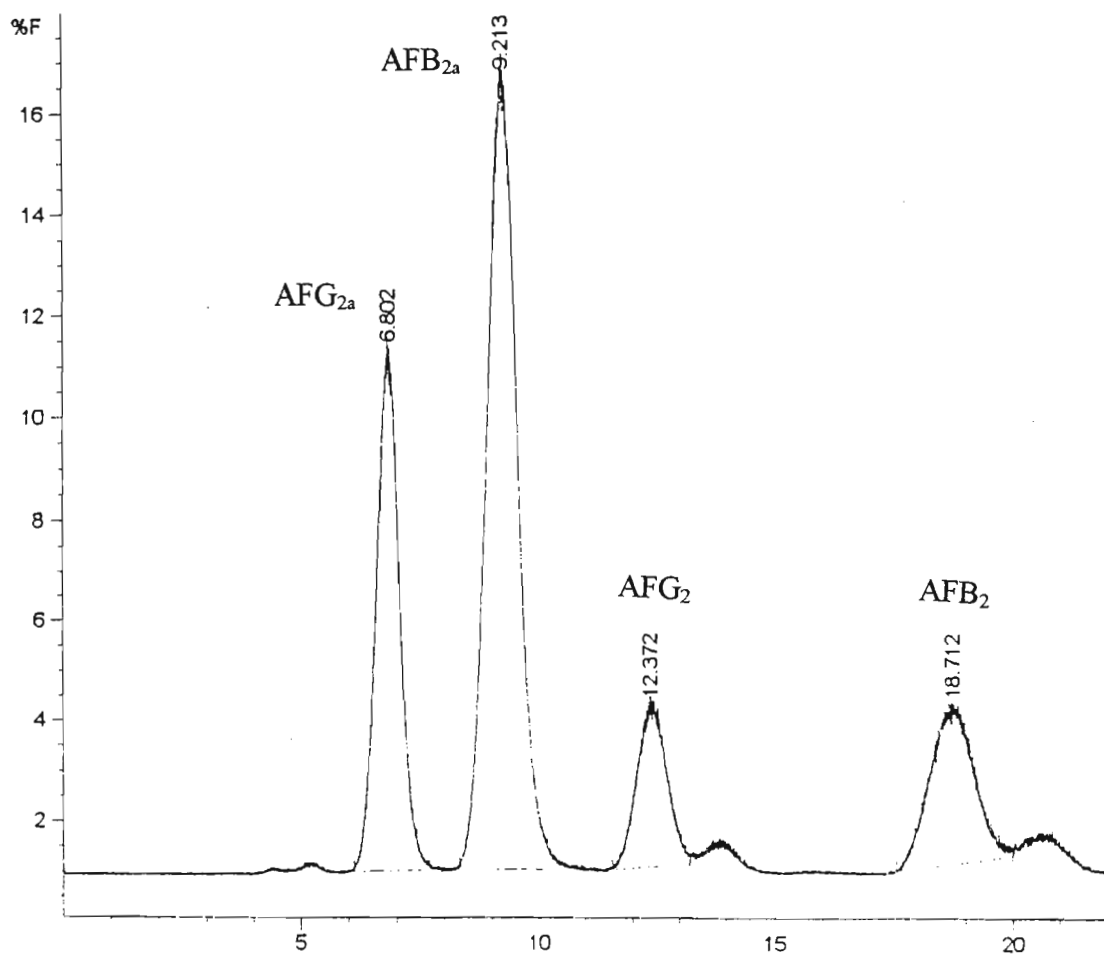


Figure 65. The Isocratic Reversed Phase Chromatogram for the Separation of Aflatoxins with the Mobile Phase of Water: Acetonitrile : Isopropanol: Acetic Acid (8: 1: 0.5: 0.5) at a Flow Rate of 1 ml/min.

It was found that the best solvent system consisted of a mobile phase of water: acetonitrile: isopropanol : acetic acid (8: 1: 0.5: 0.5). The chromatogram is presented in Figure 65. It must be mentioned that the aim in this study was to separate the four metabolites and to achieve base-line resolution of AFB<sub>2a</sub>. This was necessary since it was decided to quantify



the conversion of ST and ST derivatives to AFB<sub>1</sub> (AFB<sub>2a</sub>) in whole cells of *A. parasiticus* (Chapter 6).

The base-line resolution between AFG<sub>2a</sub> and AFB<sub>2a</sub> was calculated by using the formula :

$$R = \frac{2 (t_2 - t_1)}{(w_{b1} + w_{b2})}$$

Using a chart speed of 1 cm/min, the resolution was calculated as approximately 2.05 which indicated good base-line separation between the two peaks (R must be greater than 1.5). The base-line resolution between the other peaks were not calculated since the metabolite of concern was AFB<sub>1</sub> (see Chapter 6).

During the course of the study using whole cell feeding experiments (Chapter 6), it was found that the HPLC pump seal developed a serious leak. This resulted in the sapphire piston being scored. This meant expensive maintenance and a time delay since the sapphire piston was not available. Faced with this problem and the day to day problems that is normally experienced with HPLC systems, it was decided that the samples (Chapter 6) be re-run on a Perkin Elmer System using the same C<sub>18</sub> column and the optimised mobile phase discussed above. It was therefore not surprising that the retention time of an authentic AFB<sub>1</sub> (pre-column derivatised) standard was not affected by changing the HPLC system. A typical chromatogram of a pre-column derivatised standard AFB<sub>1</sub> (AFB<sub>2a</sub>) is presented in Figure 66 (page 76). The quantitative analysis of the conversion of ST and its derivatives to AFB<sub>1</sub> was therefore performed using this second HPLC system.

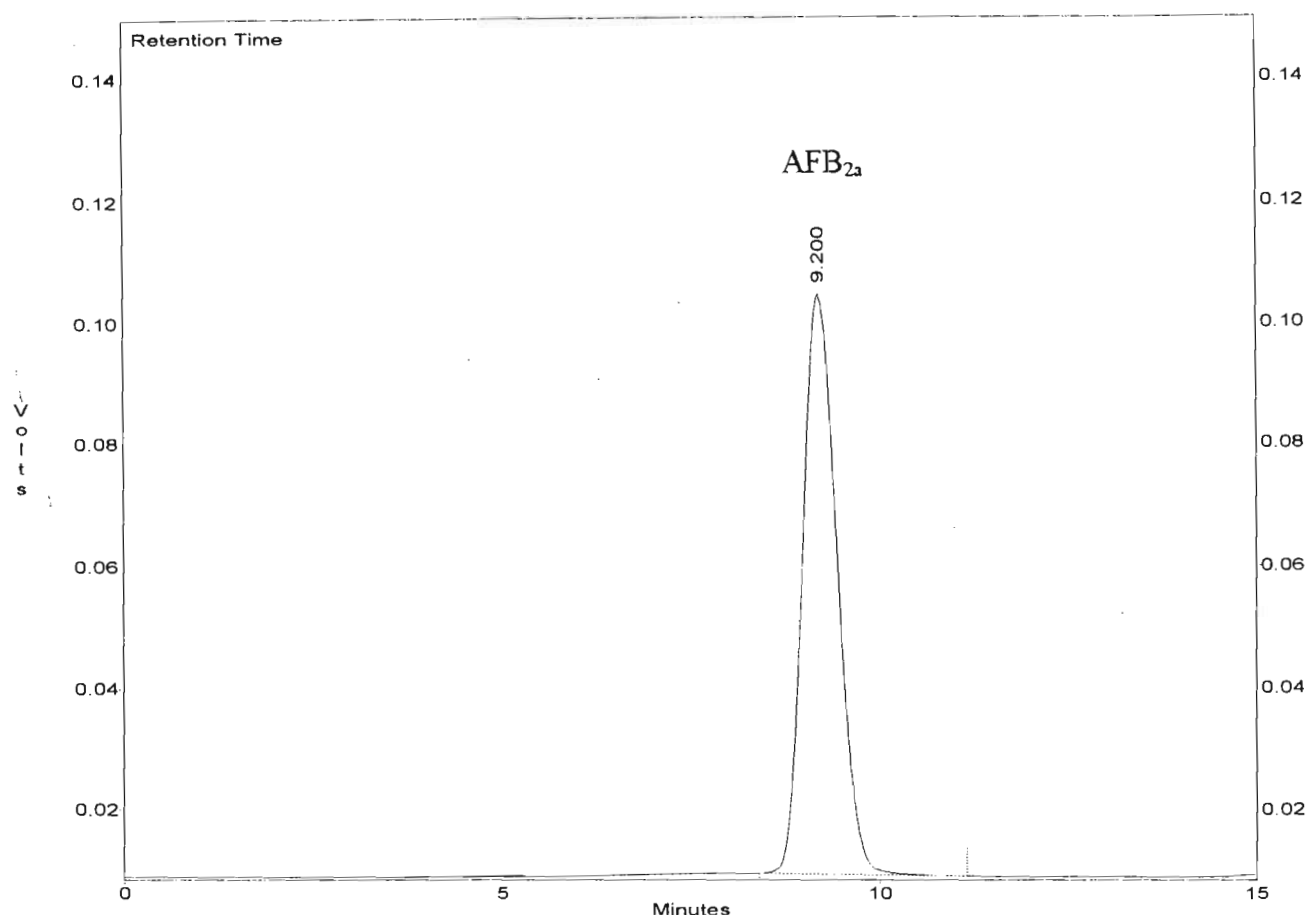


Figure 66. A Typical Isocratic Reversed Phase Chromatogram of a Pre-Column Derivatised AFB<sub>1</sub> Standard Obtained with the Mobile Phase of Water: Acetonitrile : Isopropanol: Acetic Acid (8: 1: 0.5: 0.5) at a Flow Rate of 1 ml/min.

Under the conditions used in this study, the quantitative determination of AFB<sub>2a</sub> was linear in the range 0.01 p.p.m. to 1 p.p.m. Higher concentration of AFB<sub>2a</sub> was not investigated since the quantity present in the diluted samples (see Chapter 6) occurred within this range. This result compares favourably with the research undertaken by Manabe *et al.*<sup>157</sup> who reported a linear range of 0.025 p.p.m. to 12.5 p.p.m. for the four aflatoxins with an eluting solvent of toluene: ethyl acetate: formic acid: methanol (89: 7.5: 2.0: 1.5).

The standard curve of AFB<sub>2a</sub> (Figure 57, Appendix 33, page 264) was constructed by plotting absorbance, expressed in units of area, versus concentration, expressed in p.p.b. A  $r^2$  value of 0.98 indicated a close to linear relationship between the two variables, viz., area and concentration. Statistical analysis of the results (Table 14, Appendix 36, page 266) for repeatability of retention times and peak areas of AFB<sub>2a</sub>, revealed a high degree of precision. Coefficients of variation were 3.48 % and 0.83 % for retention time and peak area, respectively. In this study, the higher variation in retention time is due to the HPLC pump which was not operating at optimum efficiency.

Each day upon HPLC start-up, the instrument was allowed to equilibrate for a minimum of 30 minutes and two injections of TFA in the injection solvent (50  $\mu$ l TFA/5ml solvent) were made to condition the column. Also an AFB<sub>2a</sub> standard was routinely run on a daily basis in order to check for slight variation of retention time which could be due to the slight differences in composition of the mobile phase and also to the HPLC pump. Also at the end of each day, methanol was pumped through the column to flush out materials still retained on the column and also to prevent algae or mould growth.

The parameters selected for optimisation of the HPLC system, using the diode array detector, were the column, mobile phase, gradient program and detection wavelength. The structures of the chemical compounds were similar and hence it was predicted that the separation of these compounds would be simple. However the presence of other aflatoxin metabolites, which are produced by the fungi, posed a problem.

The first column that was investigated was the C<sub>18</sub> Prodigy (150 x 4.60 mm) which was used in the previous HPLC method. Using an isocratic system at high solvent strength, i.e., water: acetonitrile (2: 8), a blank was run to determine the unretained peak (Figure 67, page 78). A peak at retention time less than 2 minutes was observed. This peak was either the unretained peak or more likely an impurity present in the solvent. The chromatogram was initially scanned at an absorbance of 365 nm which is one of the wavelengths at which AFB<sub>1</sub> has been reported to show good absorbance. This meant that the peak at retention time < 2 minutes was not due to acetonitrile since acetonitrile has a UV cut-off at 190 nm.

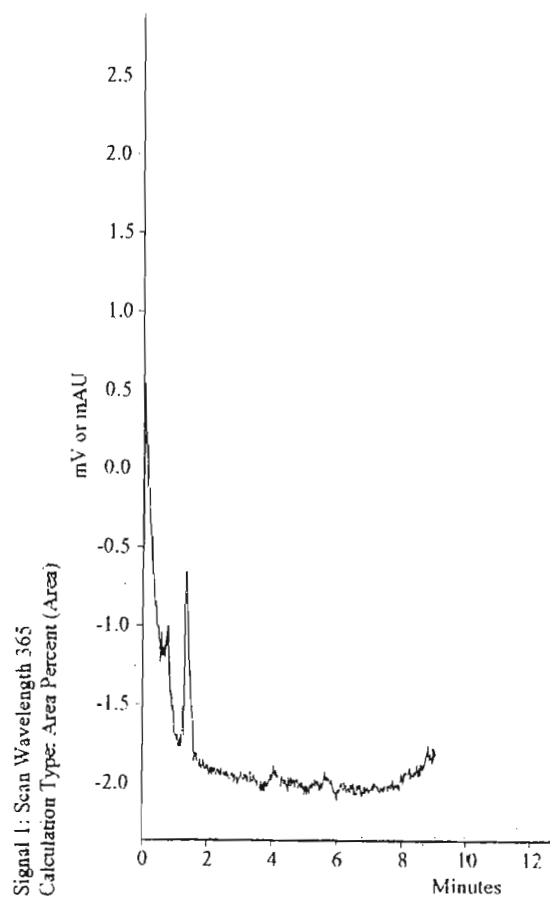


Figure 67. A Typical Isocratic Reversed Phase Chromatogram of a Blank Run with the Mobile Phase of Water: Acetonitrile (2: 8) at a Flow Rate of 1 ml/min.

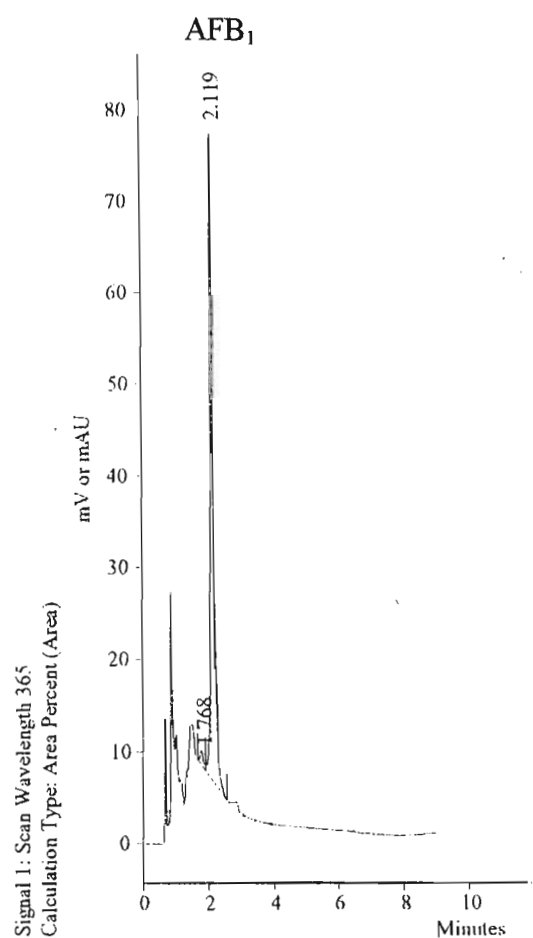


Figure 68. A Typical Isocratic Reversed Phase Chromatogram of AFB<sub>1</sub> Standard with the Mobile Phase Water: Acetonitrile (2: 8) at a Flow Rate of 1 ml/min.

A standard AFB<sub>1</sub> sample was injected (Figure 68) and its retention time was found to be 2.12 minutes. An active cell-free extract (see Chapter 7) sample was subsequently injected and a group of 4 or more unresolved peaks (Figure 69) was observed which masked the

area in which AFB<sub>1</sub> eluted (2.12). Also present in cell-free extracts were a number of compounds which eluted after AFB<sub>1</sub>. These compounds were relatively less polar than AFB<sub>1</sub> since they were retained longer on the column due to their interaction with the non-polar stationary phase. These and other compounds have been observed in all chromatograms of whole cell and cell-free reactions (Chapter 7, 8, 9 and 10) and are most probably metabolites produced by the fungi. Since the compounds of interest were AFB<sub>1</sub>, OMST and ST, the other metabolites were not identified and were therefore considered as unknown compounds.

During these initial investigations attempts were made to separate AFB<sub>1</sub> from other early eluting polar compounds.

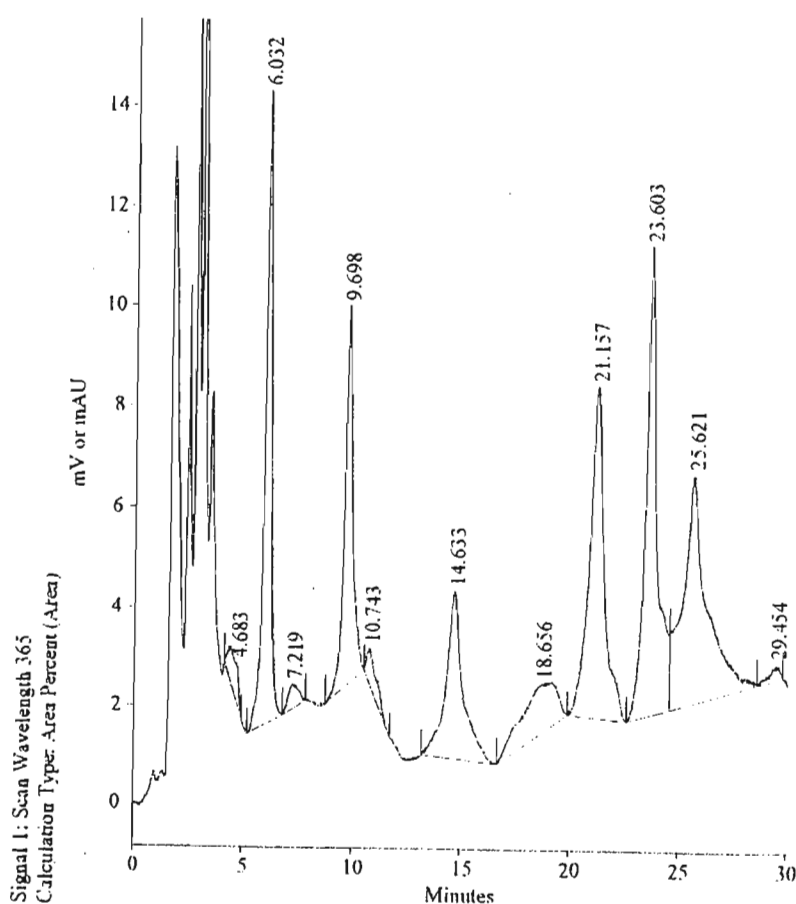


Figure 69. The Isocratic Reversed Phase Chromatogram for the Separation of AFB<sub>1</sub> in a Cell-Free Extract With the Mobile Phase of Water: Acetonitrile (2: 8) at a Flow Rate of 1 ml/min.

Since AFB<sub>1</sub> was found to co-elute with other polar metabolites, the above mentioned solvent system proved unsuccessful and it was decided to increase the solvent strength by decreasing the acetonitrile component. This change in the mobile phase would allow the early eluting compounds to be retained longer on the column due to their stronger interaction with the stationary phase. This was evident when a standard sample of AFB<sub>1</sub> was injected and the peak was found to appear at retention time 4.33 minutes for a mobile phase of water: acetonitrile (3: 7). The chromatogram is presented in Figure 70.

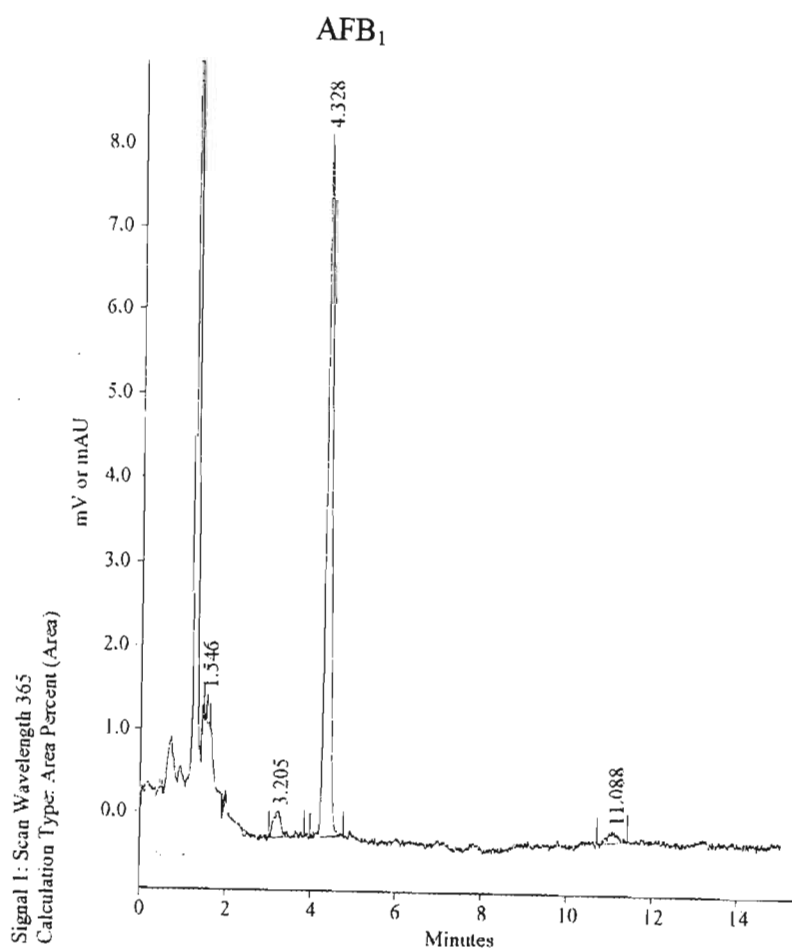


Figure 70. The Isocratic Reversed Phase Chromatogram of AFB<sub>1</sub> Standard Obtained With the Mobile Phase of Water: Acetonitrile (3: 7) at a Flow Rate of 1 ml/min.

An active cell-free extract sample was subsequently injected (Figure 71) with a mobile phase of water: acetonitrile (3: 7) in order to determine if there was any improvement in the separation of AFB<sub>1</sub> from other polar compounds. The chromatogram showed that AFB<sub>1</sub> (RT 4.23 minutes) separated out from other early eluting polar compounds. However, the AFB<sub>1</sub> peak was not base-line resolved and in addition there was interference from a shouldering peak at RT 4.95 minutes.

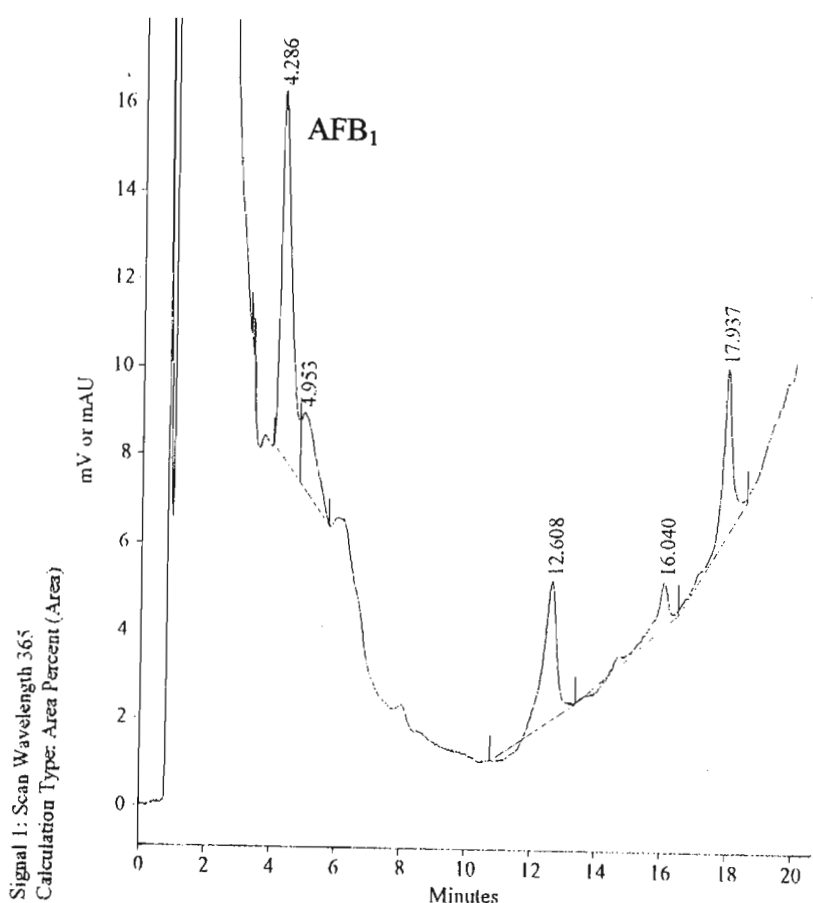


Figure 71. The Isocratic Reversed Phase Chromatogram for the Separation of AFB<sub>1</sub> in a Cell-Free Extract With the Mobile Phase of Water: Acetonitrile (3: 7) at a Flow Rate of 1 ml/min.

It was decided that another column be investigated, viz., C<sub>18</sub> Lichrosphere (250 x 4.60 mm) in order to determine if there was any improvement in the separation of AFB<sub>1</sub> from the unknown compound. This was a longer column compared to the C<sub>18</sub> Prodigy and the overall resolution of AFB<sub>1</sub> from other polar compounds was expected to improve. The

chromatogram of a cell-free extract using a mobile phase of water: acetonitrile (3: 7) is presented in Figure 72. There was a change in the retention time of AFB<sub>1</sub> (7.62 minutes) and the separation of compounds was improved. However, the retention of later eluting compounds with retention times greater than 20 minutes posed a problem. The overall analysis time was over 40 minutes since a minimum of 10 minutes was required for the instrument to equilibrate and also for any other non-polar compounds to elute. This long analysis time was not practical considering that many samples were to be analysed and this instrument was being used by other research teams on a daily basis. It was therefore decided to investigate gradient elution in order to elute the more tightly bound compounds earlier. The gradient elution program is presented in Table 17 (page 83).

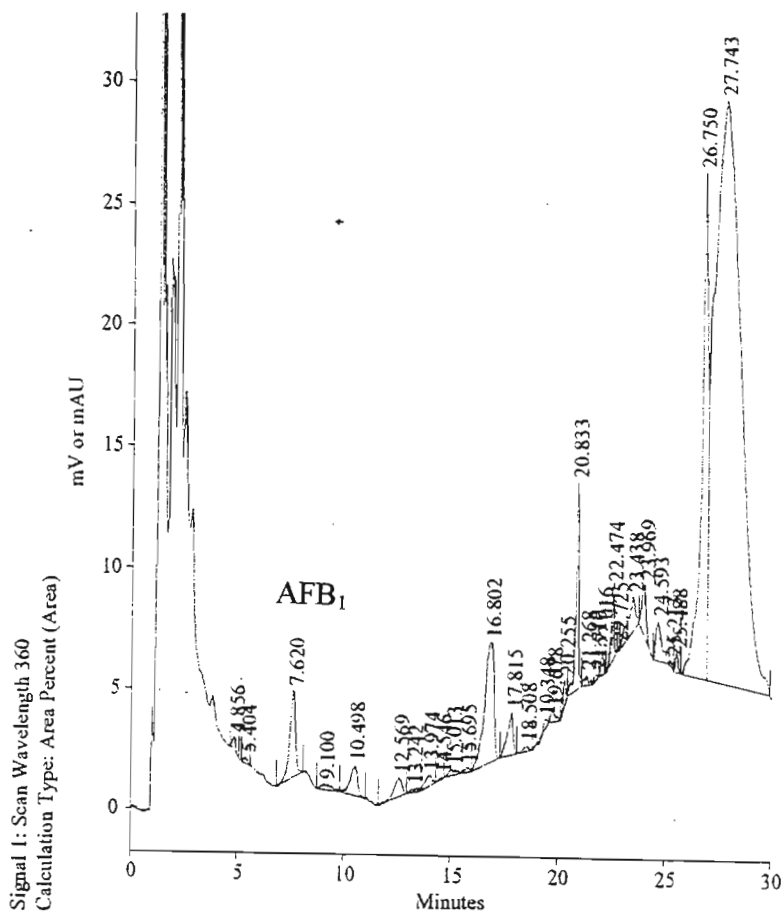


Figure 72. The Isocratic Reversed Phase Chromatogram for the Separation of AFB<sub>1</sub> in a Cell-Free Extract With the Mobile Phase of Water: Acetonitrile (3: 7) at a Flow Rate of 1 ml/min.



Table 17. The Gradient Elution Program Used for HPLC Analysis for the Conversion of ST and ST Derivatives to AFB<sub>1</sub> in Cell-Free Extracts.

Time (minutes)	% Water	% Acetonitrile
0	40	60
5	40	60
20	20	80

The chromatogram of a cell-free extract, which was spiked with ST (20.18 min.) and OMST (10.64 min.) is presented in Figure 73. This solvent system displayed good results in that AFB<sub>1</sub> was separated from an unknown compound (5.27 min.), and both ST and OMST were well separated from any interfering compounds.

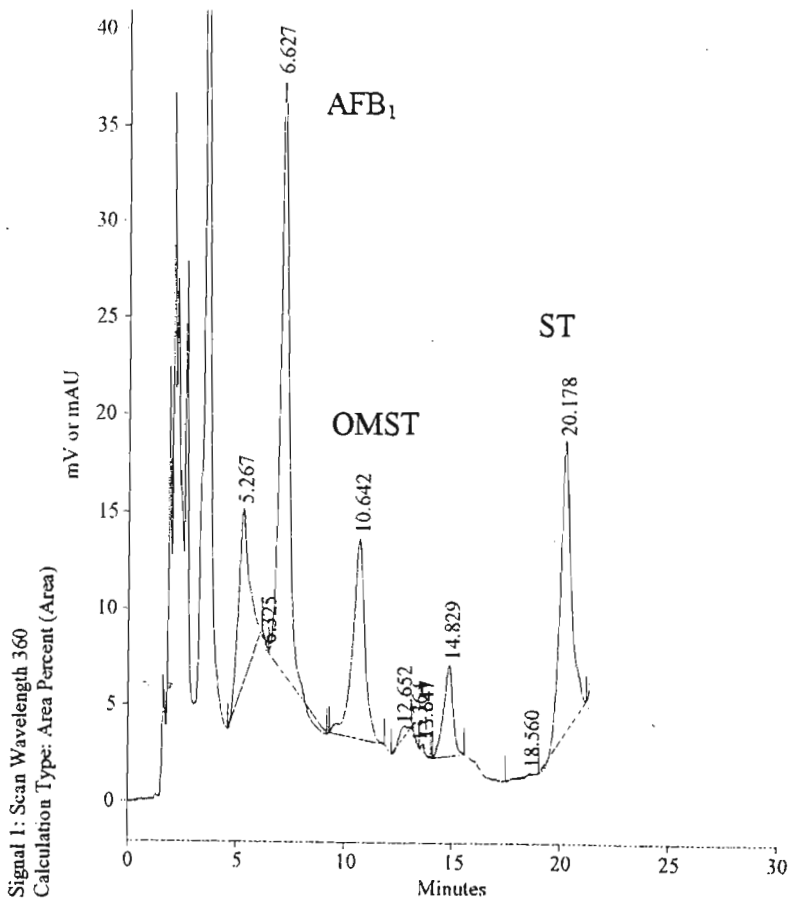


Figure 73. The Gradient Reversed Phase Chromatogram for the Separation of Aflatoxins in a Cell-Free Extract at a Flow Rate of 1 ml/min. Gradient Program: 60 % Acetonitrile (time 0); 60 % Acetonitrile (time 5 min.); 80 % Acetonitrile (time 20 min.).

Aflatoxin B<sub>1</sub>, OMST and ST were identified in the cell-free extract by comparing their retention time with standard samples and their chromatograms are presented in Figure 74, 75 and 76 (page 85), respectively.

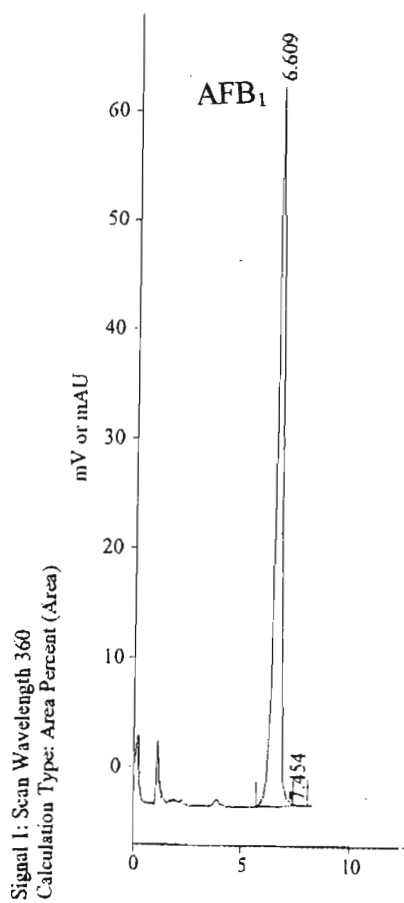


Figure 74. A Typical Gradient Reversed Phase Chromatogram of AFB<sub>1</sub> Standard at a Flow Rate of 1 ml/min.

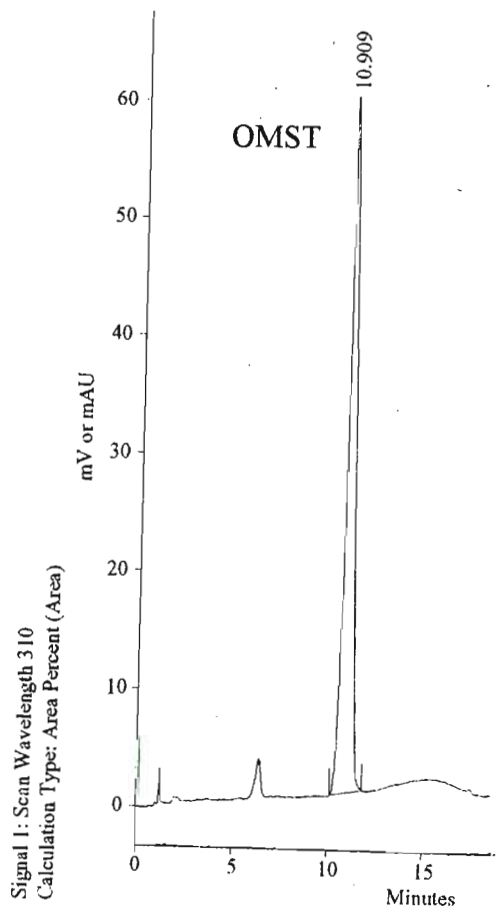


Figure 75. A Typical Gradient Reversed Phase Chromatogram of OMST Standard at a Flow Rate of 1 ml/min.

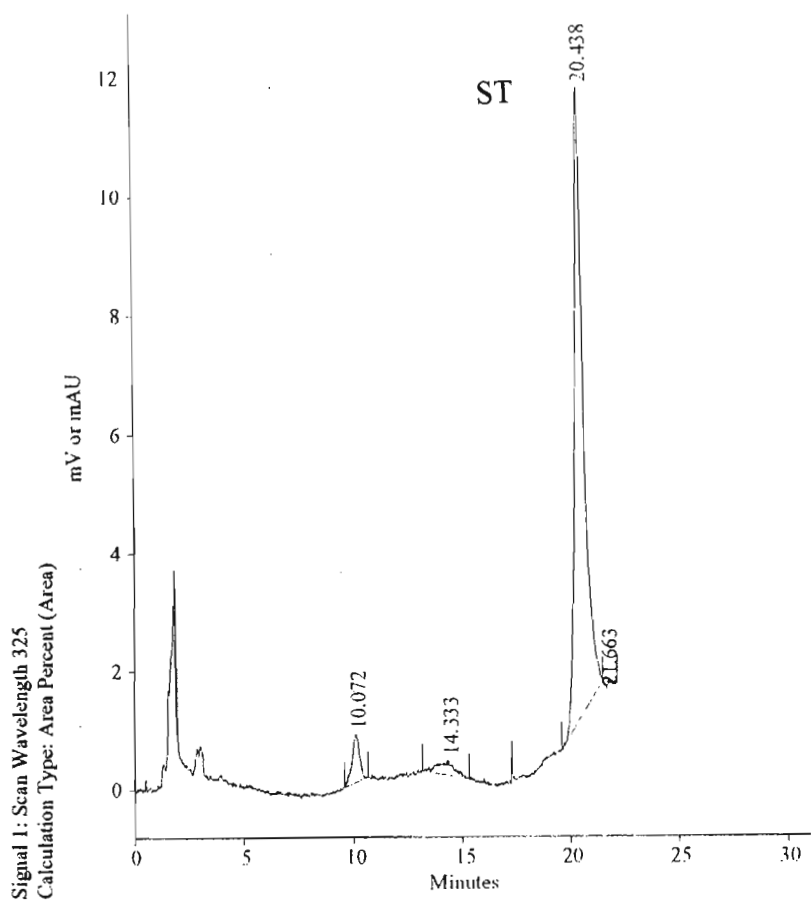


Figure 76. A Typical Gradient Reversed Phase Chromatogram of ST Standard at a Flow Rate of 1 ml/min.

The UV profile of AFB<sub>1</sub> is presented in Figure 77 (page 86). The UV profile of ST and OMST are presented in Figure 78-79 (Appendix 38-39, page 268), respectively.

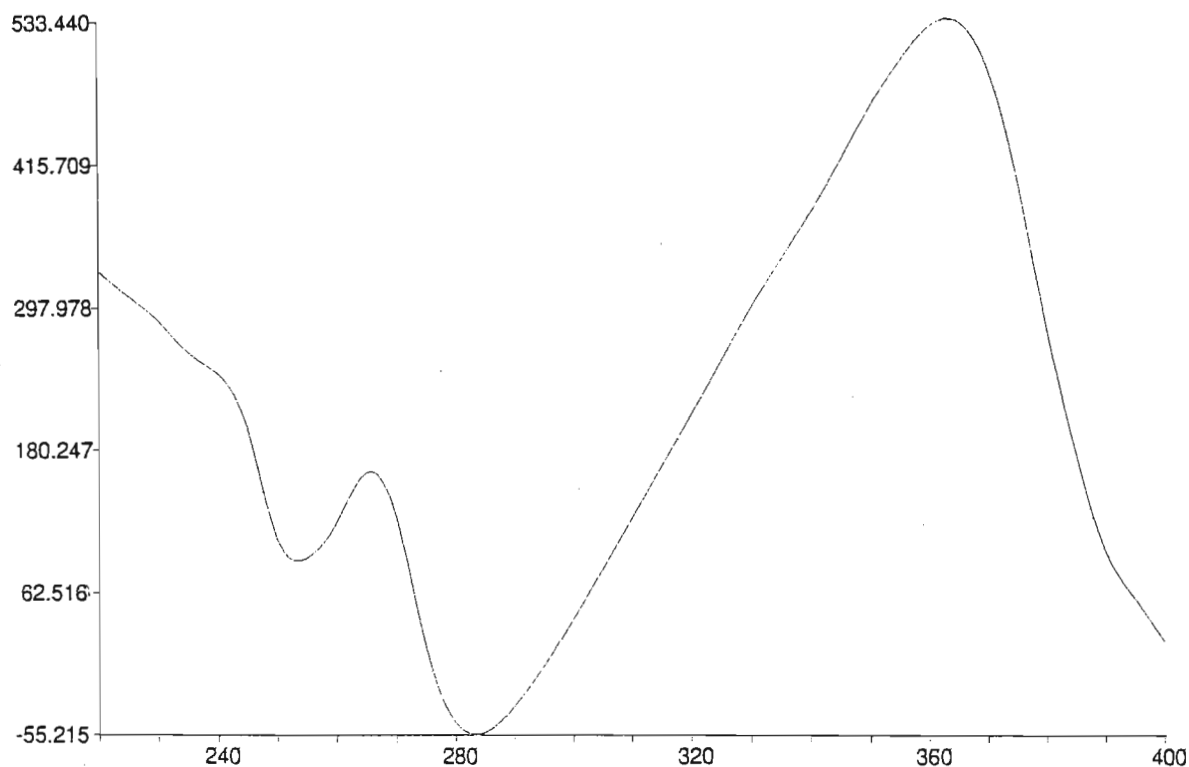


Figure 77. The UV Spectrum of AFB<sub>1</sub> Standard.

As mentioned earlier, the diode array detector used in this study contained a LightPipe flow-cell and was reported to deliver a 400 % increase in the sensitivity over other diode array detectors. This improvement in the design enabled the detection of as low as 0.01 p.p.m. AFB<sub>1</sub>. Concentrations lower than 0.01 p.p.m. AFB<sub>1</sub>, i.e., the limit of detection, were not investigated since AFB<sub>1</sub> produced by the enzyme mediated reactions (Chapters 7, 8 and 9) were not lower than 0.02 p.p.m. The detector response for AFB<sub>1</sub> was linear in the range 0.02 p.p.m. to 5.00 p.p.m. with a  $r^2$  value of 0.99 (Figure 58, Appendix 35, page 265).

Statistical analysis of the results (Table 15, Appendix 37, page 267) for repeatability of retention times and peak areas of AFB<sub>1</sub>, revealed a high degree of precision. Coefficients of

variation were 0.97 % and 3.73 % for retention time and peak area, respectively.

All quantitative analysis (Chapters 7, 8 and 9) of AFB<sub>1</sub> extracted from cell-free extracts, partially purified enzyme(s) and whole cells were performed by HPLC using the diode array detector with the gradient elution program described earlier. During the course of these studies it was found that the RP-18 guard column required changing on a weekly basis since it proved effective in the protection of the column by removing any insoluble and particulate matter. It must be mentioned that each day upon HPLC start-up, the instrument was allowed to equilibrate for a minimum of 45 minutes with the mobile phase. Also the AFB<sub>1</sub> standard was routinely run on a daily basis in order to check for slight variation of retention time which is probably due to the slight differences in composition of the mobile phase. At the end of each day, methanol was pumped through the column to flush out materials still retained on the column and also to prevent algae or mould growth.

In summary HPLC methods were developed to quantify AFB<sub>1</sub> by using:

- the Perkin Elmer System linked to a fluorescence detector and
- the Spectra Physics System linked to a diode array detector.

## CHAPTER SIX

### BIOTRANSFORMATION OF STERIGMATOCYSTIN DERIVATIVES USING WHOLE CELLS

#### 6.1 INTRODUCTION

Mutants of the fungal species *A. parasiticus* and *A. flavus*, are characterised by their impaired aflatoxin synthesis. The averantin accumulating mutant (avn-1) was isolated by Bennett *et al.*<sup>158</sup>. The averufin accumulating mutant (avr-1) was isolated by Donkersloot *et al.*<sup>159</sup>. The versicolorin A accumulating mutant was isolated by Bennett and Goldblatt<sup>160</sup> and characterised by Lee *et al.*<sup>161</sup>. These mutants have been useful in studying the aflatoxin biosynthetic pathway.

Earlier studies have shown that the incubation of putative intermediates with mutants of *A. parasiticus*, blocked early in the pathway, that generated AFB<sub>1</sub>, was indicative of their role as biogenetic precursors<sup>162</sup>. These aflatoxin precursors are placed past the site of the mutant block. The currently accepted scheme for the aflatoxin pathway (Figure 80) is based on such data obtained from feeding studies using isotopically labelled precursors<sup>163</sup>.

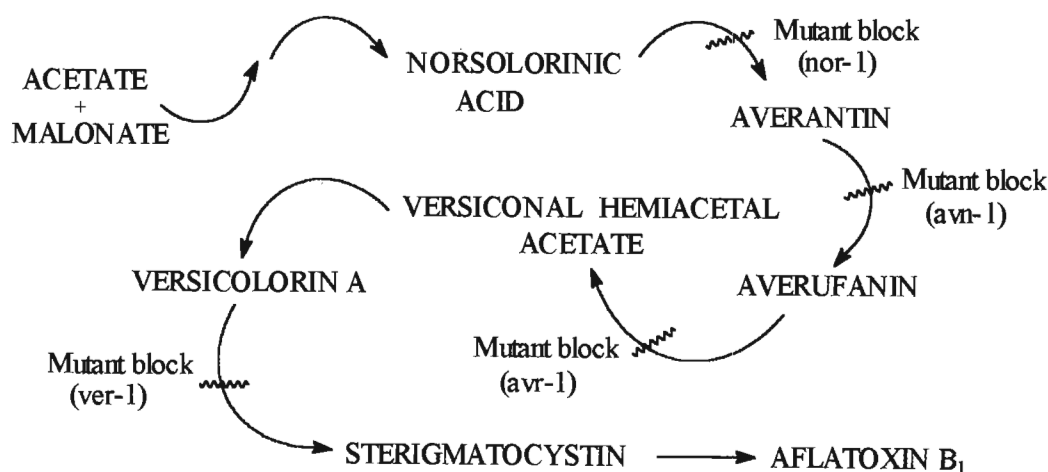


Figure 80. Scheme for Aflatoxin Biosynthesis and Sites for Blocked Mutants<sup>163</sup>.

The biosynthesis of AFB<sub>1</sub> has been the subject of conflicting speculation and numerous reviews<sup>10,94,164,165</sup>. As early as 1979, Bu'Lock<sup>101</sup> proposed that the biosynthetic pathway involves the conversion of ST to AFB<sub>1</sub> via OMST. Subsequently other research groups<sup>5-7</sup> confirmed that the addition of exogenously added OMST was converted to AFB<sub>1</sub>. Recently, several laboratories (discussed in Section 2.9, page 31-34) have focused on genetic studies in order to understand the molecular biology of the aflatoxin biosynthetic pathway. A recent study by Prieto and Woloshuk<sup>127</sup>, employing techniques of molecular biology, revealed an oxidoreductase gene *ord1*, encoding a cytochrome P-450 monooxygenase, that could mediate the conversion of exogenously supplied OMST to AFB<sub>1</sub>.

Since studies have not established the necessity for methylating ST to OMST in the AFB<sub>1</sub> biosynthetic pathway, compounds were synthesised in which the free hydroxyl group of ST was replaced by alkyl and aryl groups other than methyl. Thus compounds homologous to OMST were prepared by chemical reactions (Chapter 4).

The objective of this study was to elucidate the role of OMST in AFB<sub>1</sub> biosynthesis by examining the conversion of exogenously added ST and ST derivatives to AFB<sub>1</sub> by whole cells using a mutant of *A. parasiticus* (ver-1) (Figure 80, page 88) that blocks an earlier step in the biosynthetic pathway.

## 6.2. MATERIALS AND METHOD

### 6.2.1. Chemicals and Materials

All chemicals were of reagent grade or analytical grade. Analytical grade solvents were used for extraction and were purchased from Sigma Chemical Suppliers (SA) and Merck NT Laboratory Suppliers (SA). Petri-dishes and disposable plastic pipettes were purchased from Polychem Chemical Co. (SA). Thin layer chromatography plates containing fluorescent indicator (F<sub>254</sub>) (Merck Art:5554) were purchased from Merck NT Laboratory Suppliers (SA). Potato dextrose agar was purchased from Laboratory and Scientific Chemical Co.(SA).

### 6.2.2. Organism, Media and Culture Conditions

An aflatoxin blocked mutant *A. parasiticus* (Wh1-11-105), which accumulates versicolorin A, was maintained on PDA at 28 °C for 5-7 days. A spore suspension of approximately 10<sup>6</sup> spores, in 0.01 % SDS (1 ml), was inoculated in Reddy's medium<sup>67</sup> (100 ml) (Appendix 2, page 234) in ten conical flasks (250 ml). The growth medium (one liter, in a 4 L Erlenmeyer flask) was autoclaved (140 °C, 20 psi) for 1 hour and cooled to room temperature prior to inoculation. The conical flasks were plugged with cotton wool and incubated at 25 °C in a controlled environment incubator shaker (New Brunswick Scientific) at 180 r.p.m. for 96 hours.

After incubation, the resultant mycelia were vacuum filtered in a Buchner funnel double layered with cheese cloth and rinsed thoroughly with the resting medium (50ml) (Appendix 40, page 269). Three grams (wet weight) of mycelial pellets were added to the resting medium (50 ml) supplemented with acetone<sup>95</sup> (0.5 ml) containing 0.770 µmol of the substrate and was incubated in a controlled environment incubator shaker at 25 °C and at 180 r.p.m .

In a preliminary study, the incubation time was 48 hours. In the time course study, AFB<sub>1</sub> was monitored at regular time intervals as indicated in results and discussion (page 93).



### 6.2.3. Extraction of Aflatoxins and Sample Preparation for Thin Layer and High Pressure Liquid Chromatography

A wide bore disposable pipette was used to aliquot samples (5 ml), at regular time intervals. The culture fluid which contained mycelia, in the form of pellets, was filtered through double layered cheese-cloth. The filtrate was extracted with chloroform (3 x 5 ml), dried over a bed of anhydrous sodium sulphate, filtered and evaporated to dryness *in vacuo*. The solid residue was reconstituted in chloroform (1 ml), quantitatively transferred to vials, by means of pasteur pipettes, and evaporated to dryness under a gentle stream of nitrogen gas and heat.

The pellets were washed with 30 % acetone (3 x 5 ml), extracted with chloroform (3 x 5 ml) and treated as described above.

In the preliminary investigation, the dried residue was reconstituted in chloroform (1 ml) and a portion (20 µl) was spotted onto the origin of a t.l.c. plate (10 x 10 cm aluminium backed Kieselgel 60). The plate was developed in CEI and TEF, air dried and scanned for fluorescence under UV. The t.l.c. plates were then sprayed with aluminium chloride in ethanol (20 %, w/v) to test for the characteristic change in intensity and colour of fluorescence<sup>166,167</sup> under UV.

In the time course study, trifluoroacetic acid (500 µl) was added to the dried residue, allowed to stand for 5 minutes and made up to volume with the mobile phase (100 ml). The sample was analysed by HPLC using the Perkin Elmer chromatograph linked to a fluorescence detector (conditions described in Chapter 5).

### 6.3. RESULTS AND DISCUSSION

It was found that after an incubation time of 48 hours in the whole cell feeding experiments, ST and its alkyl derivatives (synthesis described in Chapter 4) were converted to AFB<sub>1</sub>. The identity of AFB<sub>1</sub> was established by two dimensional t.l.c. using CEI (first dimension) and TEF (second dimension) as the solvent system.

Sterigmatocystin derivatives demonstrated a characteristic pale blue fluorescence under UV illumination. Fluorescence of these compounds turned yellow-green when treated with the aluminium chloride spray reagent. Sterigmatocystin ( $R_{f1}$  0.91;  $R_{f2}$  0.83) exhibited a brick red fluorescence under UV light which changed to yellow when treated with the spray reagent. Aflatoxin B<sub>1</sub> ( $R_{f1}$  0.61;  $R_{f2}$  0.39) displayed a characteristic blue fluorescence under UV illumination and no reaction occurred upon treatment with the spray reagent.

The results from whole cell feeding experiments indicated that the blocked mutant of *A. parasiticus* was able to convert all ST derivatives to AFB<sub>1</sub>. These results, as well as those reported by other authors<sup>5,95,98,162</sup>, confirm that blocked mutants retain the remaining enzyme activities involved in the aflatoxin pathway. The transformation of ST and OMST to AFB<sub>1</sub> has been repeatedly reported<sup>100,168,169</sup> and the enzymatic activities involved in these conversions have been established<sup>7,90,101,170</sup>. The wild type blocked mutant *A. parasiticus* is able to produce all four aflatoxins, viz., AFB<sub>1</sub>, AFB<sub>2</sub>, AFG<sub>1</sub> and AFG<sub>2</sub>. The recovery of only AFB<sub>1</sub> from the whole cells indicate that OMST and ST derivatives are not precursors of the G aflatoxins and AFB<sub>2</sub>. This result therefore confirms that the aflatoxin pathway branches at the end (Figure 13, page 23). Although the position of OMST as an intermediate in AFB<sub>1</sub> biosynthetic pathway is generally agreed, it is not clear either from the point of metabolic simplicity or enzyme specificity, why methylation of ST is an obligatory process in the pathway. It is apparent from these findings that the "enzyme" responsible for the conversion of ST did not display a high degree of substrate specificity, since it was unable to recognize the difference between the various alkyl groups, either as ether or ester functional groups.

In order to investigate the question of relative specificity of the “enzyme” involved, a time course study of the various substrates was done. The substrates selected were ST, OMST, OEST, OPROST and OBzST. In this investigation both the culture fluid and mycelial (pellet) fraction were monitored by HPLC for AFB<sub>1</sub> production at regular time intervals. High pressure liquid chromatography was carried out by using the Perkin Elmer chromatogram linked to a fluorescence detector.

The quantity of AFB<sub>1</sub>, produced by whole cells, was calculated by using by the integrated peak area of the chromatogram and a back-fit straight line equation from the calibration graph of AFB<sub>1</sub> (Figure 57, Appendix 33, page 264). Preliminary investigations indicated that the quantity of AFB<sub>1</sub> produced by whole cells was sufficiently large and fell outside the linear range of the calibration graph. Therefore all samples were subsequently prepared in the mobile phase (100 ml) water: acetonitrile: isopropanol: acetic acid (8: 1: 0.5: 0.5) after derivatisation with TFA. The quantity of AFB<sub>1</sub> was calculated by using the formula :

$$\mu\text{mol AFB}_1 \text{ produced} = \frac{(\mu\text{g}/100 \text{ ml}) \text{ AFB}_1 \text{ produced} \times 100}{\text{molar mass AFB}_1}$$

and hence % conversion to AFB<sub>1</sub> was calculated by using the formula :

$$\% \text{ conversion to AFB}_1 = \frac{\mu\text{mol AFB}_1 \times 100}{\mu\text{mol substrate}}$$

The results of whole cell reaction for the conversion of different substrates to AFB<sub>1</sub> are presented in Table 18 (culture fluid fraction, page 94) and Table 19 (pellet fraction, page 96). The time course for the biotransformation of ST and ST derivatives to AFB<sub>1</sub> in the culture fluid fraction and pellet fraction is graphically presented in Figure 81 (page 95) and Figure 82 (page 97), respectively. Typical chromatograms are presented in Figure 83-85 (Appendix 41-43, page 270-272).

Table 18. The Conversion of Selected Substrates to AFB<sub>1</sub> in the Culture Fluid Fraction of Whole Cells of *A. parasiticus* (Wh1-11-105).

Time (minutes)	Substrate (0.770 $\mu$ mol)	Integrated Peak Area	AFB <sub>1</sub> Produced ( $\mu$ g/100ml)	AFB <sub>1</sub> Produced ( $\mu$ g/assay)	% Conversion to AFB <sub>1</sub>
15	ST	21698	0.068	6.8	2.83
30	ST	79152	0.227	22.7	9.48
45	ST	139056	0.394	39.4	16.41
60	ST	163852	0.463	46.3	19.28
90	ST	189304	0.534	53.4	22.23
120	ST	279877	0.786	78.6	32.71
150	ST	280890	0.789	78.9	32.83
15	OMST	31150	0.094	9.4	3.93
30	OMST	43983	0.130	13.0	5.41
45	OMST	122538	0.348	34.8	14.50
60	OMST	225950	0.636	63.6	26.47
90	OMST	280604	0.788	78.8	32.79
120	OMST	311360	0.873	87.3	36.35
150	OMST	355024	0.995	99.5	41.40
15	OEST	26514	0.081	8.1	3.39
30	OEST	134445	0.381	38.1	15.88
45	OEST	173330	0.489	48.9	20.38
60	OEST	258902	0.727	72.7	30.28
90	OEST	298831	0.838	83.8	34.90
120	OEST	350038	0.981	98.1	40.83
150	OEST	353288	0.990	99.0	41.20
15	OPROST	36587	0.109	10.9	4.56
30	OPROST	153729	0.435	43.5	18.11
45	OPROST	189304	0.534	53.4	22.23
60	OPROST	274770	0.772	77.2	32.19
90	OPROST	341369	0.957	95.7	39.82
120	OPROST	356479	0.999	99.9	41.57
150	OPROST	377748	1.057	105.7	44.03
15	OBzST	19913	0.063	6.3	2.63
30	OBzST	28066	0.086	8.6	3.57
45	OBzST	35757	0.107	10.7	4.46
60	OBzST	48357	0.142	14.2	5.92
90	OBzST	63131	0.183	18.3	7.63
120	OBzST	77938	0.224	22.4	9.34
150	OBzST	85362	0.245	24.5	10.20

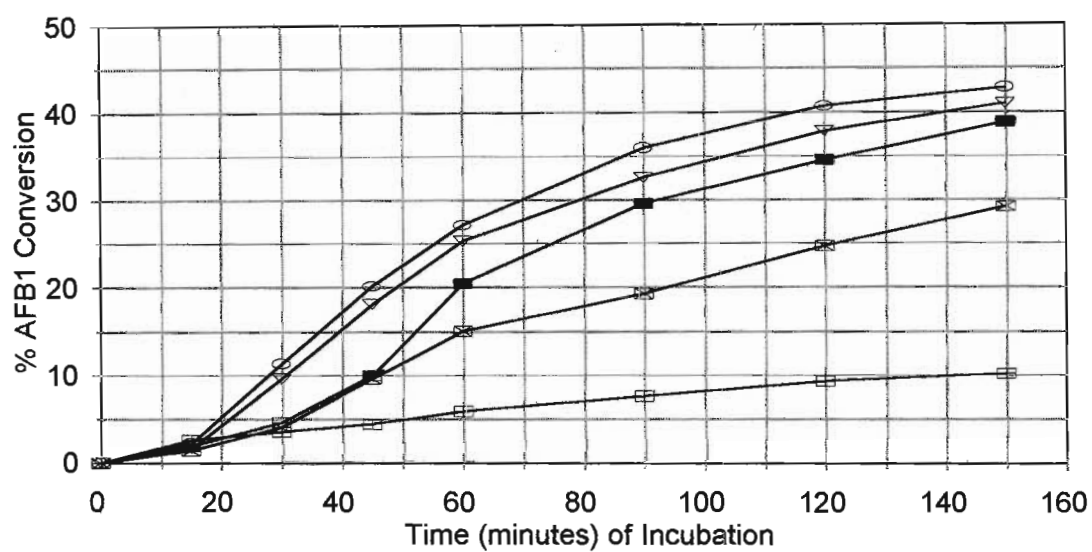


Figure 81. Time Course for the Biotransformation of ST and ST Derivatives to AFB<sub>1</sub> in the Culture Fluid Fraction.

**KEY:** OPROST (O); OEST (V); OMST (■); ST (⊗); OBzST (□)

Table 19. The Conversion of Selected Substrates to AFB<sub>1</sub> in the Pellet Fraction of Whole Cells of *A. parasiticus* (Wh1-11-105).

Time (minutes)	Substrate (0.770 $\mu$ mol)	Integrated Peak Area	AFB <sub>1</sub> Produced ( $\mu$ g/100ml)	AFB <sub>1</sub> Produced ( $\mu$ g/assay)	% Conversion to AFB <sub>1</sub>
15	ST	16486	0.017	1.7	2.23
30	ST	18515	0.059	5.9	2.47
45	ST	23222	0.072	7.2	3.01
60	ST	26086	0.080	8.0	3.34
90	ST	28349	0.087	8.7	3.60
120	ST	34344	0.103	10.3	4.30
150	ST	40692	0.121	12.1	5.03
15	OMST	12085	0.041	4.1	1.72
30	OMST	25245	0.078	7.8	3.24
45	OMST	34247	0.103	10.3	4.29
60	OMST	39466	0.117	11.7	4.89
90	OMST	50282	0.148	14.8	6.14
120	OMST	53557	0.157	15.7	6.52
150	OMST	56654	0.165	16.5	6.88
15	OEST	14546	0.048	4.8	2.09
30	OEST	21157	0.067	6.7	2.77
45	OEST	39009	0.116	11.6	4.84
60	OEST	47693	0.141	14.1	5.84
90	OEST	54316	0.159	15.9	6.61
120	OEST	64586	0.187	18.7	7.79
150	OEST	77221	0.222	22.2	9.26
15	OPROST	8049	0.030	3.0	1.26
30	OPROST	22268	0.069	6.9	2.90
45	OPROST	30771	0.093	9.3	3.88
60	OPROST	43488	0.128	12.8	5.36
90	OPROST	60192	0.175	17.5	7.29
120	OPROST	79733	0.229	22.9	9.55
150	OPROST	83718	0.241	24.1	10.01
15	OBzST	1325	0.011	1.1	0.48
30	OBzST	6875	0.027	2.7	1.12
45	OBzST	13587	0.046	4.6	1.89
60	OBzST	15842	0.052	5.2	2.15
90	OBzST	19719	0.063	6.3	2.60
120	OBzST	28019	0.086	8.6	3.56
150	OBzST	31562	0.096	9.6	3.97

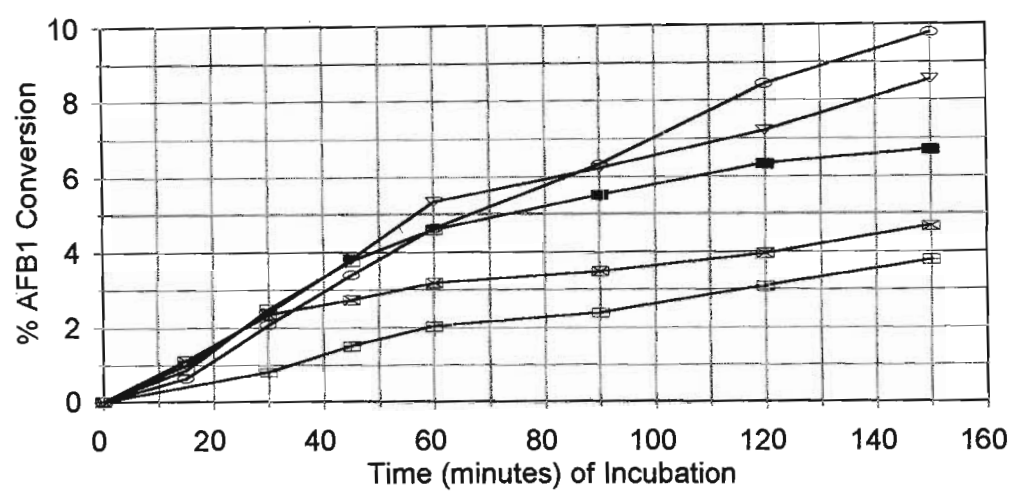


Figure 82. Time Course for the Biotransformation of ST and ST Derivatives to AFB<sub>1</sub> in the Pellet Fraction.

**KEY: OPROST (O); OEST (V); OMST (■); ST (⊗); OBzST (□)**

The data presented in Table 18 (page 94) and 19 (page 96) shows that the five substrates were converted to AFB<sub>1</sub> but they differ either in their sensitivity to enzymatic attack or are influenced by other experimental factors. The results from both the culture fluid and mycelial fractions indicate a general decrease in the rate of conversion in the order :



During the first 45 minutes of reaction, as indicated by Figures 81 and 82, there is no clear indication of a difference in AFB<sub>1</sub> conversion when ST and OMST are used as substrates, however; for a longer reaction time (> 60 minutes) there appears to be a significant difference in the conversion. The relatively slower conversion of ST to AFB<sub>1</sub>, compared to OMST as substrate, suggests that ST has to undergo an *in vivo* methylation step to OMST followed by subsequent enzymatic transformation to form AFB<sub>1</sub>.

Studies<sup>102,103</sup> have shown that electron donating alkyl groups present on a substrate can affect the catalysis of enzymes generally by increasing the rate of conversion to products. It may be possible that a similar event is occurring in this case, although the trend is reversed in that the hydroxyl group of ST is more electron donating than the alkyl groups of ST derivatives. Although the propyl group of ST, by inductive effects, is more electron donating than the other alkyl ST derivatives, it is unlikely that such minor contributions will account for the differences in the percentage conversion to AFB<sub>1</sub>.

It seems much more likely that there is a permeability effect with the uptake of the compounds through the fungal membrane even though the addition of acetone to the fungal system used in previous studies<sup>95</sup> gave satisfactory results. As the propyl derivative is the least polar of the derivatives it might be able to penetrate the cell membrane more easily and thus reach the active site for conversion to AFB<sub>1</sub>. Based on this reasoning it is not surprising that the benzoyl derivative, being the most polar derivative, is converted to AFB<sub>1</sub> at a much slower rate. The enzymatic reaction profile of OBzST, unlike the other substrates, appears to be linear thereby suggesting that a longer incubation time is required for higher conversion. Hence the effect being measured may be one of membrane permeability rather than enzyme specificity. For this reason a quantitative study was not made of the kinetics of whole cell feeding experiments. The fact that all the derivatives



were converted, however, reveals that the “enzyme” involved in the conversion of ST to AFB<sub>1</sub> are non specific as far as the alkyl side chain is concerned.

The transformation of ST and ST derivatives to AFB<sub>1</sub> has served several purposes:

- it is proof that enzymatic activities are present in the aflatoxigenic strain
- it confirms that the aflatoxin pathway branches at the end since only AFB<sub>1</sub> was detected in the transformation experiments
- it denotes that these enzymes do not distinguish between exogenous and endogenous precursors
- moreover it confirms the role of ST and OMST as late intermediates in the aflatoxin pathway

This study, however, does not resolve the question as to whether the alkylation of ST to OMST is obligatory in the biosynthesis of AFB<sub>1</sub>. Therefore further investigations are required to determine whether the permeability of the substrates is a negative factor or not. One solution is to prepare a crude “enzyme”, containing the enzymatic activity for the conversion of the substrates to AFB<sub>1</sub>, and under optimum enzymatic conditions to undertake a time course study of selected substrates.

## CHAPTER SEVEN

### ENZYMATIC CONVERSION OF STERIGMATOCYSTIN DERIVATIVES USING CELL-FREE EXTRACTS

#### 7.1. INTRODUCTION

Nearly all of the evidence in support of the biosynthetic pathway of aflatoxins has been obtained from isotopic and chemical analysis with whole mycelia or crude cell-free preparations. The individual steps in the pathway, and their mechanisms could only be conclusively proved by isolating and studying the enzymes present in the fungi.

In the study of primary metabolism, many cell-free systems and pure enzyme preparations have been used successfully. These techniques, however, have not been greatly employed in the study of secondary metabolism mainly because of the low levels of enzymes involved and the difficulty in purifying these secondary metabolic enzymes<sup>171</sup>. Such isolation is achieved physically, by “killing” and fragmenting the cells and wherever possible by fractionating the cell debris. Certainly, procedures designed to give cell-free preparations active in secondary biosynthetic processes have often proved difficult because some systems require integrated association of enzymes which are sensitive to membrane disruption.

Of the secondary metabolic enzymes studied, those involved in the biosynthesis of patulin have had considerable research centred on them. Basset and Tanenbaum<sup>171</sup> obtained the first cell-free extract capable of converting glucose acetyl CoA and 6-methylsalicylate to patulin. Lynen and Tada<sup>172</sup> obtained a similar system, which required the presence of NADPH, and speculated that a multi-enzyme complex was involved.

The first cell-free biosynthesis of aflatoxins was reported by Raj *et al.*<sup>173</sup>. These researchers found that labelled acetate, mevalonate and leucine were incorporated into AFB<sub>1</sub>. Yao and Hsieh<sup>174</sup>, using a cell-free system, suggested that the enzymes responsible for AFB<sub>1</sub> biosynthesis were located in the mitochondrial fraction, whilst Singh and Hsieh<sup>46</sup> proposed

that the conversion of ST to AFB<sub>1</sub> was carried out in the cytoplasm by an oxygenase, although no attempt was made to isolate the “enzyme” or intermediates involved.

Anderson and Dutton<sup>48</sup> found that a cell-free system derived from *A. flavus* was capable of converting ST and versiconal acetate to AFB<sub>1</sub>. Anderson and Dutton<sup>167</sup> later showed that the conversion of VA to AFB<sub>1</sub> was pH dependent and supported the view that under the proper pH condition, VA is converted to versicolorin A hemiacetal.

Cleveland *et al.*<sup>7</sup>, in 1987, established that subcellular fractionation of *A. parasiticus* mycelia resolved two enzyme fractions involved in ST to AFB<sub>1</sub> conversion:

- a post microsomal supernatant fraction (containing a methyltransferase) catalysed the conversion of ST to OMST and
- a microsomal-associated activity (containing an oxido-reductase) catalysed conversion of OMST to AFB<sub>1</sub>.

Yabe *et al.*<sup>99</sup>, in 1989, demonstrated that two *O*-methyltransferases were involved in the latter part of the aflatoxin biosynthetic pathway. *O*-methyltransferase I was involved in the conversion of DMST to ST and DHDMST to DHST. *O*-methyltransferase II was involved in the conversion of ST to OMST and DHST to DHOMST. Bhatnagar *et al.*<sup>175</sup> subsequently reported a homogeneous preparation of *O*-methyltransferase II and a partially purified preparation of the oxido-reductase. Keller *et al.*<sup>170</sup>, in 1993, reported an almost homogenous preparation of *O*-methyltransferase I by a 5 step chromatographic procedure. Yabe *et al.*<sup>90</sup> recently reported a homogenous preparation of *O*-methyltransferase I from the cytosol fraction of the mycelia of *A. parasiticus* NIAH 26, through a series of chromatographic procedures.

The objective of the present investigation was to prepare an active cell-free system, i.e., a crude “enzyme” preparation which is able to convert ST to AFB<sub>1</sub>, and to optimise conditions, viz., pH and temperature for enzyme activity. Also a time course reaction was to be investigated to monitor the conversion of ST and selected ST derivatives to AFB<sub>1</sub>.

## **7.2. MATERIALS AND METHODS**

### **7.2.1. Chemicals**

All chemicals were purchased from Sigma Chemical Suppliers (SA). Reduced nicotinamide adenine dinucleotide phosphate (NADPH) and S-adenosyl methionine (SAM) were purchased from Boehringer Mannheim (Germany).

### **7.2.2. General**

A Controlled Environment Incubator Shaker (New Brunswick Scientific) was used for incubation experiments. Mycelia were stored at -85 °C in a Ultra Low Freezer (Nuaire). A Virtis Sentry Freeze Drier was used for freeze drying mycelia at -70 °C. Centrifugation was conducted in a Beckman Model J2-21 Centrifuge. High pressure liquid chromatography analysis was carried out with the diode array detector. Ultra-violet data were obtained from a Milton Roy Spectronic 601 spectrophotometer. Mass measurements were made by means of a Mettler TG 50 Thermobalance.

### **7.2.3. Culture and Culture Conditions**

An aflatoxin blocked mutant of *A. parasiticus* (Wh1-11-105) was maintained on PDA (Appendix 1, page 234) at 28 °C for 5-7 days. The spore suspensions were prepared by the method as described in Section 3.2.3. (page 37). Conventional aseptic techniques were applied to inoculate the spore suspensions (1 ml containing approximately  $10^6$  spores) into ten Erlenmeyer flasks (250 ml) containing sterile Reddy's medium<sup>67</sup> (100 ml) (Appendix 2, page 234). The Reddy's medium (one liter, in a 4 L Erlenmeyer flask) was autoclaved (140 °C, 20 psi) for 1 hour and cooled to room temperature prior to inoculation. The ten flasks were incubated at 28 °C in shake culture at 150 r.p.m. The flasks were removed after 96 hours.

#### **7.2.4. The Preparation of Cell-Free Extracts**

The mycelial pellets were harvested by vacuum filtration in a Buchner funnel through a double layered cheesecloth. The mycelia were rinsed thoroughly with ice cold 20 mM phosphate buffer (pH 7.2) (Appendix 44, page 273) and the excess wash solution was removed by vacuum filtration. The damp mycelial cake was freeze dried for 48 hours at -70 °C, transferred into an air tight container and stored in a freezer at -85 °C.

The dried mycelia (0.5 g) were gently ground to a fine powder in a dry, chilled pestle and mortar at 4 °C. The powdered mycelia was suspended in ice cold, 20 mM phosphate buffer (10 ml) and gently stirred for 15 minutes. The homogenate was centrifuged at 20 000 x g for 20 minutes at 4 °C. The resulting supernatant was filtered with glass wool and used as the cell-free extract.

#### **7.2.5. The Method Used for Enzyme Assays**

Enzyme activity was assayed by adding the cell-free extract (500 µl; final protein concentration 1 mg/ml) to the phosphate buffer (400 µl) (pH 7.5) in a 10 ml glass test tube. To the mixture was added NADPH (50 µl, 1.5 µmol) and/or SAM (50 µl, 1.5 µmol) to give a final concentration of 1.5 mM. The mixture was then incubated in the shaker at 27 °C and at 100 r.p.m for 5 minutes. Thereafter the enzymatic reaction was initiated by adding the substrates (30.86 nmol), dissolved in acetone (50 µl). The reaction was stopped after 1 hour by adding chloroform (3 ml).

The effect of cell-free extract protein concentration on the production of AFB<sub>1</sub> from ST was monitored at enzyme concentration of 0.5-3.0 mg/ml. The protein content of the cell-free extract was determined by the Bradford method<sup>176</sup> (Section 7.2.8., page 105).

During pH optima determinations, the pH of each assay buffer was varied from pH 6.4 to 7.6 and the reaction was carried out at 27 °C for 1 hour. Studies were carried out in triplicate.

For temperature optima determinations, the reaction temperature was varied from 22 °C to 32 °C and the reaction was carried out in the buffer solution (pH 7.2) for 1 hour. Studies were carried out in triplicate.

For the time course reaction, the reactions were carried out at 28 °C, pH 7.2 and a protein concentration of 1 mg/ml. All experiments were conducted in triplicate and the results are expressed as a mean, unless otherwise indicated.

After different incubation times, the reaction was stopped by adding chloroform (3 ml). The chloroform layer was separated from the aqueous portion by extraction. The extraction was repeated twice more with further chloroform (3 ml). The total extract was then dried over a bed of anhydrous sodium sulphate, filtered and evaporated to dryness under a stream of nitrogen gas and gentle heat.

#### **7.2.6. Qualitative Analysis by Thin Layer Chromatography**

The dried residue was reconstituted in chloroform (100 µl) and a 20 µl portion was spotted onto the origin of a t.l.c. plate (10 x 10 cm aluminium backed Kieselgel 60). The plate was developed in CEI, air dried and scanned for fluorescence under UV. The t.l.c. plates were then sprayed with aluminium chloride (20 %) and heated to test for the characteristic change in intensity and colour of fluorescence<sup>166,167</sup> under UV.

#### **7.2.7. Quantification by High Pressure Liquid Chromatography**

The dried residue was made to volume in acetonitrile (10 ml) and analysed by HPLC (250 x 4.6 mm C<sub>18</sub> Lichrosphere column) using a gradient elution program of water and acetonitrile (described in Chapter 5, page 83).

## **7.2.8. Determination of the Protein Content of the Cell-Free Extract**

### **7.2.8.1. Preparation of the Bradford Reagent**

Serva Blue G (25.00 mg) was dissolved in phosphoric acid (25 ml, 85 %, w/v). To this solution absolute ethanol (12 ml) was added and the solution thoroughly mixed<sup>176</sup>. This solution was accurately diluted with deionised water to a volume of 250 ml in a volumetric flask.

### **7.2.8.2. Preparation of the Protein Standard Calibration Graph**

Solution A: Ovalbumin (10.00 mg) was dissolved and made up to 10 ml in 0.15 M sodium chloride to give a standard solution containing 1 mg/ml protein. An aliquot (1 ml) was diluted to 10 ml with a 0.15 M sodium chloride solution to give a solution containing 100 µg/ml protein.

Typical procedure: Solution A (100 µl) was added to the Bradford reagent (5ml). The mixture was vortexed and allowed to stand for 2 minutes. The solution was then transferred to glass cuvettes and its absorbance measured at  $A_{595}$  using 0.15 M sodium chloride as a blank. Similarly standard solutions of ovalbumin were prepared in the concentration range 20-100 µg/ml. The UV data obtained for the calibration graph of protein is presented in Table 20 (Appendix 45, page 274). A standard calibration curve was plotted from quintuplicate assays (Figure 86, Appendix 46, page 274). The protein content of the cell-free extract was determined as described above.

### 7.3. RESULTS AND DISCUSSION

The results reported in Chapter 6 indicated that in whole cell studies, ST and its derivatives were subject to, at different extents, a permeability effect, i.e., the cell wall and cell membrane serve as barriers between the culture fluid and the cytoplasm. The reasoning is based on the fact that each compound has different polarities, as indicated e.g., in their migration on t.l.c. plates (Table 4, page 50). Thus the actual rate of conversion could not be compared because of the time delay to penetrate the barrier in order to reach the active enzyme site. Thus to obviate this problem, an investigation was undertaken to prepare an active cell-free system and to examine the time course reaction with selected ST derivatives.

In order to disrupt the cell wall and hence prepare an active cell-free extract, the freeze dried mycelia were gently ground at 4 °C, using a pestle and mortar, transferred into the buffer solution and stirred gently. The mixture was then centrifuged to remove any debris and insoluble particulates. The supernatant, after filtration, was used as the cell-free extract. It must be mentioned that when the ground mycelia was vigorously stirred in the buffer, the solution started to “froth” and was subsequently found to be inactive, i.e., ST was not converted to AFB<sub>1</sub>. Also if the mycelia were not adequately freeze dried or properly stored, the cell-free extract was found to be inactive. One other point, which requires mentioning, is that the freeze dried mycelia could be stored for a maximum of 1 month after which the activity of the “enzyme” decreased. Therefore it is advisable that cell-free extracts should be prepared from fresh mycelia.

The buffer solution, containing the disodium salt of ethylene diamine tetraacetic acid (1 mM), was reported to enhance enzymatic activity perhaps through inactivation of metal dependent proteases or by aiding the solubility of weakly membrane bound proteins<sup>73</sup>. Also glycerol (10 %) was added to support enzymatic activity.

The preparation of active cell-free extracts posed a problem because the “enzyme” were probably membrane bound and were easily disrupted, however, after several attempts the finer details of the technique of preparing active “enzyme” extract was learnt. Initial



investigations were carried out by using the enzymatic conditions reported by Singh and Hsieh<sup>46</sup>, i.e., temperature of 27 °C at pH 7.5 in the presence of 50 times more co-factors than the substrate.

Total protein concentration of the cell-free extract was determined by the Bradford method with ovalbumin as standard<sup>176</sup>. The standard calibration graph, presented in Figure 86 (Appendix 46, page 274) was obtained by measuring the absorbance of the protein at A<sub>595</sub>. Linear regression analysis of the data gave a  $r^2$  value of 0.85 thereby indicating a close to linear relationship between the two variables.

It was necessary to dilute the cell-free extract in order to obtain an absorbance reading which falls within the range of the calibration graph. The effect of cell-free extract protein concentration, from 0.5 to 3.0 mg/ml, on the conversion of ST to AFB<sub>1</sub> is presented in Table 21 (page 108). The results of this investigation are presented graphically in Figure 87 (page 108). A typical chromatogram is presented in Figure 88 (Appendix 47, page 275).

The metabolites were quantified by HPLC using the diode array detector. The quantity of AFB<sub>1</sub>, produced by the cell-free reaction, was calculated by using the integrated peak area of the chromatogram and a back-fit straight line equation from the calibration graph of AFB<sub>1</sub> (Figure 58, Appendix 35, page 265). The % conversion of ST to AFB<sub>1</sub> was calculated by means of the formula:

$$\% \text{ conversion of ST to AFB}_1 = [(\mu\text{mol AFB}_1 \text{ produced}) / (\mu\text{mol substrate added})] \times 100$$

Linear regression analysis of the data (Table 21, page 108) gave a  $r^2$  value of 0.98 thereby indicating a close to linear relationship between the two variables, viz., cell-free extract protein concentration and quantity of AFB<sub>1</sub> produced. The best fit straight line graph is presented in Figure 87 (page 108). Singh and Hsieh<sup>46</sup> reported a curvilinear response, for a similar investigation, and suggested that this was possibly due to a reduced oxygen supply. This result confirms that a true enzyme catalysed reaction was occurring inspite of the small quantities of substrate involved.

Table 21. The Effect of Cell-Free Extract Protein Concentration on the Conversion of ST (10 µg) to AFB<sub>1</sub> in Cell-Free Extracts, in the Presence of NADPH (1.5 mM) and SAM (1.5 mM), at pH 7.5 and 27 °C for an Incubation Time of 1 Hour.

Enzyme Protein (mg/ml)	Integrated Peak Area	AFB <sub>1</sub> Produced (ng/10 ml)	AFB <sub>1</sub> Produced (µg/ml)	% Conversion to AFB <sub>1</sub>
0.5	27204	112	1.12	11.63
1.0	58210	250	2.50	25.96
1.5	76799	328	3.28	34.06
2.0	98744	420	4.20	43.61
2.5	120102	510	5.10	52.96
3.0	128392	545	5.45	56.60

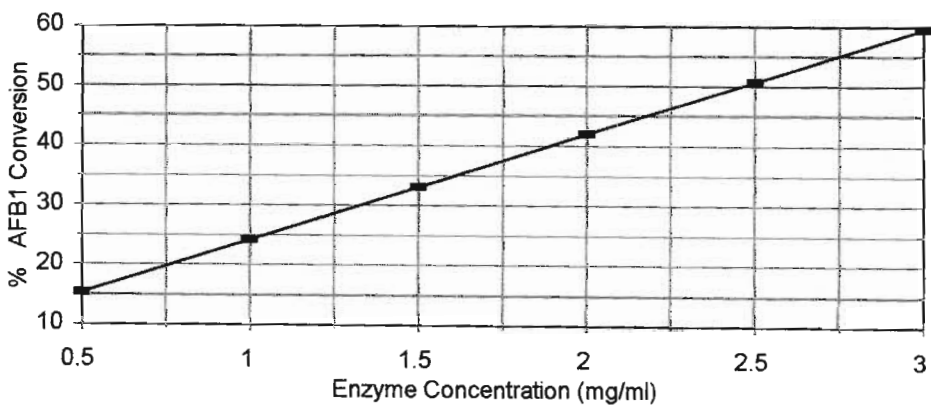


Figure 87. The Effect of Cell-Free Extract Protein Concentration on the Conversion of ST to AFB<sub>1</sub> at pH 7.5 and 27 °C for an Incubation Time of 1 Hour.

A previous study<sup>46</sup> showed that the “enzyme” present in the cell-free extract depended on two factors viz., the pH of the solution and the temperature of incubation. Thus it was essential that these factors be optimised to give the best conversion results for the cell-free extract. The results for an investigation of pH in the range 6.4 to 7.6 is presented in Table 22 (page 109) and graphically presented in Figure 89 (page 110). Typical chromatograms are presented in Figures 90-91 (Appendix 48-49, page 276-277).

In this investigation the highest conversion of ST to AFB<sub>1</sub> (23.68 %) was recorded at pH 7.2. There was a decrease in the activity of the enzyme above and below pH 7.2 and a narrow pH range was evident which seemed to follow the typical “bell shaped” curve of many enzyme systems. The sensitivity of the enzyme system towards small pH changes may be accounted for by the removal of the insulating effect of the membrane and thus the internal buffering capacity of the cytoplasm. It thus appears that slightly alkaline pH seems to be a general characteristic of enzymes involved in the biosynthesis of fungal metabolites, e.g. a pH optimum<sup>177</sup> of 7.5 was required for the mixed function oxidase involved in patulin biosynthesis and pH 7.8 was found to be the optimum<sup>178</sup> for the biosynthesis of 6-methyl-salicylic acid.

Table 22. The Effect of pH of Incubation on the Conversion of ST (10 µg) to AFB<sub>1</sub> in Cell-Free Extracts, in the Presence of NADPH (1.5 mM) and SAM (1.5 mM) at 27 °C for an Incubation Time of 1 Hour.

Incubation pH	Integrated Peak Area	AFB <sub>1</sub> Produced (ng/10 ml)	AFB <sub>1</sub> Produced (µg/assay)	AFB <sub>1</sub> Produced (µg/assay) <sup>a</sup>	% Conversion to AFB <sub>1</sub>
6.8	9378	45	0.45	0.43 ± 0.08	4.47
	6731	34	0.34		
	10423	49	0.49		
7.0	22098	98	0.98	1.17 ± 0.16	12.15
	29505	129	1.29		
	28034	123	1.23		
7.1	41462	179	1.79	1.69 ± 0.11	17.55
	39074	169	1.69		
	36322	158	1.58		
7.2	47915	207	2.07	2.28 ± 0.27	23.68
	60177	258	2.58		
	50756	219	2.19		
7.3	30850	135	1.35	1.27 ± 0.13	13.19
	30656	134	1.34		
	25485	112	1.12		
7.4	8116	39	0.39	0.47 ± 0.11	4.88
	9260	44	0.44		
	13107	60	0.60		

<sup>a</sup>Values for AFB<sub>1</sub> represents the mean and standard deviation of experiments conducted in triplicate.

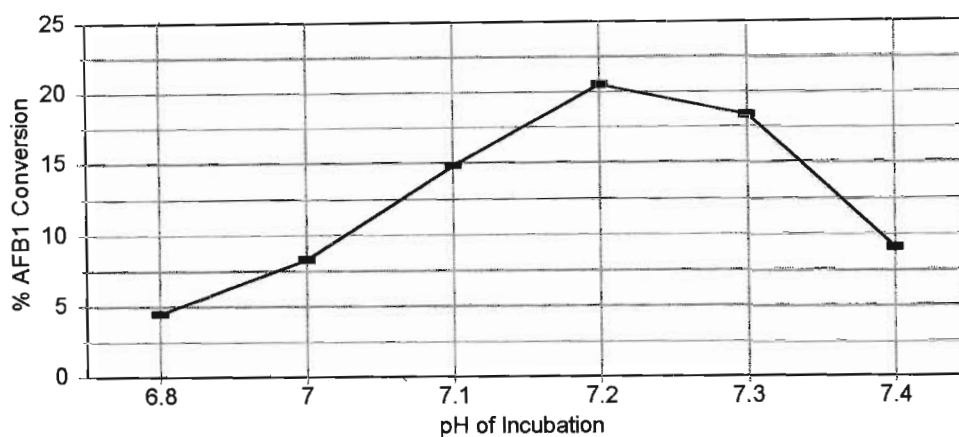


Figure 89. The Effect of pH of Incubation for the Enzymatic Conversion of ST to AFB<sub>1</sub> at 27 °C for an Incubation Time of 1 Hour. The Enzyme Concentration is 1 mg/ml.

Having determined the pH for optimum conversion of ST to AFB<sub>1</sub> by the cell-free extract, a study was undertaken to determine the optimum temperature, at pH 7.2, for optimum enzyme activity. The results obtained are presented in Table 23 (page 111) and Figure 92 (page 112) graphically presents the effect of temperature of incubation on the conversion of ST to AFB<sub>1</sub>. A typical chromatogram is presented in Figure 93 (Appendix 50, page 278).

Table 23. The Effect of Temperature of Incubation on the Conversion of ST (10  $\mu$ g) to AFB<sub>1</sub> in Cell-Free Extracts, in the Presence of NADPH (1.5 mM) and SAM (1.5 mM) at pH 7.2 for an Incubation Time of 1 Hour.

Incubation Temperature	Integrated Peak Area	AFB <sub>1</sub> Produced (ng/10 ml)	AFB <sub>1</sub> Produced ( $\mu$ g/assay)	AFB <sub>1</sub> Produced ( $\mu$ g/assay) <sup>a</sup>	% Conversion to AFB <sub>1</sub>
24	16141	73	0.73	0.75 $\pm$ 0.11	7.79
	19467	87	0.87		
	14093	64	0.64		
26	27246	120	1.20	1.32 $\pm$ 0.13	13.71
	33407	146	1.46		
	29577	130	1.30		
27	54630	235	2.35	2.51 $\pm$ 0.14	26.07
	59835	257	2.57		
	60574	260	2.60		
28	73199	313	3.13	3.13 $\pm$ 0.15	32.50
	69293	297	2.97		
	76711	328	3.28		
29	68199	292	2.92	2.75 $\pm$ 0.26	28.56
	56923	244	2.44		
	67452	289	2.89		
30	43277	187	1.87	2.04 $\pm$ 0.19	21.18
	46319	200	2.00		
	52229	225	2.25		
32	36728	160	1.60	1.76 $\pm$ 0.19	18.28
	45843	198	1.98		
	38901	169	1.69		

<sup>a</sup>Values for AFB<sub>1</sub> represents the mean and standard deviation of experiments conducted in triplicate.

It is apparent that the “enzyme” system is very sensitive to temperature change as it was found that a change of temperature by  $\pm 1$  °C caused a substantial change in the percentage of conversion of ST to AFB<sub>1</sub>. This is understandable since the “enzyme” system had become directly exposed to the environment by the removal of the protective cell wall and cell membrane.

It was found that the best conversion of ST to AFB<sub>1</sub> (32.50 %) was recorded at 28 °C and pH 7.2. This result compares favourably with an investigation by Singh and Hsieh<sup>46</sup> who reported a cell-free reaction at 27 °C with an optimum pH between 7.5-7.8. These researchers, however, did not determine the best pH for optimum enzyme activity which implies that investigations undertaken in our laboratory are more reliable.

Cleveland *et al.*<sup>7</sup> reported an optimum enzyme activity:

- for a post microsomal supernatant enzyme fraction at pH 8.0-8.5 and 35- 40 °C and
- for a microsomal enzyme fraction at pH 7.0 and 17- 23 °C.

In the case of these experiments a total crude extract was used so no distinction between free and membrane bound “enzyme” was made. Since in these investigations the optimum enzyme activity for the conversion of ST to AFB<sub>1</sub> was found to occur at pH 7.2 and 28 °C, all subsequent enzymatic reactions (Chapters 7, 8, 9 and 10) were conducted under these conditions of pH and temperature.

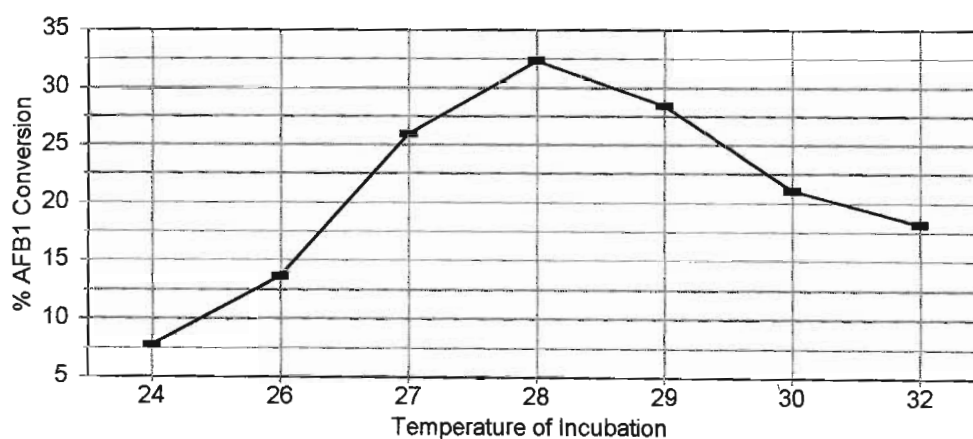


Figure 92. The Effect of Temperature of Incubation for the Enzymatic Conversion of ST to AFB<sub>1</sub> at pH 7.2 for an Incubation Time of 1 Hour.

Thus having optimised conditions for the enzymatic conversion of ST to AFB<sub>1</sub> in cell-free extracts, it was decided to investigate the presence of endogenous co-factors, viz., SAM and NADPH. This was necessary since the centrifugation process, in the preparation of the cell-free extract, had previously been reported<sup>46</sup> to have stopped the regeneration of the co-factors into the required form i.e.  $\text{NADP}^+ \rightarrow \text{NADPH}$  and



The data for the study is presented in Table 24 (page 113) and is graphically presented in Figure 94 (page 113). A typical chromatogram is presented in Figure 95 (Appendix 51, page 279).

Table 24. The Effect of the Addition of Co-Factors on the Conversion of ST (10 µg) to AFB<sub>1</sub> in Cell-Free Extracts, in the Presence of Co-Factors (1.5 mM) at pH 7.2 and 28 °C for an Incubation Time of 1 Hour.

Co-Factors Added (1.5 mM)	Integrated Peak Area	AFB <sub>1</sub> Produced (ng/10 ml)	AFB <sub>1</sub> Produced (µg/assay)	AFB <sub>1</sub> Produced (µg/assay) <sup>a</sup>	% Conversion to AFB <sub>1</sub>
NONE	23030	102	1.02	1.08 ± 0.09	11.21
	26112	115	1.15		
SAM	29733	130	1.30	1.32 ± 0.03	13.71
	30627	134	1.34		
NADPH	31379	137	1.37	1.49 ± 0.16	15.47
	36874	160	1.60		
SAM + NADPH	56003	241	2.41	2.61 ± 0.28	27.10
	65303	280	2.80		

<sup>a</sup>Values for AFB<sub>1</sub> represents the mean and standard deviation of experiments conducted in duplicate.

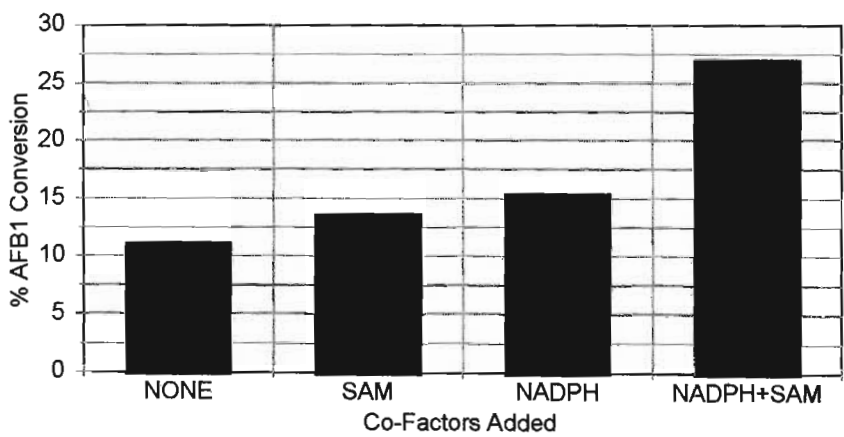


Figure 94. The Effect of the Addition of Co-Factors (1.5 mM) on the Conversion of ST to AFB<sub>1</sub> in a Cell-Free Extract at pH 7.2 and 28 °C for an Incubation Time of 1 Hour.

It was not surprising to find that ST was converted to AFB<sub>1</sub> (11.21 %) by the cell-free reaction even without the addition of exogenous co-factors thereby confirming earlier reports<sup>46</sup>. This meant that either the centrifugation step, in the preparation of the cell-free extract, did not completely stop the regeneration of these two co-factors or the reaction might be able to proceed slowly from ST to AFB<sub>1</sub> without these co-factors. However, the most likely proposition is the former since it has been shown by research teams<sup>7,175</sup> that an oxido-reductase, which requires NADPH, is involved in the enzymatic reaction. Although

the percentage conversion of ST to AFB<sub>1</sub> was low (11.21 % versus 27.10 %) without the addition of exogenous co-factors, this result indicates the presence of SAM and NADPH in the cell-free extract. The enhancement is greater by the addition of NADPH (15.47 % conversion to AFB<sub>1</sub>) than SAM (13.71 % conversion to AFB<sub>1</sub>) but greatest when both are added (27.10 % conversion to AFB<sub>1</sub>). Lower conversion rates as compared to other experiments reported here, are due to variation in the activity of the cell-free extract. As mentioned earlier (page 106), the freeze dried mycelia lose enzyme activity on storage and therefore it is important that enzymatic reactions with cell-free extract be carried out with freshly prepared mycelia. For the experiments reported in this study it was not practically possible because of the large number of samples which was required to be analysed by HPLC, with the Spectra Physics System, since this instrument was shared amongst other research teams.

Thus having found that the percentage conversion to AFB<sub>1</sub> increased with the addition of SAM and NADPH, all subsequent cell-free reactions were conducted by adding an excess of these exogenous co-factors, i.e., 50 times more than the substrate, unless their effect was being investigated.

A time course study with selected substrates, viz. ST, OMST and OPROST, was undertaken to determine whether the results of the time course study (discussed in Chapter 6) was in part a measure of membrane permeability. The results of the time course reaction of cell-free extracts are presented in Table 25 (page 115) and graphically presented in Figure 96 (page 116). Typical chromatograms are presented in Figure 97-98 (Appendix 52-53, page 280-281).



Table 25. The Conversion of Selected Substrates (30.86 nmol) to AFB<sub>1</sub> in Cell-Free Extracts, in the Presence of NADPH (1.5 mM) and SAM (1.5 mM) at pH 7.2 and 28 °C.

Substrate Added	Time (minutes)	Integrated Peak Area	AFB <sub>1</sub> Produced (ng/10 ml)	AFB <sub>1</sub> Produced (μg/assay)	AFB <sub>1</sub> Produced (μg/assay) <sup>a</sup>	% Conversion to AFB <sub>1</sub>
ST	15	10782	51	0.51	0.5 ± 0.15	5.19
		7163	35	0.35		
		14116	65	0.65		
ST	30	23765	105	1.05	0.89 ± 0.23	9.24
		13507	62	0.62		
		23003	101	1.01		
ST	45	42365	183	1.83	1.67 ± 0.15	17.34
		35036	152	1.52		
		38357	166	1.66		
ST	60	58358	251	2.51	2.56 ± 0.19	26.58
		55887	240	2.40		
		64869	278	2.78		
OMST	15	6953	34	0.34	0.55 ± 0.21	5.71
		11850	55	0.55		
		16502	75	0.75		
OMST	30	25234	111	1.11	1.23 ± 0.21	12.77
		25244	111	1.11		
		33644	147	1.47		
OMST	45	42259	183	1.83	1.99 ± 0.18	20.67
		45223	195	1.95		
		50920	219	2.19		
OMST	60	60514	260	2.60	2.66 ± 0.07	27.62
		61790	265	2.65		
		63870	274	2.74		
OPROST	15	6425	32	0.32	0.44 ± 0.12	4.57
		12357	57	0.57		
		8676	42	0.42		
OPROST	30	14504	66	0.66	0.63 ± 0.13	6.54
		16566	75	0.75		
		10432	49	0.49		
OPROST	45	26600	117	1.17	1.08 ± 0.08	11.21
		22777	101	1.01		
		24296	107	1.07		
OPROST	60	27435	121	1.21	1.59 ± 0.56	16.51
		30347	133	1.33		
		52007	224	2.24		

<sup>a</sup>Values for AFB<sub>1</sub> represents the mean and standard deviation of experiments conducted in triplicate.

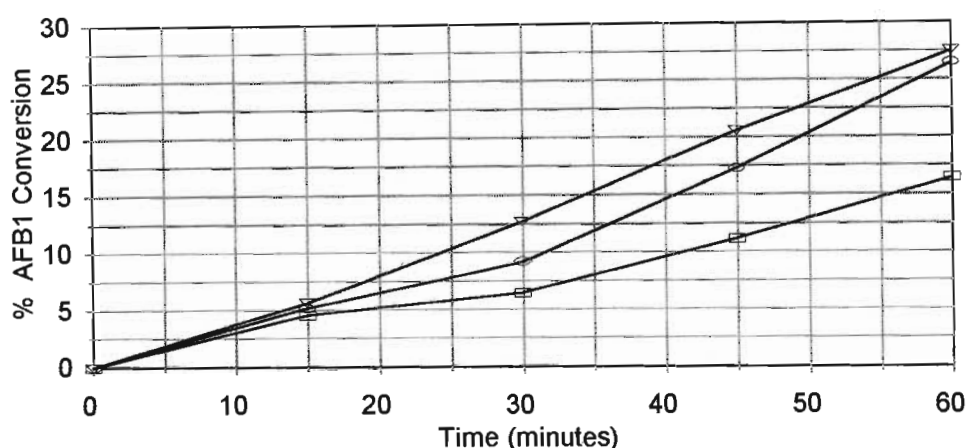


Figure 96. The Conversion of ST, OMST and OPROST to AFB<sub>1</sub> in a Cell-Free Extract, in the Presence of NADPH (1.5 mM) and SAM (1.5 mM) at pH 7.2 and 28 °C.

KEY: ST (o); OMST( ∇ ); OPROST(□)

The results of this investigation provide clear evidence for an enzymatic conversion of ST, OMST and OPROST to AFB<sub>1</sub> and hence confirms that OMST is a definite metabolite in the AFB<sub>1</sub> biosynthetic pathway. Under the experimental condition, the rate of conversion is close to linear for up to 60 minutes of incubation. Cleveland and Bhatnagar<sup>98</sup>, in an investigation with the partially purified “enzyme”, reported that the enzyme catalysed reaction was linear for up to 2 hours of incubation. On inspection of the reaction profile it appears that the enzymatic reactivity of OPROST is slower than ST and OMST. There is a possibility that the conditions were optimised for the overall conversion of ST to AFB<sub>1</sub> and may not be ideal for the conversion of OMST and OPROST to AFB<sub>1</sub>. However, if the above reasoning is not true and conditions are equally suited for all three substrates, then the results of this study is contrary to the findings made in the preceding Chapter, viz., the approximate rate, in decreasing order, was given as:

$$\text{OPROST} > \text{OMST} \cong \text{ST}$$

The results of this investigation indicates an approximate rate, in decreasing order, as:

$$\text{OMST} \cong \text{ST} > \text{OPROST}$$

These results would thus confirm that the time course reaction using whole cells (Chapter 6) was in part a measure of membrane permeability rather than substrate specificity. Therefore it may be concluded that the more rapid conversion of OPROST, observed in whole cell experiments (Chapter 6), were due to its higher hydrophobicity and ability to penetrate the membrane quicker than the other ST derivatives. Also the results of this investigation confirms the conclusion made in the previous Chapter, viz., the enzymatic system is non specific to the different alkyl functional groups. The results may also indicate that the groups are good leaving groups and hence may not affect the ring cleavage process.

It seems as if steric effects play a negligible part in the formation of the enzyme-substrate complex and may be influenced by some form of electron-displacement effects. If such is the case then interaction of the substrate with the enzyme system must take place in a part of the molecule remote from the ether group of ST. The most likely form of such interaction subject to polar influences is hydrogen bonding between the hydrogen accepting groups in ST and hydrogen in the enzyme. A question which arises is whether an electron donating alkyl group is able to activate the aromatic ring to such an extent so as to enhance subsequent oxidation and ring cleavage?

It should be mentioned that the substrate specificity of the enzyme, i.e., either the enzyme is displaying relative specificity or an *O*-alkyl ST derivative is an obligatory intermediate between ST and AFB<sub>1</sub>, is not clearly evident in this study. This is because the cell-free extracts contains sub-optimal concentrations of endogenous co-factors which are used for the conversion of substrate to product. The conversion of OPROST to AFB<sub>1</sub>, although at a slower rate, also clouds the issue. Two explanations are possible: either the "enzyme" responsible for the conversion exhibit relative specificity whereby a series of ST derivatives can be converted to AFB<sub>1</sub> but at different rates; or all the derivatives are converted to a common intermediate, e.g., ST, prior to conversion. The former hypothesis is favoured from these results which is in keeping with certain secondary metabolic enzymes, i.e., relative specificity.

As long as the co-factors SAM and NADPH are present in the crude “enzyme” preparation, the role of OMST as a metabolite in the AFB<sub>1</sub> biosynthetic pathway, i.e., either it is part of a metabolic grid or a compulsory metabolite, cannot be established. Therefore the total elimination of indigenous co-factors from the crude “enzyme” preparation and hence control of the enzymatic reaction, by the addition of exogenous co-factors and substrates, would give a better understanding of enzyme specificity and the role of OMST in the AFB<sub>1</sub> biochemical pathway.

## CHAPTER EIGHT

### PARTIAL PURIFICATION OF THE CELL-FREE EXTRACT AND ITS ENZYMATIC REACTION

#### 8.1. INTRODUCTION

There are numerous methods available for the purification of enzymes from crude extracts. These include fractional precipitation with ammonium sulphate, ion exchange chromatography and molecular exclusion chromatography.

As mentioned earlier (page 101), Cleveland *et al.*<sup>7</sup> reported that fractionation of the cell-free extract gave two crude enzyme fractions, viz., a methyl transferase and an oxido-reductase which catalysed the conversion of ST to OMST and OMST to AFB<sub>1</sub>, respectively. Subsequently Bhatnagar *et al.*<sup>100</sup> reported a homogenous preparation of the methyltransferase by a scheme involving a cellulosic weak anion exchanger, chromatofocusing and fracto-gel filtration chromatography. Attempts, by the same research team, to purify the oxido-reductase were unsuccessful due to the rapid degeneration of the enzyme(s). However, Bhatnagar *et al.*<sup>175</sup> reported the preparation of a non-homogenous oxido-reductase by a scheme involving a cellulosic weak anion exchanger, ammonium sulphate precipitation, ion-exchange and fracto-gel filtration chromatography.

Since one of the objectives in this study was to separate the enzymatic protein from smaller molecules in particular indigenous co-factors that could influence the course of an enzyme catalysed reaction, molecular exclusion chromatography was chosen since it is a simple and efficient method. In this method the separating mechanism is dependant on differences in molecular size of the solute. The partitioning of the solute molecules occurs between the stationary phase (gel beads) and the mobile phase (buffer solution). Since large molecules are excluded from the stationary phase to a greater extent, the order of elution from the chromatographic column is therefore in order of decreasing molecular size.

In view of the small differences in sensitivity exhibited by the substrates, viz., ST, OMST and OPROST as represented by the time course reaction (Chapter 7, Figure 96, page 116), it seemed desirable to ascertain whether the conversion of several of these substrates is affected by a single enzyme or by a number of closely related enzymes present in the cell-free extract. Therefore, the removal of primary and secondary metabolites, co-factors and small biomolecules from the cell-free extract would allow the effects of added substrates and co-factors to be assayed against no background reactions. This would allow the determination of the role of OMST in the AFB<sub>1</sub> biosynthetic pathway i.e., either it is a compulsory intermediate in the conversion of ST to AFB<sub>1</sub> or one of a set of related substrates displaying the enzyme catalysis effect known as relative specificity.

## **8.2. MATERIALS AND METHODS**

### **8.2.1. General**

Ultra-violet data were obtained from a Milton Roy Spectronic 601 spectrophotometer. A Controlled Environment Incubator Shaker (New Brunswick Scientific) was used for enzymatic reactions. A Beckman Model J2-21 Centrifuge and a Virtis Sentry Freeze Drier were also used.

### **8.2.2. Chemicals**

Sephadex G-25, of particle size 100-300 microns, was purchased from Pharmacia Fine Chemicals (SA). Dialysis tube ( i.d. 10 mm ; molecular weight retention >10000 ) and all other chemicals were purchased from Sigma Chemical Suppliers (SA). The Ordinary protein marker was purchased from Combitek Co.(SA).

### **8.2.3. Preparation of Sephadex Gel**

Using the bed volume of 5 ml per gram dry gel, the mass of Sephadex was calculated and 36 grams was weighed and added to phosphate buffer (200 ml)(Appendix 44, page 273). The buffer was stirred gently and the resulting slurry was heated in a boiling water bath for one hour to de-aerate the gel. The gel was kept undisturbed for 24 hours to effect final swelling of the beads.

### **8.2.4. Preparation of the Column for Chromatography**

A glass column (280 mm x 33 mm) was packed with the swollen gel. The packed column was equilibrated with phosphate buffer (400 ml) at a flow rate of 30 ml per hour. The cell-free extract (6 ml) (preparation is described in Section 7.2.5, page 103) was applied directly to the column and then eluted with buffer at a flow rate of 25 ml per hour at 4°C. Fractions (1.5 ml) were collected in glass test tubes (10 ml) and then transferred into glass

cuvettes. The protein content of each fraction was monitored at  $A_{280}$  nm by a UV spectrophotometer and the active fractions pooled (see results and discussion).

#### **8.2.5. The Method of Dialysis for Concentrating the Enzyme**

The dialysis tubing (2 m length) was soaked for 24 hours in deionised water after which the pooled active “enzyme” fractions (obtained as above) were transferred into the tubing. This was placed in solid sucrose for 3 hours at 4 °C. The concentrated protein solution containing the enzyme activity (250 µg/ml) was used in conversion experiments.

#### **8.2.6. The Method Used for Enzyme Assays**

The concentrated enzyme protein fraction (250 µg/ml) was tested for activity with 30.86 nmole of the substrates ST, OMST, OPROST, and OBzST (synthesis is described in Chapter 4) at pH 7.2 and 28 °C. In these experiments the effect of the addition of the co-factors NADPH (1.5 mM) and SAM (1.5 mM) were investigated.

The method used for the enzymatic reactions is described in Chapter 7 (page 103-104). The metabolites were extracted and dried as described on page 104. The dried residue was made to volume in acetonitrile (1 ml) and analysed by HPLC using a gradient elution program as described on page 83.

#### **8.2.7. The Method Used for Polyacrylamide Gel Electrophoresis**

The active partially purified enzyme were analysed by non-denaturing polyacrylamide gel electrophoresis (PAGE). The solutions required for this experiment is presented in Appendix 54 (page 282-283). The following procedure was followed:

The glass cells of the electrophoresis unit were cleaned with ethanol, dried and assembled in a vertical position. The lower ends were sealed with parafilm. The freshly prepared running gel solution was introduced into the tube to a level 3 cm from the top. The gel was overlaid with water and allowed to polymerise for 30 minutes. The water layer was then removed.



Freshly prepared stacking gel (0.25 ml) solution was overlaid on the running gel. The combs were placed in the sandwiches to cast lanes for the loading of the sample. The combs were removed and the wells rinsed with deionised water. Excess water was removed. The wells and upper chamber were filled with tank buffer. Samples (250  $\mu$ l) were mixed with treatment buffer (250  $\mu$ l) and bromophenol blue was added. Aliquots of 50-100  $\mu$ l of the sample were loaded into the wells.

Electrophoresis was performed at 30 mA/gel until the bromophenol front reached the bottom of the gel. The gels were removed intact and the separated protein bands stained for 6 hours. The protein bands were then destained in solution I (1 hr) and solution II (6 hours). The gels were then photographed.

### 8.3. RESULTS AND DISCUSSION

The chromatography technique, i.e., molecular exclusion chromatography does not represent a classical enzyme purification procedure because the enzyme of interest elutes in the void volume (discussed below). However, this technique was used since the objective was to remove the co-factors, viz., NADPH and SAM which were found in sub-optimal concentration in cell-free extracts.

Gel filtration was carried out with a Sephadex G-25 column and the protein content of each fraction, collected at 4 °C, was recorded at an absorbance of 280 nm by the UV spectrophotometer. A plot of fraction collected versus absorbance of protein at 280 nm for the separation of the protein from active cell-free extract by molecular exclusion chromatography is graphically presented in Figure 99. On examination of the profile, it seemed most likely that the pooling of fractions 9-17 would have given the correct fraction for the enzymatic conversion of ST to AFB<sub>1</sub>. These fractions were turbid, suggesting that the particles were extremely large, possibly because of conglomeration or the commonly de-salting out effects on the protein.

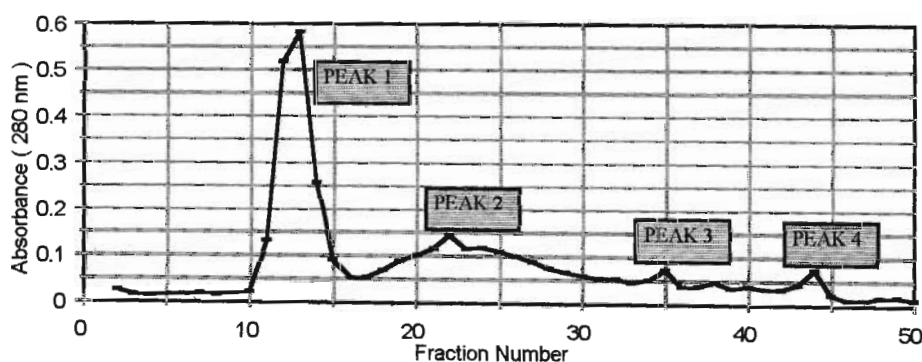


Figure 99. Protein Elution Profile after Separation of the Cell-Free Extract by Gel Chromatography with Sephadex G-25.

When the enzyme fraction 9-17 was incubated for 5 hours with the substrate ST, in the presence of the co-factors SAM and NADPH, it was found that no AFB<sub>1</sub> was produced. This was established by HPLC analysis of the metabolites. The experiment was repeated with a new batch of the enzyme fraction 9-17. A typical chromatogram is presented in Figure 100 (Appendix 55, page 284). This implied that either a crucial enzyme fraction

was missing or the “enzyme” system had lost its activity. It was therefore decided that the enzyme fraction 9-30 be pooled together and enzyme activity be investigated in the presence of NADPH and SAM. The results are presented in Table 26. The % conversion of ST and ST derivatives to AFB<sub>1</sub> was calculated by means of the formula:

$$\% \text{ conversion to AFB}_1 = [(\mu\text{mol AFB}_1 \text{ produced}) / (\mu\text{mol substrate added})] \times 100$$

It was found that although the conversion of ST to AFB<sub>1</sub> was low (3.22 %), the correct “enzyme” fraction was determined and this “enzyme” fraction (9-30) was therefore used for all subsequent enzymatic reactions.

Table 26 : The Conversion of ST (10  $\mu\text{g}$ ) to AFB<sub>1</sub> in Enzyme Fraction 9-30, in the Presence of NADPH (1.5 mM) and SAM (1.5 mM) at pH 7.2 and 28 °C for an Incubation Time of 5 Hours.

Integrated Peak Area	AFB <sub>1</sub> Produced (ng/ml)	AFB <sub>1</sub> Produced ( $\mu\text{g}/\text{assay}$ )	AFB <sub>1</sub> Produced ( $\mu\text{g}/\text{assay}$ ) <sup>a</sup>	% Conversion to AFB <sub>1</sub>
71269	304	0.30	0.31 $\pm$ 0.01	3.22
72569	310	0.31		

<sup>a</sup>Values for AFB<sub>1</sub> represents the mean and standard deviation of experiment conducted in duplicate.

It thus became apparent from the low conversion (3.22 % AFB<sub>1</sub>) that there was a loss of enzyme activity due to the lack of certain other factors, possibly metal ions, eg., iron, which were being removed by the chromatographic method. Also during the chromatographic separation procedure, the “enzyme” was diluted with the buffer solution thereby resulting in the protein and hence the “enzyme” undergoing to some extent denaturing effects. It was therefore decided that the enzyme fraction 9-30 would be concentrated to try and increase the percentage conversion of ST to AFB<sub>1</sub>.

The partially purified “enzyme” was subsequently concentrated by dialysis against solid sucrose<sup>23</sup> which would tend to remove excess water. Dialysis of the combined “enzyme” fraction 9-30 was conducted at 4 °C in order to minimize denaturing of the “enzyme”.

This dialysed fraction was subsequently tested for enzyme activity with exogenously added ST and co-factors. Also the dialysed “enzyme” fraction 9-30 was subjected to non-

denaturing PAGE and the bands compared to that of Ordinary protein marker. The crude enzyme fraction from chromatography (Figure 101) was found to represent many functional activities in secondary metabolism , i.e., units ranging from 26 kDa to over 200 kDa. Bhatnagar *et al.*<sup>100</sup> characterised the methyltransferase by SDS-PAGE and reported two sub-units of 58 kDa and 110 kDa. The authors were not able to purify the oxido-reductase to homogeneity since denaturing PAGE did not exhibit a single protein band. Analysis by SDS-PAGE revealed that the “enzyme” was found to exist as a multi sub-unit complex greater than 150 kDa.

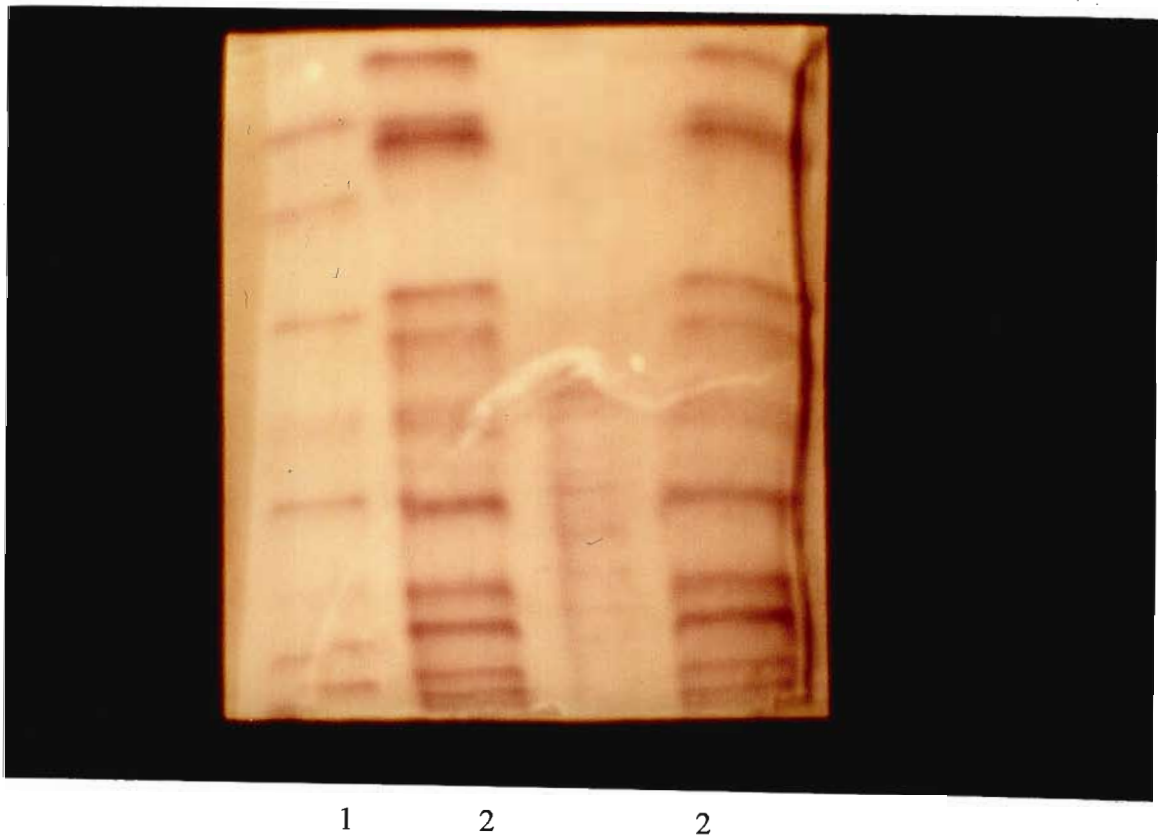


Figure 101. Polyacrylamide Gel Electrophoresis of the Partially Purified Enzyme(s) Fraction 9-30.

KEY: 1 = partially purified “enzyme”; 2 = Protein marker.

The results for the enzymatic conversion of ST to AFB<sub>1</sub>, using the dialysed “enzyme” fraction 9-30, is presented in Table 27. A typical chromatogram is presented in Figure 102 (Appendix 56, page 285).

Table 27. The Conversion of ST (10µg) to AFB<sub>1</sub> in Enzyme Fraction 9-30, After Dialysis, in the Presence of NADPH (1.5 mM) and SAM (1.5 mM) at pH 7.2 and 28 °C for an Incubation Time of 3 Hours.

Integrated Peak Area	AFB <sub>1</sub> Produced (ng/ml)	AFB <sub>1</sub> Produced (µg/assay)	AFB <sub>1</sub> Produced (µg/assay) <sup>a</sup>	% Conversion to AFB <sub>1</sub>
322431	1361	1.36	1.31 ± 0.08	13.61
295883	1249	1.25		

<sup>a</sup> Values for AFB<sub>1</sub> represents the mean and standard deviation of experiment conducted in duplicate.

It is clear from the increased percentage conversion of ST to AFB<sub>1</sub> (13.61 % versus 3.22 %), that the dialysis method with solid sucrose was an appropriate technique for concentrating the partially purified “enzyme” and for retention of enzyme activity. It must be mentioned that the chromatographic separation procedure, conducted at approximately 4 °C, was extremely time consuming bearing in mind that only 1 ml was finally obtained, after dialysis, for enzymatic reaction.

Further investigations were carried out with the substrate ST, by varying the two co-factors, to determine the intermediacy of OMST in the aflatoxin biochemical pathway. The results are presented in Table 28 (page 128). A typical chromatogram is presented in Figure 103 (Appendix 57, page 286).

Table 28. <sup>a</sup> The Enzymatic Reaction of ST (10 µg) in Enzyme Fraction 9-30 , After Dialysis, at pH 7.2 and 28 °C for an Incubation Time of 3 Hours.

Substrate (30.86 nmol)	Co-factors Added (1.5 mM)	% Conversion to AFB <sub>1</sub>
ST	None	ND
ST	SAM	ND
ST	NADPH	ND
ST (BOILED ENZYME)	SAM + NADPH	ND

<sup>a</sup> Enzymatic reaction conducted in duplicate.

ND = not detected

From these results it was concluded that :

- the separation by molecular exclusion chromatography removed the endogenous co-factors which were present in the cell-free extract. This is indicated by the absence of AFB<sub>1</sub> when no co-factors were added to the partially purified “enzyme” (Table 28).
- the reaction was enzyme mediated as shown by the absence of AFB<sub>1</sub> when the enzyme was boiled even though co-factors were added (Table 28).
- the transformation of ST to AFB<sub>1</sub> only occurs when both NADPH and SAM are added (Table 27).
- the intermediate OMST is a compulsory intermediate in the biosynthesis of ST to AFB<sub>1</sub>. This is indicated by the absence of AFB<sub>1</sub> in the enzymatic reaction when only NADPH was added to ST as substrate.

Thus it became clear that the enzymatic conversion of ST to AFB<sub>1</sub> could be promoted only by the addition of both exogenous co-factors SAM and NADPH. An interesting fact which emerged was that ST could not be converted to AFB<sub>1</sub> with the addition of exogenous NADPH alone, but only with a combination of SAM. This finding resolved the conflicting speculations with respect to OMST, i.e., either it is a true intermediate between ST and AFB<sub>1</sub> or part of a metabolic grid. It would appear that the oxido-reductase “enzyme”, present in the cell-free extract, has an active site which is unable to recognize the underivatised phenolic group. Therefore for ST to be converted to AFB<sub>1</sub>, the methyltransferase together with SAM must first transform the phenolic group of ST to a methyl ether derivative. This raised the question of whether methyl was the mandatory

alkyl group or whether other alkyl groups such as propyl could substitute. The latter seemed a likely proposition considering that in earlier investigations :

- the seven ST derivatives were converted to AFB<sub>1</sub> in whole cell reactions (Chapter 6) and
- the propyl derivative was converted to AFB<sub>1</sub> in cell-free extracts (Chapter 7).

An investigation was therefore undertaken to determine the specificity of the partially purified “enzyme” by using selected ST derivatives, viz., OMST, OPROST and OBzST, as substrates. An earlier investigation has shown that the endogenous co-factors were removed by molecular exclusion chromatography. Also other research teams<sup>7,175</sup> have reported the conversion of OMST to AFB<sub>1</sub> in the presence of NADPH. Therefore this study was undertaken to determine the specificity of the oxido-reductase in the presence of NADPH. The results of an investigation for the enzymatic conversion of selected ST derivatives to AFB<sub>1</sub> at 28 °C and pH 7.2, for a reaction time of 3 hours, is presented in Table 29. Typical chromatograms are presented in Figure 104-105 (Appendix 58-59, page 287-288).

Table 29. The Conversion of Selected Substrates (10 µg) to AFB<sub>1</sub> in Enzyme Fraction 9-30 , After Dialysis, in the Presence of NADPH (1.5 mM) at pH 7.2 and 28 °C for an Incubation Time of 3 Hours.

Substrate	Integrated Peak Area	AFB <sub>1</sub> Produced (ng/ml)	AFB <sub>1</sub> Produced (µg/assay)	AFB <sub>1</sub> Produced (µg/assay) <sup>a</sup>	% Conversion to AFB <sub>1</sub>
OMST	468573	1975	1.98	1.97 ± 0.02	20.46
OMST	462997	1952	1.95		
OPROST	897993	3780	3.78	3.77 ± 0.02	39.15
OPROST	891679	3754	3.75		
OBzST	72629	311	0.31	0.32 ± 0.01	3.32
OBzST	73703	315	0.32		

<sup>a</sup> Values for AFB<sub>1</sub> represents the mean and standard deviation of experiment conducted in duplicate.

From the results presented above, it can be concluded that all the derivatives, viz., OMST, OPROST and OBzST, were converted to AFB<sub>1</sub> in the presence of exogenously added

NADPH thereby suggesting that the “enzyme” displays relative specificity. There is no obvious answer to the question as to why ST has to be alkylated prior to conversion to AFB<sub>1</sub>. Usually free phenols are preferred substrates for oxygenase(s) involved in aromatic cleavage since *O*-alkyl ethers are more recalcitrant towards metabolic conversion.

It appears that the rate of conversion of the ST derivatives to AFB<sub>1</sub> follows the decreasing order :



The interesting observation was that OPROST is more rapidly converted than OMST itself, in these experiments, which is contrast to previous results with a crude cell-free extract (Chapter 7). Speculations on the reason(s) for these observations is as follows: the converting “enzyme” has a hydrophobic patch around the active site that recognises longer alkyl chains, e.g., propyl, better than shorter ones, i.e., methyl; or propyl is a better leaving group than methyl in the enzyme catalysed reaction, where the alkyl group is lost. Also from these experiments and previous investigations (Chapters 6 and 7) it is clear that the aryl derivative, viz., OBzST is not a favoured substrate for the “enzyme”.

From these conclusions, it is evident that the conversion of ST to AFB<sub>1</sub> in *A. parasiticus* is not simple. From the point of view of the simplest scheme, i.e., the principle of Ochaum’s Razor, ST should be directly converted to AFB<sub>1</sub> by the action of an appropriate oxygenase(s) as proposed in earlier schemes<sup>87</sup>. The proposal that methylation is a mandatory step in this sequence seems an unnecessary complication and it is tempting to suggest that this metabolite is a side shunt or at the best one of a series of substrates that can be converted by the oxygenase(s) exhibiting relative specificity. The discovery that other alkyl derivatives can also be converted to AFB<sub>1</sub> by whole cells and cell-free extracts supported the latter suggestion.

A proposed scheme (Figure 106, page 131) such as the following could be envisaged:



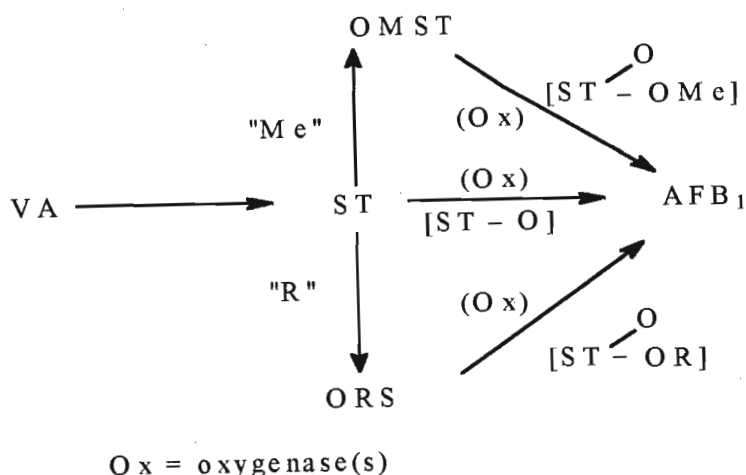
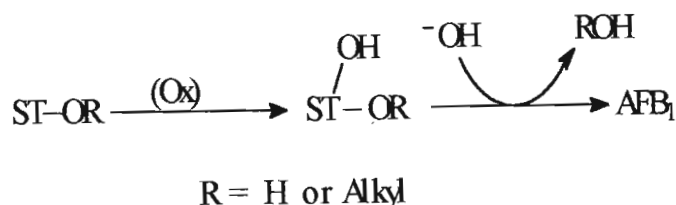


Figure 106. A Proposed Scheme for the Conversion of ST and ST Derivatives to AFB<sub>1</sub>.

The relative rates of the reactions would be controlled by affinity of substrate for enzyme and by suitability of the leaving group H<sup>+</sup> or R as presented by Reaction 1:



### Reaction 1

The finding that OMST is an obligatory intermediate as previously proposed<sup>5,7</sup> and more recently confirmed<sup>127</sup> by molecular biology investigation modifies Reaction 1 to Reaction 2:



### Reaction 2

In spite of the biochemically unsatisfying nature of reaction 2, the experiments done here strongly support it. However other questions are raised. Why must the fungi expend more energy by an additional methylation step? What is the nature of the oxygenase(s)? How do they function when the activating phenol group is methylated? Is there more than one

enzyme, e.g., a de-alkylating enzyme, an oxidase and a ring cleavage one? It is therefore obvious that further investigations are warranted to address some of these questions.

In summary, the partially purified “enzyme” system displays relative specificity for ST derivatives and the intermediate OMST is a compulsory metabolite for the conversion of ST to AFB<sub>1</sub> which occurs in the latter part of the biosynthetic pathway of aflatoxins. The results of this study are encouraging in that a suitable crude “enzyme”, from which indigenous co-factors have been removed, can be routinely prepared for studying the final stages of AFB<sub>1</sub> biosynthesis.

## CHAPTER NINE

### SYNTHESIS OF SIMPLE XANTHONES AND THEIR INHIBITION OF AFLATOXIN BIOSYNTHESIS

#### 9.1. INTRODUCTION

Among the various naturally occurring  $\gamma$ -pyrone derivatives such as flavanoids and chromones, xanthenes form an important class of compounds. The term xanthone designates the chemical compound dibenzo- $\gamma$ -pyrone (Figure 107).

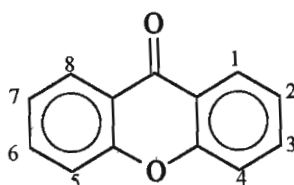


Figure 107. The Structure of the Xanthone Nucleus.

The parent substance is almost colourless and does not, so far as it is known, occur in nature. However, many of its oxygenated derivatives such as 1,5-dihydroxyxanthone and 1,7-dihydroxyxanthone have been isolated from natural sources, including medicinal plants<sup>179,180</sup>.

During the past thirty years, a large number of xanthenes have been isolated from the higher plants. The reviews by Roberts<sup>181</sup> in 1961 and by Dean<sup>182</sup> in 1963 refer to the natural occurrence of twelve xanthenes in higher plants and four xanthenes which have been described as fungal metabolites. In 1968, Gottlieb<sup>183</sup> reported the isolation of six xanthenes from higher plants and seven xanthenes as fungal metabolites. In 1969, Carpenter *et al.*<sup>184</sup> listed eight xanthenes from higher plants. The importance of their work on the isolation and synthesis of naturally occurring xanthenes has also been recognised and communicated in a review by Sultanbawa<sup>185</sup>.

Surveys of the structures of a large number of naturally occurring xanthenes indicate that such compounds contain from one to five hydroxy and/or methoxy groups<sup>183,184</sup>. Although the xanthone nucleus contains only four different locations for substituents, these being duplicated symmetrically, even with just five hydroxy and/or methoxy groups to place around the periphery, one is faced with numerous possible structures. Looking at the structures of such xanthenes, it becomes clear that selectivity and orientation control would be a major problem in the synthesis of xanthenes. It simplifies matters somewhat, that while each benzene ring in a xanthone interacts strongly with the central pyrone nucleus, there seems little transmission of effects across this nucleus from one benzene ring to the other. The xanthone nucleus is normally stable to both acids and bases. The stronger acids merely protonate the carbonyl oxygen atom (reversibly) giving hydroxyxanthylum salts.

A number of methods have been recommended for the synthesis of xanthenes. A review by Roberts<sup>181</sup> is an excellent source of information on general methods for the synthesis of xanthenes that appeared in the literature up to 1960. Subsequently, a few more methods have also been recommended for the purpose.

The methods used for the synthesis of the xanthone derivatives may be broadly classified into three groups involving:

- (I) condensation of *o*-hydroxybenzoic acid derivatives with reactive phenols
- (II) cyclisation of 2,2'-dihydroxybenzophenone derivatives and  
2,3'-dihydroxybenzophenone derivatives
- (III) approaches, which are different to those given under I and II.

The methods included under I, which are used for the synthesis of xanthenes, refer mainly to the synthesis of xanthenes by Grover *et al.*<sup>186</sup>. The reaction involves condensation of a salicylic acid derivative and a suitable phenol by utilising acid catalysed experimental conditions. This method by far enjoys the greatest popularity<sup>187,188</sup>. The substrates are heated together with zinc chloride in phosphorus oxychloride. Reaction times vary from 0.5 to 24 hours. In a few cases polyphosphoric acid has been preferred to the zinc chloride mixture<sup>187,188</sup>.

The reaction by Grover *et al.*<sup>186</sup> provides a variety of simple polyhydroxyxanthenes and their ethers which are not unduly sensitive to acids. The methoxy group is usually stable unless they occupy position 1 or 8 in the final xanthone, in which case they tend to be lost, as they would be from any other *o*-alkoxycarbonyl compound and hence mixtures may be produced. Sometimes the solvent, i.e., phosphorus oxychloride, is omitted from the reaction conditions so as to raise the reaction temperature above 60 °C. This is comparatively an older technique and is known as the Nencki reaction<sup>189</sup>. One of the disadvantages of the Nencki reaction is that demethylation of the methoxy group occurs as the reaction components are heated with zinc chloride at higher temperatures (above 180 °C).

Recently Nevreker *et al.*<sup>190</sup> suggested the use of an effective reaction medium containing equimolar quantities of phosphorus oxychloride and phosphoric acid (producing polymeric phosphoric acid) in the presence of anhydrous zinc chloride. For optimal condensation of *o*-hydroxybenzoic acid derivatives with reactive phenols to give xanthenes in better yields, a reaction temperature of 110 °C was used. The reaction medium had an advantage over the one suggested by Grover *et al.*<sup>186</sup>, as the former could be employed for condensation of *o*-hydroxybenzoic acid with reactive phenols at even higher temperatures (above 60 °C) to give 1-hydroxyxanthone derivatives in better yields. It also had an advantage over Nencki's method since it can be used at higher temperatures thereby keeping the reaction medium homogeneous.

As the synthesis of simple xanthenes was required in this study, the reaction conditions suggested by Nevreker *et al.*<sup>190</sup> were adopted. It has been mentioned in the literature review (Section 2.8, page 29) that much research has focused on inhibition studies using synthetic and natural products. However, the effect of simple xanthenes on AFB<sub>1</sub> production has not been researched. This therefore prompted an investigation into the study of xanthenes. The objective of synthesising simple substituted xanthenes was to generate compounds that could compete with the natural xanthone substrate OMST, produced by *A. parasiticus*, for the enzyme site and hence determine their inhibitory and other metabolic effects.

There are various ways to regulate enzyme activity, viz., through chemical modification of the enzyme, control of enzyme synthesis and degradation. A mode of enzyme regulation that has been useful to biochemists studying enzymes is inhibition which is the decrease in enzyme activity caused by the binding of a molecule (an inhibitor) to the enzyme.

Many different kinds of molecules can inhibit enzymes and they act in a variety of different ways. There are two classes of inhibition, viz., reversible and irreversible inhibition. In the case of reversible inhibition the inhibitor forms non-covalent bonds with the enzyme. In this form of inhibition the catalytic action of the enzyme can be restored by removing the inhibitor. In the case of irreversible inhibition the inhibitor forms covalent bonds with the enzyme which results in permanent change to the enzyme.

There are various types of reversible inhibition and they differ in the mechanisms by which they decrease the enzyme's activity and how they affect the kinetics of the reaction. In competitive inhibition the inhibitor closely resembles the substrate and therefore occupies the enzyme active site. For whatever fraction of time the inhibitor occupies the active site, the enzyme is unavailable for catalysis. In competitive inhibition the enzyme can transform the substrate to products whereas the inhibitor remains unchanged (Figure 108).

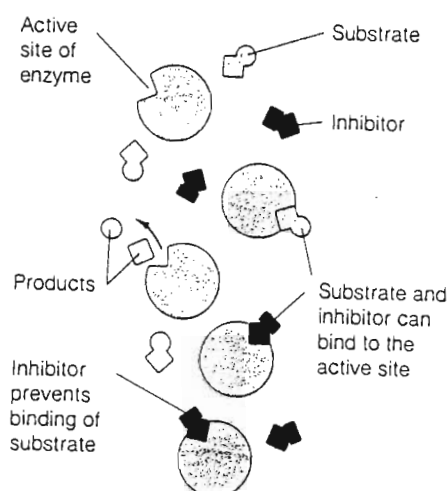
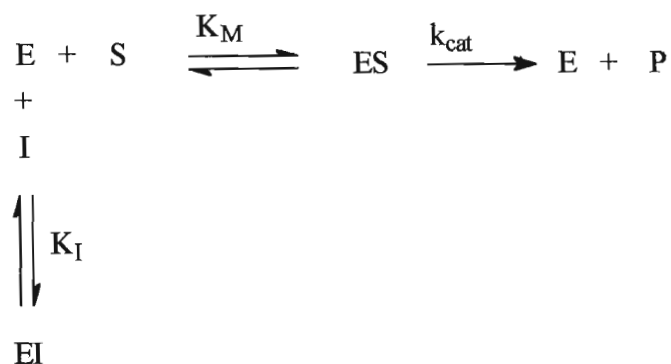


Figure 108. The Effect of the Inhibitor on the Enzyme in Competitive Inhibition<sup>191</sup>.

The reaction scheme<sup>191</sup> for competitive inhibition is written as :



where I represents the inhibitor, E is the enzyme, S is the substrate, ES is the enzyme-substrate complex,  $K_M$  is termed the Michaelis constant and  $K_I$  is the dissociation constant for inhibitor binding which is expressed as :

$$K_I = [\text{E}] [\text{I}] / [\text{EI}]$$

where [I] is the concentration of the free inhibitor.

For the reaction :

$$[\text{E}]_t = [\text{E}] + [\text{ES}] + [\text{EI}]$$

Total	Free	Enzyme	Enzyme
Enzyme	Enzyme	bound to	bound to
		Substrate	Inhibitor

The rate equation<sup>191</sup> is written as :

$$\begin{aligned}
 V &= \frac{k_{\text{cat}} [\text{E}]_t [\text{S}]}{[\text{S}] + K_M} \\
 &= \frac{V_{\text{max}} [\text{S}]}{[\text{S}] + K_M}
 \end{aligned}$$

where V represents the reaction velocity.

The effect of competitive inhibition is presented graphically in Figure 109. A plot of  $V$  versus  $S$  shows that the addition of inhibitor causes a decrease in the rate but  $V_{\max}$  at high substrate concentration does not change. Also the  $K_M$  is higher in the presence of the inhibitor. The Line-Weaver Burk plot ( $1/V$  versus  $1/S$ ) is a linear graph which clearly shows that  $K_M$  is changed by the inhibitor.

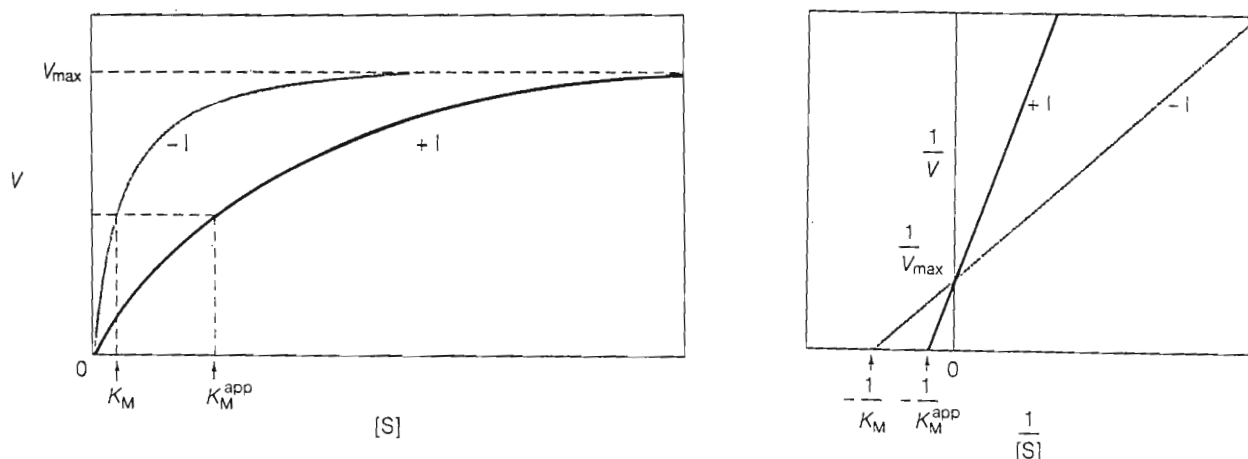


Figure 109. Effects of Competitive Inhibition on Enzyme Kinetics<sup>191</sup>.

In the case of non-competitive inhibition the molecule or ion binds to a second site on the enzyme (not the active site) in such a way that it modifies  $k_{\text{cat}}$  (Figure 110).

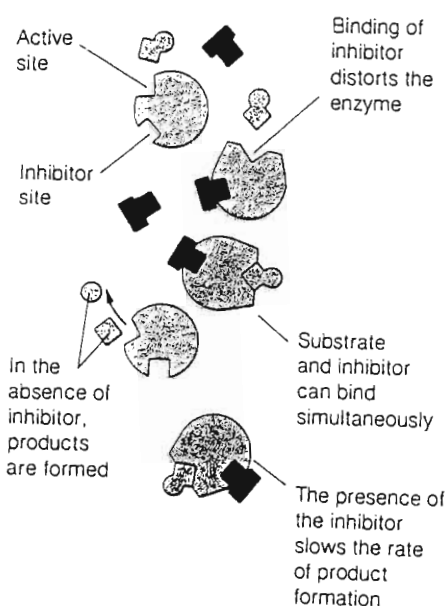
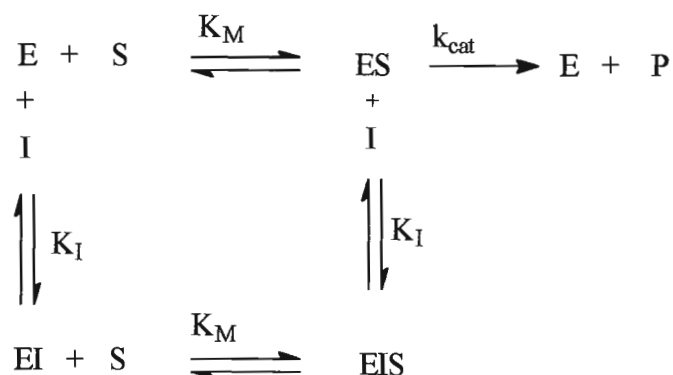


Figure 110. The Effect of the Inhibitor on the Enzyme in Non-Competitive Inhibition<sup>191</sup>.



Such an inhibitor does not resemble the substrate at all but has a strong affinity for a second binding site. In this type of inhibition the inhibitor binds equally well with the enzyme and the enzyme-substrate complex.

The reaction scheme<sup>191</sup> for non-competitive inhibition is written as :



The rate equation is written as :

$$\begin{aligned}
 V &= \frac{\{k_{\text{cat}}/(1 + [\text{I}] / K_I)\}[\text{E}]_t [\text{S}]}{[\text{S}] + K_M} \\
 &= \frac{k_{\text{cat}} [\text{E}]_t [\text{S}]}{[\text{S}] + K_M}
 \end{aligned}$$

The effect of non-competitive inhibition is presented graphically (Figure 111, page 140). The apparent  $K_M$  is not influenced by the inhibitor but  $V_{\text{max}}$  is decreased because the enzyme is not as catalytically efficient in the presence of the inhibitor.

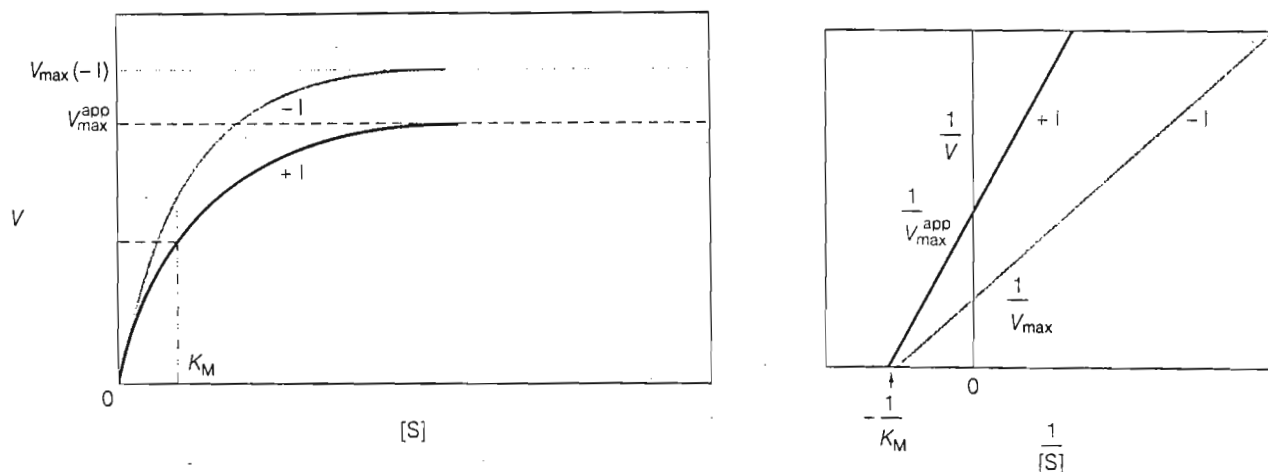


Figure 111. The Effect of Non-Competitive Inhibition on Enzyme Kinetics<sup>191</sup>.

In the case of uncompetitive inhibition the molecule binds only to the enzyme-substrate complex (Figure 112).

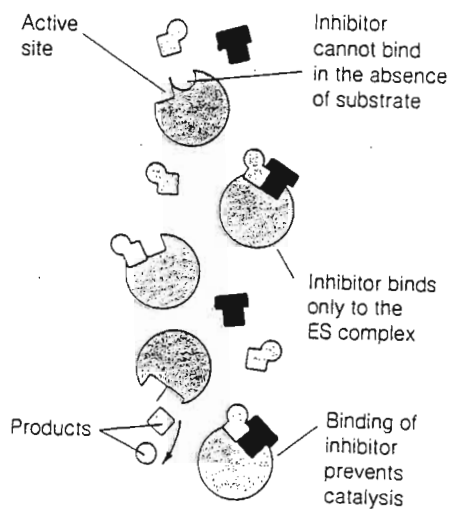
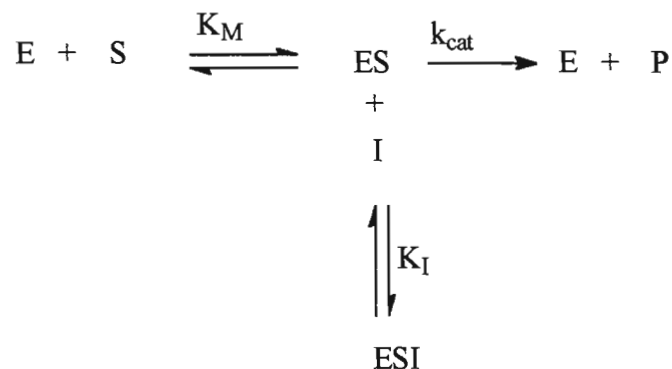


Figure 112. The Effect of the Inhibitor on the Enzyme in Uncompetitive Inhibition<sup>191</sup>.

The reaction scheme<sup>191</sup> for uncompetitive inhibition is written as :



The effect of uncompetitive inhibition is presented graphically (Figure 113). Since the inhibitor effectively “siphons off” some of the enzyme-substrate complex, this leads to a decrease in  $K_M$  in the presence of the inhibitor. Also  $V_{\text{max}}$  decreases because the enzyme is not catalytically efficient in the presence of the inhibitor.

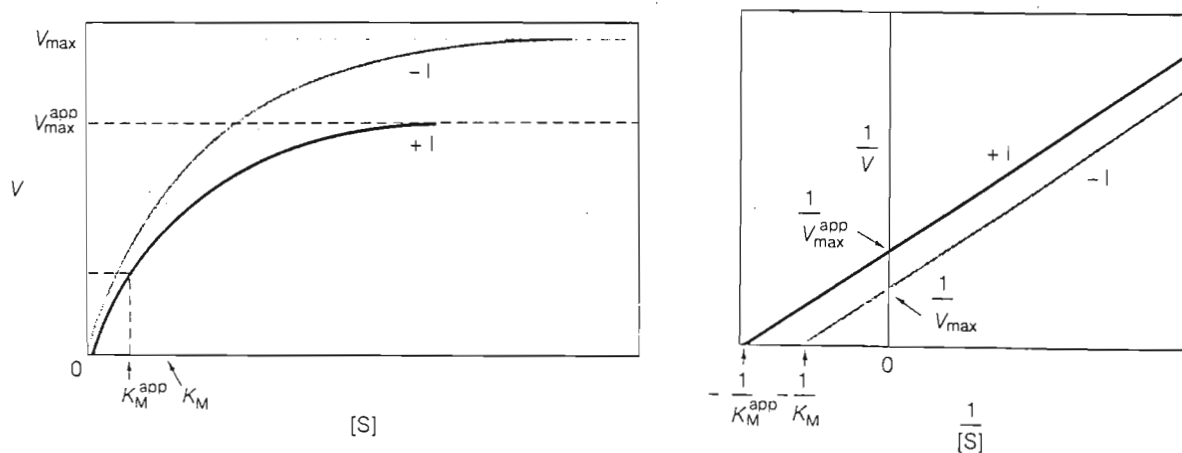


Figure 113. The Effect of Uncompetitive Inhibition on Enzyme Kinetics<sup>191</sup>.

To begin with, this study was initiated by selecting four simple xanthenes which could be synthesised by known synthetic methods. The four xanthenes were 1-methoxyxanthone (1), 1,8-dimethoxyxanthone (2), 1,6,8-trimethoxyxanthone (3) and 1-methoxy-3,6-dimethyl-xanthone (4) (Figure 114). Each of the four compounds contain the xanthone nucleus and the methoxy functional group thereby showing some resemblance in structure to the natural metabolite produced by *A. parasiticus*, viz., OMST.

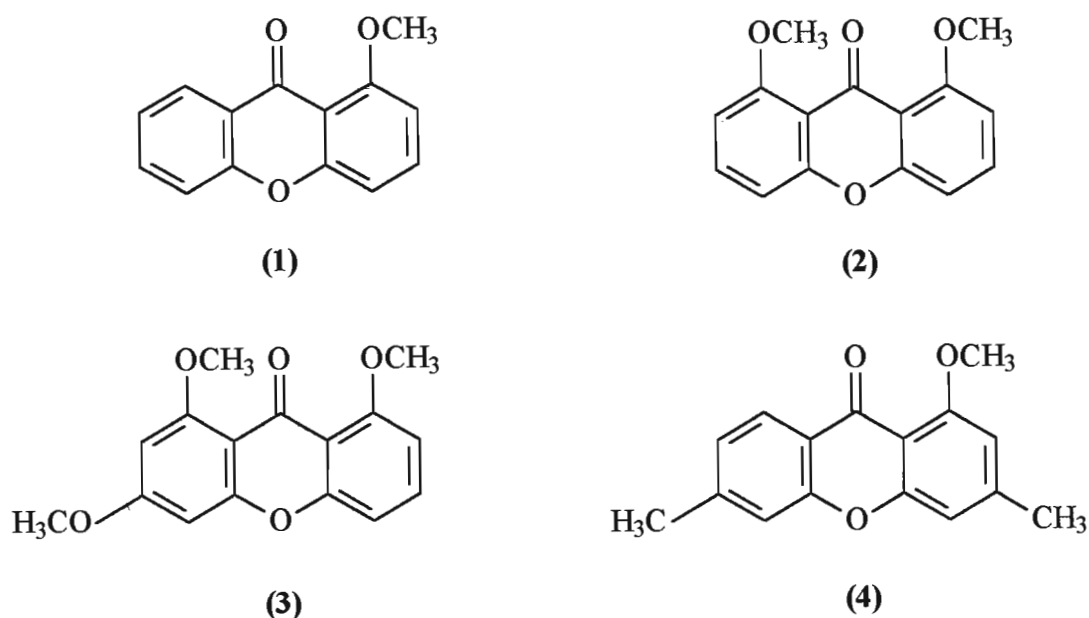


Figure 114. The Structures of Four Simple Xanthenes.

The method by Patel and Trivedi<sup>192</sup> was selected for the synthesis of 1-hydroxyxanthone (7) (Figure 115, page 143) which could thereafter be methylated by a modified Williamson synthesis (described in Section 4.2.3., page 47) to form 1-methoxyxanthone (1). The formation of 1-hydroxyxanthone is a one-pot reaction involving the thermal condensation of 4-hydroxyphenol (5) with ethyl salicylate (6). This method of synthesis was initially chosen as it seemed to be a quick and simple reaction and this would have been advantageous if industrial scale production was required once the compound was found to be an effective inhibitor. The scheme for the reaction is presented in Figure 115 (page 143). The formation of (7) is rather unusual and can be explained by a mechanism shown in Figure 116 (page 144).

Transesterification of ethyl salicylate with 4-hydroxyphenol results in the formation of 4'-hydroxyphenyl salicylate (**8**) which undergoes thermal Fries rearrangement giving 2,5,2'-trihydroxy benzophenone (**9**). This is followed by transformation involving free radicals generated at high temperature to give the 1-hydroxyxanthone.

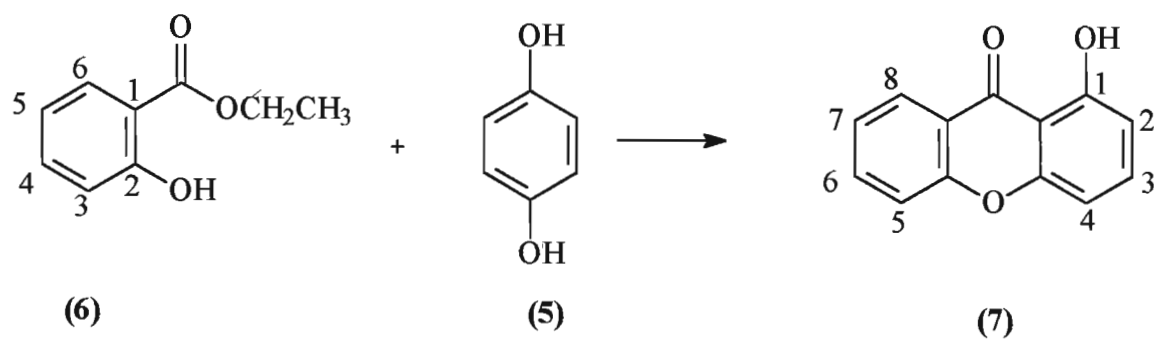


Figure 115. The Reaction Scheme for the Synthesis of 1-Hydroxyxanthone.

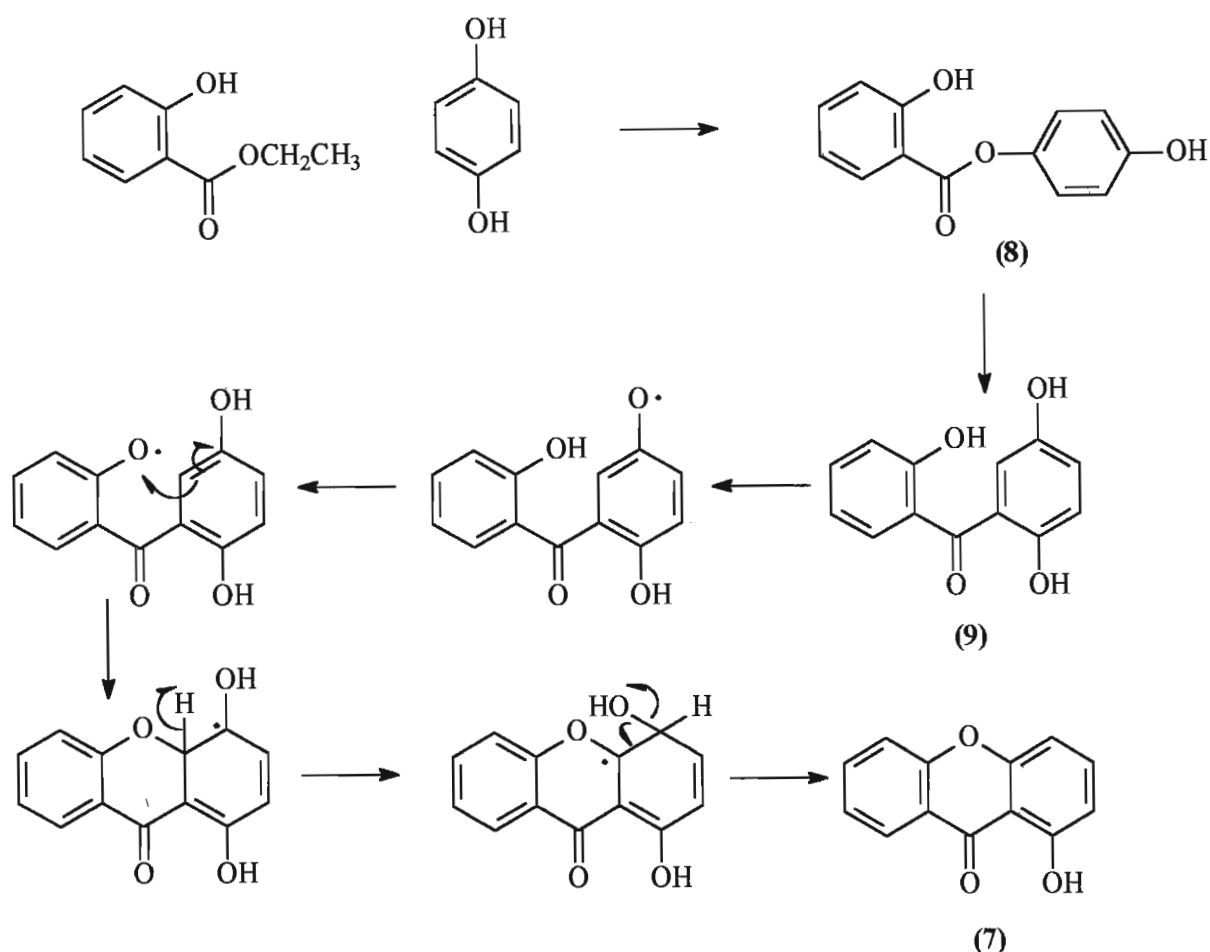


Figure 116. The Mechanism proposed by Patel and Trivedi<sup>192</sup> for the Formation of 1-Hydroxyxanthone.

The simple xanthenes 1,8-dihydroxyxanthone, 1-hydroxy-6,8-dimethoxyxanthone and 1-hydroxy-3,6-dimethylxanthone could be synthesised by means of the method used by Nevreker *et al.*<sup>190</sup>. This reaction involves the condensation of *o*-hydroxybenzoic acid derivatives with reactive phenols in a mixture of phosphorus oxychloride, phosphoric acid and zinc chloride. The methoxy derivative of each of the xanthone could be prepared by the modified Williamson synthesis as described in Section 4.2.3. (page 47). A reaction scheme which shows the formation of the selected hydroxyxanthenes is presented in Figure 117 (page 145).

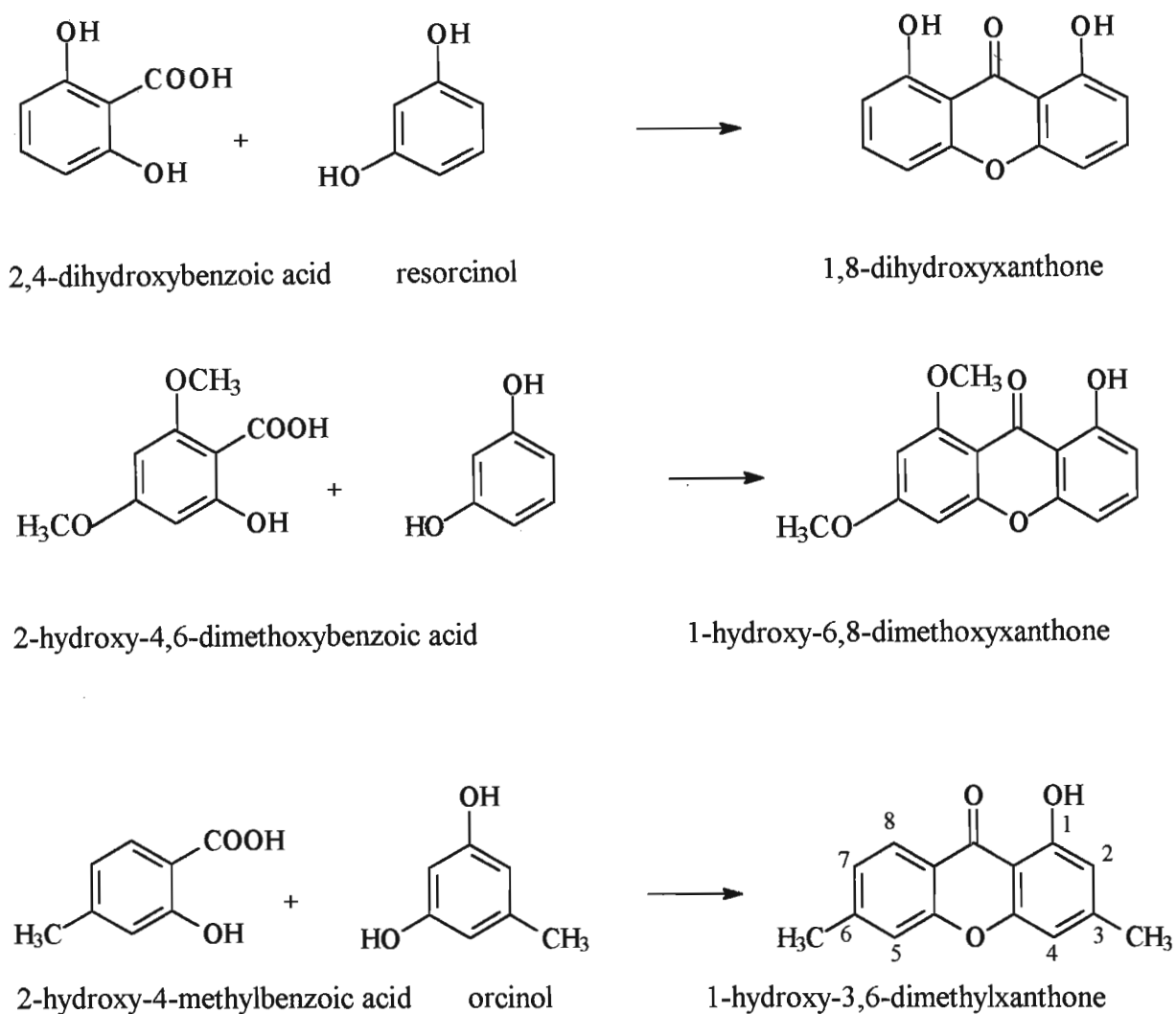


Figure 117. The Reaction Scheme for the Condensation Reaction in the Formation of Simple Xanthenes.

The objectives of this study were to :

- synthesise, purify and characterise simple xanthone derivatives
- determine the effect of the simple xanthenes on AFB<sub>1</sub> production and
- determine the type of inhibition caused by the simple xanthenes.

## 9.2. MATERIALS AND METHODS

### 9.2.1. General

Melting points are uncorrected and obtained using an Electrothermal IA 9000 digital melting point apparatus. Low resolution mass spectra were recorded on a Hewlett Packard 518A mass spectrometer operating at an ionization potential of 70 eV. The infra-red spectrum was recorded using potassium bromide discs on a Shimadzu 470 spectrometer.  $^1\text{H}$ -NMR spectra were recorded in  $\text{CDCl}_3$  on a Varian Gemini 300 NMR spectrometer (300 MHz). The spectra were referenced against the central line of deuteriochloroform singlet at  $\delta_{\text{H}}$  7.24 p.p.m. for  $^1\text{H}$ -NMR.

### 9.2.2. Chemicals

2-Hydroxybenzoic acid (salicylic acid), 4-hydroxyphenol (quinol), 2,6-dihydroxybenzoic acid, 3-hydroxyphenol (resorcinol), 2-hydroxy-4,6-dimethoxybenzoic acid, anhydrous zinc chloride, 3-hydroxy-5-methylphenol (orcinol), diphenylether, phosphorus oxychloride, 2-hydroxy-4-methylbenzoic acid and all reagent grade solvents were purchased from Sigma Chemical Suppliers (SA). Ethyl salicylate could not be purchased and was synthesised.

### 9.2.3. Synthesis of Ethyl Salicylate

In a 500 ml round-bottom flask was placed a mixture of 2-hydroxybenzoic acid (28 g ; 0.2 mol), absolute ethanol (116 ml ; 2.0 mol) and concentrated sulphuric acid (2 ml). The mixture was heated under refluxed for 5 hours. The excess ethanol was removed *in vacuo* and the residue poured into a beaker containing deionised water (250 ml). The mixture was stirred and poured into a separating funnel. The lower organic layer was collected and washed with a saturated solution of sodium bicarbonate (3 x 25 ml) until evolution of carbon dioxide ceased. The combined organic fractions were washed with deionised water (25 ml), separated from water and dried over magnesium sulphate for half an hour. The ethyl salicylate solution was filtered through a fluted filter-paper directly into a round



bottom flask fitted with a still-head carrying a 360 °C thermometer and an air condenser. The colourless ester, b.p. 231-234 °C, was collected ( 6.34 g ; 69 %). The <sup>1</sup>H-NMR and expanded <sup>1</sup>H-NMR spectra are presented in Figure 118 (Appendix 60, page 289) and Figure 119 (Appendix 61, page 290), respectively.  $\delta_{\text{H}}$  (300 MHz) 7.83 (dd,  $J$  1.65,  $J$  7.92, H-3) 6.84 (dt,  $J$  1.17,  $J$  8.04, H-4) 7.4 (dt,  $J$  1.65,  $J$  8.61, H-5) 6.95 (d,  $J$  8.25, H-6) 4.38 (q,  $J$  7.14, CH<sub>2</sub>) 1.39 (t,  $J$  7.14, CH<sub>3</sub>).

#### 9.2.4. Attempted Synthesis of 1-Hydroxyxanthone

A mixture of 4-hydroxyphenol (2 g ; 0.018 mol), ethyl salicylate (2 g ; 0.012 mol) and diphenyl ether (5 ml) was refluxed for 40 hours<sup>192</sup>. The reaction mixture was thereafter subjected to steam distillation to produce a pasty mass which was dissolved in petroleum ether (b.p. 60 °C) and filtered by gravity filtration. The filtrate was evaporated *in vacuo* to produce an orange coloured residue. Preparative t.l.c. of the mixture using silica gel as an adsorbent and hexane: ethyl acetate: acetic acid (20: 3: 2) as the solvent system gave a yellow coloured compound. The compound was insoluble in aqueous sodium bicarbonate. A reddish-brown colour was obtained with concentrated sulphuric acid and no colour change occurred with alcoholic ferric chloride solution. The yield of the unknown compound (m.p. 153-156 °C) was 0.056 g. The <sup>1</sup>H-NMR spectrum is presented in Figure 120 (Appendix 62, page 291). This compound was not identified since it lacked the aromatic protons of 1-hydroxyxanthone (see results and discussion, page 155).

#### 9.2.5. Attempted Synthesis of 1,8-Dihydroxyxanthone

2,6-Dihydroxybenzoic acid was condensed with resorcinol following the procedure described by Nevreker *et al.*<sup>190</sup>. This involved the use of a mixture of polymeric phosphoric acid and zinc chloride.

Polymeric phosphoric acid was prepared<sup>190</sup> by treating phosphorus oxychloride (10 ml, 0.10 mol) with orthophosphoric acid (8 ml, 0.10 mol). During the addition of these reagents, brisk evolution of gaseous hydrochloric acid was observed. The reaction mixture was refluxed at 50 °C for 1.5 hour to remove the gaseous hydrochloric acid. The

above treatment resulted in a colourless liquid which was used as polymeric phosphoric acid.

A mixture of polymeric phosphoric acid (30.00 g), anhydrous zinc chloride (6.00 g), 2,6-dihydroxybenzoic acid (1.54 g, 0.01 mol) and resorcinol (1.10 g, 0.01 mol) was heated at 120 °C for 6 hours resulting in the reaction mixture attaining a dark red colour. The reaction mixture was cooled and crushed ice (10 g) was added. The aqueous mixture was extracted with ethyl acetate (3 x 50 ml). The combined ethyl acetate extracts were washed with brine solution (1x 25 ml) and extracted with a saturated solution of sodium bicarbonate (2 x 25 ml). The bicarbonate extract was subsequently neutralised with 6 M hydrochloric acid and the neutral solution obtained was extracted with ethyl acetate (3 x 50 ml). The combined ethyl acetate extracts (150 ml) were washed with brine (1 x 25 ml), dried over anhydrous sodium sulphate and concentrated *in vacuo* to give a pale brown solid (0.983 g). Thin layer chromatography of the solid using silica gel t.l.c. plates and benzene: ethyl acetate: acetic acid (20: 20: 1) as the solvent system did not show any spot corresponding to the 1-hydroxyxanthone derivative as indicated by the negative colour tests (alcoholic ferric chloride- no green colour; aqueous sodium hydroxide solution- no yellow or orange colour; concentrated sulphuric acid- no yellow or orange colour), on the other hand it showed a major spot corresponding to 2,6-dihydroxybenzoic acid, the unreacted starting material.

#### 9.2.6. Attempted Synthesis of 1-Hydroxy-6,8-dimethoxyxanthone

A mixture of polymeric phosphoric acid (30.00 g), anhydrous zinc chloride (6.00 g), 2-hydroxy-4,6-dimethoxybenzoic acid (1.96 g, 0.01 mol) and resorcinol (1.10 g, 0.01 mol) was heated at 120 °C for 6 hours resulting in the reaction mixture attaining a dark red colour. The reaction mixture was cooled and crushed ice (10 g) was added. The aqueous mixture was extracted with ethyl acetate (3 x 50 ml). The combined ethyl acetate extracts were washed with brine solution (1x 25 ml) and extracted with a saturated solution of sodium bicarbonate (2 x 25 ml). The bicarbonate extract was subsequently neutralised with 6 M hydrochloric acid and the neutral solution thus obtained was extracted with ethyl acetate (3 x 50 ml). The combined ethyl acetate extracts (150 ml) were washed with brine (1 x 25 ml), dried over anhydrous sodium sulphate and

concentrated *in vacuo* to give a dark red liquid (0.818 g). Thin layer chromatography of the solid using silica gel t.l.c. plates and benzene: ethyl acetate: acetic acid (20: 20: 1) as the solvent system did not show any spot corresponding to the 1-hydroxyxanthone derivative as indicated by the negative colour tests (alcoholic ferric chloride- no green colour ; aqueous sodium hydroxide solution- no yellow or orange colour ; concentrated sulphuric acid- no yellow or orange colour), on the other hand it showed a major spot corresponding to 2-hydroxy-4,6-dimethoxybenzoic acid, the unreacted starting material.

### 9.2.7. Synthesis of 1-Hydroxy-3,6-dimethylxanthone

A mixture of polymeric phosphoric acid (30.00 g), anhydrous zinc chloride (6.00 g), 2-hydroxy-4-methylbenzoic acid (1.52 g, 0.01 mol) and orcinol (1.24g, 0.01 mol) was heated at 120 °C for 5 hours resulting in the reaction mixture attaining a dark red colour. The reaction mixture was cooled and crushed ice (10 g) was added. The aqueous mixture was extracted with ethyl acetate (3 x 50 ml). The combined ethyl acetate extracts were washed with brine solution (1x 25 ml) and extracted with a saturated solution of sodium bicarbonate (2 x 25 ml). The bicarbonate extract was subsequently neutralised with 6 M hydrochloric acid and the neutral solution thus obtained was extracted with ethyl acetate (3 x 50 ml). The combined ethyl acetate extracts (150 ml) were washed with brine (1 x 25 ml), dried over anhydrous sodium sulphate and concentrated *in vacuo* to give an orange coloured solid (0.119 g). Preparative t.l.c. of the mixture using silica gel as an adsorbent and benzene: ethyl acetate: acetic acid (20: 20: 1) as the solvent system gave a pale yellow coloured compound. The compound was soluble in aqueous sodium bicarbonate and gave an orange colour with aqueous sodium hydroxide. A deep yellow colour was obtained with concentrated sulphuric acid and a green colour with alcoholic ferric chloride solution. The compound was recrystallised from methanol: benzene (50:50) to yield (0.066 g ; 2.75 %) of light yellow needles, m.p. 146-147°C (Literature value<sup>193</sup> 147-148 °C). EIMS *m/z* 240 (Figure 121, page 159) corresponds to C<sub>15</sub>H<sub>12</sub>O<sub>3</sub>. The <sup>1</sup>H-NMR and expanded <sup>1</sup>H-NMR spectra are presented in Figure 122 (Appendix 63, page 292) and Figure 123 (Appendix 64, page 293), respectively. The COSY spectrum is presented in Figure 124 (Appendix 65, page 294).  $\delta_H$  (300MHz) 6.72 (broad s, H-2) 6.60 (broad s, H-4) 7.23 (broad s, H-5) 7.16 (d, *J* 8.40, H-7) 8.12 (d, *J* 8.70, H-8)

2.41 (s, CH<sub>3</sub>) 2.50 (s, CH<sub>3</sub>). The IR spectrum is presented in Figure 125 (Appendix 66, page 295).

#### 9.2.8. Alkylation of 1-Hydroxy-3,6-dimethylxanthone to 1-Methoxy-3,6-dimethylxanthone

1-Hydroxy-3,6-dimethylxanthone (20.00 mg, 83  $\mu$ mol), anhydrous potassium carbonate (34.40 mg, 249  $\mu$ mol) and methyl iodide (23.4  $\mu$ l, 165  $\mu$ mol) were heated under reflux in dry acetone (10 ml) for 8 hours. The cooled solution was filtered, poured into deionised water (5 ml) and extracted with chloroform (3 x 5 ml). The combined extracts were then dried over anhydrous sodium sulphate and concentrated *in vacuo* to give 16.50 mg of crude product. Preparative t.l.c. of the mixture using silica gel as an adsorbent and benzene: ethyl acetate: acetic acid (20: 20: 1) as the solvent system gave a pale brown compound. The compound was recrystallised from methanol: benzene (50:50) to yield (12.60 mg ; 59.5 %) colourless crystals, m.p. 173-174 °C (Literature value<sup>191</sup> 174-175 °C). EIMS *m/z* 254 (Figure 126, page 160) corresponds to C<sub>16</sub>H<sub>14</sub>O<sub>3</sub>. The <sup>1</sup>H-NMR and expanded <sup>1</sup>H-NMR spectra are presented in Figure 127 (Appendix 67, page 296) and Figure 128 (Appendix 68, page 297), respectively.  $\delta_{\text{H}}$  (300 MHz) 6.83 (broad s, H-2) 6.57 (broad s, H-4) 7.16 (broad s, H-5) 7.11 (d, *J* 8.07, H-7) 8.15 (d, *J* 7.8, H-8) 4.0 (s, OCH<sub>3</sub>) 2.46 (s, CH<sub>3</sub>) 2.42 (s, CH<sub>3</sub>).

#### 9.2.9. Acetylation of 1-Hydroxy-3,6-dimethylxanthone to 1-Acetyl-3,6-dimethylxanthone

1-Hydroxy-3,6-dimethylxanthone (20.00 mg, 83  $\mu$ mol) was dissolved in dry pyridine (5 ml) and the solution was treated with acetic anhydride (1 ml). The mixture was warmed gently on a water bath and kept at room temperature for 24 hours. The reaction mixture was cooled and crushed ice (2 g) was added. The aqueous solution was subsequently extracted with ethyl acetate (3 x 10 ml). The combined ethyl acetate extracts were successively washed with dilute hydrochloric acid and water, dried over anhydrous sodium sulphate and concentrated *in vacuo* to give a yellow solid (14.00 mg ; 59.60 %). The compound was recrystallised from methanol: benzene (50:50) to give pale yellow

crystals, m.p. 151-152 °C (Literature value<sup>191</sup> 151-152 °C). EIMS  $m/z$  282 (Figure 129, page 161) corresponds to  $C_{17}H_{14}O_4$ . The  $^1H$ -NMR and expanded  $^1H$ -NMR spectra are presented in Figure 130 (Appendix 69, page 298) and Figure 131 (Appendix 70, page 299), respectively.  $\delta_H$  (300 MHz) 6.78 (broad s, H-4) 7.19 (broad s, H-2) 7.16 (broad s, H-5) 7.13 (d,  $J$  8.1, H-7) 8.09 (d,  $J$  8.1, H-8) 2.47 (s,  $CH_3$ ) 2.46 (s,  $CH_3$ ) 2.15 (s,  $OCOCH_3$ ).

#### 9.2.10. Organism, Media and Culture Conditions for Whole Cell Reactions

The method used in the preparation of whole cells is described in Section 6.2.2. (page 90). *Aspergillus parasiticus* (CMI 91019b) and *A. parasiticus* (Wh1-11-105) were used.

For the high aflatoxin producing strain (CMI 91019b), the chemically defined medium of Reddy *et al.*<sup>67</sup> (Appendix 2, page 234) was used as the standard liquid culture medium. A spore suspension of approximately  $10^6$  spores, in 1 ml of 0.01 % SDS, was inoculated in ten conical flasks (250 ml) containing the sterile liquid medium (50 ml) which was supplemented with acetone (0.5 ml)<sup>95</sup>. Aliquots containing 2.0, 2.5 and 3.0  $\mu$ mol of 1-hydroxy-3,6-dimethylxanthone (in 0.5 ml acetone) were added into 3 separate conical flasks containing the spores in the liquid medium. This procedure was repeated for the methoxy and acetyl derivatives in 6 additional conical flasks. The control flask was prepared by adding acetone (0.5 ml) to the liquid medium containing spores. The ten flasks were incubated in a rotary shaker at 25 °C and 180 r.p.m. for 96 hours. The metabolites were extracted and quantified as described in Section 9.2.11. (page 152).

For the aflatoxin blocked mutant fungi (Wh1-11-105) the following modifications were made to the method described in Section 6.2.2. (page 90). Three grams (wet weight) of mycelial pellets were added into seven conical flasks (250 ml) containing the resting medium (50 ml) (Appendix 40, page 269) which was supplemented with acetone (0.5 ml)<sup>95</sup>. Aliquots containing 2.5 and 3.0  $\mu$ mol of 1-hydroxy-3,6-dimethylxanthone (in 0.5 ml acetone) were added into 2 separate conical flasks in the liquid medium containing the mycelia. This procedure was repeated for the methoxy and acetyl derivatives in 4 additional conical flasks. The control flask was prepared by adding acetone (0.5 ml) to the

liquid medium containing the mycelia. The substrate OMST was dissolved in acetone (100  $\mu$ l). The reactions were initiated by the addition of OMST (1.0  $\mu$ mol) to each of the 7 conical flasks. The flasks were then incubated in a rotary shaker at 25 °C and 180 r.p.m. for 3 hours. The metabolites were extracted and quantified as described in Section 9.2.11.

#### **9.2.11. Extraction of Aflatoxins and Sample Preparation for Thin Layer and High Pressure Liquid Chromatography**

Acetone (30 ml) was added to each flask, the flasks were vigorously shaken and the metabolites were extracted with chloroform (3 x 30 ml). The chloroform extracts were dried over anhydrous sodium sulphate, filtered and concentrated *in vacuo*. The solid residue was dissolved in chloroform (1 ml), quantitatively transferred to vials and evaporated to dryness under a gentle stream of nitrogen gas and heat.

For t.l.c. analysis, the method is described in Section 6.2.3. (page 91).

For HPLC analysis, the metabolites obtained from *A. parasiticus* (CMI 91019b) were dissolved in acetonitrile (250 ml) and analysed by means of the diode array detector using a gradient elution of water and acetonitrile (described in Chapter 5, page 83). These studies were carried out in duplicate.

The metabolites obtained from *A. parasiticus* (Wh1-11-105) were dissolved in acetonitrile (10 ml) and analysed by means of the diode array detector using a gradient elution of water and acetonitrile. The metabolites obtained from the control were dissolved in acetonitrile (75 ml). These studies were carried out in duplicate.

#### **9.2.12. Preparation of the Cell-Free Extract**

The method for the preparation of the cell-free extract is described in Section 7.2.4. (page 103).

### 9.2.13. The Method Used for Enzyme Assay

Enzyme activity was assayed by adding the cell-free extract (500  $\mu$ l, final protein 1 mg/ml) to the phosphate buffer pH 7.2 (400  $\mu$ l) (Appendix 44, page 273) in a glass test tube (10 ml). To the mixture was added NADPH (50  $\mu$ l; 0.15  $\mu$ mol). The mixture was incubated in a rotary shaker at 28 °C and at 100 r.p.m. for 5 minutes. The reaction was subsequently initiated by adding the xanthone (5.92 nmol) dissolved in acetone (50  $\mu$ l) and OMST (2.96 nmol) dissolved in acetone (50  $\mu$ l). The mixture, incubated in a rotary shaker at 28 °C and at 100 r.p.m., was allowed to react for 3 hours. The reaction was stopped by adding chloroform (3 ml). The chloroform layer was separated from the aqueous layer by extraction. The extraction was repeated with chloroform (2 x 3 ml). The combined chloroform extracts were dried over anhydrous sodium sulphate, filtered and evaporated to dryness under a stream of nitrogen gas and gentle heat.

The dried residue was dissolved in acetonitrile (1 ml) and analysed by HPLC with the diode array detector (see Chapter 5, page 83). These studies were carried out in triplicate.

### 9.2.14. Kinetic Studies of Cell-Free Extracts

Enzyme activity was assayed by adding the cell-free extract (500  $\mu$ l; final protein 1.25 mg/ml) to the phosphate buffer (pH 7.2) (400  $\mu$ l) containing NADPH (50  $\mu$ l; 0.15  $\mu$ mol) in a glass test tube (10 ml). The mixture was incubated in a rotary shaker at 28 °C and 100 r.p.m. for 5 minutes. The reaction was initiated by adding OMST, dissolved in acetone (50  $\mu$ l), and allowed to react for 10 minutes. The concentration of metabolite substrate, i.e., OMST was varied from 0.73  $\mu$ M to 25.2  $\mu$ M and the concentration of 1-methoxy-3,6-dimethylxanthone was 2.75  $\mu$ M for  $K_m$  determination and substrate competition studies. The rest of the procedure is described in Section 9.2.13.

For HPLC analysis with the diode array detector, the extract was dissolved in acetonitrile (1 ml). These studies were carried out in triplicate.

### 9.3. RESULTS AND DISCUSSION

The reason for studying the simple xanthenes is because part of their structures is similar to that of the metabolite OMST and therefore these compounds have the potential of “mimicking” the natural substrate *in vivo*. It was shown in the earlier study (Chapter 8) that OMST is a compulsory metabolite found between ST and AFB<sub>1</sub> in the aflatoxin biochemical pathway. As discussed previously (Chapter 8) the conversion of OMST to AFB<sub>1</sub> is catalysed by a complex yet very efficient enzyme system displaying relative specificity, viz., an oxido-reductase. Bhatnagar *et al.*<sup>175</sup> reported that the partially purified oxido-reductase existed as a multi sub-unit complex but these researchers were unable to purify the enzyme to homogeneity. Therefore a study was undertaken to synthesise simple xanthenes and to determine their effect on AFB<sub>1</sub> production. The results thereof would provide more information on the mechanism of enzyme-substrate binding.

None of the simple xanthenes, selected for this study, were available commercially and therefore it was decided these compounds be synthesised by known chemical methods. An attempt was made to synthesise 1-hydroxyxanthone by the method used by Patel and Trivedi<sup>192</sup>. This reaction required the use of ethyl salicylate as a starting compound which was not available commercially. Therefore ethyl salicylate was synthesised by the esterification of 2-hydroxybenzoic acid with ethanol in an acid catalysed reaction. This compound was easily characterised by <sup>1</sup>H-NMR. The <sup>1</sup>H-NMR spectrum of ethyl salicylate is presented in Figure 118 (Appendix 60, page 289) and the expanded <sup>1</sup>H-NMR spectrum is presented in Figure 119 (Appendix 61, page 290).

The next step in the synthesis involved the thermal condensation reaction which was reported by Patel and Trivedi<sup>192</sup>. This step in the reaction proved problematic. According to literature, the xanthone was separated from a pasty mass by column chromatography with petroleum ether (b.p. 60-80 °C) as the eluting solvent. In this investigation, a pasty mass was produced which was partially soluble in petroleum ether. The main problem with a one-pot synthesis is that many by-products can be formed thereby making purification difficult. The pasty mass was dissolved in petroleum ether, as cited in the literature, and filtered by gravity filtration. The filtrate was evaporated *in vacuo* to



produce an orange colour residue. Preparative t.l.c. of the mixture using silica gel as an adsorbent and hexane: ethyl acetate: acetic acid (20: 3: 2) as the solvent system gave a yellow coloured compound. Thin layer chromatography analysis of the solid did not show any spot corresponding to 1-hydroxyxanthone derivative as indicated by the negative colour tests (alcoholic ferric chloride- no green colour; aqueous sodium hydroxide solution- no yellow or orange colour; concentrated sulphuric acid- no yellow or orange colour). The <sup>1</sup>H-NMR spectrum of the yellow compound (Figure 120, Appendix 62, page 291) was compared with the expected 1-hydroxyxanthone <sup>1</sup>H-NMR data<sup>189</sup> (Table 30) and it was found that the synthesised yellow compound was not an hydroxyxanthone since the protons presented in the table were not identified in the <sup>1</sup>H-NMR spectrum of the yellow compound.

Table 30. The <sup>1</sup>H-NMR Data of 1-Hydroxyxanthone.

Proton atom	Chemical shift δ <sub>H</sub> (p.p.m.)	Splitting Pattern	Coupling Constant <i>J</i> (H,H) Hz
H-2	6.78	triplet doublet	9.2
H-3	7.60	triplet	9.0
H-4	6.91	double doublet	9.2
H-5	7.48	double doublet	9.2
H-6	7.75	triplet doublet	9.9
H-7	7.40	triplet doublet	9.9
H-8	8.25	double doublet	9.2

The yellow compound, however, contained the CH<sub>3</sub>CH<sub>2</sub>COO group as indicated by the appearance of the CH<sub>2</sub> group at δ<sub>H</sub> 4.18 (quartet) and the CH<sub>3</sub> group appears at δ<sub>H</sub> 1.43 (triplet). It is possible that the free hydroxyl group of ethyl salicylate reacted with 4-hydroxy-phenol to form the yellow compound. The identity of the yellow compound was not further investigated since it was obvious that the compound lacked the protons of the xanthone nucleus. A second attempt at the synthesis of 1-hydroxyxanthone also proved futile and this method of synthesis was therefore abandoned.

At this stage an attempt was made to synthesise 1,8-dihydroxyxanthone and 1-hydroxy-6,8-dimethoxyxanthone by using the method reported by Nevreker *et al.*<sup>190</sup>. However, in both cases no reaction occurred under the experimental conditions used and the starting

material was recovered. Two further attempts also proved futile. The synthesis of 1,8-dihydroxyxanthone was expected to be difficult since Nevreker *et al.*<sup>190</sup>, who pioneered this reaction, obtained a maximum yield of 475 mg (10.4 %) thereby indicating the difficulty of the reaction. This failure in the synthesis could probably be due to the difficulty to reproduce literature conditions and not due to the reagents since these were freshly prepared or purchased as required.

These results were disappointing especially the reaction to produce 1-hydroxy-6,8-dimethoxyxanthone which could have been easily converted to the methoxy derivative. The successful synthesis would have been very useful since 1,6,8-trimethoxyxanthone possess the correct functional groups at the correct position to mimic OMST and hence possibly compete for the “active enzyme” site by the process known as competitive inhibition. It is therefore recommended that other methods be investigated to synthesise these additional compounds for it is possible that they may be more potent inhibitors of AFB<sub>1</sub> production than the compound successfully synthesised in this study (see later).

Fortunately, the synthesis of 1-hydroxy-3,6-dimethylxanthone (Figure 117, page 145) by the method used by Nevreker *et al.*<sup>190</sup> was successful as indicated by preliminary qualitative tests. The pale yellow coloured compound was soluble in aqueous sodium bicarbonate and gave an orange colour with aqueous sodium hydroxide. A deep yellow colour was obtained with concentrated sulphuric acid and a green colour with alcoholic ferric chloride solution. These tests indicated a positive reaction for a 1-hydroxyxanthone derivative.

A preliminary investigation of AFB<sub>1</sub> inhibition by a partially purified sample of 1-hydroxy-3,6-dimethylxanthone was undertaken. This feeding study with the whole cells of *A. parasiticus* (CMI 91019b) indicated promising results, viz., AFB<sub>1</sub> production was inhibited in the presence of the xanthone. This result was not surprising, since many kinds of molecules can inhibit enzymes and in particular, 1-hydroxy-3,6-dimethylxanthone contained the key xanthone nucleus which therefore had some resemblance to OMST. This initial investigation was monitored by t.l.c. by comparing the intensity of the blue AFB<sub>1</sub> spot ( $R_f$  0.61; CEI) of the metabolites extracted from the reaction flask, viz., the

flask in which the xanthone was added, with that of the control, viz., the flask in which no xanthone was added.

Having established that the partially purified 1-hydroxy-3,6-dimethylxanthone could inhibit AFB<sub>1</sub> production, the xanthone was subsequently purified by preparative t.l.c. to give crystalline 1-hydroxy-3,6-dimethylxanthone (66 mg; 2.75 %). Although the % yield was lower than that obtained by Nevreker *et al.*<sup>190</sup> (10.62 %), it was sufficient to carry out micro-scale reactions in the preparation of two derivatives, viz., 1-methoxy-3,6-dimethylxanthone and 1-acetyl-3,6-dimethylxanthone. A possible reason for the low yield of 1-hydroxy-3,6-dimethylxanthone is the instability of *o*-hydroxybenzoic acid at high temperature and hence decarboxylation occurs.

The methoxy derivative, i.e., 1-methoxy-3,6-dimethylxanthone was prepared by the modified Williamson synthesis and purified by preparative t.l.c. to give crystalline product (12.60 mg; 59.50 %). The acetyl derivative, i.e., 1-acetyl-3,6-dimethylxanthone was prepared by the esterification reaction and purified by preparative t.l.c. to give crystalline product (14.00 mg; 59.60 %). The scheme for the reactions is presented in Figure 132.

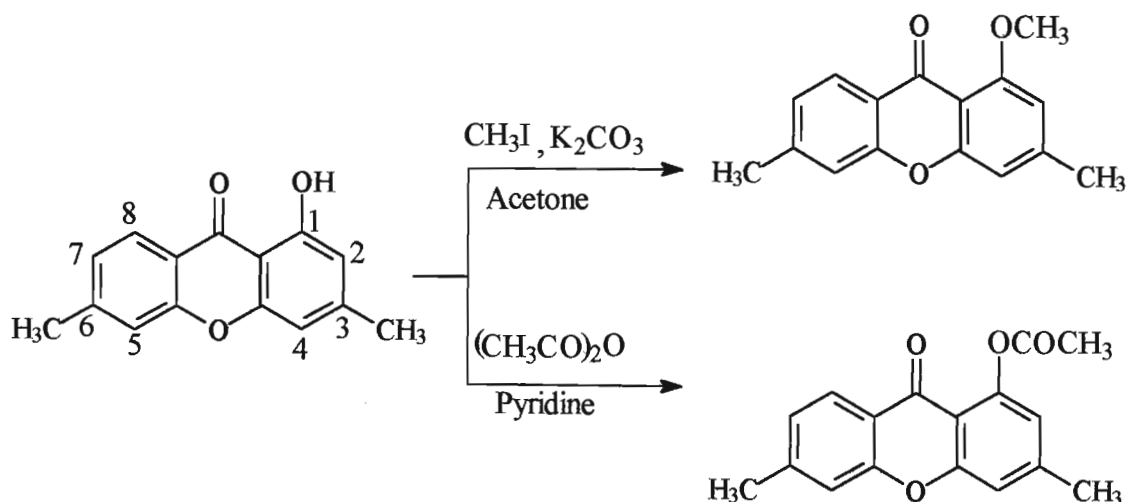


Figure 132. The Reaction Scheme for the Synthesis of Xanthone Derivatives.

A comparison of the structure of 1-methoxy-3,6-dimethylxanthone with that of OMST (Figure 133, page 158) shows that they are not entirely compatible. The xanthone

carbonyl group in relation to the 1-methoxy derivative is the same as that for OMST but the 3-methyl group is different. The other phenyl ring is also substituted at the 6 position.

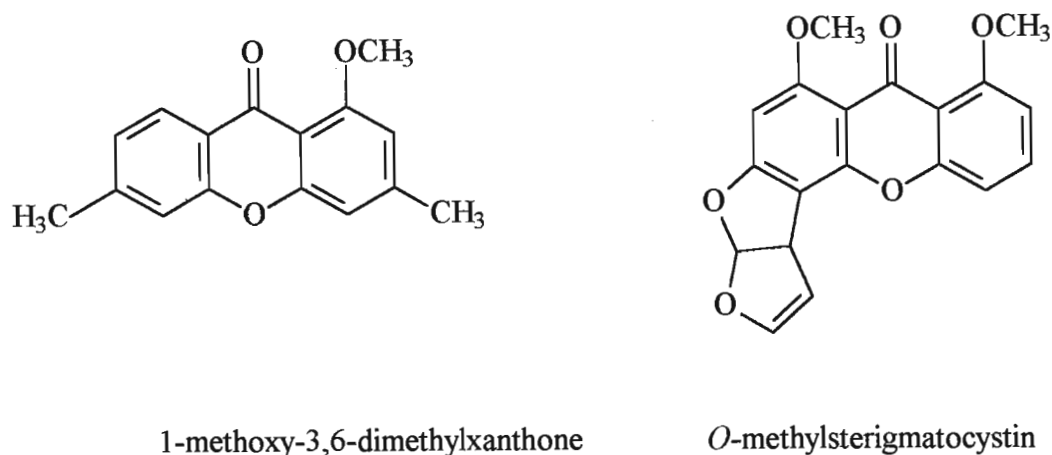


Figure 133. The Structures of 1-Methoxy-3,6-dimethylxanthone and OMST.

After having synthesised and purified the three xanthones, spectroscopic techniques were used for their characterisation. Nuclear magnetic resonance spectroscopy was selected as the main technique to characterise the compounds. Mass spectrometry and infra-red spectrometry were also used.

The <sup>1</sup>H-NMR spectrum of 1-hydroxy-3,6-dimethylxanthone (Figure 122, Appendix 63, page 292) showed two singlets at  $\delta$  2.40 and  $\delta$  2.50 which were assigned to the methyl groups at C-6 and C-3, respectively. The expanded <sup>1</sup>H-NMR spectrum (Figure 123, Appendix 64, page 293) and the COSY spectrum (Figure 124, Appendix 65, page 295) were used to assign the five aromatic protons, viz., the three singlets at  $\delta$  6.72,  $\delta$  6.60, and  $\delta$  7.23 were assigned to H-2, H-4 and H-5, respectively. The two doublets at  $\delta$  7.16 and  $\delta$  8.12 were assigned to H-7 and H-8, respectively.

After having established the structure by using <sup>1</sup>H and COSY NMR spectra, MS was used to confirm the correct molecular mass. The normalised mass spectrum of 1-hydroxy-3,6-dimethylxanthone (Figure 121, page 159) showed the molecular ion peak [ $M^+$ ] at  $m/z$  240 which corresponds to a molecular formula C<sub>15</sub>H<sub>12</sub>O<sub>3</sub>.

The IR spectrum (Figure 125, Appendix 66, page 295) was used to determine the carbonyl and hydroxyl groups. The carbonyl stretch appeared at  $1652\text{ cm}^{-1}$  and a broad band at  $3001\text{ cm}^{-1}$  indicated the intermolecular hydrogen bonded hydroxyl group. This group was confirmed by the appearance of the C-O stretching band at  $1190\text{ cm}^{-1}$ .

Since the structure of the parent compound, viz., 1-hydroxy-3,6-dimethylxanthone was established earlier, only  $^1\text{H}$ -NMR and mass spectra were used to characterise the two xanthone derivatives.

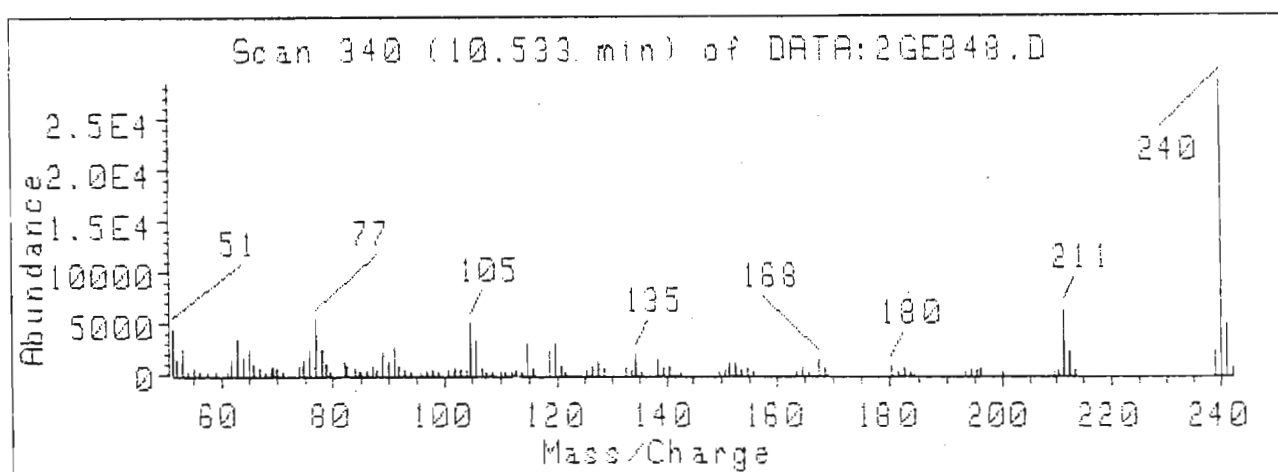


Figure 121. The Normalised Mass Spectrum of 1-Hydroxy-3,6-dimethylxanthone.

The  $^1\text{H}$ -NMR spectrum of 1-methoxy-3,6-dimethylxanthone is presented in Figure 127 (Appendix 67, page 296) and the expanded  $^1\text{H}$ -NMR spectrum is presented in Figure 128 (Appendix 68, page 297). The singlet at  $\delta$  4.0 was assigned to the methoxy protons and the two singlets at  $\delta$  2.46 and  $\delta$  2.42 were assigned to the methyl protons at C-3 and C-6 (protons are interchangeable). The three singlets at  $\delta$  6.83,  $\delta$  6.57 and  $\delta$  7.16 were assigned to H-2, H-4 and H-5, respectively. The two doublets at  $\delta$  7.11 and  $\delta$  8.16 were assigned to H-7 and H-8, respectively. The normalised mass spectrum (Figure 126, page 160) showed the molecular ion  $[\text{M}^+]$  at  $m/z$  254 which corresponds to a molecular formula of  $\text{C}_{16}\text{H}_{14}\text{O}_3$ .

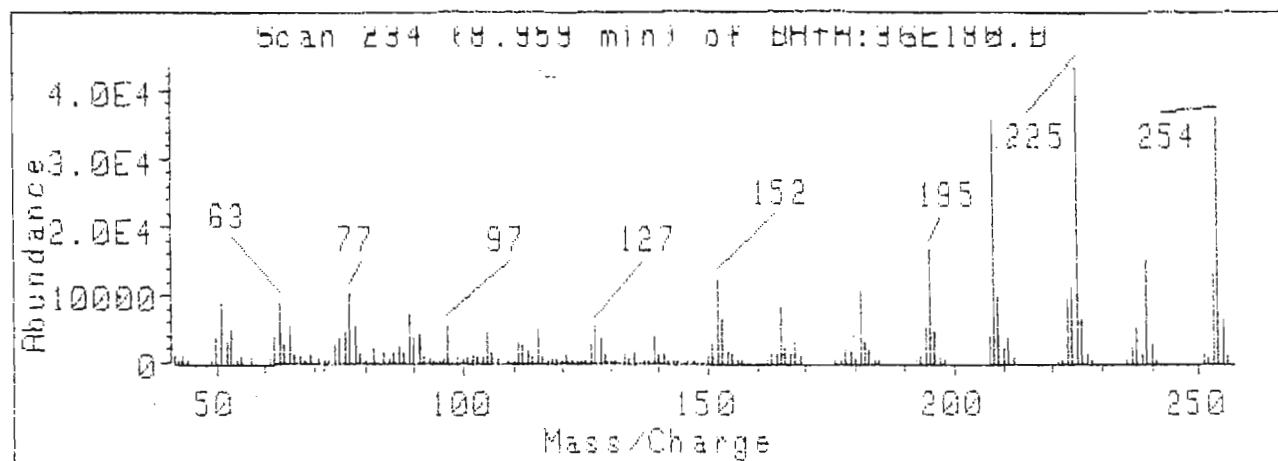


Figure 126. The Normalised Mass Spectrum of 1-Methoxy-3,6-dimethylxanthone.

The  $^1\text{H}$ -NMR spectrum of 1-acetyl-3,6-dimethylxanthone is presented in Figure 130 (Appendix 69, page 298) and the expanded  $^1\text{H}$ -NMR spectrum is presented in Figure 131 (Appendix 70, page 299). The two singlets at  $\delta$  2.46 and  $\delta$  2.45 were assigned to the methyl protons at C-3 and C-6 (protons are interchangeable). A further singlet integrating to three protons at  $\delta$  2.15 was assigned to the acetyl protons at C-1. The three singlets at  $\delta$  7.19,  $\delta$  6.78 and  $\delta$  7.16 were assigned to H-2, H-4 and H-5, respectively. The two doublets at  $\delta$  7.13 and  $\delta$  8.09 were assigned to H-7 and H-8, respectively. The normalised mass spectrum (Figure 129, page 161) showed the molecular ion  $[\text{M}^+]$  at  $m/z$  282 which corresponds to a molecular formula of  $\text{C}_{17}\text{H}_{14}\text{O}_4$ .

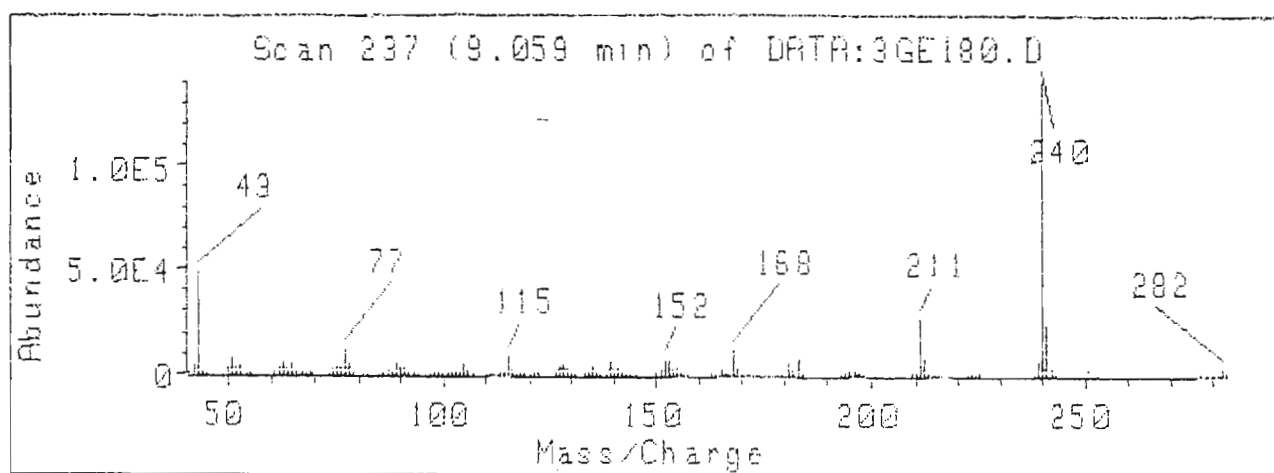


Figure 129. The Normalised Mass Spectrum of 1-Acetyl-3,6-dimethylxanthone.

The effect of the three simple xanthenes on the production of AFB<sub>1</sub> was investigated in whole cells of *A. parasiticus* (CMI 91019b), a fungus which has all the necessary enzymes to produce AFB<sub>1</sub>. Each of the three xanthenes was dissolved in acetone and incubated in whole cells of *A. parasiticus* for 96 hours. The metabolites were then isolated and analysed by t.l.c. which indicated different colored pigments viz., blue, green, yellow, red and orange under UV irradiation. This indicated that a variety of metabolites were present in the extract and these metabolites were not identified because they were in too small amounts for isolation and also a liquid chromatography mass spectrometer was not available. However, the metabolites which are found to occur in the latter part of the AFB<sub>1</sub> biochemical pathway, viz., ST, OMST and AFB<sub>1</sub> were identified by comparing their  $R_f$  value with those of authentic standards. Two dimensional t.l.c. using CEI (first dimension) and TEF (second dimension) was used to identify ST, OMST and AFB<sub>1</sub>. Sterigmatocystin ( $R_{f1}$  0.91;  $R_{f2}$  0.83) exhibited a brick red fluorescence under UV which changed to yellow when the t.l.c. plate was sprayed with aluminium chloride spray reagent and heated gently. *O*-methylsterigmatocystin ( $R_{f1}$  0.54;  $R_{f2}$  0.44) exhibited a blue fluorescence under UV which changed to yellow when the t.l.c. plate was sprayed with aluminium chloride spray reagent and heated gently. Aflatoxin B<sub>1</sub> ( $R_{f1}$  0.62;  $R_{f2}$  0.39) displayed a characteristic blue fluorescence under UV and no change occurred upon treatment with the aluminium chloride spray reagent. Also relatively small amounts of

yellow and orange pigments were observed thereby indicating some typical metabolites produced by the fungi. These metabolites were not investigated further since these pigments did not accumulate when the quantity of exogenously added xanthenes was increased.

Quantification of AFB<sub>1</sub> in each assay was obtained by HPLC with the diode array detector. The calibration graph of AFB<sub>1</sub> (Figure 58, Appendix 35, page 265) was used to determine the quantity of AFB<sub>1</sub> from the integrated peak area of the chromatogram. For this purpose, the extracts were appropriately diluted (specified in experimental section) so that the integrated area of AFB<sub>1</sub> in the extract fell within the range of the calibration graph of AFB<sub>1</sub>. Having determined the quantity of AFB<sub>1</sub> (taking into account the dilution factor) in each extract, the % conversion to AFB<sub>1</sub> and % inhibition of AFB<sub>1</sub> were calculated. The quantity of AFB<sub>1</sub> obtained from the control experiment, in which no xanthone was added, was assumed to be 100 % conversion to AFB<sub>1</sub>. Based on this assumption, the % conversion to AFB<sub>1</sub> and % inhibition of AFB<sub>1</sub> were calculated as follows:

$$\% \text{ Conversion to AFB}_1 = (\mu\text{mol AFB}_1 \text{ in extract} / \mu\text{mol AFB}_1 \text{ in control}) \times 100$$

$$\text{and } \% \text{ Inhibition of AFB}_1 = 100 - \% \text{ conversion to AFB}_1$$

The results of whole cell feeding experiments with the three xanthenes, viz., 1-hydroxy-3,6-dimethylxanthone, 1-methoxy-3,6-dimethylxanthone and 1-acetyl-3,6-dimethylxanthone, for an incubation period of 96 hours, are presented in Table 31 (page 163). Typical chromatograms are presented in Figure 134-136 (Appendix 71-73, page 300-302).



Table 31. The Whole Cell Reaction of *A. parasiticus* (CMI 91019b) , in the Presence of Different Quantities of Xanthone Derivatives for an Incubation Time of 96 Hours.

Compound Added ( $\mu\text{mol}$ )	Integrated Peak Area	AFB <sub>1</sub> Produced (ng) <sup>a</sup>	AFB <sub>1</sub> Produced ( $\mu\text{g}/\text{assay}$ )	AFB <sub>1</sub> Produced ( $\mu\text{g}/\text{assay}$ ) <sup>b</sup>	% Conversion to AFB <sub>1</sub>	% Inhibition of AFB <sub>1</sub>
Control	424646 426104	1790 1797	447.50 449.25	448.37 $\pm 1.24$	100.00	0
<b>RSK 9</b>						
2.00	122479 132976	520 564	130.00 141.00	135.50 $\pm 7.78$	30.22	69.78
2.50	119757 115971	509 493	127.25 123.25	125.25 $\pm 2.83$	27.93	72.07
3.00	90759 97853	387 417	96.75 104.25	100.50 $\pm 5.30$	22.41	77.59
<b>RSK 10</b>						
2.00	119581 126255	508 536	127.00 134.00	130.5 $\pm 4.95$	29.11	70.89
2.50	111211 111646	473 475	118.25 118.75	118.5 $\pm 0.35$	26.43	73.57
3.00	96732 84938	412 362	103.00 99.50	101.25 $\pm 2.47$	22.58	77.42
<b>RSK 3</b>						
2.00	168107 169209	712 717	178.00 179.25	178.63 $\pm 0.88$	39.84	60.16
2.50	151849 146346	644 620	161.00 155.00	158.00 $\pm 4.24$	35.24	64.76
3.00	133398 120757	566 513	141.50 128.25	134.88 $\pm 9.37$	30.08	69.92

<sup>a</sup> Values for AFB<sub>1</sub> in a 250 times diluted assay. <sup>b</sup> Values of AFB<sub>1</sub> represents the mean and standard deviation of experiments conducted in duplicate.

KEY: RSK 9 = 1-hydroxy-3,6-dimethylxanthone; RSK 10 = 1-methoxy-3,6-dimethylxanthone ; RSK 3 = 1-acetyl-3,6-dimethylxanthone

It was initially anticipated that there might be permeability problems associated with the uptake of polar compounds such as the xanthenes, but the whole cell system apparently had little difficulty with these compounds. The permeability of the xanthenes through the cellular membrane could in part be due to the acetone carrier system<sup>95</sup> which was being used.

In the absence of the xanthone, a large quantity of AFB<sub>1</sub> was produced (448.37 µg/assay). Addition of each of the three synthesised xanthenes gave varying degree of inhibition. In this investigation, it was unclear as to which of these compounds displayed the strongest inhibitory effect on the production of AFB<sub>1</sub>. However, it was evident that there was a slight increase in the inhibitory effect as the quantity of xanthenes were increased.

Having determined that the xanthenes were capable of inhibiting the production of AFB<sub>1</sub> in a wild strain of fungi, it was decided to investigate the effect in whole cells of a mutant *A. parasiticus* (Wh1-11-105). Quantification of AFB<sub>1</sub> in each assay was obtained by HPLC with the diode array detector. The calibration graph of AFB<sub>1</sub> (Figure 58, Appendix 35, page 265) was used to determine the quantity of AFB<sub>1</sub> from the integrated peak area of the chromatogram. For this purpose, the extracts were appropriately diluted (specified in experimental section) so that the integrated area of AFB<sub>1</sub> in the extract fell within the range of the calibration graph of AFB<sub>1</sub>. Having determined the quantity of AFB<sub>1</sub> (taking into account the dilution factor) in each extract, the % AFB<sub>1</sub> conversion and % AFB<sub>1</sub> inhibition were calculated as follows:

$$\% \text{ Conversion to AFB}_1 = (\mu\text{mol AFB}_1 \text{ in extract} / \mu\text{mol OMST added}) \times 100$$

$$\% \text{ Inhibition of AFB}_1 = 100 - (\% \text{ AFB}_1 \text{ in extract} / \% \text{ AFB}_1 \text{ in control}) \times 100$$

The result of whole cell feeding experiments with OMST as the substrate, in the presence of the three xanthenes for an incubation time of 3 hours is presented in Table 32 (page 165). Typical chromatograms are presented in Figure 137-139 (Appendix 74-76, page 303-305). The results of this investigation showed that the production of AFB<sub>1</sub> was inhibited by the synthesised compounds in cultures of *A. parasiticus* (Wh1-11-105). In the absence of the xanthone, there was an adequate conversion of OMST to AFB<sub>1</sub> (79.33 %). There was no significant difference in the inhibitory effect of the three synthesised compounds. The results of this investigation could not be used to determine which xanthone of the three has a greater inhibiting capacity. Although the three

xanthenes have slightly different polarity, it is obvious that the xanthenes were permeable through the cellular membrane. This permeability could in part be due to the acetone carrier system<sup>95</sup> which was being used, as mentioned earlier.

Table 32. The Enzymatic Conversion of OMST (1.00  $\mu$ mol) to AFB<sub>1</sub> in Whole-Cells of *A. parasiticus* (Wh1-11-105), in the Presence of Different Quantities of Xanthone Derivatives, for an Incubation Time of 3 Hours at 25 °C.

Compound Added ( $\mu$ mol)	Integrated Peak Area	AFB <sub>1</sub> Produced (ng)	AFB <sub>1</sub> Produced ( $\mu$ g/assay)	AFB <sub>1</sub> Produced ( $\mu$ g/assay) <sup>c</sup>	% Conversion to AFB <sub>1</sub>	% Inhibition of AFB <sub>1</sub>
Control	783847	3300 <sup>a</sup>	247.50		79.33	0
<b>RSK 9</b>						
2.5	1141027 920720	4802 <sup>b</sup> 3876 <sup>b</sup>	48.02 38.76	43.39 $\pm$ 6.54	13.91	82.47
3.0	847867 634123	3570 <sup>b</sup> 2671 <sup>b</sup>	35.70 26.71	31.20 $\pm$ 6.35	10.00	87.40
<b>RSK 10</b>						
2.5	450961 539529	1901 <sup>b</sup> 2273 <sup>b</sup>	19.01 22.73	20.87 $\pm$ 2.63	6.69	91.57
3.0	633669 786812	2669 <sup>b</sup> 3313 <sup>b</sup>	26.69 33.13	29.91 $\pm$ 4.55	9.59	87.91
<b>RSK 3</b>						
2.5	1094377 982791	4606 <sup>b</sup> 4137 <sup>b</sup>	46.06 41.37	43.71 $\pm$ 3.31	14.00	82.33
3.0	637038 545908	2683 <sup>b</sup> 2300 <sup>b</sup>	26.83 23.00	24.91 $\pm$ 2.71	7.98	89.93

<sup>a</sup> Values for AFB<sub>1</sub> in a 75 times diluted assay. <sup>b</sup> Values for AFB<sub>1</sub> in a 10 times diluted assay. <sup>c</sup> Values for AFB<sub>1</sub> represents the mean and standard deviation of experiments conducted in duplicate.

KEY: RSK 9 = 1-hydroxy-3,6-dimethylxanthone; RSK 10 = 1-methoxy-3,6-dimethylxanthone ; RSK 3 = 1-acetyl-3,6-dimethylxanthone

Having established that the addition of the three xanthenes to whole cell of the mutant fungal strain successfully inhibited AFB<sub>1</sub> production, an investigation was undertaken on cell-free extracts. This required the addition of each of the xanthenes to the active cell-free extract containing OMST and NADPH. The result of inhibition studies in cell-free extracts is presented in Table 33 (page 166). Typical chromatograms are presented in Figure 140-141 (Appendix 77-78, page 306-307).

Table 33. The Enzymatic Conversion of OMST (2.96 nmol) to AFB<sub>1</sub> in Cell-Free Extracts, in the Presence of Xanthone Derivatives and NADPH (1.5 mM) at pH 7.2 and 28 °C for an Incubation Time of 1 Hour.

Compound Added (nmol)	Integrated Peak Area	AFB <sub>1</sub> Produced (ng/ml)	AFB <sub>1</sub> Produced (µg/assay)	AFB <sub>1</sub> Produced (µg/assay) <sup>a</sup>	% Conversion to AFB <sub>1</sub>	% Inhibition of AFB <sub>1</sub>
Control	128436 130689 120177	545 555 510	0.545 0.555 0.510	0.537 ± 0.02	57.19	0
<b>RSK 9</b>						
5.92	31264 23308 41972	137 103 182	0.137 0.103 0.182	0.141 ± 0.04	15.10	73.58
<b>RSK 10</b>						
5.92	55949 69882 79245	240 299 338	0.240 0.299 0.338	0.292 ± 0.05	31.29	45.28
<b>RSK 3</b>						
5.92	111266 89932 64258	473 383 275	0.473 0.383 0.275	0.377 ± 0.10	39.92	30.19

<sup>a</sup>Values for AFB<sub>1</sub> represents the mean and standard deviation of experiments conducted in triplicate.

The enzyme concentration is 1 mg/ml.

RSK 9 = 1-hydroxy-3,6-dimethylxanthone ; RSK 10 = 1-methoxy-3,6-dimethylxanthone

RSK 3 = 1-acetyl-3,6-dimethylxanthone

In the absence of xanthone, OMST was converted to AFB<sub>1</sub> (57.19 %). The addition of the three xanthenes inhibited the production of AFB<sub>1</sub> to different extent. It was evident that 1-hydroxy-3,6-dimethylxanthone displayed the largest inhibitory effect on AFB<sub>1</sub> production and the order of decreasing inhibition is:

1-hydroxy-3,6-dimethylxanthone > 1- methoxy-3,6-dimethylxanthone > 1-acetyl-3,6-dimethyl-xanthone.

Based on the difference in structure of OMST to the three xanthenes, the lowest inhibitory effect of the acetyl derivative is predictable since the acetyl group in the xanthone makes it even less like OMST which contains the methoxy group. However, it is surprising that the methoxy derivative has a lower inhibitory effect than the hydroxyl

derivative. It is most likely that due to the smaller size of the hydroxyl group, the hydroxyl derivative is able to fit easily in a recess of an enzyme site thereby preventing the normally easy access of OMST to the enzyme site for conversion to AFB<sub>1</sub>.

For kinetic studies based on AFB<sub>1</sub> inhibition, the xanthone used was 1-methoxy-3,6-dimethylxanthone since it showed structural features (Figure 133, page 158) that could mimic OMST, the metabolite of concern.

The time course study (Chapter 7) with cell-free extracts indicated a close to linear relationship between time of incubation of OMST and percentage conversion to AFB<sub>1</sub> for up to 1 hour of incubation. Cleveland and Bhatnagar<sup>98</sup> reported a linear relationship for up to 2 hours of incubation. Therefore in this investigation  $V_o$ , the initial reaction velocity, was measured in terms of the quantity of AFB<sub>1</sub> (nmol) produced for a fixed period of time, viz., 10 minutes.

The results of substrate competition studies with cell-free extracts are presented in Table 34 (page 168) and Table 35 (page 169). Typical chromatograms are presented in Figure 142-143 (Appendix 79-80, page 308-309). Using the data from these Tables, the substrate concentration  $S_o$  ( $\mu$ M), the product concentration  $V_o$  ( $\mu$ M/min),  $1/S_o$  and  $1/V_o$  were calculated and these values are presented in Table 36 (page 169). A plot of  $S_o$  versus  $V_o$  is presented in Figure 144 (page 172).

Table 34. The Enzymatic Conversion of OMST to AFB<sub>1</sub> in Cell-Free Extracts, in the Presence of NADPH (0.15 mM) at pH 7.2 and 28 °C for an Incubation Time of 10 Minutes.

OMST Added (nmol)	Integrated Peak Area	AFB <sub>1</sub> Produced (ng/assay)	AFB <sub>1</sub> Produced (µg/assay)	AFB <sub>1</sub> Produced (µg/assay) <sup>a</sup>
0.73	32817	143	0.14	0.16 ± 0.02
	37172	161	0.16	
	42000	182	0.18	
1.68	81195	346	0.35	0.37 ± 0.02
	89401	381	0.38	
	89371	381	0.38	
2.75	127043	539	0.54	0.53 ± 0.03
	130690	555	0.56	
	116546	495	0.50	
4.20	138068	586	0.59	0.63 ± 0.04
	15833	671	0.67	
	148676	630	0.63	
12.65	194279	822	0.82	0.84 ± 0.02
	201883	854	0.85	
	202918	858	0.86	
16.81	209908	888	0.89	0.90 ± 0.02
	210968	892	0.89	
	221107	835	0.84	
21.01	221556	937	0.94	0.93 ± 0.05
	205814	870	0.87	
	229665	971	0.97	

<sup>a</sup> Values for AFB<sub>1</sub> in a 1 ml assay represent the mean and standard deviation of experiments conducted in triplicate.

Table 35. The Enzymatic Conversion of OMST to AFB<sub>1</sub> in Cell-Free Extracts, in the Presence of NADPH (0.15 mM) and 1-Methoxy-3,6-dimethylxanthone (2.75  $\mu$ M) at pH 7.2 and 28 °C for an Incubation Time of 10 Minutes.

OMST Added (nmol)	Integrated Peak Area	AFB <sub>1</sub> Produced (ng/assay)	AFB <sub>1</sub> Produced ( $\mu$ g/assay)	AFB <sub>1</sub> Produced ( $\mu$ g/assay) <sup>a</sup>
0.73	23650	105	0.10	0.11 $\pm$ 0.01
	25455	112	0.11	
	27703	122	0.12	
1.68	66111	283	0.28	0.29 $\pm$ 0.01
	65379	280	0.28	
	67647	290	0.29	
2.75	81647	348	0.35	0.36 $\pm$ 0.03
	91167	388	0.39	
	77462	331	0.33	
4.20	94149	401	0.40	0.40 $\pm$ 0.01
	92960	396	0.40	
	91189	389	0.39	
12.65	123569	525	0.53	0.55 $\pm$ 0.02
	132753	563	0.56	
	133017	564	0.56	
16.81	117410	499	0.50	0.56 $\pm$ 0.06
	140145	594	0.59	
	142384	604	0.60	
21.01	143565	609	0.61	0.57 $\pm$ 0.04
	133616	567	0.57	
	124410	528	0.53	

<sup>a</sup> Values for AFB<sub>1</sub> in a 1 ml assay represent the mean and standard deviation of experiments conducted in triplicate.

Table 36. The Data<sup>a</sup> Obtained for the Line-Weaver Burk Plot.

So ( $\mu$ M)	<sup>b</sup> V <sub>o</sub> ( $\mu$ M/min)	<sup>c</sup> V <sub>o</sub> ( $\mu$ M/min)	(1/So)	<sup>b</sup> (1/V <sub>o</sub> )	<sup>c</sup> (1/V <sub>o</sub> )
0.73	0.05	0.03	1.37	20.00	33.33
1.68	0.12	0.09	0.60	8.33	11.11
2.75	0.17	0.11	0.36	5.88	9.09
4.20	0.20	0.13	0.24	5.00	7.69
12.65	0.27	0.17	0.08	3.70	5.88
16.81	0.29	0.18	0.06	3.45	5.56
21.01	0.30	0.18	0.05	3.33	5.56
25.2	0.31	0.19	0.04	3.22	5.26

<sup>a</sup>Values for AFB<sub>1</sub> produced are based on the mean of three independent determinations. <sup>b</sup>AFB<sub>1</sub> concentration in the absence of inhibitor. <sup>c</sup>AFB<sub>1</sub> concentration in the presence of inhibitor (2.75  $\mu$ M).

It is evident from Figure 144 (page 172) that the addition of 1-methoxy-3,6-dimethylxanthone caused a decrease of  $V_{\max}$  because the enzyme(s) is not as catalytically efficient in the presence of the inhibitor. Although Figure 144 (page 172) indicates that 1-methoxy-3,6-dimethylxanthone inhibits the production of AFB<sub>1</sub>, it is not clear as to the type of inhibition that was occurring, i.e., is it competitive, non-competitive or uncompetitive inhibition. Linear regression analysis of the data  $1/S_0$  and  $1/V_0$  from inhibition studies gave  $r^2$  values of 0.98 and 0.95 for the reaction without inhibitor and with inhibitor, respectively. These two values indicate a close to linear relationship between the two variables. The Line-Weaver Burk plot<sup>194</sup> was constructed by graphing  $1/V_0$  versus  $1/S_0$  (Figure 145, page 172). The  $K_m$  value was calculated from the  $1/S_0$  versus  $1/V_0$  plot for the control, i.e., the reaction in the absence of the inhibitor.

$$\begin{aligned} K_m / V_0 &= \text{slope} \\ &= 19.25 - 6.67 / 1.37 - 0.36 \\ &= 12.58 / 1.01 \end{aligned}$$

$$\begin{aligned} \text{and from the regression constant} \quad 1/V &= 2.2 \\ \text{therefore} \quad K_m &= 5.66 \end{aligned}$$

The  $K_m$  value for OMST, using the cell-free extract at pH 7.2 and temperature 28 °C, is approximately 5.66  $\mu\text{M}$  which compares favourably with the value of 1.2  $\mu\text{M}$  for a partially purified oxido-reductase at pH 7.5 and 29 °C for an incubation time of 10 minutes as reported by Bhatnagar *et al.*<sup>175</sup>. The  $K_m$  value is a fundamental characteristic of an enzyme, therefore the discrepancy of the results in these investigations is suggestive of the dependence of the availability of oxygen and probably to other co-factors. The former seems a plausible suggestion since the “enzyme” responsible for the conversion of OMST to AFB<sub>1</sub> is an oxido-reductase which contains an oxygenase (discussed in Chapter 10) responsible for the formation of intermediates in the latter part of the AFB<sub>1</sub> biosynthetic pathway.

The  $K_m$  value of 5.66  $\mu\text{M}$  is not affected by the addition of the inhibitor 1-methoxy-3,6-dimethylxanthone as indicated by Figure 145 (page 172). This means that non-competitive inhibition is being displayed and the Lineweaver-Burk equation for this type of inhibition



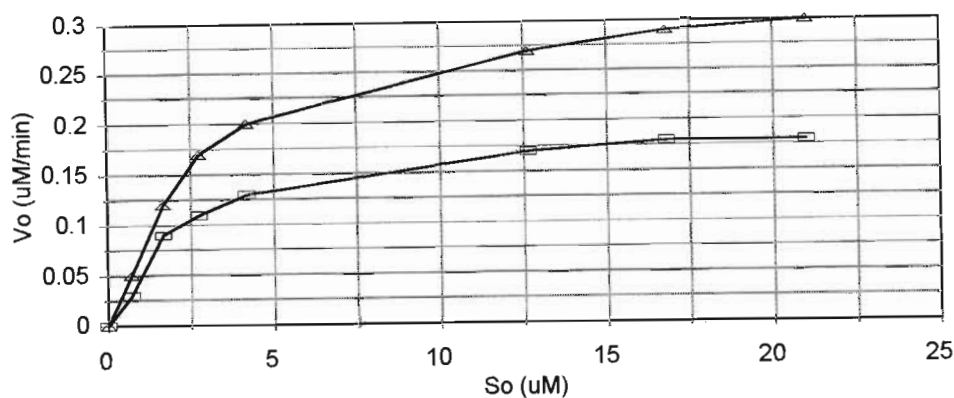
is:

$$1/v = [1 + (I)/K_i] [1/V + (K_m/V) (1/S)]$$

As seen from Figure 145 (page 172), the effect of a non-competitive inhibitor is to increase both the slope and the Y intercept.

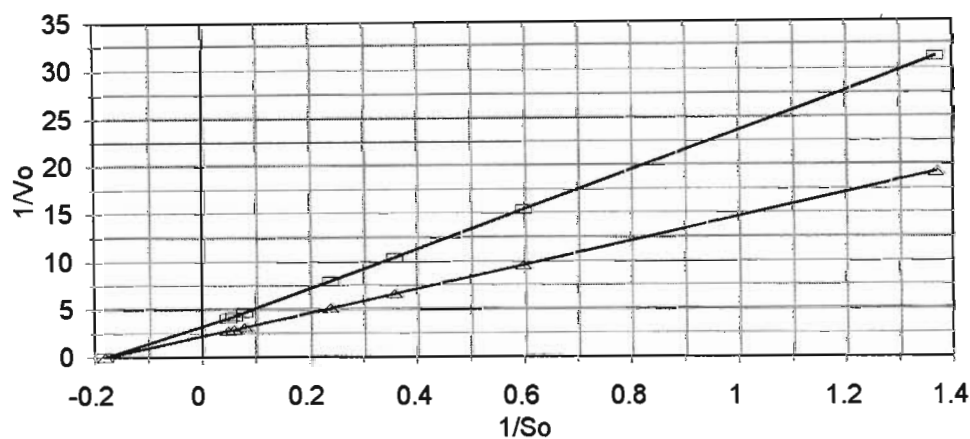
Classical non-competitive inhibition occurs because of strong binding of the inhibitor to the enzyme, e.g., by covalent bonds, which the normal substrate cannot dislodge no matter what concentration is used. The inhibitor can either block the active site by binding irreversibly to an active residue or at a place remote from the active site which either hinders or distorts it. In the case of 1-methoxy-3,6-dimethylxanthone, it is difficult to imagine a covalent linkage being introduced and one must therefore presume a very stable complex formed at the active site analogous to the normal substrate binding. Alternatively the formation of a stable complex at a site removed from the active site, which in terms of amino acid residues is not directly involved with the catalytic process. This is supported by the fact that no coumarin or intermediate reaction product from 1-methoxy-3,6-dimethylxanthone was observed, although an analogous ring system was present for such a reaction to take place.

These experimental results are predictable since the xanthone does not completely resemble the substrate and therefore has the possibility to bind at a second enzyme site thereby distorting the "active enzyme" site which is responsible for converting OMST to AFB<sub>1</sub>.



KEY: OMST ( $\Delta$ ) ; OMST + 1-methoxy-3,6-dimethylxanthone ( $\square$ )

Figure 144. The Effect of OMST Concentration and of the Addition of 1-methoxy-3,6-dimethylxanthone (2.75  $\mu$ M ) on the Production of AFB<sub>1</sub> in Cell-Free Extracts, in the Presence of NADPH (1.5 mM) for an Incubation Time of 10 minutes at pH 7.2 and 28 °C. The Enzyme concentration was 1.00 mg/ml.



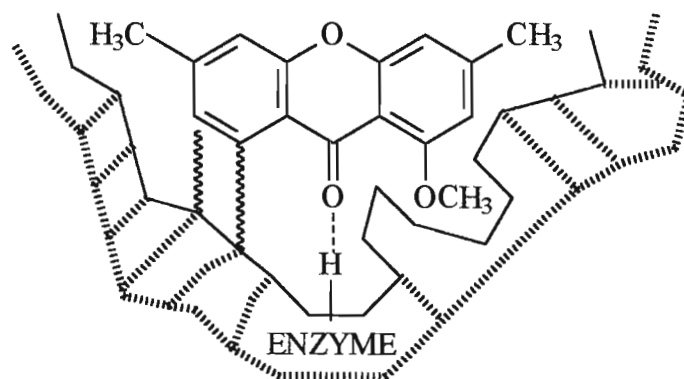
KEY: OMST ( $\Delta$ ) ; OMST + 1-methoxy-3,6-dimethylxanthone ( $\square$ )

Figure 145. The Lineweaver-Burk Plot.

It cannot be concluded from kinetic data alone whether the inhibitor has become part of the “active enzyme” site or not. However, it is most likely that the inhibitor may combine with an enzymatic site different from the site at which the substrate is bound. This would then distort the “active enzyme” site and would subsequently change the catalytic

properties of the “active enzyme” site.

If one considers substrate-enzyme binding based on the polyaffinity theory, then the combination of a substrate of OMST with the “active centre” of the enzyme would involve at least two structural elements of the substrate. In the case of 1-methoxy-3,6-dimethylxanthone, one likely form of interaction, subject to polar influences, is hydrogen bonding involving the hydrogen accepting group of the inhibitor and hydrogens of the enzyme. Another possible form of interaction is van der Waals forces involving the aryl group. Based on the above reasoning, a partial representation (Figure 146) may be advanced as at least a plausible working hypothesis:



KEY: Hydrogen bond (-----); van der Waals forces (~~~~~)

Figure 146. A Possible Mode of Attachment of 1-Methoxy-3,6-dimethylxanthone to an Enzyme Center.

In the above figure, the hydrogen bond is intended to represent bonds of this type between the enzyme and the substrate. The weak van der Waals forces of attraction may exist between the enzyme and the aryl groups. It is tempting to speculate that the size of the substituent, viz., the methoxy group, rather than the electronic property of the substituent is of importance. It maybe possible that the orientation of the inhibitor at the enzyme complex, aided by the close fitting of the substituent into a recess in the enzyme of about the size of a methoxy group, results in the key group of OMST becoming less

accessible to the enzyme. It is, however, difficult to imagine that the oxygen groups on the inhibitor have sufficient hydrogen bonding capacity to cause sufficient attachment to the enzyme for inhibition to take place. A more likely explanation is that the inhibitor combines with a hydrophobic region of the enzyme complex. This might either distort the enzyme tertiary structure, as such areas are usually internalised, or displace the non-reactive part of the normal substrate assuming that requires such a hydrophobic area for recognition and binding. This is a plausible hypothesis, however it is difficult to examine experimentally because such catalytic centers, if they exist, are parts of complex protein molecules. This task is made even more difficult by the fact that the catalytic action of an enzyme protein is usually observed only when the protein is in the native state; treatment that leads to denaturation of the protein also destroys the enzyme activity.

It is not possible to generalise extensively about the mode of action of the inhibitor and discussion of this question may be postponed until some other individual enzymes that exhibit such inhibition behaviour are considered. Since the nature of the actual binding site of the oxido-reductase is still unknown, it is suggested that isotopic techniques be investigated to test hypothesis about the nature of the enzyme-substrate intermediates in this enzyme catalysed reaction.

A question which arose is the nature of the oxygenase involved in the final mechanistic pathway, viz., the conversion of OMST to AFB<sub>1</sub>. Is the 'oxido-reductase' a monooxygenase, a dioxygenase or both? There are conflicting speculations on the nature of the oxygenase and this question warranted further investigation. One way to resolve this question is to monitor the quantity of oxygen consumed by a partially purified "enzyme" which is responsible for the conversion of OMST to AFB<sub>1</sub>.

## CHAPTER TEN

### THE NATURE OF THE OXYGENASE(S) INVOLVED IN THE CONVERSION OF OMST TO AFB<sub>1</sub>

#### 10.1 INTRODUCTION

##### 10.1.1. The Metabolic Mechanism

Among the most important biological conversions in the initial metabolic degradation of many substances, are those in which molecular oxygen is incorporated into the substrate molecule. These oxygen-fixing reactions are ubiquitous in nature, occurring in plants, animals and micro-organisms. As mentioned in Section 2.5.1. (page 8), the oxygenases are categorized as monooxygenase, if one oxygen atom is incorporated into the substrate, or dioxygenase if two oxygen atoms are incorporated into the substrate. The monooxygenases are characterised by the cleavage of molecular oxygen with the subsequent incorporation of one atom into the substrate and the other to produce water. The reactions catalysed by this mechanism include hydroxylation, epoxidation and conversion of ketones to esters, including lactonization. With some substrates several oxygenations may occur in sequence, one such reaction generating the substrate for a subsequent one. In addition to molecular oxygen, a two-electron donor molecule is required and water is formed from the atom of oxygen that is not incorporated into the substrate.

With respect to the latter part of the aflatoxin biochemical pathway, i.e., the conversion of OMST to AFB<sub>1</sub>, it has been postulated<sup>23</sup> that the 'oxido-reductase' may be composed of at least two enzymes, one of which is likely to be monooxygenase requiring NADPH for activity and the other a dioxygenase requiring the presence of ferrous ions. Bhatnagar *et al.*<sup>175</sup> used a partially purified enzyme to show that NADPH is required for enzyme activity; however, the presence of ferrous ion was not found to be stimulatory for

the activity of the 'oxido-reductase' at this stage of enzyme purification. Bhatnagar *et al*<sup>87,100</sup> proposed two tentative mechanisms for the conversion of OMST to AFB<sub>1</sub> (page 24-27). Recently, Chatterjee and Townsend<sup>136</sup> suggested that a single enzyme might be possible to execute this seemingly multi-step reaction as outlined in Figure 147.

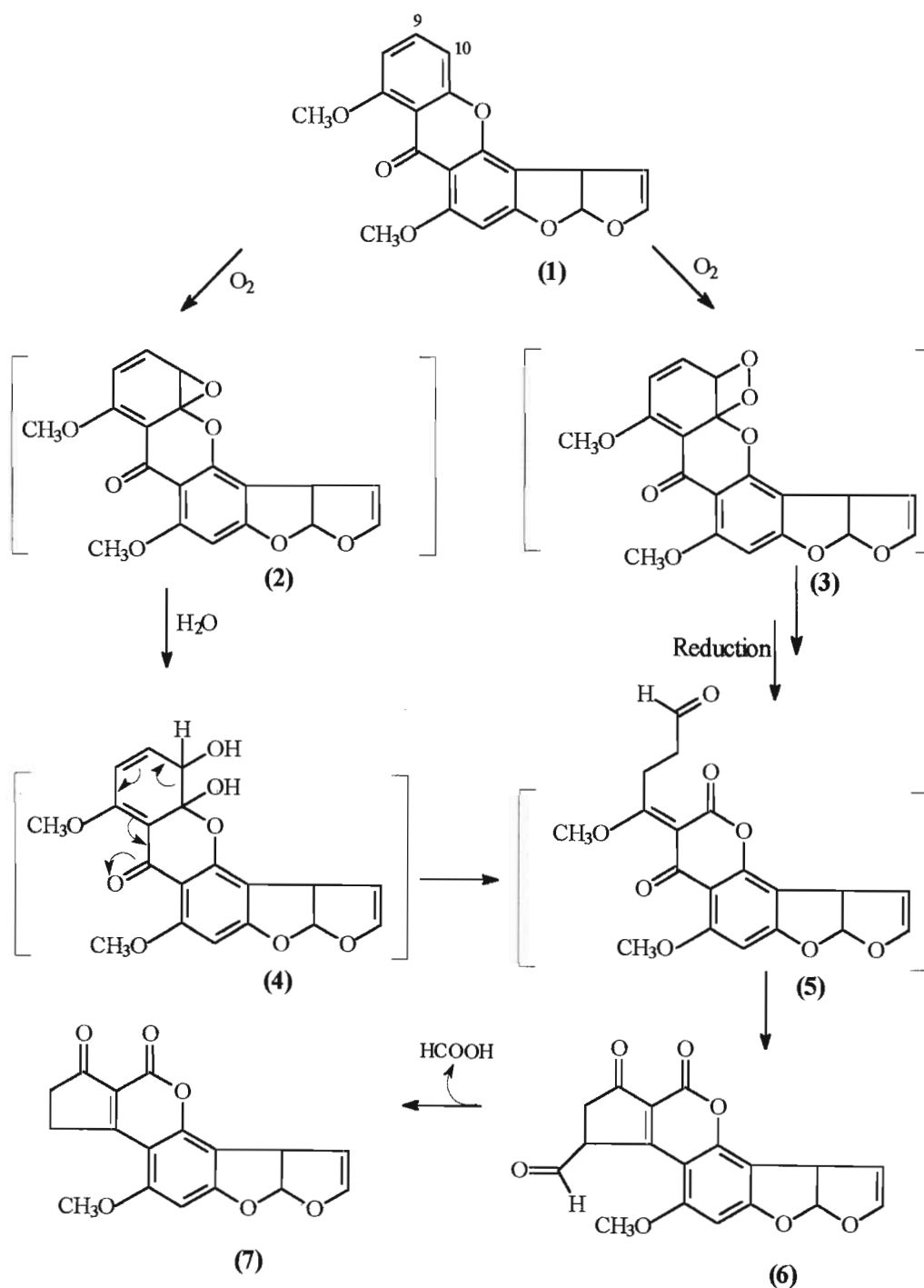


Figure 147. The Mechanism Proposed by Chatterjee and Townsend<sup>136</sup> in the Formation of Aflatoxin B<sub>1</sub>.

In this proposal OMST (**1**) undergoes a monooxygenase reaction in keeping with the observed requirement of NADPH for enzymatic activity. The reactive epoxide (**2**) hydrates to form a diol (**4**) which cleaves to form a stable  $\beta$ -ketone lactone (**5**). An aldol condensation of the lactone produces a coumarin (**6**) which would undergo a retro-aldol reaction to release C-10 of **1** as formic acid and AFB<sub>1</sub> (**7**). An alternative pathway was also suggested, which uses a dioxygenase to produce an intermediate (**3**) which would subsequently undergo a reduction reaction to produce the aldehyde (**5**). However, further research by the same authors showed radiolabelled  $^{14}\text{CO}_2$  was generated from the  $^{14}\text{C}$ -10 of **1**. This finding indicated that 10-hydroxy-OMST (**8**) (Figure 148) was a possible intermediate involved in the oxidative rearrangement process. Using the important finding made by Simpson *et al.*<sup>195</sup> that  $^2\text{H}$  at C-10 of **1** underwent deuterium migration (Figure 149) in the course of the biosynthesis, it was proposed that the epoxide was formed at C-9/C-10 of **1**. This would then result in the formation of **4** with subsequent loss of water to **8**. Subsequent cleavage by either a monooxygenase or a dioxygenase and reclosure by loss of  $\text{CO}_2$  could occur as shown in Figure 148.

The mechanism proposed by Chatterjee and Townsend (Figure 147) is obscure in that :

- the rearrangement of intermediate **4** does not produce intermediate **5** and
- the rearrangement of intermediate **5** to intermediate **6** does not indicate the loss of the methyl group.

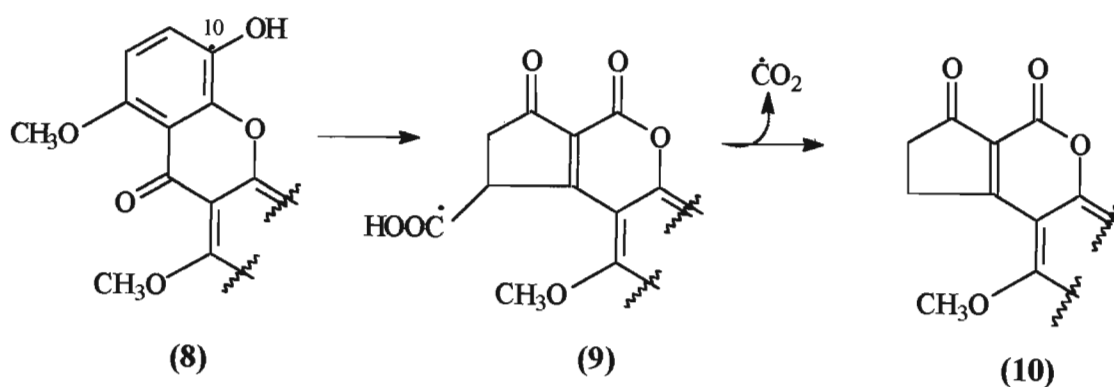


Figure 148. The Mechanism Proposed by Chatterjee and Townsend<sup>136</sup> in the Formation of Aflatoxin B<sub>1</sub>.

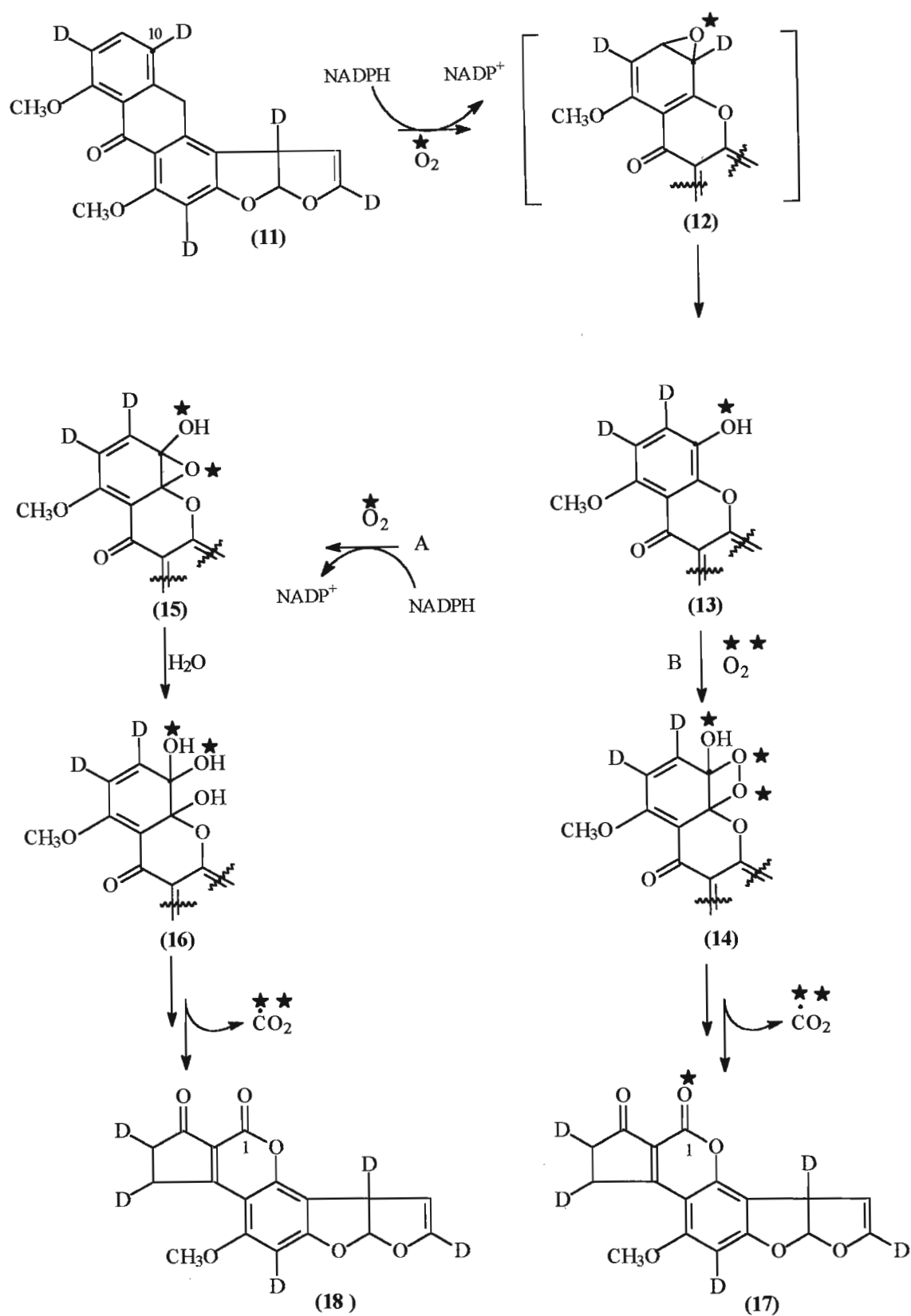


Figure 149. The Mechanism Proposed by Watanabe and Townsend<sup>196</sup> in the Formation of Aflatoxin B<sub>1</sub>.

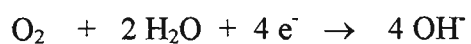


Watanabe and Townsend<sup>196</sup> reported the incorporation of molecular oxygen as  $^{18}\text{O}_2$  into AFB<sub>1</sub>. It was reported that  $^{18}\text{O}$  was incorporated at carbon one of compound **17** and a mechanism was proposed which is presented in Figure 149 (page 178). It was suggested that the first step involved a monooxygenase reaction in the formation of an epoxide (**12**) which subsequently formed the 10-hydroxy-OMST (**13**) derivative thereby indicating a “NIH shift” (the shift of deuterium from the site of hydroxylation to an adjacent site during the oxidation of aromatic compounds). Further oxidation could involve a second monooxygenase (path A) or a dioxygenase (path B). These researchers have suggested that the enzymatic reaction would follow path B, i.e., a monooxygenase mediated reaction followed by a dioxygenase reaction. This mechanism, however, is not fully explained since the formation of intermediate **13** requires some type of rearrangement. Therefore the final mechanism involving oxidative cleavage and rearrangement reactions of OMST to AFB<sub>1</sub> has not been adequately resolved.

The objective of this study was to determine the type of oxygenases, i.e., a monooxygenase or a dioxygenase or both, involved in the conversion of OMST to AFB<sub>1</sub>. In order to answer this question it was decided to monitor the consumption of molecular oxygen by a polarographic technique using a Clark oxygen electrode.

#### 10.1.2. The Oxygen Electrode

Oxygen measurement by polarographic techniques is based on the polarization of two electrodes with a potential of slightly less than negative one volt in a solution containing electrolytes and dissolved oxygen. The Clark oxygen electrode (Figure 150, page 180) normally consists of a platinum cathode and a silver anode both immersed in the same solution of potassium chloride (a drop of saturated solution) and separated from the test solution by a membrane. Oxygen diffuses through the membrane, which prevents contamination of the electrode by chemicals present in the test solution, to the cathode. Reduction occurs at the cathode (negatively polarized) surface resulting in a flow of current. This reaction at the cathode is expressed as :



At the other electrode (anode), described as the reference electrode, oxidation takes place.

For a Ag/AgCl reference, the reaction is :

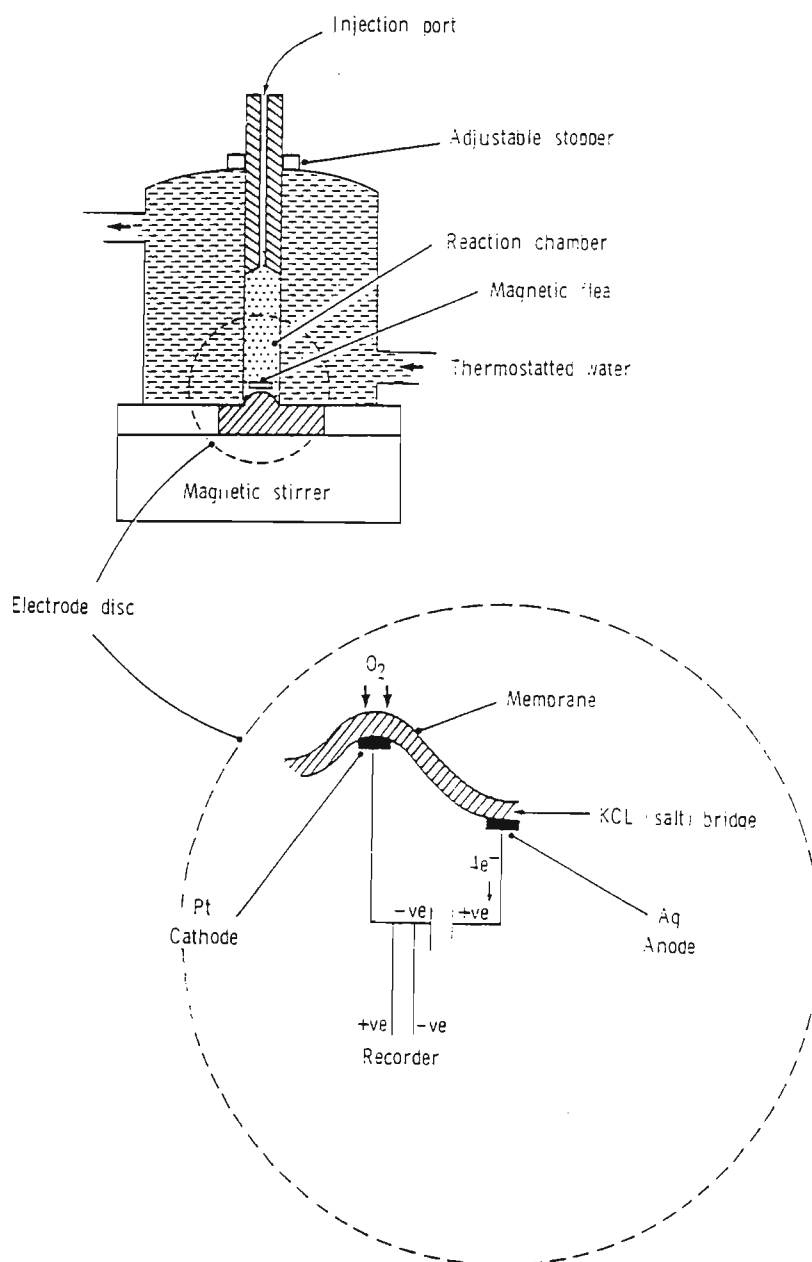
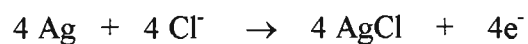


Figure 150. A Schematic Diagram of a Clark Oxygen Electrode.

The voltage-current relationship for a polarographic oxygen electrode, is represented by the characteristic curve (Figure 151).

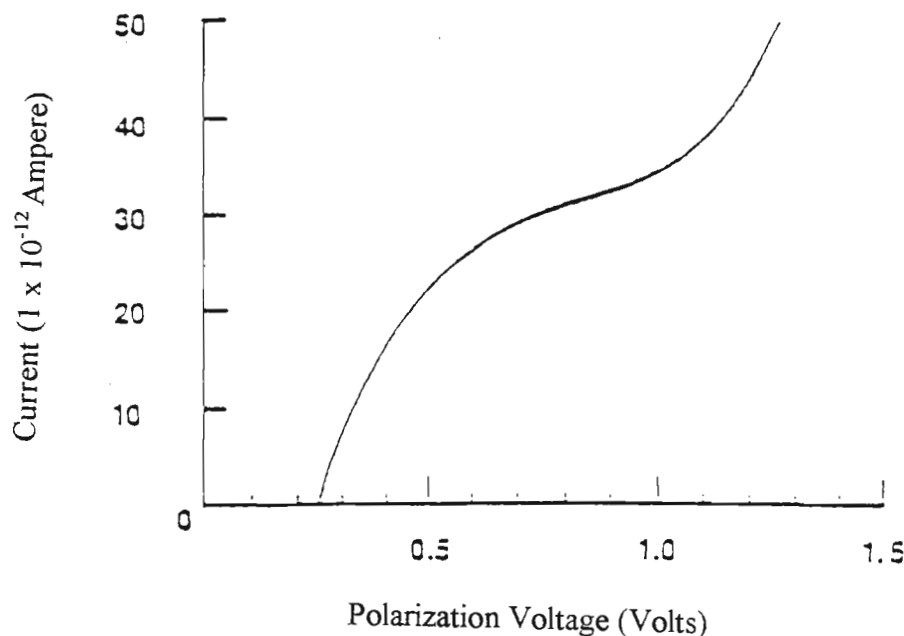


Figure 151. The Characteristic Polarographic Curve.

In the region below approximately - 0.5 volt (V), there is a reasonably linear voltage-current relationship. As the polarization voltage is increased beyond - 0.5 V, the current will tend to reach a plateau at which changes in V have little effect on current. The electrode is normally operated with the polarization voltage set to the midpoint of the plateau region, in which case the current is diffusion limited. In a diffusion limited condition virtually all of the oxygen molecules which reach the cathode are immediately reduced, resulting in a zero oxygen concentration at the cathode surface, and a current which is limited by the rate at which oxygen can diffuse to this zero concentration region. The diffusion rate is a function of the oxygen diffusion coefficient of the membrane and media surrounding the cathode and the dissolved oxygen concentration, which is proportional to the oxygen partial pressure ( $pO_2$ ) and temperature. The result is that, for a

constant temperature, current flow through the electrode will be directly proportional to  $pO_2$  and hence the percentage oxygen concentration.

A plot of the relationship between current and  $pO_2$ , for a fixed polarization voltage, is called the standard curve as shown in Figure 152. For most electrodes the curve is linear.

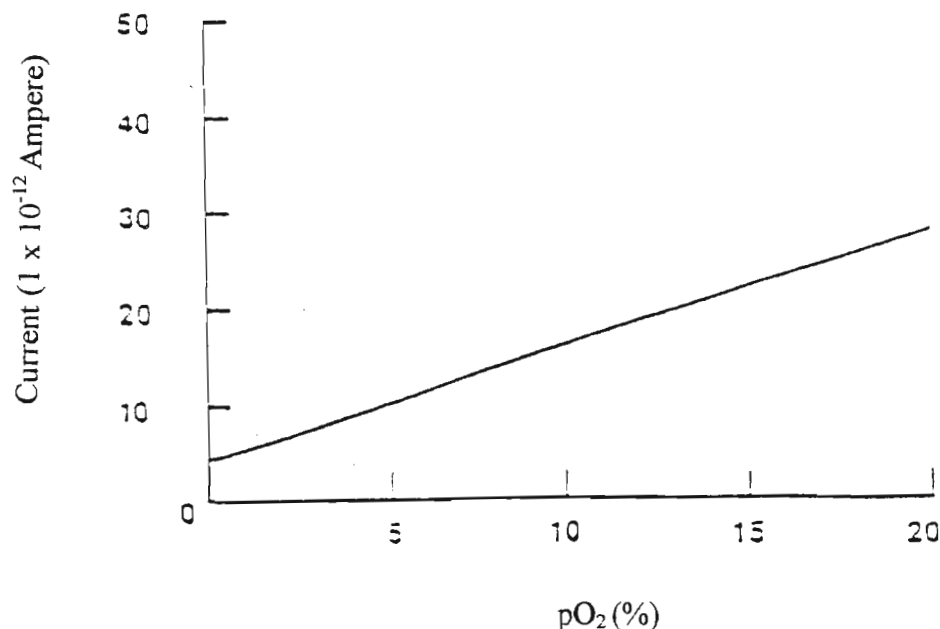


Figure 152. The Standard Curve of Current and Partial Pressure of Oxygen.

It should be noted that the curve does not intersect the origin but rather indicates a small current, the “dark” current, at zero potential. This current results from electrical leakage through insulating materials in the system and reduction of oxygen which was absorbed into the electrode materials.

As the bulk fluid continually moves past the cathode surface, a “stirring” artifact is created. Therefore, large variations in readings will result from bulk flow in an unstirred solution. In a stirred solution, at a fixed oxygen tension, current increases as the velocity of the fluid across the electrode increases to a point when it becomes independent of the stirring velocity. For this reason, best results are obtained in a well stirred system, since

oxygen current becomes independent of stirring velocity once the critical stirring speed is determined (Figure 153).

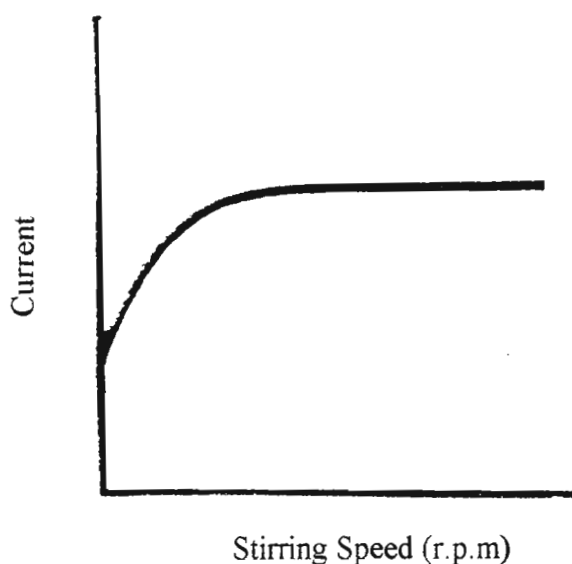


Figure 153. The Effect of Stirring Speed on Current.

The thickness of the electrolyte behind the membrane is important to the electrode response time and is affected by two factors. The first is the surface of the electrode. This surface must be smooth and flat in the vicinity of the cathode in order to achieve a thin electrolyte layer. The second factor, which affects the thickness of the electrolyte layer behind the membrane, is the way in which the membrane is installed. The membrane must be installed in a manner to avoid creases, air pockets, punctures and minimum membrane stretch.

The time constant of the electrode depends on the time required to establish the various oxygen gradients in the electrolyte. This depends mainly on the permeability of the membrane and the mobility of oxygen in the sample. To increase the electrode response time, a thin membrane with a high oxygen diffusion constant is used in a rapidly stirred system.

The Clark oxygen electrode is mounted on a stirring motor and a magnetic flea (stirrer bar) inserted into the reaction vessel (600  $\mu$ l). Since the solubility and rate of diffusion of oxygen are both temperature dependent, water from a temperature controller is pumped through the outer compartment of the oxygen electrode. In order to obtain a continuous trace of the oxygen content, a recorder is attached.

## 10.2. MATERIALS AND METHODS

### 10.2.1. General

Ultra-violet data were obtained from a LKB Ultrospec II 4050 UV/VIS spectrophotometer. A Controlled Environment Incubator Shaker (New Brunswick Scientific) was used for incubation experiments to test the activity of enzymes. Mycelia were stored at -85 °C in a Ultra Low Freezer (Nuaire). A Virtis Sentry Freeze Drier was used for freeze drying mycelia at -70 °C. Centrifugation was conducted in a Beckman Model J2-21 Centrifuge. High pressure liquid chromatography analysis was carried out with a Spectra System (Thermo Separation Product) with a P 2000 Pump, AS 3000 Auto-Injector, a Spectra Focus Optical Scanning Detector linked to a Pentium Computer and IBM 4029 Printer and a C<sub>18</sub> Waters reversed phase column fitted with a guard column. Mass measurements were made by means of a Mettler TG 50 Thermobalance. A 730 Clark Style oxygen electrode (Diamond General Development Corp. (USA)) linked to a Chemical Microsensor, an Instech 1060 stirrer, a Water Bath (set at 25 °C) and a CR 600 Recorder (JJ Instruments) were used. The oxygen uptake chamber was stainless steel (600 µl, volume) and was teflon coated. The electrode specifications were :

- Length 32 mm
- Diameter (with O-ring installed) 3.2 mm
- Typical current (ambient pO<sub>2</sub>) 20 nanoamps
- Time constant < 4 seconds
- O<sub>2</sub> consumption rate 15.6 x 10<sup>10</sup> O<sub>2</sub> molecules per second
- Membrane thickness 0.025 mm polyethylene

### 10.2.2. Chemicals

All chemicals were of reagent grade or analytical grade. Analytical grade solvents were purchased from Sigma Chemical Suppliers (SA) and used for extraction and HPLC analysis. Petri-dishes and disposable plastic pipettes were purchased from Polychem

Chemical Co. (SA). Thin layer chromatography plates containing fluorescent indicator (F<sub>254</sub>) (Merck Art: 5554) were purchased from Merck NT Laboratory Suppliers (SA). Sephadex G-25, of particle size 100-300 microns, was purchased from Pharmacia Fine Chemicals (SA). Dialysis tube ( i.d. 10 mm ; molecular weight retention >10000 ) and all other chemicals were purchased from Sigma Chemical Suppliers (SA). Reduced nicotinamide adenine dinucleotide phosphate and S-adenosyl methionine were purchased from Boehringer Mannheim (Germany).

### 10.2.3. Preparation of the Concentrated Dialysed Enzyme(s)

An AFB<sub>1</sub> blocked mutant of *A. parasiticus* (Wh1-11-105) was maintained on PDA for 5-7 days. A spore suspension (1 ml)(described in Section 6.2.2, page 90) was inoculated into five Erlenmeyer flasks (250 ml) containing sterile Reddy's medium<sup>67</sup> (100 ml). The flasks were incubated at 28 °C in shake culture at 150 rpm for 96 hours and harvested by filtering through double layer cheesecloth. The mycelia was washed with ice cold 20 mM phosphate buffer (pH 7.2) (Appendix 44, page 273) dried by vacuum filtration, freeze-dried and stored in an airtight container at -78 °C.

A sample of freeze-dried mycelium (0.5 g) was gently ground to a fine powder in a dry chilled mortar. The powdered mycelium was suspended in ice cold 20 mM phosphate buffer (10 ml) and gently stirred for 15 minutes. The homogenate was centrifuged at 20 000 x g for 20 minutes at 4 °C and filtered through glass wool. The supernatant, i.e., the cell free extract, was loaded into the glass column (described in Section 8.2.4, page 121) and run at 4 °C at a flow rate of 25 ml per hour with the phosphate buffer solution. The active fraction was collected and dialysed against solid sucrose for 3 hours. The concentrated partially purified "enzyme" protein fraction (1 ml) was tested for activity with 3.09 nmole of the substrate OMST at 28 °C and pH 7.2. in the presence of NADPH (0.15 mM).



#### 10.2.4. Qualitative Analysis by Thin Layer Chromatography

The metabolites were extracted from the aqueous solution with chloroform, passed through anhydrous sodium sulphate and evaporated to dryness with nitrogen and gentle heat. The dried residue was re-dissolved in chloroform (100  $\mu$ l) and a portion (20  $\mu$ l) was spotted onto the origin of a t.l.c. plate (10 x 10 cm aluminium backed Kieselgel 60). The plate was developed in CEI, air dried and scanned for fluorescence under UV. The t.l.c. plates were then sprayed with aluminium chloride (20 %, m/v) and heated to test for the characteristic change in intensity and colour of fluorescence<sup>166,167</sup> under UV.

#### 10.2.5. Quantification by High Pressure Liquid Chromatography

Standard solutions of AFB<sub>1</sub> were prepared in the range 50-1000 p.p.b. in 5.00 ml volumetric flasks by serial dilution with the mobile phase consisting of acetonitrile: water (40: 60, v/v). The external calibration method was used by plotting concentration in p.p.b. versus average integrated peak area in mV.s. The best fit straight line was obtained by using linear regression analysis. The data and calibration graph of AFB<sub>1</sub> are presented in Table 37 (Appendix 81, page 310) and Figure 154 (Appendix 82, page 310), respectively.

The dried residue was dissolved in the mobile phase (500  $\mu$ l) and made to volume in a 1 ml volumetric flask, filtered through Whatmann LC (0.2  $\mu$ m) filter and analysed by HPLC using a mobile phase of acetonitrile : water (40 : 60).

#### 10.2.6. Quantification of NADPH by Ultra-Violet Spectroscopy

An accurate volume (50  $\mu$ l) of a stock solution of NADPH (1 mg/ml) was pipetted, by means of a micro-pipette, into a 5.00 ml volumetric flask and brought to mark with deionised water. This solution of NADPH (50  $\mu$ g/5 ml) was used to prepare standard solutions of NADPH in the range 2.5- 40  $\mu$ g per 5 ml by pipetting an accurate volume and diluting the solution to 5.00 ml in a volumetric flask. The solution was transferred into

a glass cuvette and the absorbance was read at 340 nm against deionised water as blank. The data is presented in Table 38 (Appendix 83, page 311) and the calibration graph is presented in Figure 155 (Appendix 84, page 311).

### **10.2.7. The Method Used for Oxygen Consumption Studies**

#### **10.2.7.1. The Operation of the Oxygen Uptake Chamber**

The window valve, made of an optical glass, of the uptake chamber was used as a 3-position stopcock to control the flow of fluid, viz., when rinsing, loading and emptying the chamber. This was achieved by aligning the two depressions on the inside of the glass window with the two holes in front of the sample cup. The three possible alignment positions is presented in Figure 156 (page 189).

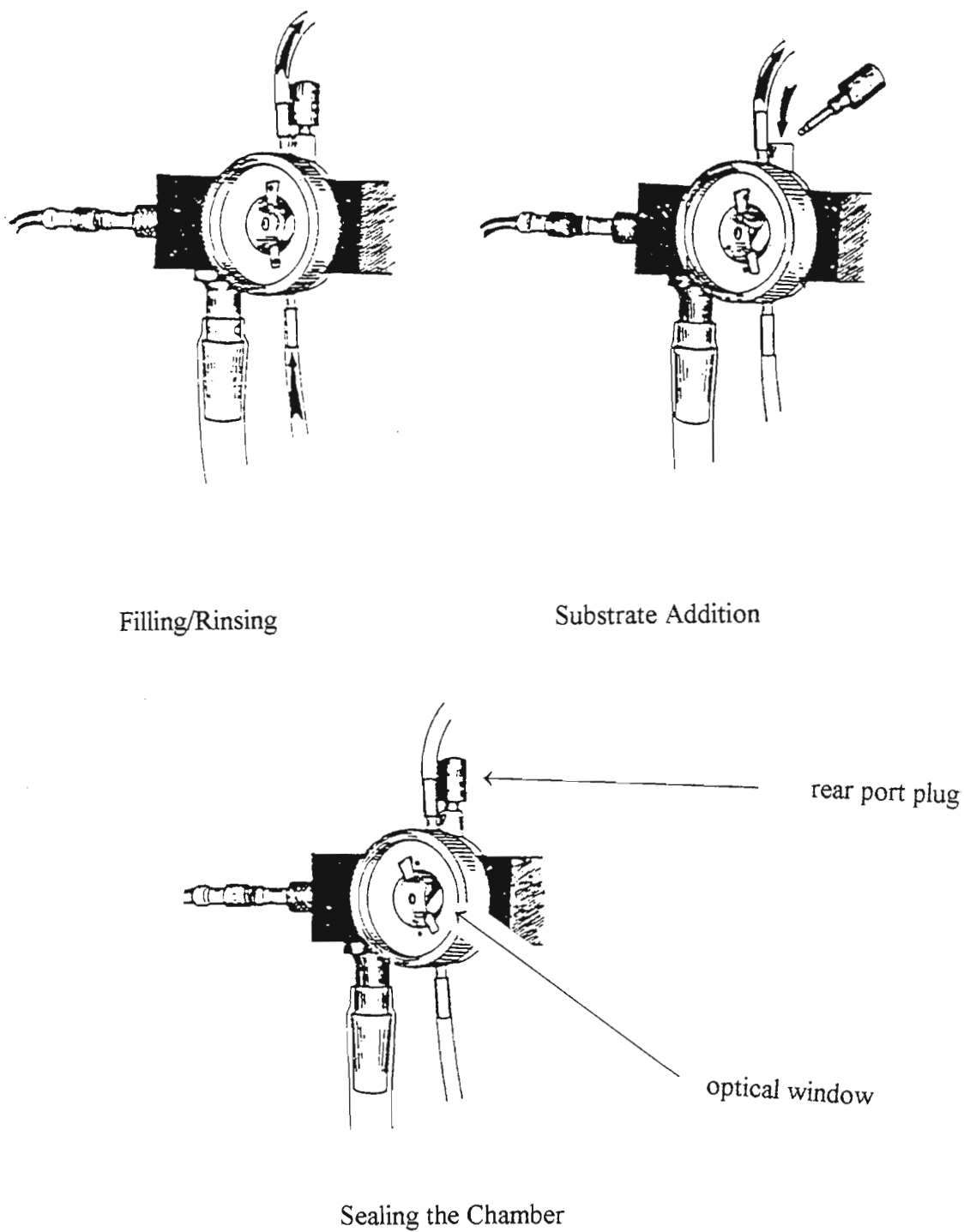


Figure 156. The Three Alignment Positions of the Window Valve of the Oxygen Uptake Chamber.

With the valve aligned in a vertical position, i.e., with the top and bottom port open, the chamber was flushed with either deionised water or the calibration solution. This was carried out by means of a modified set-up (described in Section 11.2.7.3). When taking measurements, the ports were closed by rotating the glass window anti-clockwise so as to misalign the two depressions inside the glass. In order to rinse (flush) the uptake cell with the “enzyme” the upper port, which is larger than the bottom port, was aligned with the depression and addition was made via the rear port. The plug was then inserted so as to seal the chamber from the outside. For substrate, co-factor or solvent addition, the rear port was opened and a Hamilton syringe was used such that the needle made contact with the bottom of the uptake cell. Immediately after addition, the rear port plug was inserted.

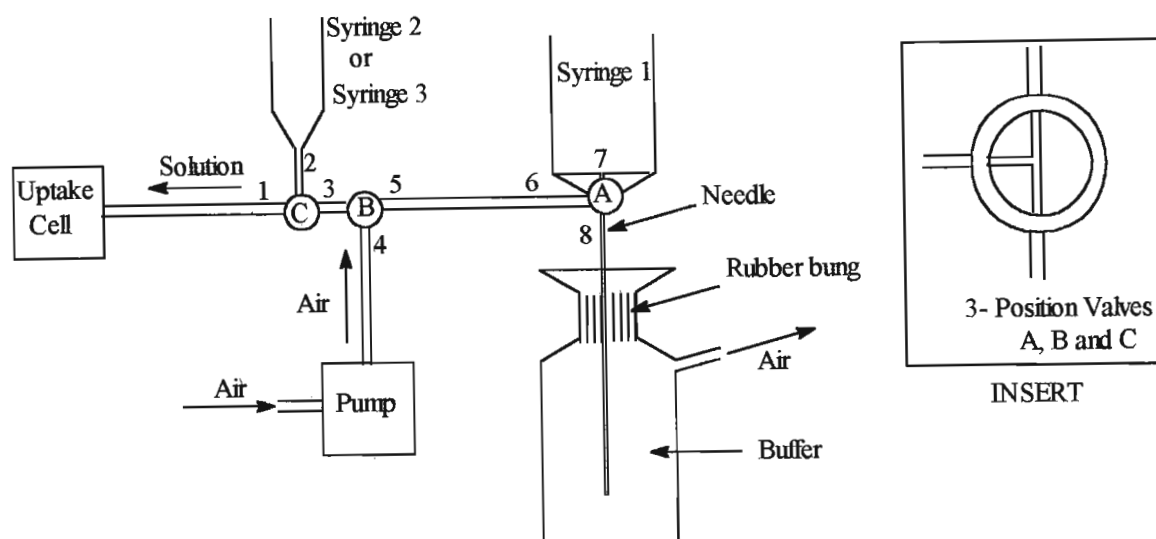
#### **10.2.7.2. The Installation of the Membrane**

Using an installation tool, the O-ring was inserted into the narrow end of the tool. The O-ring was then rolled to the opposite end of the tool. Thereafter the membrane was placed carefully on the end of the tool containing the O-ring. The tip of the electrode was dipped into a saturated solution of potassium chloride and whilst holding the membrane onto the tool, the electrode was placed on the membrane and the O-ring was rolled into the groove of the electrode. The electrode was then examined to ensure that a drop of potassium chloride was visible on the electrode. The excess overlapping membrane was trimmed with a scissor and the electrode was inserted into the uptake chamber and hand tightened.

#### **10.2.7.3. Calibration of the Instrument.**

The chemical microsensor was set-up as follows: The negative electrode polarization position was selected and a polarization voltage of  $-0.75\text{ V}$  was set by adjusting the polarization control knob. The coarse gain was set at  $10^{-7}$  ampere and the coarse zero was set at  $10^{-11}$  ampere. The output selector was set to allow  $\text{O}_2$  to be measured as percentage  $\text{O}_2$ .

A calibration system (Figure 157) was designed in order to calibrate the Clark oxygen electrode. The system consisted of three 3-position valves (see insert) A, B and C which were used to control the flow of either air or the liquid, viz., deionized water, the 0 % O<sub>2</sub> solution or the 21 % O<sub>2</sub> solution.



j

Figure 157. A Diagrammatic Representation of a Modified Calibration Cell for the Clark Oxygen Electrode.

Note : This diagram is not drawn to scale.

The instrument was calibrated as follows :

- calibration of the instrument with 21 % O<sub>2</sub> solution : Phosphate buffer (100 ml, 20 mM, pH 7.2, 25 °C) was introduced into the glass flask, via the hypodermic syringe 1, by closing position 6 of valve A. Thereafter positions 3 and 7 of valves B and A, respectively were closed and the pump switched on for approximately 30 minutes. The pump was switched off, position 6 was closed and the saturated buffer solution was withdrawn into syringe 1. Positions 2, 4 and 8 were closed and the buffer solution, in syringe 1, was slowly introduced into the uptake cell with it's valve in the open position. Having rinsed (flushed) the uptake cell with approximately 30 ml of the buffer solution, the valve in the uptake cell was closed and the stirrer was switched on

and set to control 6, which gave the highest % O<sub>2</sub> reading. The fine gain was adjusted to read 21 % O<sub>2</sub>. After a stabilisation period of approximately 20 minutes, the fine gain was readjusted to read 21 % O<sub>2</sub> and the recorder pen was set at a convenient point on the graph paper to read 21 % O<sub>2</sub>. The exact point on the graph paper, viz., either 20 mm representing 4 % O<sub>2</sub> or 20 mm representing 5 % O<sub>2</sub>, was established after preliminary investigations with the enzyme in the uptake cell. After ensuring that there was no further current drift, the stirrer was stopped and the uptake cell was flushed with deionised water.

- rinsing of the uptake cell with deionised water : deionised water was placed in the hypodermic syringe 2 and the syringe was then inserted into valve C. With position 3 closed and the uptake cell valve open, deionised water was slowly introduced into the uptake cell.
- 0 % O<sub>2</sub> : a freshly prepared solution of sodium sulphite (2 %, 100 ml) was prepared in a 100 ml plastic bottle. The cap was screwed tightly and shaken vigorously for approximately 5 minutes. The sodium sulphite solution was placed in the hypodermic syringe 3 and the syringe was then inserted into valve C. With position 3 closed and the valve of the uptake cell open, the solution was slowly introduced into the uptake cell. Thereafter the valve in the uptake cell was closed and the stirrer was set to control 6. The fine zero was then adjusted to read 0 % O<sub>2</sub>. After a stabilisation period of approximately 20 minutes, the fine zero was readjusted to read 0 % O<sub>2</sub> and the recorder pen was set at zero on the graph paper. The stirrer was stopped.

After flushing the cell with deionised water, the 21 % O<sub>2</sub> solution was introduced into the uptake cell. The stirrer was set and the fine gain and recorder were readjusted to read 21 % O<sub>2</sub>. Similarly, the 0 % O<sub>2</sub> solution was used to retune the fine zero and the recorder readjusted. The uptake cell was flushed thoroughly with deionised water.

#### **10.2.7.4. The Method Used to Determine the Electrode Response to Organic Solvents**

The uptake cell was flushed with the phosphate buffer and the valves were closed. The rear port plug was removed and the organic solvent (50  $\mu$ l) was injected at the bottom of the uptake cell by means of a Hamilton syringe. The plug was immediately inserted and the stirrer and recorder started. The stirrer and recorder were stopped after base-line stabilisation was achieved. The uptake cell was flushed, first, with deionised water and followed by the phosphate buffer. The following solvents were used to determine their effect on electrode response: acetone, ethanol, dioxane, acetonitrile and dimethyl sulphoxide.

Dimethyl sulphoxide (100 ml) was placed into the 100 ml flask and helium was gently bubbled into the solvent for approximately 30 minutes. An aliquot (50  $\mu$ l) was injected at the bottom of the uptake cell, containing the phosphate buffer, by means of a Hamilton syringe. The plug was immediately inserted and the stirrer and recorder started. The stirrer and recorder were stopped after base-line stabilisation was achieved.

#### **10.2.7.5. The Method Used For Enzyme Assay with the Clark Oxygen Electrode**

The uptake cell was flushed with deionised water and the valves were closed. The rear port plug was removed and the uptake cell was flushed with the partially purified "enzyme" by means of a 1000  $\mu$ l micro-pipette. The plug was inserted and the uptake cell, which was free of air bubbles, was stirred and the recorder started. Stirring was allowed to continue until the system equilibrated at 25 °C. The stirrer was stopped, the plug was removed and the co-factor(s) (50  $\mu$ l, 50  $\mu$ g) was added by means of the Hamilton syringe. The plug was inserted and stirring continued. The stirrer was stopped, the plug removed and the substrate (50  $\mu$ l, 3.09 nmol) which was dissolved in dimethyl sulphoxide, was added. The plug was inserted and stirring continued until a steady base-line was obtained.

The following four reactions were carried out with the partially purified “enzyme” and using ST as substrate:

- co-factors SAM and NADPH were added followed by deionised water (50  $\mu$ l).
- co-factors SAM and NADPH were added followed by dimethyl sulphoxide (50  $\mu$ l).
- deionised water (50  $\mu$ l) followed by dimethyl sulphoxide (50  $\mu$ l).
- co-factors SAM and NADPH were added followed by ST (50  $\mu$ l, 3.09 nmol).

For the three reactions mentioned above, SAM (50  $\mu$ l, 0.15  $\mu$ mol) and NADPH (50  $\mu$ l, 0.15  $\mu$ mol) were added.

After each reaction the stirrer and recorder were stopped, and the contents of the uptake cell was collected in a 10 ml beaker by flushing it with deionised water (approximately 5 ml).

The following four reactions were carried out with the partially purified “enzyme” and using OMST as substrate:

- co-factor NADPH was added followed by deionised water (50  $\mu$ l).
- co-factor NADPH was added followed by dimethyl sulphoxide (50  $\mu$ l). This reaction was carried out in triplicate.
- co-factor NADPH was added followed by OMST. This reaction was carried out in quintuplicate.

For the three reactions mentioned above, NADPH (50  $\mu$ l, 0.15  $\mu$ mol) was added.

After each reaction the stirrer and recorder were stopped, and the contents of the uptake cell was collected in a volumetric flask (5 ml) by flushing it with deionised water. The volumetric flask was made up to 5.00 ml and UV measurements were made at 340 nm to monitor the quantity of NADPH which was consumed by the reaction.

The metabolites were extracted as described in Section 7.2.5 (page 103). Qualitative analysis of the metabolites were carried out by t.l.c. as described in Section 10.2.4. (page 187) and quantitative analysis of AFB<sub>1</sub> was carried out by HPLC as described in Section 10.2.5. (page 187).



### 10.3. RESULTS AND DISCUSSION

The oxygen consumption studies were initially based on the enzymatic study undertaken by Del Rio *et al.*<sup>197</sup> because no known enzymatic studies involving an oxygen electrode were previously undertaken with aflatoxins. Furthermore, the Clark oxygen electrode was a new unstandardised instrument. The research reported by Del Rio *et al.*<sup>197</sup> is based on measurement of the initial rate at which oxygen is released by the enzyme catalase, derived from plant leaves, in an oxygen-free phosphate buffer. However, since the present study undertaken required that the initial rate of oxygen consumed by the enzyme was to be monitored, small changes were made with regards to the method (discussed below) although, overall, the technique remained the same.

The first problem which had to be addressed was to design a system which could be used to calibrate the instrument. This is described under methods (Section 10.2.7.3, page 191). The instrument was calibrated with the two calibrating solutions, viz., 21 % O<sub>2</sub> and 0 % O<sub>2</sub>, sequentially and the fine gain or the fine zero and the recorder pen deflection adjusted accordingly. This process was repeated several times until there was no base-line drift. Also, the instrument was checked for any base-line drift after a few hours of enzymatic reaction.

Preliminary investigations of the enzymatic reaction, by means of the Clark oxygen electrode, were undertaken by following the method of Del Rio *et al.*<sup>197</sup>, viz., the phosphate buffer was added first and after a few minutes of equilibration, the substrate (OMST in acetone) and the co-factor (NADPH in deionised water) were added followed by the partially purified "enzyme" (100 µl; 100 µg). Two problems became evident, i.e., the electrode gave a response of approximately 6 % O<sub>2</sub> when acetone (50 µl) was added and AFB<sub>1</sub> was not produced by the enzymatic reaction. The latter problem was not surprising considering that, firstly, an impure "enzyme" was being used and, secondly, this "enzyme" was being further diluted by the buffer in the uptake cell. The problem of an impure "enzyme" could not be resolved since several attempts<sup>175</sup> were unsuccessful in

purifying the “enzyme” to homogeneity by a 4-step procedure. However, the second problem could be addressed by using a larger volume of the “enzyme”, i.e., by adding the “enzyme” preparation first followed by NADPH and OMST. Subsequently, another preliminary investigation was carried out by adding the “enzyme” (600  $\mu$ l; 600  $\mu$ g), followed by NADPH (dissolved in deionised water) and OMST (dissolved in acetone). A typical recorder trace (Figure 158) is explained sequentially:

- the “enzyme” (E), stored at 4 °C, is added and the system equilibrates at 25 °C
- the stirrer is stopped (Ss) resulting in a decrease in % O<sub>2</sub> (see Figure 153, page 183)
- the co-factor (N) is added, the stirrer is started (Sp) and the system equilibrates
- the stirrer is stopped, the substrate (OMST) is added and the stirrer is re-started resulting in an immediate increase in % O<sub>2</sub>. This increase in % O<sub>2</sub> was unexpected. It was initially speculated that this was a result of the “enzyme” releasing any bound molecular oxygen; however subsequent investigations showed that the % O<sub>2</sub> response was due to the organic solvent (discussed later)
- the reaction proceeds until the recorder pen reaches base-line stabilisation.

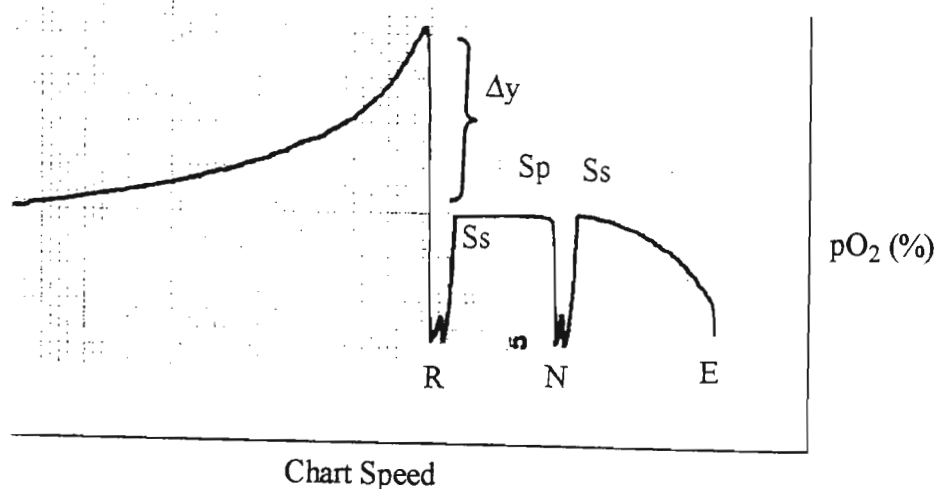


Figure 158. A Recorder Trace of the Enzymatic Conversion of OMST to AFB<sub>1</sub> by a Partially Purified Enzyme, in the Presence of NADPH (0.15 mM), by the Clark Oxygen Electrode.

E = Enzyme added ; S<sub>s</sub> = stirrer stopped ; S<sub>p</sub> = stirrer started ; N = NADPH added ; R = OMST added ;  $\Delta y$  = height above base-line.

Thin layer chromatography was used to determine the conversion of OMST to AFB<sub>1</sub>. *O*-methylsterigmatocystin ( $R_f$  0.54; CEI) exhibited a blue fluorescence under UV which changed to yellow when the t.l.c. plate was sprayed with the aluminium chloride spray reagent and heated gently. Aflatoxin B<sub>1</sub> ( $R_f$  0.62; CEI) displayed a characteristic blue spot which did not undergo any colour change with the spray reagent.

Having found that OMST was converted to AFB<sub>1</sub> within the first 10 minutes of the reaction, i.e., the reaction was monitored until base-line stabilisation was reached, the problem of the electrode response (height above baseline;  $\Delta y$ ) towards acetone had to be addressed. Since OMST is insoluble in water, a water miscible organic solvent had to be used to dissolve this substrate. It was therefore decided to investigate some common water miscible organic solvents in order to determine the one which would produce the smallest electrode response. The effect of organic solvents (50  $\mu$ l) on the response of the electrode is presented in Table 39. A typical recorder trace of the effect of deionised water (50  $\mu$ l), acetone (50  $\mu$ l) and dimethyl sulphoxide (50  $\mu$ l) on the response of the electrode is presented in Figures 159, 160 and 161, respectively (page 198-199).

Table 39. The Effect of Organic Solvents (50  $\mu$ l) on Electrode Response.

Solvent System	Electrode Response
Deionised water	1 mm ; 0.25 % Oxygen <sup>a</sup>
Dimethyl sulphoxide	17 mm ; 4.25 % Oxygen <sup>a</sup>
Acetonitrile	20 mm ; 5.00 % Oxygen <sup>a</sup>
Ethanol	36 mm ; 9.00 % Oxygen <sup>a</sup>
Dioxane	22 mm ; 5.50 % Oxygen <sup>a</sup>
Acetone	27 mm ; 6.75 % Oxygen <sup>a</sup>

<sup>a</sup>The Y-axis is calibrated with 5 % O<sub>2</sub> representing 20 mm and the percentage oxygen is based on the assumption that the electrode does not respond to the organic solvent but is a measure of oxygen present.

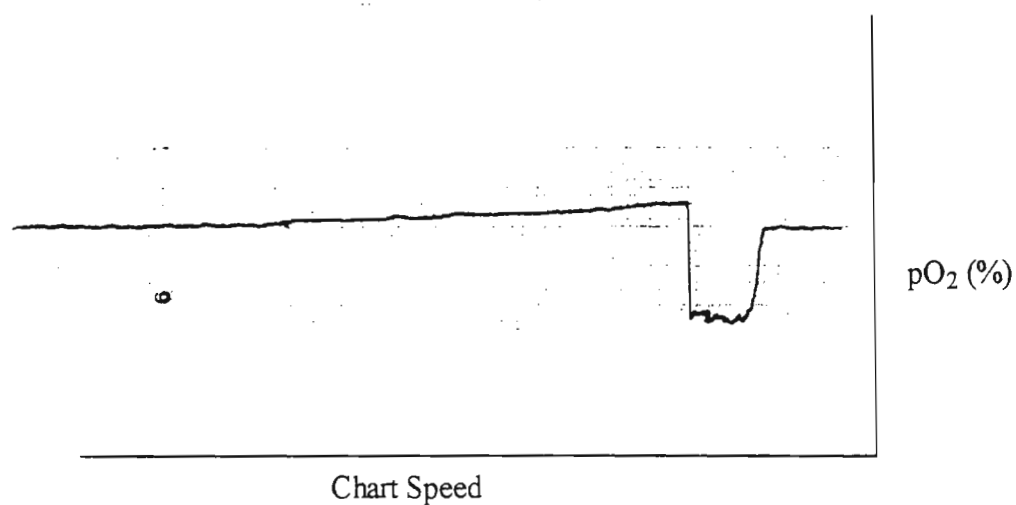


Figure 159. A Recorder Trace Showing the Response of the Electrode by the Addition of Deionised Water (50  $\mu$ l).

Chart speed 10 mm/minute. Y-axis 5 %  $O_2$  = 20 mm.

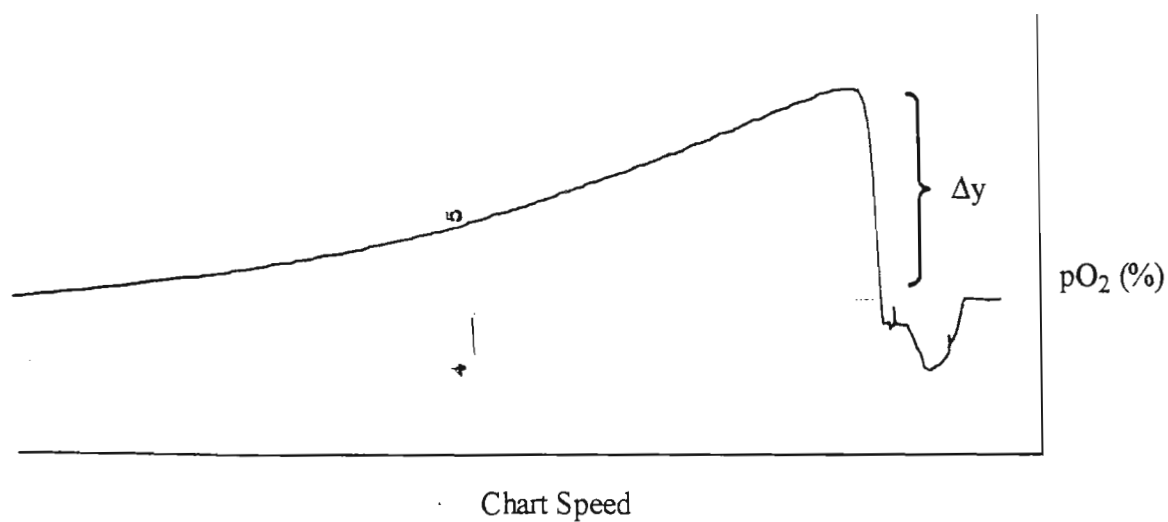


Figure 160. A Recorder Trace Showing the Response of the Electrode by the Addition of Acetone (50  $\mu$ l).

Chart speed 10 mm/minute. Y-axis 5 %  $O_2$  = 20 mm.

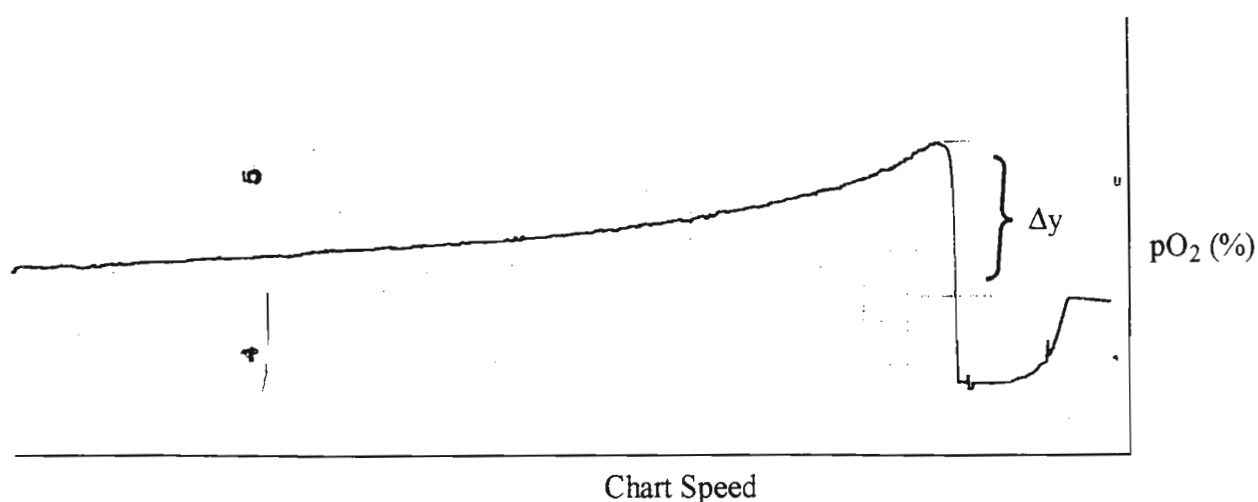


Figure 161. A Recorder Trace Showing the Response of the Electrode by the Addition of Dimethyl sulphoxide (50  $\mu$ l).

Chart speed 10 mm/minute. Y-axis 5 %  $O_2$  = 20 mm.

It was found that dimethyl sulphoxide produced the smallest electrode response ( $\Delta y$ ). This solvent was therefore chosen to dissolve OMST in all subsequent reactions. Since a preliminary investigation, discussed earlier, indicated that the reaction occurred in the first 10 minutes and that the base-line was stabilised in this period, it showed that the organic solvent contained sufficient dissolved oxygen to support an oxygenase catalysed reaction, the solubility in most organic solvents is more than in water. An investigation was undertaken to determine the approximate percentage of oxygen present in dimethyl sulphoxide. This was achieved by adding dimethyl sulphoxide (50  $\mu$ l), containing dissolved oxygen, to the phosphate buffer and comparing the electrode response with a dimethyl sulphoxide solution which was bubbled with helium for approximately 30 minutes to remove any dissolved oxygen. The results are presented in Table 40 (page 200) and the recorder traces are presented in Figure 162, 163 and 164 (page 200-201).

Table 40. The Effect of Dimethyl Sulphoxide on Electrode Response.

Solvent added (50 µl)	Height of Response (mm)
dimethyl sulphoxide	22
dimethyl sulphoxide	22
dimethyl sulphoxide (bubbled with helium)	17.5
dimethyl sulphoxide (bubbled with helium)	17.5

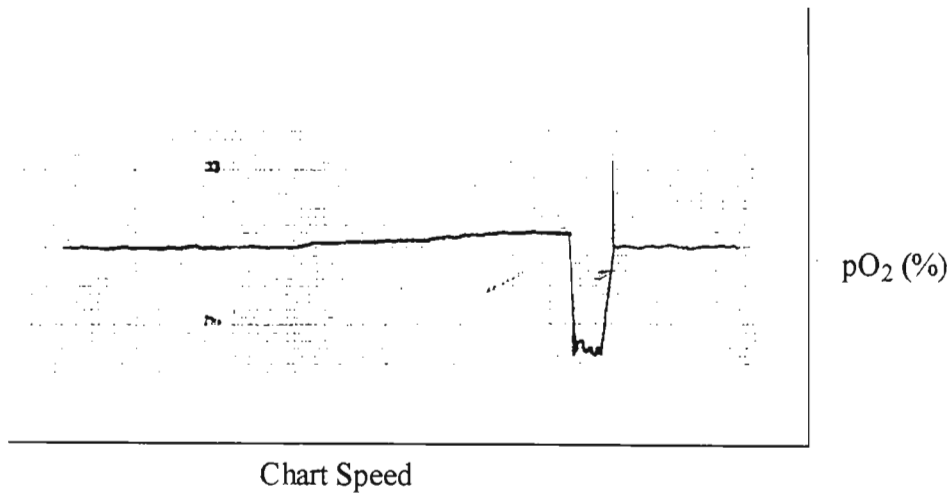


Figure 162. A Recorder Trace Showing the Response of the Electrode by the Addition of Deionised Water (50 µl).

Chart speed 0.5 mm/second. Y-axis 4 %  $O_2$  = 20 mm.

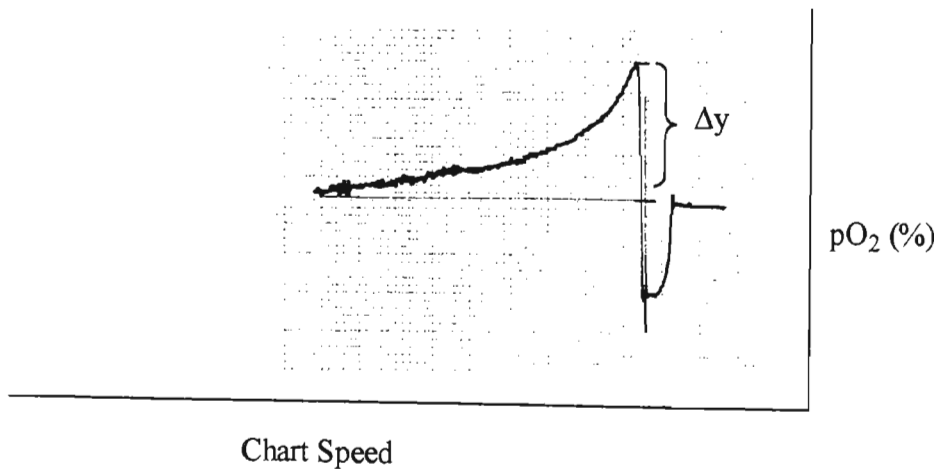


Figure 163. A Recorder Trace Showing the Response of the Electrode by the Addition of Dimethyl Sulphoxide (50 µl) Free of Dissolved Oxygen.

Chart speed 0.5 mm/second. Y-axis 4 %  $O_2$  = 20 mm.

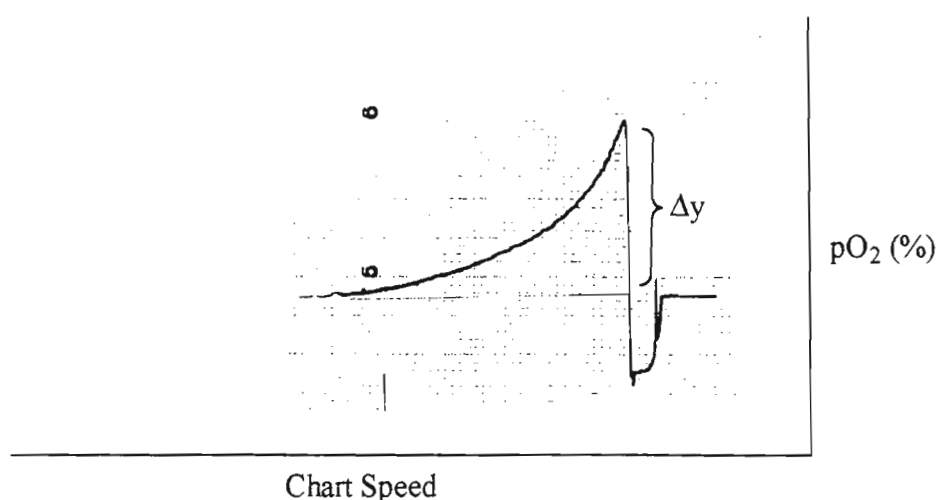


Figure 164. A Recorder Trace Showing the Response of the Electrode by the Addition of Dimethyl Sulphoxide (50  $\mu$ l) Containing Oxygen.

Chart speed 0.5 mm/second. Y-axis 4 %  $O_2$  = 20 mm.

The percentage of oxygen present in dimethyl sulphoxide was calculated from the difference in the height of the electrode response as follows :

$$\begin{aligned}\text{change in height} &= 22 - 17.5 \\ &= 4.5 \text{ mm}\end{aligned}$$

Since the recorder paper was calibrated for a height of 20 mm representing 4 %  $O_2$  (v/v),

$$\text{therefore } \% O_2 = 0.9$$

A value of 0.9 %  $O_2$  was anticipated to be sufficient for the “enzyme” to convert nanogram quantities of OMST to AFB<sub>1</sub> thereby indicating that the enzymatic conversion, in the preliminary investigation (Figure 158, page 196), occurred in the time interval before the base-line could be stabilised. This was confirmed by t.l.c. analysis (discussed earlier). Supporting evidence for the rapid enzymatic conversion of substrate to product is given by Del Rio *et al.*<sup>197</sup> who reported that in their enzymatic system, the enzymatic reaction was rapid and occurred in 140 seconds.

In order to confirm that the initial rate of conversion was rapid and therefore occurred within the first ten minutes of the reaction, an investigation was undertaken with ST as substrate in the presence of NADPH and SAM. The results are presented in Table 41

(page 202) and the recorder traces are presented in Figure 165-168 (page 203-204). An explanation of the different sections of the recorder trace is given on page 196.

The quantity of oxygen consumed in the enzymatic reaction was calculated by using the method of Del Rio *et al.*<sup>197</sup>, viz., the initial velocity of the reaction is calculated from the change in the slope of the first-order curve which is the equilibration period after the addition of the substrate.

$$\begin{aligned}\text{Initial velocity of control} &= 24/10.25 \\ &= 2.34 \text{ mm/min} \\ &= v_1\end{aligned}$$

$$\begin{aligned}\text{Initial velocity of reaction} &= 23.5/8.5 \\ &= 2.76 \text{ mm/min} \\ &= v_2\end{aligned}$$

The slope value for the reaction was corrected for the contribution by the non-enzymatic reaction (control). Therefore:

$$\begin{aligned}\text{Initial velocity of reaction} &= v_2 - v_1 \\ &= 0.42 \text{ mm/min}\end{aligned}$$

Thin layer chromatography was used to confirm the identity of AFB<sub>1</sub> as described earlier. It was found that ST was converted to AFB<sub>1</sub> only when all the requirements for an enzymatic reaction were satisfied, viz., using an active “enzyme” preparation and the presence of the co-factors (NADPH and SAM) and the substrate (ST).

Table 41. The Conversion of ST (3.09 nmol) to AFB<sub>1</sub> in a Partially Purified Enzyme, in the Presence of NADPH (0.15 mM) and SAM (0.15 mM) at pH 7.2 and 28 °C.

Substrate Added	Height of Response (mm)	Time (min)	Initial Velocity (mm/min)	AFB <sub>1</sub> Produced
SAM + NADPH + H <sub>2</sub> O	1.0	NIL	NIL	ND
ST + H <sub>2</sub> O	24	10.45	<sup>a</sup> 2.30	ND
SAM+NADPH +DMSO (Control)	24	10.25	<sup>a</sup> 2.34	ND
ST + NADPH + SAM (Reaction)	23.5	8.5	2.76	++

<sup>a</sup>Values represent the drift experienced by the electrode in order to reach base-line stability; ND = not detected; ++ = AFB<sub>1</sub> detected by t.l.c.



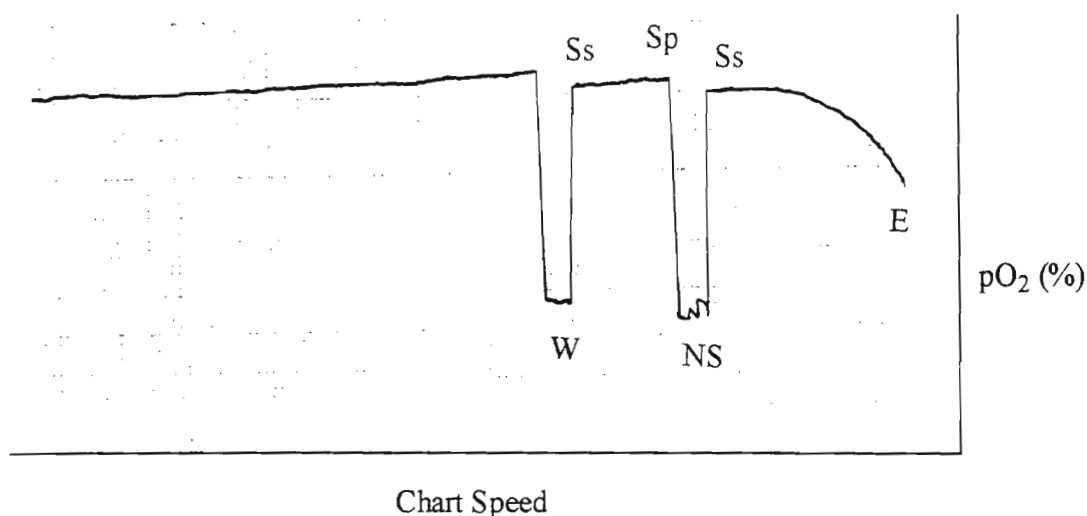


Figure 165. A Recorder Trace of the Partially Purified Enzyme in the Presence of SAM (0.15 mM) and NADPH (0.15 mM).

Chart speed 10 mm/minute. Y-axis 4 %  $O_2$  = 20 mm.

E = Enzyme added; Ss = stirrer stopped; Sp = stirrer started; W = deionised water added; NS = NADPH and SAM added.

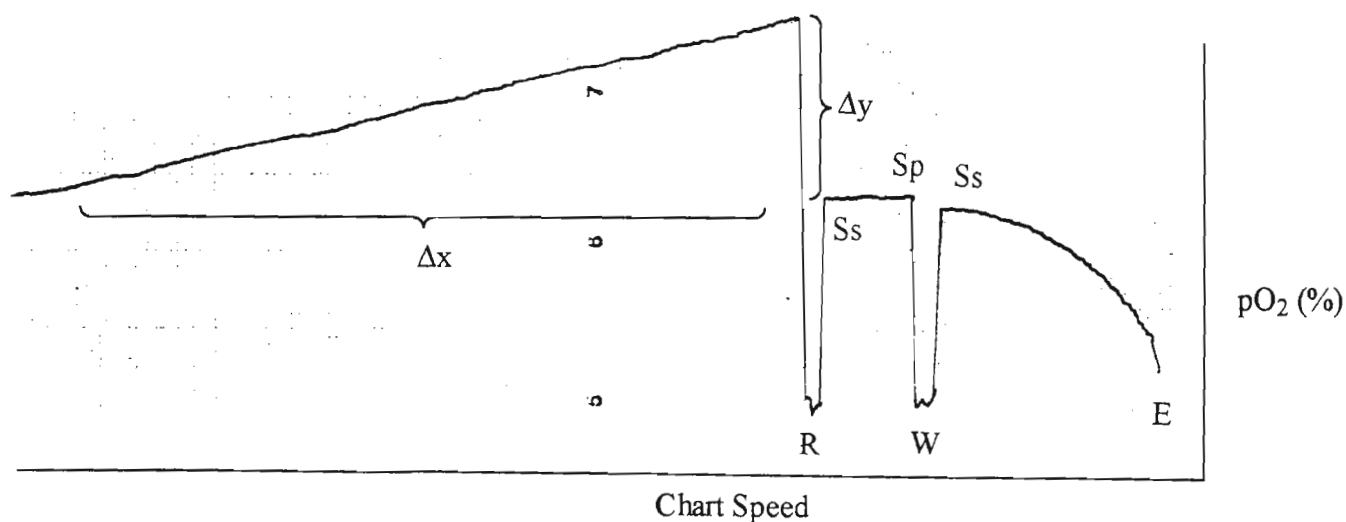


Figure 166. A Recorder Trace of the Partially Purified Enzyme in the Presence of ST and Deionised water (50  $\mu$ l).

Chart speed 10 mm/minute. Y-axis 4 %  $O_2$  = 20 mm.

E = Enzyme added; Ss = stirrer stopped; Sp = stirrer started; W = deionised water added; R = ST added.

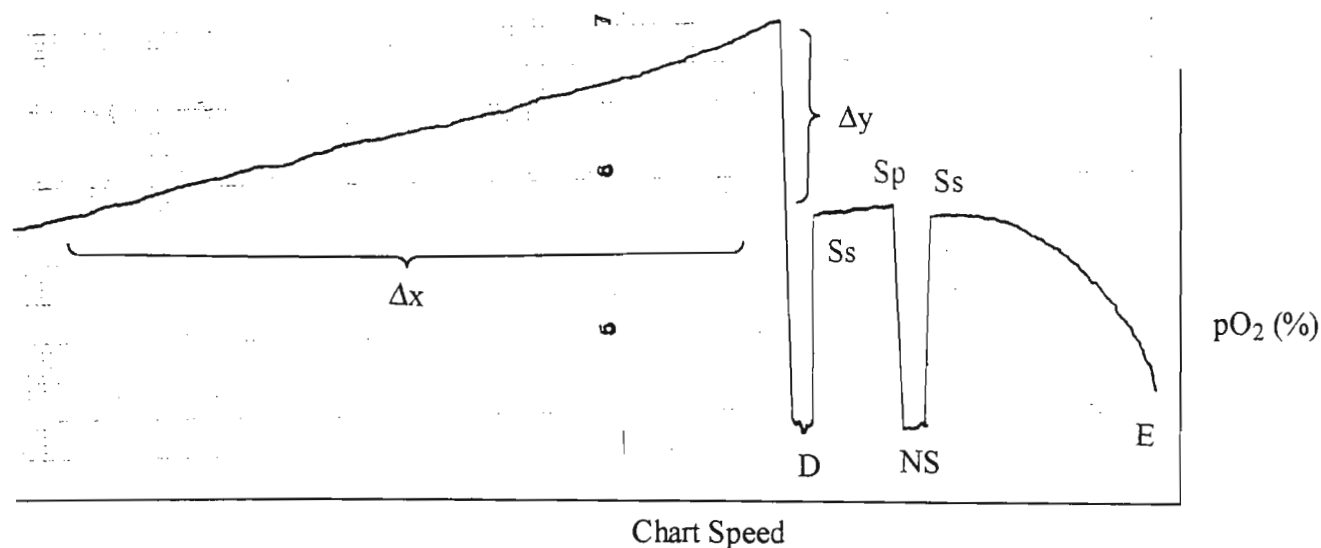


Figure 167. A Recorder Trace of the Partially Purified Enzyme in the Presence of SAM (0.15 mM), NADPH (0.15 mM) and DMSO (50  $\mu$ l).

Chart speed 10 mm/minute. Y-axis 4 %  $O_2$  = 20 mm.

**E** = Enzyme added; **S<sub>s</sub>** = stirrer stopped; **S<sub>p</sub>** = stirrer started; **NS** = NADPH and SAM added; **D** = DMSO added.

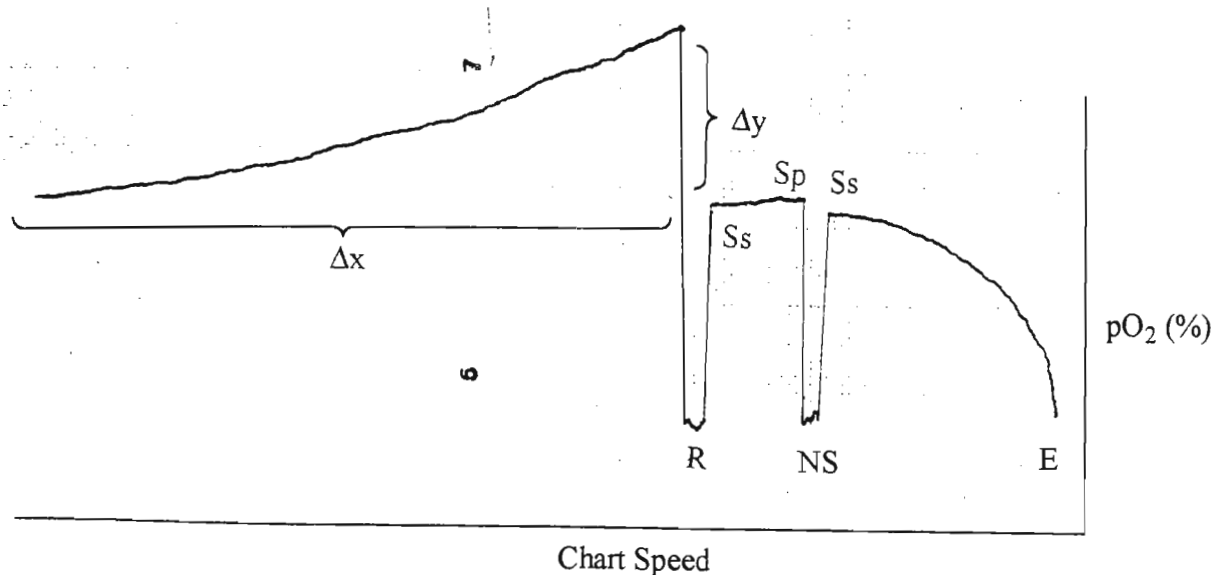


Figure 168. A Recorder Trace for the Conversion of ST to AFB<sub>1</sub> by a Partially Purified Enzyme in the Presence of SAM (0.15 mM) and NADPH (0.15 mM).

Chart speed 10 mm/minute. Y-axis 4 %  $O_2$  = 20 mm.

**E** = Enzyme added; **S<sub>s</sub>** = stirrer stopped; **S<sub>p</sub>** = stirrer started; **NS** = NADPH and SAM added; **R** = ST added.

Thus having determined that ST was converted to AFB<sub>1</sub> by the partially purified “enzyme”, an investigation was undertaken with OMST as a substrate in the presence of NADPH (50 µg/50 µl). The results are presented in Table 42 (page 206). Typical recorder traces are presented in Figure 169-171 (page 207-208). An explanation of the different sections of the recorder trace is given on page 196.

As mentioned earlier the method used by Del Rio *et al.*<sup>197</sup> was used to quantify the consumption of molecular oxygen in the enzymatic reaction. The corrected initial velocity of the reaction was calculated from the difference in the slope, of the first-order curve, of the reaction and control (described earlier, page 202), i.e.,

$$\begin{aligned}\text{corrected initial velocity} &= v_2 - v_1 \\ &= 2.71 - 2.26 \text{ mm/min.} \\ &= 0.45 \text{ mm/min.}\end{aligned}$$

where  $v_1$  = mean value of the slope for the control reaction.

Since the recorder paper was calibrated for a height of 20 mm representing 4 % O<sub>2</sub>, therefore:

$$\begin{aligned}\text{corrected initial velocity of the reaction} &= 0.45 \times 4/20 \\ &= 0.09 \text{ \% oxygen/min.}\end{aligned}$$

The total % oxygen consumed in the reaction was calculated by the formula:

$$\begin{aligned}\text{total \% oxygen consumed} &= \text{corrected initial velocity} \times \text{time} \\ &= 0.09 \times 8.5 \\ &= 0.77 \text{ \% O}_2\end{aligned}$$

The 21 % O<sub>2</sub> calibration solution was corrected to read 20.37 % O<sub>2</sub> by using the formula :

$$\% \text{ O}_2 (\text{corrected}) = \% \text{ O}_2 (\text{dry}) (1 - P_v / P_{\text{atm}})$$

where % O<sub>2</sub> (corrected) = the percentage of oxygen with respect to total dissolved gases

% O<sub>2</sub> (dry) = the percentage oxygen in the dry gas mixture

$P_v$  = the current atmospheric pressure = 756 mm mercury

$P_{\text{atm}}$  = the vapour pressure of water at 25 °C = 23 mm mercury

The percentage oxygen values of Table 42 were converted to oxygen concentration on the basis<sup>197</sup> of the air-saturated phosphate buffer of 0.250  $\mu\text{mol}$  of  $\text{O}_2/\text{ml}$  at 25 °C. Since the uptake cell was of 600  $\mu\text{l}$  capacity, this meant that 0.150  $\mu\text{mol}$  of  $\text{O}_2$  represented 20.37 %  $\text{O}_2$ . Therefore the total oxygen consumed ( $\mu\text{mol}$ ) in the reaction was calculated as:

$$\begin{aligned}\text{Total oxygen consumed} &= 0.150 \times \text{total \% O}_2 / 20.37 \\ &= 5.67 \times 10^{-3} \mu\text{mol} \\ &= 5.67 \text{ nmol}\end{aligned}$$

The results are presented in Table 43 (page 208).

Table 42. The Conversion of OMST (3.09 nmol) to  $\text{AFB}_1$  in a Partially Purified Enzyme, in the Presence of NADPH (50  $\mu\text{g}/50 \mu\text{l}$ ) at pH 7.2 and 28 °C.

Substrates Added	Height of Response (mm)	<sup>a</sup> Reaction Time (mm; min)	Initial Velocity (mm/min)	Initial Velocity (% $\text{O}_2/\text{min}$ )	Total % $\text{O}_2$ consumed
NADPH + $\text{H}_2\text{O}$ (Blank)	1.0	85; 8.5	0.12		
NADPH + DMSO (Control)	23	103; 10.3	2.23	-	-
	23.5	104; 10.4	2.26	-	-
	23	101; 10.1	2.28 Mean 2.26	-	-
OMST + NADPH (Reaction)	23	85; 8.5	<sup>b</sup> 2.71	<sup>c</sup> 0.45	0.77
	23.5	86; 8.6	<sup>b</sup> 2.73	<sup>c</sup> 0.47	0.77
	23.5	90; 9.0	<sup>b</sup> 2.61	<sup>c</sup> 0.35	0.63
	23	89; 8.9	<sup>b</sup> 2.58	<sup>c</sup> 0.32	0.53
	23	92; 9.2	<sup>b</sup> 2.50	<sup>c</sup> 0.24	0.46

<sup>a</sup>Chart speed was 10 mm/min. <sup>b</sup>Values uncorrected. <sup>c</sup>Values corrected.

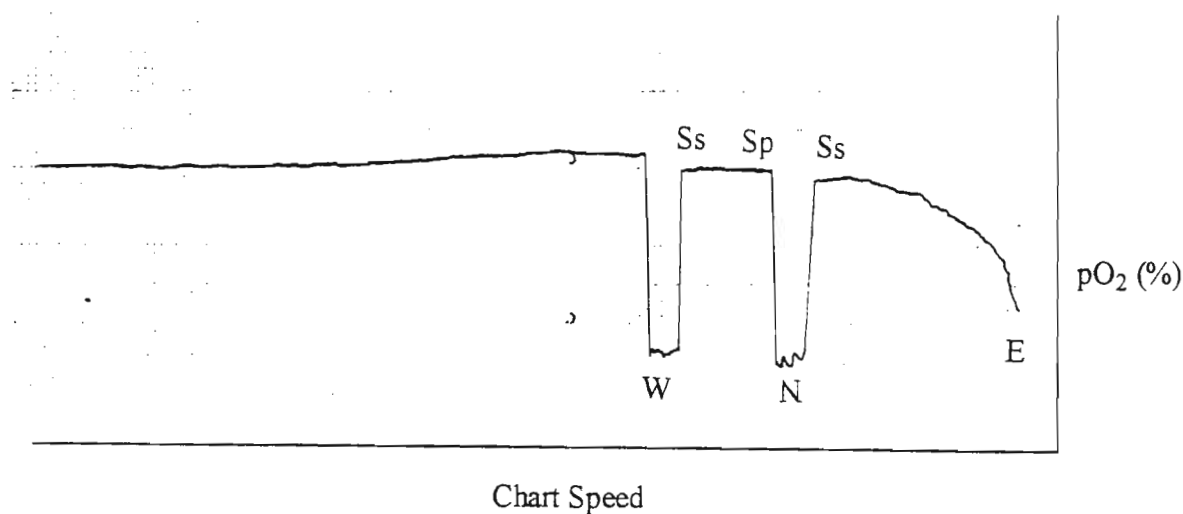


Figure 169. A Recorder Trace of the Partially Purified Enzyme in the Presence of NADPH (50  $\mu$ g/50  $\mu$ l).

Chart speed 10 mm/minute. Y-axis 4 %  $O_2$  = 20 mm.

E = Enzyme added ; Ss = stirrer stopped ; Sp = stirrer started ; N = NADPH added.

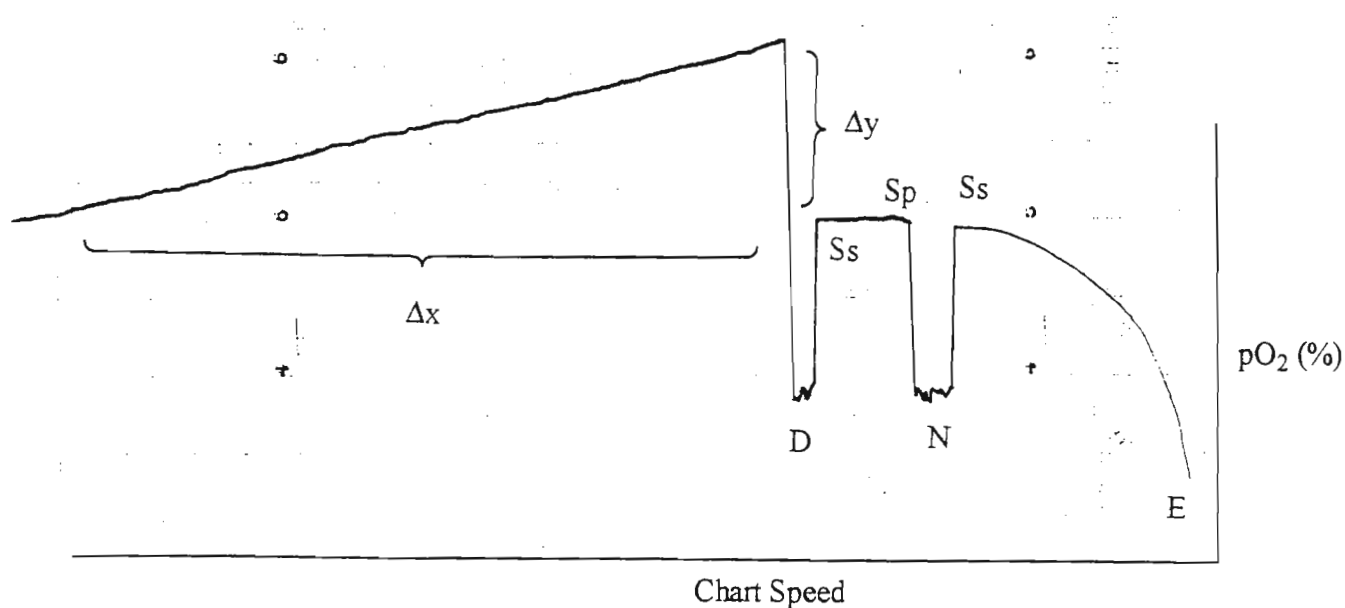


Figure 170. A Recorder Trace of the Partially Purified Enzyme in the Presence of NADPH (50  $\mu$ g/50  $\mu$ l) and DMSO (50  $\mu$ l).

Chart speed 10 mm/minute. Y-axis 4 %  $O_2$  = 20 mm.

E = Enzyme added ; Ss = stirrer stopped ; Sp = stirrer started ; N = NADPH added ; D = DMSO added.

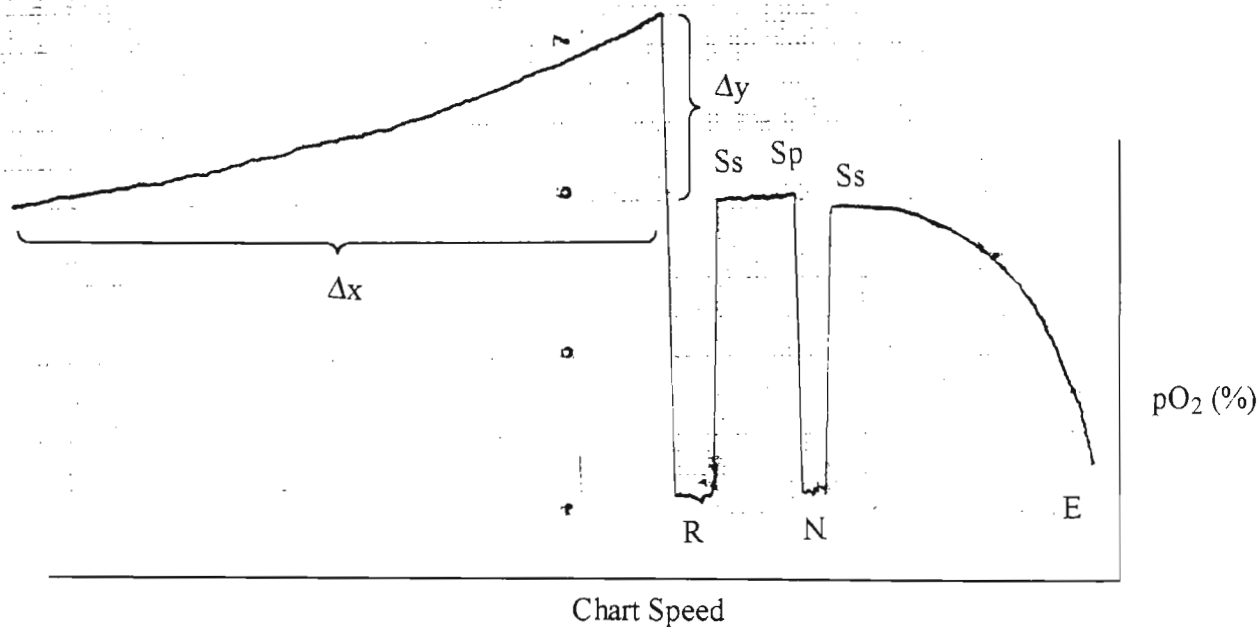


Figure 171. A Recorder Trace for the Conversion of OMST to AFB<sub>1</sub> by a Partially Purified Enzyme in the Presence of NADPH (50 μg/50 μl). Chart speed 10 mm/minute. Y-axis 4 % O<sub>2</sub> = 20 mm. E = Enzyme added ; S<sub>s</sub> = stirrer stopped ; S<sub>p</sub> = stirrer started ; N = NADPH added ; R = OMST added.

Table 43. The Enzymatic Conversion of OMST (3.09 nmol) to AFB<sub>1</sub> in a Partially Purified Enzyme, in the Presence of NADPH (50 μg/50 μl) at pH 7.2 and 28 °C.

Substrate added	Oxygen consumed (nmol)	AFB <sub>1</sub> Produced	AFB <sub>1</sub> Produced (nmol)	NADPH absorbance at 340 nm	NADPH reacted (nmol)
OMST + NADPH	5.67	<sup>a</sup> 52196 ; <sup>b</sup> 786	2.52	0.055	2.73
	5.67	<sup>a</sup> 58344 ; <sup>b</sup> 874	2.80	0.055	2.73
	4.64	<sup>a</sup> 43422 ; <sup>b</sup> 660	2.12	0.056	1.67
	3.90	<sup>a</sup> 43036 ; <sup>b</sup> 655	2.10	0.056	1.67
	3.39	<sup>a</sup> 40514 ; <sup>b</sup> 619	1.98	0.056	1.67
Mean ± STD	4.64 ± 1.03		2.30 ± 0.34		1.91 ± 0.68

<sup>a</sup>Peak Area of AFB<sub>1</sub>. <sup>b</sup>Mass of AFB<sub>1</sub> (nanogram).

Aflatoxin B<sub>1</sub> was quantified by HPLC using the variable optical scanning detector. The quantity of AFB<sub>1</sub>, produced by the enzymatic reaction, was calculated by using the

integrated peak area of the chromatogram and a back-fit straight line equation from the calibration graph of AFB<sub>1</sub> (Figure 154, Appendix 82, Page 310). A typical chromatogram of standard AFB<sub>1</sub> is presented in Figure 172 (Appendix 85, page 312). The results are presented in Table 43 (page 208). Typical chromatograms for the enzymatic conversion of OMST to AFB<sub>1</sub> is presented in Figure 173-174 (Appendix 86-87, page 313-314).

It must be mentioned (discussed in Section 7.3, page 107) that an excess of NADPH was used in these enzymatic reactions and therefore the unreacted NADPH was quantified by monitoring the absorbance at 340 nm by UV. The quantity of NADPH, not used in the enzymatic reaction, was calculated by using a back-fit straight line equation from the calibration graph of NADPH (Figure 155, Appendix 84, page 311). An absorbance reading of 0.055 indicated that 0.047719 mg/5ml remained after enzymatic reaction. Therefore the quantity of NADPH which was used in the reaction was calculated as :

$$\begin{aligned} \text{NADPH consumed} &= \text{NADPH added} - \text{NADPH unreacted} \\ &= 50\,000 - 47719 \text{ ng} \\ &= 2\,281 \text{ ng} = 2.73 \text{ nmol} \end{aligned}$$

The results are presented in Table 43 (page 208). Since small quantities of NADPH were consumed in the enzymatic reaction, changes in the absorbance of unreacted NADPH were not easily detected. This would account for the large variation in the quantity of NADPH consumed in the enzymatic reaction.

Using the data from Table 43 (page 208), the mole ratio was calculated (Table 44).

Table 44. The Mole Ratio of Substrates for the Enzymatic Conversion of OMST to AFB<sub>1</sub>.

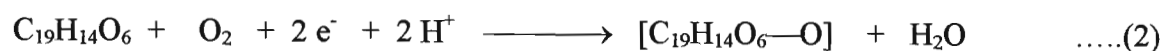
O <sub>2</sub> /AFB <sub>1</sub>	O <sub>2</sub> /NADPH	AFB <sub>1</sub> /NADPH
2.25	2.08	0.92
2.03	2.08	1.03
2.19	2.78	1.27
1.86	2.36	1.26
1.72	2.03	1.19
2.01 ± 0.22	2.27 ± 0.32	1.13 ± 0.15

From these results the following stoichiometric relationship was determined:

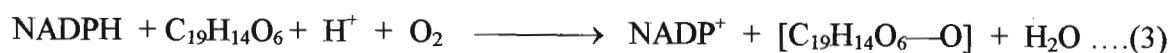


The oxygen stoichiometry observed during this study can be explained by considering the possibility of the “enzyme” preparation containing both a monooxygenase and a dioxygenase which is essential for the biotransformation of OMST to AFB<sub>1</sub>. The presence of a monooxygenase is supported by various research groups, including the experiments conducted in Chapter 7 (page 100). As mentioned earlier the involvement of a dioxygenase was first proposed by Dutton<sup>23</sup> and supported by Watanabe and Townsend<sup>196</sup>.

Chatterjee and Townsend<sup>136</sup> suggested (Figure 147, page 176) that biological hydroxylation of OMST (1) to a diol 4 via the epoxide 2 could be achieved by a monooxygenase. This, therefore, requires that one oxygen atom, from molecular oxygen, would be inserted into the substrate whilst the other would be used to form water. It is most likely that molecular oxygen is cleaved by the two electrons produced by NADPH as illustrated by the following equations :

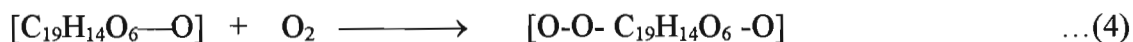


The overall net equation can be written as :

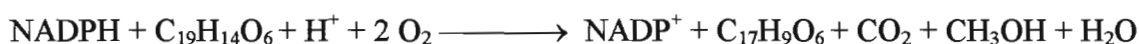


According to the above equation, the number of moles of oxygen consumed will be equal to the number of moles of AFB<sub>1</sub> (C<sub>17</sub>H<sub>9</sub>O<sub>6</sub>) produced in the reaction. However, the stoichiometric relationship indicates that a dioxygenase may be involved by using a second mole of oxygen to produce AFB<sub>1</sub> from an intermediate [O-O- C<sub>19</sub>H<sub>14</sub>O<sub>6</sub> -O]. Therefore, the following equations can be written :





The overall net equation for the conversion of OMST to AFB<sub>1</sub> is obtained by adding equation 3, 4 and 5 :



The overall net equation can be used to explain the stoichiometric relationship obtained in this study. Based on the above chemical equation and the stoichiometric relationship, it is evident that in the formation of water one proton is supplied by NADPH whilst the second proton comes from the medium. This finding is supported by the research of Gunsalus *et al.*<sup>198</sup> who reported a monooxygenase activity of a keto-lactonising complex extracted from *Pseudomonas* cells.

It is most likely that the soluble preparation of the partially purified “enzyme” contains a close association of the monooxygenase and dioxygenase in the microsomal portion of the cell. This provides an explanation for the difficulty of purifying the “enzyme” to homogeneity since these “enzymes” would be membrane bound and hence labile.

Based on these experimental results, a possible mechanism is presented (Figure 175, page 215) for the conversion of OMST to AFB<sub>1</sub>, which occurs in the latter part of the aflatoxin biochemical pathway. It is not possible at this moment to furnish further evidence of the proposed mechanism beyond the essentiality of the stoichiometric relationship, deuterium migration and oxygen labeling investigations and, therefore, this mechanism serves as a model compatible with the facts, in untangling this rather complex series of events.

It has been reported by Daly *et al.*<sup>199</sup> that the shift of deuterium from the site of hydroxylation to an adjacent site during the oxidation of aromatic compounds (the “NIH shift”) is a characteristic of monooxygenase enzymes. Vannelli and Hooper<sup>200</sup> recently reported the migration of deuterium in the hydroxylation of monosubstituted benzene

catalysed by ammonia monooxygenase of *Nitrosomonas europaea*. It was found that the phenolic products of the hydroxylation of aromatics containing *ortho-para* directing substituents, viz., OH, NH<sub>2</sub>, Cl and OCH<sub>3</sub>, were primarily *para* phenols. Based on the above reports, we now postulate (Figure 175, page 215) that the first step in the mechanism would require one oxygen atom to be inserted into the substrate to form an unstable epoxide **12** which undergoes a 'NIH shift' to form a phenol **13**. Although *para*-hydroxylation activity has been demonstrated in *Aspergillus* and related fungi<sup>201</sup>, the possibility of the electron donor, the substrate and oxygen involved in the formation of a complex through which hydroxylation could occur directly to **13**, by means of a concerted movement of electrons, without the participation of any other discrete oxidation levels is ruled out on the basis of the deuterium incorporation study by Simpson *et al.*<sup>195</sup>. Their study of the pattern of deuterium incorporation, from [2-<sup>2</sup>H<sub>3</sub>] acetate, into AFB<sub>1</sub> is consistent with the action of a monooxygenase (i.e., \*O from <sup>18</sup>O<sub>2</sub>) involved in the first oxidative cleavage process. Although phenol **13** has not been isolated and its intermediacy in the biochemical pathway has not been investigated, its role in the overall cleavage process is consistent with the observed NADPH dependence of the partially purified "enzyme" discussed in Section 8.3 (page 124).

According to the mechanism (Figure 175, page 215), the epoxide **12** opens to form a cationic intermediate and hence a *para* ketone intermediate. The ketone then tautomerizes to a phenol and the *para* deuterium shifts to the adjacent carbon. Thus the 'NIH' shift provides a *priori* evidence for the intermediacy of an epoxide intermediate. The present observation also suggests that OMST binds in the "enzyme" in a way that the methoxy group is placed away from the site of hydroxylation leaving the *para* position available for hydroxylation.

Also, oxygen is most likely reduced to an active form by NADPH, which supplies the necessary electrons to cleave the oxygen molecule. It is further suggested that an oxene (:O:), an analog of carbene, is formed whilst NADPH is oxidized to NADP<sup>+</sup>. If such is the case then the oxene maybe inserted into the substrate to form **12**. However, this

suggestion would require further examination since a direct insertion reaction of this type into an aromatic C-H bond would probably be as unselective as the insertion of a carbene.

The third step, according to the proposed mechanism, requires a dioxygenase to insert two oxygen atoms to form an unstable dioxetane intermediate **18** which would then undergo step-wise rearrangement and cyclization to finally produce AFB<sub>1</sub>. The combination of the oxygen consumption studies and the <sup>18</sup>O labelling data argue strongly in favour of the dioxetane intermediate **18**. It is possible that the phenolic substrates maybe activated through their ready capacity for electron donation. The unstable intermediate **18** then undergoes rearrangement to form an intermediate **19** which probably loses the methoxy group to form an enol **20** and finally carbon dioxide to form AFB<sub>1</sub>. However, evidence for the rearrangement steps still remains open for discussion and hence further investigations.

The mechanism proposed for the conversion of OMST to AFB<sub>1</sub> lacks much of the ambiguity associated with the mechanisms proposed by other research teams. It is clear that the function of the “enzyme” system is to generate an active oxygen species and to exert the specificity observed in the final metabolic pathway.

Supporting evidence for the results of this study is based on the research by Watanabe and Townsend<sup>196</sup>, who reported the incorporation of <sup>18</sup>O in AFB<sub>1</sub>. Therefore, according to the mechanism proposed here, two oxygen atoms from O<sub>2</sub> molecule will be lost as carbon dioxide whilst the second oxygen atom from another O<sub>2</sub> molecule will be present in AFB<sub>1</sub>. The role of oxygen in these oxidative biotransformation therefore places limits on the final mechanistic steps leading to the formation of AFB<sub>1</sub>. Thus the mechanism proposed is introduced as a working hypothesis which covers the requisites of the oxygen-reducing reactions and coupling to a substrate. Nonetheless, it is hoped that the final mechanistic resolution of these remarkable oxidative cleavage and rearrangement processes may become accessible from future studies at the genetic level. It is recommended that the “enzyme” be purified to homogeneity in order to undertake spectroscopic investigations

and determine the crystal structure of these enzymes. It is also recommended that similar oxygen consumption studies be undertaken with OMST labelled with deuterium, at the appropriate positions, to monitor the isotopic ratio of the product AFB<sub>1</sub>. The data so obtained will provide more information regarding the mechanism for the conversion of OMST to AFB<sub>1</sub>.

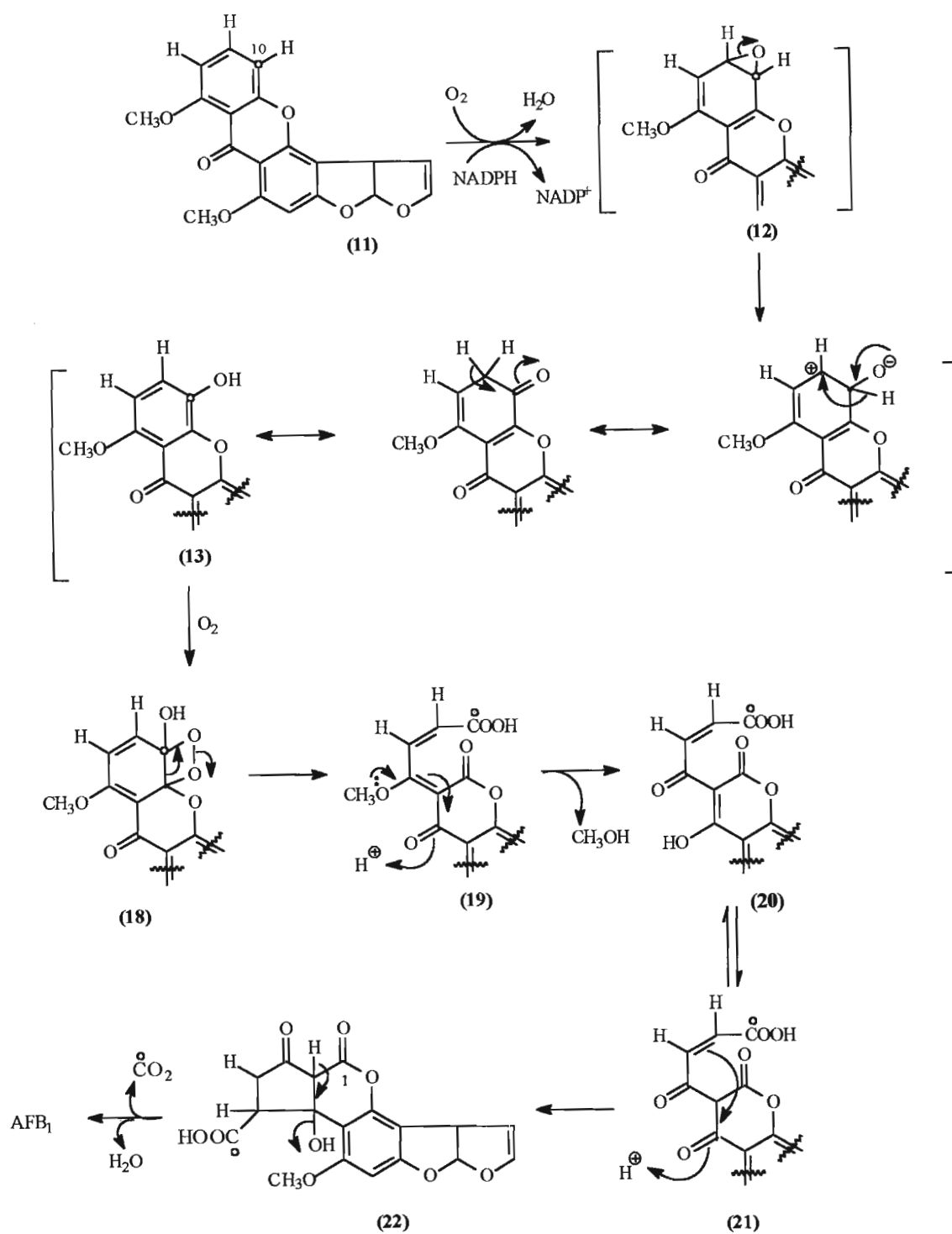


Figure 175. A Mechanism Proposed by Gengan *et al.* for the Conversion of OMST to AFB<sub>1</sub>.

## CHAPTER ELEVEN

### GENERAL DISCUSSION

Although the enzymes used in secondary metabolism are produced by the same biosynthetic machinery as those of primary metabolism, they have not received the same attention as those used in primary metabolism. A reason why studies on the enzymology of secondary metabolism has had a slow start is the difficulty of obtaining active cell-free extracts. The first problem was to determine when to harvest and extract the cells. The second was to use a gentle technique to disrupt the cell wall because the “enzyme” could easily undergo denaturing effects. However, after many years of intensive studies these two problems have been solved.

Many secondary metabolites have been found to have economic significance, e.g., the antibiotic compounds such as penicillin<sup>202</sup> and tetracycline<sup>203</sup> which are commercially available. Hence it is important to investigate the “enzyme” which are involved in their production.

Recently with the advent of the new technology in genetic engineering, the study of the enzymology of secondary metabolism has attracted greater interest. A variety of experimental approaches, viz., reverse genetics, differential screening of cDNA libraries and complementation in mutant strains have led to the identification and characterisation of genes involved in aflatoxin biosynthesis, eg., the gene<sup>127</sup> *ord1* corresponding to a transcript of about 2 kb was identified within the 3.3 kb DNA fragment isolated from the protoplast of *A. flavus*. It has been suggested that *ord1* encodes a cytochrome P-450 type monooxygenase responsible for the conversion of OMST to AFB<sub>1</sub>.

Since aflatoxins have been recognized for over 30 years as fungal contaminants of foodstuffs, it is understandable that the production of these secondary metabolites should be prevented rather than promoted and thus an understanding of their formation is of importance. The biosynthesis of aflatoxins, however, has been the subject of conflicting speculations and numerous reviews. While great progress was made in determining the chemistry, toxicity and biological activities of aflatoxins, research in their biosynthesis

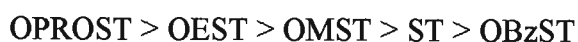
only became a dynamic field of interest with the advancement of scientific procedures, viz., the use of radio-labelled precursors, blocked mutants, cell-free extracts and metabolic inhibitors. Currently there is now agreement on the identity of most of the intermediates involved in the biosynthesis of AFB<sub>1</sub>. However, there is a lack of clarity on the details of AFB<sub>1</sub> biosynthesis including the conversion of ST to AFB<sub>1</sub>. While cell-free conversions of ST and OMST to AFB<sub>1</sub> have been reported<sup>5-7</sup>, these final stages of the biosynthesis have not been understood despite several mechanistic proposals<sup>86,100,101</sup>. There is no clear cut metabolic evidence of the intermediacy of OMST, i.e., either it is a compulsory intermediate or a shunt metabolite and hence part of a metabolic grid. The question of the specificity of the “enzyme” and the nature of the oxygenase(s) involved in the latter part of the biosynthesis of AFB<sub>1</sub> has also not been adequately addressed. This study therefore investigates the latter part of the aflatoxin biosynthetic pathway and the “enzyme” responsible for the biotransformation of OMST to AFB<sub>1</sub>.

In order to study the specificity of the “enzyme” it is necessary to determine the effect of substrates, of known chemical structures, on purified or non-homogenous enzyme systems. Only when such substrates are available is it possible to establish unequivocally the nature of the chemical reaction that is being catalysed. Since studies have not established the necessity for methylating ST to OMST in the AFB<sub>1</sub> biosynthetic pathway, compounds were synthesised in which the free hydroxyl group of ST was replaced by alkyl and aryl group other than methyl. Thus substrates, homologous to OMST, were produced and as none of these compounds were available, it was necessary to prepare these novel compounds by chemical reactions. In order to prepare these compounds sufficient quantities of ST were required. However, due to ST being expensive to purchase it had to be produced in-house from fungal cultures. In order to study the action of the “enzyme” on different substrates and to carry out investigation on enzyme kinetics and oxygen consumption, reliable methods were required for the quantification of enzyme catalysed reactions. These include HPLC, spectroscopy and an oxygen electrode.

To begin this study *A. versicolor*, a fungus known to be a producer of ST, was used to produce ST by standard protocols. After extracting and purifying ST (110 mg) by column chromatography and recrystallisation, it was characterised by spectroscopic techniques.

Although the quantity of ST (6 mg/100ml medium) was lower than the yield (14 mg/100ml medium) reported by Chatterjee and Townsend<sup>136</sup>, it was sufficient to carry out micro-scale reactions. Seven novel ST derivatives were prepared by converting the phenolic group of ST to compounds analogous to OMST. In spite of the difficulty of using small quantities (10 mg) of ST for each reaction, these seven derivatives were synthesised, purified and characterised by spectroscopic techniques.

The next stage was to determine the metabolism of these novel compounds in whole cells of *A. parasiticus*. Feeding studies were undertaken and it was found that all seven derivatives were converted to AFB<sub>1</sub>. This meant that these compounds were suitable substrates for the “enzyme” and could be involved in the latter part of the biosynthetic pathway. It was decided that a time course study be undertaken, using whole cells and selected substrates, in order to compare the rate of AFB<sub>1</sub> production. To achieve this, quantification of AFB<sub>1</sub> was necessary and a HPLC method was developed. The method involved a pre-column derivatisation technique with TFA as the derivatising reagent. The mobile phase water: acetonitrile: isopropanol: acetic acid (8: 1: 0.5: 0.5, v/v) of the HPLC method was different from those normally used in reversed phase chromatography, in that it contained a substantial quantity of acetic acid which was reported<sup>157</sup> to enhance the fluorescence of aflatoxins. After having set up a suitable method for quantification of AFB<sub>1</sub>, a time course study for the conversion of ST and ST derivatives to AFB<sub>1</sub> was then undertaken with the mutant fungus. The results from both the culture fluid and mycelial fractions indicated a general decrease in the rate of conversion in the order:



It was found that the rate of conversion of each of the tested substrates to AFB<sub>1</sub> was not comparable since there was a permeability effect with the uptake of the compounds through the fungal membrane, even though the addition of acetone to the fungal system used in previous studies<sup>95</sup> gave satisfactory results. The propyl derivative (OPROST) was converted more rapidly than the others, including the natural substrates ST and OMST. This did not resolve the question of which of the putative intermediates were involved in AFB<sub>1</sub> biosynthesis, as all were converted. The fact that OPROST was converted the quickest of the substrates could be explained on the basis of polarity. It being the least polar, meant that it could penetrate the cellular membrane more rapidly. The question as to whether the alkylation of ST to OMST is obligatory in the biosynthesis of AFB<sub>1</sub> was



also left unresolved and kinetic studies were not undertaken with whole cell feeding experiments since permeability was a factor. One of the solution to this problem was to remove the rigid cell wall of the fungus and extract the crude “enzyme”.

At this stage a newly acquired chromatographic equipment, linked to a diode array detector, was used and thus improved quantification of AFB<sub>1</sub>. An HPLC method was developed for the separation of AFB<sub>1</sub> from interfering metabolites. This study was problematic because various metabolites, which are usually produced in the AFB<sub>1</sub> biosynthetic pathway, were found to co-elute with AFB<sub>1</sub>. Two columns, viz., a C<sub>18</sub> Lichrosphere and C<sub>18</sub> Prodigy, and various composition of the mobile phase acetonitrile: water were investigated. The best column was found to be a C<sub>18</sub> Lichrosphere (250 x 4.60 mm) and a gradient elution program was used for the separation of AFB<sub>1</sub> from other metabolites.

A few techniques were available to prepare active cell-free extracts. However, in this study the method of lyophilisation was selected as this was the common method used by other research groups, who were studying the latter part of the biosynthetic pathway. The preparation of active cell-free extracts posed a problem because some of the “enzyme” are probably membrane bound and therefore were easily disrupted. After numerous attempts, the finer details of the technique of preparing active “enzyme” extracts was learnt and initial investigation with this preparation was done using the conditions reported by Singh and Hsieh<sup>46</sup>, i.e., at pH 7.5 and 27 °C using 50 times more co-factors (NADPH and SAM) than substrate. This established that the cell-free extract was capable of converting ST to AFB<sub>1</sub> as shown by t.l.c. and quantitated by HPLC. A control with no substrate added indicated that the cell-free extract was not capable of producing AFB<sub>1</sub> without the addition of ST. On incubating ST with the cell-free extract and co-factors over a pH range, the optimum was found to be pH 7.2. Similarly the optimum temperature was found to be 28 °C, which is in agreement with that found by Singh and Hsieh<sup>46</sup> who reported a cell-free reaction at 27 °C with an optimum pH between 7.5-7.8. These researchers, however, did not determine the best pH for optimum enzyme activity which implies that investigations undertaken in our laboratory are more reliable. It was also important to investigate the effect of co-factors, because it is known<sup>98</sup> that NADPH and

SAM are required for the conversion of ST to AFB<sub>1</sub>. It was found that the cell-free extract was capable of converting ST to AFB<sub>1</sub> without added co-factors but their addition does increase the rate of conversion. Enhancement is greater with the addition of NADPH than SAM but greatest when both are added. The requirement for NADPH is not unexpected, as the type of monooxygenase proposed in the conversion<sup>23</sup> would require it, and the favourable effects of SAM suggest that OMST is an intermediate in the pathway, as it is the source of the methyl group. In subsequent experiments both these co-factors were added in excess to ensure optimum conversion rates. Time course experiments for the three substrates, viz., ST, OMST and OPROST using the determined optimum conditions were then carried out. The results indicated that the rate of conversion, in decreasing order, was :

$$\text{OMST} \cong \text{ST} > \text{OPROST}$$

The rates of conversion for ST and OMST were statistically indistinguishable although the rate for OMST was marginally higher. The conversion of OPROST was slower, confirming the speculation that the time course studies undertaken earlier with whole cells was in part a measure of membrane permeability.

The results of this study were encouraging in that a suitable cell-free extract can be routinely prepared which is useful for studying the final stages of AFB<sub>1</sub> biosynthesis. The addition of exogenous co-factor indicates that OMST is an intermediate in the pathway, although the presence of sub-optimal concentration of co-factors does not allow a clear-cut answer. The conversion of the propyl analogue, although at a slower rate, also clouds the issue. Two explanations are possible: either the "enzyme" responsible for the conversion exhibit relative specificity, whereby a series of ST homologues can be converted to AFB<sub>1</sub> but at different rates; or all the homologues are converted to a common intermediate, e.g., ST, prior to conversion. The former hypothesis is favoured from these results, which is in keeping with the characteristics of certain secondary metabolic enzymes, i.e., relative specificity.

Although the results of cell-free extract investigations were more reliable than that of whole cell feeding experiments, these results could not be used to determine the specificity of the "enzyme". The problem, firstly, is that the enzymatic conditions were

optimised for ST which may not be the optimum condition for the ST derivatives. Secondly, it was found that the endogenous co-factors SAM and NADPH were present in the cell-free extract and these co-factors were necessary for the enzyme catalysed reactions. As long as these co-factors were present in the cell-free extract, the intermediacy of OMST could not be established. A solution to this problem was to remove these co-factors so as to have total control of the enzymatic reaction.

The next stage in this study was devoted to preparing a partially purified “enzyme” which is responsible for the conversion of ST to AFB<sub>1</sub>, but which lacked the two co-factors. It was surprising that a study of this type was not attempted by previous researchers in order to resolve the role of OMST in the biosynthetic pathway. The results of this study were encouraging in that a new protocol of a partially purified “enzyme” preparation has been developed from the fungus *A. parasiticus* which carries out the transformation of ST and ST derivatives to AFB<sub>1</sub>. The new method entails, first, the generation of a crude cell-free extract by lyophilisation, followed by molecular exclusion chromatography and conventional dialysis against solid sucrose. Molecular exclusion chromatography (at 4 °C) efficiently removes small molecules and co-factors (MW < 10 000) from the protein suspension whereas dialysis concentrates the proteins. The “enzyme” of the aflatoxin pathway have been stabilised by this procedure and the effects of added substrates and co-factors were assayed against virtually no background reactions. This enzyme system, however, was not homogenous since the objective was to remove the low molecular weight components, usually present in cell-free extracts, and hence it was not possible to compare the results, i.e., characterisation by PAGE, with a previous investigation<sup>100</sup>.

On incubating pooled “enzyme” fractions 9-30, viz., after separation by molecular exclusion chromatography, with ST as the substrate, only 3 % conversion to AFB<sub>1</sub> was obtained. On concentrating the “enzyme” by dialysis against sucrose, a conversion of 13.6 % for ST to AFB<sub>1</sub>, in the presence of NADPH and SAM was obtained. On incubating ST under the same conditions with either SAM or NADPH or no co-factor at all, no conversion was observed. This result was critical in that it demonstrated that gel filtration had removed co-factors from the mycelial extract and that ST is not converted to AFB<sub>1</sub> in the absence of NADPH or SAM. It can, therefore, be concluded that in the natural

pathway to AFB<sub>1</sub> biosynthesis, OMST is an obligatory intermediate. As OPROST had been converted to AFB<sub>1</sub> in crude cell-free extracts in previous experiments, various *O*-alkyl derivatives were tested for conversion by the partially purified “enzyme” in the presence of NADPH but in absence of SAM. All three substrates (OMST, OPROST and OBzST) were metabolised to AFB<sub>1</sub> at different rates, hence the “enzyme” was displaying relative specificity, a well known phenomena in secondary metabolism. As might have been anticipated, the aryl group as represented by OBzST, is not a favoured substrates, as the natural one OMST has a small alkyl group. The interesting observation was that OPROST is more rapidly converted than OMST itself, in these experiments, which is in contrast to previous results with a crude cell-free extract. Speculations on the reason(s) for these observations are as follows: the converting “enzyme” has a hydrophobic patch around the active site that recognises longer alkyl chains, e.g. propyl, better than shorter ones, i.e., methyl; or propyl is a better leaving group than methyl in the enzyme catalysed reaction, where the alkyl group is lost. Further work using other homologues is required to resolve this question. There is no obvious answer to the question posed earlier as to why ST has to be alkylated prior to conversion to AFB<sub>1</sub>. Usually free phenols are preferred substrates for oxygenases involved in aromatic cleavages since *O*-alkyl ethers are more recalcitrant towards metabolic conversions. It may be that methylation under natural conditions is part of a detoxification mechanism and that the oxygenases involved in the conversion are also responsible for the metabolism of other substituted aromatic compounds that the fungus comes into contact with. This latter suggestion can only be resolved once we have a full understanding of fungal oxygenase systems involved in the breakdown of aromatic compounds.

The question that arose was whether the enzymatic reaction was carried out by a single enzyme or by more than one closely related “enzyme”. This can only be elucidated if the oxido-reductase can be purified to homogeneity. Other questions also arose, viz., what is the nature of the oxido-reductase? What type of binding occurs between the enzyme and substrate? The latter question could be investigated by studying the regulation of the activity of the “enzyme”.

The next stage in this study was devoted to synthesising simple xanthone derivatives which could “mimic” OMST and hence compete for the “enzyme” site. The type of

interaction between the xanthone, OMST and “enzyme” could be obtained from kinetic investigation. The simple xanthenes chosen for this study were not available commercially and were therefore prepared by synthesis from simple reactants. A simple xanthone, viz., 1-hydroxy-3,6-dimethylxanthone, was synthesised, purified by preparative t.l.c. (yield 2.75 %) and characterised by spectroscopic techniques. Two derivatives were subsequently prepared, viz., 1-methoxy-3,6-dimethylxanthone (yield 59.50 %) and 1-acetyl-3,6-dimethylxanthone (yield 59.60 %), purified by preparative t.l.c. and characterised by spectroscopic techniques. On incubating the three compounds in whole cells of *A. parasiticus* (NIX) it was found that these compounds inhibited AFB<sub>1</sub> production. A similar effect was obtained in whole cells of *A. parasiticus* (Wh1-11-105) with OMST as substrate. On incubating OMST in a cell-free extract, in the presence of NADPH, at pH 7.2 and 28 °C it was found that OMST was converted to AFB<sub>1</sub> (57.19 % conversion). On incubating the cell-free extract with the three xanthenes, under similar enzymatic conditions, it was found that 1-hydroxy-3,6-dimethylxanthone (15.10 % conversion to AFB<sub>1</sub>) had a greater inhibitory effect than 1-methoxy-3,6-dimethylxanthone (31.29 % conversion to AFB<sub>1</sub>) and 1-acetyl-3,6-dimethylxanthone (39.92 % conversion to AFB<sub>1</sub>). These results indicated that the xanthenes were competing with OMST for the “enzyme”. However, it was not clearly evident what type of inhibition took place therefore a kinetic study was undertaken. The xanthone which was chosen for competition studies was 1-methoxy-3,6-dimethylxanthone because it resembled OMST. The results from a kinetic investigation showed that 1-methoxy-3,6-dimethylxanthone was a non-competitive inhibitor. A  $K_M$  value of 5.60  $\mu$ M for OMST was calculated from a Line-Weaver Burk plot. This result indicated that 1-methoxy-3,6-dimethylxanthone was probably binding at a second enzyme site thereby distorting the active site. However, a more likely explanation is that the inhibitor could combine with the hydrophobic region of the “enzyme” complex and either distorts the “enzyme” tertiary structure or displaces the non-reactive part of OMST assuming that such hydrophobic regions are required for enzymatic biotransformation. This is a plausible hypothesis, which is difficult to investigate, because active enzyme sites are in fact a part of complex protein molecules. This hypothesis can only be resolved if isotopic labelling techniques are investigated in order to determine the nature of enzyme-substrate intermediates.

A question which arose was what is the nature of the oxygenase involved in the final mechanistic pathway, i.e., the conversion of OMST to AFB<sub>1</sub>? Is the 'oxido-reductase' a monooxygenase, a dioxygenase or both? There are conflicting speculations on the nature of the oxygenase and therefore warranted further investigation. Oxygen consumption studies were undertaken using a Clark oxygen electrode, a new unstandardised instrument. Due to budgetary constraints, a calibrating cell was not purchased and therefore a calibrating system was designed. Initial investigations were undertaken by following the method of Del Rio *et al.*<sup>197</sup> but this method was subsequently modified because the "enzyme" used was impure and therefore required larger concentration of total protein. A major problem arose, i.e., the organic solvent acetone, which was used to dissolve the substrate, caused the electrode to give a response of 6 % oxygen. This problem was resolved by investigating other water miscible organic solvents and selecting one which caused the smallest electrode response, viz., dimethyl sulphoxide. Enzymatic reactions were carried out with the partially purified "enzyme" by means of the Clark oxygen electrode at pH 7.2 and 25 °C. Sterigmatocystin was used as the substrate in the presence of SAM and NADPH. It was established that the partially purified "enzyme" was capable of converting ST to AFB<sub>1</sub>, as shown by t.l.c., within 10 minutes. Similarly, the above enzymatic reactions were carried out with OMST as the substrate, in the presence of NADPH, at pH 7.2 and 25 °C. Aflatoxin B<sub>1</sub> and NADPH were quantitated by HPLC and UV spectroscopy, respectively. From the results of enzymatic reactions, the following stoichiometric relationship was determined:



Based on the above experimental evidence, a mechanism was proposed for the conversion of OMST to AFB<sub>1</sub> which utilized two closely associated "enzyme", viz., a monooxygenase, which required NADPH for activity, and a dioxygenase as proposed by Dutton<sup>23</sup> and by Watanabe and Townsend<sup>196</sup>. The role of oxygen in these oxidative biotransformation places limits on the final mechanistic pathway leading to the formation of AFB<sub>1</sub>. The mechanism proposed, however, is a working hypothesis which covers the requisites of the oxygen-reducing reactions and coupling to OMST. Nonetheless, it is hoped that the final mechanistic resolution of these remarkable oxidative cleavage and rearrangement processes may become accessible from future studies at the genetic level.

## REFERENCES

1. Murakami, H., Takase, S. and Ishii, T. 1976. *J. Gen. Microbiol.*, 13: 513.
2. Goldblatt, L.A. and Dollear, F.G. 1977. *Pure Appl. Chem.*, 49: 1759.
3. Townsend, C.A. and Christensen, S.B. 1983. *Tetrahedron*, 21: 3575.
4. Townsend, C.A., Christensen, S.B. and Trautwein, K. 1984. *Am. Chem. Soc.*, 106: 3868.
5. Bhatnagar, D., McCormick, S. P., Lee, L. S. and Hill, R.A. 1987. *Appl. Environ. Microbiol.*, 53: 1028.
6. Jeenah, M. S. and Dutton, M.F. 1983. *Biochem. Biophys. Commun.*, 116: 1114.
7. Cleveland, T.E., Lax, A.R., Lee, L. S. and Bhatnagar, D. 1987. *Appl. Environ. Microbiol.*, 53: 1711.
8. Burkhardt, T.V. and Forgacs, J. 1968. *Tetrahedron*, 24: 717.
9. Bennett, J.W. and Christensen, S.B. 1983. *Adv. Appl. Microbiol.*, 29: 53.
10. Maggon, K.K., Gupta, S. K. and Venkitasubramanian, T. A. 1977. *Bacteriol. Rev.*, 41: 822.
11. Sargeant, K. , Sheridan, A., O' Kelly, J. and Carnaghan, R.B.A. 1961. *Nature*, 192: 1095.
12. Allcroft R., Carnaghan, R.B.A., Sargeant, K. and O' Kelly, J. 1961. *Vet. Rec.*, 73: 428.
13. Asplin, F.D. and Carnaghan, R.B.A. 1961. *Vet. Rec.*, 73: 1215.
14. Nesbitt, B.F. , O' Kelly , J., Sargeant, K. and Sheridan, A. 1962. *Nature*, 195:1062.
15. Hartley, R.D., Nesbitt, B.F. and O'Kelly, J. 1963. *Nature*, 198: 1056.
16. Asao, T., Buchi, G., Abdel-Kader, M.M., Chang, S.B., Wick, E.L. and Wogan, G.N. 1963. *J. Amer. Chem. Soc.*, 85: 1706.
17. Asao, T., Buchi, G., Abdel-Kader, M.M., Chang, S.B., Wick, E.L. and Wogan, G.N. 1965. *J. Amer. Chem. Soc.*, 87: 882.
18. Van Soest, T.C. and Peerdeman, A.F. 1970. *Acta. Crystalogr.*, 26: 1940.
19. Van Soest, T.C. and Peerdeman, A.F. 1970. *Acta. Crystalogr.*, 26: 1956.
20. Cheung, K.K. and Sim, G.A. 1964. *Nature*, 201: 1185.
21. Brechbuhler, S., Buchi, G. and Milne, G. 1967. *J. Org. Chem.*, 32: 2641.
22. Dutton, M.F. and Heathcote, J.G. 1966. *J. Biochem.*, 101: 21.
23. Dutton, M.F. 1988. *Microbiol. Rev.*, 52: 274.
24. Hsieh, D.P.H. and Yang, S.L. 1975. *Appl. Microbiol.*, 29: 17.

25. Hatsuda, Y. and Kuyama, S. 1954. *J. Agric. Chem. Soc. Japan*, 28: 989.
26. Bullock, E., Roberts, J.C. and Underwood, J.G. 1962. *J. Chem. Soc.*, 4179.
27. Tanaka, N., Katsube, Y., Hatsuda, Y., Hamasaki, T. and Ishida, M. 1970. *Bull. Chem. Soc. Japan*, 11: 3635.
28. Fukuyama, K., Tsukihara, K., Katsube, Y., Hamasaki, T., Hatsuda, Y., Tanaka, N. and Ashida, T. 1975. *Bull. Chem. Soc. Japan*, 48: 1639.
29. Seto, H., Cary, L.W. and Tanabe, M. 1974. *Tetrahedron Letter*, 4491.
30. Pachler, K.G.R., Steyn, P.S., Vleggaar, R., Wessels, P.L. and Scott, B. 1976. *J. Chem. Soc. Perkin Trans.*, 1: 1182.
31. Hatsuda, Y., Hamasaki, T., Ishida, M. and Hara, S. 1972. *Agric. Biol. Chem.*, 36: 521.
32. Hamasaki, T., Hatsuda, Y., Matsui, K. and Isono, K. 1973. *Agric. Biol. Chem.*, 37: 1769.
33. Bullock, E., Kirkaldy, D., Roberts, J.C. and Underwood, J.G. 1963. *J. Chem. Soc.*, 829.
34. Elsworthy, G.C., Holker, J.S.E., Mckeown, L.J., Robinson, J.B. and Mulhein, L.J. 1970. *J. Chem. Soc. Chem. Commun.*, 1069.
35. Drew, S.W. and Demain, A.L. 1977. *Annu. Rev. Microbiol.*, 31: 343.
36. Behal, V. 1986. *Trends Biochem. Sci.*, 11: 88.
37. Malik, V.S. 1980. *Trends Biochem. Sci.*, 5: 68.
38. Mathews, C.K. and van Holde, K.E. 1990. *Biochemistry, Benjamin Cummings, New York*, 593.
39. Prairie, R.L. and Talalay, P. 1963. *Biochem.*, 2: 203.
40. Dagley, S. 1967. In: *Soil Biochemistry, Edwards Arnold, London*, 287.
41. Feigelson, P. and Greengard, O. 1961. *J. Biol. Chem.*, 236 : 153.
42. Nagami, K. and Miyake, Y. 1971. *Biochem. Biophys. Res. Comm.*, 42: 497.
43. Oka, T. and Simpson, F.G. 1971. *Biochem. Biophys. Res. Comm.*, 43 : 1
44. Hirata, F. and Hayaishi, O. 1971. *J. Biol. Chem.*, 246: 7825.
45. Wan, N.C. and Hsieh, D.P.H. 1980. *Appl. Environ. Microbiol.*, 39: 109.
46. Singh, R. and Hsieh, D.P.H. 1976. *Appl. Environ. Microbiol.*, 31: 743.
47. Chuturgoon, A.A. and Dutton, M.F. 1991. *Mycopath.*, 113: 41.
48. Anderson, M.S. and Dutton, M.F. 1979. *Experientia*, 35: 21.



49. Bajpai, P., Agrawala, P.K. and Viswanathan, L. 1981. *J. Gen. Microbiol.*, 127: 131.
50. Rao, V.M., Maggon, K.K. and Venkitasubramanian, T.A. 1980. *Toxicon.*, 18: 279.
51. Kumar, A.A., Vaidyanathan, C.S. and Rao, N.A. 1978. *Indian J. Biochem. Biophys.*, 15: 5.
52. Ghosh, D. and Samantha, T.B. 1981. *J. Steroid Biochem.*, 14: 1063.
53. Higgins, E.S. 1961. *Enzymologia*, 23: 176.
54. Kiser, R.C. and Niehaus, W.G. 1981. *Arch. Biochem. Biophys.*, 21: 613.
55. Niehaus, W.G. and Dilts, R.P. 1982. *J. Bacteriol.*, 151: 243.
56. Allen, C.M. 1972. *Biochemistry*, 11: 2154.
57. Minamikawa, T., Jayasankar, B.A., Bohm, I.E., Taylor, I.E.P. and Towers, G.H.N. 1970. *Biochem. J.*, 116: 889.
58. Scott, A.I., Beadling, L.C., Georgopapadakou, N.H. and Subbarayan, C.R. 1974. *Bioorg. Chem.*, 3: 238.
59. Forrester, P.I. and Gaucher, G.M. 1972. *Biochem.*, 11: 1108.
60. Gupta, S.K., Maggon, K.K. and Venkitasubramanian, T.A. 1977. *Microbios*, 18: 27.
61. Gupta, S.K., Maggon, K.K. and Venkitasubramanian, T.A. 1972. *Microbios*, 19: 7.
62. Bhatnagar, D., Ahmad, S., Mukerji, K.G. and Venkitasubramanian, T.A. 1986. *J. Appl. Bacteriol.*, 60: 135.
63. Rao, V.M., Saraswathy, S., Maggon, K.K. and Venkitasubramanian, T.A. 1980. *J. Food. Sci.*, 45: 1031.
64. Marsh, P.B., Simpson, M.E. and Truckses, M.W. 1975. *Appl. Microbiol.*, 30: 52.
65. Davis, N.D., Diener, U.L. and Agnihotri, V.P. 1967. *Mycopathol. Mycol. Appl.*, 3: 251.
66. Payne, G.A. and Hagler, W.M. 1983. *Appl. Environ. Microbiol.*, 46: 805.
67. Reddy, T.V., Viswanathan, L. and Venkitasubramanian, T.A. 1971. *Appl. Microbiol.*, 22: 393.
68. Davis, N.D., Diener, U.L. and Eldridge, D.W. 1966. *Appl. Microbiol.*, 14: 378.
69. Mateles, R.I. and Adye, J.C. 1965. *Appl. Microbiol.*, 13: 208.
70. Niehaus, W.G. and Dilts, R.P. 1984. *Arch. Biochem. Biophys.*, 228: 113.
71. Abdollahi, A. and Buchanan, R.L. 1981. *J. Food. Sci.*, 46: 633.
72. Buchanan, R.L. and Lewis, D.F. 1984. *Appl. Environ. Microbiol.*, 48: 306.
73. Tyagi, J.S. and Venkitasubramanian, T.A. 1981. *Can. J. Microbiol.*, 27: 1276.

74. Bhatnagar, D., Ahmad, S., Mukerji, K.G. and Venkitasubramanian, T.A. 1986. *J. Appl. Bacteriol.*, 60: 203.
75. Turner, W.B and Aldridge, D.C. 1983. *In: Fungal Metabolites, Academic Press, London*, 2: 189.
76. Steyn, P.S., Vlegaar, R. and Wessels, P.L. 1980. *In: The Biosynthesis of Mycotoxins, Academic Press, Inc., New York*, 105.
77. Silva, J.C., Minto, R.E., Barry, C.E. and Holland, K.A. 1996. *J. Biol. Chem.*, 271: 13600.
78. Harris, T.M. and Harris, C.M. 1977. *Tetrahedron*, 33: 159.
79. Collie, J.N. 1907. *Proc. Chem. Soc.*, 23: 230.
80. Birch, A.J. and Donovan, F.W. 1953. *Austral. J. Chem.*, 6: 360.
81. Richards, J.H and Hendrickson, J.B. 1964. *In: The Biosynthesis of Steroids, Terpenes and Acetogenins, Benjamin, New York*, 16.
82. Wakil, S.J., Stoops, J.K. and Joshi, V.C. 1983. *Ann. Res. Biochem.*, 52: 537.
83. Behal, V., Jehova, V., Vanek, Z. and Hostalek, Z. 1977. *Phytochemistry*, 16: 347.
84. Lynen, F. 1967. *Pure Appl. Chem.*, 14: 137.
85. Hopwood, D.A. and Sherman, D.H. 1990. *Annu. Rev. Genet.*, 24: 37.
86. Packter, N. M. 1973. *In: Biosynthesis of Acetate Derived Compound, John Wiley & Sons, New York*, 112.
87. Bhatnagar, D., Ehrlich, K.C. and Cleveland, T.E. 1992. *Handbook of Applied Mycology*, 255.
88. McGuire, G.M., Brobst, S.W., Graybill, T.M., Pal, K. and Townsend, C.A. 1989. *J. Am. Chem. Soc.*, 111: 8308.
89. Yabe, K., Ando, Y. and Hamasaki, T. 1991. *Agric. Biol. Chem.*, 55: 1907.
90. Yabe, K., Matsushima, K.E., Koyama, T. and Hamasaki, T. 1998. *Appl. Environ. Microbiol.*, 64: 166.
91. Yabe, K., Ando, Y. and Hamasaki, T. 1988. *Appl. Environ. Microbiol.*, 54: 2101.
92. Holker, J.S.E. and Mulheirn, L.J. 1968. *J. Chem. Soc. Chem. Commun.*, 1576.
93. Tanabe, M., Hamasaki, T. and Seto, H. 1970. *J. Chem. Soc. Chem. Commun.*, 1539.
94. Biollaz, M., Buchi, G. and Milne, G. 1970. *J. Am. Chem. Soc.*, 92: 1043.
95. Hsieh, D.P.H., Lin, M.T. and Yao, R.C. 1973. *Biochem. Biophys. Res. Commun.*, 52: 992.

96. Zamir, L.O. and Hufford, K.D. 1981. *Appl. Environ. Microbiol.*, 42: 168.
97. Lax, A.R., Cleveland, T.E., Bhatnagar, D. and Lee, L.S. 1986. *Plant Physiol.*, 80: 19.
98. Cleveland, T.E. and Bhatnagar, D. 1987. *Can. J. Microbiol.*, 33: 1108.
99. Yabe, K., Ando, Y., Hashimoto, J. and Hamasaki, T. 1989. *Appl. Environ. Microbiol.*, 55: 2172.
100. Bhatnagar, D., Cleveland, T.E. and Lillehoj, E.B. 1989. *Mycopath.*, 107: 75.
101. Bu' Lock, J.D. 1979. In: *Comprehensive Organic Chemistry*, Oxford, Pergamon Press, 5: 927.
102. Machinist, J.M., Dehner, E.W. and Ziegler, D.M. 1968. *Arch. Biochem. Biophys.*, 125: 858.
103. Ziegler, D.M. and Mitchell, C.H. 1972. *Arch. Biochem. Biophys.*, 150: 116.
104. Elliott, M. and Janesin N.F. 1978. *Chem. Soc. Rev.*, 7: 473.
105. Zaika, L.L. and Buchanan, R.L. 1987. *J. Food Protection*, 50 : 691.
106. Rao, H.R.G. and Harein, P.K. 1972. *J. Econ. Entomol.*, 65: 988.
107. Cox, R.H.F., Churchill, R.J. and Dorner, J.W. 1977. *J. Am. Chem. Soc.*, 99: 3159.
108. Anderson, M.S. and Dutton, M.F. 1980. *J. Food. Prot.*, 43: 381.
109. Uraih, N., Cassity, T.R. and Chipley, J.R. 1977. *Canad. J. Microbiol.*, 23: 1580.
110. Wheeler, M.H., Bhatnagar, D. and Rojas, M.G. 1989. *Pest. Biochem. Physiol.*, 35: 315.
111. Wheeler, M.H., Bhatnagar, D. and Klich, M.A. 1991. *Pest. Biochem. Physiol.*, 41: 190.
112. Mahmoud, Q.L.E. 1994. *Lett. App. Microbiol.*, 19: 110.
113. Minto, R.E and Townsend, C.A. 1997. *Chem. Rev.*, 97: 2537.
114. Chang, P.K., Skory, C.D and Linz, J.E. 1992. *Curr. Genet.*, 21: 231.
115. Trail, F., Mahanti, N., Raraick, M., Mehig, R and Linz, J.E. 1995. *Appl. Environ. Microbiol.*, 61: 2665.
116. Yu, J., Chang, P.K., Cary, J.W., Bhatnagar, D. and Cleveland, T.E. 1997. *Appl. Environ. Microbiol.*, 63: 1349.
117. Foutz, K.R., Woloshuk, C.P. and Payne, G.A. 1995. *Mycopath.*, 87: 787.
118. Yu, J., Chang, P.K., Cary, J.W., Wright, M., Bhatnagar, D., Cleveland, T.E., Payne, G.A. and Linz, J.E. 1995. *Appl. Environ. Microbiol.*, 61: 2365.
119. Keller, N.P., Kantz, N.J. and Adams, T.H. 1994. *Appl. Environ. Microbiol.*, 60: 1444.

120. Chang, P.K., Cary, J.W., Yu, J., Bhatnagar, D. and Cleveland, T.E. 1995. *Mol. Gen. Genet.*, 248: 270.
121. Mahanty, N., Bhatnagar, D., Carey, J.W., Joubran, J. and Linz, J.E. 1996. *Appl. Environ. Microbiol.*, 62: 191.
122. Trail, F., Chang, P.K., Carey, J. and Linz, J.E. 1994. *Appl. Environ. Microbiol.*, 60: 4078.
123. Cary, J.W., Wright, M., Bhatnagar, D., Lee, R. and Chu, F.S. 1996. *Appl. Environ. Microbiol.*, 62: 360.
124. Prieto, R., Yousibova, G.L. and Woloshuk, C.P. 1996. *Appl. Environ. Microbiol.*, 62: 3567.
125. Skory, C.D., Chang, P.K. and Linz, J.E. 1992. *Appl. Environ. Microbiol.*, 58: 3527.
126. Yu, J., Cary, J.W., Bhatnagar, D., Cleveland, T.E., Keller, N.P and Chu, F.S. 1993. *Appl. Environ. Microbiol.*, 59: 3564.
127. Prieto, R. and Woloshuk, C.P. 1997. *Appl. Environ. Microbiol.*, 63: 1661.
128. Payne, G.A., Nystrom, G.J., Bhatnagar, D., Cleveland, T.E. and Woloshuk, C.P. 1993. *Appl. Environ. Microbiol.*, 59: 156.
129. Chang, P.K., Carey, J., Bhatnagar, D., Cleveland, T.E., Bennet, J.W., Linz, J.E., Woloshuk, C.P. and Payne, G.A. 1993. *Appl. Environ. Microbiol.*, 59: 3273.
130. Keller, N.P. and Hohn, T.M. 1997. *Fungal Genet. Biol.*, 21: 17.
131. Payne, G.A. and Brown, M.P. 1998. *Annu. Rev. Phytopathol.*, 36: 392.
132. Schroeder, H.W. and Kelton, W.H. 1975. *Appl. Microbiol.*, 30: 589.
133. Rabie, C.J., Lubben, A. and Steyn, M. 1976. *Appl. Environ. Microbiol.*, 32: 206.
134. Davies, J.E., Kirkaldy, D. and Roberts, J.C. 1960. *J. Chem. Soc.*, 54: 2169.
135. Halls, N.A. and Ayres, C.J. 1975. *J. Chem. Soc.*, 30: 702.
136. Chatterjee, M. and Townsend, C.A. 1994. *J. Org. Chem.*, 59: 4424.
137. Barnes, S.E., Dola, T.P., Bennett, J.W. and Bhatnagar, D. 1994. *Mycopath.*, 125: 173.
138. Steyn, P.S. and Maes, C.M. 1984. *J. Chem. Soc. Perkin. Trans. I.*, 1137.
139. Salhab, A.S., Russell, G.F., Coughlin, J.R. and Hsieh, D.P.H. 1976. *JAOAC.*, 59(5): 1037.
140. Bullock, E., Roberts, J.C and Underwood, J.G. 1962. *J. Chem. Soc.*, 479.
141. Birkinshaw, J.H. and Hammady, I.M.M. 1957. *Biochem. J.*, 65: 162.
142. Hatsuda, Y., Juyama, S and Terashima, N. 1954. *J. Agr. Chem. Soc. Japan*, 28: 989.

143. Pons, W.A. and Goldblatt, L.A. 1969. In: *Aflatoxins*, Academic Press, New York, 86.
144. Anderillos, P.J., Beckwith, A.C. and Eppley, R.M. 1967. *JAOAC.*, 50: 346.
145. Lillard, D.A. and Lantrin, R.S. 1971. *JAOAC.*, 53: 1060.
146. Horwitz, W. (Ed.) 1970. "*Official Methods of Analysis*", Assoc. Off. Anal. Chem., Washington, D.C., 426.
147. Stubblefield, R.D. and Shotwell, O.D. 1977. *JAOAC.*, 60: 784.
148. Garner, R.C. 1975. *J. Chromatogr.*, 103: 186.
149. Takahashi, D.M. 1977. *J. Chromatogr.*, 131: 147.
150. Takahashi, D.M. 1977. *JAOAC.*, 60: 799.
151. Pons, W.A. and Franz, A.O. 1978. *JAOAC.*, 61: 793.
152. Hurst, W.J. and Toomey, P.B. 1978. *J. Chromatogr. Sci.*, 16: 372.
153. Lansden, J.A. 1977. *J. Agr. Food Chem.*, 25: 969.
154. Kok, W. Thu. 1994. *J. Chromatogr. B.*, 659: 127.
155. Kuronen, P. 1989. *Arch. Environ. Contam. Toxicol.*, 18: 336.
156. Tarter, E.J., Hanchay, J.P. and Scott, P.M. 1984. *JAOAC.*, 67: 597.
157. Manabe, M., Goto, T. and Matura, S. 1978. *Agric. Biol. Chem.*, 42(11): 2003.
158. Bennett, J.W., Lee, L.S., Shoss, S.M. and Boudreaux, G.H. 1980. *Appl. Environ. Microbiol.*, 39: 835.
159. Donkersloot, J.A., Mateles, R.I. and Yang, S.S. 1972. *Biochem. Biophys. Res. Commun.*, 47: 1051.
160. Bennett, J.W. and Goldblatt, L.A. 1973. *Sabouraudia*, 11: 235.
161. Lee, L.S., Bennett, J.W., Cucullu, A.F. and Ory, R.L. 1975. *J. Agric. Food. Chem.*, 24: 1167.
162. Singh, R. and Hsieh, D.P.H. 1977. *Arch. Biochem. Biophys.*, 178: 285.
163. Bennett, J.W., Floyd, J.C. and Mills, J.C. 1986. *Experimental Mycol.*, 11: 109.
164. Dutton, M. F., Heathcote, J.G. and Hibbert, J.R. 1976. *Chem. Ind.*, 1976: 270.
165. Venkitasubramanian, T.A. and Gupta, S. K. 1977. *Ann. Nutr. Alim.*, 31: 635.
166. Stack, M. and Rodricks, J.V. 1971. *JAOAC.*, 54: 85.
167. Dutton, M.F. and Anderson, M.S. 1982. *Appl. Environ. Microbiol.*, 43: 548.
168. Cleveland, T.E., Bhatnagar, D., Foell, C.J. and McCormick, S.P. 1987. *Appl. Environ. Microbiol.*, 53: 1028-1033.

169. Dutton, M.F., Ehrlich, K. and Bennett, J.W. 1985. *Appl. Environ. Microbiol.*, 49: 1392.
170. Keller, N.P., Dischinger, H.C., Bhatnagar, D., Cleveland, T.E. and Ullah, A.H.J. 1993. *Appl. Environ. Microbiol.*, 59: 479.
171. Basset, E.W. and Tanenbaum, S.W. 1960. *Biochem. Biophys. Acta.*, 40: 535.
172. Lynen, F. and Tada, M. 1961. *Angew. Chem.*, 73: 513.
173. Raj, F.G., Viswanathan, L., Murphy, H.S.R. and Venkitasubramanian, T.A. 1965. *Experientia*, 15: 1141.
174. Yao, R.C. and Hsieh, D.P.H. 1974. *Appl. Microbiol.*, 28: 52.
175. Bhatnagar, D., Cleveland, T.E. and Kingston, D.G.T. 1991. *Biochem.*, 30: 4343.
176. Bradford, M. M. 1976. *Anal. Biochem.*, 72: 248.
177. Murphy, G., Vogel, G., Krippahl, G. and Lynen, F. 1974. *Eur. J. Biochem.*, 49: 443.
178. Dimorth, P., Walter, H. and Lynen, F. 1970. *Eur. J. Biochem.*, 13: 98.
179. Finnegan, R.A., Patel, J.K. and Bachman, L. 1966. *Tetrahedron Letters*, 49: 6087.
180. Govindachari, T.A., Pai, B.R. and Rao, V.R. 1971. *Ind. J. Chem.*, 9(8): 772.
181. Roberts, J.C. 1961. *Chem. Rev.*, 61: 591.
182. Dean, F.M. 1963. *In: Naturally Occurring Oxygen Ring Compounds. Butterworth, London*, 175.
183. Gottlieb, O.R. 1968. *Phytochem.*, 7: 411.
184. Carpenter, I., Locksley, H.D. and Scheinmann, F. 1969. *Phytochem.*, 8: 2013.
185. Sultanbawa, M.U.S. 1980. *Tetrahedron*, 36: 1465.
186. Grover, P.K., Shah, G.D. and Shah, R.D. 1955. *J. Chem. Soc.*, 3932.
187. Locksley, H.D., Moore, I. and Scheinmann, F. 1966. *J. Chem. Soc. (C).*, 430.
188. Jackson, B., Locksley, H.D. and Scheinmann, F. 1967. *J. Chem. Soc. (C).*, 785.
189. Desai, B.M., Desai, P.R. and Desai, R.D. 1960. *J. Indian Chem. Soc.*, 37: 53.
190. Nevrekar, N.B., Lele, B.V., Mucheli, M.V.R. and Kudav, N.A. 1983. *Chem. Ind.*, 479.
191. Mathews, C.K. and van Holden, K.E. 1990. *Biochemistry*, Benjamin/Cummings Co., 381.
192. Patel, G.N. and Trivedi, K. 1988. *Indian J. Chem.*, 27B: 458.
193. Kane, V.V., Kulkarni, A.B. and Shah, R.C. 1959. *J. Sci. Ind. Res.*, 18B, 28.
194. Dixon, M. and Webb, E.C. 1964. *In: Enzymes, Longmans, Green and Co., London*, 54.

195. Simpson, T.E., de Jesus, A.E., Steyn, P.S. and Vleggar, R.E. 1983. *J. Chem. Soc. Chem. Comm.*, 338.
196. Watanabe, C.M.H. and Townsend, C.A. 1996. *J. Org. Chem.*, 61: 1990.
197. Del Rio, L.A., Ortega, R.G., Lopez, A.L. and Gorge, J.L. 1977. *Anal. Biochem.*, 80: 409.
198. Gunsalus, I.C., Conrad, H.E. and Trudgill, P.W. 1964. *Oxidases and Redox Systems*. John Wiley & Sons, New York, 1: 440.
199. Daly, J., Jerima, D. and Witkop, B. 1972. *Experientia*, 28: 1129.
200. Vannelli, T. and Hooper, A.B. 1995. *Biochem.*, 34: 11743.
201. Fried, R., Thomas, R.W., Gerke, J.R., Herz, J.E. and Donin, M.N. 1952. *J. Am. Chem. Soc.*, 74: 3962.
202. Hollander, I.J., Shen, Y.G., Hein, J. and Demain, A.L. 1984. *Science*, 224: 610.
203. Hostalek, Z. and Vanek, Z. 1979. *Biotechnol. Lett.*, 1 : 177.

## APPENDIX 1

### Preparation of Potato Dextrose Agar

Commercial grade of potato dextrose (15 g) was dissolved in 300 ml of hot deionised water. The solution was transferred to a 1 L volumetric flask and diluted to mark with deionised water. The medium was sterilized in an autoclave for 1 hour at 120 °C.

## APPENDIX 2

### The Preparation of Reddys Medium

The chemicals listed below were weighed by means of a Mettler TG 50 Thermobalance and dissolved in 1 L deionised water.

Potassium dihydrogen orthophosphate	0.75 g
Magnesium sulphate septahydrate	0.35 g
Disodium tetraborate decahydrate	2.0 mg
Ammonium molybdate	2.0 mg
Ferrous sulphate septahydrate	2.0 mg
Zinc sulphate septahydrate	10.0 mg
Manganous chloride dihydrate	5.0 mg
Calcium chloride dihydrate	75.0 mg
L-Asparagine	10.0 mg
Ammonium sulphate	3.5 g
Sucrose	85.0 g

L-asparagine was dissolved in 250 ml deionised water. The compounds were added with stirring and the solution made up to 1 L with deionised water. The medium (100 ml) was transferred to 250 ml Erlenmeyer flasks and sterilised in an autoclave for 1 hour at 120 °C.



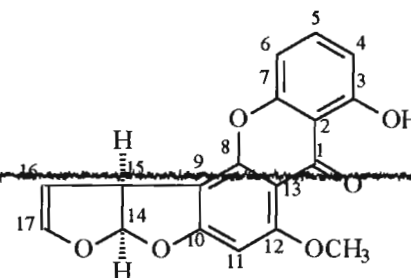
DRG1:STERIGMATOCYSTIN IN CDCL3

C H 3

C H 2

C H

C H n



APPENDIX 3

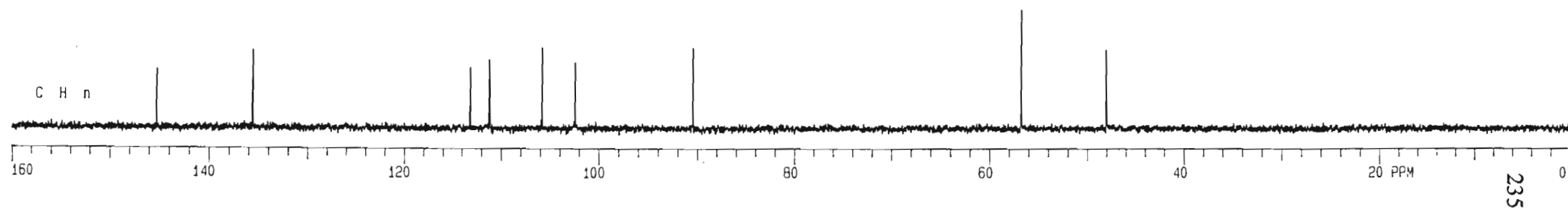
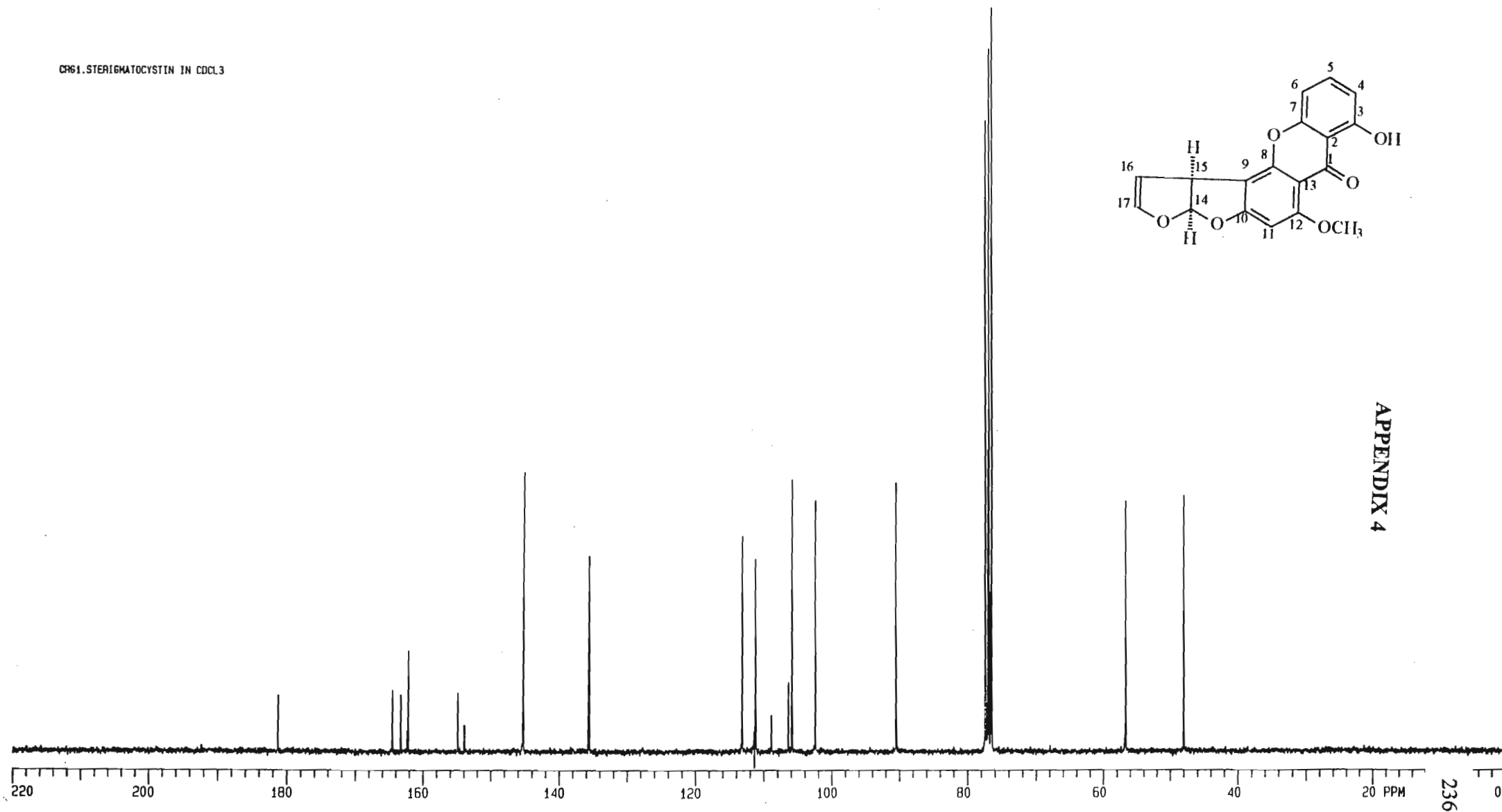
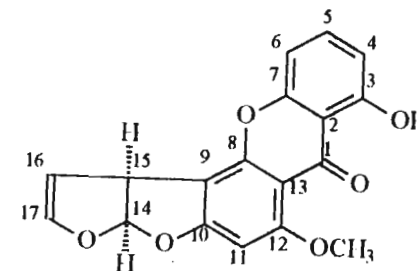


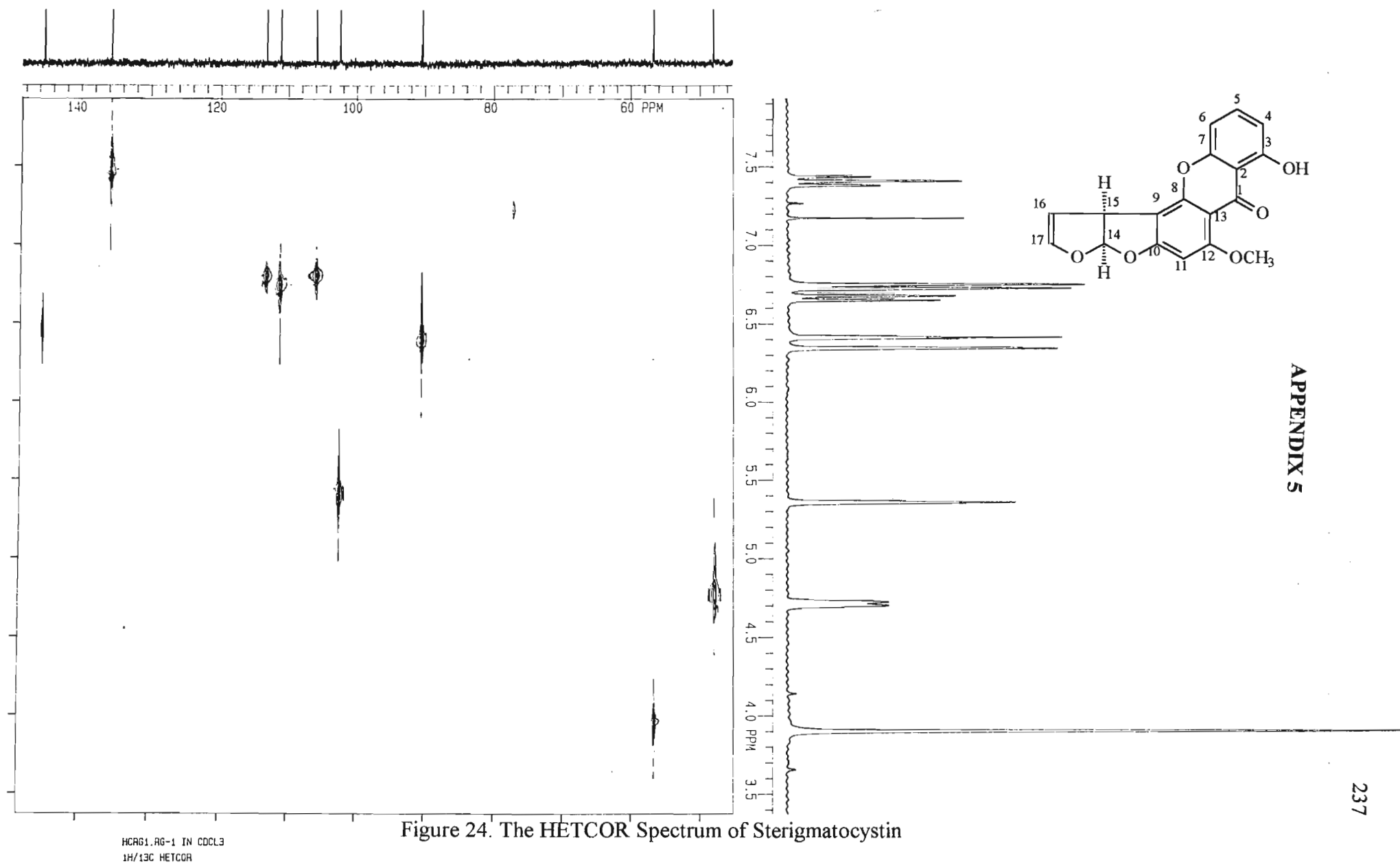
Figure 22. The DEPT Spectrum of Sterigmatocystin

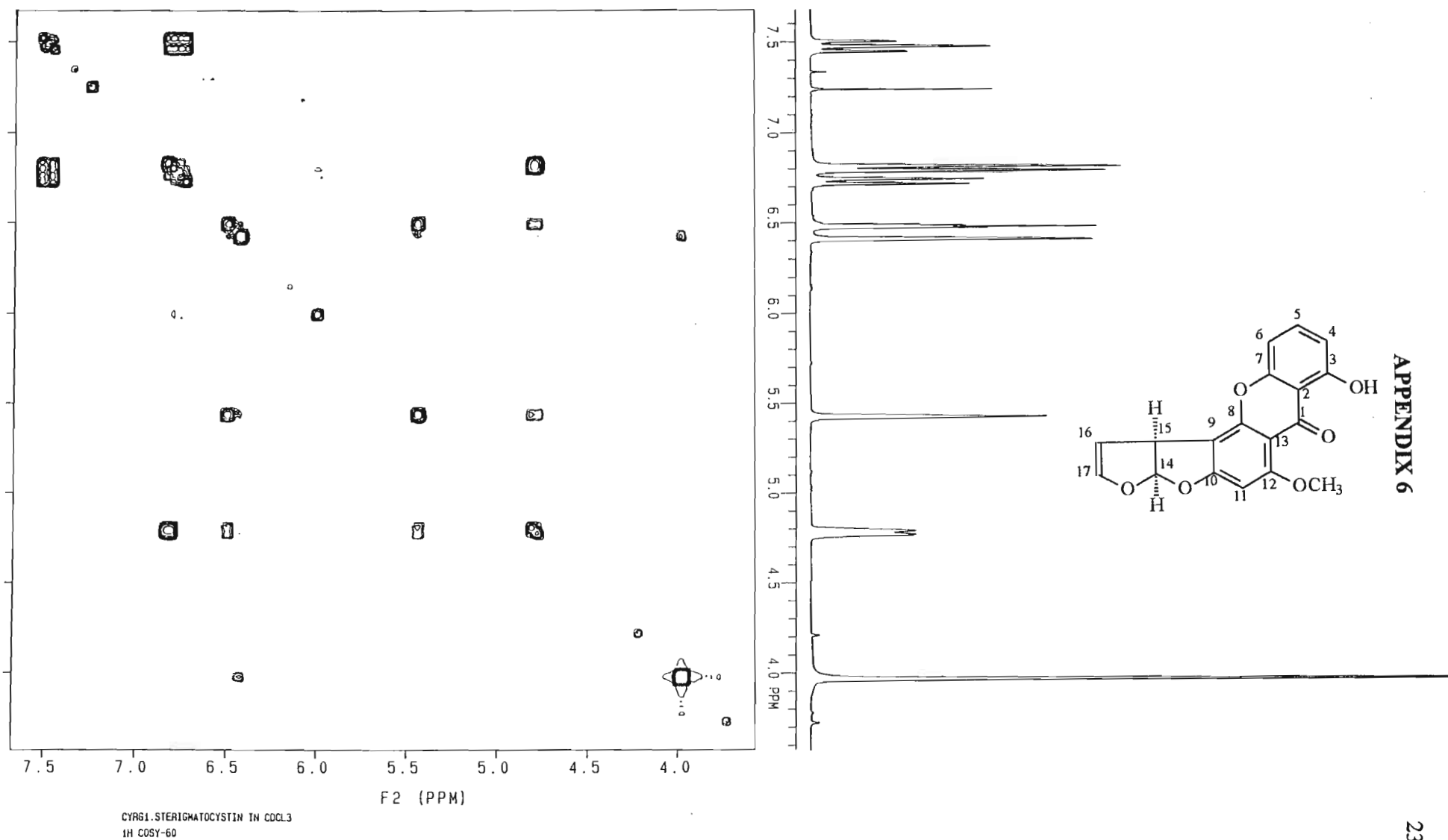
CR61. STERIGMATOCYSTIN IN CDCL<sub>3</sub>



APPENDIX 4

Figure 23. The <sup>13</sup>C-NMR Spectrum of Sterigmatocystin





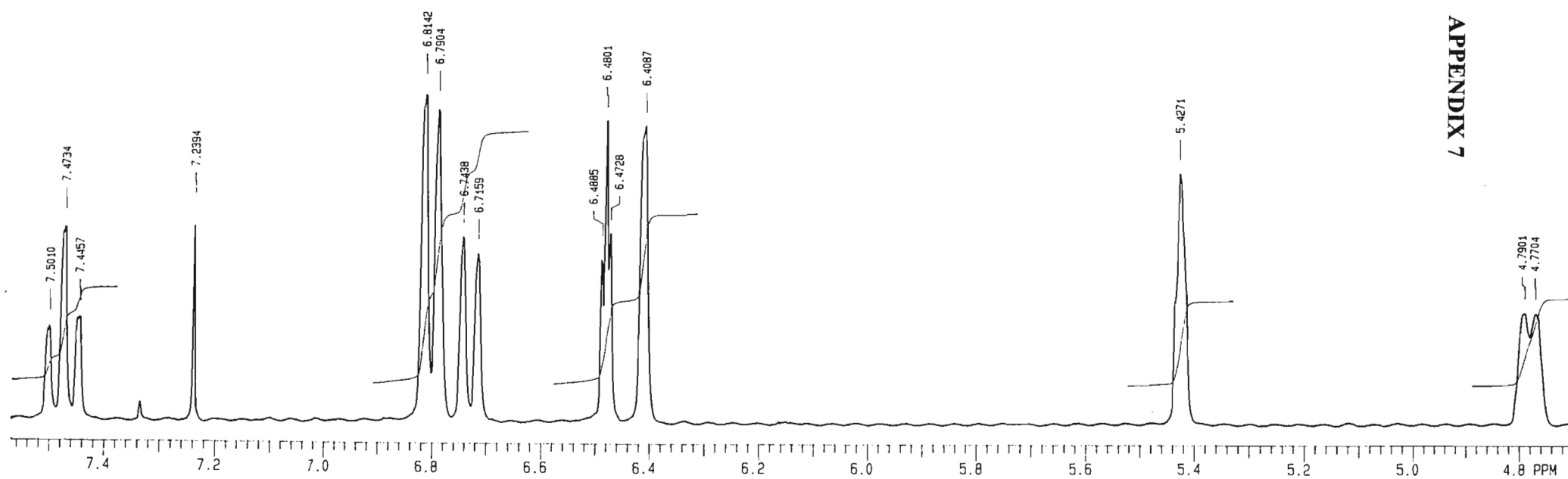
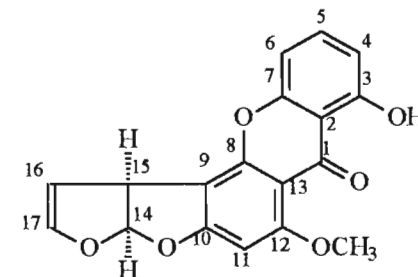


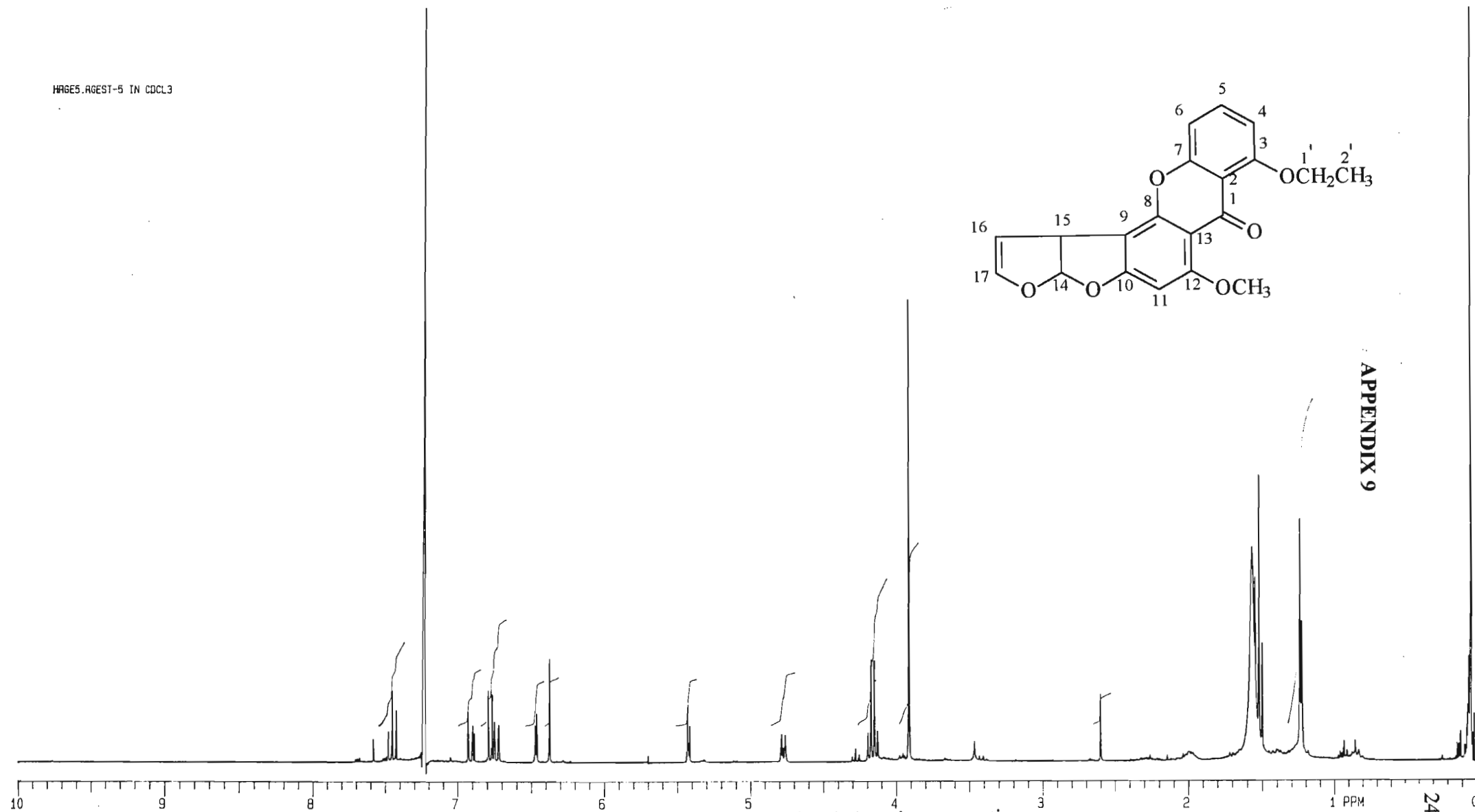
Figure 27. The Expanded  $^1\text{H}$ -NMR Spectrum of Sterigmatocystin

## APPENDIX 8

Table 5. The  $^1\text{H}$ -NMR Data of *O*-Ethyl sterigmatocystin

Proton atom	Chemical Shift $\delta$ H (ppm)	Splitting Pattern	Coupling constant J ( H,H ) Hz
H-4	6.91	doublet	7.8
H-5	7.48	triplet	8.5
H-6	6.74	doublet	7.2
H-11	6.38	singlet	-
H-14	6.78	doublet	7.1
H-15	4.79	triplet	7.1
H-16	5.43	triplet	2.5
H-17	6.47	triplet	2.7
OCH <sub>3</sub>	3.92	singlet	-
-CH <sub>2</sub>	4.16	quartet	7.0
-CH <sub>3</sub>	1.53	triplet	7.1

HAGERST-5 IN CDCL<sub>3</sub>



APPENDIX 9

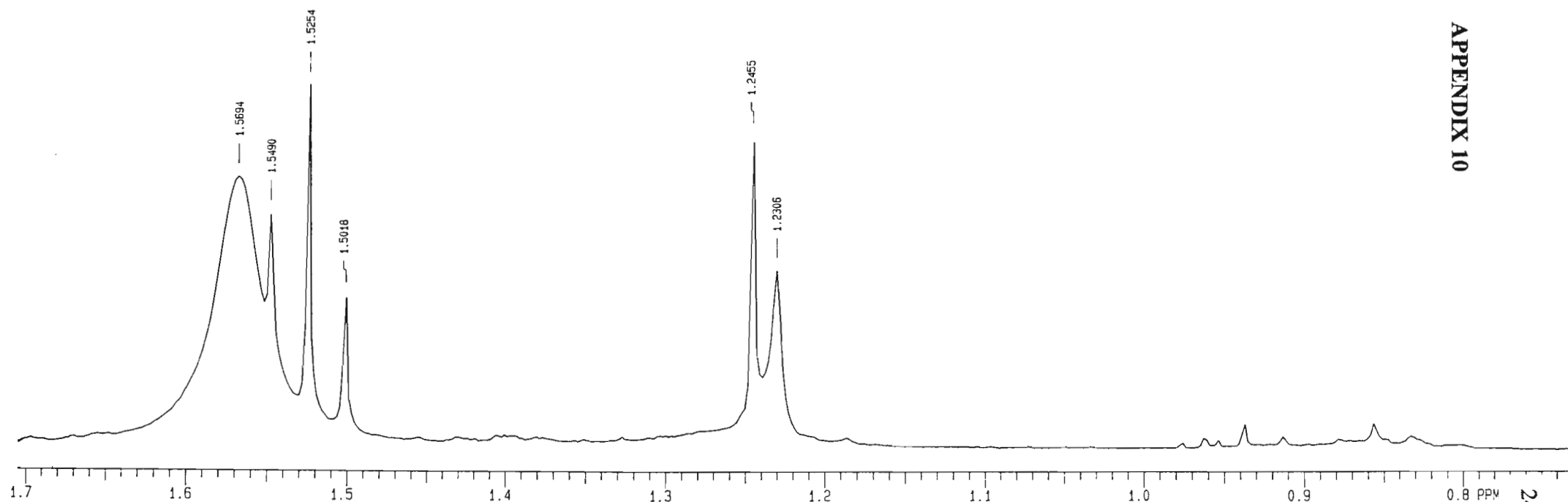
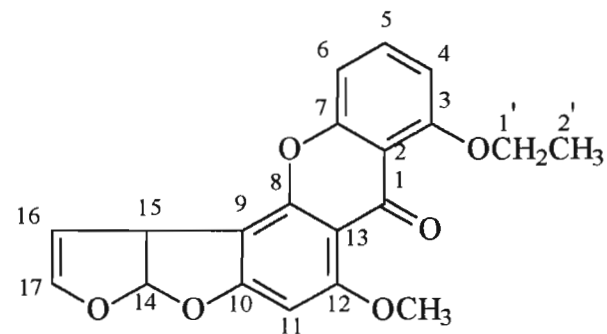
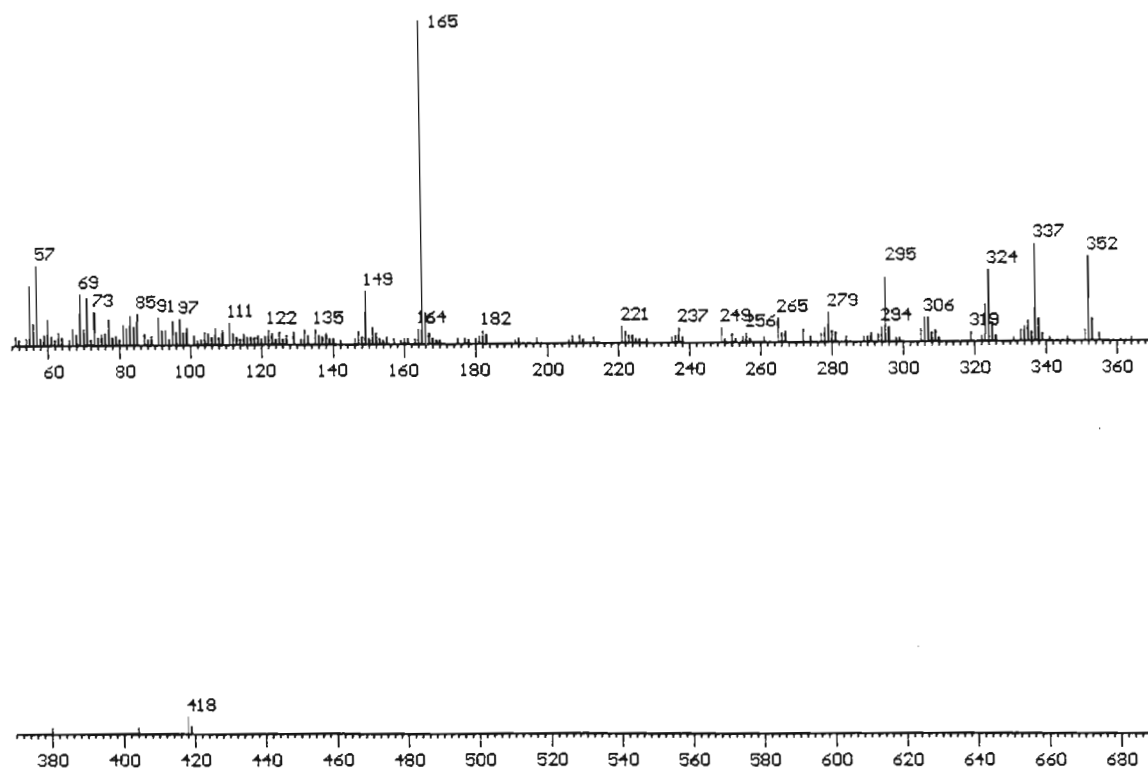
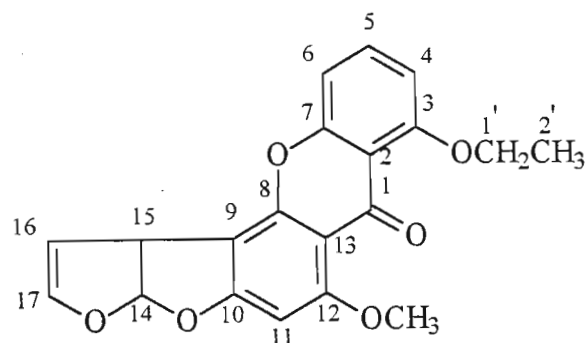


Figure 34. The Expanded  $^1\text{H}$ -NMR Spectrum of *O*-Ethyl sterigmatocystin



## APPENDIX 11

Figure 35. The Normalised Mass Spectrum of *O*-Ethyl sterigmatocystin

## APPENDIX 12

Table 6. The  $^1\text{H}$ -NMR Data of *O*-Propyl sterigmatocystin.

Proton atom	Chemical Shift $\delta$ H (ppm)	Splitting Pattern	Coupling constant J ( H,H ) Hz
H-4	6.90	doublet	7.8
H-5	7.45	triplet	8.3
H-6	6.73	doublet	8.3
H-11	6.38	singlet	-
H-14	6.78	doublet	7.1
H-15	4.77	triplet	7.1
H-16	5.43	triplet	2.7
H-17	6.47	triplet	2.1
OCH <sub>3</sub>	3.92	singlet	-
-CH <sub>2</sub>	4.04	triplet	6.6
-CH <sub>2</sub>	1.95	multiplet	6.8
-CH <sub>3</sub>	1.10	triplet	7.3

HAG251.AGCPA-25T IN CDCL3

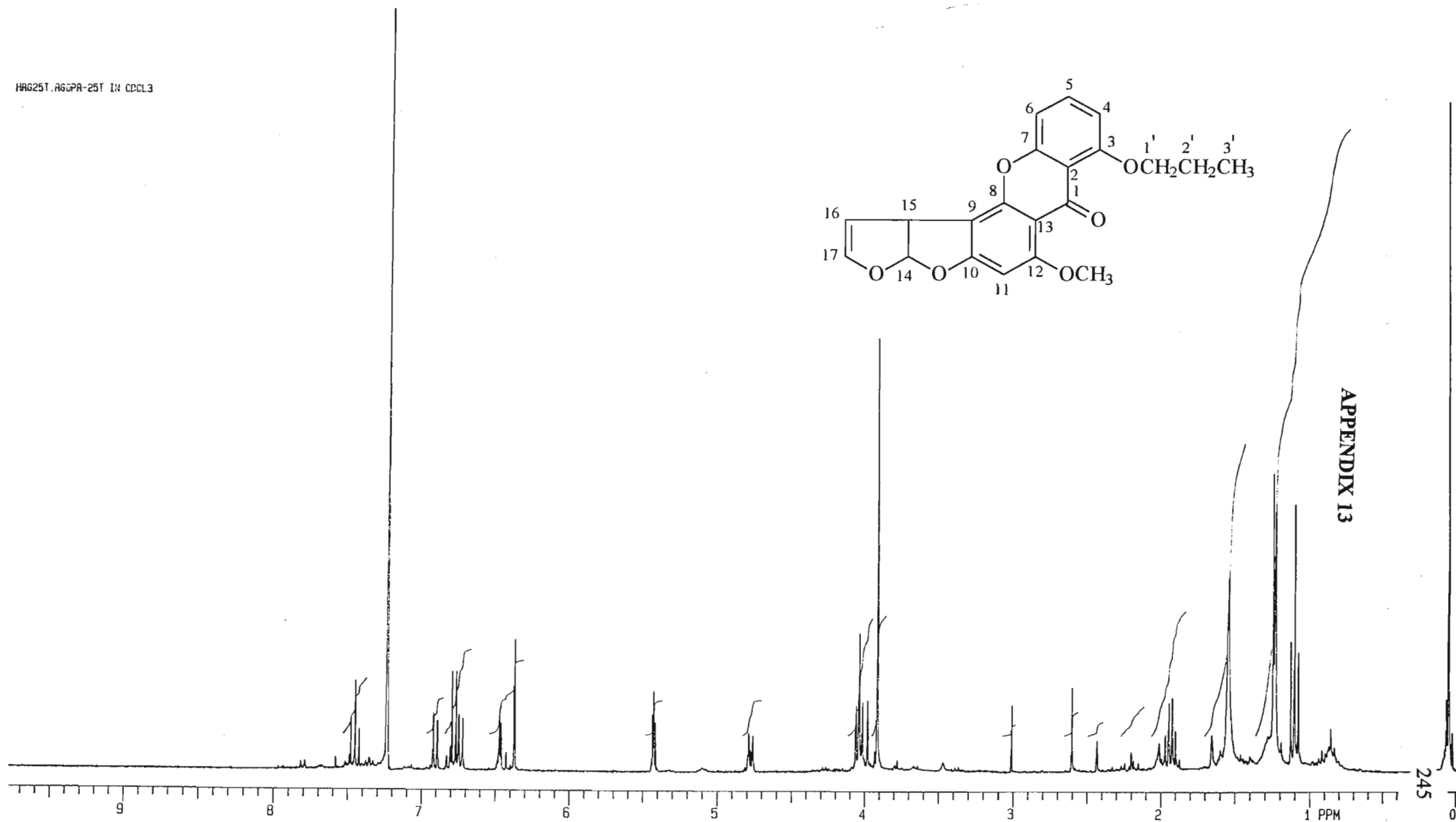


Figure 36. The <sup>1</sup>H-NMR Spectrum of *O*-Propyl sterigmatocystin

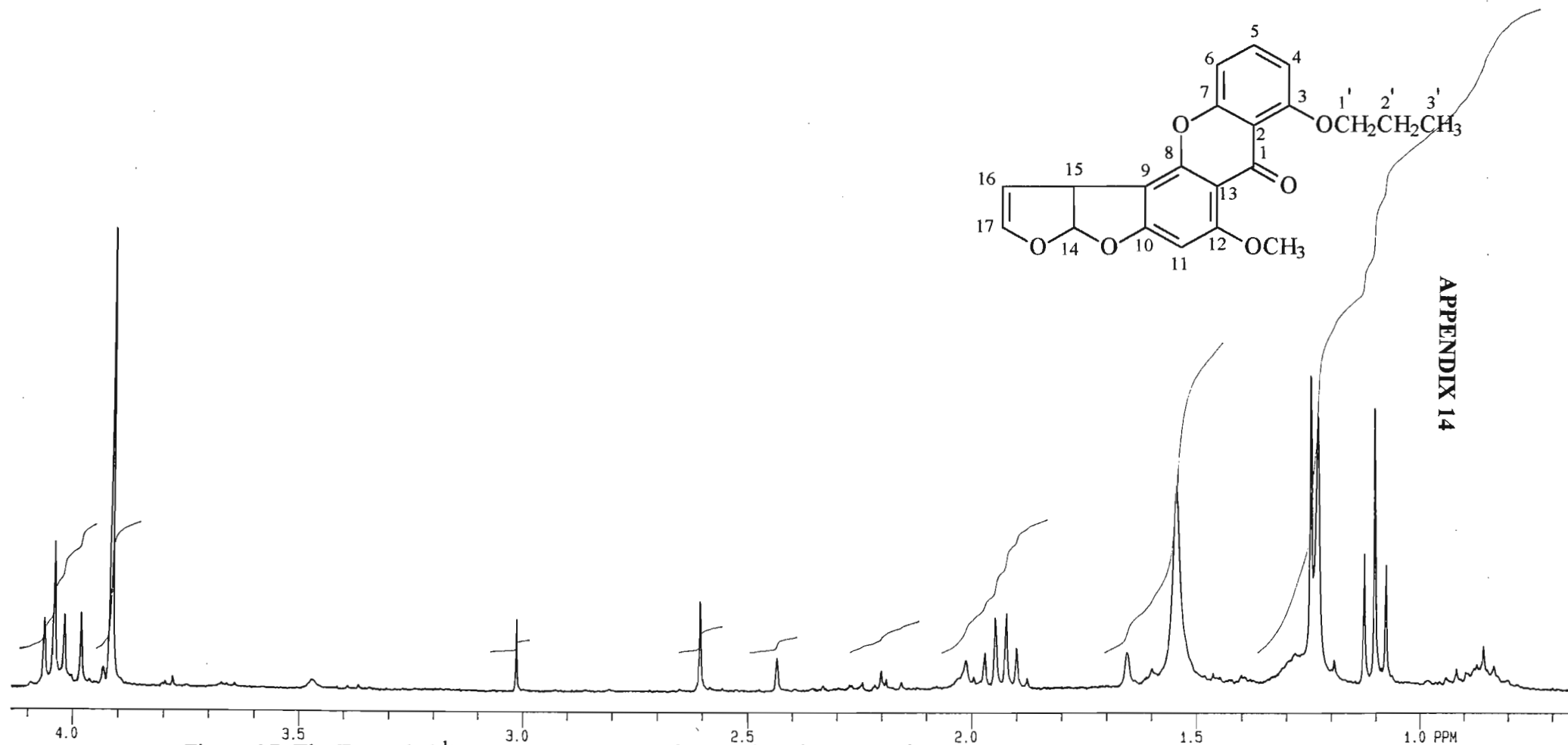
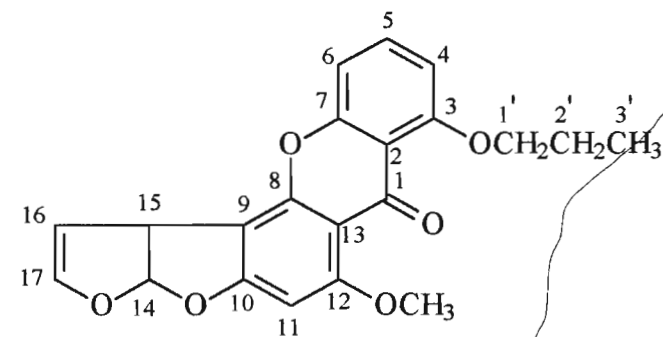
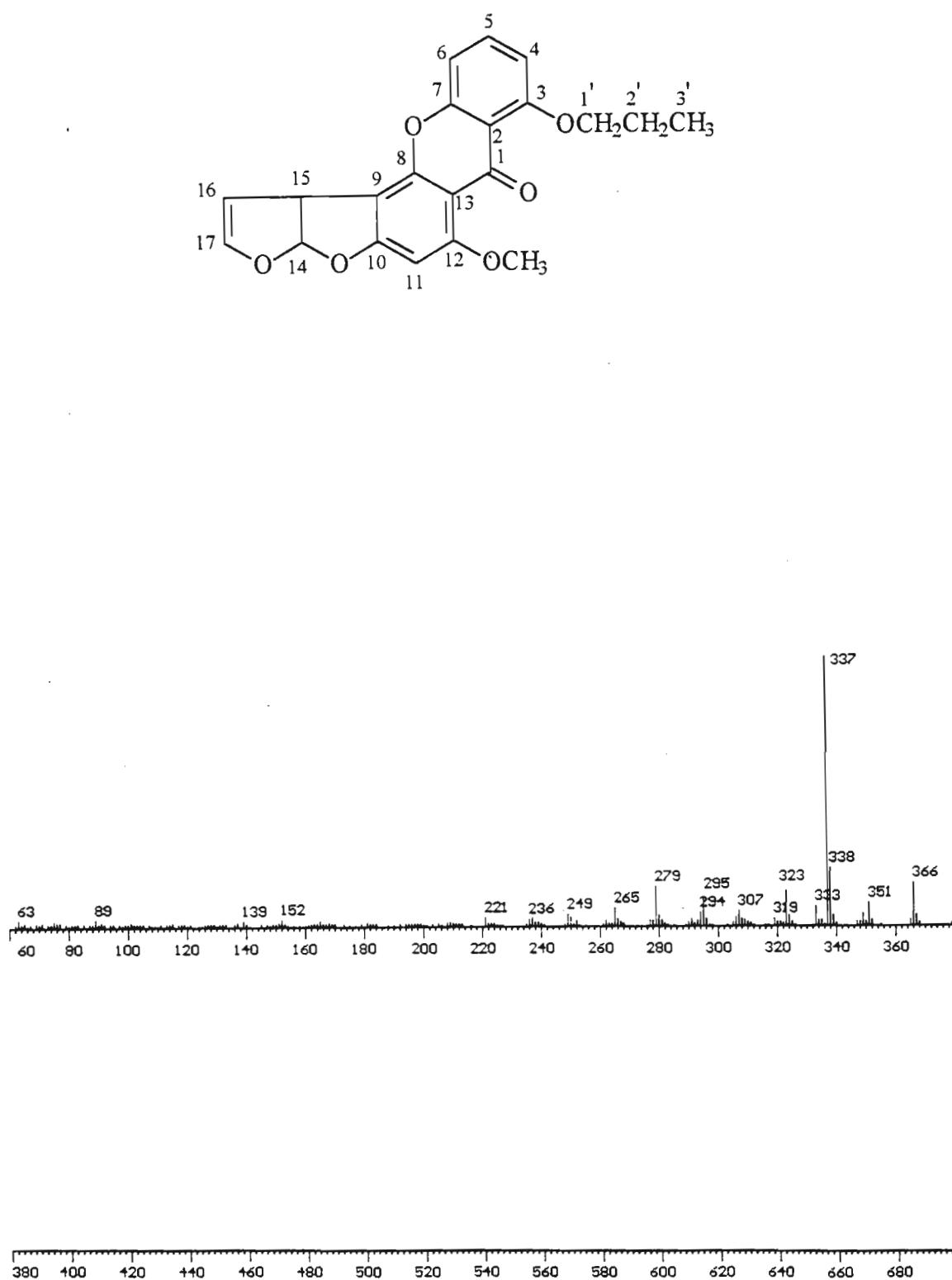


Figure 37. The Expanded <sup>1</sup>H-NMR Spectrum of *O*-Propyl sterigmatocystin

## APPENDIX 15

Figure 38. The Normalised Mass Spectrum of *O*-Propyl sterigmatocystin

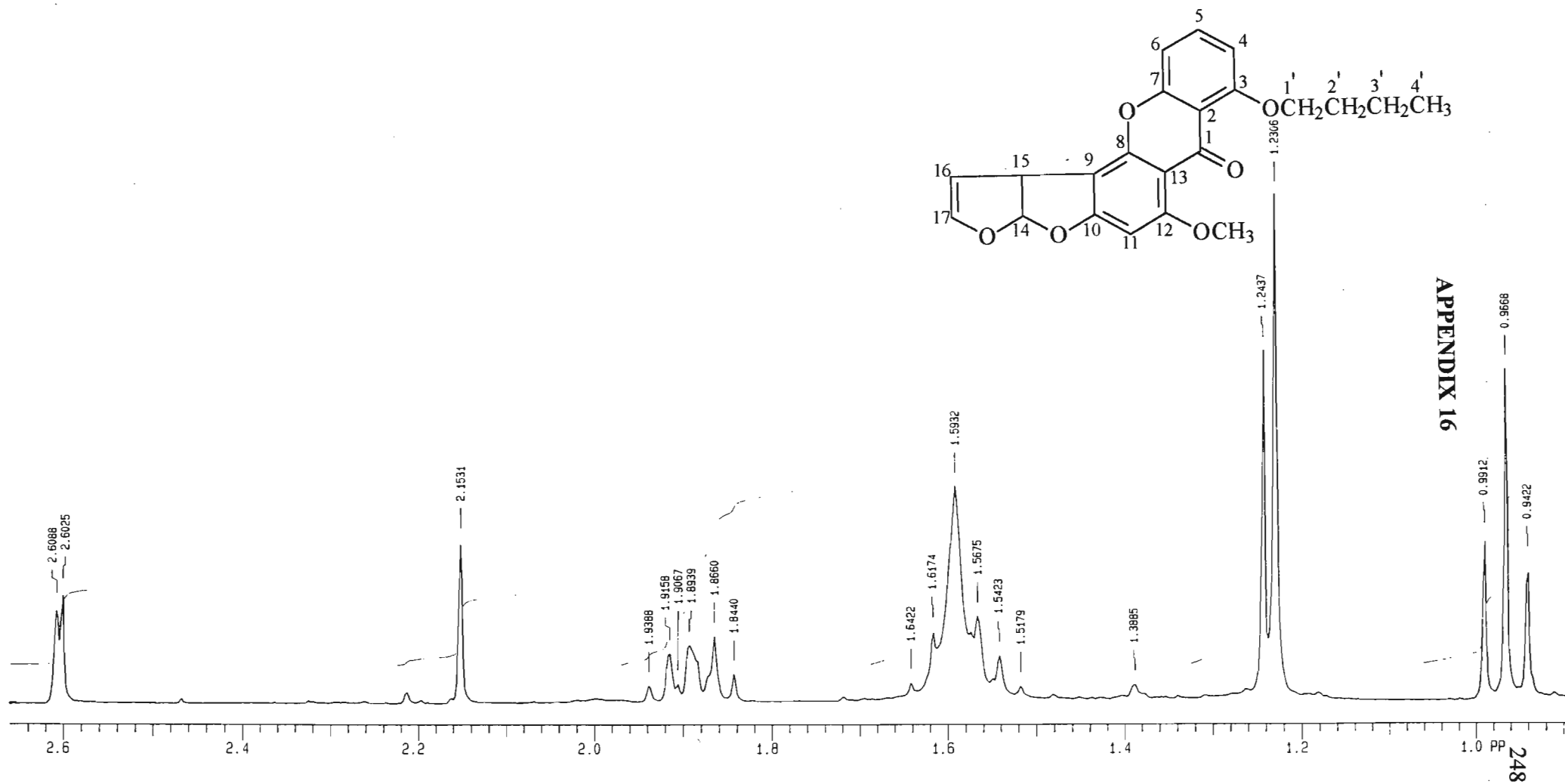


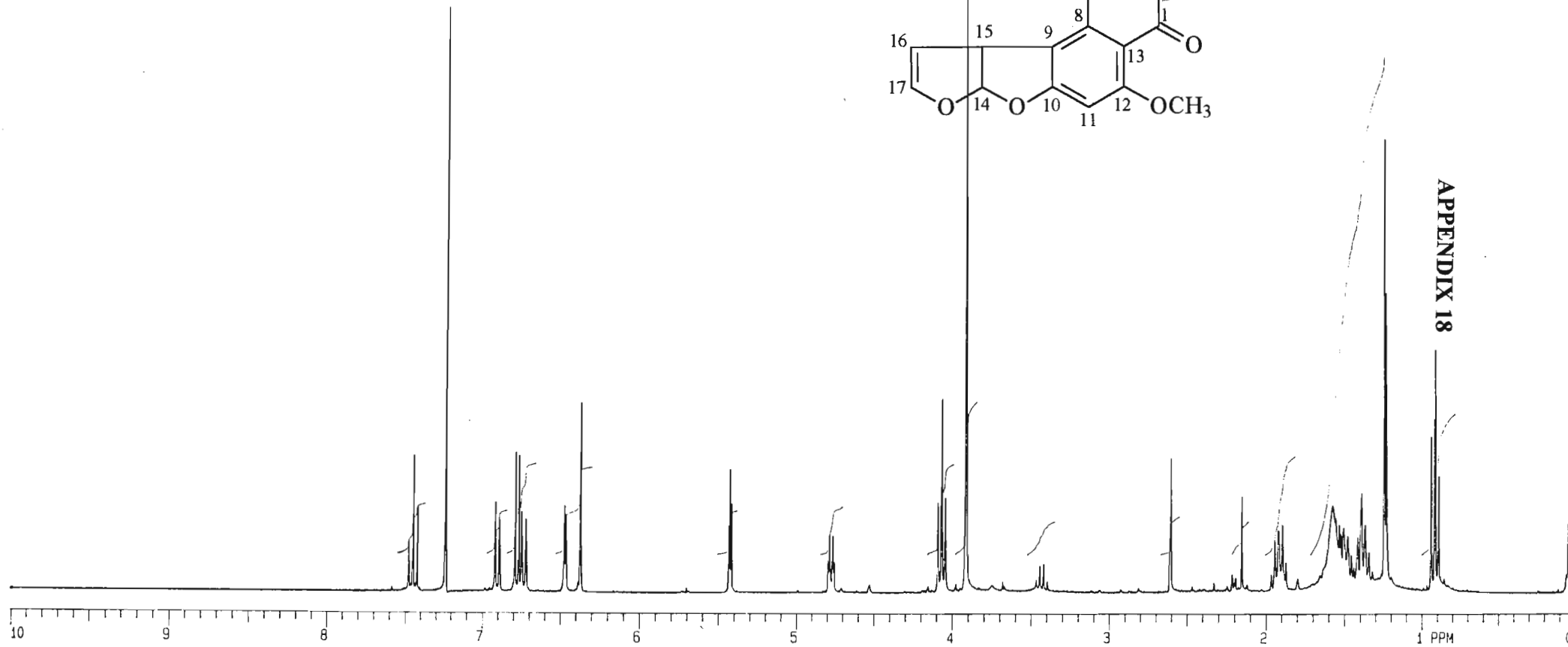
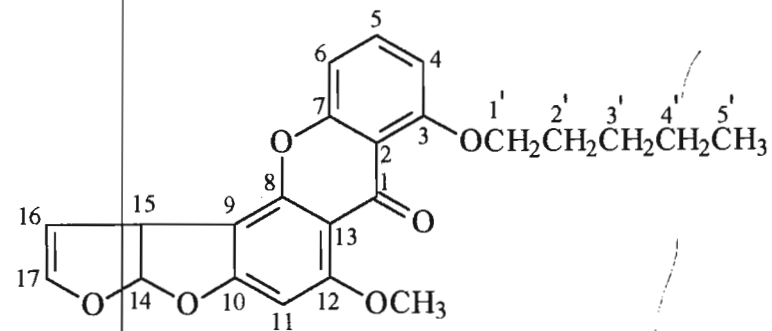
Figure 40. The Expanded <sup>1</sup>H-NMR Spectrum of *O*-Butyl sterigmatocystin

## APPENDIX 17

Table 8. The  $^1\text{H}$ -NMR Data of *O*-Pentyl sterigmatocystin.

Proton atom	Chemical Shift $\delta$ H (ppm)	Splitting Pattern	Coupling constant J ( H,H ) Hz
H-4	6.90	doublet	8.2
H-5	7.45	triplet	8.4
H-6	6.74	doublet	8.2
H-11	6.37	singlet	-
H-14	6.77	doublet	7.1
H-15	4.78	triplet	7.1
H-16	5.43	triplet	2.6
H-17	6.47	triplet	2.1
OCH <sub>3</sub>	3.92	singlet	-
-CH <sub>2</sub>	4.07	triplet	6.8
-CH <sub>2</sub>	1.92	multiplet	6.8
-CH <sub>2</sub>	1.49	multiplet	2.1
-CH <sub>2</sub>	1.39	multiplet	8.3
-CH <sub>3</sub>	0.92	triplet	7.3

HAGPE1.AGPEST-1 IN CDCL3



APPENDIX 18

Figure 42. The <sup>1</sup>H-NMR Spectrum of *O*-Pentyl sterigmatocystin



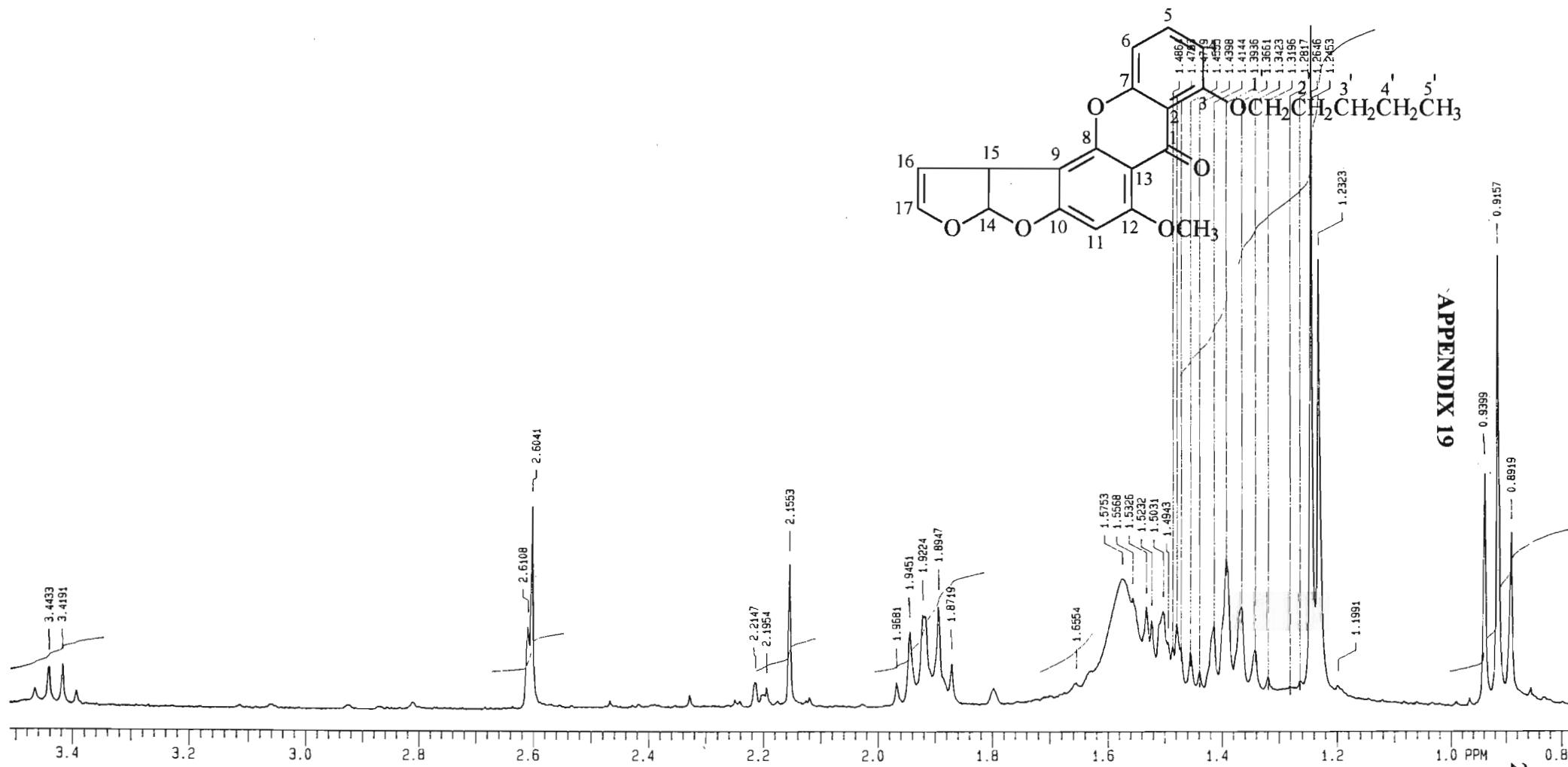
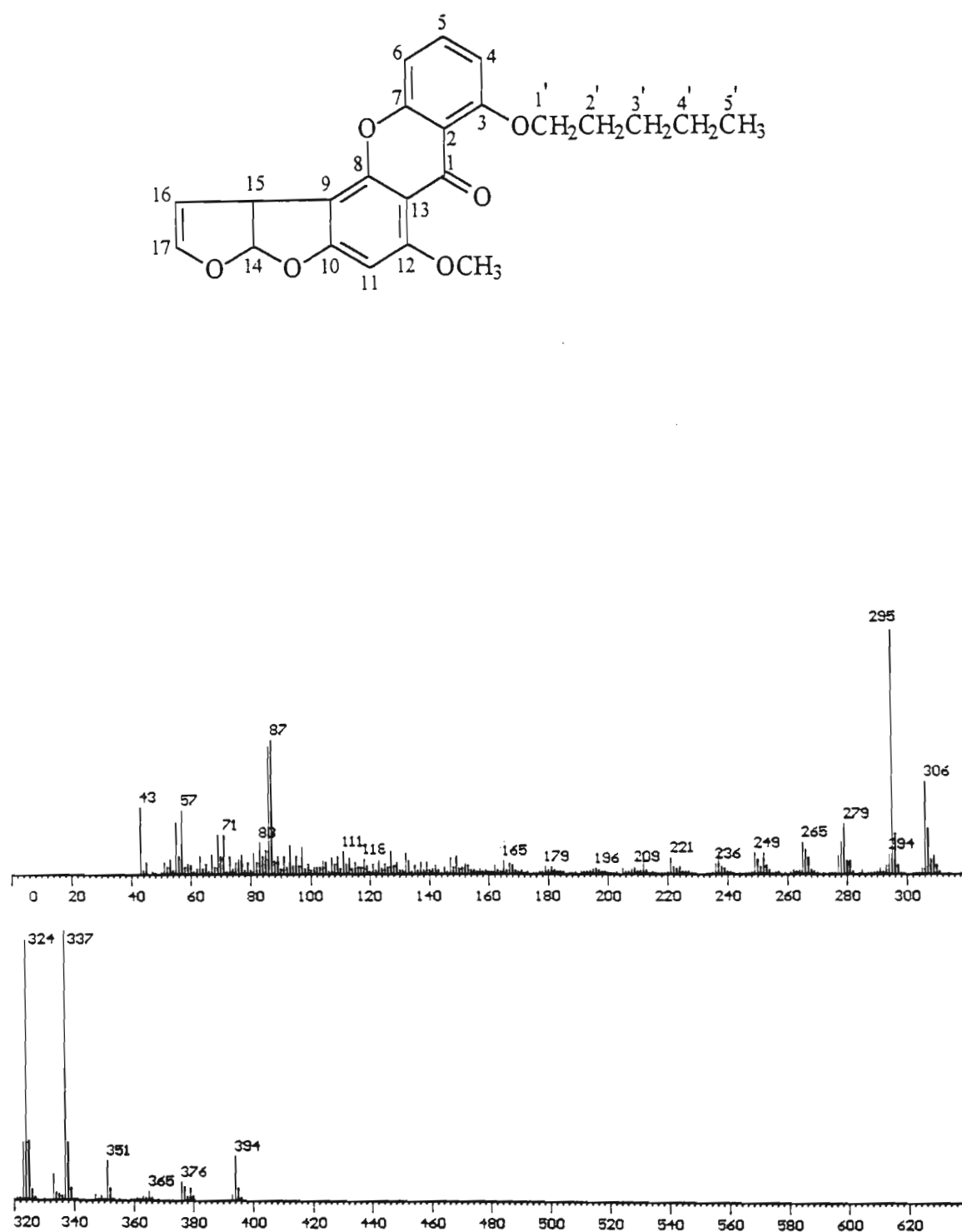


Figure 43. The Expanded <sup>1</sup>H-NMR Spectrum of *O*-Pentyl sterigmatocystin

## APPENDIX 20

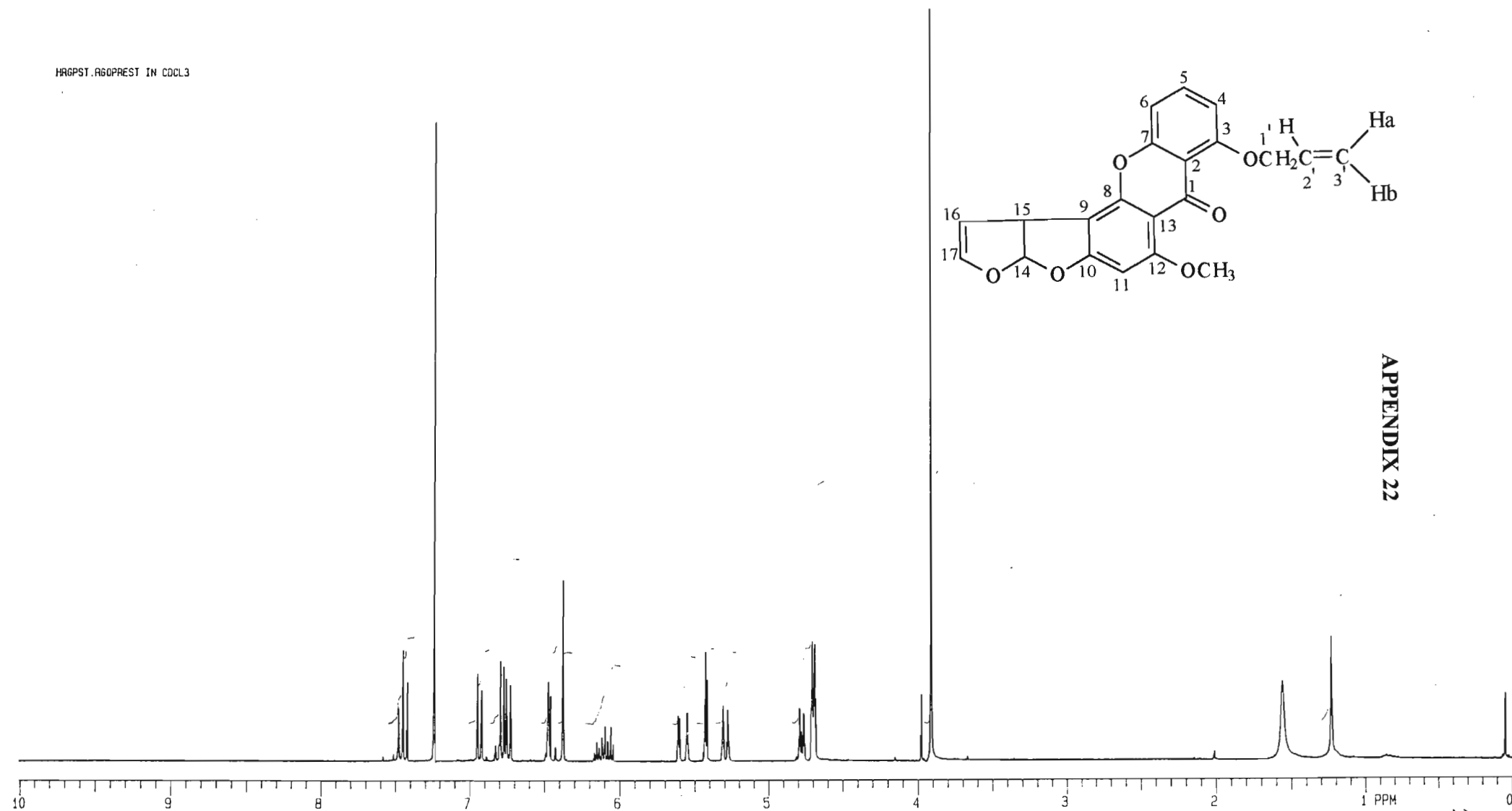
Figure 44. The Normalised Mass Spectrum of *O*-Pentyl sterigmatocystin

## APPENDIX 21

Table 9. The  $^1\text{H}$ -NMR Data of *O*- Propenyl sterigmatocystin.

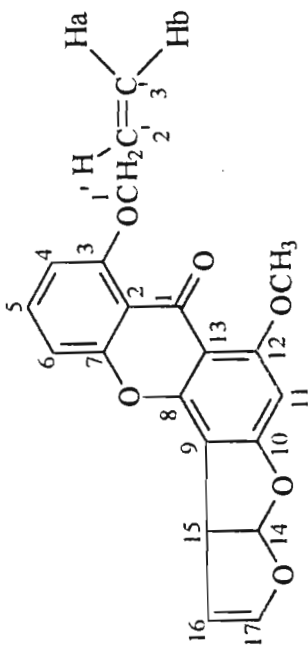
Proton atom	Chemical Shift $\delta$ H (ppm)	Splitting Pattern	Coupling constant J ( H,H ) Hz
H-4	6.93	doublet	8.2
H-5	7.45	triplet	8.5
H-6	6.74	doublet	8.2
H-11	6.38	singlet	-
H-14	6.78	doublet	7.2
H-15	4.78	triplet	7.1
H-16	5.43	triplet	2.6
H-17	6.47	triplet	2.6
OCH <sub>3</sub>	3.92	singlet	-
H-1'	4.70	doublet-doublet	4.9; 5.25
H-2'	6.09	multiplet	
H-3a'	5.60	doublet-doublet	15.57; 1.59
H-3b'	5.30	doublet-doublet	9.21; 1.47

HAGPST.A60PREST IN CDCL3



APPENDIX 22

Figure 45. The <sup>1</sup>H-NMR Spectrum of *O*-Propenyl sterigmatocystin



# APPENDIX 23

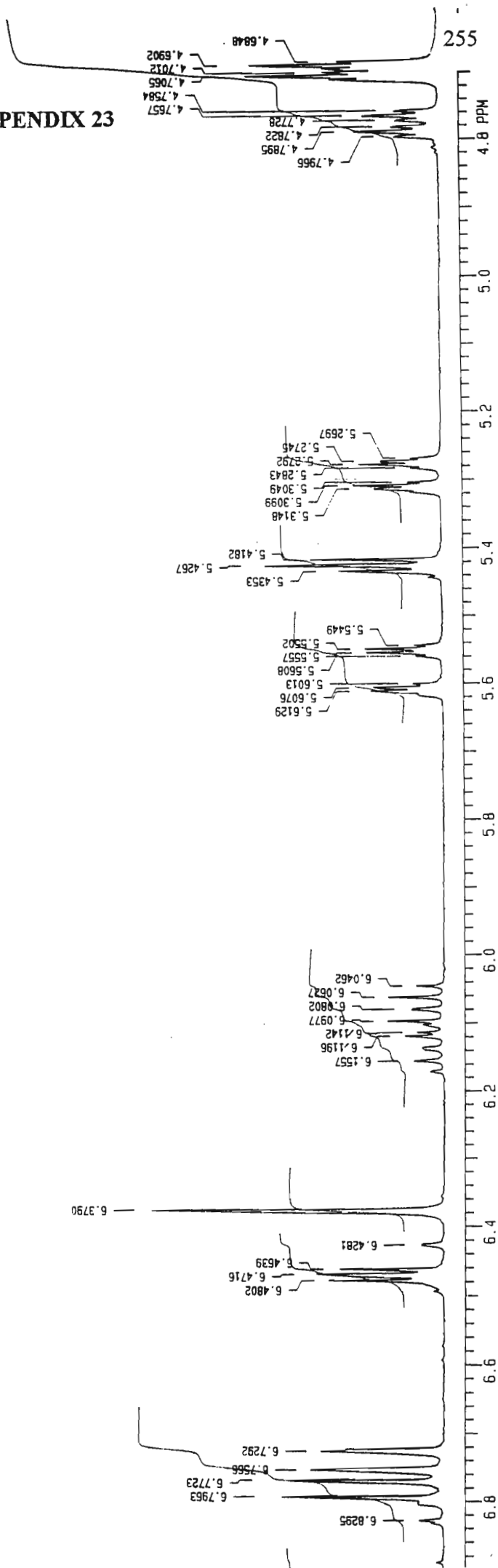
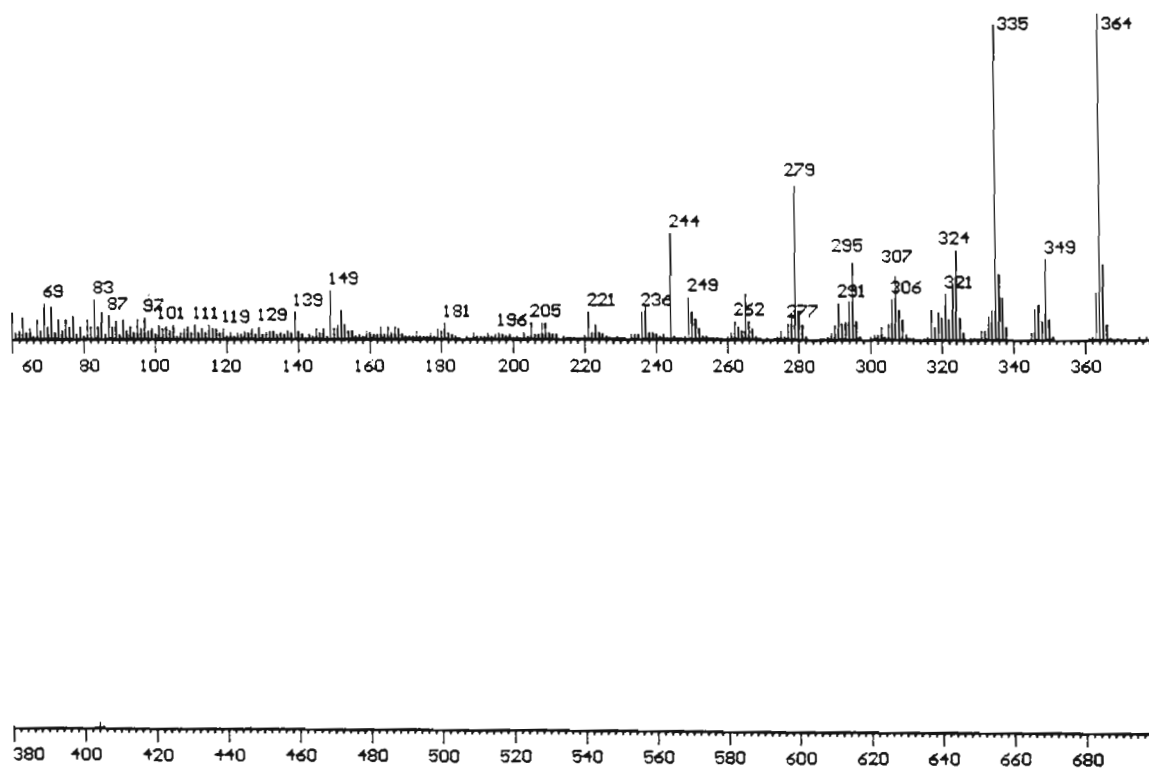
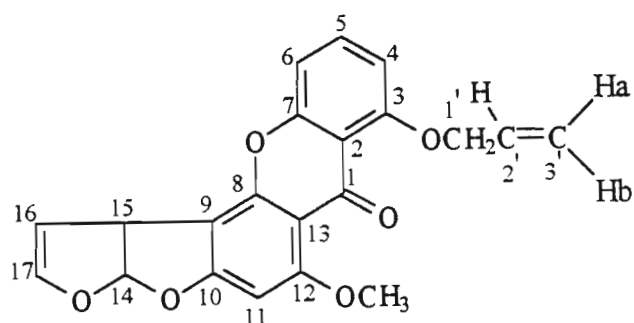


Figure 46. The Expanded <sup>1</sup>H-NMR Spectrum of *O*-Propenyl sterigmatocystin

## APPENDIX 24

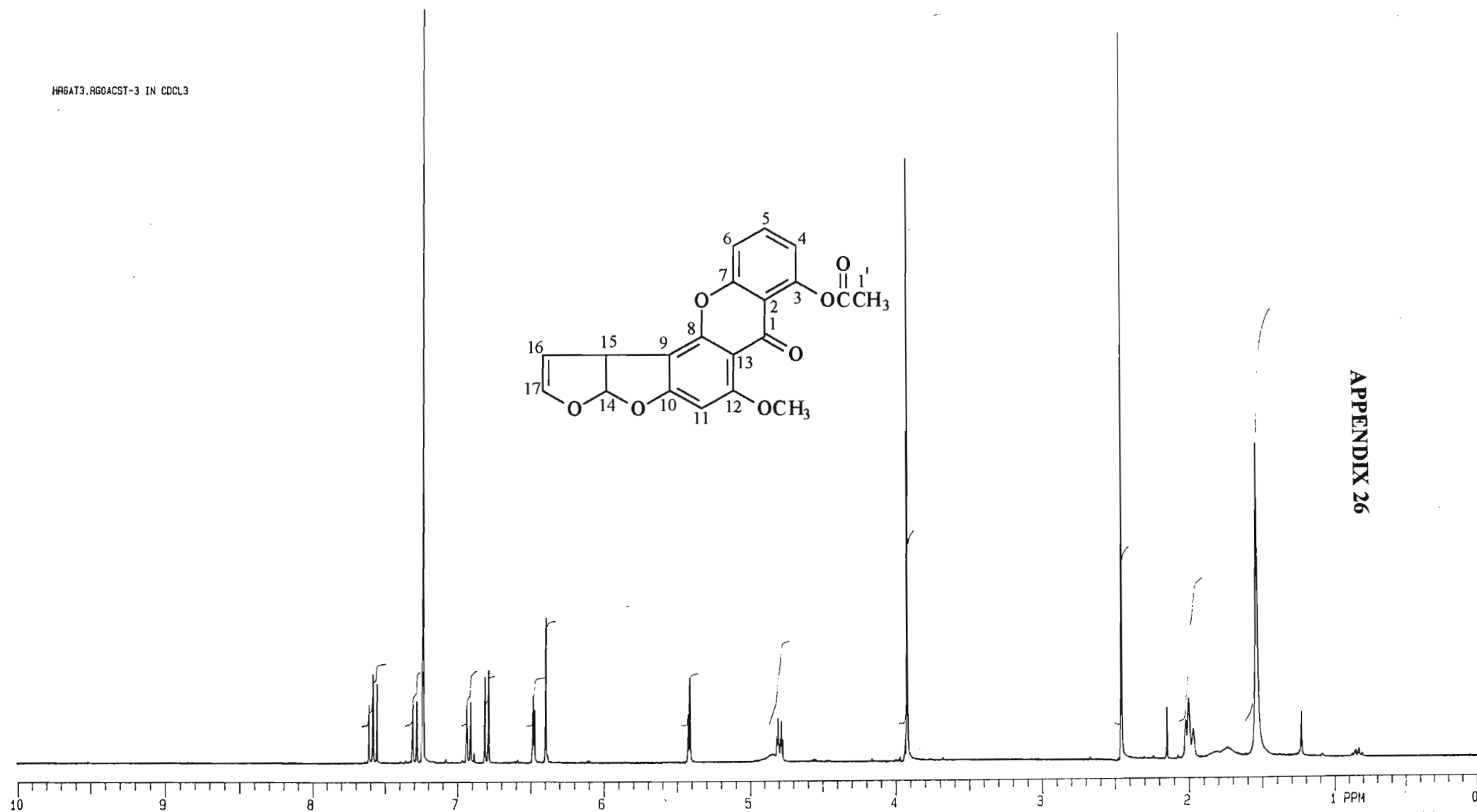
Figure 47. The Normalised Mass Spectrum of *O*-Propenyl sterigmatocystin

## APPENDIX 25

Table 10. The  $^1\text{H}$ -NMR data of *O*-Acetyl sterigmatocystin.

Proton atom	Chemical Shift $\delta$ H (ppm)	Splitting Pattern	Coupling constant J ( H,H ) Hz
H-4	7.30	doublet	1.1
H-5	7.59	triplet	8.3
H-6	6.92	doublet	1.2
H-11	6.40	singlet	-
H-14	6.91	doublet	1.1
H-15	4.79	triplet	7.1
H-16	5.42	triplet	2.7
H-17	6.49	triplet	7.1
OCH <sub>3</sub>	3.93	singlet	-
H-3'	2.46	singlet	-

HR6AT3.R60ACST-3 IN CDCL3

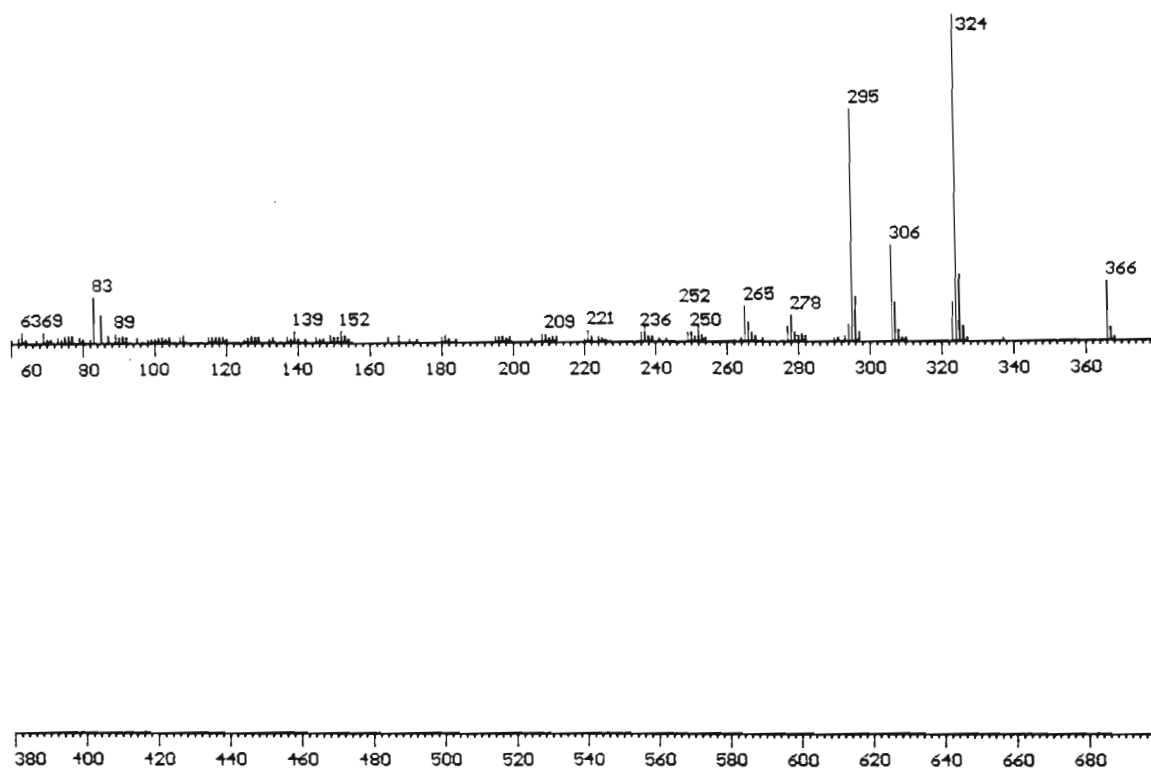
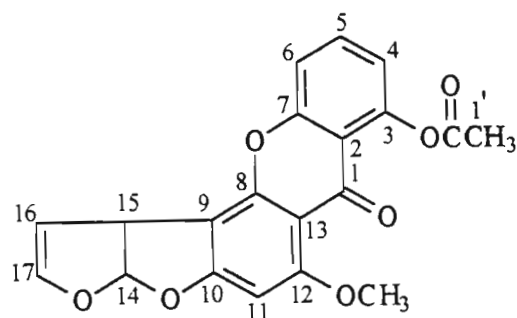


APPENDIX 26

Figure 48. The <sup>1</sup>H-NMR Spectrum of *O*-Acetyl sterigmatocystin



## APPENDIX 27

Figure 49. The Normalised Mass Spectrum of *O*-Acetyl sterigmatocystin

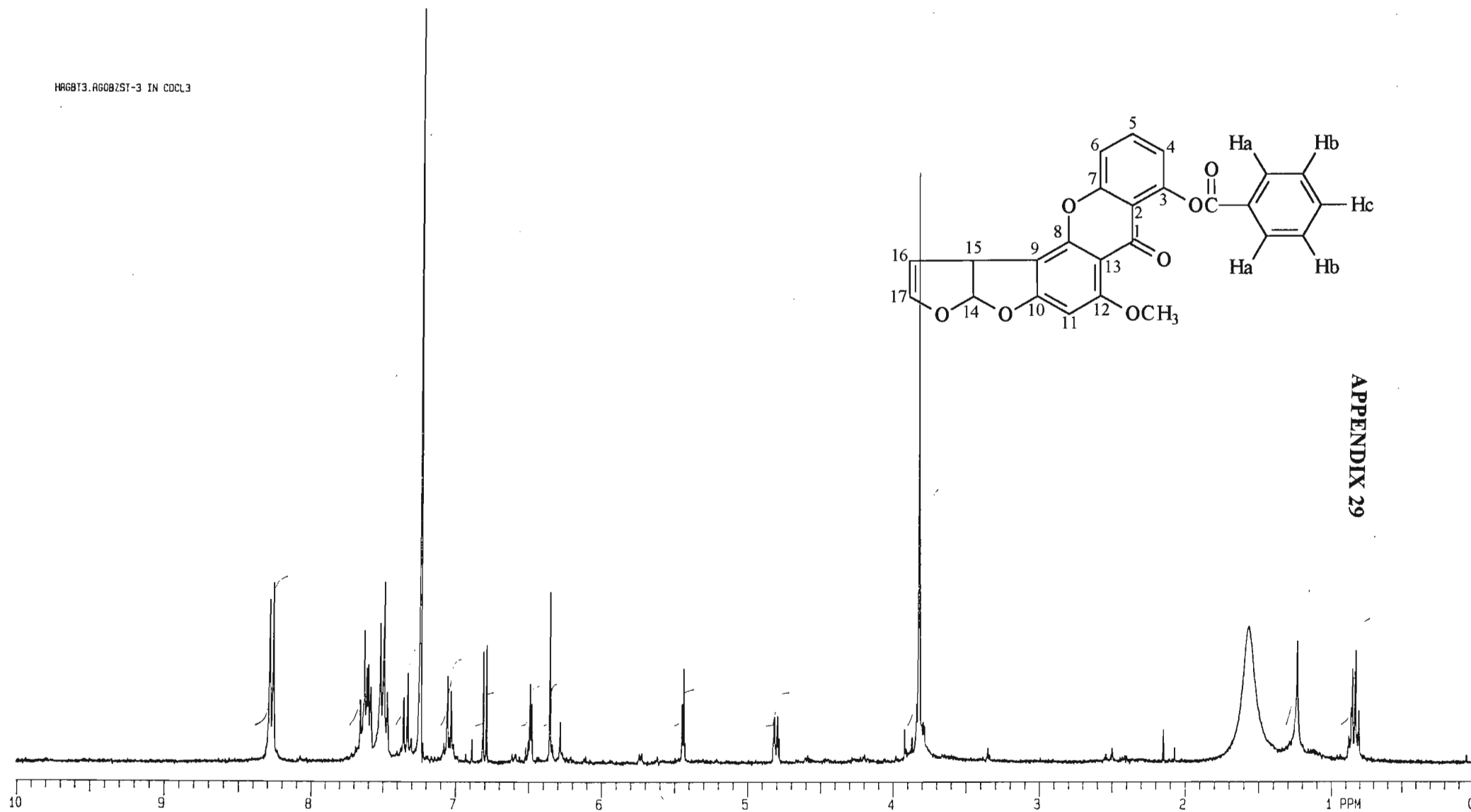
## APPENDIX 28

Table 11. The  $^1\text{H}$ -NMR data of *O*-Benzoyl sterigmatocystin.

Proton atom	Chemical Shift $\delta$ H (ppm)	Splitting Pattern	Coupling constant J ( H,H ) Hz
H-4	7.33	doublet	7.1
H-5	7.50	triplet	7.8
H-6	7.04	doublet	6.6
H-11	6.35	singlet	-
H-14	6.80	doublet	7.1
H-15	4.81	triplet	7.2
H-16	5.44	triplet	2.5
H-17	6.49	triplet	6.49
OCH <sub>3</sub>	3.83	singlet	-
2 x Ha	8.27	doublet	7.2
2 x Hb	*	multiplet	*
1 x Hc	*	multiplet	*

\*The chemical shift and coupling constant of the proton could not be easily determined

H86BT3.A60BZST-3 IN CDCL3



APPENDIX 29

Figure 50. The  $^1\text{H}$ -NMR Spectrum of *O*-Benzoyl sterigmatocystin

APPENDIX 30

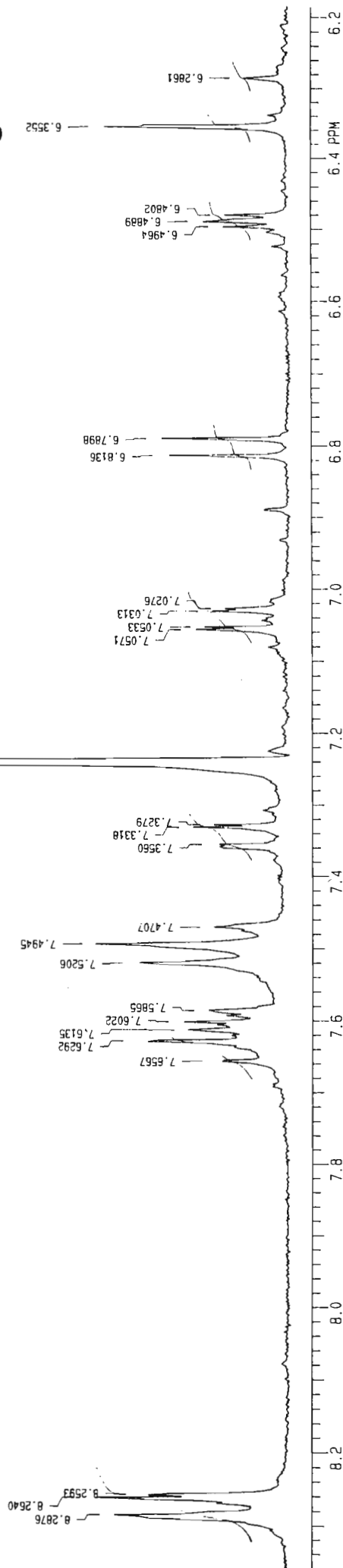
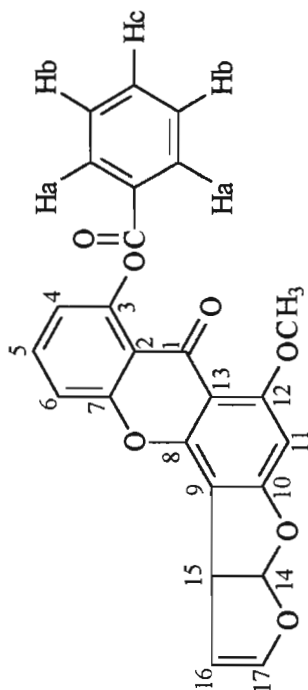
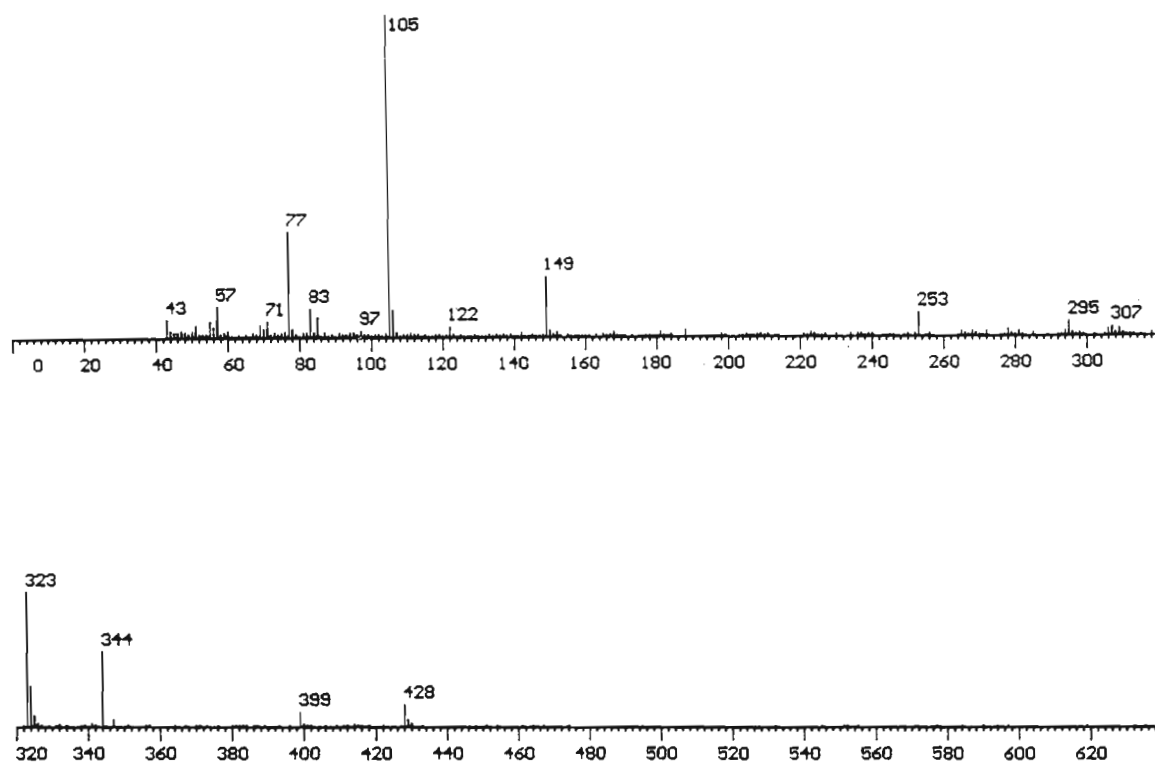
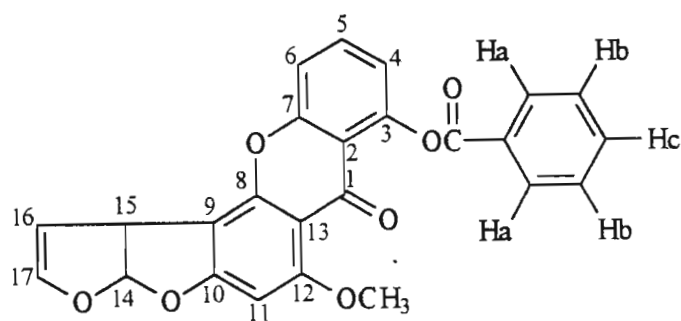


Figure S1. The Expanded <sup>1</sup>H-NMR Spectrum of *O*-Benzoyl sterigmatocystin

## APPENDIX 31

Figure 52. The Normalised Mass Spectrum of *O*-Benzoyl sterigmatocystin

APPENDIX 32

Table 12. The Data for the Calibration Graph of AFB<sub>1</sub> Using the Fluorescence Detector.

Concentration (p.p.b.)	Average Integrated Peak Area of AFB <sub>1</sub>
10	1490
50	15523
100	33399
250	87736
500	173653
1000	358432

APPENDIX 33

R squared = 0.99

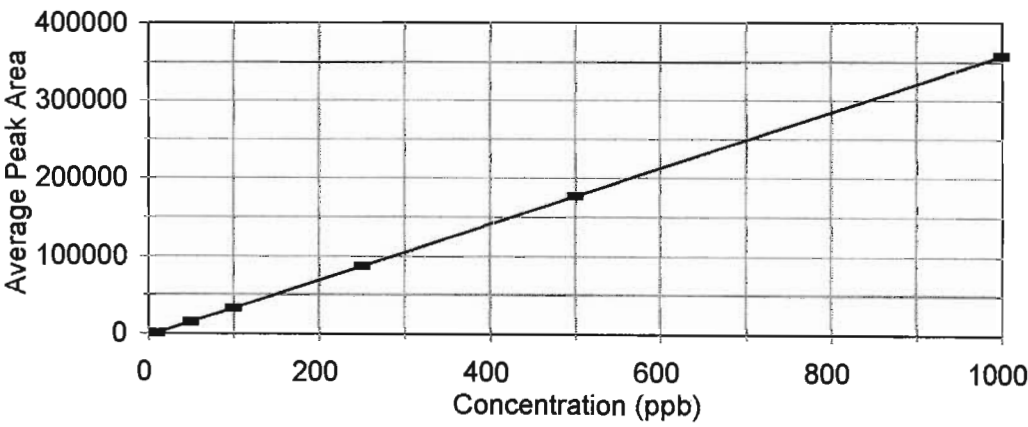


Figure 57. The Calibration Graph of AFB<sub>1</sub> Using the Fluorescence Detector.

APPENDIX 34

Table 13. The Data for the Calibration Graph of AFB<sub>1</sub> using the Diode Array Detector.

Concentration (p.p.b.)	Average Integrated Peak Area of AFB <sub>1</sub>
20	3533
50	10131
100	27509
300	65256
500	127400
1000	225955
5000	1189444

APPENDIX 35

R squared = 0.99

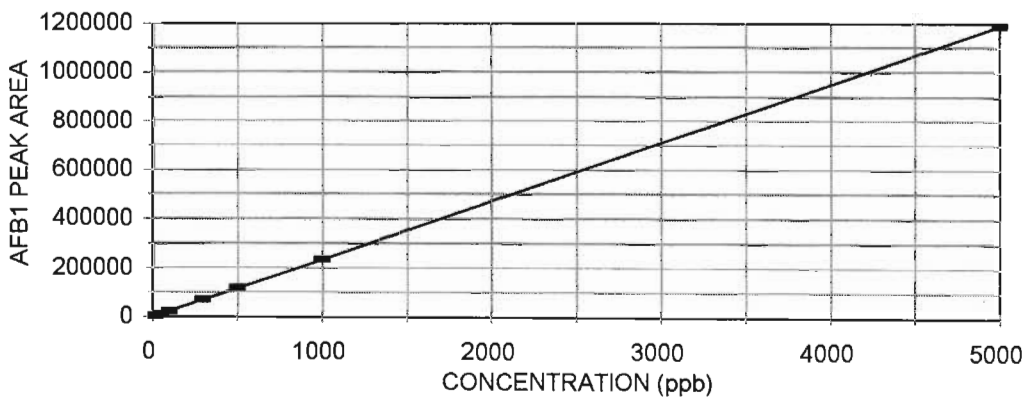


Figure 58. The Calibration Graph of AFB<sub>1</sub> Using the Diode Array Detector.

### APPENDIX 36

Table 14. The HPLC Data for Repeatability of Peak Areas and Retention Times with the Fluorescence Detector.

Injection number	Peak Area	Retention Time
1	110390	8.183
2	109359	7.933
3	110343	7.400
4	109383	8.183
5	110392	8.233
6	110261	8.167
7	110067	8.133
8	107734	8.183
Mean	109741.1	8.050
Standard Deviation	916.99	0.28
% Coefficient of Variation	0.83	3.48

Eight 20  $\mu$ l injections were made of a 300 ppb derivatized AFB<sub>1</sub> standard solution. Fluorescence detection, excitation at 325 nm and emission at 420 nm, was used.



### APPENDIX 37

Table 15. The HPLC Data for Repeatability of Peak Areas and Retention Times with the Diode array Detector.

Injection number	Peak Area	Retention Time
1	123695	6.392
2	125290	6.405
3	114113	6.413
4	127447	6.279
5	128896	6.363
6	123500	6.389
7	127242	6.286
8	126955	6.357
Mean	120622	6.348
Standard Deviation	8479	0.062
% Coefficient of Variation	3.73	0.97

Eight 20  $\mu$ l injections were made of a 500 ppb AFB<sub>1</sub> standard solution. The diode array detector was used.

## APPENDIX 38

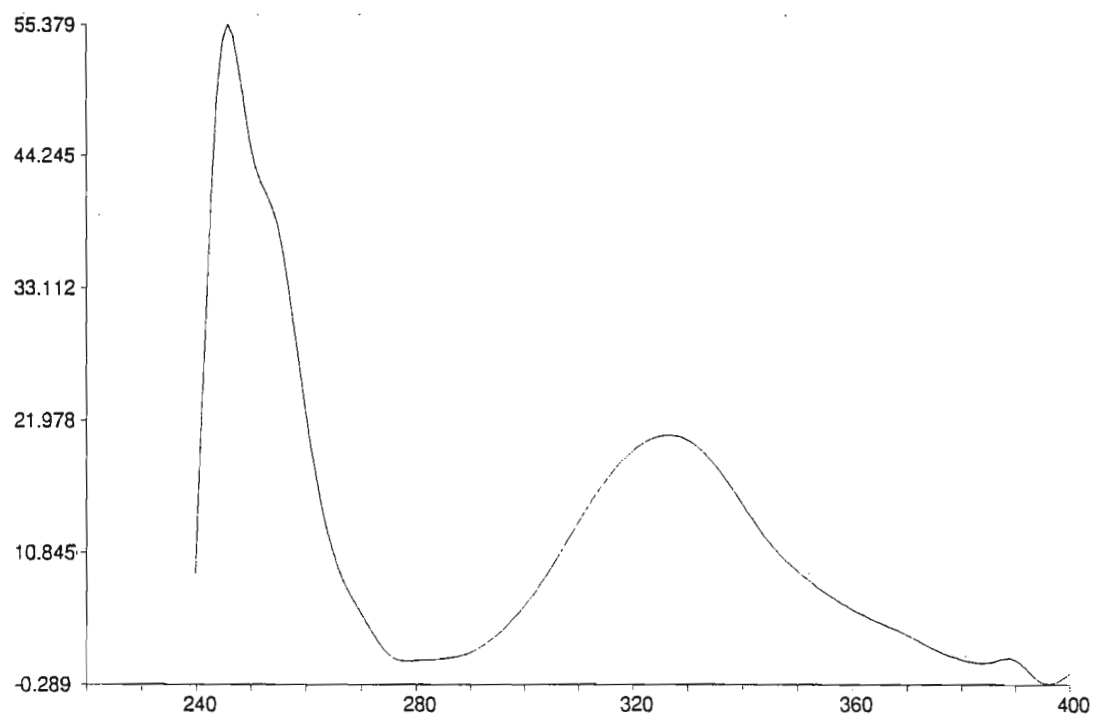
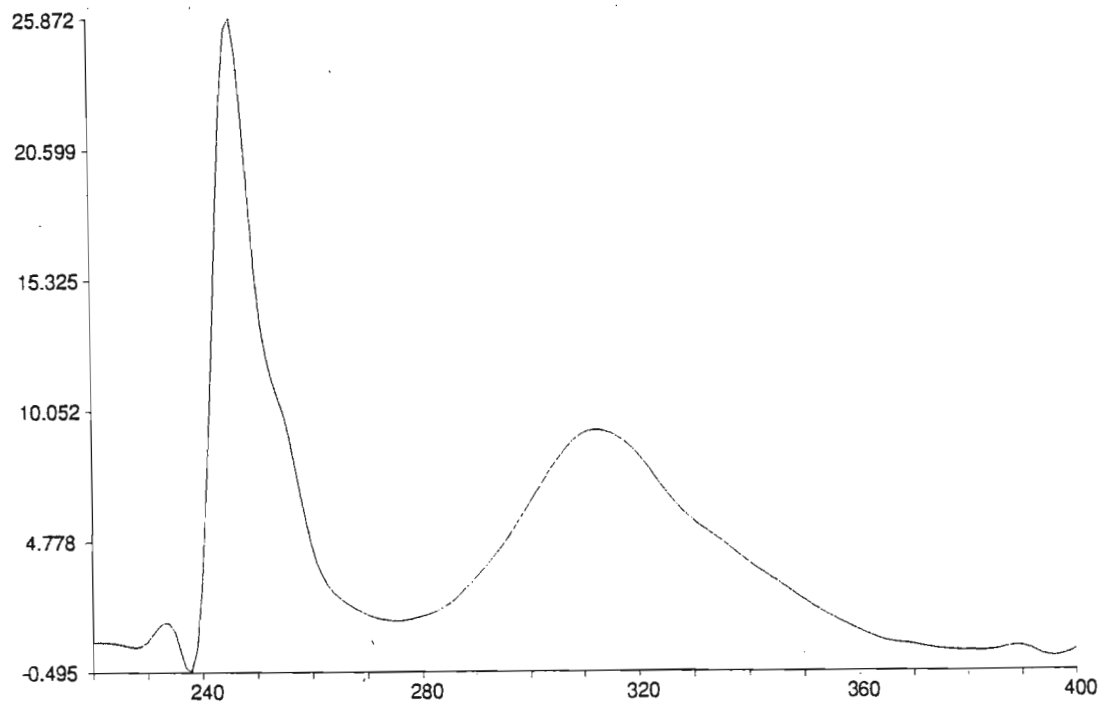


Figure 78. The UV Spectrum of Standard Sterigmatocystin

## APPENDIX 39

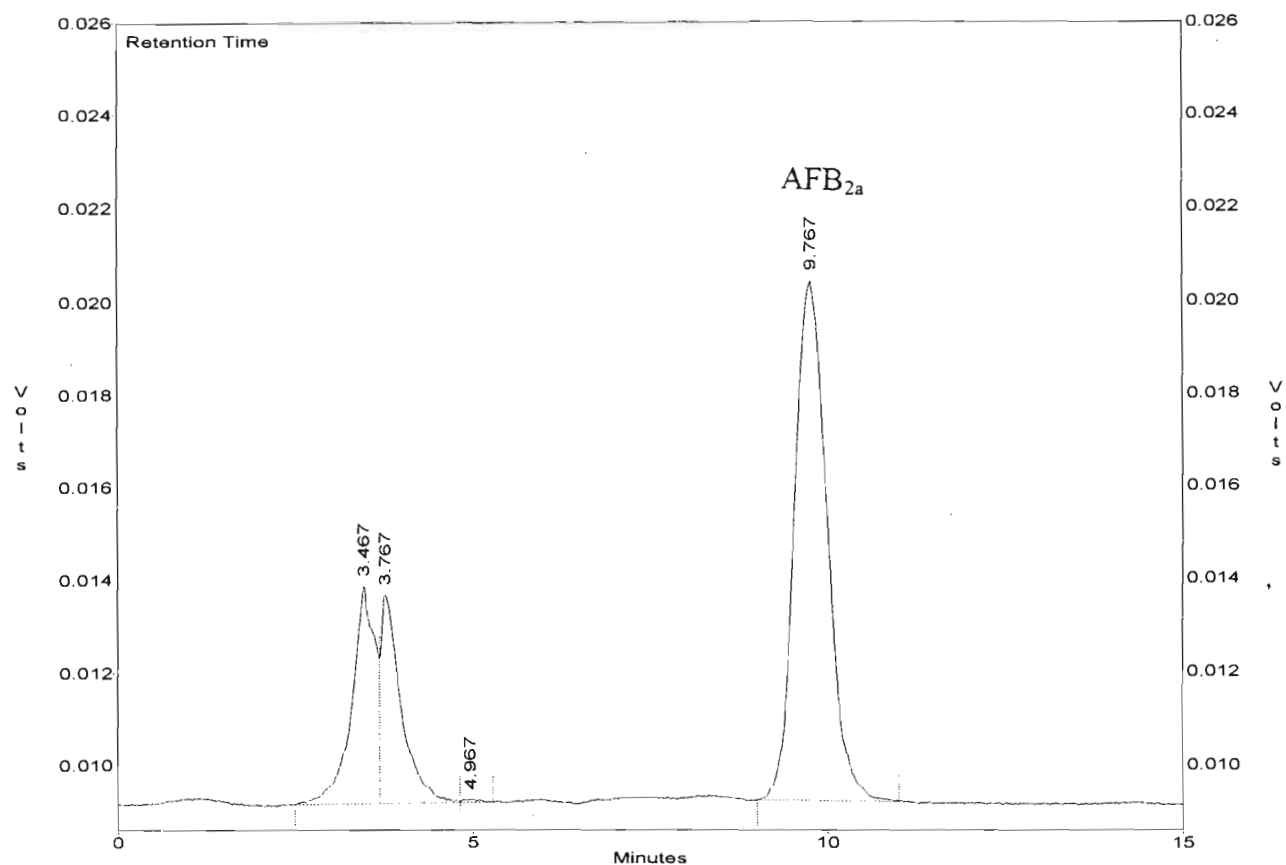
Figure 79. The UV Spectrum of Standard *O*-Methyl sterigmatocystin

**APPENDIX 40****Preparation of the Resting Medium**

The chemicals listed below were weighed by means of a Mettler TG 50 Thermobalance and dissolved in 1 L deionised water.

Potassium dihydrogen orthophosphate	5.0 g
Magnesium sulphate septahydrate	0.5 g
Potassium chloride	0.5 g
Disodium tetraborate decahydrate	0.7 mg
Ammonium molybdate	0.5 mg
Copper sulphate quinhhydrate	0.3 mg
Ferrous sulphate septahydrate	10.0 mg
Manganous sulphate quadrahydrate	0.11 mg
Zins sulphate septahydrate	17.6 mg

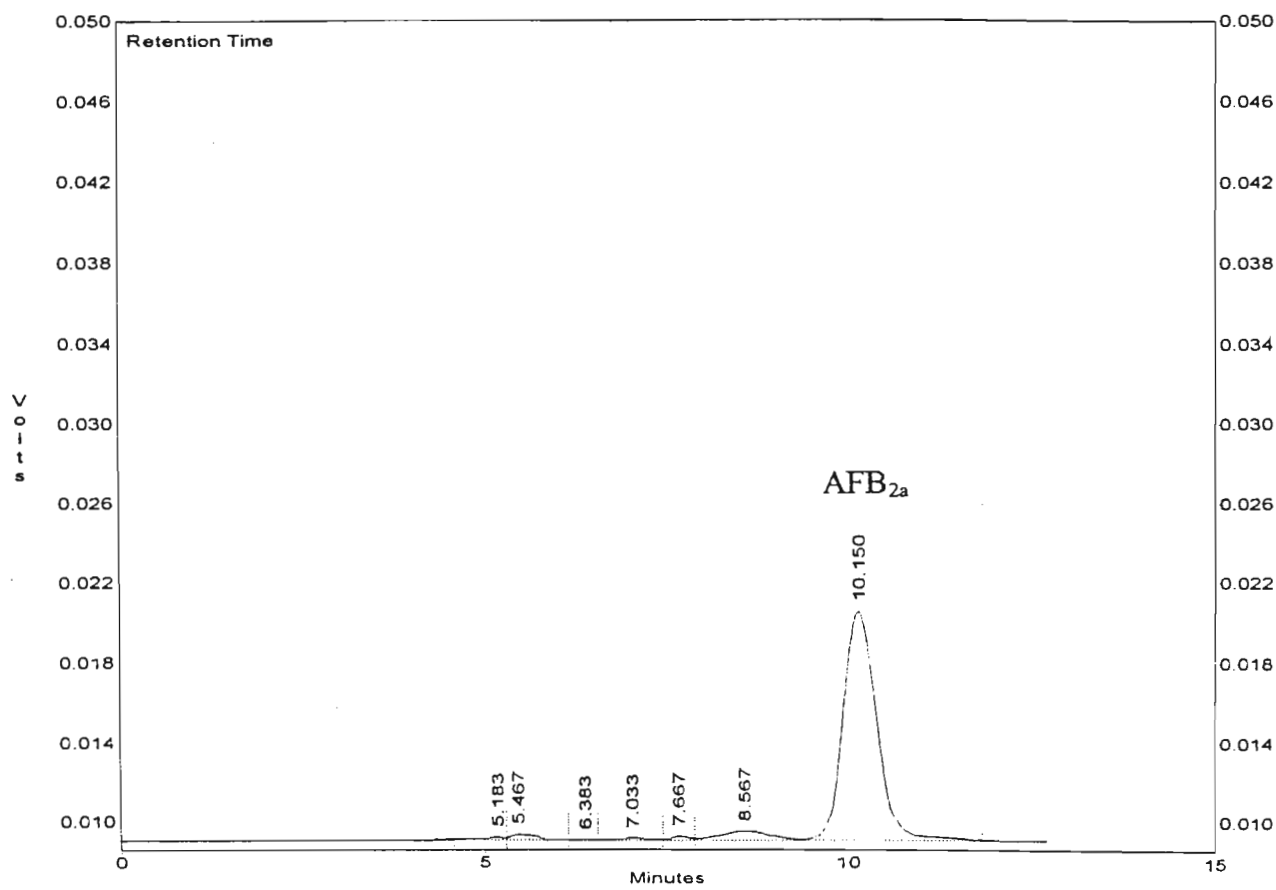
## APPENDIX 41



Pkno	Min. Time	Area	Area%	Height	Height%	Flags
1	3.467	107154	19.364	4697	22.929	BV
2	3.767	90039	16.271	4504	21.987	VV
3	4.967	1156	0.209	79	0.386	VV
4	9.767	355024	64.156	11205	54.699	BV
Totals		553373	100.000	20485	100.000	

Figure 83. The Liquid Chromatogram for the Conversion of OMST to AFB<sub>1</sub> in Whole Cells of *A. parasiticus* (Wh1)

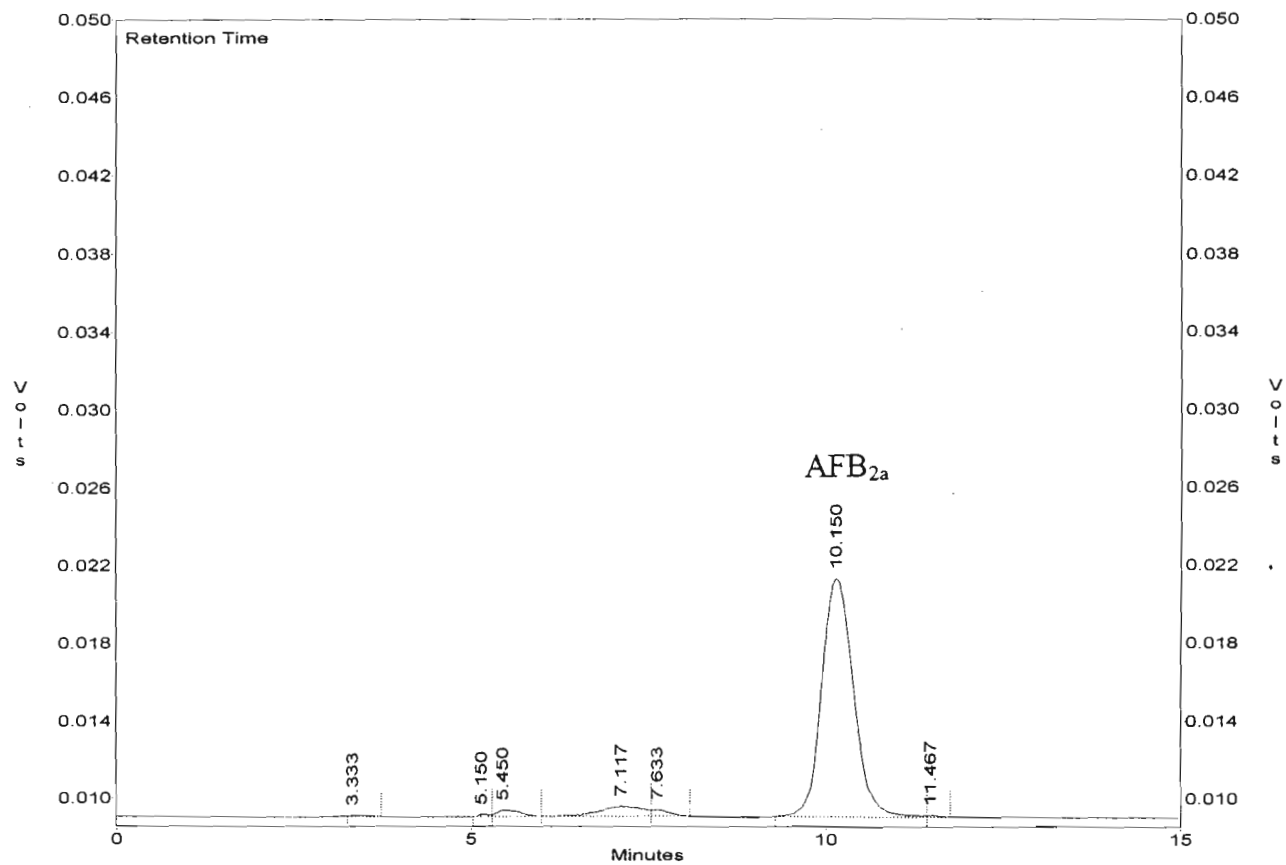
APPENDIX 42



Pkno	Miq. Time	Area	Area%	Height	Height%	Flags
1	5.183	2796	0.713	142	1.114	BV
2	5.467	6616	1.686	281	2.204	VV
3	6.383	694	0.177	55	0.431	VV
4	7.033	3143	0.801	136	1.067	VV
5	7.667	3264	0.832	215	1.687	VV
6	8.567	22534	5.744	470	3.687	VV
7	10.150	353288	90.048	11449	89.810	VV
Totals		392335	100.000	12748	100.000	

Figure 84. The Liquid Chromatogram for the Conversion of OPROST to AFB<sub>1</sub> in Whole Cells of *A. parasiticus* (Wh1)

APPENDIX 43



Pkno	Miq. Time	Area	Area%	Height	Height%	Flags
1	3.333	822	0.197	33	0.241	BV
2	5.150	1342	0.322	135	0.985	BV
3	5.450	7819	1.875	347	2.532	VV
4	7.117	22646	5.430	516	3.765	VV
5	7.633	5683	1.363	340	2.481	VB
6	10.150	377748	90.568	12234	89.273	BV
7	11.467	1028	0.246	99	0.722	VV
Totals		417088	100.000	13704	100.000	

Figure 85. The Liquid Chromatogram for the Conversion of OEST to AFB<sub>1</sub> in Whole Cells of *A. parasiticus* (Wh1)

**APPENDIX 44****Preparation of the Phosphate Buffer Solution**

A 1 litre solution of a 20 mM phosphate buffer was prepared by dissolving the compounds listed below in minimum deionised water. The solution was diluted to approximately 980 ml with deionised water. The pH of the solution was adjusted using either 0.100 M hydrochloric acid or 0.100 M sodium hydroxide solution. The solution was then made up to the 1 litre mark with deionised water.

Chemical	Quantity Added
disodium hydrogen phosphate	1.8767 g
sodium dihydrogen phosphate	1.0582 g
ethylene diamine tetraacetic acid (disodium salt)	0.3722 g
magnesium chloride hexahydrate	0.4066 g
glycerol	100 ml
monothioglycerol	0.216 g

APPENDIX 45

Table 20. The Data for the Calibration Graph of Protein using the Bradford Assay Method

Protein Concentration (ug/ml)	Average Absorbance at A <sub>595</sub>
20	1.023
40	1.077
60	1.087
80	1.094
100	1.114

APPENDIX 46

R squared = 0.85

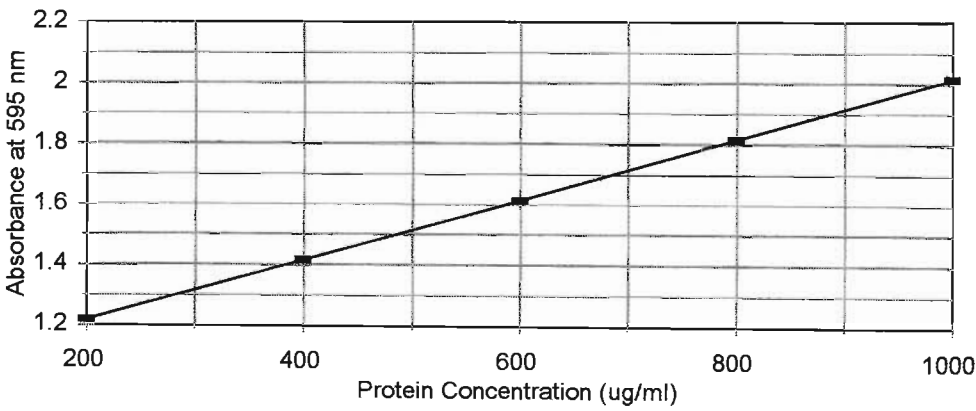


Figure 86. The Calibration Graph of the Protein Ovalbumin.



APPENDIX 47

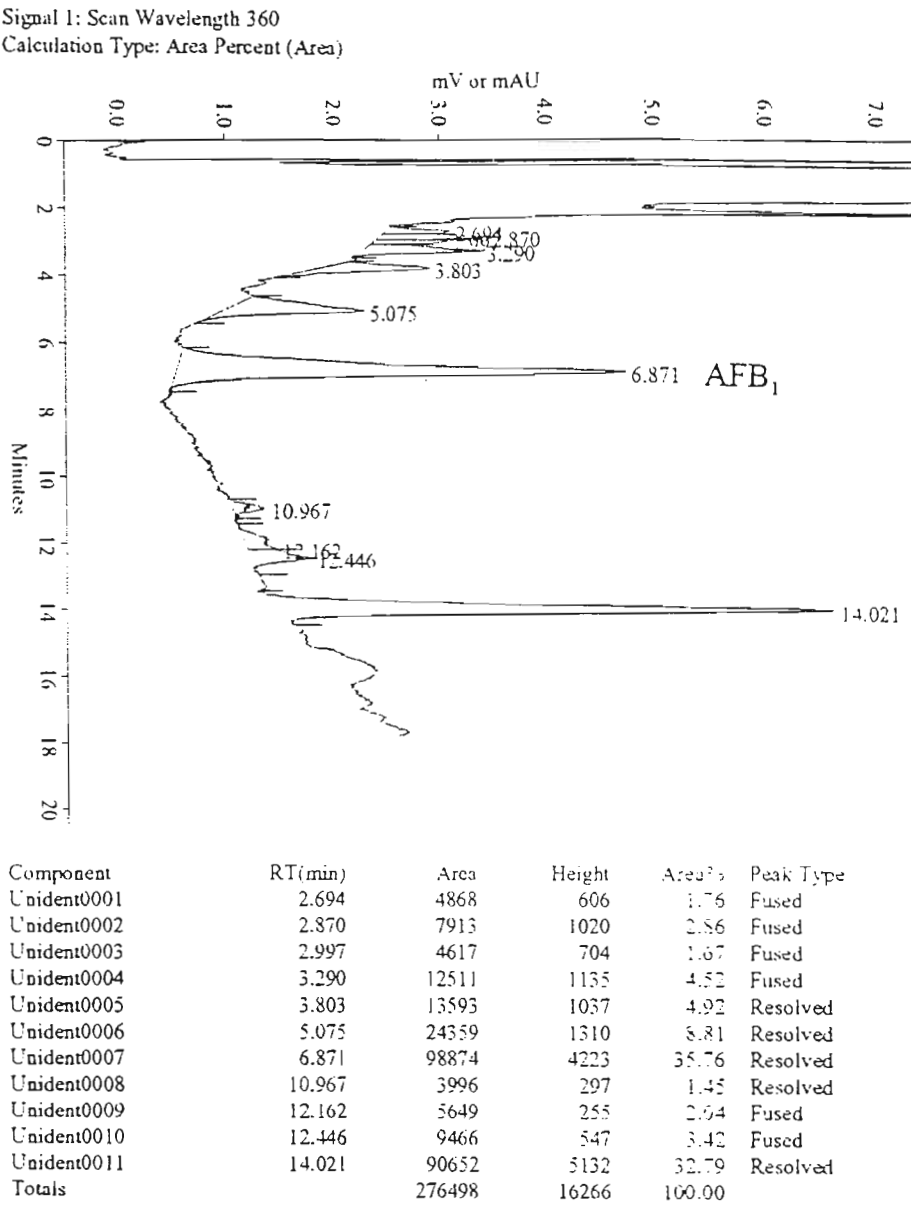


Figure 88. A Typical Liquid Chromatogram for the Conversion of ST to AFB<sub>1</sub> in a Cell-Free Extract at pH 7.5 and 27 °C for an Incubation Time of 1 Hour

## APPENDIX 48

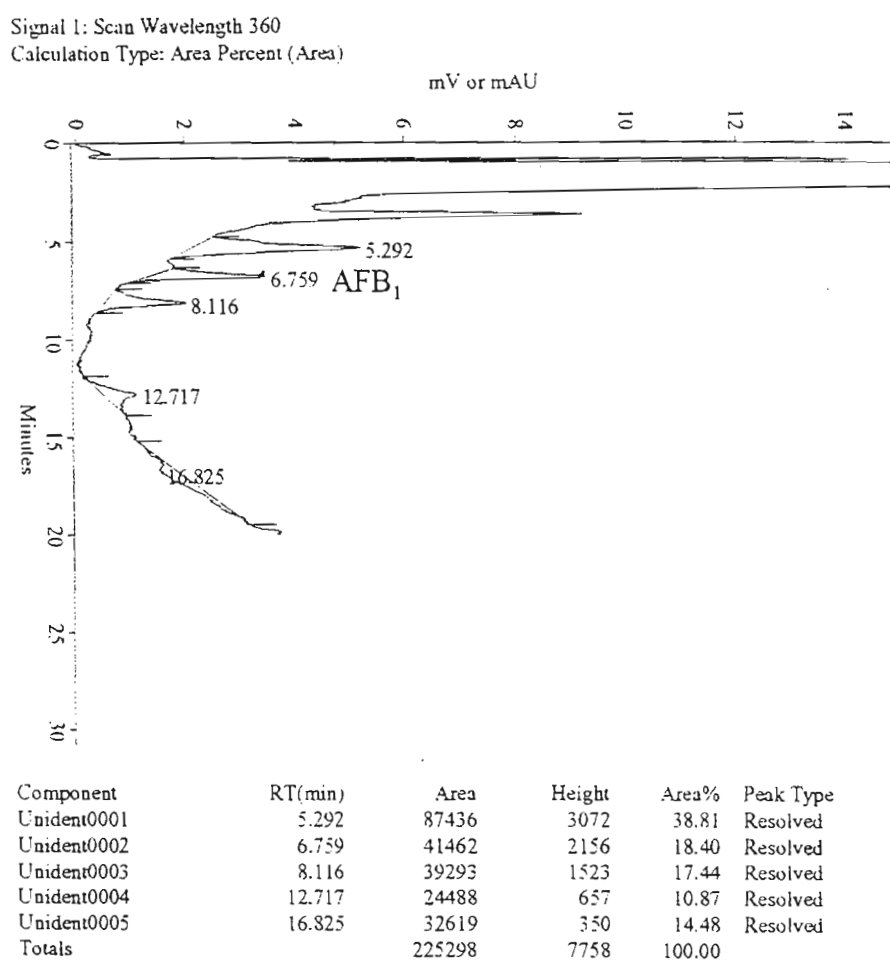


Figure 90. A Typical Liquid Chromatogram for the Conversion of ST to AFB<sub>1</sub> in a Cell-Free Extract at pH 7.1 and 27 °C for an Incubation Time of 1 Hour

APPENDIX 49

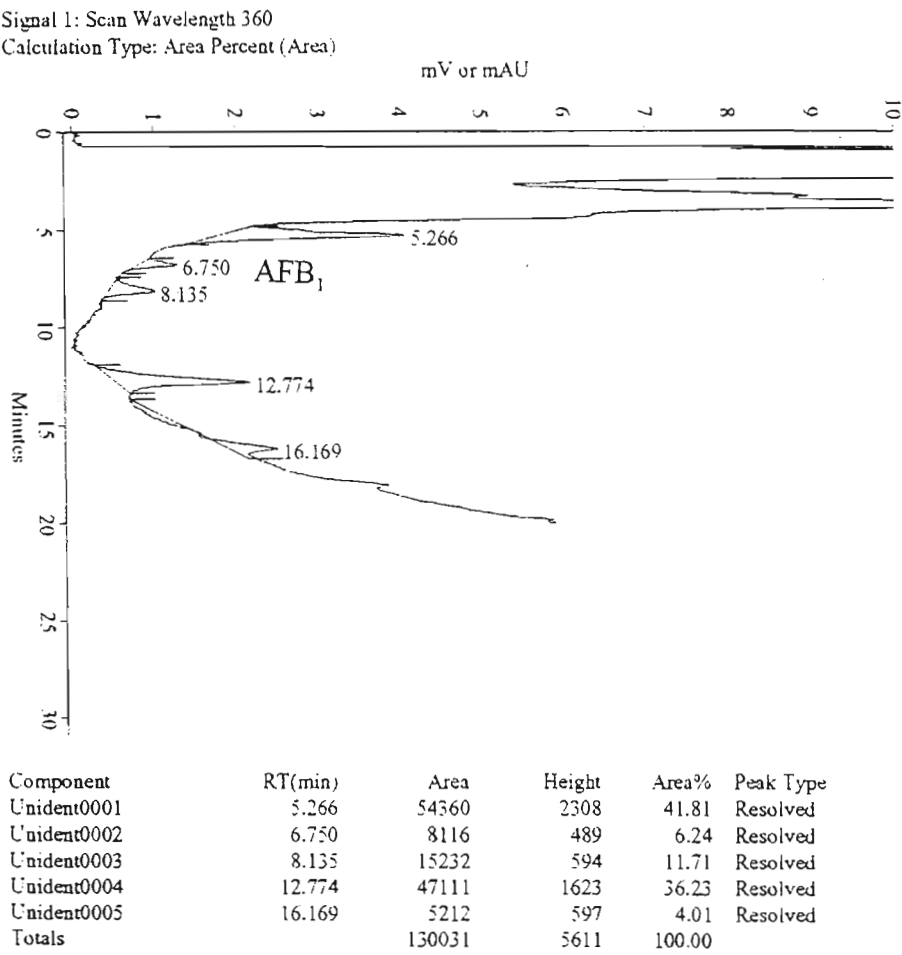


Figure 91. A Typical Liquid Chromatogram for the Conversion of ST to AFB<sub>1</sub> in a Cell-Free Extract at pH 7.4 and 27 °C for an Incubation Time of 1 Hour

APPENDIX 50

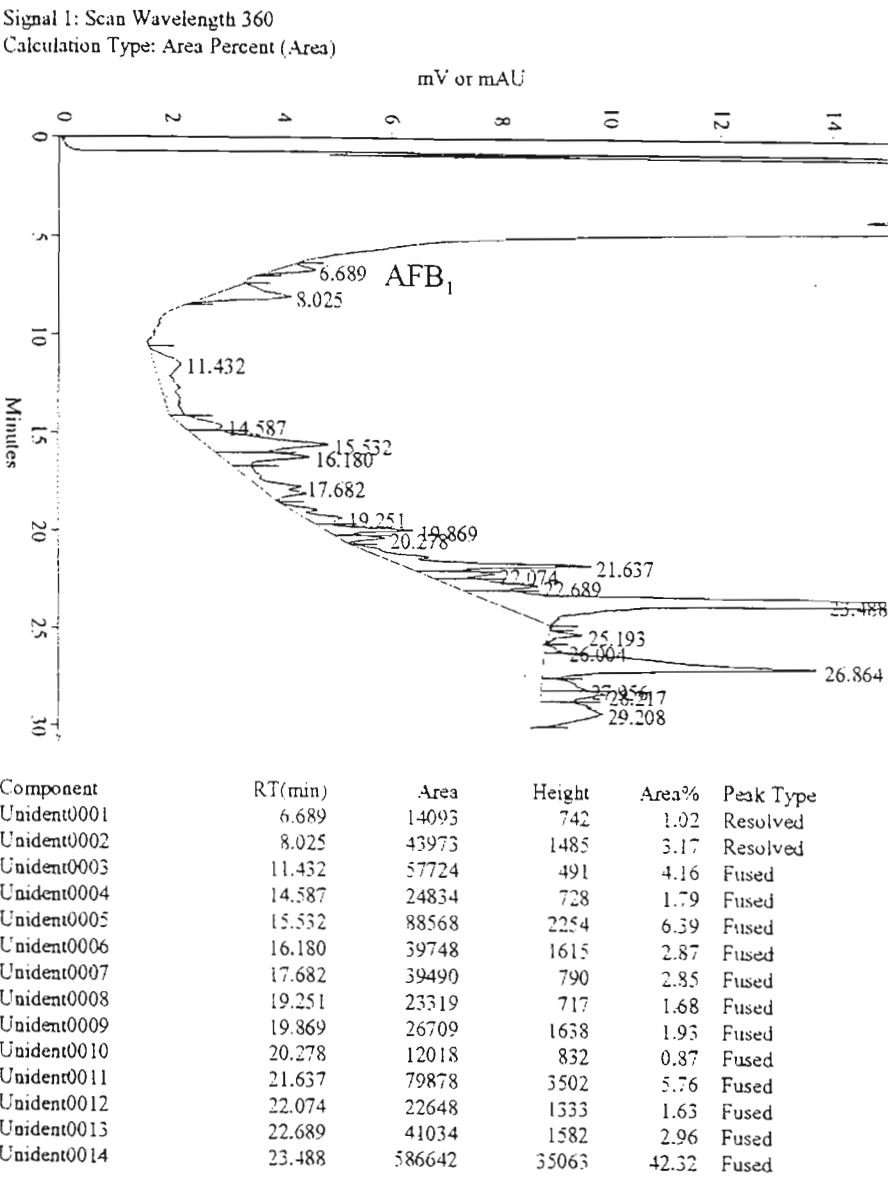


Figure 93. A Typical Liquid Chromatogram for the Conversion of ST to AFB<sub>1</sub> in a Cell-Free Extract at pH 7.2 and 24 °C for an Incubation Time of 1 Hour

APPENDIX 51

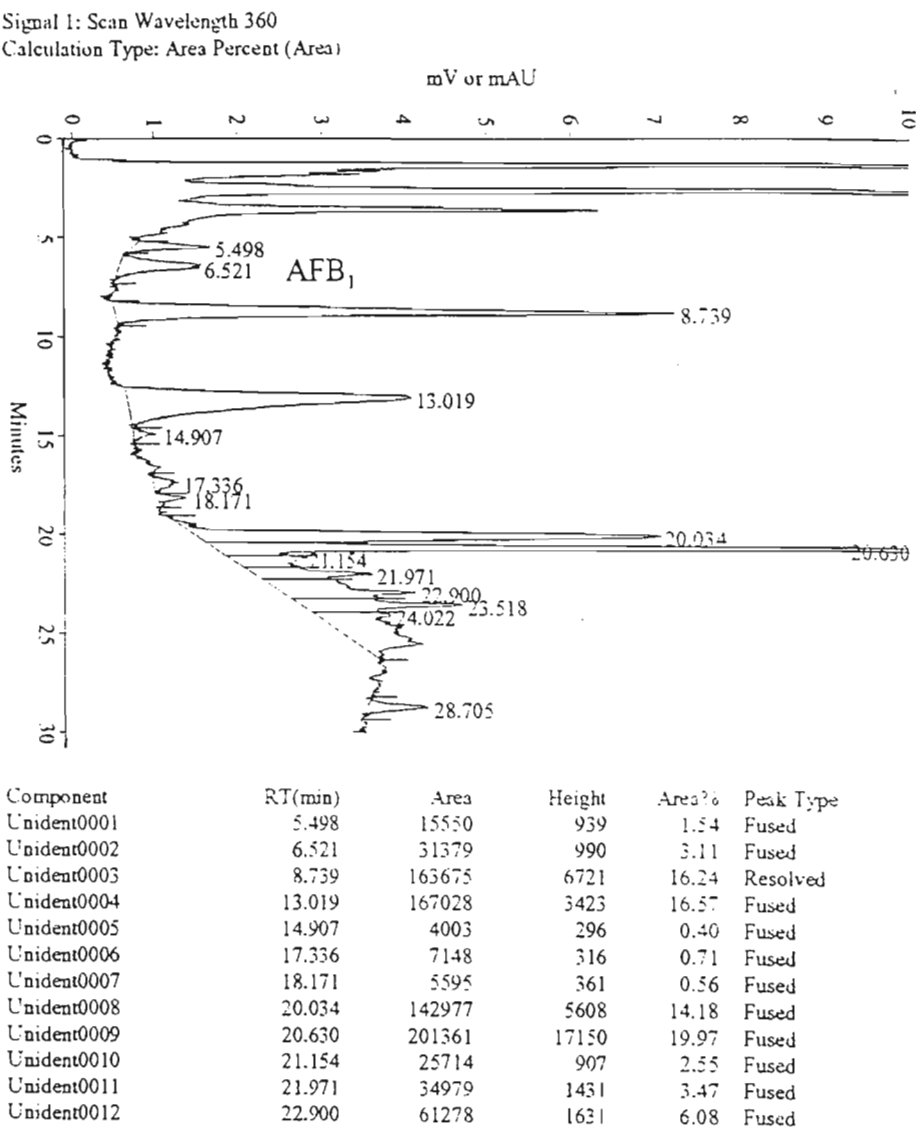


Figure 95. A Typical Liquid Chromatogram for the Conversion of ST to AFB<sub>1</sub> in a Cell-Free Extract, in the Presence of NADPH (1.5 mM), at pH 7.2 and 28 °C for an Incubation Time of 1 Hour

APPENDIX 52

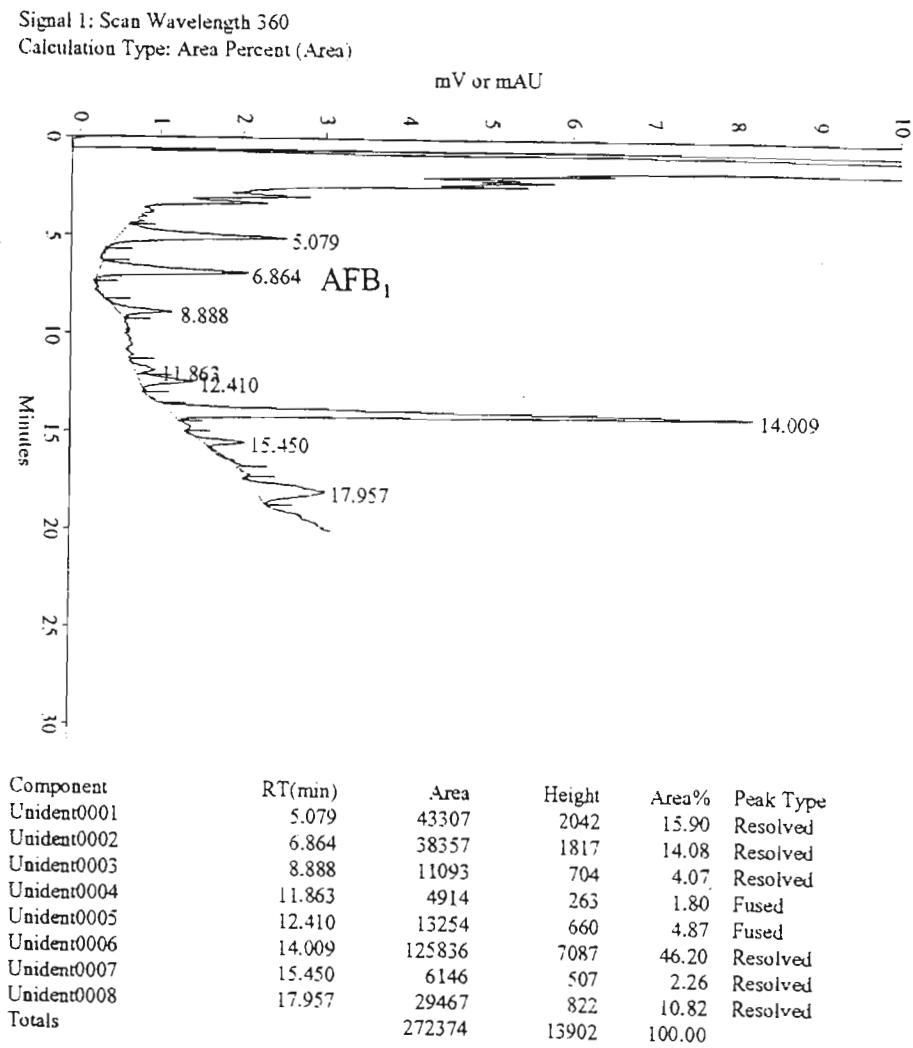


Figure 97. A Typical Liquid Chromatogram for the Conversion of ST to AFB<sub>1</sub> in a Cell-Free Extract at pH 7.2 and 28 °C for an Incubation Time of 45 Minutes

APPENDIX 53

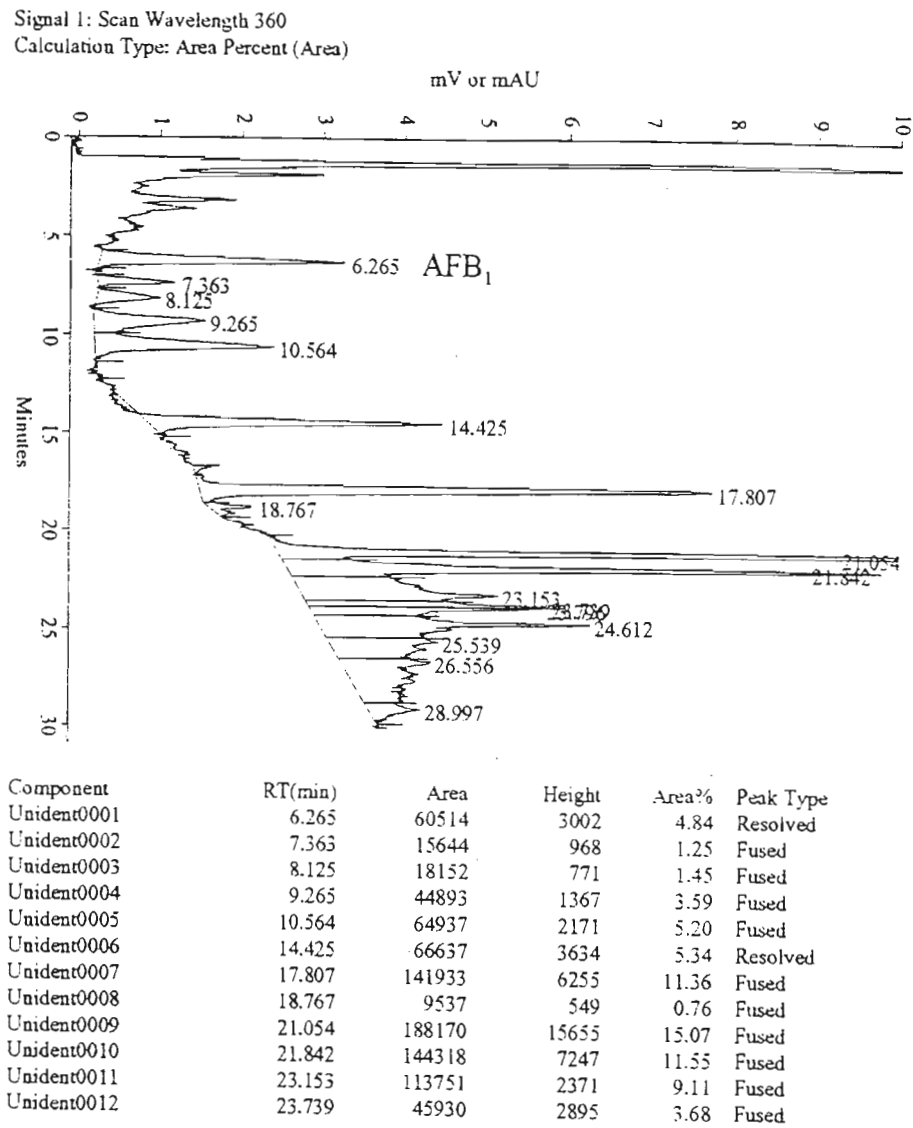


Figure 98. A Typical Liquid Chromatogram for the Conversion of OMST to AFB<sub>1</sub> in a Cell-Free Extract at pH 7.2 and 28 °C for an Incubation Time of 60 Minutes

## APPENDIX 54

### The Preparation of Solutions for PAGE

**Monomer Solution:** To 75 ml of deionised water was added 29.20 g of acrylamide and 0.80 g of Bis (N,N'- methylene- bisacrylamide), with stirring. The solution was made up to 100 ml with deionised water.

**Running Gel Buffer:** Tris base (18.10 g) was dissolved in 90 ml of deionised water. The pH of the solution was adjusted to 8.9 with a 6M HCl solution and thereafter diluted to 100 ml with deionised water.

**Stacking Gel Buffer:** Tris base (3.0 g) were dissolved in 40 ml of deionised water. The pH of the solution was adjusted to 6.8 and made up to 50.00 ml with deionised water.

**Tank Buffer:** Tris base (3.0 g) and glycine (14.4 g) were dissolved and made up to 1 L . The pH of the buffer was 8.9.

**Treatment Buffer:** Stacking gel buffer (2.5 ml) was added to 2 ml of glycerol and diluted to 10 ml with deionised water.

**Initiator:** Ammonium persulphate (0.5 g) was dissolved in 5.0 ml water just before use.

**Staining Solution:** Coomassie blue (1.0 g) was dissolved in 100 ml of deionised water. The solution was filtered and a 31.30 ml aliquot was transferred to a solution containing 175 ml methanol and 25 ml acetic acid. The solution was diluted to 250 ml with deionised water.

**Destaining Solution I:** Methanol (50 ml) and 1 ml of acetic acid were made up to 100 ml with deionised water.



**Destaining Solution II:** Acetic acid (70 ml) and 5 ml of methanol were made up to 100 ml with deionised water.

#### **Preparation of the Separating Gel**

To 10.0 ml of the monomer solution was added 7.5 ml of the running gel buffer and 12.5 ml of deionised water. The solution was gently swirled. The initiator (150  $\mu$ l) and 10  $\mu$ l of N,N,N',N'-tetramethyl-1,2-diaminoethane (TEMED) solution were then added..

#### **Preparation of the Stacking Gel**

To 2.6 ml of the monomer solution was added, with stirring, 5 ml of stacking gel buffer, 12.4 ml of deionised water, 100  $\mu$ l of the initiator and 10  $\mu$ l of TEMED.

APPENDIX 55

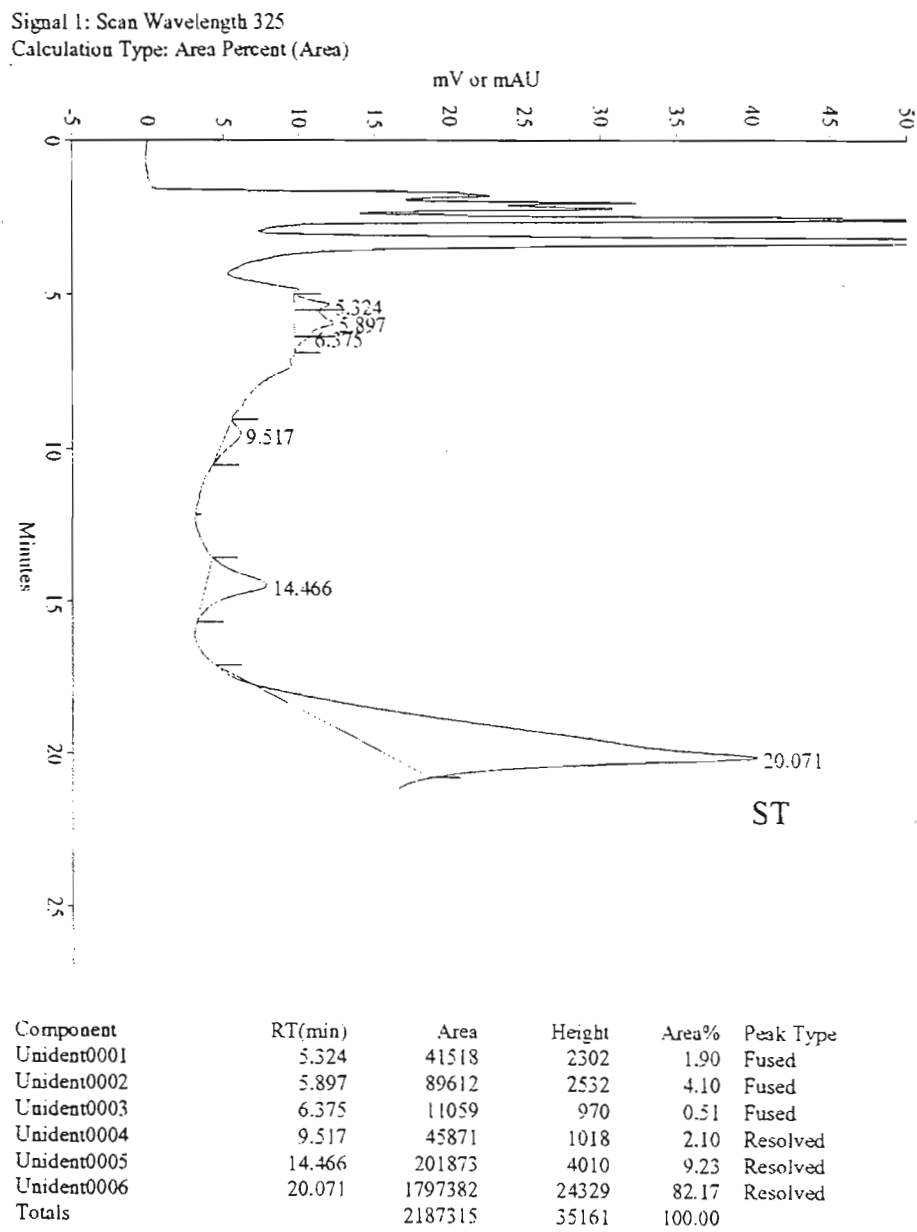


Figure 100. A Typical Liquid Chromatogram of ST in Enzyme Fraction 9-17, in the Presence of NADPH (1.5 mM) and SAM (1.5 mM), at pH 7.2 and 28 °C for an Incubation Time of 5 Hours

APPENDIX 56

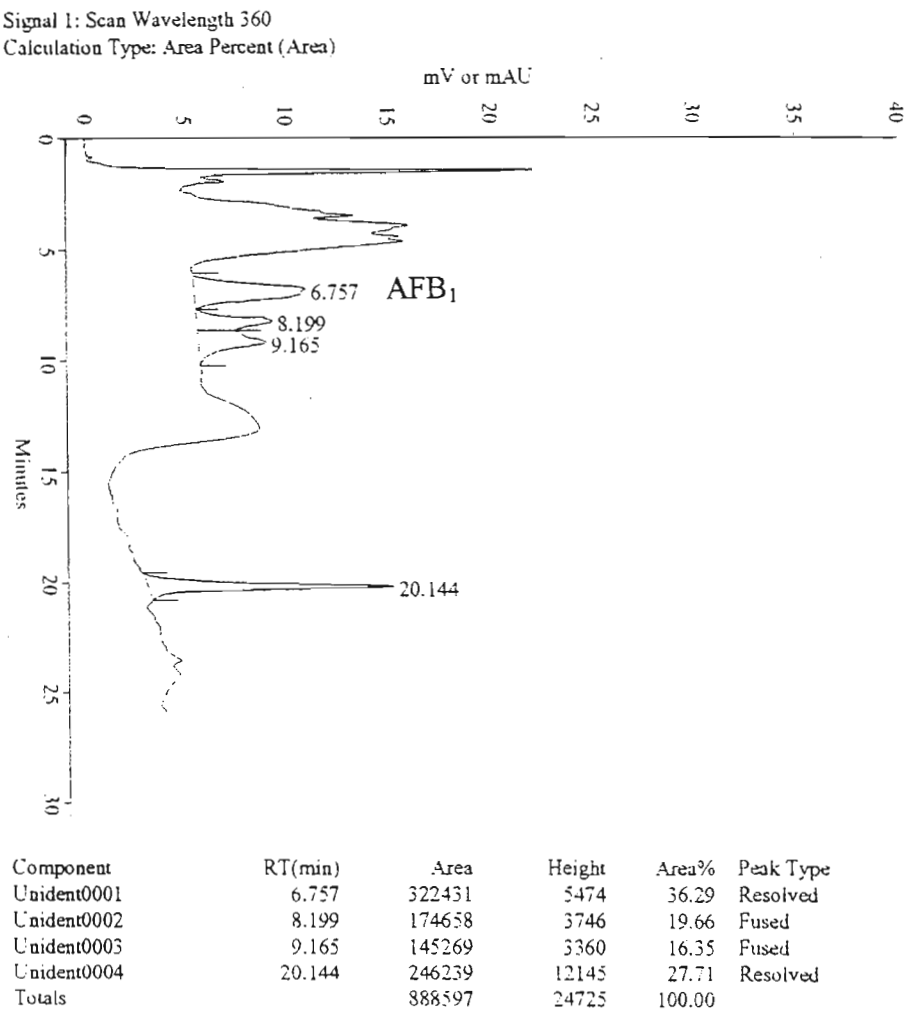


Figure 102. A Typical Liquid Chromatogram for the Conversion of ST to AFB<sub>1</sub> in Enzyme Fraction 9-30, after Dialysis, in the Presence of NADPH (1.5 mM) and SAM (1.5 mM), at pH 7.2 and 28 °C for an Incubation Time of 3 Hours

APPENDIX 57

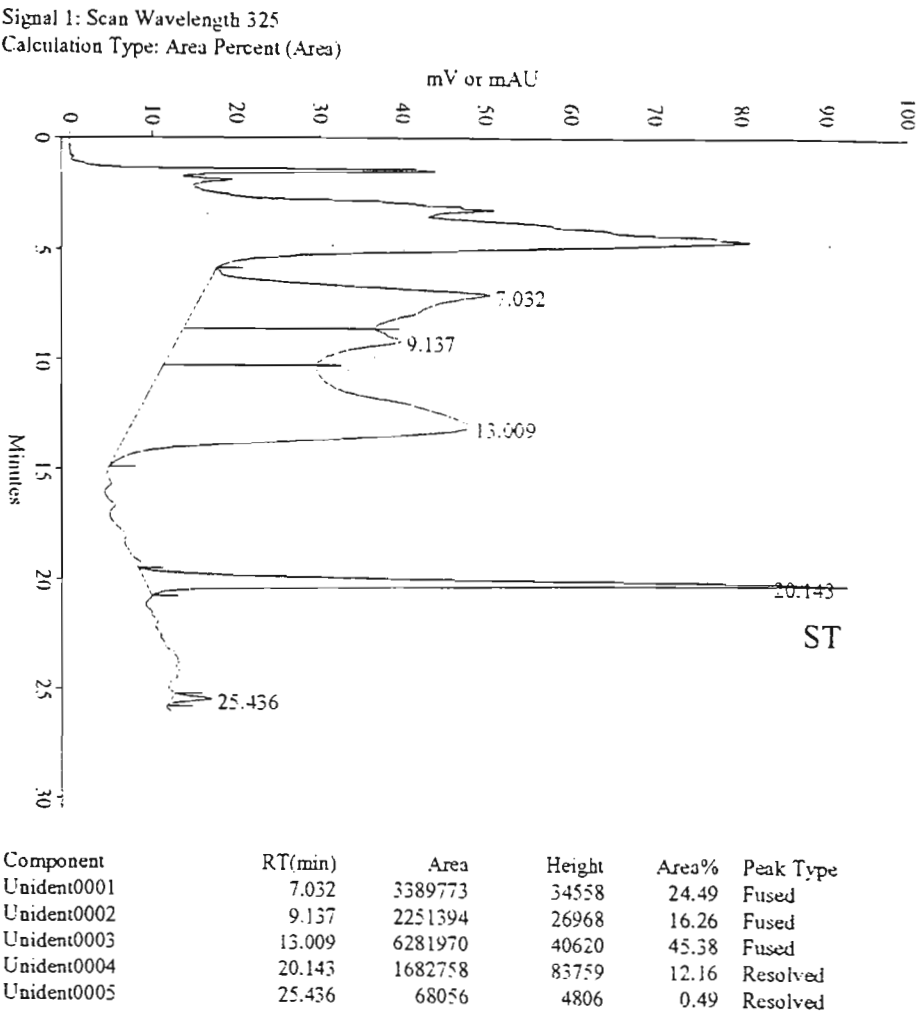
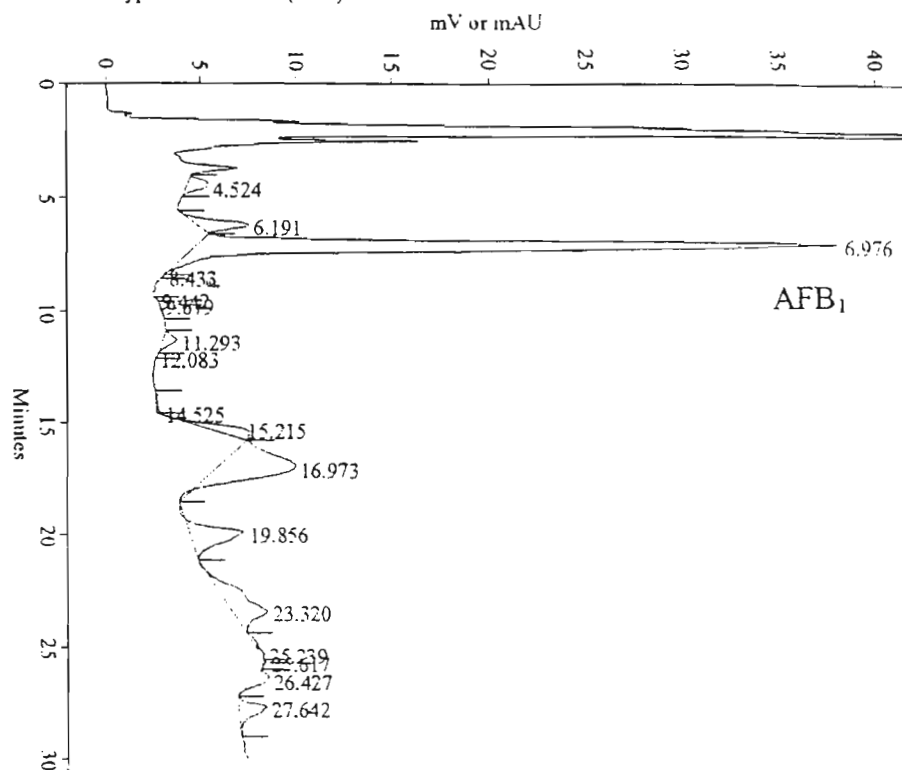


Figure 103. A Typical Liquid Chromatogram of ST in Enzyme Fraction 9-30, in the Presence of NADPH (1.5 mM), at pH 7.2 and 28 °C for an Incubation Time of 3 Hours

## APPENDIX 58

Signal 1: Scan Wavelength 360

Calculation Type: Area Percent (Area)



Component	RT(min)	Area	Height	Area%	Peak Type
Unident0001	4.524	33038	1092	1.90	Resolved
Unident0002	6.191	67664	2660	3.89	Fused
Unident0003	6.976	897993	33211	51.68	Fused
Unident0004	8.433	130	54	7.48e-03	Fused
Unident0005	9.442	140	64	8.06e-03	Fused
Unident0006	9.679	891	101	0.05	Fused
Unident0007	11.293	21181	730	1.22	Fused
Unident0008	12.083	333	66	0.02	Fused
Unident0009	14.525	5117	203	0.29	Fused
Unident0010	15.215	59948	1901	3.45	Fused
Unident0011	16.973	290574	4094	16.72	Fused
Unident0012	19.856	123129	2826	7.09	Fused
Unident0013	23.320	144084	1820	8.29	Fused
Unident0014	25.239	11673	256	0.67	Fused

Figure 104. A Typical Liquid Chromatogram for the Conversion of OPROST to AFB<sub>1</sub> in Enzyme Fraction 9-30, in the Presence of NADPH (1.5 mM), at pH 7.2 and 28 °C for an Incubation Time of 3 Hours

APPENDIX 59

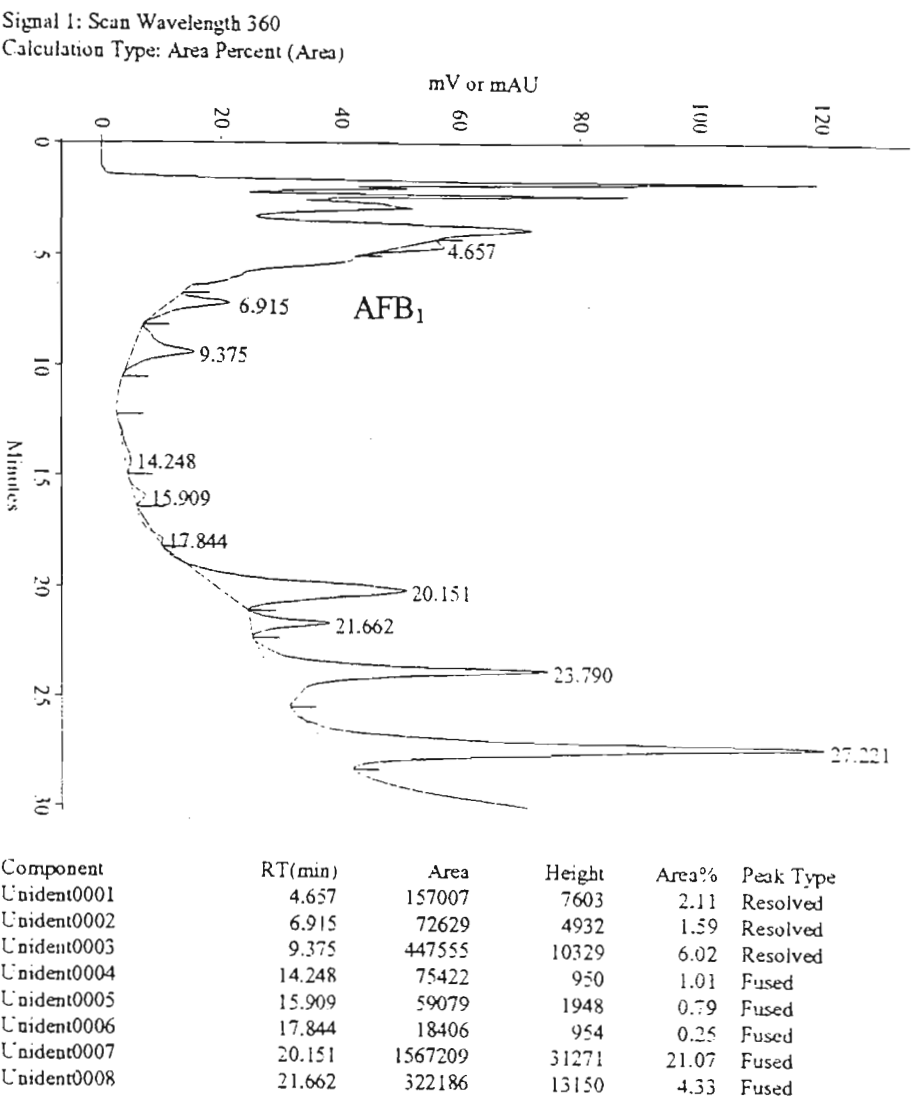
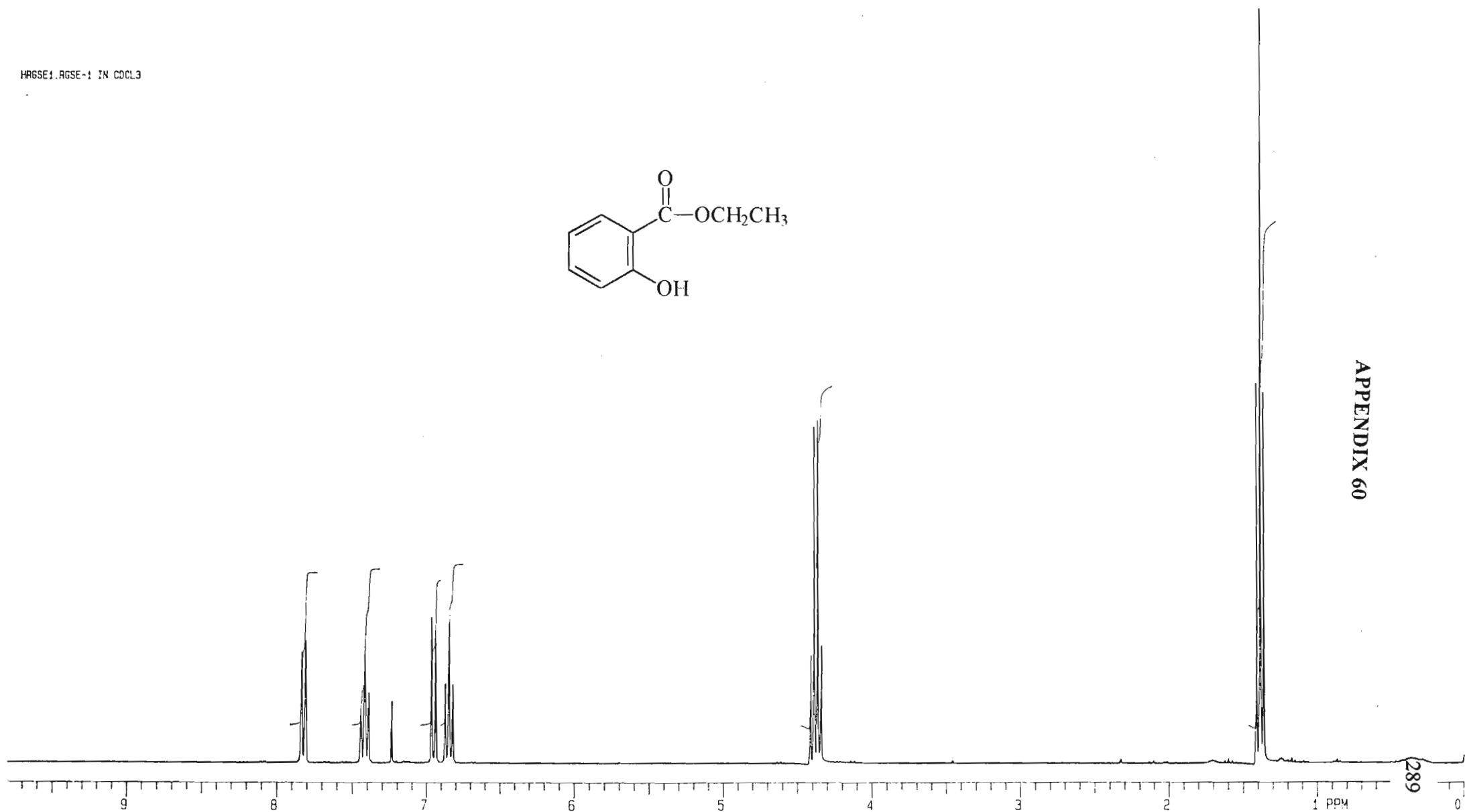
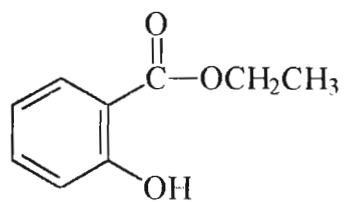


Figure 105. A Typical Liquid Chromatogram for the Conversion of OBzST to AFB<sub>1</sub> in Enzyme Fraction 9-30, in the Presence of NADPH (1.5 mM), at pH 7.2 and 28 °C for an Incubation Time of 3 Hours

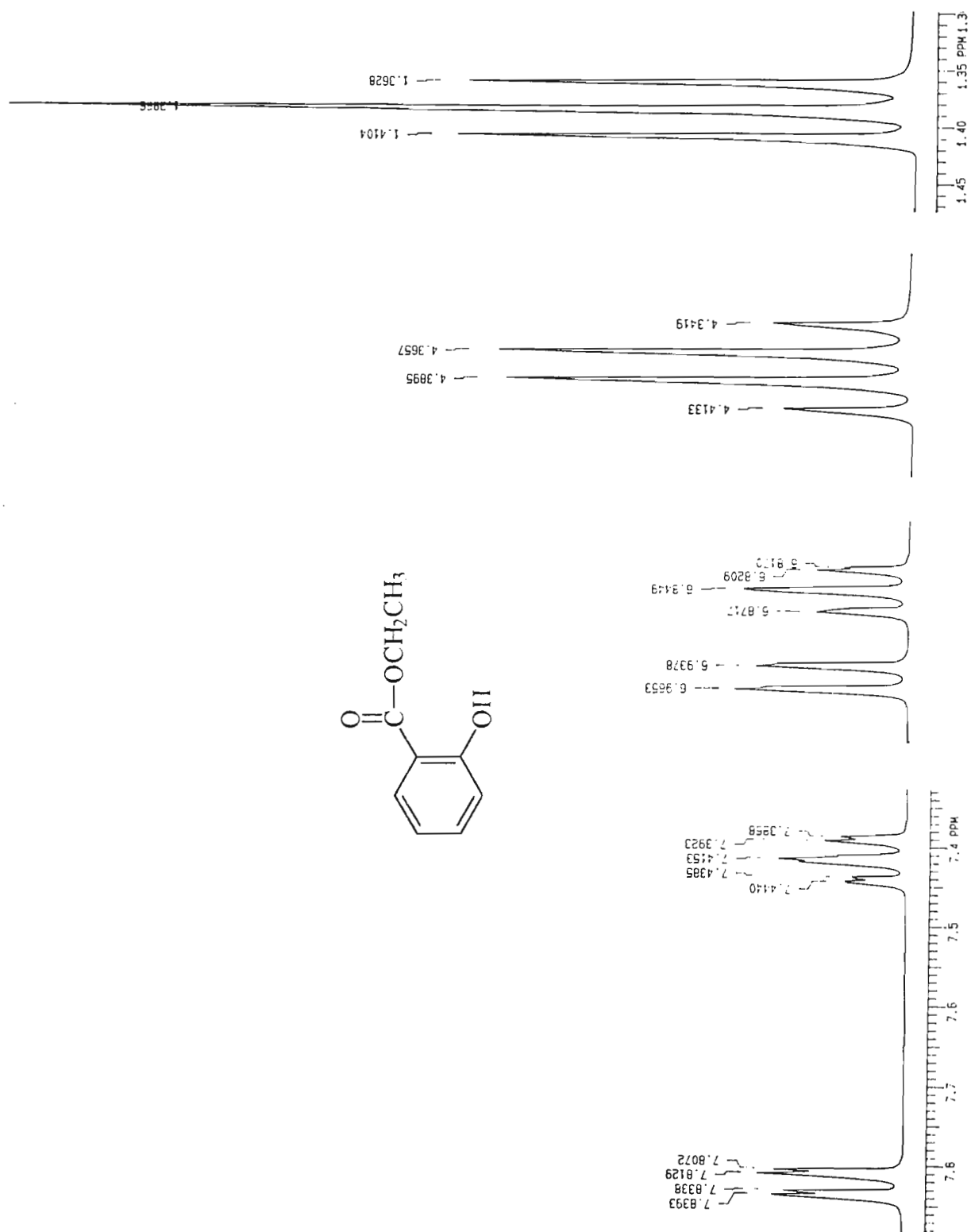
HR6SE1. RGSE-1 IN CDCL3



APPENDIX 60

Figure 118. The  $^1\text{H}$ -NMR Spectrum of Ethyl Salicylate

## APPENDIX 61

Figure 119. The Expanded  $^1\text{H}$ -NMR Spectrum of Ethyl Salicylate



HR6XN3.RGXAN-3 IN CDCL3

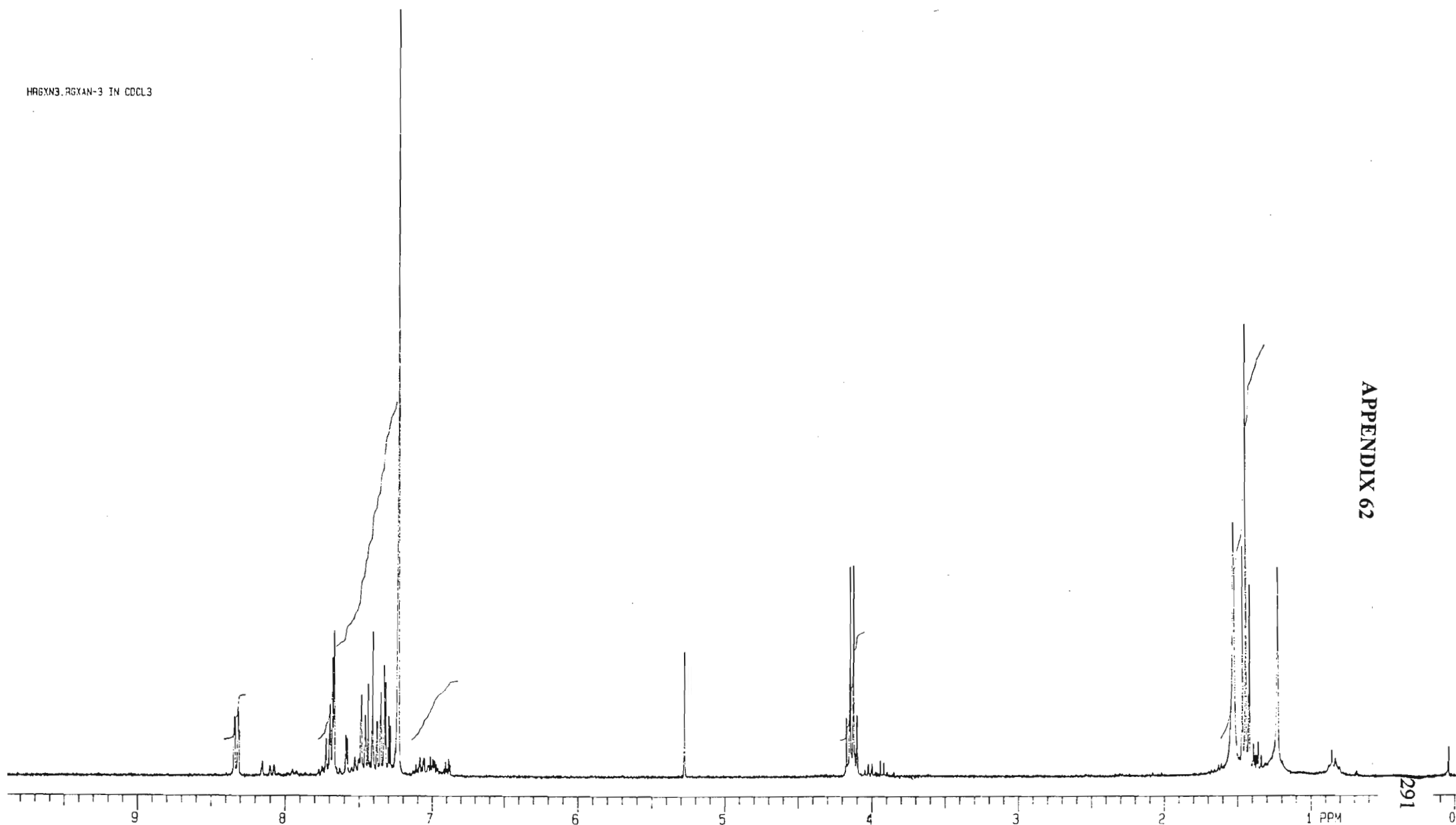


Figure 120. The  $^1\text{H}$ -NMR Spectrum of the Compound Obtained from the Condensation of Ethyl Salicylate with Hydroquinone

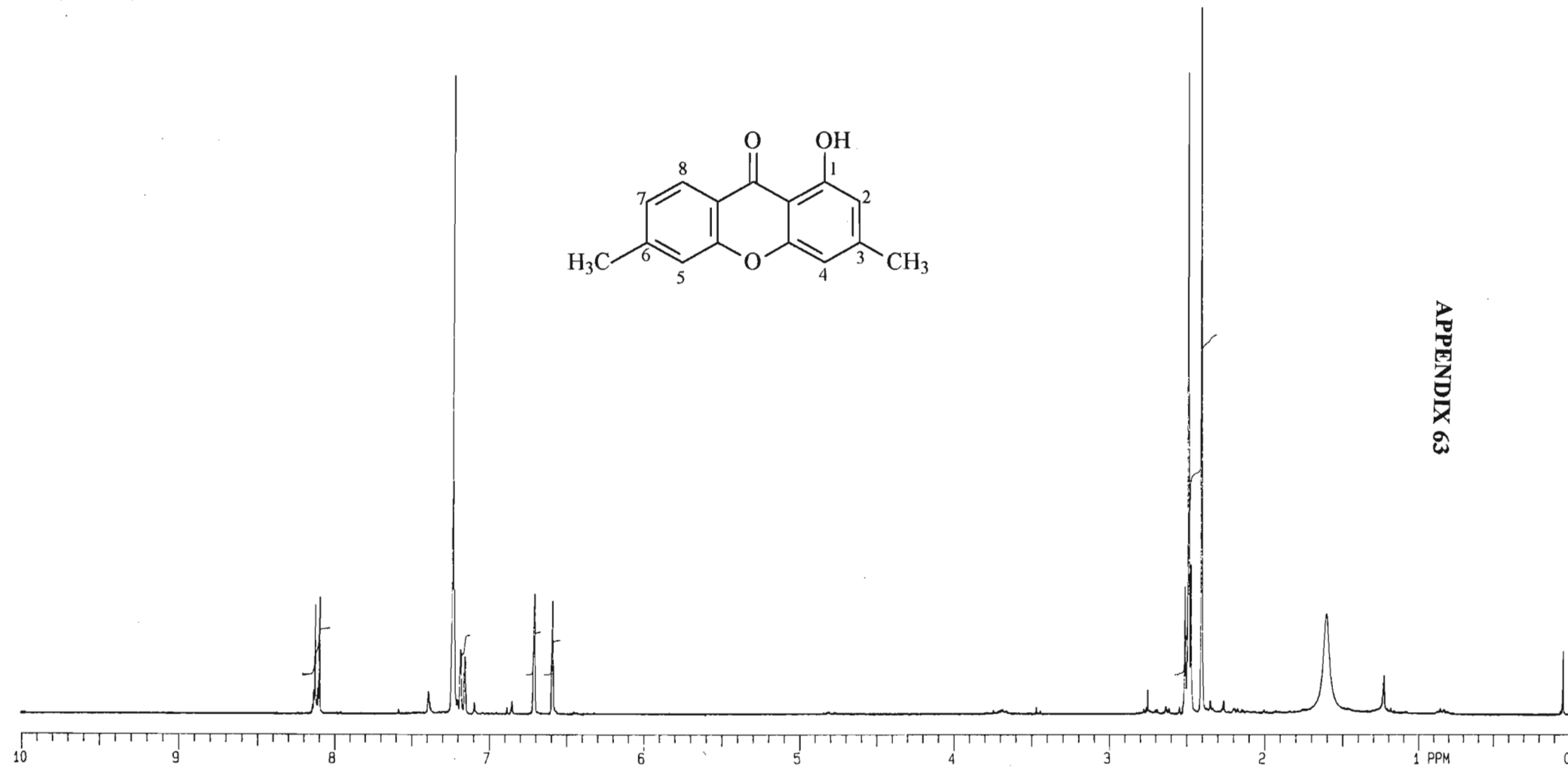
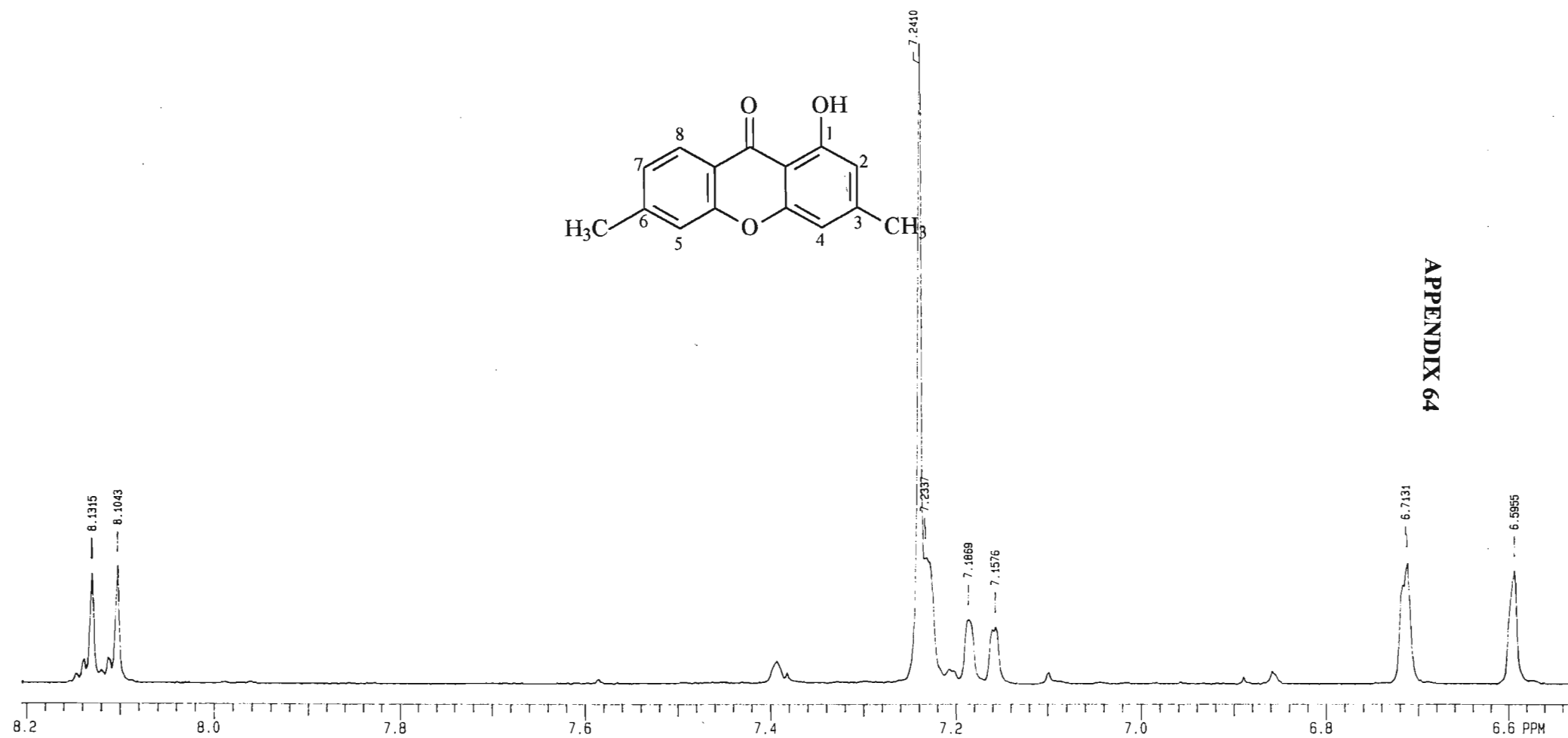
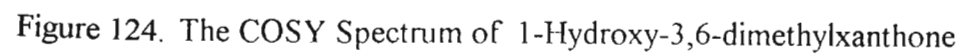


Figure 122. The <sup>1</sup>H-NMR Spectrum of 1-Hydroxy-3,6-dimethylxanthone

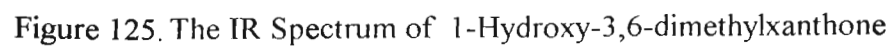


APPENDIX 64

Figure 123. The Expanded <sup>1</sup>H-NMR Spectrum of 1-Hydroxy-3,6-dimethylxanthone



295



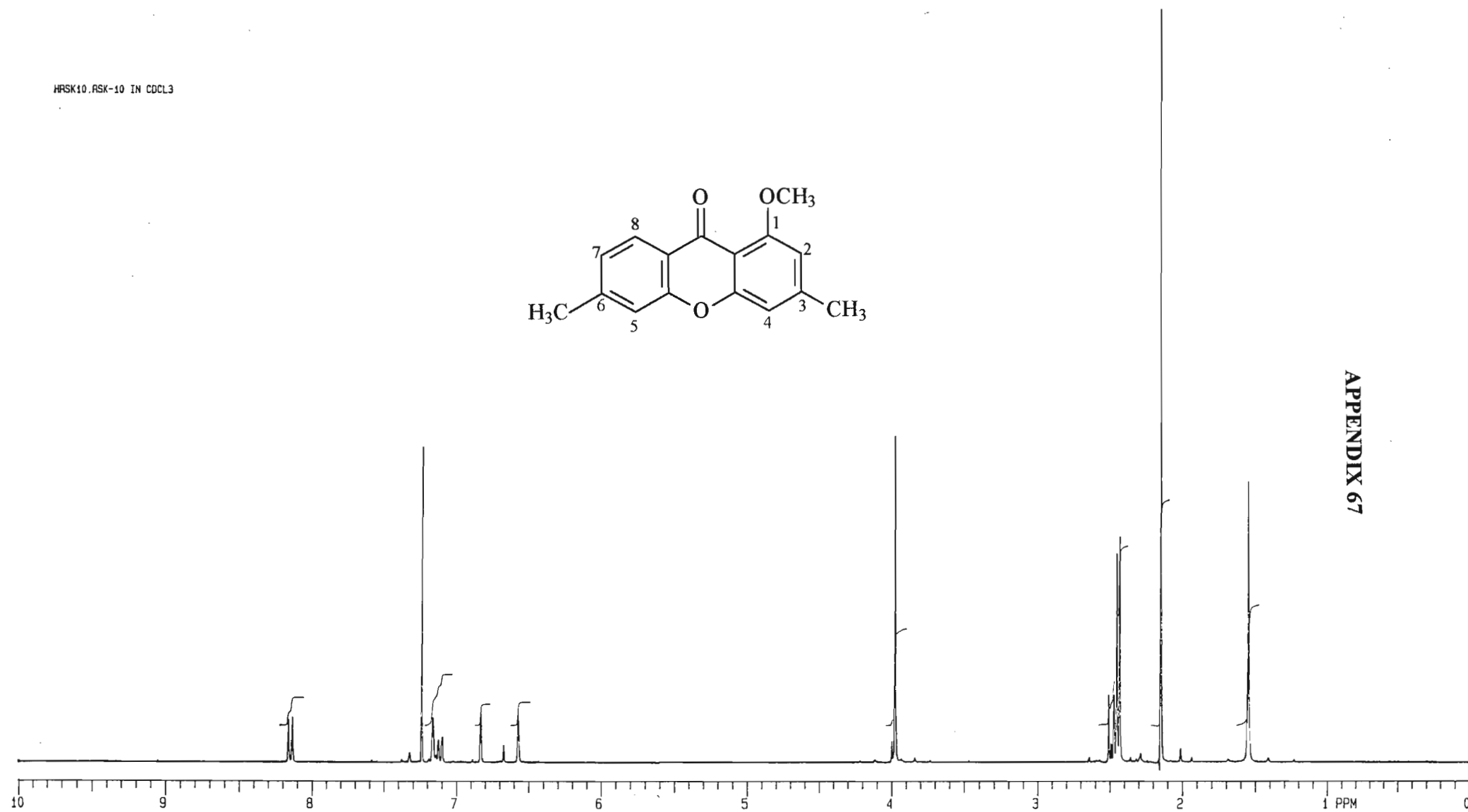
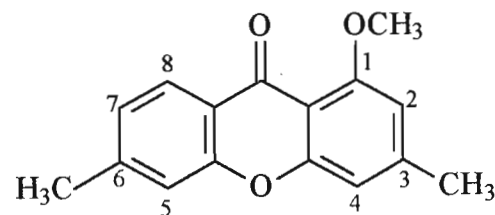


Figure 127. The <sup>1</sup>H-NMR Spectrum of 1-Methoxy-3,6-dimethylxanthone

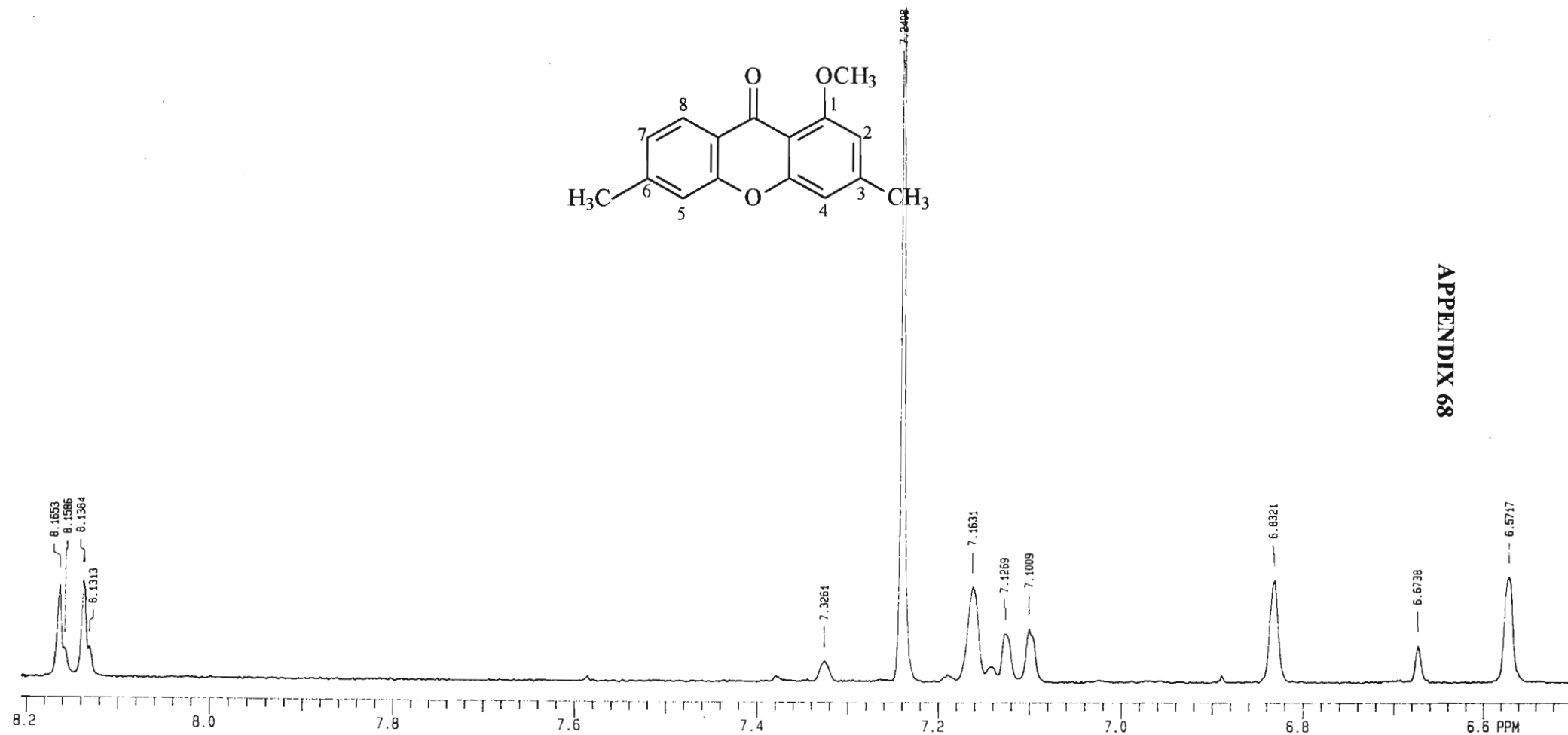


Figure 128. The Expanded <sup>1</sup>H-NMR Spectrum of 1-Methoxy-3,6-dimethylxanthone

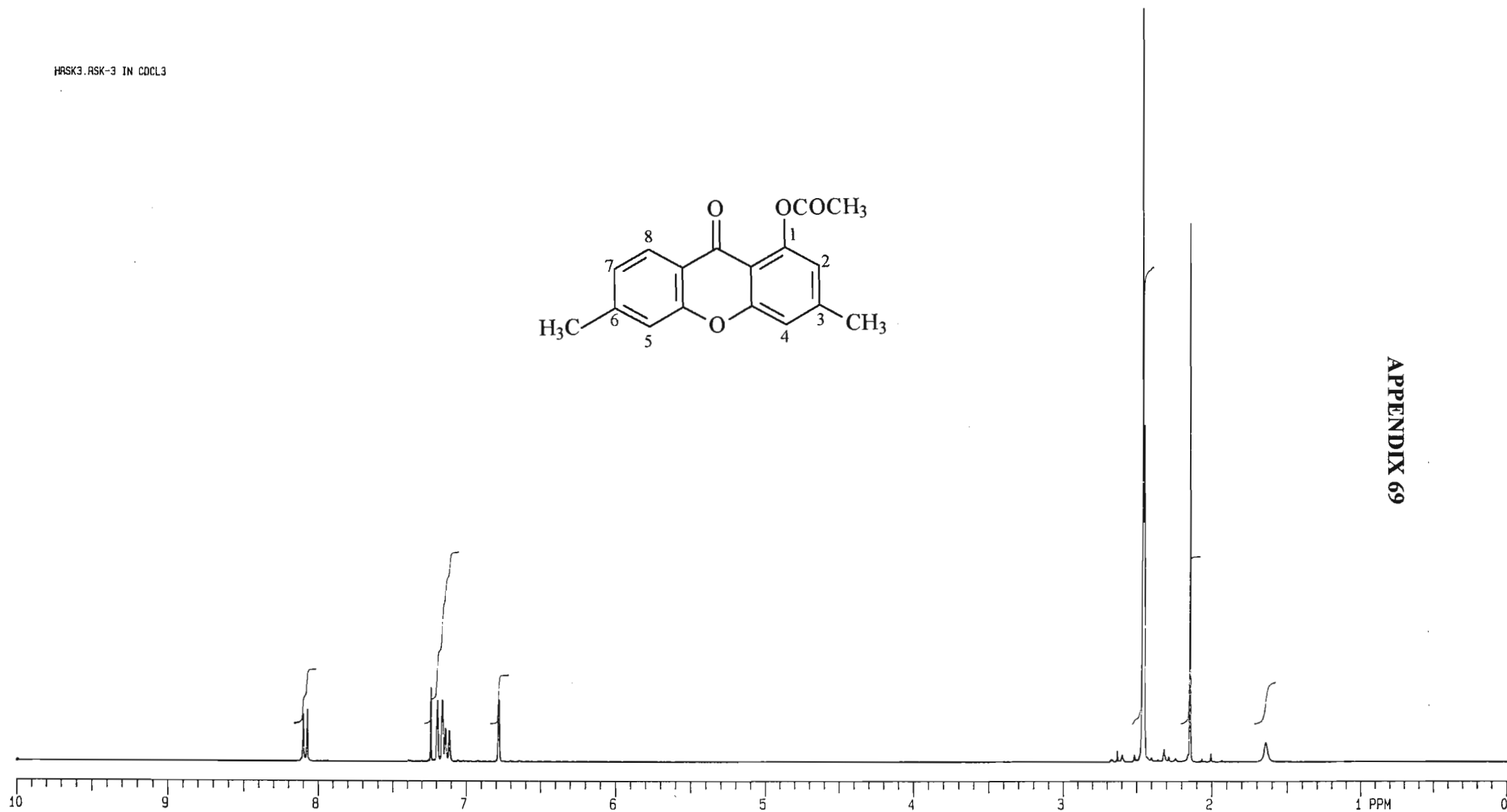
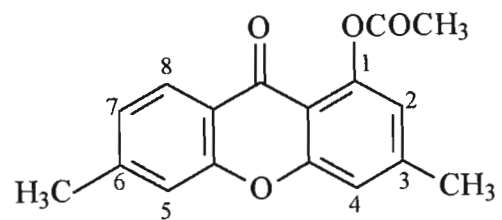


Figure 130. The  $^1\text{H}$ -NMR Spectrum of 1-Acetyl-3,6-dimethylxanthone



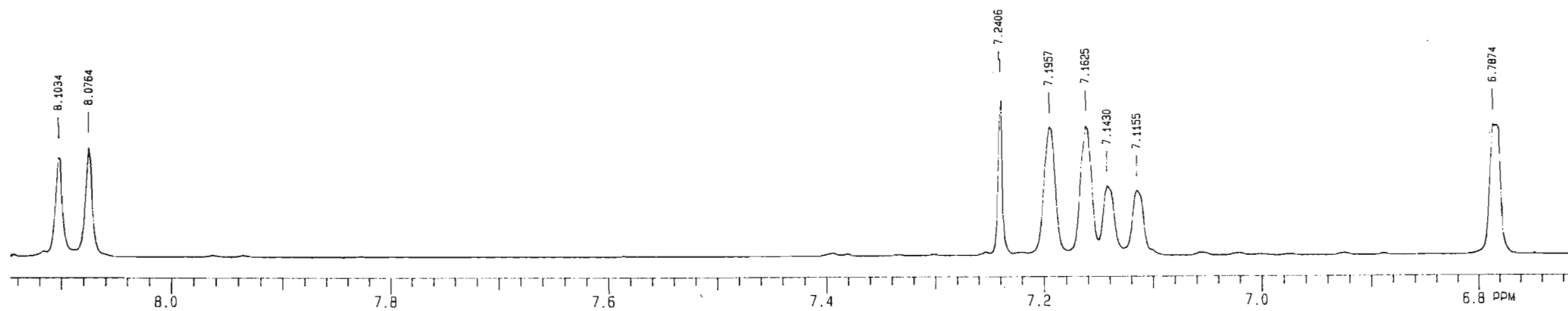
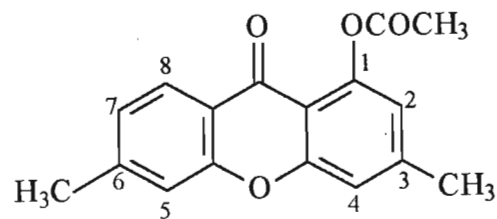


Figure 131. The Expanded <sup>1</sup>H-NMR Spectrum of 1-Acetyl-3,6-dimethylxanthone

APPENDIX 71

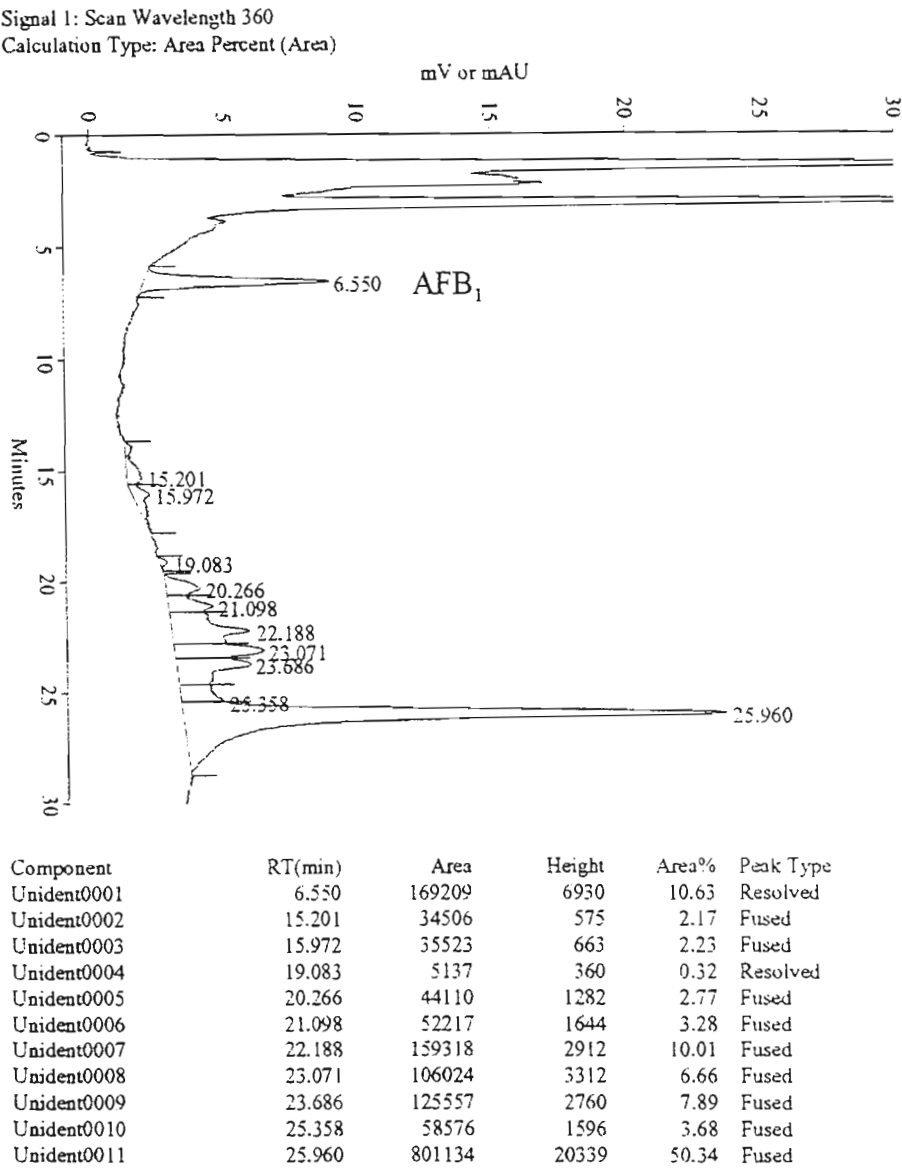
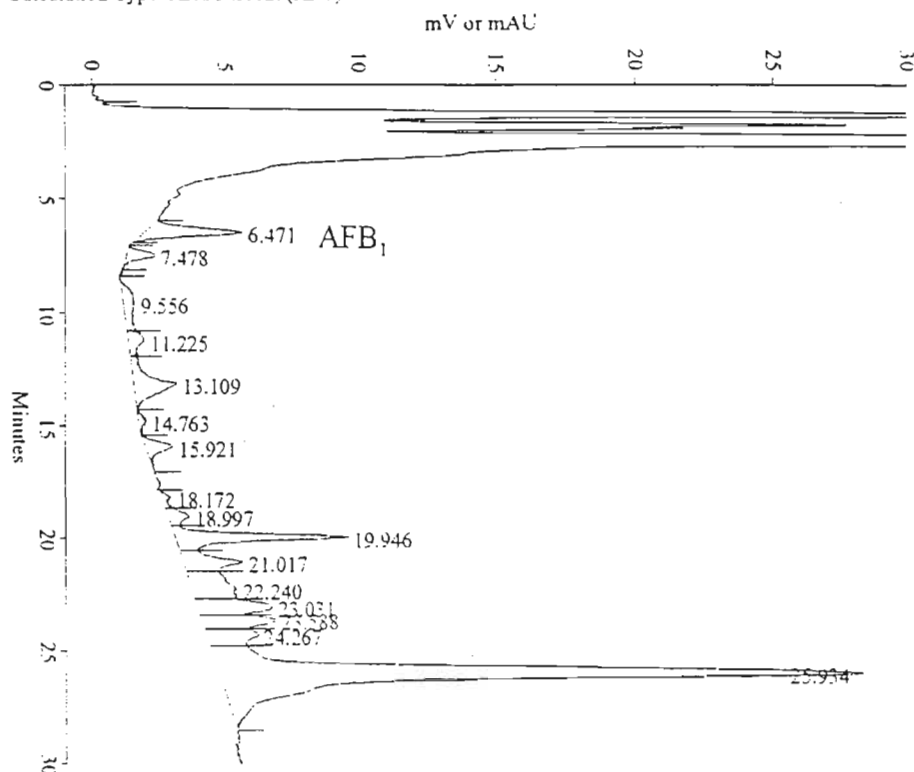


Figure 134. A Typical Liquid Chromatogram for the Production of AFB<sub>1</sub> in Whole Cells of *A. parasiticus* (NIX) in the Presence of 1-Acetyl-3,6-dimethylxanthone

## APPENDIX 72

Signal 1: Scan Wavelength 360

Calculation Type: Area Percent (Area)



Component	RT(min)	Area	Height	Area%	Peak Type
Unident0001	6.471	90759	3652	4.61	Resolved
Unident0002	7.478	26054	1109	1.32	Resolved
Unident0003	9.556	39193	475	1.99	Fused
Unident0004	11.225	27567	632	1.40	Fused
Unident0005	13.109	83422	1642	4.24	Fused
Unident0006	14.763	7705	294	0.39	Fused
Unident0007	15.921	32318	1067	1.64	Fused
Unident0008	18.172	7550	346	0.38	Fused
Unident0009	18.997	24450	801	1.24	Fused
Unident0010	19.946	156183	6521	7.94	Fused
Unident0011	21.017	75455	2261	3.83	Fused
Unident0012	22.240	106304	1668	5.40	Fused
Unident0013	23.031	97852	2775	4.97	Fused
Unident0014	23.588	85375	2739	4.34	Fused
Unident0015	24.267	73475	1922	3.73	Fused
Unident0016	25.934	1034432	23637	52.56	Fused
Totals		1968094	51541	100.00	

Figure 135. A Typical Liquid Chromatogram for the Production of AFB<sub>1</sub> in Whole Cells of *A. parasiticus* (NIX) in the Presence of 1-Hydroxy-3,6-dimethylxanthone

APPENDIX 73

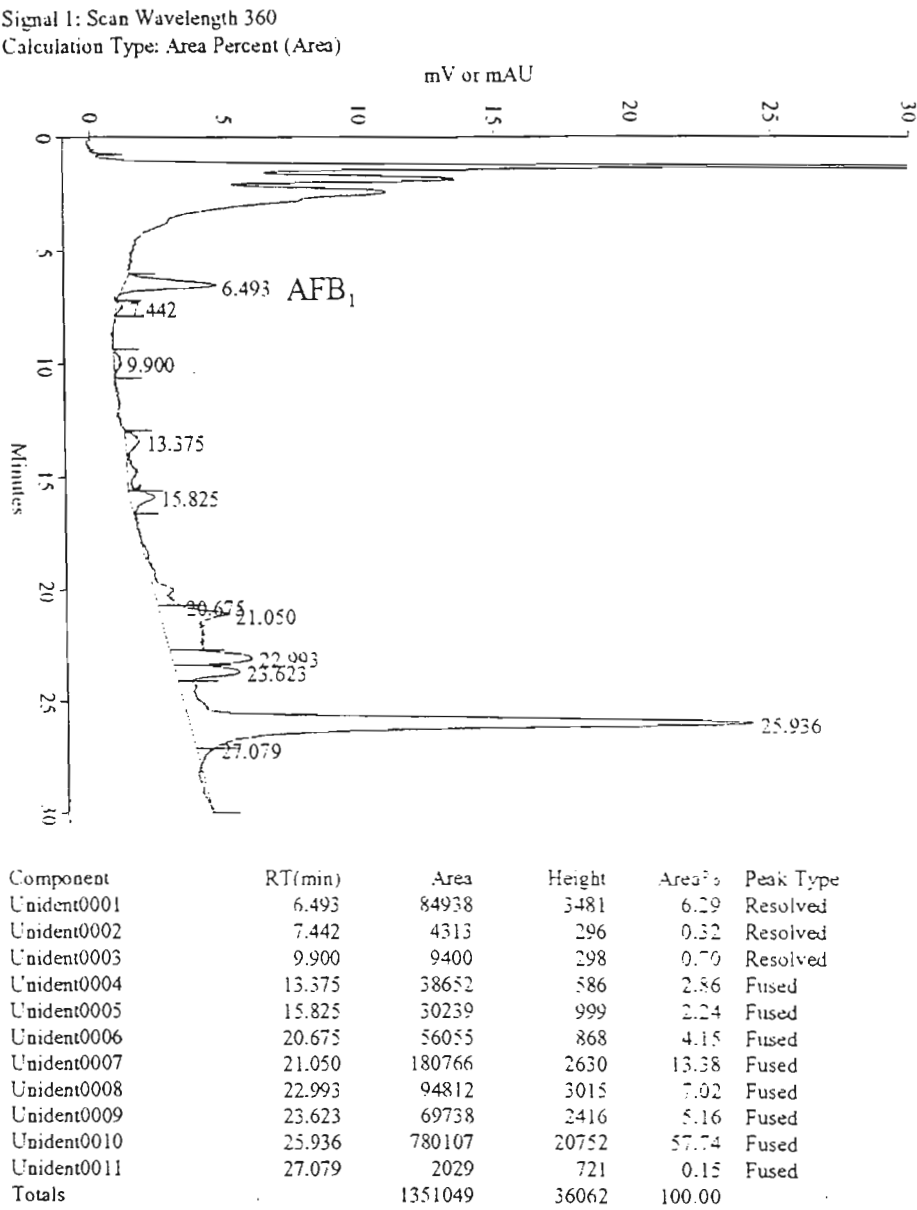


Figure 136 . A Typical Liquid Chromatogram for the Production of AFB<sub>1</sub> in Whole Cells of *A. parasiticus* (NIX) in the Presence of 1-Methoxy-3,6-dimethylxanthone

## APPENDIX 74

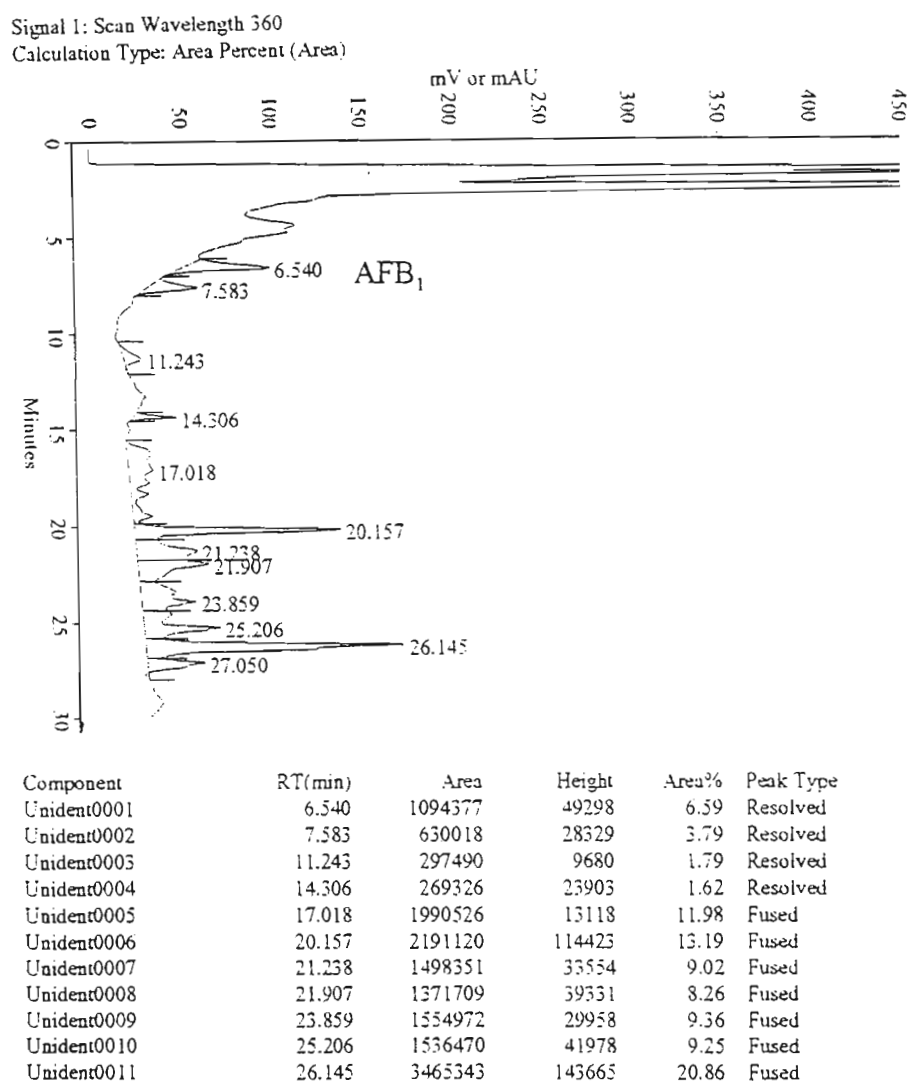


Figure 137. A Typical Liquid Chromatogram for the Conversion of OMST to AFB<sub>1</sub> in Whole Cells of *A. parasiticus* (Wh1) in the Presence of 1-Acetyl-3,6-dimethylxanthone

APPENDIX 75

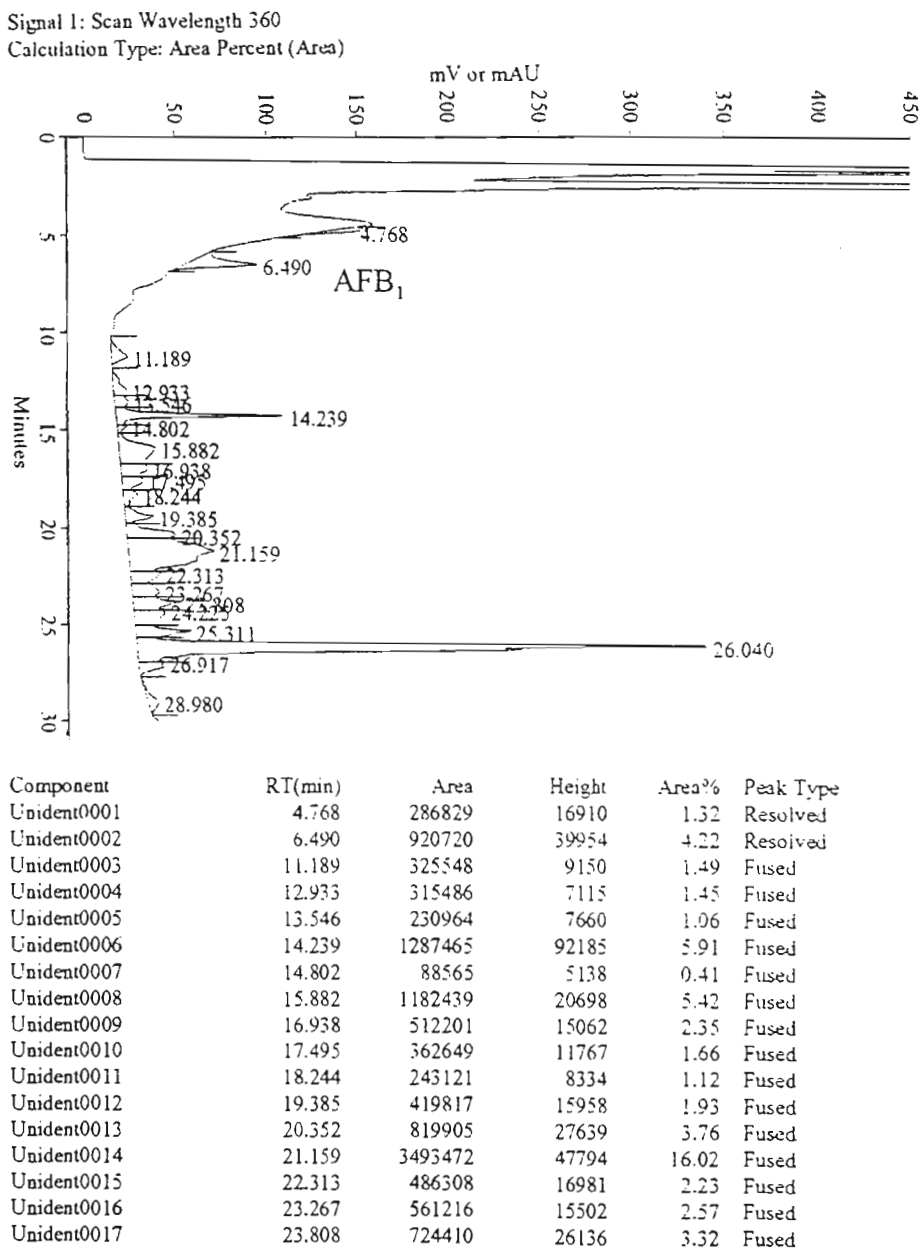


Figure 138. A Typical Liquid Chromatogram for the Conversion of OMST to AFB<sub>1</sub> in Whole Cells of *A. parasiticus* (Wh1) in the Presence of 1-Hydroxy-3,6-dimethylxanthone

APPENDIX 76

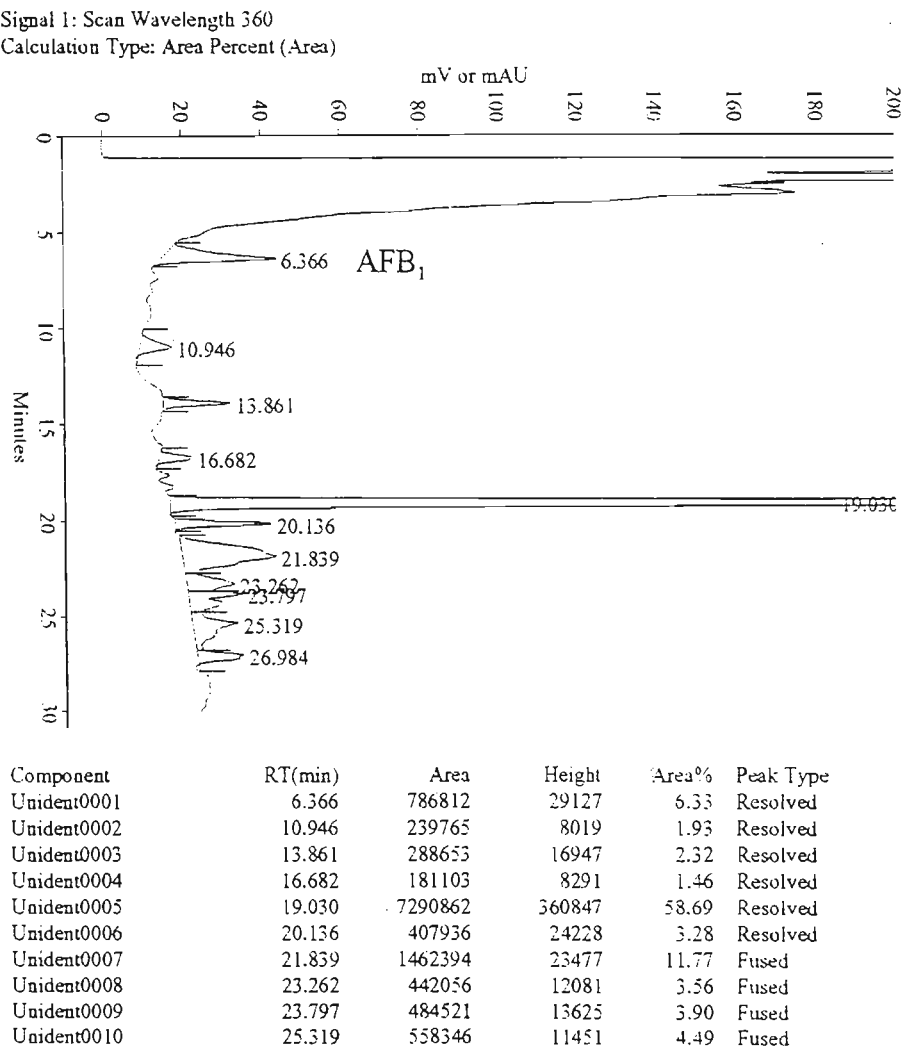


Figure 139. A Typical Liquid Chromatogram for the Conversion of OMST to AFB<sub>1</sub> in Whole Cells of *A. parasiticus* (Wh1) in the Presence of 1-Methoxy-3,6-dimethylxanthone

APPENDIX 77

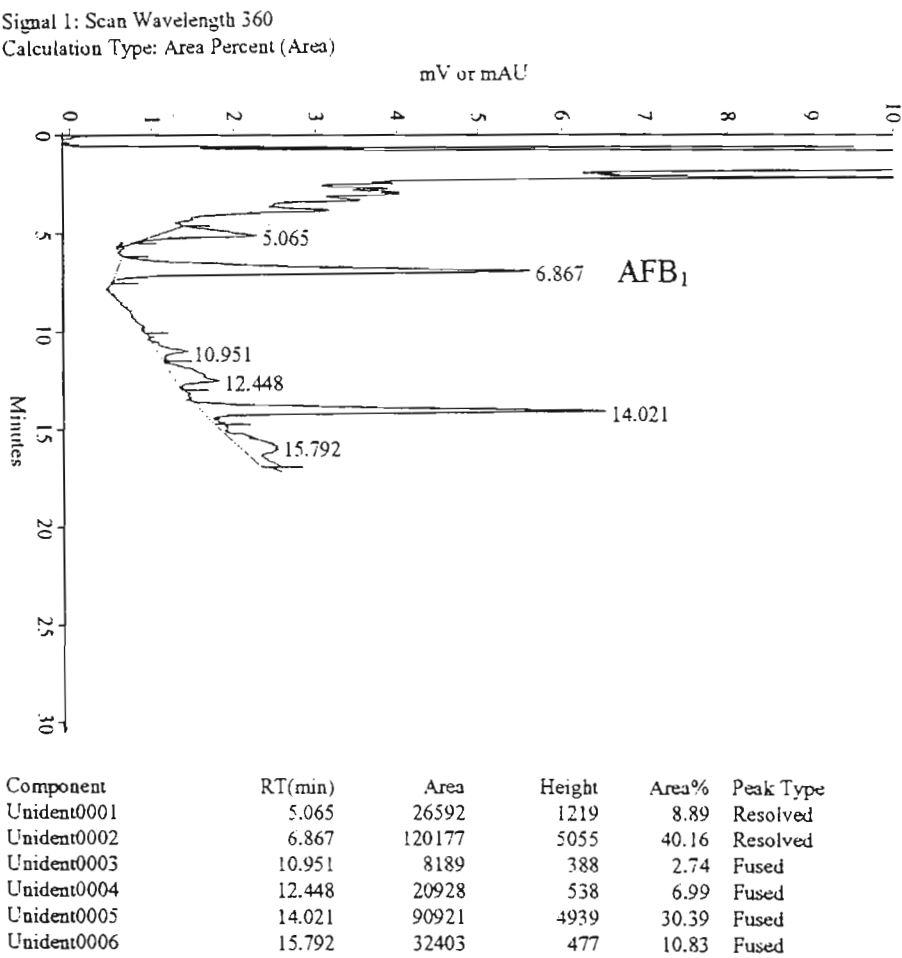


Figure 140. A Typical Liquid Chromatogram for the Conversion of OMST to AFB<sub>1</sub> in a Cell-Free Extract at pH 7.2 and 28 °C for an Incubation Time of 1 Hour



APPENDIX 78

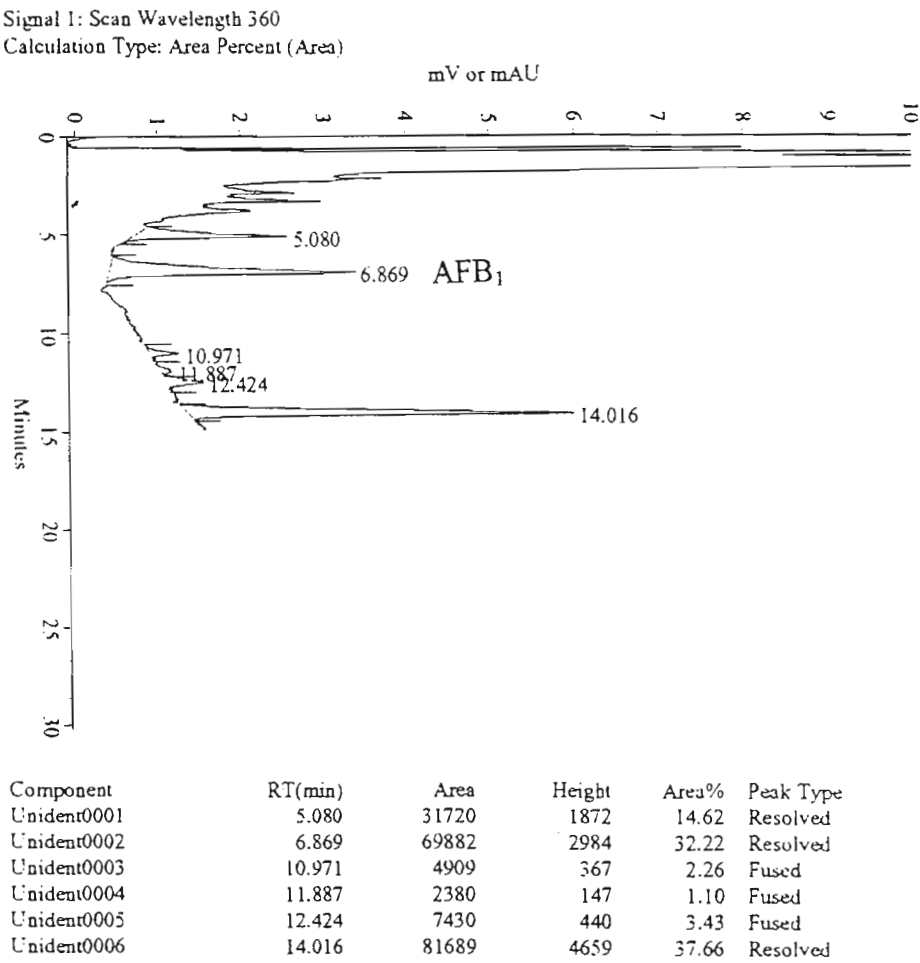
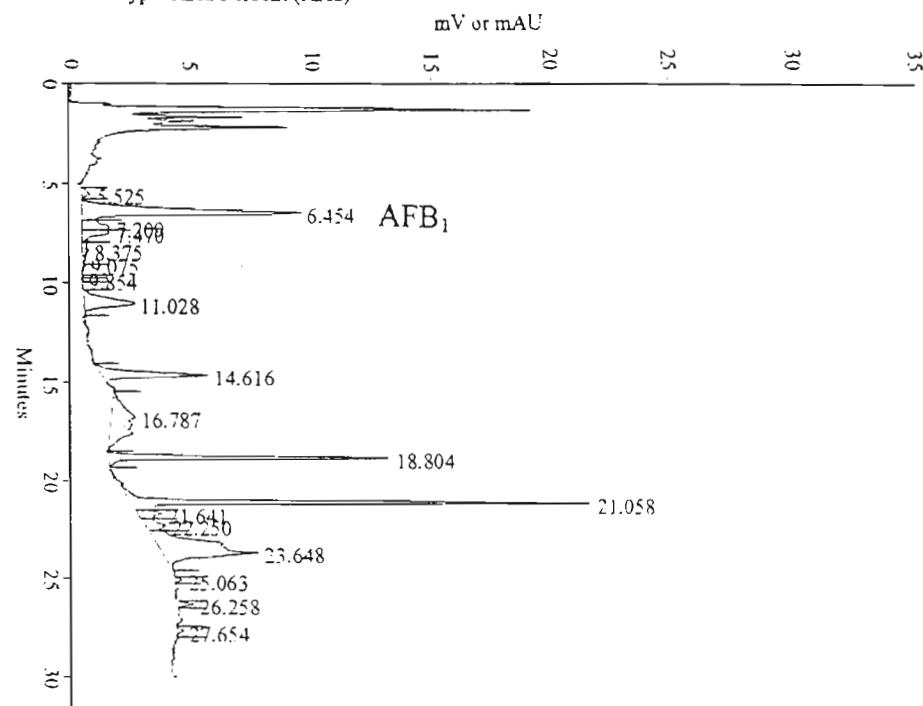


Figure 141. A Typical Liquid Chromatogram for the Conversion of OMST to AFB<sub>1</sub> in a Cell-Free Extract, in the Presence of 1-Methoxy-3,6-dimethylxanthone, at pH 7.2 and 28 °C for an Incubation Time of 1 Hour

## APPENDIX 79

Signal 1: Scan Wavelength 360

Calculation Type: Area Percent (Area)



Component	RT(min)	Area	Height	Area%	Peak Type
Unident0001	5.525	6049	419	0.56	Fused
Unident0002	6.454	194279	9103	17.95	Fused
Unident0003	7.209	27236	1203	2.52	Fused
Unident0004	7.470	23666	1220	2.19	Fused
Unident0005	8.375	10266	306	0.95	Fused
Unident0006	9.075	925	159	0.09	Fused
Unident0007	9.854	167	101	0.02	Resolved
Unident0008	11.028	61399	2138	5.67	Resolved
Unident0009	14.616	78012	4448	7.21	Fused
Unident0010	16.787	94516	1051	8.73	Fused
Unident0011	18.804	133846	11701	12.37	Fused
Unident0012	21.058	216347	19253	19.99	Fused
Unident0013	21.641	18365	1036	1.70	Fused
Unident0014	22.250	21926	890	2.03	Fused
Unident0015	23.648	185682	3943	17.16	Fused

Figure 142. A Typical Liquid Chromatogram for the Conversion of OMST to AFB<sub>1</sub> in a Cell-Free Extract at pH 7.2 and 28 °C for an Incubation Time of 10 Minutes

APPENDIX 80

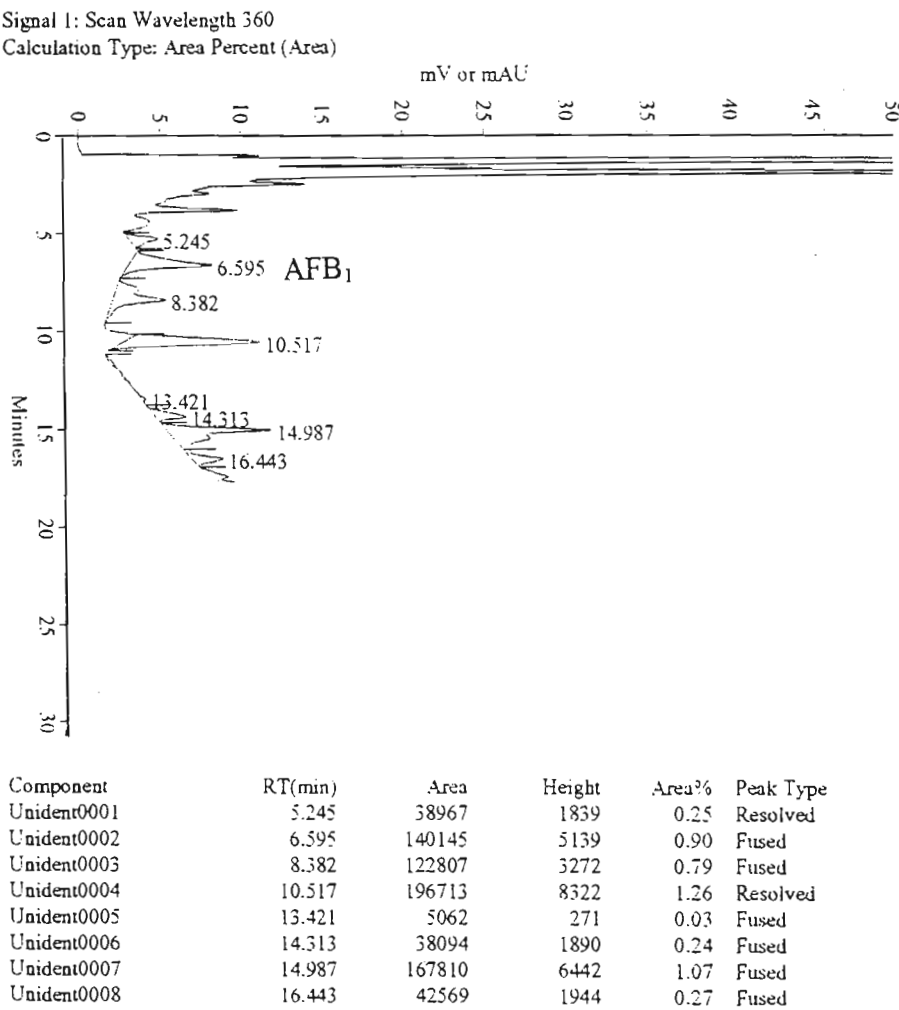


Figure 143. A Typical Liquid Chromatogram for the Conversion of OMST to AFB<sub>1</sub> in a Cell-Free Extract, in the Presence of 1-Methoxy-3,6-dimethylxanthone, at pH 7.2 and 28 °C for an Incubation Time of 10 Minutes

APPENDIX 81

Table 37. The Data for the Calibration Graph of AFB<sub>1</sub>.

Concentration (p.p.b.)	Peak Area
40	1922
50	2439
100	4602
500	25026
1000	70543

APPENDIX 82

R squared = 0.97

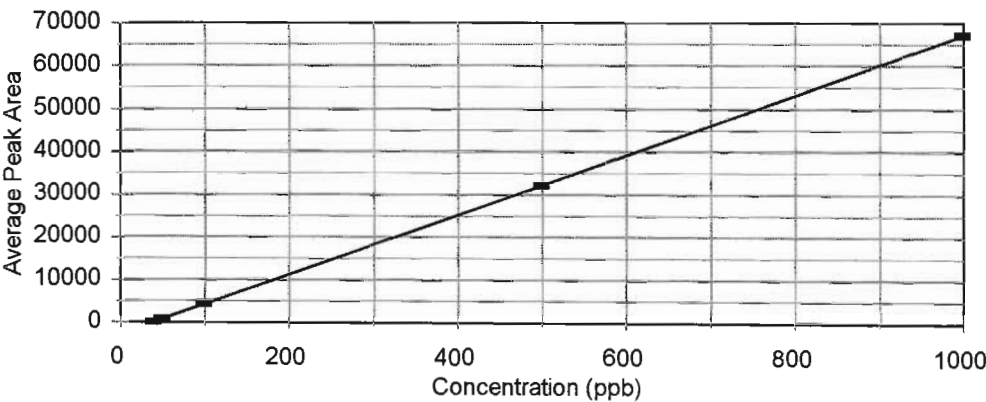


Figure 154. The Calibration Graph of AFB<sub>1</sub>.

APPENDIX 83

Table 38. The Data for the Calibration Graph of NADPH.

Concentration of NADPH (mg /5ml)	Absorbance at 340 nm
0.005	0.008
0.01	0.011
0.02	0.025
0.03	0.037
0.04	0.043
0.05	0.059

APPENDIX 84

R squared = 0.98

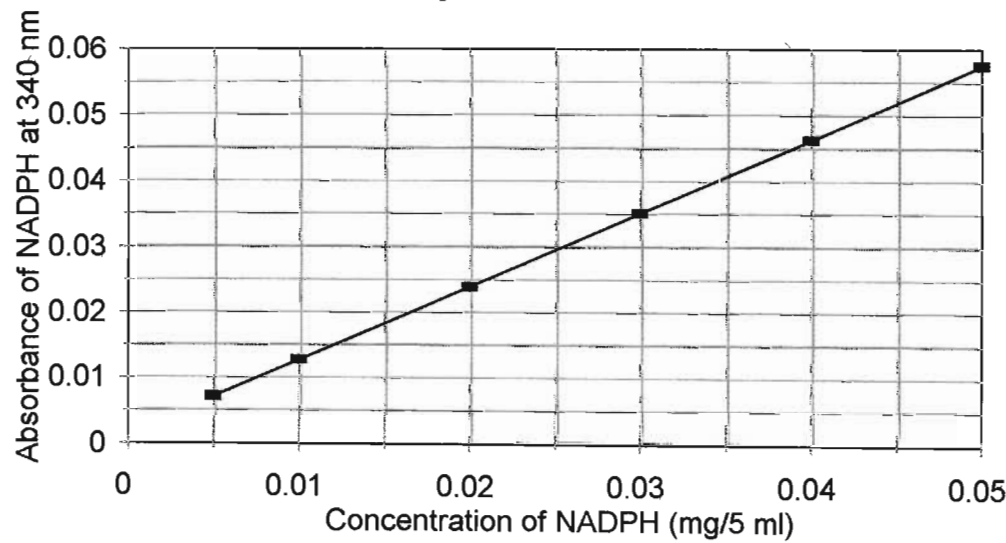


Figure 155. The Calibration Graph of NADPH.

APPENDIX 85

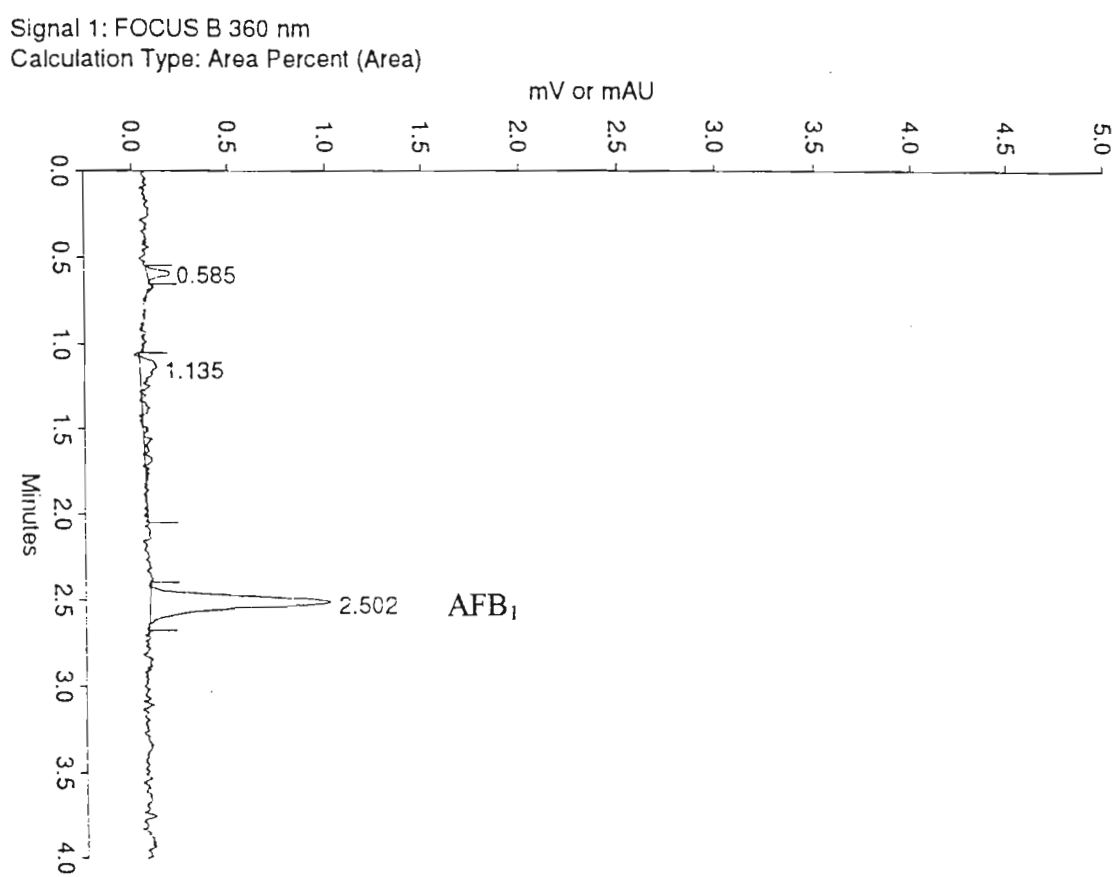


Figure 172. A Typical Liquid Chromatogram of Standard AFB<sub>1</sub> with an Aqueous Mobile Phase of Acetonitrile (60 %) at a Flow Rate of 1 ml/min.

APPENDIX 86

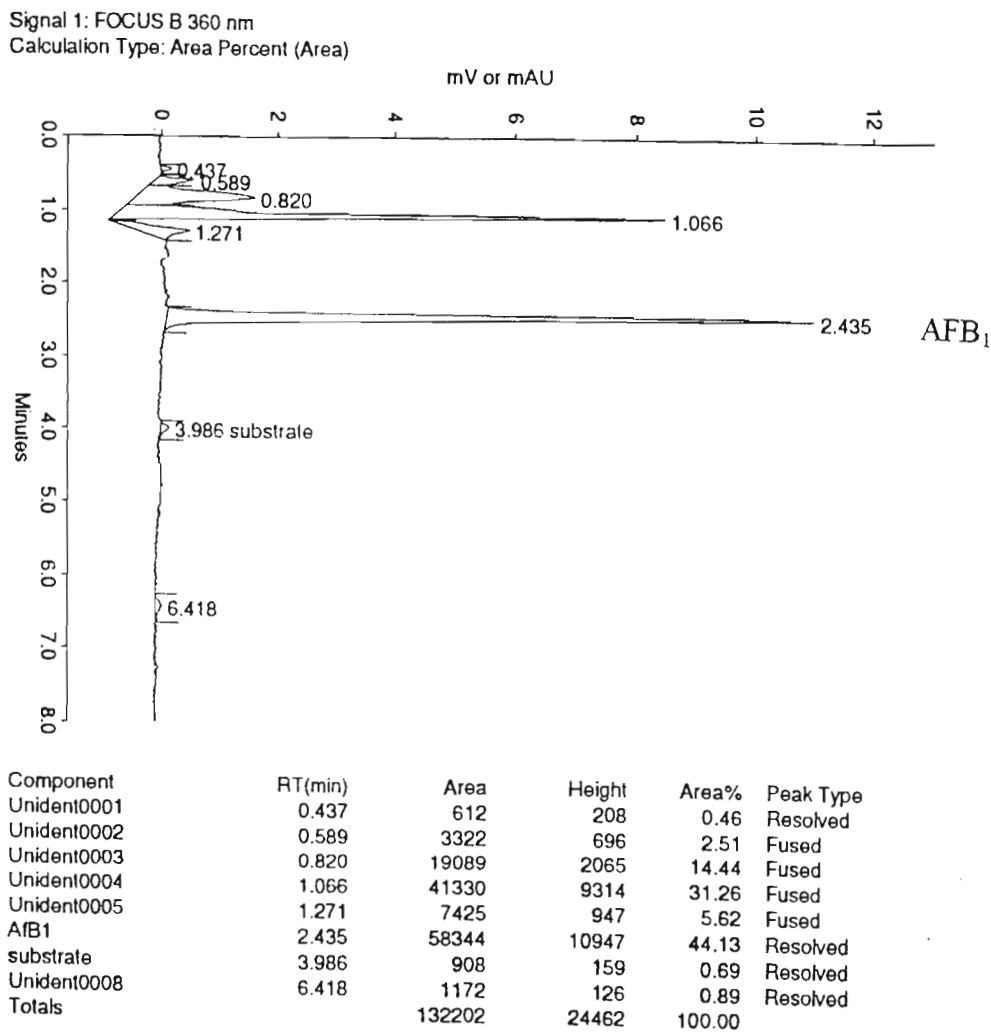


Figure 173. A Typical Liquid Chromatogram for the Conversion of OMST to AFB<sub>1</sub> in a Partially Purified Enzyme(s) Fraction 9-30 in the Presence of NADPH (50 µg/50 µl)

APPENDIX 87

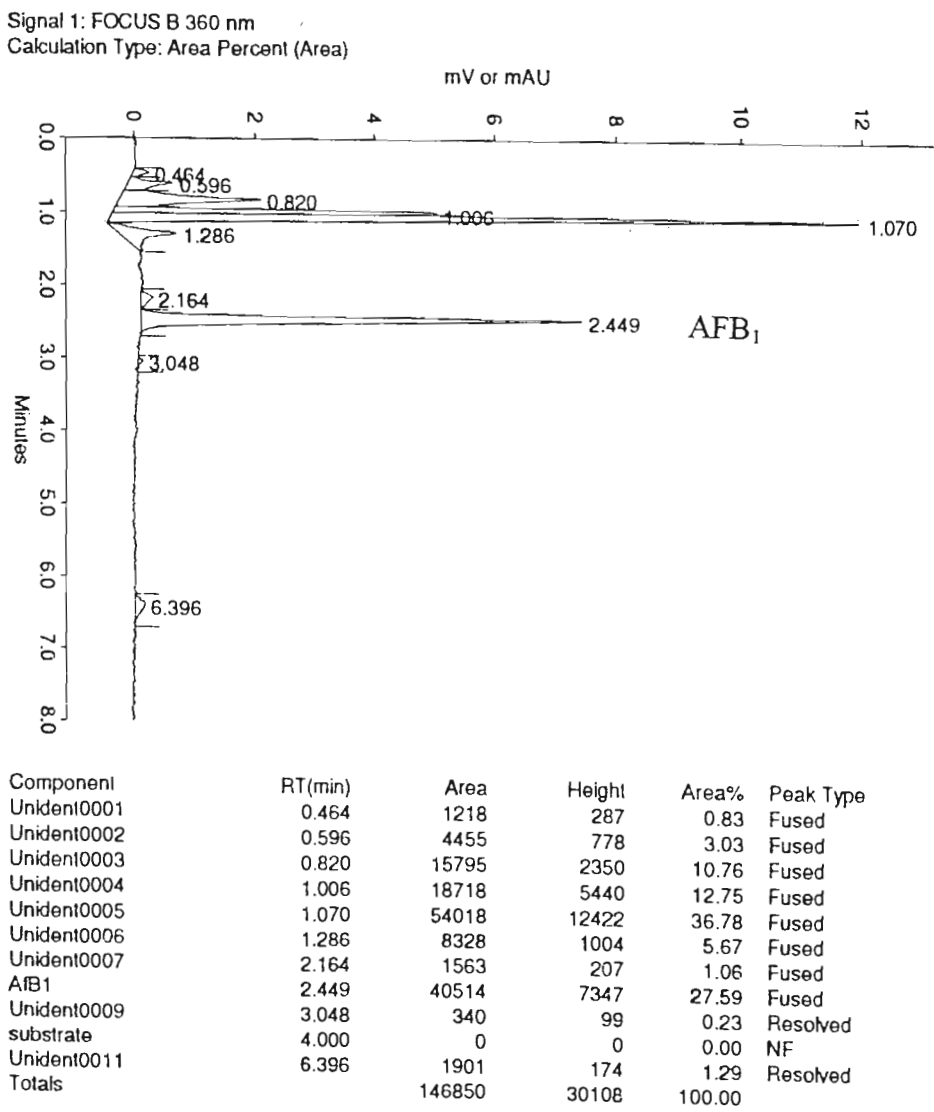


Figure 174. A Typical Liquid Chromatogram for the Conversion of OMST to AFB<sub>1</sub> in a Partially Purified Enzyme(s) Fraction 9-30 in the Presence of NADPH (50 µg/50 µl)